


Methods in
Molecular Biology 720

Springer Protocols

Anthony E. Pegg
Robert A. Casero, Jr. *Editors*

Polyamines

Methods and Protocols

 Humana Press

METHODS IN MOLECULAR BIOLOGY™

Series Editor
John M. Walker
School of Life Sciences
University of Hertfordshire
Hatfield, Hertfordshire, AL10 9AB, UK

For other titles published in this series, go to
www.springer.com/series/7651

Polyamines

Methods and Protocols

Edited by

ANTHONY E. PEGG

*Department of Cellular and Molecular Physiology, Milton S. Hershey Medical Center,
Pennsylvania State University College of Medicine, Hershey, PA, USA*

ROBERT A. CASERO, Jr.

*The Sidney Kimmel Comprehensive Cancer Center, Johns Hopkins University
School of Medicine, Baltimore, MD, USA*

 **Humana Press**

Editors

Anthony E. Pegg, Ph.D.
College of Medicine
Milton S. Hershey Medical Center
Pennsylvania State University
University Drive 500
Hershey, PA 17033-0850, USA
apegg@psu.edu

Robert A. Casero, Jr., Ph.D.
School of Medicine
Sidney Kimmel Comprehensive Cancer Center
Johns Hopkins University
Orleans St. 1650
Baltimore, MD 21231, USA
rcasero@jhmi.edu

ISSN 1064-3745 e-ISSN 1940-6029
ISBN 978-1-61779-033-1 e-ISSN 978-1-61779-034-8
DOI 10.1007/978-1-61779-034-8
Springer New York Dordrecht Heidelberg London

Library of Congress Control Number: 2011921314

© Springer Science+Business Media, LLC 2011

All rights reserved. This work may not be translated or copied in whole or in part without the written permission of the publisher (Humana Press, c/o Springer Science+Business Media, LLC, 233 Spring Street, New York, NY 10013, USA), except for brief excerpts in connection with reviews or scholarly analysis. Use in connection with any form of information storage and retrieval, electronic adaptation, computer software, or by similar or dissimilar methodology now known or hereafter developed is forbidden.

The use in this publication of trade names, trademarks, service marks, and similar terms, even if they are not identified as such, is not to be taken as an expression of opinion as to whether or not they are subject to proprietary rights.

Printed on acid-free paper

Humana Press is part of Springer Science+Business Media (www.springer.com)

Preface

Polyamines are ubiquitous cellular components that perform multiple functions and are essential for normal growth and development. Polyamine biosynthesis and the regulation of polyamine levels, which are closely linked to cell growth, have been the subject of many studies over the past 40 years. A volume of this series (Vol. 79, *Polyamine Protocols*) was published in 1998 and described some methods for assays of biosynthetic and catabolic enzymes, measurement of polyamine levels, and transport measurements. In the last decade, there have been important new findings in the polyamine field and a variety of new experimental systems have become available. These include studies with animal models and human patients, which indicate that polyamines play a critical role in normal development and in the development of neoplasia. Therapeutic roles for polyamine inhibitors and analogs have been established and more are under investigation. Polyamine metabolism is now recognized as a significant source of oxidative damage. Polyamines are now established as regulators of critical ion channels. Polyamine transport systems have been characterized much more fully. The polyamine family has been expanded to include compounds present in plants, thermophilic microorganisms, and protozoal parasites that play essential roles in their physiology. Methods for identifying polyamine-responsive genes are now available. The proposed volume will cover methodologies for studies in these areas.

Anthony E. Pegg, PhD
Robert A. Casero, Jr., PhD

Contents

<i>Preface</i>	v
<i>Contributors</i>	xi
PART I INTRODUCTION	
1 Current Status of the Polyamine Research Field <i>Anthony E. Pegg and Robert A. Casero, Jr.</i>	3
PART II IDENTIFICATION OF POLYAMINE METABOLIC ENZYMES AND CHARACTERIZATION OF POLYAMINE-REGULATED GENES AND ION CHANNELS	
2 Exploring Polyamine Biosynthetic Diversity Through Comparative and Functional Genomics <i>Anthony J. Michael</i>	39
3 Characterization of Genes for Polyamine Modulon <i>Kazuei Igarashi and Keiko Kashiwagi</i>	51
4 Posttranscriptional Regulation of Gene Expression in Epithelial Cells by Polyamines <i>Lan Xiao and Jian-Ying Wang</i>	67
5 Identification, Chemical Synthesis, and Biological Functions of Unusual Polyamines Produced by Extreme Thermophiles <i>Tairo Oshima, Toshiyuki Moriya, and Yusuke Terui</i>	81
6 Polyamine Block of Inwardly Rectifying Potassium Channels <i>Harley T. Kurata, Wayland W.L. Cheng, and Colin G. Nichols</i>	113
PART III TRANSGENIC MODELS FOR STUDY OF POLYAMINE FUNCTION	
7 Carcinogenesis Studies in Mice with Genetically Engineered Alterations in Polyamine Metabolism <i>David J. Feith</i>	129
8 Transgenic Rodents with Altered SSAT Expression as Models of Pancreatitis and Altered Glucose and Lipid Metabolism <i>Anne Uimari, Mervi T. Hyvönen, Eija Pirinen, and Leena Alhonen</i>	143
9 Use of (Gyro) Gy and Spermine Synthase Transgenic Mice to Study Functions of Spermine <i>Xiaojing Wang and Anthony E. Pegg</i>	159

PART IV ENZYMES INVOLVED IN POLYAMINE CATABOLISM
AND POSTTRANSLATIONAL PROTEIN MODIFICATION

- 10 A Simple Assay for Mammalian Spermine Oxidase: A Polyamine
Catabolic Enzyme Implicated in Drug Response and Disease 173
Andrew C. Goodwin, Tracy R. Murray-Stewart, and Robert A. Casero, Jr.
- 11 Characterization, Assay, and Substrate Specificity of Plant
Polyamine Oxidases 183
Panagiotis N. Moschou and Kalliopi A. Roubelakis-Angelakis
- 12 Assay of Deoxyhypusine Synthase Activity 195
Edith C. Wolff, Seung Bum Lee, and Myung Hee Park
- 13 Assay of Deoxyhypusine Hydroxylase Activity 207
Jong Hwan Park, Edith C. Wolff, and Myung Hee Park

PART V REGULATION OF POLYAMINE CONTENT

- 14 Identification and Assay of Allosteric Regulators of S-Adenosylmethionine
Decarboxylase 219
Erin K. Willert, Lisa N. Kinch, and Margaret A. Phillips
- 15 Protocols for Studying Antizyme Expression and Function 237
Noriyuki Murai, Yasuko Murakami, and Senya Matsufuji
- 16 Identification, Assay, and Functional Analysis of the Antizyme
Inhibitor Family 269
Chaim Kahana
- 17 Posttranscriptional Regulation of Ornithine Decarboxylase 279
Shannon L. Nowotarski, Sofia Origanti, and Lisa M. Shantz

PART VI POLYAMINE TRANSPORT AND UPTAKE

- 18 Identification and Assays of Polyamine Transport Systems
in *Escherichia coli* and *Saccharomyces cerevisiae*. 295
Keiko Kashiwagi and Kazuei Igarashi
- 19 Genetic and Biochemical Analysis of Protozoal Polyamine Transporters 309
Marie-Pierre Hasne and Buddy Ullman
- 20 Heparan Sulfate Proteoglycan-Mediated Polyamine Uptake 327
*Johanna Welch, Katrin Svensson, Paulina Kucharzewska,
and Mattias Belting*
- 21 Polyamine Transport Systems in Mammalian Cells and Tissues 339
Takeshi Uemura and Eugene W. Gerner
- 22 Procedures to Evaluate the Importance of Dietary Polyamines 349
Paul Acheampong, Mary J. Macleod, and Heather M. Wallace

PART VII POLYAMINES AND DISEASE

- 23 Determination of N^1, N^{12} -Diacetylspermine in Urine: A Novel
Tumor Marker 367
*Masao Kawakita, Kyoko Hiramatsu, Mari Yanagiya, Yosuke Doi,
and Mieko Kosaka*

24	Spermidine/Spermine-N ¹ -Acetyltransferase in Kidney Ischemia Reperfusion Injury	379
	<i>Kamyar Zahedi and Manoocher Soleimani</i>	
25	Use of Polyamine Metabolites as Markers for Stroke and Renal Failure	395
	<i>Kazuei Igarashi and Keiko Kashiwagi</i>	
26	Methods to Evaluate Alterations in Polyamine Metabolism Caused by <i>Helicobacter pylori</i> Infection	409
	<i>Alain P. Gobert, Rupesh Chaturvedi, and Keith T. Wilson</i>	
27	High-Resolution Capillary Gas Chromatography in Combination with Mass Spectrometry for Quantification of Three Major Polyamines in Postmortem Brain Cortex	427
	<i>Gary Gang Chen, Laura M. Fiori, Orval A. Mamer, and Gustavo Turecki</i>	
28	Spermine Synthase Deficiency Resulting in X-Linked Intellectual Disability (Snyder–Robinson Syndrome)	437
	<i>Charles E. Schwartz, Xiaojing Wang, Roger E. Stevenson, and Anthony E. Pegg</i>	
PART VIII CHEMISTRY AND ANALYSIS		
29	Methylated Polyamines as Research Tools	449
	<i>Alex R. Khomutov, Janne Weisell, Maxim A. Khomutov, Nikolay A. Grigorenko, Alina R. Simonian, Merja R. Häkkinen, Tuomo A. Keinänen, Mervi T. Hyvönen, Leena Alhonen, Sergey N. Kochetkov, and Jouko Vepsäläinen</i>	
30	Fluorescent Substrates for Polyamine Catabolic Enzymes and Transport	463
	<i>Koichi Takao and Akira Shirahata</i>	
31	Use of Polyamine Derivatives as Selective Histone Deacetylase Inhibitors	475
	<i>Patrick M. Woster</i>	
32	Measurement of Polyamine pK _a Values	493
	<i>Ian S. Blagbrough, Abdelkader A. Metwally, and Andrew J. Geall</i>	
33	Polyamine Analysis by LC-MS	505
	<i>Merja R. Häkkinen</i>	
	<i>Index</i>	519

Contributors

- PAUL ACHEAMPONG • *Division of Applied Medicine, University of Aberdeen, Aberdeen, Scotland, UK*
- LEENA ALHONEN • *A.I. Virtanen Institute for Molecular Sciences, Biocenter Kuopio, University of Eastern Finland, Kuopio, Finland*
- MATTIAS BELTING • *Department of Clinical Sciences, Section of Oncology, Lund University and Lund University Hospital, Lund, Sweden*
- IAN S. BLAGBROUGH • *Department of Pharmacy and Pharmacology, University of Bath, Bath, UK*
- ROBERT A. CASERO, JR. • *School of Medicine, Sidney Kimmel Comprehensive Cancer Center, Johns Hopkins University, Baltimore, MD, USA*
- RUPESH CHATURVEDI • *Division of Gastroenterology, Hepatology, and Nutrition, Department of Medicine, Vanderbilt University Medical Center, Nashville, TN, USA*
- GARY GANG CHEN • *McGill Group for Suicide Studies, Douglas Mental Health University Institute, McGill University, Montreal, QC, Canada*
- WAYLAND W.L. CHENG • *Department of Cell Biology and Physiology, Washington University School of Medicine, St. Louis, MO, USA*
- YOSUKE DOI • *Alfresa Pharma Corporation, Osaka, Japan*
- DAVID J. FEITH • *Department of Cellular and Molecular Physiology, Pennsylvania State University College of Medicine, Hershey, PA, USA*
- LAURA M. FIORI • *McGill Group for Suicide Studies, Douglas Mental Health University Institute, McGill University, Montreal, QC, Canada*
- ANDREW J. GEALL • *Department of Pharmacy and Pharmacology, University of Bath, Bath, UK*
- EUGENE W. GERNER • *Arizona Cancer Center, University of Arizona, Tucson, AZ, USA*
- ALAIN P. GOBERT • *UR454 Unite de Microbiologie, INRA, Saint-Genes-Champagnelle, France*
- ANDREW C. GOODWIN • *The Sidney Kimmel Comprehensive Cancer Center, Johns Hopkins University School of Medicine, Baltimore, MD, USA*
- NIKOLAY A. GRIGORENKO • *BASF, GVP/SI, Basel, Switzerland*
- MERJA R. HÄKKINEN • *Department of Biosciences, Laboratory of Chemistry, Biocenter Kuopio, University of Kuopio, Kuopio, Finland*
- MARIE-PIERRE HASNE • *Department of Biochemistry and Molecular Biology, Oregon Health and Science University, Portland, OR, USA*
- KYOKO HIRAMATSU • *Department of Molecular Medical Research, Tokyo Metropolitan Institute of Medical Science, Tokyo, Japan*
- MERVI T. HYVÖNEN • *Department of Biotechnology and Molecular Medicine, A.I. Virtanen Institute for Molecular Sciences, Biocenter Kuopio, University of Kuopio, Kuopio, Finland*

- KAZUEI IGARASHI • *Graduate School of Pharmaceutical Sciences, Chiba University, Chiba, Japan; Amine Pharma Research Institute, Innovation Plaza at Chiba University, Chiba, Japan*
- CHAIM KAHANA • *Department of Molecular Genetics, The Weizmann Institute of Science, Rehovot, Israel*
- KEIKO KASHIWAGI • *Faculty of Pharmacy, Chiba Institute of Science, Chiba, Japan*
- MASAO KAWAKITA • *Department of Molecular Medical Research, Tokyo Metropolitan Institute of Medical Science, Tokyo, Japan*
- TUOMO A. KEINÄNEN • *Department of Biotechnology and Molecular Medicine, A.I. Virtanen Institute for Molecular Sciences, Biocenter Kuopio, University of Kuopio, Kuopio, Finland*
- LISA N. KINCH • *Department of Biochemistry, University of Texas Southwestern Medical Center at Dallas, Dallas, TX, USA*
- ALEX R. KHOMUTOV • *Engelhardt Institute of Molecular Biology, Russian Academy of Sciences, Moscow, 119991, Russia*
- MAXIM A. KHOMUTOV • *Engelhardt Institute of Molecular Biology, Russian Academy of Sciences, Moscow, Russia*
- SERGEY N. KOCHETKOV • *Engelhardt Institute of Molecular Biology, Russian Academy of Sciences, Moscow, Russia*
- MIEKO KOSAKA • *Alfresa Pharma Corporation, Osaka, Japan*
- PAULINA KUCHARZEWSKA • *Department of Clinical Sciences, Section of Oncology, Lund University and Lund University Hospital, Lund, Sweden*
- HARLEY T. KURATA • *Department of Anesthesiology, Pharmacology, and Therapeutics, University of British Columbia, Vancouver, BC, Canada*
- SEUNG BUM LEE • *The Oral and Pharyngeal Cancer Branch, NIDCR, National Institutes of Health, Bethesda, MD, USA*
- MARY J. MACLEOD • *Division of Applied Medicine, University of Aberdeen, Aberdeen, Scotland, UK*
- ORVAL A. MAMER • *Mass Spectrometry Unit, McGill University, Montreal, QC, Canada*
- SENYA MATSUFUJI • *Department of Molecular Biology, The Jikei University School of Medicine, Tokyo, Japan*
- ABDELKADER A. METWALLY • *Department of Pharmacy and Pharmacology, University of Bath, Bath, UK*
- ANTHONY J. MICHAEL • *University of Texas Southwestern Medical Center, Department of Pharmacology, Forest Park, Dallas, TX, USA*
- TOSHIYUKI MORIYA • *Institute of Environmental Microbiology, Kyowa-kako Co., Machida, Tokyo, Japan; Department of Molecular Biology, Tokyo University of Pharmacy and Life Science, Hachioji, Tokyo, Japan*
- PANAGIOTIS N. MOSCHOU • *Department of Biology, University of Crete, Heraklion, Greece*
- NORIYUKI MURAI • *Department of Molecular Biology, The Jikei University School of Medicine, Tokyo, Japan*
- YASUKO MURAKAMI • *Department of Molecular Biology, The Jikei University School of Medicine, Tokyo, Japan*

- TRACY R. MURRAY-STEWART • *The Sidney Kimmel Comprehensive Cancer Center, Johns Hopkins University School of Medicine, Baltimore, MD, USA*
- COLIN G. NICHOLS • *Department of Cell Biology and Physiology, Washington University School of Medicine, St. Louis, MO, USA*
- SHANNON L. NOWOTARSKI • *Department of Cellular and Molecular Physiology, Milton S. Hershey Medical Center, Pennsylvania State University College of Medicine, Hershey, PA, USA*
- SOFIA ORIGANTI • *Department of Cellular and Molecular Physiology, Milton S. Hershey Medical Center, Pennsylvania State University College of Medicine, Hershey, PA, USA*
- TAIRO OSHIMA • *Institute of Environmental Microbiology, Kyowa-kako Co., Machida, Tokyo, Japan*
- JONG HWAN PARK • *The Oral and Pharyngeal Cancer Branch, NIDCR, National Institutes of Health, Bethesda, MD, USA*
- MYUNG HEE PARK • *The Oral and Pharyngeal Cancer Branch, NIDCR, National Institutes of Health, Bethesda, MD, USA*
- ANTHONY E. PEGG • *College of Medicine, Milton S. Hershey Medical Center, Pennsylvania State University, Hershey, PA, USA*
- MARGARET A. PHILLIPS • *Department of Pharmacology, University of Texas Southwestern Medical Center at Dallas, Dallas, TX, USA*
- EIJA PIRINEN • *A.I. Virtanen Institute for Molecular Sciences, Biocenter Kuopio, University of Kuopio, Kuopio, Finland*
- KALLIOPI A. ROUBELAKIS-ANGELAKIS • *Department of Biology, University of Crete, Heraklion, Greece*
- CHARLES E. SCHWARTZ • *J.C. Self Research Institute, Greenwood Genetic Center, Greenwood, SC, USA*
- LISA M. SHANTZ • *Department of Cellular and Molecular Physiology, Milton S. Hershey Medical Center, Pennsylvania State University College of Medicine, Hershey, PA, USA*
- AKIRA SHIRAHATA • *Department of Clinical Dietetics and Human Nutrition, Laboratory of Cellular Physiology, Josai University, Saitama, Japan*
- ALINA R. SIMONIAN • *Engelhardt Institute of Molecular Biology, Russian Academy of Sciences, Moscow, Russia*
- MANOOCHER SOLEIMANI • *Department of Surgery, Division of Nephrology and Hypertension, University of Cincinnati College of Medicine, Cincinnati, OH, USA*
- ROGER E. STEVENSON • *J.C. Self Research Institute, Greenwood Genetic Center, Greenwood, SC, USA*
- KATRIN SVENSSON • *Department of Clinical Sciences, Section of Oncology, Lund University and Lund University Hospital, Lund, Sweden*
- KOICHI TAKAO • *Laboratory of Cellular Physiology, Department of Clinical Dietetics and Human Nutrition, Faculty of Pharmaceutical Sciences, Josai University, Saitama, Japan*
- YUSUKE TERUI • *Faculty of Pharmacy, Chiba Institute of Science, Choshi, Chiba, Japan*

- GUSTAVO TURECKI • *Douglas Mental Health University Institute, McGill University, Montreal, QC, Canada*
- TAKESHI UEMURA • *Arizona Cancer Center, University of Arizona, Tucson, AZ, USA*
- ANNE UIMARI • *A.I. Virtanen Institute for Molecular Sciences, Biocenter Kuopio, University of Kuopio, Kuopio, Finland*
- BUDDY ULLMAN • *Department of Biochemistry and Molecular Biology, Oregon Health and Science University, Portland, OR, USA*
- JOUKO VEPSÄLÄINEN • *Department of Biosciences, Biocenter Kuopio, University of Kuopio, Kuopio, Finland*
- HEATHER M. WALLACE • *Division of Applied Medicine, University of Aberdeen, Aberdeen, Scotland, UK*
- JIAN-YING WANG • *Baltimore Veterans Affairs Medical Center, Baltimore, MD, USA*
- XIAOJING WANG • *Department of Cellular and Molecular Physiology, Milton S. Ebersole Medical Center, Pennsylvania State University College of Medicine, Hershey, PA, USA*
- JANNE WEISELL • *Department of Biosciences, Biocenter Kuopio, University of Kuopio, Kuopio, Finland*
- JOHANNA WELCH • *Department of Clinical Sciences, Section of Oncology, Lund University and Lund University Hospital, Lund, Sweden*
- ERIN K. WILLERT • *Department of Pharmacology, University of Texas Southwestern Medical Center at Dallas, Dallas, TX, USA*
- KEITH T. WILSON • *Division of Gastroenterology, Hepatology, and Nutrition, Department of Medicine, Vanderbilt University Medical Center, Nashville, TN, USA; Veterans Affairs Tennessee Valley Healthcare System, Nashville, TN, USA*
- EDITH C. WOLFF • *The Oral and Pharyngeal Cancer Branch, NIDCR, National Institutes of Health, Bethesda, MD, USA*
- PATRICK M. WOSTER • *Department of Pharmaceutical Sciences, Wayne State University, Detroit, MI, USA*
- LAN XIAO • *Baltimore Veterans Affairs Medical Center, Baltimore, MD, USA*
- MARI YANAGIYA • *Alfresa Pharma Corporation, Osaka, Japan*
- KAMYAR ZAHEDI • *Department of Surgery, Division of Nephrology and Hypertension, University of Cincinnati College of Medicine, Cincinnati, OH, USA*

Part I

Introduction

Chapter 1

Current Status of the Polyamine Research Field

Anthony E. Pegg and Robert A. Casero, Jr.

Abstract

This chapter provides an overview of the polyamine field and introduces the 32 other chapters that make up this volume. These chapters provide a wide range of methods, advice, and background relevant to studies of the function of polyamines, the regulation of their content, their role in disease, and the therapeutic potential of drugs targeting polyamine content and function. The methodology provided in this new volume will enable laboratories already working in this area to expand their experimental techniques and facilitate the entry of additional workers into this rapidly expanding field.

Key words: Putrescine, Spermidine, Spermine, Hypusine, Antizyme, Polyamine transport

1. Structure of Physiological Polyamines

Mammalian tissues contain putrescine (1,4-diaminobutane), which is strictly speaking a diamine, spermidine, and spermine (1), while a wider spectrum of natural polyamines exists in other organisms (Fig. 1). Plants have these three polyamines and also thermospermine (2, 3) and agmatine. Some fungi and some, but not all, bacteria contain only putrescine and spermidine since they lack a spermine synthase. Specific organisms also contain other diamines such as 1,3-diaminopropane and cadaverine (1,5-diaminopentane) and *sym*-norspermidine (caldine). Thermophilic bacteria and archaea are a rich source of polyamines including these compounds and a wide variety of other polyamines. Since thermophiles were the first source for isolation of polyamines such as thermospermine, caldine, and thermine (Fig. 1) this explains their trivial names, but these polyamines are not unique to organisms living at high temperature. Similarly, spermidine and spermine are so named because the first report of crystals in seminal plasma by Leeuwenhoek was subsequently shown to be due to the precipitation of insoluble

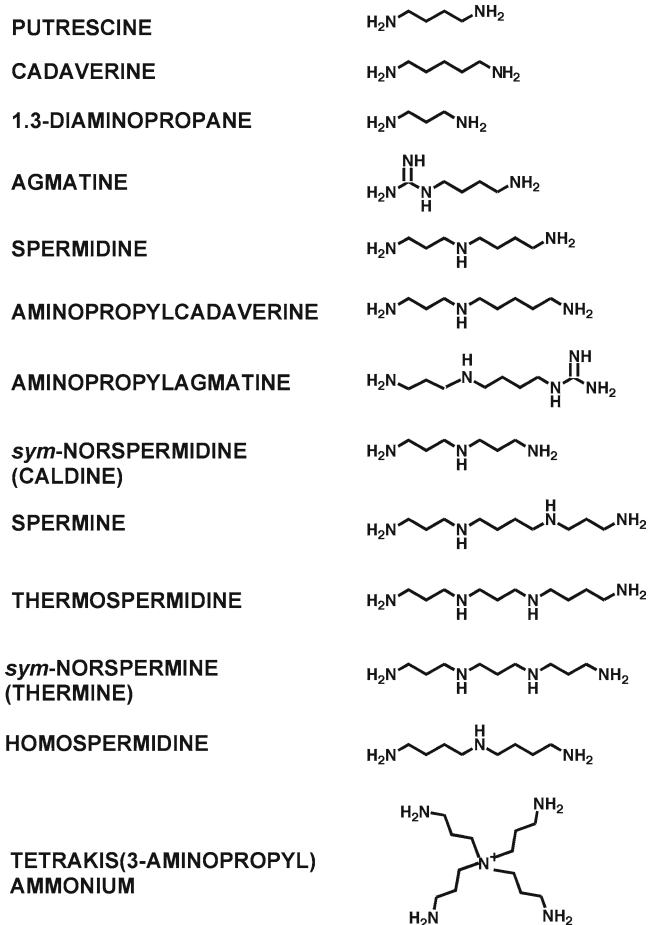


Fig. 1. Structures of some naturally occurring polyamines. It should be noted that at physiological pH values the nitrogen atoms in these structures (and in subsequent figures) would be predominantly protonated (see Chapter 32). Additional polyamines found in thermophiles are described in Chapter 5.

spermine phosphate, but these polyamines are present in all tissues and many extracellular fluids of mammals (4).

2. Synthesis of Polyamines

Diamines such as putrescine, cadaverine, and 1,3-diaminopropane are formed by the decarboxylation of the relevant amino acid (L-ornithine, L-lysine and L-1,4-diaminobutyric acid respectively); reactions catalyzed by pyridoxal phosphate-dependent decarboxylases (Fig. 2a) (5). An alternative pathway to putrescine occurs in plants and microorganisms in which L-arginine is decarboxylated forming agmatine (6). This can then be converted to

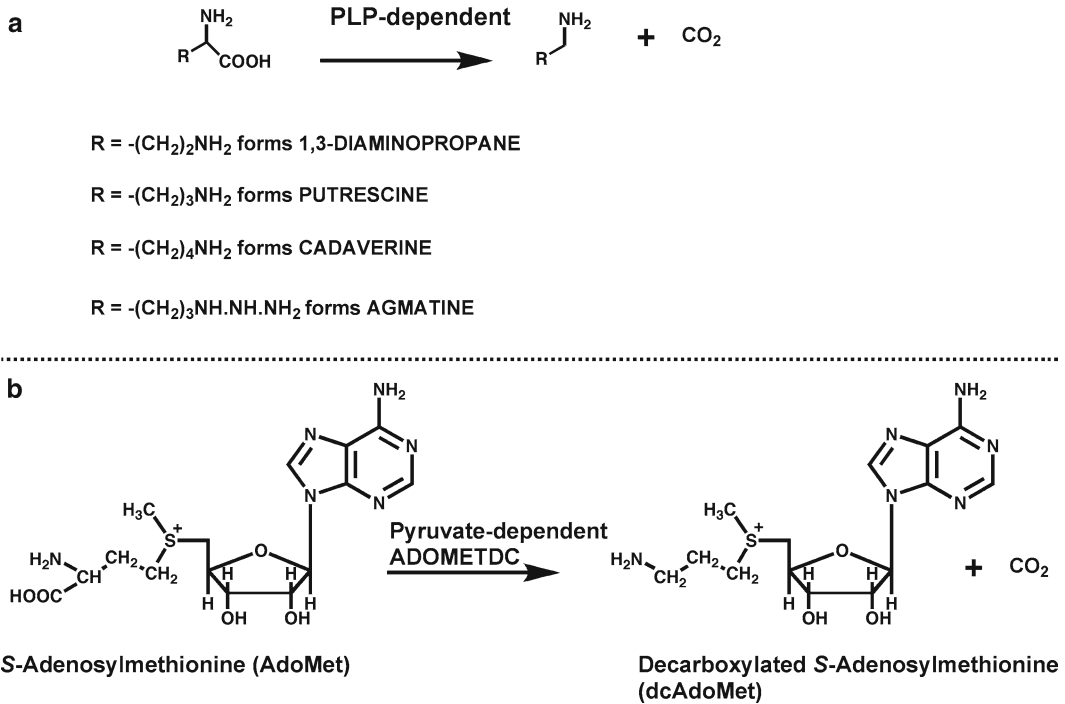
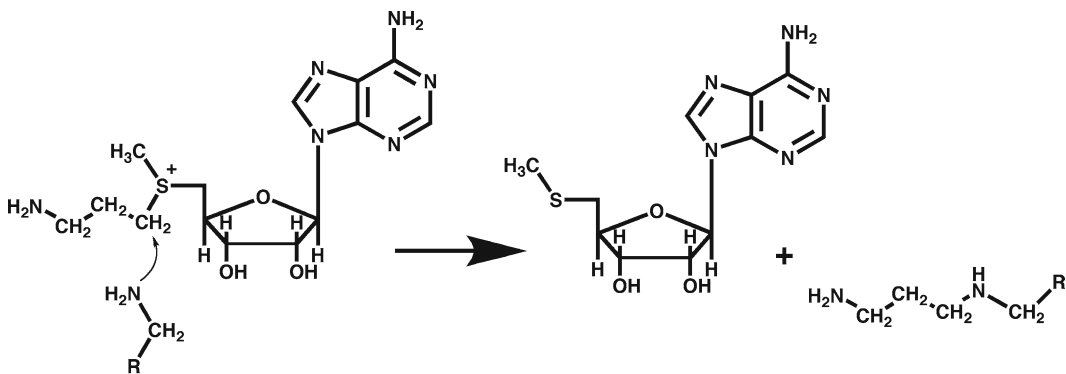


Fig. 2. Decarboxylases involved in polyamine synthesis. (a) Pyridoxal phosphate (PLP)-dependent decarboxylases [L -1,4-diaminobutyric acid decarboxylase, L -ornithine decarboxylase (ODC), L -lysine decarboxylase and L -arginine decarboxylase]. (b) S -adenosylmethionine decarboxylase, which contains a covalently bound pyruvate group essential for activity.

putrescine either by the reaction of agmatinase releasing urea, as in *E. coli*, or by the combined actions of agmatine deiminase releasing ammonia forming N -carbamoylputrescine and N -carbamoylputrescine amidase as in plants.

There are two pathways for the addition of aminopropyl groups to form the higher polyamines. By far the most extensively studied is that first demonstrated by the Tabors (7), which occurs in mammals, plants, fungi, and many bacteria including *E. coli*, where decarboxylated S -adenosylmethionine (dcAdoMet) is used as the aminopropyl donor. This nucleoside is produced by the action of the pyruvoyl-dependent S -adenosylmethionine decarboxylase (AdoMetDC) (8, 9). Enzymes termed aminopropyltransferases (10–12) use dcAdoMet and an amine acceptor to form the higher polyamines (Fig. 3). Thus, putrescine is used as a substrate by the aminopropyltransferase, termed spermidine synthase, to form spermidine. A distinct aminopropyltransferase, spermine synthase, then uses a second dcAdoMet molecule to add the aminopropyl group to the N^8 of spermidine forming spermine. In addition to a spermine synthase, plants contain a thermospermine synthase that attacks the N^1 end of spermidine producing thermospermine. The aminopropyltransferases mentioned above in mammals and plants, and in some bacteria and fungi, are



R = - (CH₂)₃NH₂ forms spermidine

R = - (CH₂)₂NH(CH₂)₃NH₂ forms thermine

R = - (CH₂)₃NH (CH₂)₃NH₂ forms spermine

R = - (CH₂)₃NH.N=H.NH₂ forms aminopropylagmatine

R = - (CH₂)₂NH(CH₂)₄NH₂ forms thermospermidine

R = - (CH₂)₄NH₂ forms aminopropylcadaverine

R = - (CH₂)₂NH₂ forms caldine

Fig. 3. Aminopropyltransferases involved in polyamine synthesis. The reaction catalyzed by these enzymes involves the attack by the unprotonated terminal N of the amine substrate on the methylene C atom adjacent to the sulfonium center of the dcAdoMet aminopropyl donor. The deprotonation of the attacking N, which is facilitated by residues in the enzyme, and the positive charge on the sulfonium S of dcAdoMet allow the reaction to proceed forming the polyamine product. The reactions shown have all been demonstrated by purified aminopropyltransferases. Other members of this family of enzymes may occur to bring about the synthesis of longer chain polyamines.

quite specific for the amine acceptor (13). Other organisms including the thermophiles have less specific aminopropyltransferases that can make a variety of polyamines including thermine. Some contain an enzyme that uses agmatine to produce aminopropylagmatine (Fig. 3), which is then converted into spermidine and urea by an agmatinase-like enzyme allowing for the production of spermidine without a putrescine intermediate. It is likely that some thermophiles and some other organisms such as diatoms where very long chain polyamines are involved in biomineralization of the shell contain additional aminopropyltransferases supporting their synthesis but these enzymes have not been characterized.

The polyamine biosynthetic pathway dependent on dc-AdoMet described above is very well understood and methods for the assay of these enzymes including L-ornithine decarboxylase (ODC), AdoMetDC, and aminopropyltransferases were provided in Volume 79 of this series published in 1998.

There is, however, a second pathway for the synthesis of polyamines containing aminopropyl moieties in which L-aspartic- β -semialdehyde is used to provide the aminopropyl group (14, 15) (Fig. 4). The condensation of this molecule with putrescine forms carboxyspermidine, which is then decarboxylated to form spermidine. Similar reactions using 1,3-diaminopropane form *sym*-norspermidine and the same enzymes (termed

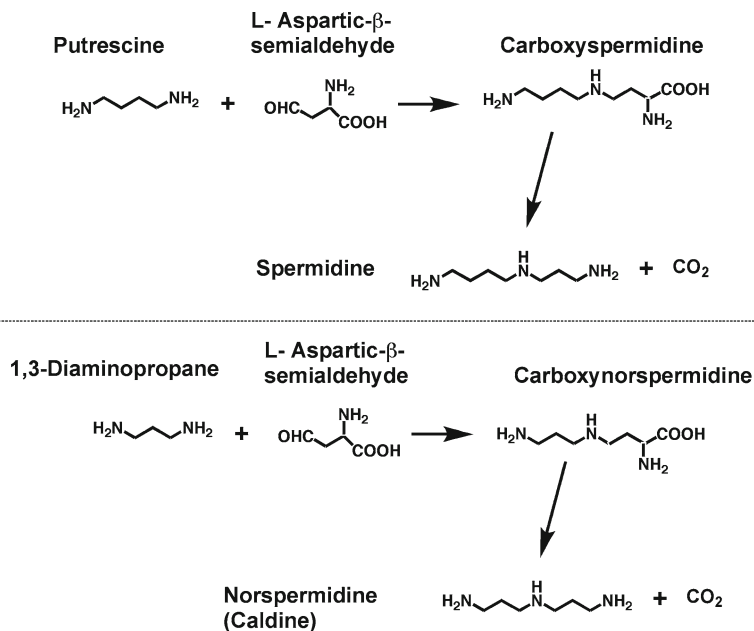


Fig. 4. Condensation reactions forming polyamines from L-aspartic-β-semialdehyde. Reaction of L-aspartic-β-semialdehyde with putrescine or 1,3-diaminopropane by carboxynorspermidine synthase forms carboxyspermidine or carboxynorspermidine, which are decarboxylated by carboxynorspermidine decarboxylase to form spermidine or *sym*-norspermidine, respectively.

carboxynorspermidine synthase and carboxynorspermidine decarboxylase) are able to bring about both syntheses (Fig. 4). This pathway is used in many microbes.

Finally, there is also a pathway for the synthesis of *sym*-homospermidine, which involves the use of NAD and putrescine with either a second molecule of putrescine or spermidine to generate the product via condensation with 4-aminobutyraldehyde intermediate (16, 17) (Fig. 5a). In plants, the homospermidine synthase, which is responsible for the latter reaction, is derived from deoxyhypusine synthase (18), a critical enzyme for a posttranslational modification, which involves polyamines and is described below.

The second chapter of this volume describes genomic methods for identifying key polyamine biosynthetic genes and thus determination of the pathways used in particular organisms. This is a very important area since polyamines are essential for normal growth and their biosynthetic pathways provide targets for drug development. Organisms such as *Vibrio cholerae* that use the L-aspartic-β-semialdehyde condensation pathway may be sensitive to potential therapeutics that are innocuous to host organisms that do not depend on these reactions.

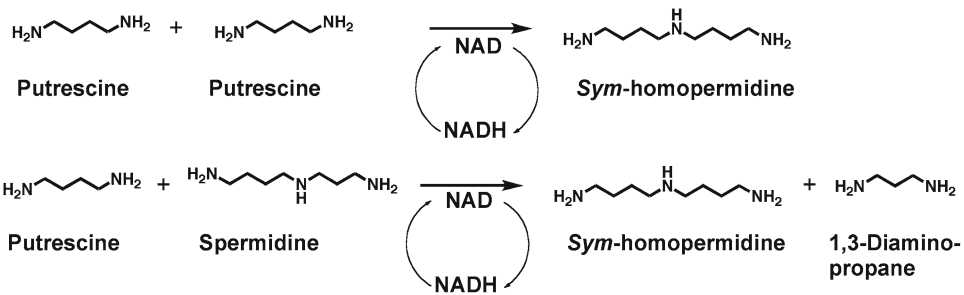
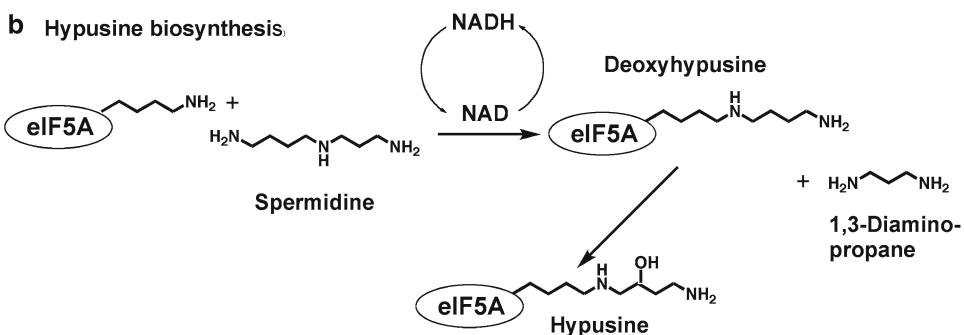
a Sym-homospermidine biosynthesis.**b Hypusine biosynthesis.**

Fig. 5. Synthesis of *sym*-homospermidine and of hypusine. *sym*-Homospermidine can be formed from two molecules of putrescine or from putrescine and spermidine as shown in (a). In both cases, NAD is needed for hydrogen extraction, but is regenerated in the second half of the reaction. The reaction using spermidine and putrescine, which also generates 1,3-diaminopropane, is similar to that used for the hypusine modification of eIF5A shown in (b). In this case, a lysine residue in eIF5A is used instead of putrescine forming deoxyhypusine in eIF5A and free 1,3-diaminopropane. A second enzyme hydroxylates the deoxyhypusine to form the complete hypusine modification (see Chapters 12 and 13 for more details of the reactions forming hypusine).

Polyamines with quaternary ammonium centers such as tetrakis(3-aminopropyl)ammonium (Fig. 1) or tertiary N atoms such as mitsubishine (see Chapter 5) respectively are found in acute thermophiles and are needed for growth at extreme temperatures (19, 20). The biosynthetic reactions leading to these polyamines have not yet been elucidated.

3. Functions of Polyamines

Polyamines have a multitude of functions affecting growth and development, and these pleiotropic effects complicate efforts to understand the physiological and pathophysiological effects of perturbing polyamine content. Recent studies have identified a number of key areas in which polyamine effects are initiated (21–23). These include regulation of gene transcription, multiple effects on posttranscriptional regulation, control of the activity of ion channels as well as modulation of protein kinase activities, the cell cycle, membrane structure/function, and nucleic acid structure and stability.

A critical new concept increasing understanding of the role of polyamines in maintaining optimal growth rates and cell viability has been provided by studies showing that there is a bacterial “polyamine modulon” that consists of a set of genes whose expression is increased by polyamines as a result of increased translation (24, 25). Polyamines stimulate translation in a number of ways including alteration of mRNA structure allowing initiation of protein synthesis encoded by genes that lack Shine–Dalgarno sequences or have them placed at nonoptimal positions. The proteins whose synthesis is directly stimulated by polyamines also include transcription factors and kinases that can in turn enhance gene expression of other proteins. The polyamine modulon concept has been extended to yeast (26) and is likely to also apply to mammalian cells (27). Methods for identifying members of the polyamine modulon are described in Chapter 3.

In eukaryotes, another factor is also involved in the role of polyamines in stimulating gene expression. This is the protein eIF5A, which is only active after a posttranslational modification to form hypusine (Fig. 5b). This reaction has an absolute requirement for spermidine as a precursor. The functions of eIF5A have been the subject of considerable debate and it may have multiple functions, but recent studies indicate that it is a translation elongation factor (28–30). Many other sites of post-transcriptional gene regulation, such as mRNA transport, and turnover are also influenced by polyamines either via eIF-5A or other proteins. These include RNA-binding proteins such as the HuR family (31–33). The HuR proteins are highly regulated by polyamines and methods for their study are described in Chapter 4.

The novel polyamines present in thermophiles are essential for growth at higher temperatures and have effects on nucleic acid stability and structure, and in protein synthesis (19, 20). Methods for the synthesis and the study of the function of these polyamines are described in Chapter 5.

A new and critically important area in polyamine research was revealed when it was observed that the steep voltage-dependence of the inwardly rectifying potassium (Kir) channels is caused by the binding of polyamines (34) and that polyamines profoundly affect the activities of NMDA receptors (35). Subsequent studies have shown that a wide variety of ion channels are affected by polyamines including the Kir potassium channels, which control membrane potential and potassium homeostasis in many cell types, glutamate receptors that mediate excitatory synaptic transmission in the mammalian brain, as well as other channels affecting intracellular calcium signaling, Na⁺ transport, and some connexin-linked gap junctions (22, 23). Chapter 6 describes methodology characterizing polyamine interactions with both prokaryotic and eukaryotic Kir channels.

4. Use of Transgenics to Investigate Polyamine Function

The ability to generate transgenic rodents that have reductions or increases in polyamine content due to alteration in the activities of key enzymes has now provided important tools to evaluate polyamine function in mammals (36–38). Various aspects of these studies are covered in Chapters 7–9.

There is much evidence linking elevated polyamine content to tumor growth and development. Consequently a number of animal models have been developed in which polyamine content is disturbed and studies are carried out on their susceptibility to tumor induction by chemicals, oncogene activation, UV radiation, and other stimuli. Remarkably, even the small reduction in ODC activity brought about by the *Odc* heterozygosity in *ODC*^(+/-) transgenic mice reduced lymphoma and skin tumor development (39, 40). Similarly, moderately increased levels of antizyme (AZ), which as described below is a negative regulator of ODC, dramatically lowered skin carcinogenesis in response to two-stage carcinogenesis protocols (37, 41). The use of these and other models for studying the role of polyamines in neoplasia is described in Chapter 7.

These studies correlate well with a number of investigations using human patients that show that interference with polyamine synthesis by drugs such as DFMO (an irreversible inactivator of ODC) has a profound cancer preventative effect (42). Thus, clinical trials examining the reoccurrence of colonic polyps have shown that prolonged treatment with this drug combined with sulindac caused a 70% reduction of recurrence of all adenomas, and over a 90% reduction in advanced and/or multiple adenomas (43). Treatment with DFMO also reduced the development of non-melanoma skin cancer in subjects with a previous history of this disease (44). Some encouraging results in a Phase IIb clinical trial suggest that DFMO may be useful for chemoprevention of prostate cancer (45). At present, all of the clinical data supporting the use of the polyamine pathway for cancer chemoprevention are derived from studies with DFMO, but animal studies suggest that polyamine analogs described below and the targeting of drugs to other enzymes in the pathway, such as spermidine synthase (which like ODC is regulated by the oncogene *c-myc*), may also be successful (46).

Remarkable phenotypic changes occur in rodents in which the activity of the catabolic enzyme spermidine/spermine-*N*¹-acetyltransferase (SSAT) (Fig. 6) is increased. This contrasts to the relatively minimal effects in untreated mice with inactivation of the *Sat1* gene. The lack of significant changes in these mice is consistent with the concept that normally SSAT levels are very low and that physiological and pathophysiological effects of SSAT occur in response to its induction (47, 48). Multiple lines

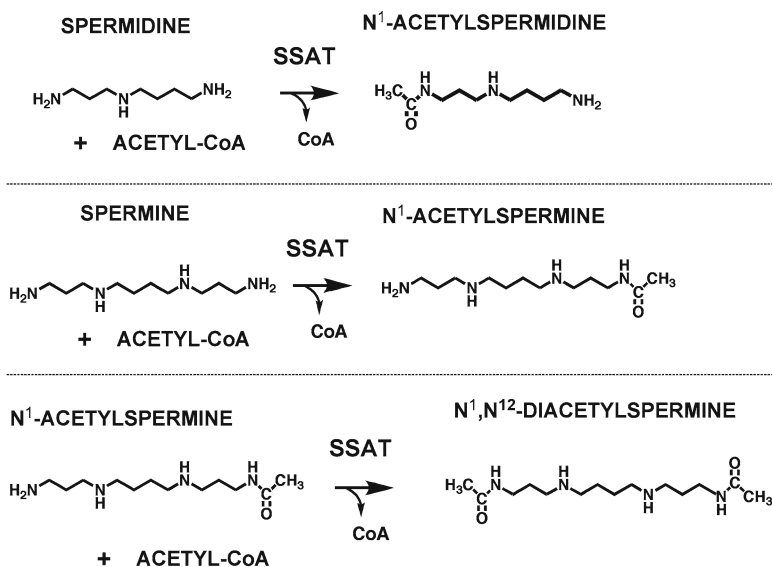


Fig. 6. Reactions catalyzed by SSAT.

of transgenic mice and transgenic rats overexpressing SSAT have been described (47, 49). These mice also show a wide variety of other defects including hair loss, female infertility, weight loss, CNS effects, altered carbohydrate and lipid metabolism, a tendency to develop pancreatitis and altered responses to chemical carcinogens. These effects are related not only to the alterations in polyamine content, but also to the effects on levels of acetyl-CoA, ATP, and oxidative damage associated with the increased activity of the SSAT/APAO pathway (Fig. 4) described below, and the increased metabolic flux through the polyamine pathway due to the futile cycle set up by compensatory increases in polyamine synthesis in response to constitutively elevated SSAT levels (48). Chapter 7 describes methods to study pancreatitis and altered lipid and carbohydrate metabolism in rodents with elevated expression of SSAT.

The critical importance of polyamines for mammalian development is shown by studies with mouse knockouts of the *ODC* or *AdoMetDC* genes, which are lethal at very early embryonic stages. Spermidine synthase knockouts would almost certainly also be lethal since spermidine is essential for viability in yeast (50). In contrast, mice lacking spermine synthase do survive on an appropriate strain background and can be used to evaluate the specific functions of spermine (51). Chapter 9 describes the phenotypic changes in these mice and their use to evaluate the role of spermine in growth, behavior, fertility, hearing, and cardiac function.

Transgenic approaches have also been used to evaluate the functions of polyamines in plants. It is noteworthy that although many plants contain both ODC and arginine decarboxylase, the

former is not required in all species since there is no gene for ODC in *Arabidopsis thaliana* (52). Genes for AdoMetDC and arginine decarboxylase are essential for normal plant development as is the gene for thermospermine synthase (2, 3, 13, 53, 54).

5. Polyamine Catabolism

The enzymatic reactions forming polyamines are effectively irreversible. Polyamines are interconverted and removed by a combination of acetylation, oxidation, and excretion to vacuoles or extracellular fluids. Putrescine can be attacked by diamine oxidase and other copper-dependent enzymes that oxidize the terminal amino groups of spermidine and spermine are well known (55–57). These enzymes are present extracellularly in mammals. The products of their reaction, which can rearrange to form acrolein, are highly toxic (58, 59) and this reaction is the basis of many publications that erroneously claim that polyamines exert direct toxic effects on the basis of observations that addition of polyamines to cell cultures causes cell death. The observed toxicity in such systems is due to the formation of toxic metabolites by enzymes in the serum used to support cell culture. Although elevated levels of intracellular polyamines can lead to apoptosis or increased formation of reactive oxygen species, the polyamine transport systems are highly regulated to avoid uptake of excess polyamines.

Interconversion of polyamines in mammals is brought about by two FAD-dependent oxidases (Fig. 7). Spermine oxidase (SMO), first described in 2001, is specific for spermine acting on it to produce spermine, H_2O_2 , and 3-aminopropanal (48, 60). It exists as multiple forms due to splicing variations and is highly inducible by polyamine analogs and other stimuli. The other oxidase, N^1 -acetylpolyamine oxidase (APAO), is generally a constitutively expressed enzyme that has minimal activity on free polyamines, but is highly active on N^1 -acetylspermidine (forming putrescine) and N^1 -acetylspermine (forming spermidine). With both substrates, H_2O_2 and N -acetyl-3-aminopropanal are produced (48, 61). The substrates for APAO are produced by SSAT (Fig. 6), which is very highly regulated and inducible by polyamines (48). Therefore, the SSAT/APAO pathway acts to prevent the overaccumulation of polyamines. This occurs at the expense of the generation of reactive oxygen species (ROS) and potentially toxic aldehydes. Such damage may be limited by the subcellular localization of APAO, which is a peroxisomal enzyme, whereas similar production of ROS by SMO may be more damaging due to its nuclear and cytoplasmic localization. Assay of SMO is described in Chapter 10.

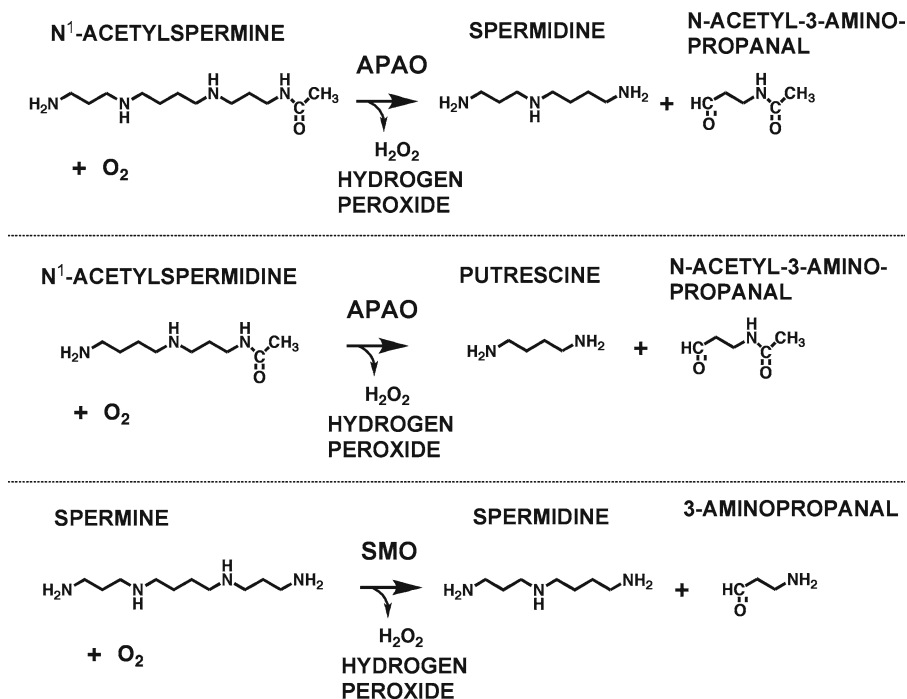


Fig. 7. Reactions catalyzed by APAO and SMO. APAO has a strong preference for N^1 -acetylated polyamines formed by SSAT releasing N -acetyl-3-aminopropanal and SMO is specific for spermine releasing 3-aminopropanal. Both reactions also generate hydrogen peroxide.

Plants also use polyamine oxidation to interconvert polyamines and regulate polyamine content and also to form H_2O_2 that may act as a signaling molecule (54, 62–64). Methods for the investigation of these enzymes are described in Chapter 11.

6. Formation and Function of Hypusine

One essential function of polyamines in eukaryotes, as stated above, is to serve as a precursor of hypusine [N^ϵ -(4-amino-2-hydroxybutyl)lysine] (Fig. 5b). Hypusine production is a posttranslational modification of the protein eIF5A. This modification is essential for the activity of eIF5A, which as described above is needed for protein synthesis at the elongation step and probably also for other functions essential for growth and for viral replication (29, 50, 65–67). Drugs preventing the hypusination of eIF5A inhibit the expression of HIV-1 genes (68). The ability to serve as the source of hypusine can only be fulfilled by spermidine, which is used as a substrate by the enzyme deoxyhypusine synthase (66). This enzyme attaches the aminobutyl group of spermidine to a specific lysine residue in the protein eIF5A forming deoxyhypusine (Fig. 5b). This

protein is then further modified by deoxyhypusine hydroxylase (69) to produce the complete hypusinated eIF5A. Assays for these enzymes are described in Chapters 12 and 13.

7. Regulation of Polyamine Content

In mammals, polyamine content is controlled primarily by alterations in the activity of the key enzymes ODC, AdoMetDC, and SSAT, along with alterations in efflux and uptake (22, 70, 71). Changes in ODC and SSAT activity are brought about by alterations in the content of enzyme protein and this level is controlled at the levels of transcription, mRNA stability, translation, and protein turnover (47, 48, 71–73). AdoMetDC is formed as a proenzyme that undergoes an autocatalytic cleavage to form its pyruvoyl cofactor and its two subunits (8, 22, 71). AdoMetDC activity is also varied by alterations in the level of the processed protein and, additionally, by activation of the protein by putrescine in mammals, yeast, and some other organisms (8, 22, 74) and by binding of an activating protein (75–77) in trypanosomes. This protein, which was discovered in 2007, has been named prozyme. Methods to identify and assay this important regulatory molecule in these parasites that are responsible for major human diseases including African sleeping sickness, Chagas disease, and Leishmaniasis are described in Chapter 14. DFMO is highly effective as a therapeutic agent for some forms of African sleeping sickness, but other forms and other parasitic diseases are less susceptible to DFMO and AdoMetDC may be a critical target for their treatment (78, 79).

It has been known for 40 years that ODC protein has a very rapid rate of turnover (80). More recent studies have shown that a key part of the regulation of ODC content is due to two proteins that influence the proteasomal degradation of ODC termed antizyme (AZ) and antizyme inhibitor (AZIn) (71, 72, 81, 82). AZ was first described and named in 1976 as an inducible protein inhibitor of ODC (83). It does act as an inhibitor by binding to the ODC monomer. ODC functions as a homodimer with two active sites formed at the dimer interface. Association between the two subunits is quite weak and the dimers are in rapid equilibrium with inactive monomers. Therefore, binding of AZ causes loss of ODC activity, but more importantly it targets the protein for degradation by the 26S proteasome. AZ acts in a catalytic manner in this reaction since most of the AZ is released and can cause further ODC degradation (72, 84). AZ is not restricted to mammals having been found in yeast and many other species (85, 86).

AZ synthesis is increased in response to high polyamine levels predominantly via increasing a +1 frameshifting mechanism,

which is needed to allow read-through of a stop codon that prevents AZ synthesis (87, 88). Polyamines stimulate this frame-shifting, hence increasing the level of AZ and providing a regulatory feedback to control polyamine levels. Procedures for quantifying, assay, and characterization of AZ, which has at least four isoforms, some of which may be phosphorylated (89), are described in Chapter 15. AZ-3 is expressed specifically in germ line cells during spermatogenesis and is needed for haploid germ cell differentiation (90).

A second component of the system regulating ODC protein stability is AZIn (22, 73, 91). This protein, which has a structure similar to that of ODC itself, but does not dimerize or have any activity (92), binds to AZ more tightly than ODC. It can therefore displace ODC from the ODC:AZ complex or prevent this complex from forming, thus preventing ODC degradation. There are two *AZIn* genes (91, 93) and inactivation of the *AZIn-1* gene is lethal (94). Methods for the study of AZIn are covered in Chapter 16.

The ODC gene promoter region contains sequences including E-boxes, a cAMP response element, CAAT and LSF motifs, AP-1 and AP-2 sites, GC-rich Sp1 binding sites, and a TATA box. These binding sites allow for regulation of the synthesis of ODC mRNA by many factors including oncogenes such as *c-Myc*, hormones, tumor promoters, and other growth factors (21, 22, 36, 65, 95, 96). There are also many studies showing that translational regulation of ODC synthesis via the long 5'UTR of its mRNA affects ODC production. Both cap-dependent and internal ribosome entry site (IRES)-mediated translation have been reported with the initiation factor eIF4E playing an important regulatory role (97, 98). Early studies also suggested that the 3'UTR of the ODC mRNA might exert regulatory activity (99) and this possibility has now been confirmed with studies showing that mRNA content is also regulated at the level of mRNA stability via interactions of key proteins with this region. Chapter 17 describes methods for studying the posttranscriptional regulation of ODC.

8. Polyamine Transport

The polyamines exist predominantly in a charged form at physiological pH and are excluded by cell membranes. The existence of transport systems underlying both uptake and efflux has been known for many years and several chapters outlining methods to determine polyamine transport into and out of the cell were included in Volume 79 of this series. At that time, almost nothing was known about the mechanism of this transport and the

components of the transporters. Recently, great progress has been made in the characterization and study of these systems. This work has been led by a series of elegant studies in which the components of the carrier-mediated systems for both uptake and efflux of polyamines in bacteria have been fully characterized using proteins from *E. coli* (100, 101). Detailed studies of these transport systems in yeast have also been published (101–103). Chapter 18 describes methods for investigating these transporters in detail.

Specific polyamine transporters have also been isolated from protozoan parasites (104, 105) and methods for investigation of these proteins are covered in Chapter 19. Some protozoa such as *T. cruzi*, which causes Chagas disease, lack enzymes capable of putrescine synthesis and uptake is therefore essential for their ability to possess adequate polyamines to maintain viability. Even in those parasites possessing a complete polyamine synthesis system, a full understanding of the uptake systems and methods for their inhibition or down-regulation may be needed to maintain the therapeutic activity of drugs targeting the polyamine pathway. Some progress has been made on the synthesis of inhibitors of polyamine transport using amino acid-spermidine conjugates (106–108). Lipophilic polyamine analogs where a C16-lipophilic substituent is attached to a Lys-spermine conjugate have been shown to have considerable promise, but reports so far have been limited to studies of inhibition of transport into cancer cells (108).

Many attempts to isolate similar carrier-mediated systems from higher organisms have not yet been successful, although recently a transporter protein CATP-5, a P5B-type ATPase associated with the plasma membrane that is involved in polyamine transport, has been identified in *C. elegans* (109). It should be noted that mammalian polyamine transport system can transport a number of related compounds including paraquat (110, 111), antiproliferative agents such as MGBG (112–114) and mepacrine (115), and synthetic drugs conjugated with a polyamine (115–118). The latter property may be valuable to deliver drugs to tumor cells, although obvious problems such as maintaining the tumor-killing properties of the drug or making a version cleavable inside the cell, as well as imparting tumor selectivity, since the uptake systems are not unique to tumor cells, must be overcome. An additional difficulty when reactive drugs are attached to polyamines is that these drugs may inactivate the carrier and thus rapidly inactivate the uptake process.

The polyamine transport system in mammals is also responsible for the uptake of many polyamine analogs, which, as described below, are under investigation and in some cases detailed clinical trials as antitumor agents. AZ (Chapter 15) has a dual function in maintaining polyamine homeostasis (72). It not only reduces putrescine synthesis by its effects reducing ODC activity, but also inhibits polyamine transport. The molecular mechanism

for this inhibition is not yet understood. Many of the polyamine analogs also induce AZ synthesis and thus limit their own accumulation (119, 120). Finding an analog that lacks this property but is still actively transported is an important goal, although providing selectivity towards tumors is also a key limiting issue.

Many attempts to isolate mammalian carrier-mediated uptake systems similar to those characterized from bacteria, fungi, and protozoal parasites have not yet been successful. However, endocytic pathways for polyamine transport have been described and fluorescent polyamine derivatives have been localized in discrete vesicles (121). Polyamine transport can follow a dynamin-dependent and clathrin-independent endocytic uptake pathway.

Cell surface heparin sulfate proteoglycans have been implicated in polyamine transport (122–124), and uptake of polyamines was blocked by a single chain variable fragment antiheparin sulfate antibody (125). Such uptake mechanisms are covered in Chapter 20. A caveolin-regulated system that transports polyamines in colon cancer cells has been described (126). Phosphorylation of caveolin-1 at Tyr¹⁴ is stimulated by the oncogene *k-Ras* and increases the activity of this system (126).

There is also compelling evidence for a polyamine efflux system which excretes excess putrescine and the acetylpolyamines formed by SSAT (127–129). Important recent studies have identified SLC3A2, previously known as a glycosylated heavy chain of a cationic amino acid transporter and its partner y+ LAT light chain, as a part of a putrescine and acetylpolyamine efflux system. This complex supports coupled arginine uptake and putrescine efflux, indicating that there is a putrescine/arginine exchange reaction (130). Methods for the study of these mammalian transport systems are included in Chapter 21. Interestingly, SSAT was colocalized with SLC3A2, so this efflux system may be closely linked to polyamine acetylation. Expression of SLC3A2 was negatively regulated by *k-Ras* (130). Thus, this oncogene can increase polyamine content by affecting both influx and efflux.

Since polyamines are ubiquitous components of plant and animal cells and are produced by intestinal microorganisms, there is substantial dietary exposure to polyamines (131). Uptake from this source is a significant potential problem leading to resistance to drugs that block endogenous polyamine synthesis which are used for cancer chemotherapy or chemoprevention (124, 132). Diets low in polyamines and supplemented with antibiotics to reduce synthesis by intestinal organisms have been designed to overcome this problem (133–135). On the other hand, enhanced use of dietary polyamines may be helpful in some conditions in which pathology is associated with depleted polyamines (136, 137). Detailed descriptions of the polyamine contents of various foodstuffs are available to aid in the design of diets with appropriate polyamine content (131, 138). Chapter 22 details simple and

reliable methods for precisely measuring dietary polyamines from a number of food sources. Understanding the variety of dietary sources and their actual content of polyamines will be critical as chemotherapeutic and chemopreventive strategies using polyamine-like molecules move forward.

9. Deranged Polyamine Metabolism and Human Disease

There is an increasing realization that polyamines and/or their metabolites may have critical roles in human disease. Conditions causing reduced polyamine content, increased polyamine oxidation, or overproduction of certain polyamines are associated causatively in a number of conditions. In some cases, it is not entirely clear how the changes seen are produced or how they are linked to the conditions, but they provide an important diagnostic test. For example, urinary excretion of N^1, N^{12} -diacetylspermine has now been shown to be a valuable marker for a variety of cancers (139). The possible value of polyamine measurements in cancer diagnosis and monitoring of therapy was first proposed by Russell and colleagues (140, 141) who showed that increased extracellular polyamines were associated with neoplasia, but was not generally useful. The rationale/explanation for such increases was that the rapid turnover of cancerous cells led to release of increased polyamines that were found in blood and urine. However, many other conditions where there was increased cell proliferation/turnover, tissue damage, pregnancy, and dietary considerations can all influence such polyamine levels leading to a far more variation than is acceptable for such tests. More recent studies in which the focus has been on N^1, N^{12} -diacetylspermine have provided a more reliable assay (139). This product can be formed by SSAT as shown in Fig. 6 and is readily excreted from cells (142), but it is not clear how the N^1, N^{12} -diacetylspermine found in urine of cancer patients originates. Another advantage of N^1, N^{12} -diacetylspermine is that antibodies to this polyamine can be produced that have adequate specificity for analytical use (143), whereas it is difficult to produce antibodies for a free polyamines, such as spermine, which have sufficient selectivity over closely related molecules such as spermidine. Chapter 23 gives full details of this method and its diagnostic applicability.

Polyamine oxidation and the subsequent production of H_2O_2 (Fig. 7) leading to cell death by apoptosis may be an important tissue-remodeling event during development (144, 145). However, inadequately regulated oxidative damage caused by the production of H_2O_2 and/or aldehydes produced by the APAO and the SMO reactions may be involved in the initiation of cancer and the etiology of several other pathologies (48, 60). High levels

of SMO may be particularly damaging since this enzyme is not located in peroxisomes as is APAO.

Recent work clearly implicates a significant role for ROS generated via the SSAT/APAO, and possibly SMO, pathway in ischemia reperfusion injury (IRI) (48, 146–148). SSAT was one of the genes that was significantly up-regulated in a mouse model of IRI (149) and plasmid-derived induction of SSAT in kidney epithelial cells (which also leads to SMO induction) showed ROS production leading to injury that could be prevented by catalase. H₂O₂-mediated DNA damage leads to decreased proliferation and repair capability in injured kidneys (148). Confirmation that SSAT plays an important role in kidney IRI has been provided by studies using the *SSAT* knockout mouse, which was less sensitive to both liver and kidney IRI (150). These results clearly have important implications in the treatment and prevention of IRI, and methods to study the role of ROS in IRI, which have more general potential for study of tissue damage related to increased polyamine catabolism, are described in Chapter 24.

Further studies in human renal failure (151, 152) and cerebral stroke (153, 154) have also focused on the role of the polyamine oxidation. These studies have shown that the metabolite, acrolein, may be of particular importance (154–157). The acute toxicity of acrolein, which can be formed from spermine by extracellular Cu-dependent oxidases present in serum, has been known for many years (58, 59, 158), but only recently this metabolite been demonstrated to be an important potential cause and biomarker for ischemic disease. Methods for these assays are given in Chapter 25.

SMO is likely to provide an important mechanistic link between infection, inflammation, and carcinogenesis (48). It is induced in ulcerative colitis leading to increased oxidative stress and altered immune responses (159). Infection of gut macrophages with *Helicobacter pylori*, which causes gastric ulcers and stomach cancer, induced arginase II and ODC increasing polyamine content and also induced SMO producing ROS including H₂O₂ leading to DNA damage and apoptosis (160–163). Thus, *H. pylori* infection may escape the immune system by killing the immune cells responsible for eradicating the infection. Furthermore, the increased SMO expression in the gastric epithelial cells could result in ROS production leading to mutagenic DNA damage and initiation of neoplastic transformation (163). Chapter 26 describes procedures for these investigations.

As mentioned above, animal models with increased SSAT activity have suggested that this enzyme may be involved in a wide variety of other conditions including pancreatitis, blockage of regenerative tissue growth, obesity, diabetes, and carcinogenesis. Such SSAT overexpression leads to a variety of biochemical alterations that may cause pathogenesis. These include: the loss of

polyamines and the reduction in acetyl-CoA and ATP due to the futile cycle set up by increased degradation causing increased synthesis of polyamines and the formation of ROS (47, 49, 164–168). Human genetic studies also suggest that the SSAT/APAO and SMO pathways may be involved in heritable disease. One form of keratosis follicularis spinulosa decalvans (KFSD), a rare X-linked inherited disease affecting primarily the skin and eyes, may be associated with an increased gene copy of the *Sat1* gene encoding SSAT (169). KFSD is characterized by keratosis and hair loss and elevated SSAT in mouse models does cause such changes (49, 170). Cells from patients with the neurodegenerative lysosomal storage disease Niemann–Pick type C are more sensitive to the toxic effects of aldehydes formed by the polyamine catabolic pathways (171). Low SSAT activity may be related to behavioral changes particularly a propensity to suicide (172–174). Decreased *Sat1* gene expression due to reduced levels of SSAT mRNA that may be imparted by the C allele of the *Sat1* 342A/C gene polymorphism has been correlated to depression and a propensity to suicide. Microarray analyses indicating a link between decreased SSAT expression and suicide were supported by studies with reverse transcription-polymerase chain reaction; immunohistochemistry and Western blotting for SSAT have been used to show that SSAT content was lower in the brains of persons committing suicide than in normal controls. Alterations in polyamine levels in such depressive patients have also been reported (175) and methods to examine this and relate it to disease are described in Chapter 27.

The mechanism by which SSAT is linked to behavioral effects is not understood, but may be linked to polyamine-mediated alterations in ion channels including NMDA receptors, AMPA receptors, K⁺ channels, and Ca²⁺ in the brain. Kainate-induced seizures increase SSAT activity (176) and transgenic overexpression of SSAT protects from kainate (177), and epilepsy-like seizure activity induction by pentylentetrazol (177). These SSAT transgenic mice also showed a reduced activity and spatial learning impairment (36, 178). The critical role of polyamines in cognitive function is shown most clearly by the finding that an inherited defect in spermine synthase causes Snyder–Robinson syndrome (SRS) (179). SRS is an X-linked recessive disease that causes mild-to-moderate mental retardation as well as hypotonia, cerebellar circuitry dysfunction, thin habitus and kyphoscoliosis. The first gene alteration shown to cause this condition was a splice variant of the *SMS* gene that resulted in an inactive truncated protein. Subsequent studies showed that similar phenotypes were associated with point mutations in the coding region that produce virtually complete loss of spermine synthase activity (13, 180, 181). The analysis of human samples to determine SRS is covered in Chapter 28.

10. Polyamine Analogs and Derivatives as Research Tools and Therapeutics

A wide variety of polyamines have been produced by synthetic chemists and these have been used for a variety of experimental and therapeutic experiments. One interesting series of compounds first described by the laboratories of Coward and of Ganem has methyl substituents on the α carbon atom or both the terminal carbon atoms of spermidine or spermine (182–186). Such substitution does not interfere with the uptake or many physiological functions of the polyamines, but renders them resistant to some oxidative catabolism and as substrates for acetylation and the generation of ROS (187–189). They can therefore be used to investigate polyamine function and to replace polyamines in conditions of polyamine deficiency (188, 190). More recent studies, in which (S)- and (R)- isomers of α -methylspermidine and (S,S)-, (R,S)-, and (R,R)-diastereomers of α,α' -(dimethyl)spermine have been used, have confirmed and extended these important findings (67, 191–196). Such studies have shown the maintenance of nucleic acid structure (196, 197), the stereospecificity of oxidation reactions (192, 194), the ability of derivatives that can support hypusine synthesis to support growth (67, 188, 190), and the role of polyamines in other growth processes including hair synthesis (198), liver regeneration, and adipocyte differentiation (199). Of particular interest is the ability to overcome acute liver damage and pancreatitis related to polyamine depletion by provision of α -methylspermidine or α,α' -(dimethyl)spermine (168, 193, 195, 200, 201). The synthesis of such derivatives is covered by Chapter 29. Other active polyamine analogs have also been produced that contain unsaturated moieties leading to structural changes that can be used to investigate polyamine function (185, 186, 190, 202). *N*-(3-aminopropyl)-1,4-diamino-*cis*-but-2-ene [the *cis* isomer of the alkene analog of spermidine] was a good substrate for spermine synthase, but that the *trans* isomer and the alkyne analog [*N*-(3-aminopropyl)-1,4-diaminobut-2-yne] were not substrates. Only the *cis* isomer was able to act as a precursor of hypusine and support sustained growth in cells treated with an inhibitor of polyamine synthesis (190).

Other very useful polyamine derivatives involve substitution at N-groups. Such derivatives of both the terminal and internal N atoms have been used to provide analogs that are transported by the polyamine transport system and thus can be used to study this system (121, 203–206). Fluorescent derivatives have been particularly useful in this regard (121, 204, 206). They have been used to study transport and to provide useful assay substrates for polyamine metabolic enzymes as described in Chapter 30, and also to study the binding of polyamines to receptors and ion channels. Polyamines with N-substitutions are also potentially useful

as delivery vehicles for drugs. They can incorporate additions that are known antitumor agents (118, 204, 207–209).

Many synthetic polyamine analogs are profoundly antiproliferative and/or cause apoptosis in cancer cells and some are at various stages of development as antitumor agents (210–216). Addition of terminal alkyl groups renders the analogs more resistant to metabolism and large numbers of analogs with both symmetrical terminal substituents and unsymmetrical terminal substituents have been made by the laboratories of Samejima, Bergeron, Woster, Frydman, and others (211, 217–223). Other internal modifications leading to conformational restriction of bis(ethyl) polyamines have provided particularly promising derivatives that are currently in clinical trials (224, 225).

The original hypothesis underlying the production of these *N*-alkyl substituted analogs was related to the homeostatic regulation of polyamine content and the importance of polyamines for neoplastic growth. Thus, it was hypothesized that if analogs could be developed, which did not themselves act in the roles of polyamine essential for cell growth, but were able to down-regulate polyamine synthesis and upregulate degradation/excretion, these would prevent tumor growth. Remarkably, many polyamine analogs such as *N*¹, *N*¹¹-bis(ethyl)norspermine and *N*¹, *N*¹²-bis(ethyl)spermine do indeed seem to have these properties being strong inducers of antizyme and of SSAT, thus leading to a drastic fall in polyamine content and apoptosis (119, 226–228). Induction of high levels of SSAT also may exert antitumor effects via ROS production through the activated SSAT/APAO pathways (60, 229, 230) or a reduction in acetyl-CoA and malonyl-CoA, which would decrease fatty acid synthesis (231, 232).

However, many analogs that are also effective against human tumor cells in xenografts and cell cultures do not cause as large an increase in SSAT (213, 214, 224, 233–236). They may act by directly inducing SMO, which is highly responsive to many analogs, and thus reduce spermine and increase ROS (48, 60, 229), by metabolism generating toxic metabolites via SMO or the SSAT/APAO pathways (60, 237) or by additional mechanisms such as blocking binding of polyamines to key sites for normal effects on growth, interfering with polyamine-mediated cell signaling (238) or by acting on the cytoskeleton (230). It should also be noted that the potential of polyamine analogs for therapeutic use is not limited to cancer therapy. A variety of analogs have been shown to have antiparasitic activity (216, 239–242).

Recently, a novel use of polyamine analogs for therapy has been developed based on the observations that some of these compounds are potent and specific inactivators of enzymes that play key roles in chromatin modification (215, 238, 243). Alteration of chromatin structure to reverse epigenetic changes leading to neoplastic growth is a major current focus of the development of novel

therapeutics. The synthesis of polyaminohydroxamic acid and polyaminobenzamide derivatives that selectively inactivate histone deacetylase isoforms is described in Chapter 31.

11. Chemical Properties and Analysis of Polyamines

It is important to realize that the properties of polyamines are not simply due to their total charge but that the spatial distribution of this charge and the abilities of cellular macromolecules to interact, not only via electrostatic interactions, but also by hydrophobic interactions with the aliphatic moieties, are critical to understanding their effects. The many crystal structures of proteins and nucleic acids complexed with polyamines that are now available show clearly the importance of both types of interaction.

Early studies with polyamine analogs containing fluorine substituents also demonstrate the importance of the charged nitrogen atoms in the ability of these analogs to fulfill polyamine functions (244–247), but with some exceptions (196) this aspect of the potential effects of synthetic substitutions of the polyamine backbone is not often explored. Other considerations of the charge distribution in the naturally occurring polyamines are of great importance and Chapter 32 provides a comprehensive discussion of this topic and the measurement of the pK_a values of individual polyamines.

It is a critical part of experiments on polyamine metabolism and function to measure the content of polyamines. Many methods are available for this assay and, depending on the polyamines to be assayed and the equipment available, an appropriate method can be selected. Acid extraction followed by deproteinization provides a suitable starting material. Very early methods involved separation by thin layer chromatography of either the amines followed by detection with reagents such as ninhydrin (248) or of fluorescent derivatives formed by dansylation (249, 250) or use of an amino acid analyzer with modified elution to release the more basic polyamines (251). These have largely been replaced by HPLC separation, which can be carried out with either postcolumn derivatization using *o*-phthalaldehyde (252) or by precolumn derivatization to form dansyl or benzoyl- or other readily quantifiable derivatives (253, 254). These methods are covered in Volume 79 of this series. One advantage of the precolumn dansylation procedure is that polyamine analogs with terminal alkyl or acetyl substituents can still be detected. Extension of HPLC analysis to separation of the wider variety of polyamines first characterized in thermophiles is covered in Chapter 5 of the present volume.

More recent analytical methods have employed gas chromatography/mass spectrometry (255–257). These assays, detailed procedures for which are described in Chapter 33 and for human samples in Chapter 27, are the method of choice with respect to specificity and sensitivity as long as the required equipment, marker compounds, and expertise are available and the extensive development of these assays has been a major advance.

In summary, it is hoped that the detailed methods provided in this new volume will facilitate the work in the many laboratories currently interested in polyamine function and metabolism and will foster a new generation of researchers interested in this exciting and challenging field. As we have entered a new era of polyamine research with our better understanding of their molecular functions, many challenges lie ahead. Our goal is to make meeting those challenges somewhat easier.

Acknowledgements

Research in the authors' laboratories on polyamines has been supported by NIH (CA-018138 and GM-26290 to AEP; CA-51085 and CA-98454 to RAC) and by grants from Komen for the Cure KG08923, and the Samuel Waxman Cancer Research Foundation (to RAC).

References

1. Cohen SS (1998) A guide to the polyamines. Oxford University Press, New York
2. Naka Y, Watanabe K, Sagor GH, Niitsu M, Pillai MA, Kusano T, Takahashi Y (2010) Quantitative analysis of plant polyamines including thermospermine during growth and salinity stress. *Plant Physiol Biochem* 48:527–533
3. Takahashi T, Kakehi JI (2010) Polyamines: ubiquitous polycations with unique roles in growth and stress responses. *Ann Bot (Lond)* 105:1–6
4. Williams-Ashman HG (1965) NICOLAS LOUIS VAUQUELIN (1763-1829). *Invest Urol* 2:605–613
5. Lee J, Michael AJ, Martynowski D, Goldsmith EJ, Phillips MA (2007) Phylogenetic diversity and the structural basis of substrate specificity in the beta/alpha-barrel fold basic amino acid decarboxylases. *J Biol Chem* 282:27115–27125
6. Morris DR, Pardee AB (1966) Multiple pathways of putrescine biosynthesis in *Escherichia coli*. *J Biol Chem* 241:3129–3135
7. Tabor H, Rosenthal SM, Tabor CW (1958) The biosynthesis of spermidine and spermine from putrescine and methionine. *J Biol Chem* 233:907–914
8. Pegg AE (2009) S-adenosylmethionine decarboxylase, vol 46. Portland, London
9. Bale S, Ealick SE (2010) Structural biology of S-adenosylmethionine decarboxylase. *Amino Acids* 38:451–460
10. Ikeguchi Y, Bewley M, Pegg AE (2006) Aminopropyltransferases: function, structure and genetics. *J Biochem* 139:1–9
11. Wu H, Min J, Ikeguchi Y, Zeng H, Dong A, Loppnau P, Pegg AE, Plotnikov AN (2007) Structure and mechanism of spermidine synthases. *Biochemistry* 46:8331–8339
12. Wu H, Min J, Zeng H, McCloskey DE, Ikeguchi Y, Loppnau P, Michael AJ, Pegg AE, Plotnikov AN (2008) Crystal structure of human spermine synthase: implications of substrate binding and catalytic mechanism. *J Biol Chem* 283:16135–16146
13. Pegg AE, Michael AJ (2010) Spermine synthase. *Cell Mol Life Sci* 67:113–121

14. Lee J, Sperandio V, Frantz DE, Longgood J, Camilli A, Phillips MA, Michael AJ (2009) An alternative polyamine biosynthetic pathway is widespread in bacteria and essential for biofilm formation in *Vibrio cholerae*. *J Biol Chem* 284:9899–9907
15. Tait GH (1976) A new pathway for the biosynthesis of spermidine. *Biochem Soc Trans* 4:610–612
16. Yamamoto S, Nagata S, Kusaba K (1993) Purification and characterization of homospermidine synthase in *Acinetobacter tartarogenes* ATCC 31105. *J Biochem* 114:45–49
17. Ober D, Harms R, Witte L, Hartmann T (2003) Molecular evolution by change of function. alkaloid-specific homospermidine synthase retained all properties of deoxyhypusine synthase except binding the eIF5A precursor protein. *J Biol Chem* 278:12805–12812
18. Shaw FL, Elliott KA, Kinch LN, Fuell C, Phillips MA, Michael AJ (2010) Evolution and multifarious horizontal transfer of an alternative biosynthetic pathway for the alternative polyamine sym-homospermidine. *J Biol Chem* 285:14711–14723
19. Oshima T (2007) Unique polyamines produced by an extreme thermophile *Thermus thermophilus*. *Amino Acids* 33:367–372
20. Terui Y, Ohnuma M, Hiraga K, Kawashima E, Oshima T (2005) Stabilization of nucleic acids by unusual polyamines produced by an extreme thermophile. *Biochem J* 388:427–433
21. Gerner EW, Meyskens FL Jr (2004) Polyamines and cancer: old molecules, new understanding. *Nat Rev Cancer* 4:781–792
22. Pegg AE (2009) Mammalian polyamine metabolism and function. *IUBMB Life* 61:880–894
23. Igarashi K, Kashiwagi K (2010) Modulation of cellular function by polyamines. *Int J Biochem Cell Biol* 42:39–51
24. Yoshida M, Kashiwagi K, Shigemasa A, Taniguchi S, Yamamoto K, Makinoshima H, Ishihama A, Igarashi K (2004) A unifying model for the role of polyamines in bacterial cell growth, the polyamine modulon. *J Biol Chem* 279:46008–46013
25. Igarashi K, Kashiwagi K (2006) Polyamine modulon in *Escherichia coli*: genes involved in the stimulation of cell growth by polyamines. *J Biochem (Tokyo)* 139:11–16
26. Uemura T, Higashi K, Takigawa M, Toida T, Kashiwagi K, Igarashi K (2009) Polyamine modulon in yeast-stimulation of COX4 synthesis by spermidine at the level of translation. *Int J Biochem Cell Biol* 41:2538–2545
27. Nishimura K, Okudaira H, Ochiai E, Higashi K, Kaneko M, Ishii I, Nishimura T, Dohmae N, Kashiwagi K, Igarashi K (2009) Identification of proteins whose synthesis is preferentially enhanced by polyamines at the level of translation in mammalian cells. *Int J Biochem Cell Biol* 41:2251–2261
28. Saini P, Eylar DE, Green R, Dever TE (2009) Hypusine-containing protein eIF5A promotes translation elongation. *Nature* 459:118–121
29. Park MH, Nishimura K, Zanelli CF, Valentini SR (2010) Functional significance of eIF5A and its hypusine modification in eukaryotes. *Amino Acids* 41:2538–2545
30. Landau G, Bercovich Z, Park MH, Kahana C (2010) The role of polyamines in supporting growth of mammalian cells is mediated through their requirement for translation initiation and elongation. *J Biol Chem* 285:12474–12481
31. Zou T, Mazan-Mamczarz K, Rao JN, Liu L, Marasa BS, Zhang AH, Xiao L, Pullmann R, Gorospe M, Wang JY (2006) Polyamine depletion increases cytoplasmic levels of RNA-binding protein HuR leading to stabilization of nucleophosmin and p53 mRNAs. *J Biol Chem* 281:19387–19394
32. Zou T, Liu L, Rao JN, Marasa BS, Chen J, Xiao L, Zhou H, Gorospe M, Wang JY (2008) Polyamines modulate the subcellular localization of RNA-binding protein HuR through AMP-activated protein kinase-regulated phosphorylation and acetylation of importin alpha1. *Biochem J* 409:389–398
33. Liu L, Rao JN, Zou T, Xiao L, Wang PY, Turner DJ, Gorospe M, Wang JY (2009) Polyamines regulate c-Myc translation through Chk2-dependent HuR phosphorylation. *Mol Biol Cell* 20:4885–4898
34. Lopatin AN, Makhina EN, Nichols CG (1994) Potassium channel block by cytoplasmic polyamines as the mechanism of intrinsic rectification. *Nature* 372:366–369
35. Williams K (1997) Modulation and block of ion channels: a new biology of polyamines. *Cell Signal* 9:1–13
36. Jänne J, Alhonen L, Pietilä M, Keinänen T (2004) Genetic approaches to the cellular functions of polyamines in mammals. *Eur J Biochem* 271:877–894
37. Pegg AE, Feith DJ, Fong LYY, Coleman CS, O'Brien TG, Shantz LM (2003) Transgenic mouse models for studies of the role of polyamines in normal, hypertrophic and neoplastic growth. *Biochem Soc Trans* 31:356–360
38. Alhonen L, Uimari A, Pietilä M, Hyvonen MT, Pirinen E, Keinänen TA (2009) Transgenic animals modelling polyamine metabolism-related diseases. *Essays Biochem* 46:125–144

39. Nilsson JA, Keller UB, Baudino TA, Yang C, Norton S, Old JA, Nilsson LM, Neale G, Kramer DL, Porter CW, Cleveland JL (2005) Targeting ornithine decarboxylase in Myc-induced lymphomagenesis prevents tumor formation. *Cancer Cell* 7:433–444
40. Guo Y, Cleveland JL, O'Brien TG (2005) Haploinsufficiency for ODC modifies mouse skin tumor susceptibility. *Cancer Res* 65:1146–1149
41. Feith DJ, Fong LYY, Pegg AE (2005) Antizyme inhibits N-nitrosomethylbenzylamine-induced mouse forestomach carcinogenesis in a p53-independent manner. *Proc Am Assoc Cancer Res* 46:A3887
42. Rial NS, Meyskens FL, Gerner EW (2009) Polyamines as mediators of APC-dependent intestinal carcinogenesis and cancer chemoprevention. *Essays Biochem* 46:111–124
43. Gerner EW, Meyskens FL Jr (2009) Combination chemoprevention for colon cancer targeting polyamine synthesis and inflammation. *Clin Cancer Res* 15:758–761
44. Bailey HH, Kim K, Verma AK, Sielaff K, Larson PO, Snow S, Lenaghan T, Viner JL, Douglas J, Dreckschmidt NE, Hamielec M, Pomplun M, Sharata HH, Puchalsky D, Berg ER, Havighurst TC, Carbone PP (2010) A randomized, double-blind, placebo-controlled phase 3 skin cancer prevention study of α -difluoromethylornithine in subjects with previous history of skin cancer. *Cancer Prev Res* 3:35–47
45. Simoneau AR, Gerner EW, Nagle R, Ziogas A, Fujikawa-Brooks S, Yerushalmi H, Ahlering TE, Lieberman R, McLaren CE, Anton-Culver H, Meyskens FL Jr (2008) The effect of difluoromethylornithine on decreasing prostate size and polyamines in men: results of a year-long phase IIb randomized placebo-controlled chemoprevention trial. *Cancer Epidemiol Biomarkers Prev* 17:292–299
46. Forshell TP, Rimpi S, Nilsson JA (2010) Chemoprevention of B-cell lymphomas by inhibition of the Myc target spermidine synthase. *Cancer Prev Res* 3:140–147
47. Pegg AE (2008) Spermidine/spermine N¹-acetyltransferase: a key metabolic regulator. *Am J Physiol Endocrinol Metab* 294:E995–E1010
48. Casero RA Jr, Pegg AE (2009) Polyamine catabolism and disease. *Biochem J* 421:323–338
49. Jänne J, Alhonen L, Pietila M, Keinänen TA, Uimari A, Hyvonen MT, Pirinen E, Jarvinen A (2006) Genetic manipulation of polyamine catabolism in rodents. *J Biochem (Tokyo)* 139:155–160
50. Chattopadhyay MK, Park MH, Tabor H (2008) Hypusine modification for growth is the major function of spermidine in *Saccharomyces cerevisiae* polyamine auxotrophs grown in limiting spermidine. *Proc Natl Acad Sci USA* 105:6554–6559
51. Pegg AE, Wang X (2009) Mouse models to investigate the function of spermine. *Commun Integr Biol* 2:271–274
52. Hanfrey C, Sommer S, Mayer MJ, Burtin D, Michael AJ (2001) Arabidopsis polyamine biosynthesis: absence of ornithine decarboxylase and the mechanism of arginine decarboxylase activity. *Plant J* 27:551–560
53. Hanfrey C, Franceschetti M, Mayer MJ, Illingworth C, Michael AJ (2002) Abrogation of upstream open reading frame-mediated translational control of a plant S-adenosylmethionine decarboxylase results in polyamine disruption and growth perturbations. *J Biol Chem* 277:44131–44139
54. Vera-Sirera F, Minguet EG, Singh SK, Ljung K, Tuominen H, Blazquez MA, Carbonell J (2010) Role of polyamines in plant vascular development. *Plant Physiol Biochem* 48:534–539
55. Seiler N, Bolkenius FN, Knodgen B (1985) The influence of catabolic reactions on polyamine excretion. *Biochem J* 225:219–226
56. Morgan DM (1998) Polyamine oxidases—enzymes of unknown function? *Biochem Soc Trans* 26:586–591
57. Seiler N (2004) Catabolism of polyamines. *Amino Acids* 26:217–233
58. Kimes BW, Morris DR (1971) Inhibition of nucleic acid and protein synthesis in *Escherichia coli* by oxidized polyamines and acrolein. *Biochim Biophys Acta* 228:235–244
59. Kimes BW, Morris DR (1971) Preparation and stability of oxidized polyamines. *Biochim Biophys Acta* 228:223–234
60. Wang Y, Casero RA Jr (2006) Mammalian polyamine catabolism: a therapeutic target, a pathological problem, or both? *J Biochem (Tokyo)* 139:17–25
61. Adachi MS, Juarez PR, Fitzpatrick PF (2010) Mechanistic studies of human spermine oxidase: kinetic mechanism and pH effects. *Biochemistry* 49:386–392
62. Moschou PN, Sanmartin M, Andriopoulou AH, Rojo E, Sanchez-Serrano JJ, Roubelakis-Angelakis KA (2008) Bridging the gap between plant and mammalian polyamine catabolism: a novel peroxisomal polyamine oxidase responsible for a full back-conversion pathway in *Arabidopsis*. *Plant Physiol* 147:1845–1857

63. Cona A, Rea G, Angelini R, Federico R, Tavladoraki P (2006) Functions of amine oxidases in plant development and defence. *Trends Plant Sci* 11:80–88
64. Rodriguez AA, Maiale SJ, Menendez AB, Ruiz OA (2009) Polyamine oxidase activity contributes to sustain maize leaf elongation under saline stress. *J Exp Bot* 60:4249–4262
65. Childs AC, Mehta DJ, Gerner EW (2003) Polyamine-dependent gene expression. *Cell Mol Life Sci* 60:1394–1406
66. Park MH (2006) The post-translational synthesis of a polyamine-derived amino acid, hypusine, in the eukaryotic translation initiation factor 5A (eIF5A). *J Biochem (Tokyo)* 139:161–169
67. Hyvönen MT, Keinänen TA, Cerrada-Gimenez M, Sinervirta R, Grigorenko N, Khomutov AR, Vepsäläinen J, Alhonen L, Jänne J (2007) Role of hypusinated eukaryotic translation initiation factor 5A in polyamine depletion-induced cytostasis. *J Biol Chem* 282:34700–34706
68. Hoque M, Hanauske-Abel HM, Palumbo P, Saxena D, D'Alliessi-Gandolfi D, Park MH, Pe'ery T, Mathews MB (2009) Inhibition of HIV-1 gene expression by Ciclopirox and Deferiprone, drugs that prevent hypusination of eukaryotic translation initiation factor 5A. *Retrovirology* 6:90
69. Vu VV, Emerson JP, Martinho M, Kim YS, Munck E, Park MH, Que L Jr (2009) Human deoxyhypusine hydroxylase, an enzyme involved in regulating cell growth, activates O₂ with a nonheme diiron center. *Proc Natl Acad Sci USA* 106:14814–14819
70. Pegg AE (1986) Recent advances in the biochemistry of polyamines in eukaryotes. *Biochem J* 234:249–262
71. Persson L (2009) Polyamine homeostasis. *Essays Biochem* 46:11–24
72. Pegg AE (2006) Regulation of ornithine decarboxylase. *J Biol Chem* 281:14529–14532
73. Kahana C (2009) Regulation of cellular polyamine levels and cellular proliferation by antizyme and antizyme inhibitor. *Essays Biochem* 46:47–61
74. Bale S, Lopez MM, Makhatadze GI, Fang Q, Pegg AE, Ealick SE (2008) Structural basis for putrescine activation of human S-adenosylmethionine decarboxylase. *Biochemistry* 47:13404–13417
75. Willert EK, Fitzpatrick R, Phillips MA (2007) Allosteric regulation of an essential trypanosome polyamine biosynthetic enzyme by a catalytically dead homolog. *Proc Natl Acad Sci USA* 104:8275–8280
76. Willert EK, Phillips MA (2008) Regulated expression of an essential allosteric activator of polyamine biosynthesis in African trypanosomes. *PLoS Pathog* 4:e1000183
77. Willert EK, Phillips MA (2009) Cross-species activation of trypanosome S-adenosylmethionine decarboxylase by the regulatory subunit prozyme. *Mol Biochem Parasitol* 168:1–6
78. Bacchi CJ (2009) Chemotherapy of human African trypanosomiasis. *Interdiscip Perspect Infect Dis* 2009:195040
79. Barker RH Jr, Liu H, Hirth B, Celatka CA, Fitzpatrick R, Xiang Y, Willert EK, Phillips MA, Kaiser M, Bacchi CJ, Rodriguez A, Yarlett N, Klinger JD, Sybertz E (2009) Novel S-adenosylmethionine decarboxylase inhibitors for the treatment of human African trypanosomiasis. *Antimicrob Agents Chemother* 53:2052–2058
80. Russell DH, Snyder SH (1969) Amine synthesis in regenerating rat liver: extremely rapid turnover of ornithine decarboxylase. *Mol Pharmacol* 5:253–262
81. Coffino P (2001) Regulation of cellular polyamines by antizyme. *Nat Rev Mol Cell Biol* 2:188–194
82. Kahana C (2009) Antizyme and antizyme inhibitor, a regulatory tango. *Cell Mol Life Sci* 66:2479–2488
83. Heller JS, Fong WF, Canellakis ES (1976) Induction of a protein inhibitor to ornithine decarboxylase by the end products of its reaction. *Proc Natl Acad Sci USA* 73:1858–1862
84. Hayashi S, Murakami Y, Matsufuji S (1996) Ornithine decarboxylase antizyme: a novel type of regulatory protein. *TIBS* 21:27–30
85. Yamaguchi Y, Takatsuka Y, Matsufuji S, Murakami Y, Kamio Y (2006) Characterization of a counterpart to mammalian ornithine decarboxylase antizyme in prokaryotes. *J Biol Chem* 281:3995–4001
86. Ivanov IP, Matsufuji S, Murakami Y, Gesteland RF, Atkins JF (2000) Conservation of polyamine regulation by translational frameshifting from yeast to mammals. *EMBO J* 19:1907–1917
87. Howard MT, Shirts BH, Zhou J, Carlson CL, Matsufuji S, Gesteland RF, Weeks RS, Atkins JF (2001) Cell culture analysis of the regulatory frameshift event required for the expression of mammalian antizymes. *Genes Cells* 6:931–941
88. Ivanov IP, Loughran G, Atkins JF (2008) uORFs with unusual translational start codons autoregulate expression of eukaryotic ornithine decarboxylase homologs. *Proc Natl Acad Sci USA* 105:10079–10084

89. Murai N, Shimizu A, Murakami Y, Matsufuji S (2009) Subcellular localization and phosphorylation of antizyme 2. *J Cell Biochem* 108:1012–1021
90. Tokuhiro K, Isotani A, Yokota S, Yano Y, Oshio S, Hirose M, Wada M, Fujita K, Ogawa Y, Okabe M, Nishimune Y, Tanaka H (2009) OAZ-t/OAZ3 is essential for rigid connection of sperm tails to heads in mouse. *PLoS Genet* 5:e1000712
91. Lopez-Contreras AJ, Ramos-Molina B, Cremades A, Penafiel R (2009) Antizyme inhibitor 2: molecular, cellular and physiological aspects. *Amino Acids* 38:603–611
92. Su KL, Liao YF, Hung HC, Liu GY (2009) Critical factors determining dimerization of human antizyme inhibitor. *J Biol Chem* 284:26768–26777
93. Snapir Z, Keren-Paz A, Bercovich Z, Kahana C (2008) ODCp, a brain- and testis-specific ornithine decarboxylase paralogue, functions as an antizyme inhibitor, although less efficiently than Az11. *Biochem J* 410:613–619
94. Tang H, Arika K, Ohkido M, Murakami Y, Matsufuji S, Li Z, Yamamura K (2009) Role of ornithine decarboxylase antizyme inhibitor *in vivo*. *Genes Cells* 14:79–87
95. Nilsson JA, Maclean KH, Keller UB, Pendeville H, Baudino TA, Cleveland JL (2004) Mnt loss triggers Myc transcription targets, proliferation, apoptosis, and transformation. *Mol Cell Biol* 24:1560–1569
96. Shantz LM, Levin VA (2007) Regulation of ornithine decarboxylase during oncogenic transformation: mechanisms and therapeutic potential. *Amino Acids* 33:213–223
97. Pyronnet S, Pradayrol L, Sonenberg N (2005) Alternative splicing facilitates internal ribosome entry on the ornithine decarboxylase mRNA. *Cell Mol Life Sci* 62:1267–1274
98. Origanti S, Shantz LM (2007) Ras transformation of RIE-1 cells activates cap-independent translation of ornithine decarboxylase: regulation by the Raf/MEK/ERK and phosphatidylinositol 3-kinase pathways. *Cancer Res* 67:4834–4842
99. Grens A, Scheffler IE (1990) The 5'- and 3'-untranslated regions of ornithine decarboxylase mRNA affect the translational efficiency. *J Biol Chem* 265:11810–11816
100. Igarashi K, Ito K, Kashiwagi K (2001) Polyamine uptake systems in *Escherichia coli*. *Res Microbiol* 152:271–278
101. Igarashi K, Kashiwagi K (1999) Polyamine transport in bacteria and yeast. *Biochem J* 344:633–642
102. Aouida M, Leduc A, Poulin R, Ramotar D (2005) AGP2 encodes the major permease for high affinity polyamine import in *Saccharomyces cerevisiae*. *J Biol Chem* 280:24267–24276
103. Uemura T, Kashiwagi K, Igarashi K (2007) Polyamine uptake by *DUR3* and *SAM3* in *Saccharomyces cerevisiae*. *J Biol Chem* 282:7733–7741
104. Hasne MP, Ullman B (2005) Identification and characterization of a polyamine permease from the protozoan parasite *Leishmania major*. *J Biol Chem* 280:15188–15194
105. Hasne MP, Coppens I, Soysa R, Ullman B (2010) A high-affinity putrescine-cadaverine transporter from *Trypanosoma cruzi*. *Mol Microbiol* 76:78–91
106. Burns MR, Carlson CL, Vanderwerf SM, Ziemer JR, Weeks RS, Cai F, Webb HW, Graminski GF (2001) Amino acid/spermine conjugates: polyamine amides as potent spermidine uptake inhibitors. *J Med Chem* 44:3632–3644
107. Covassin L, Desjardins M, Soulet D, Charest-Gaudreault R, Audette M, Poulin R (2003) Xylylated dimers of putrescine and polyamines: influence of the polyamine backbone on spermidine transport inhibition. *Bioorg Med Chem Lett* 13:3267–3271
108. Burns MR, Graminski GF, Weeks RS, Chen Y, O'Brien TG (2009) Lipophilic lysine-spermine conjugates are potent polyamine transport inhibitors for use in combination with a polyamine biosynthesis inhibitor. *J Med Chem* 52:1983–1993
109. Heinick A, Urban K, Roth S, Spies D, Nunes F, Phanstiel O IV, Liebau E, Luersen K (2010) *Caenorhabditis elegans* P5B-type ATPase CATP-5 operates in polyamine transport and is crucial for norspermidine-mediated suppression of RNA interference. *FASEB J* 24:206–217
110. Rannels DE, Pegg AE, Clark RS, Addison JL (1985) Interaction of paraquat and amine uptake by rat lungs perfused *in situ*. *Am J Physiol* 249:E506–E513
111. Minton KW, Tabor H, Tabor CW (1990) Paraquat toxicity is increased in *Escherichia coli* defective in the synthesis of polyamines. *Proc Natl Acad Sci USA* 87:2851–2855
112. Mandel J, Flintoff WF (1978) Isolation of mutant mammalian cells altered in polyamine transport. *J Cell Physiol* 97:335–344
113. Heaton MA, Flintoff WF (1988) Methylglyoxal bis (guanyldrazone)-resistant Chinese hamster ovary cells: genetic evidence that more than a single locus controls uptake. *J Cell Physiol* 136:133–139
114. Byers TL, Kameji R, Rannels DE, Pegg AE (1987) Multiple pathways for uptake of paraquat, methylglyoxal bis(guanyldrazone),

- and polyamines. *Am J Physiol* 252:C663–C669
115. Rossi T, Coppi A, Bruni E, Ruberto A, Giudice S, Baggio G (2008) Mepacrine antagonises tumour cell growth induced by natural polyamines. *Anticancer Res* 28:2765–2768
 116. Holley JL, Mather A, Wheelhouse RT, Cullis PM, Hartley JA, Bingham JP, Cohen GM (1992) Targeting of tumor cells and DNA by a chlorambucil-spermidine conjugate. *Cancer Res* 52:4190–4195
 117. Kaur N, Delcros JG, Archer J, Weagraff NZ, Martin B, Phanstiel O IV (2008) Designing the polyamine pharmacophore: influence of *N*-substituents on the transport behavior of polyamine conjugates. *J Med Chem* 51:2551–2560
 118. Palmer AJ, Ghani RA, Kaur N, Phanstiel O, Wallace HM (2009) A putrescine-anthracene conjugate: a paradigm for selective drug delivery. *Biochem J* 424:431–438
 119. Mitchell JL, Leyser A, Holtorff MS, Bates JS, Frydman B, Valasinas A, Reddy VK, Marton LJ (2002) Antizyme induction by polyamine analogues as a factor of cell growth inhibition. *Biochem J* 366:663–671
 120. Mitchell JL, Simkus CL, Thane TK, Tokarz P, Bonar MM, Frydman B, Valasinas AL, Reddy VK, Marton LJ (2004) Antizyme induction mediates feedback limitation of the incorporation of specific polyamine analogues in tissue culture. *Biochem J* 384:271–279
 121. Soulet D, Gagnon B, Rivest S, Audette M, Poulin R (2004) A fluorescent probe of polyamine transport accumulates into intracellular acidic vesicles via a two-step mechanism. *J Biol Chem* 279:49355–49366
 122. Belting M, Persson S, Fransson L-Å (1999) Proteoglycan involvement in polyamine uptake. *Biochem J* 338:317–323
 123. Belting M, Mani K, Jonsson M, Cheng F, Sandgren S, Jonsson S, Ding K, Delcros JG, Fransson LA (2003) Glypican-1 is a vehicle for polyamine uptake in mammalian cells: a pivotal role for nitrosothiol-derived nitric oxide. *J Biol Chem* 278:47181–47189
 124. Belting M, Borsig L, Fuster MM, Brown JR, Persson L, Fransson LA, Esko JD (2002) Tumor attenuation by combined heparan sulfate and polyamine depletion. *Proc Natl Acad Sci USA* 99:371–376
 125. Welch JE, Bengtson P, Svensson K, Wittrup A, Jenniskens GJ, Ten Dam GB, Van Kuppevelt TH, Belting M (2008) Single chain fragment anti-heparan sulfate antibody targets the polyamine transport system and attenuates polyamine-dependent cell proliferation. *Int J Oncol* 32:749–756
 126. Roy UK, Rial NS, Kachel KL, Gerner EW (2008) Activated K-RAS increases polyamine uptake in human colon cancer cells through modulation of caveolar endocytosis. *Mol Carcinog* 47:538–553
 127. Hawell L, Tjandrawinata RR, Byus CV (1994) Selective putrescine export is regulated by insulin and ornithine in Reuber H35 hepatoma cells. *Biochim Biophys Acta* 1222:15–26
 128. Hawel L III, Byus CV (2002) A streamlined method for the isolation and quantitation of nanomole levels of exported polyamines in cell culture media. *Anal Biochem* 311:127–132
 129. Pastorian KE, Byus CV (1997) Tolerance to putrescine toxicity in Chinese hamster ovary cells is associated with altered uptake and export. *Exp Cell Res* 231:284–295
 130. Uemura T, Yerushalmi HF, Tsapralis G, Stringer DE, Pastorian KE, Hawel L III, Byus CV, Gerner EW (2008) Identification and characterization of a diamine exporter in colon epithelial cells. *J Biol Chem* 283:26428–26435
 131. Bardocz S, Duguid TJ, Brown DS, Grant G, Pusztai A, White A, Ralph A (1995) The importance of dietary polyamines in cell regeneration and growth. *Br J Nutr* 73:819–828
 132. Quemener V, Moulinoux JP, Havouis R, Seiler N (1992) Polyamine deprivation enhances antitumoral efficacy of chemotherapy. *Anticancer Res* 12:1447–1454
 133. Quemener V, Blancard Y, Chamaillard L, Havouis R, Cipolla B, Moulinoux J (1994) Polyamine deprivation: a new tool in cancer treatment. *Anticancer Res* 14:443–448
 134. Cipolla B, Guilli F, Moulinoux JP (2003) Polyamine-reduced diet in metastatic hormone-refractory prostate cancer (HRPC) patients. *Biochem Soc Trans* 31:384–387
 135. Estebe JP, Legay F, Gentili M, Wodey E, Leduc C, Ecoffey C, Moulinoux JP (2006) An evaluation of a polyamine-deficient diet for the treatment of inflammatory pain. *Anesth Analg* 102:1781–1788
 136. Soda K, Kano Y, Sakuragi M, Takao K, Lefor A, Konishi F (2009) Long-term oral polyamine intake increases blood polyamine concentrations. *J Nutr Sci Vitaminol (Tokyo)* 55:361–366
 137. Sabater-Molina M, Larque E, Torrella F, Plaza J, Lozano T, Munoz A, Zamora S (2009) Effects of dietary polyamines at physiologic doses in early-weaned piglets. *Nutrition* 25:940–946
 138. Zoumas-Morse C, Rock CL, Quintana EL, Neuhauser ML, Gerner EW, Meyskens FL Jr (2007) Development of a polyamine data-

- base for assessing dietary intake. *J Am Diet Assoc* 107:1024–1027
139. Kawakita M, Hiramatsu K (2006) Diacetylated derivatives of spermine and spermidine as novel promising tumor markers. *J Biochem (Tokyo)* 139:315–322
 140. Russell DH (1977) Clinical relevance of polyamines as biochemical markers of tumor kinetics. *Clin Chem* 23:22–27
 141. Durie BG, Salmon SE, Russell DH (1977) Polyamines as markers of response and disease activity in cancer chemotherapy. *Cancer Res* 37:214–221
 142. Miki T, Hiramatsu K, Kawakita M (2005) Interaction of N¹, N¹²-diacetylspermine with polyamine transport systems of polarized porcine renal cell line LLC-PK1. *J Biochem (Tokyo)* 138:479–484
 143. Hamaoki M, Hiramatsu K, Suzuki S, Nagata A, Kawakita M (2002) Two enzyme-linked immunosorbent assay (ELISA) systems for N¹, N⁸-diacetylspermidine and N¹, N¹²-diacetylspermine using monoclonal antibodies. *J Biochem* 132:783–788
 144. Parchment RE (1993) The implications of a unified theory of programmed cell death, polyamines, oxyradicals and histogenesis in the embryo. *Int J Dev Biol* 37:75–83
 145. Parchment RE, Pierce GB (1989) Polyamine oxidation programmed cell death, and regulation of melanoma in the murine embryonic limb. *Cancer Res* 49:6680–6686
 146. Zahedi K, Wang Z, Barone S, Prada AE, Kelly CN, Casero RA, Yokota N, Porter CW, Rabb H, Soleimani M (2003) Expression of SSAT, a novel biomarker of tubular cell damage, increases in kidney ischemia-reperfusion injury. *Am J Physiol Renal Physiol* 284:F1046–F1055
 147. Zhao YJ, Xu CQ, Zhang WH, Zhang L, Bian SL, Huang Q, Sun HL, Li QF, Zhang YQ, Tian Y, Wang R, Yang BF, Li WM (2007) Role of polyamines in myocardial ischemia/reperfusion injury and their interactions with nitric oxide. *Eur J Pharmacol* 562:236–246
 148. Zahedi K, Bissler JJ, Wang Z, Josyula A, Lu L, Diegelman P, Kisiel N, Porter CW, Soleimani M (2007) Spermidine/spermine N¹-acetyltransferase overexpression in kidney epithelial cells disrupts polyamine homeostasis, leads to DNA damage, and causes G2 arrest. *Am J Physiol Cell Physiol* 292:C1204–C1215
 149. Barone S, Okaya T, Rudich S, Petrovic S, Tenrani K, Wang Z, Zahedi K, Casero RA, Lentsch AB, Soleimani M (2005) Distinct and sequential upregulation of genes regulating cell growth and cell cycle progression during hepatic ischemia-reperfusion injury. *Am J Physiol Cell Physiol* 289:C826–C835
 150. Zahedi K, Lentsch AB, Okaya T, Barone SL, Sakai N, Witte DP, Arend LJ, Alhonen L, Jell J, Jänne J, Porter CW, Soleimani M (2009) Spermidine/spermine-N¹-acetyltransferase ablation protects against liver and kidney ischemia reperfusion injury in mice. *Am J Physiol Gastrointest Liver Physiol* 296:G899–G909
 151. Sakata K, Kashiwagi K, Sharmin S, Ueda S, Igarashi K (2003) Acrolein produced from polyamines as one of the uraemic toxins. *Biochem Soc Trans* 31:371–374
 152. Igarashi K, Ueda S, Yoshida K, Kashiwagi K (2006) Polyamines in renal failure. *Amino Acids* 31:477–483
 153. Tomitori H, Usui T, Saeki N, Ueda S, Kase H, Nishimura K, Kashiwagi K, Igarashi K (2005) Polyamine oxidase and acrolein as novel biochemical markers for diagnosis of cerebral stroke. *Stroke* 36:2609–2613
 154. Yoshida M, Higashi K, Jin L, Machi Y, Suzuki T, Masuda A, Dohmae N, Suganami A, Tamura Y, Nishimura K, Toida T, Tomitori H, Kashiwagi K, Igarashi K (2010) Identification of acrolein-conjugated protein in plasma of patients with brain infarction. *Biochem Biophys Res Commun* 391:1234–1239
 155. Saiki R, Nishimura K, Ishii I, Omura T, Okuyama S, Kashiwagi K, Igarashi K (2009) Intense correlation between brain infarction and protein-conjugated acrolein. *Stroke* 40:3356–3361
 156. Yoshida M, Tomitori H, Machi Y, Hagihara M, Higashi K, Goda H, Ohya T, Niitsu M, Kashiwagi K, Igarashi K (2009) Acrolein toxicity: comparison with reactive oxygen species. *Biochem Biophys Res Commun* 378:313–318
 157. Yoshida M, Tomitori H, Machi Y, Katagiri D, Ueda S, Horiguchi K, Kobayashi E, Saeki N, Nishimura K, Ishii I, Kashiwagi K, Igarashi K (2009) Acrolein, IL-6 and CRP as markers of silent brain infarction. *Atherosclerosis* 203:557–562
 158. Seiler N (1990) Polyamine metabolism. *Digestion* 46:319–330
 159. Hong SK, Chaturvedi R, Piazzuelo MB, Coburn LA, Williams CS, Delgado AG, Casero RA Jr, Schwartz DA, Wilson KT (2010) Increased expression and cellular localization of spermine oxidase in ulcerative colitis and relationship to disease activity. *Inflamm Bowel Dis* 16:1557–1566
 160. Gobert AP, Cheng Y, Wang JY, Boucher JL, Iyer RK, Cederbaum SD, Casero RA Jr, Newton JC, Wilson KT (2002) *Helicobacter pylori* induces macrophage apoptosis by activation of arginase II. *J Immunol* 168:4692–4700

161. Cheng Y, Chaturvedi R, Asim M, Bussiere FI, Scholz A, Xu H, Casero RA Jr, Wilson KT (2005) *Helicobacter pylori*-induced macrophage apoptosis requires activation of ornithine decarboxylase by c-Myc. *J Biol Chem* 280:22492–22496
162. Chaturvedi R, Cheng Y, Asim M, Bussiere FI, Xu H, Gobert AP, Hacker A, Casero RA Jr, Wilson KT (2004) Induction of polyamine oxidase 1 by *Helicobacter pylori* causes macrophage apoptosis by hydrogen peroxide release and mitochondrial membrane depolarization. *J Biol Chem* 279:40161–40173
163. Xu H, Chaturvedi R, Cheng Y, Bussiere FI, Asim M, Yao MD, Potosky D, Meltzer SJ, Rhee JG, Kim SS, Moss SF, Hacker A, Wang Y, Casero RA Jr, Wilson KT (2004) Spermine oxidation induced by *Helicobacter pylori* results in apoptosis and DNA damage: implications for gastric carcinogenesis. *Cancer Res* 64:8521–8525
164. Kee K, Foster BA, Merali S, Kramer DL, Hensen ML, Diegelman P, Kisiel N, Vujcic S, Mazurchuk RV, Porter CW (2004) Activated polyamine catabolism depletes acetyl-CoA pools and suppresses prostate tumor growth in TRAMP mice. *J Biol Chem* 279:40076–40083
165. Tucker JM, Murphy JT, Kisiel N, Diegelman P, Barbour KW, Davis C, Medda M, Alhonen L, Janne J, Kramer DL, Porter CW, Berger FG (2005) Potent modulation of intestinal tumorigenesis in *Apc^{min/+}* mice by the polyamine catabolic enzyme spermidine/spermine *N*¹-acetyltransferase. *Cancer Res* 65:5390–5398
166. Hyvonen MT, Merentie M, Uimari A, Keinanen TA, Janne J, Alhonen L (2007) Mechanisms of polyamine catabolism-induced acute pancreatitis. *Biochem Soc Trans* 35:326–330
167. Jell J, Merali S, Hensen ML, Mazurchuk R, Sperryak JA, Diegelman P, Kisiel ND, Barrero C, Deeb KK, Alhonen L, Patel MS, Porter CW (2007) Genetically altered expression of spermidine/spermine *N*¹-acetyltransferase affects fat metabolism in mice via acetyl-CoA. *J Biol Chem* 282:8404–8413
168. Merentie M, Uimari A, Pietila M, Sinervirta R, Keinanen TA, Vepsalainen J, Khomutov A, Grigorenko N, Herzog KH, Janne J, Alhonen L (2007) Oxidative stress and inflammation in the pathogenesis of activated polyamine catabolism-induced acute pancreatitis. *Amino Acids* 33:323–330
169. Gimelli G, Giglio S, Zuffardi O, Alhonen L, Suppola S, Cusano R, Lo Nigro C, Gatti R, Ravazzolo R, Seri M (2002) Gene dosage of the spermidine/spermine *N*¹-acetyltransferase (*SSAT*) gene with putrescine accumulation in a patient with a Xp21.1p22.12 duplication and keratosis follicularis spinulosa decalvans (KFSD). *Hum Genet* 111:235–241
170. Pietila M, Pirinen E, Keskitalo S, Juutinen S, Pasonen-Seppanen S, Keinanen T, Alhonen L, Janne J (2005) Disturbed keratinocyte differentiation in transgenic mice and organotypic keratinocyte cultures as a result of spermidine/spermine *N*¹-acetyltransferase overexpression. *J Invest Dermatol* 124:596–601
171. Kaufmann AM, Krise JP (2008) Niemann-Pick C1 functions in regulating lysosomal amine content. *J Biol Chem* 283:24584–24593
172. Sequeira A, Gwadyr FG, Ffrench-Mullen JM, Canetti L, Gingras Y, Casero RA Jr, Rouleau G, Benkelfat C, Turecki G (2006) Implication of *SSAT* by gene expression and genetic variation in suicide and major depression. *Arch Gen Psychiatry* 63:35–48
173. Guipponi M, Deutsch S, Kohler K, Perroud N, Le Gal F, Vessaz M, Laforge T, Petit B, Jollant F, Guillaume S, Baud P, Courtet P, La Harpe R, Malafosse A (2009) Genetic and epigenetic analysis of *SSAT* gene dysregulation in suicidal behavior. *Am J Med Genet B* 50B:799–807
174. Klempan TA, Rujescu D, Merette C, Himmelman C, Sequeira A, Canetti L, Fiori LM, Schneider B, Bureau A, Turecki G (2009) Profiling brain expression of the spermidine/spermine *N*¹-acetyltransferase 1 (*SAT1*) gene in suicide. *Am J Med Genet B Neuropsychiatr Genet* 150B:934–943
175. Chen GG, Fiori LM, Moquin L, Gratton A, Mamer O, Mechawar N, Turecki G (2010) Evidence of altered polyamine concentrations in cerebral cortex of suicide completers. *Neuropsychopharmacology* 35:1477–1484
176. Ingi T, Worley PF, Lanahan AA (2001) Regulation of *SSAT* expression by synaptic activity. *Eur J Neurosci* 13:1459–1463
177. Kaasinen SK, Grohn OH, Keinanen TA, Alhonen L, Janne J (2003) Overexpression of spermidine/spermine *N*¹-acetyltransferase elevates the threshold to pentylenetetrazol-induced seizure activity in transgenic mice. *Exp Neurol* 183:645–652
178. Kaasinen SK, Oksman M, Alhonen L, Tanila H, Janne J (2004) Spermidine/spermine *N*¹-acetyltransferase overexpression in mice induces hypoactivity and spatial learning impairment. *Pharmacol Biochem Behav* 78:35–45

179. Cason AL, Ikeguchi Y, Skinner C, Wood TC, Lubs HA, Martinez F, Simensen RJ, Stevenson RE, Pegg AE, Schwartz CE (2003) X-Linked spermine synthase gene (SMS) defect: the first polyamine deficiency syndrome. *Eur J Human Genet* 11:937–944
180. de Alencastro G, McCloskey DE, Kliemann SE, Maranduba CM, Pegg AE, Wang X, Bertola DR, Schwartz CE, Passos-Bueno MR, Sertie AL (2008) New SMS mutation leads to a striking reduction in spermine synthase protein function and a severe form of Snyder-Robinson X-linked recessive mental retardation syndrome. *J Med Genet* 45:539–543
181. Becerra-Solano LE, Butler J, Castañeda-Cisneros G, McCloskey DE, Wang X, Pegg AE, Schwartz CE, Sánchez-Corona J, Garcia-Ortiz JE (2009) A missense mutation, p.V132G, in the X-linked spermine synthase gene (SMS) causes Snyder-Robinson syndrome. *Am J Med Genet A* 149A:328–335
182. Lakanen JR, Coward JK, Pegg AE (1992) α -Methylpolyamines: metabolically stable spermidine and spermine mimics capable of supporting growth in cells depleted of polyamines. *J Med Chem* 35:724–734
183. Varnado BL, Voci CJ, Meyer LM, Coward JK (2000) Circular dichroism and NMR studies of metabolically stable α -methylpolyamines: special comparison with naturally occurring polyamines. *Bioorg Chem* 28:395–408
184. Pegg AE, Poulin R, Coward JK (1995) Use of aminopropyltransferase inhibitors and of non-metabolizable analogues to study polyamine regulation and function. *Int J Biochem* 27:425–442
185. Nagarajan S, Ganem B (1987) Chemistry of naturally occurring polyamines. II. Unsaturated spermidine and spermine derivatives. *J Org Chem* 52:5044–5046
186. Nagarajan S, Ganem B, Pegg AE (1988) Studies of non-metabolizable polyamines that support growth of SV-3T3 cells depleted of natural polyamines by exposure to α -difluoromethylornithine. *Biochem J* 254:373–378
187. Yang J, Xiao L, Berkey KA, Tamez PA, Coward JK, Casero RA Jr (1995) Significant induction of spermidine/spermine N1-acetyltransferase without cytotoxicity by the growth-supporting polyamine analogue 1, 12-dimethylspermine. *J Cell Physiol* 165:71–76
188. Byers TL, Lakanen JR, Coward JK, Pegg AE (1994) The role of hypusine depletion in cytoskeleton induced by S-adenosyl-L-methionine decarboxylase inhibition: new evidence provided by 1-methylspermidine and 1, 12-dimethylspermine. *Biochem J* 303:363–368
189. Byers TL, Wechter R, Hu R, Pegg AE (1994) Effects of the S-adenosylmethionine decarboxylase inhibitor, 5'-[[[(Z)-4-amino-2-butenyl] methylamino]-5'-deoxyadenosine, on cell growth and polyamine polyamine metabolism and transport in Chinese hamster ovary cell cultures. *Biochem J* 303:89–96
190. Byers TL, Ganem B, Pegg AE (1992) Cytostasis induced in L1210 murine leukemia cells by the S-adenosyl-L-methionine decarboxylase inhibitor 5'-[[[(Z)-4-amino-2-butenyl]methylamino]-5'-deoxyadenosine may be due to the hypusine depletion. *Biochem J* 287:717–724
191. Jarvinen A, Grigorenko N, Khomutov AR, Hyvonen MT, Uimari A, Vepsalainen J, Sinervirta R, Keinänen TA, Vujčić S, Alhonen L, Porter CW, Janne J (2005) Metabolic stability of α -methylated polyamine derivatives and their use as substitutes for the natural polyamines. *J Biol Chem* 280:6595–6601
192. Jarvinen AJ, Cerrada-Gimenez M, Grigorenko NA, Khomutov AR, Vepsalainen JJ, Sinervirta RM, Keinänen TA, Alhonen LI, Janne JE (2006) α -methyl polyamines: efficient synthesis and tolerance studies in vivo and in vitro. First evidence for dormant stereospecificity of polyamine oxidase. *J Med Chem* 49:399–406
193. Hyvonen MT, Herzig KH, Sinervirta R, Albrecht E, Nordback I, Sand J, Keinänen TA, Vepsalainen J, Grigorenko N, Khomutov AR, Kruger B, Janne J, Alhonen L (2006) Activated polyamine catabolism in acute pancreatitis: α -methylated polyamine analogues prevent trypsinogen activation and pancreatitis-associated mortality. *Am J Pathol* 168:115–122
194. Jarvinen A, Keinänen TA, Grigorenko NA, Khomutov AR, Uimari A, Vepsalainen J, Narvanen A, Alhonen L, Janne J (2006) Guide molecule-driven stereospecific degradation of α -methylpolyamines by polyamine oxidase. *J Biol Chem* 281:4589–4595
195. Jin HT, Lamsa T, Hyvonen MT, Sand J, Raty S, Grigorenko N, Khomutov AR, Herzig KH, Alhonen L, Nordback I (2008) A polyamine analog bismethylspermine ameliorates severe pancreatitis induced by intraductal infusion of taurodeoxycholate. *Surgery* 144:49–56
196. Weisell J, Hyvonen MT, Vepsalainen J, Alhonen L, Keinänen TA, Khomutov AR, Soinen P (2010) Novel isosteric charge-deficient spermine analogue-1, 12-diamino-3, 6, 9-triazadodecane: synthesis, pKa measurement

- and biological activity. *Amino Acids* 38:501–507
197. Nayvelt I, Hyvonen MT, Alhonen L, Pandya I, Thomas T, Khomutov AR, Vepsäläinen J, Patel R, Keinanen TA, Thomas TJ (2010) DNA condensation by chiral alpha-methylated polyamine analogues and protection of cellular DNA from oxidative damage. *Biomacromolecules* 11:97–105
 198. Fashe TM, Keinanen TA, Grigorenko NA, Khomutov AR, Janne J, Alhonen L, Pietila M (2010) Cutaneous application of alpha-methylspermidine activates the growth of resting hair follicles in mice. *Amino Acids* 38:583–590
 199. Vuohelainen S, Pirinen E, Cerrada-Gimenez M, Keinanen TA, Uimari A, Pietila M, Khomutov AR, Janne J, Alhonen L (2010) Spermidine is indispensable in differentiation of 3T3-L1 fibroblasts to adipocytes. *J Cell Mol Med* 14:1683–1692
 200. Räsänen T-L, Alhonen L, Sinervirta R, Keinänen T, Herzig K-H, Suppola S, Khomutov AR, Vepsäläinen J, Jänne J (2002) A polyamine analogue prevents acute pancreatitis and restores early liver regeneration in transgenic rats with activated polyamine catabolism. *J Biol Chem* 277:39867–39872
 201. Hyvonen MT, Sinervirta R, Grigorenko N, Khomutov AR, Vepsäläinen J, Keinanen TA, Alhonen L (2010) alpha-Methylspermidine protects against carbon tetrachloride-induced hepatic and pancreatic damage. *Amino Acids* 38:575–581
 202. Pegg AE, Nagarajan S, Naficy S, Ganem B (1991) Role of unsaturated derivatives of spermidine as substrates for spermine synthase and in supporting growth of SV-3T3 cells. *Biochem J* 274:167–171
 203. Holley J, Mather A, Cullis P, Symons MR, Wardman P, Watt RA, Cohen GM (1992) Uptake and cytotoxicity of novel nitroimidazole-polyamine conjugates in Ehrlich ascites tumour cells. *Biochem Pharmacol* 43:763–769
 204. Cullis PM, Green RE, Merson-Davies L, Travis N (1999) Probing the mechanism of transport and compartmentalisation of polyamines in mammalian cells. *Chem Biol* 6:717–729
 205. Wang C, Delcros JG, Biggerstaff J, Phanstiel O IV (2003) Molecular requirements for targeting the polyamine transport system. Synthesis and biological evaluation of polyamine-anthracene conjugates. *J Med Chem* 46:2672–2682
 206. Soulet D, Covassin L, Kaouass M, Charest-Gaudreault R, Audette M, Poulin R (2002) Role of endocytosis in the internalization of spermidine-C(2)-BODIPY, a highly fluorescent probe of polyamine transport. *Biochem J* 367:347–357
 207. Wang C, Delcros JG, Biggerstaff J, Phanstiel O IV (2003) Synthesis and biological evaluation of N1-(anthracen-9-ylmethyl)triamines as molecular recognition elements for the polyamine transporter. *J Med Chem* 46:2663–2671
 208. Gardner RA, Delcros JG, Konate F, Breitbeil F III, Martin B, Sigman M, Huang M, Phanstiel O IV (2004) N1-substituent effects in the selective delivery of polyamine conjugates into cells containing active polyamine transporters. *J Med Chem* 47:6055–6069
 209. Kaur N, Delcros JG, Imran J, Khaled A, Chehtane M, Tschammer N, Martin B, Phanstiel O IV (2008) A comparison of chloroambucil- and xylene-containing polyamines leads to improved ligands for accessing the polyamine transport system. *J Med Chem* 51:1393–1401
 210. Porter CW, McManis J, Casero RA Jr, Bergeron RJ (1987) Relative abilities of bis(ethyl) derivatives of putrescine spermidine and spermine to regulate polyamine biosynthesis and inhibit cell growth. *Cancer Res* 47:2821–2825
 211. Bergeron RJ, Neims AH, McManis JS, Hawthorne TR, Vinson JRT, Bortell R, Ingho MJ (1988) Synthetic polyamine analogues as antineoplastics. *J Med Chem* 31:1183–1190
 212. Bergeron RJ, McManis JS, Liu CZ, Feng Y, Weimar WR, Luchetta GR, Wu Q, Ortiz-Ocasio J, Vinson JRT, Kramer D, Porter C (1994) Antiproliferative properties of polyamine analogues: a structure-activity study. *J Med Chem* 37:3464–3476
 213. Casero RA Jr, Frydman B, Stewart TM, Woster PM (2005) Significance of targeting polyamine metabolism as an antineoplastic strategy: unique targets for polyamine analogues. *Proc West Pharmacol Soc* 48:24–30
 214. Casero RA Jr, Marton LJ (2007) Targeting polyamine metabolism and function in cancer and other hyperproliferative diseases. *Nat Rev Drug Discov* 6:373–390
 215. Casero RA Jr, Woster PM (2009) Recent advances in the development of polyamine analogues as antitumor agents. *J Med Chem* 52:4551–4573
 216. Senanayake MD, Amunugama H, Boncher TD, Casero RA, Woster PM (2009) Design of polyamine-based therapeutic agents: new targets and new directions. *Essays Biochem* 46:77–94

217. Basu HS, Feuerstein BG, Deen DF, Lubich WP, Bergeron RJ, Samejima K, Marton LJ (1989) Correlation between the effects of polyamine analogues on DNA conformation and cell growth. *Cancer Res* 49:5591–5597
218. Chang BK, Bergeron RJ, Porter CW, Vinson JRT, Liang V (1992) Regulatory and anti-proliferative effects of N-alkylated polyamine analogues in human and hamster pancreatic adenocarcinoma cell lines. *Cancer Chemother Pharmacol* 30:183–188
219. Saab NH, West EE, Bieszk NC, Preuss CV, Mank AR, Casero RA Jr, Woster PM (1993) Synthesis and evaluation of unsymmetrically substituted polyamine analogues as modulators of human spermidine/spermine-*N*¹-acetyltransferase (SSAT) and as potential antitumor agents. *J Med Chem* 36:2998–3004
220. Reddy VK, Valasinas A, Sarkar A, Basu HS, Marton LJ, Frydman B (1998) Conformationally restricted analogues of IN, 12N-bisethylspermine: synthesis and growth inhibitory effects on human tumor cell lines. *J Med Chem* 41:4723–4732
221. Casero RA Jr, Woster PM (2001) Terminally alkylated polyamine analogues as chemotherapeutic agents. *J Med Chem* 44:1–26
222. Valasinas A, Reddy VK, Blokhin AV, Basu HS, Bhattacharya S, Sarkar A, Marton LJ, Frydman B (2003) Long-chain polyamines (oligoamines) exhibit strong cytotoxicities against human prostate cancer cells. *Bioorg Med Chem* 11:4121–4131
223. Frydman B, Blokhin AV, Brummel S, Wilding G, Maxuitenko Y, Sarkar A, Bhattacharya S, Church D, Reddy VK, Kink JA, Marton LJ, Valasinas A, Basu HS (2003) Cyclopropane-containing polyamine analogues are efficient growth inhibitors of a human prostate tumor xenograft in nude mice. *J Med Chem* 46:4586–4600
224. Carew JS, Nawrocki ST, Reddy VK, Bush D, Rehg JE, Goodwin A, Houghton JA, Casero RA Jr, Marton LJ, Cleveland JL (2008) The novel polyamine analogue CGC-11093 enhances the antimyeloma activity of bortezomib. *Cancer Res* 68:4783–4790
225. Frydman B, Porter CW, Maxuitenko Y, Sarkar A, Bhattacharya S, Valasinas A, Reddy VK, Kisiel N, Marton LJ, Basu HS (2003) A novel polyamine analog (SL-11093) inhibits growth of human prostate tumor xenografts in nude mice. *Cancer Chemother Pharmacol* 51:488–492
226. Casero RA Jr, Celano P, Ervin SJ, Porter CW, Bergeron RJ, Libby P (1989) Differential induction of spermidine/spermine *N*¹-acetyltransferase in human lung cancer cells by the bis(ethyl)polyamine analogues. *Cancer Res* 49:3829–3833
227. McCloskey DE, Pegg AE (2003) Properties of the spermidine/spermine *N*¹-acetyltransferase mutant L156F that decreases cellular sensitivity to the polyamine analogue *N*¹, *N*¹¹-bis(ethyl)norspermine. *J Biol Chem* 278:13881–13887
228. McCloskey DE, Pegg AE (2000) Altered spermidine/spermine *N*¹-acetyltransferase activity as a mechanism of cellular resistance to bis(ethyl)polyamine analogues. *J Biol Chem* 275:28708–28714
229. Pledgie A, Huang Y, Hacker A, Zhang Z, Woster PM, Davidson NE, Casero RA Jr (2005) Spermine oxidase SMO(PAOh1), not *N*¹-acetyl polyamine oxidase PAO, is the primary source of cytotoxic H₂O₂ in polyamine analogue-treated human breast cancer cell lines. *J Biol Chem* 280:39843–39851
230. Jiang R, Choi W, Hu L, Gerner EW, Hamilton SR, Zhang W (2007) Activation of polyamine catabolism by *N*¹, *N*¹¹-diethylnorspermine alters the cellular localization of mTOR and downregulates mTOR protein level in glioblastoma cells. *Cancer Biol Ther* 6:1644–1648
231. Beckers A, Organe S, Timmermans L, Scheys K, Peeters A, Brusselmans K, Verhoeven G, Swinnen JV (2007) Chemical inhibition of acetyl-CoA carboxylase induces growth arrest and cytotoxicity selectively in cancer cells. *Cancer Res* 67:8180–8187
232. Celik A, Kano Y, Tsujinaka S, Okada S, Takao K, Takagi M, Chohnan S, Soda K, Kawakami M, Konishi F (2009) Decrease in malonyl-CoA and its background metabolic alterations in murine model of cancer cachexia. *Oncol Rep* 21:1105–1111
233. Boncher T, Bi X, Varghese S, Casero RA Jr, Woster PM (2007) Polyamine-based analogues as biochemical probes and potential therapeutics. *Biochem Soc Trans* 35:356–363
234. Huang Y, Pledgie A, Casero RA Jr, Davidson NE (2005) Molecular mechanisms of polyamine analogs in cancer cells. *Anticancer Drugs* 16:229–241
235. Wallace HM, Niiranen K (2007) Polyamine analogues – an update. *Amino Acids* 33:261–265
236. Hacker A, Marton LJ, Sobolewski M, Casero RA Jr (2008) In vitro and in vivo effects of the conformationally restricted polyamine analogue CGC-11047 on small cell and non-small cell lung cancer cells. *Cancer Chemother Pharmacol* 63:45–53

237. Hakkinen MR, Hyvonen MT, Auriola S, Casero RA Jr, Vepsalainen J, Khomutov AR, Alhonen L, Keinanen TA (2010) Metabolism of N-alkylated spermine analogues by polyamine and spermine oxidases. *Amino Acids* 38:369–381
238. Huang Y, Greene E, Murray Stewart T, Goodwin AC, Baylin SB, Woster PM, Casero RA Jr (2007) Inhibition of lysine-specific demethylase 1 by polyamine analogues results in reexpression of aberrantly silenced genes. *Proc Natl Acad Sci USA* 104:8023–8028
239. Bitonti AJ, Dumont JA, Bush TL, Edwards ML, Stemerick DM, McCann PP, Sjoerdsma A (1989) Bis(benzyl)polyamine analogs inhibit the growth of chloroquine-resistant human malaria parasites (*Plasmodium falciparum*) in vitro and in combination with α -difluoromethylornithine cure murine malaria. *Proc Natl Acad Sci USA* 86:651–655
240. Edwards ML, Stemerick DM, Bitonti AJ, Dumont JA, McCann PP, Bey P, Sjoerdsma A (1991) Antimalarial polyamine analogues. *J Med Chem* 34:569–574
241. Zou Y, Sirisoma N, Woster PM, Casero RA Jr, Weiss LM, Rattendi D, Lane S, Bacchi CJ (2001) Novel alkylpolyamine analogues that possess both antitrypanosomal and antimicrosporidial activity. *Bioorg Med Chem Lett* 11:1613–1617
242. Woster PM (2001) New therapies for parasitic Infection. *Annu Rep Med Chem* 36:99–108
243. Huang Y, Marton LJ, Woster PM, Casero RA (2009) Polyamine analogues targeting epigenetic gene regulation. *Essays Biochem* 46:95–110
244. Seiler N, Sarhan S, Knödgen B, Gerhart F (1988) Chain-fluorinated polyamines as tumor markers. II. Metabolic aspects in normal tissues. *J Cancer Res Clin Oncol* 114:71–80
245. Hull WE, Kunz W, Port RE, Seiler N (1988) Chain-fluorinated polyamines as tumor markers-III. Determination of geminal difluoropolyamines and their precursor 2, 2-difluoroputrescine in normal tissues and experimental tumors by in vitro and in vivo ^{19}F NMR spectroscopy. *NMR Biomed* 1:11–19
246. Dezeure F, Sarhan S, Seiler N (1988) Chain-fluorinated polyamines as tumor markers. IV. Comparison of 2-fluoroputrescine and 2, 2-difluoroputrescine as substrates of spermidine synthase in vitro and in vivo. *Int J Biochem* 20:1299–1312
247. Sarhan S, Knödgen B, Gerhart F, Seiler N (1987) Chain-fluorinated polyamines as tumor markers-I. In vivo transformation of 2, 2-difluoroputrescine into 6, 6-difluorospermidine and 6, 6-difluorospermine. *Int J Biochem* 19:843–852
248. Hammond JE, Herbst EJ (1968) Analysis of polyamines by thin-layer chromatography. *Anal Biochem* 22:474–484
249. Seiler N, Wiechmann M (1965) Determination of amines on the 10⁻¹⁰-mole scale. Separation of 1-dimethylamino-naphthalene-5-sulfonyl amides by thin-layer chromatography. *Experientia* 21:203–204
250. Fleisher JH, Russell DH (1975) Estimation of urinary diamines and polyamines by thin-layer chromatography. *J Chromatogr* 110:335–340
251. Marton LJ, Russell DH, Levy CC (1973) Measurement of putrescine, spermidine, and spermine in physiological fluids by use of an amino acid analyzer. *Clin Chem* 19:923–926
252. Seiler N, Knödgen B (1985) Determination of polyamines and related compounds by reversed-phase high-performance liquid chromatography: improved separation systems. *J Chromatogr* 339:45–57
253. Kabra PM, Lee HK, Lubich WP, Marton LW (1986) Solid-phase extraction and determination of dansyl derivatives of unconjugated and acetylated polyamines by reversed-phase liquid chromatography; improved separation systems for polyamines in cerebrospinal fluid, urine and tissue. *J Chromatogr Biomed Appl* 380:19–32
254. Morgan DM (1998) Determination of polyamines as their benzoylated derivatives by HPLC. *Methods Mol Biol* 79:111–118
255. Häkkinen MR, Keinanen TA, Vepsalainen J, Khomutov AR, Alhonen L, Janne J, Auriola S (2007) Analysis of underivatized polyamines by reversed phase liquid chromatography with electrospray tandem mass spectrometry. *J Pharm Biomed Anal* 45:625–634
256. Häkkinen MR, Keinanen TA, Vepsalainen J, Khomutov AR, Alhonen L, Janne J, Auriola S (2008) Quantitative determination of underivatized polyamines by using isotope dilution RP-LC-ESI-MS/MS. *J Pharm Biomed Anal* 48:414–421
257. Chen GG, Turecki G, Mamer OA (2009) A quantitative GC-MS method for three major polyamines in postmortem brain cortex. *J Mass Spectrom* 44:1203–1210

Part II

Identification of Polyamine Metabolic Enzymes and Characterization of Polyamine-Regulated Genes and Ion Channels

Chapter 2

Exploring Polyamine Biosynthetic Diversity Through Comparative and Functional Genomics

Anthony J. Michael

Abstract

The existence of multiple, alternative pathways for polyamine biosynthesis, and the presence of alternative polyamine structural analogs, is an indication of the physiological importance of polyamines and their long evolutionary history. Polyamine biosynthesis is modular: diamines are synthesized directly or indirectly from amino acids, and triamines are synthesized from diamines by transfer of aminopropyl, carboxyaminopropyl, or aminobutyl groups to the diamine. Diversification of polyamine biosynthesis has depended on gene duplication and functional divergence, on gene fusion, and on horizontal gene transfer. Four examples of polyamine biosynthetic diversification are presented here with a discussion of methodological and conceptual approaches for identification of new pathways.

Key words: Polyamine, Evolution, Biosynthetic diversity, Metabolic pathway, Operon, Comparative genomics, Functional genomics

1. Introduction

Most studies of polyamine metabolism have been motivated by biomedical considerations focused on preventing growth of cancer cells through disruption of polyamine homeostasis (1). Although the cancer intervention strategy has turned out to be a far more frustrating endeavor than initially conceived, polyamine metabolism appears to be a promising target for intervention in parasite diseases, especially in kinetoplastidia such as trypanosomes and leishmania (2). Study of the regulation of polyamine metabolism in mammalian cells and in the budding yeast *Saccharomyces cerevisiae* has revealed an extraordinarily complex hierarchy of polyamine-responsive feedback systems based on posttranscriptional mechanisms (3). There is a wide evolutionary conservation of the

polyamine-responsive feedback systems, exemplified by the ornithine decarboxylase antizyme programmed frameshifting mechanism that is found in both fungi and animal cells. The antizyme system does not appear to be present in plants, or green and red algae, but plants and animals do share a polyamine-responsive feedback mechanism convergently centered on the translational regulation of *S*-adenosylmethionine decarboxylase (AdoMetDC; EC 4.1.1.50) mRNA by a ribosome-stalling peptide.

Polyamine biosynthesis in animal cells and yeasts is very similar. The committing step in polyamine biosynthesis in both systems is decarboxylation of ornithine by ornithine decarboxylase (ODC; EC 4.1.1.17) to produce putrescine (1,4-diaminobutane). Spermidine is synthesized from putrescine by the transfer of an aminopropyl group donated from decarboxylated *S*-adenosylmethionine, accomplished by the aminopropyltransferase spermidine synthase (SpdSyn; EC 2.5.1.16). In most animal cells, spermine can be formed from spermidine by transfer of an aminopropyl group to the aminobutyl end of spermidine, carried out by spermine synthase (EC 2.5.1.22). Some animal cells such as nematode worms have lost spermine synthase (4). Most fungi except the closely related true yeasts (Saccharomycotina), such as *S. cerevisiae* and *Candida albicans*, do not possess a spermine synthase gene (4) and, in the Basidiomycota, spermidine synthase is fused to the lysine biosynthetic enzyme saccharopine dehydrogenase. In plants, and green and red algae, spermine synthase is found only in the flowering plants (angiosperms). Spermine synthase has evolved independently on at least three occasions, in the ancestor of animal and choanoflagellates, in the ancestor of flowering plants, and in the ancestor of Saccharomycotina yeasts. Thus, the spermine synthase of plants has evolved within the last 200 million years, whereas the animal spermine synthase predates the origin of the metazoa and may have arisen in the pre-Cambrian (4). In contrast, plants and algae can synthesize a spermine structural analog, thermospermine, which is synthesized from spermidine by transfer of an aminopropyl group to the N¹-aminopropyl end of spermidine. The aminopropyltransferase responsible for the synthesis of thermospermine (EC 2.5.1.B4), thermospermine synthase, is evolutionarily much more ancient than the plant spermine synthase.

Plant polyamine metabolism differs from that in animals and fungi, not just because of thermospermine biosynthesis but because plants can also synthesize putrescine from arginine via a pathway consisting of arginine decarboxylase (ADC; EC 4.1.1.19), agmatineiminohydrolase (EC 3.5.3.12), and *N*-carbamoylputrescine amidohydrolase (EC 3.5.1.53) (5). Both thermospermine synthase and the ADC pathway were likely derived from the cyanobacterial ancestor of the chloroplast, and through endosymbiotic gene transfer, the two pathways were transferred from the chloroplast ancestral genome to the host nuclear genome. Subsequently,

ADC was retargetted back to the chloroplast. Plants also possess a wide variety of enzymes that *N*-acylate polyamines for the synthesis of alkaloids and hydroxycinnamic amides, e.g., putrescine *N*-methyltransferase and spermidine disinapoyltransferase.

The polyamine biosynthetic strategies used by animals, fungi, and plants may seem quite different, but phylogenetically, animals and fungi are sister groups within the same eukaryotic supergroup known as the Opisthokonta. Plants and red and green algae, along with glaucocystophyte algae, are in another supergroup, the Archaeplastidia. There are four other eukaryotic supergroups: the Amoebozoa, including true amoebae and slime molds, which are the group closest to the Opisthokonta; the Chromalveolata, which includes the Apicomplexan parasites such as *Plasmodium* and *Toxoplasma*; the Excavata, containing other well-known parasites such as the kinetoplastid trypanosomes and the diplomonad *Giardia* and the parabasalid *Trichomonas*; and finally the Rhizaria supergroup including foraminiferans and radiolarians (6). Polyamine metabolism is poorly sampled and characterized in the Amoebozoa, Chromalveolata, Rhizaria, and Excavata because these supergroups are relatively poorly understood at a biological level and sparsely sampled at a genomic level. It can be seen therefore that there probably remains significant uncharted polyamine biosynthetic diversity within eukaryotes. Many bacteriovorous single-celled eukaryotes have acquired genes from bacteria by horizontal gene transfer and so part of the uncharted polyamine biosynthetic diversity may be based on bacterial-derived acquisitions.

Although there is considerable polyamine biosynthetic diversity within the eukaryotes, there is far greater diversity among the prokaryotes, which consist of the other two domains of life, the bacteria and archaea (7, 8). There are now over a thousand published prokaryotic genomes, with several thousand other genomes in preparation. As a generalization, it is thought that eukaryotes share more in common with bacterial operational genes, i.e., metabolism, and with archaeal informational genes, i.e., translation and transcription. Much of the analysis of bacterial polyamine metabolism has been performed with the γ -proteobacterium *Escherichia coli* (9). Like eukaryotes, *E. coli* synthesizes putrescine and employs AdoMetDC and SpdSyn to make spermidine from putrescine. However, *E. coli* synthesizes putrescine from both ornithine and arginine. The *E. coli* biosynthetic ODC is an entirely different fold of enzyme to the eukaryotic ODC and is similar to the *Lactobacillus* ODC (10). Eukaryotic and *E. coli* ODC are an example of convergent biosynthetic evolution. The biosynthetic ADC of *E. coli* is similar to the plant ADC (11) and is related to the eukaryotic ODC. However, *E. coli* also contains a biodegradative ADC, a large decameric complex activated by acid stress (12), is and involved in acid resistance. It also possesses a biodegradative ODC, very similar to the biosynthetic ODC, and is

involved in acid stress resistance (13). Adding complexity to this picture is the fact that in *E. coli*, a structural analog of spermidine, aminopropylcadaverine, can be synthesized when putrescine is limiting (14). Cadaverine can be synthesized by an acid-inducible lysine decarboxylase and a constitutively expressed paralog (15). The AdoMetDC/SpdSyn pathway for spermidine biosynthesis is found in many bacteria and archaea. However, there are many bacteria that contain spermidine but do not contain AdoMetDC/SpdSyn orthologs, and there are many bacteria that contain *sym*-homospermidine rather than spermidine (16). Some bacteria also contain *sym*-norspermidine. The exploration of polyamine biosynthetic diversity through comparative and functional genomics has been made easier because of prior published detailed biochemical analyses of what was at the time regarded as unusual or unique polyamine biosynthetic enzymes and pathways. With the benefit of complete genome sequences, the development of molecular biological approaches in diverse organisms, and the availability of commercial gene synthesis, comparative genomic approaches for exploring polyamine biosynthetic diversity can now be biochemically validated through functional genomics and recombinant enzymology.

2. Methods and Notes: Four Vignettes

To illustrate the methods and conceptual approaches used for exploring alternative polyamine biosynthetic pathways, four biosynthetic vignettes are presented below. The first is the characterization of the alanine racemase-fold family of amino acid decarboxylases that consists of arginine, ornithine, carboxynorspermidine, and diaminopimelate decarboxylases (17). Secondly, a consideration of the aminopropyltransferase family, which includes spermidine, norspermidine, spermine, thermospermine, norspermine, and aminopropylagmatine synthases, is shown. Thirdly, an alternative pathway for norspermidine and spermidine biosynthesis based on carboxypolyamine intermediates is discussed, and lastly, the identification of spermidine *N*-acyltransferases in plants is described.

2.1. The Alanine Racemase-Fold Family of Amino Acid Decarboxylases

1. One of the driving forces in evolution is the expansion of gene families through gene duplication and subsequent divergence. Horizontal gene transfer allows the dissemination of individual members of gene families. The alanine racemase-fold family of enzymes, which includes the biosynthetic ADC, ODC (EC 4.1.1.17), carboxynorspermidine decarboxylase (CANSDC; EC 4.1.1.), and the lysine biosynthetic enzyme diaminopimelate decarboxylase (DAPDC; EC 4.1.1.20), is a typical example of the evolution of enzyme catalytic diversity through gene duplication. Each member of the family uses pyridoxal

5' phosphate as a cofactor and binds similar substrates. Key residues in the active site of each enzyme are conserved and the enzymes are of roughly the same size except for arginine decarboxylase, which is approximately 50% bigger than the others. The AR-fold ODC was thought to be a eukaryotic-specific ODC. Another class of ODC belonging to the aspartate aminotransferase fold had been described in *Lactobacillus sp.* and *E. coli*. However, a eukaryotic-type ODC was identified and characterized in the firmicute bacterium *Selenomonas ruminantium* (ODC) and was found to be active as both an ODC and lysine decarboxylase (LDC) (18).

2. To explore the prevalence of the AR-fold ODC in bacteria, a phylogenetic analysis was performed on this family of enzymes (17). The main tool for the phylogenetic analysis was BLASTP (19). Several validated ODC proteins were used to screen the protein database, including mammalian, plant, fungal, trypanosome, and *S. ruminantium* enzymes. In addition, the functionally validated ADC proteins of Arabidopsis and *E. coli*, multiple, characterized DAPDC proteins, and the *Vibrio alginolyticus* CANSDC were also used to screen the protein database by BLASTP. A quick phylogenetic tree of the related sequences can be obtained using the fast minimum evolution tree of the BLASTP results (Fig. 1). A subset of proteins exhibiting similarity to the probe sequences was collected and all sequences were aligned using the alignment program CLUSTALW (20) in the CLUSTALX package. After automated alignment, the N- and C-termini of the amino acid sequences were trimmed to optimize the alignment and then, after another automated round of sequence alignment, some manual adjustment was performed to optimize the alignment. The alignment was then used to build a Neighbor Joining tree using the program PAUP* (21). However, this approach has been superseded by the phylogenetic package MEGA Version 4.0 (22), which is free and can be downloaded from <http://www.megasoftware.net>. For an excellent explanation of the use of MEGA and of phylogenetic methods for nonspecialists, an inexpensive, how-to manual, "Phylogenetic Trees Made Easy," third edition, is available and I highly recommend this concise and readable paperback book (23). The phylogenetic tree figure configuration was modified using the program TREEVIEW (24) and the cladogram image imported into a graphics program for further annotation. Confidence levels for clades, i.e., the bootstrap supports, were calculated separately using PAUP* and the bootstrap values were added manually to the phylogenetic tree using the graphics program.
3. Based on the prominent clades of enzymes in the NJ tree, and cross-validation with known substrate preferences of some of the proteins in the tree, a number of bacterial putative ODCs

Results of PBLAST search

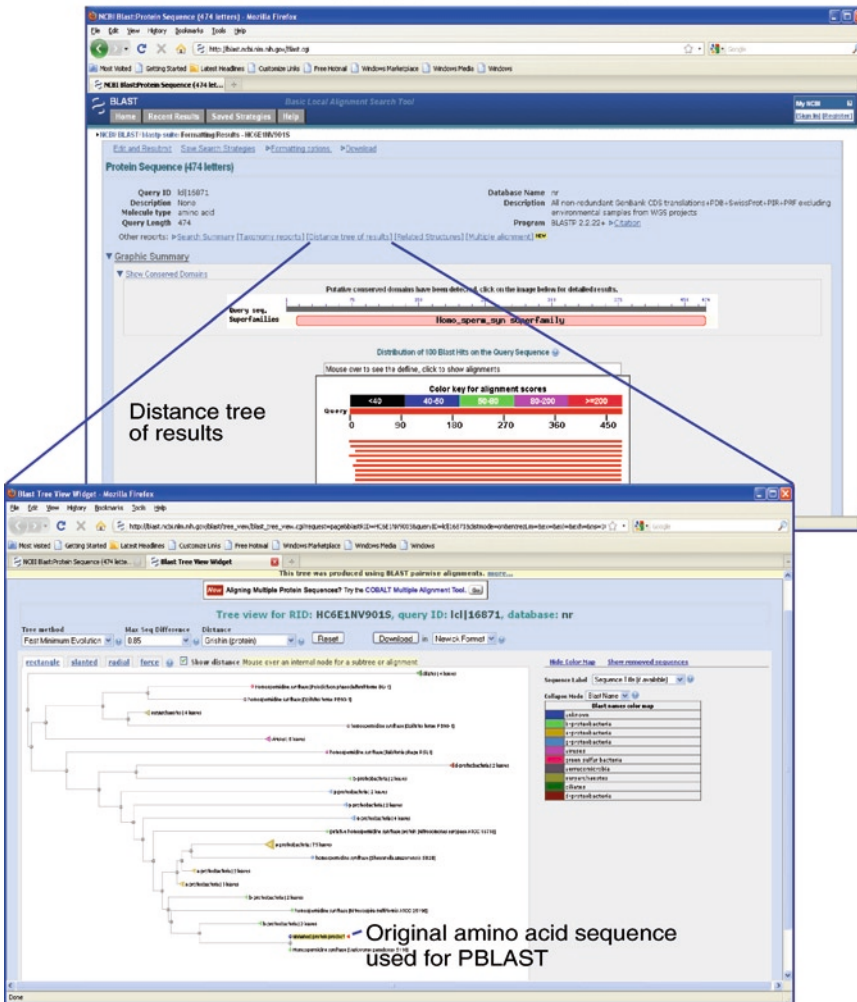


Fig. 1. Fast Minimal Evolution tree from a BLASTP search. A quick phylogenetic tree analysis can be obtained from a BLASTP search by clicking on the “distance tree of results” button at the top of the BLASTP results page. The fast minimum evolution tree individual clades and species can be clicked on to reveal subclades and species, and sequence alignments of the subtrees.

were chosen for biochemical characterization. Within the putative ODC clade, there were three subclades: one clade was comprised of the eukaryotic ODCs containing enzymes with confirmed biochemical function, another small subclade contained the bifunctional *S. ruminatum* ODC/LDC, and a third subclade contained bacterial enzymes of unknown function. Genomic DNA samples of bacterial and eukaryotic species were obtained and putative ODC and ODC/LDC genes were cloned and expressed in *E. coli* (from the eukaryotic protist parasite *Giardia lamblia*, the euryarchaeote *Methanosarcina*

mazei, and the bacterial species *Aquifex aeolicus*, *Thermotoga maritima*, *Nitrosomonas europea*, *Bartonella henselae*, *Pseudomonas aeruginosa*, and *Vibrio vulnificus*). Each enzyme was biochemically determined to be a specific ODC except for the *V. vulnificus* enzyme, which was a bifunctional ODC/LDC. A crystal structure was determined for the bifunctional *V. vulnificus* ODC/LDC protein and the mechanistic basis of the bifunctional nature of the enzyme was shown to be dependent on the presence or absence of a well-ordered water molecule in the active site. The ADC and DAPDC clades were further validated by cloning and expression in *E. coli* of the *V. vulnificus* orthologs from those clades. An additional validation of the CANSDC clade was provided later, by the characterization of the *Vibrio cholerae* ortholog (25).

2.2. Aminopropyltransferases

1. Aminopropyltransferases are typified by spermidine and spermine synthases. However, there are also recently characterized thermospermine synthases, norspermidine and norspermine synthases, as well as agmatine aminopropyl transferases and long-chain polyamine synthases. The recently solved crystal structure of the human spermine synthase revealed that there is an N-terminal domain that has structural homology to the bacterial S-adenosylmethionine decarboxylase; no corresponding catalytic activity but the domain is required for dimerization of spermine synthase and so is essential for spermine synthase activity (26). The rest of the human spermine synthase structure is very similar to spermidine synthase.
2. To investigate the evolution of aminopropyltransferases, the spermidine synthase-like domains of various functionally validated aminopropyltransferase amino acid sequences were used to screen the protein database and expressed sequence tag databases. A file of diverse aminopropyltransferase sequences was aligned as described in Figure 1. The NJ tree produced based on the alignment revealed a number of important evolutionary developments of the aminopropyltransferase gene family. A key finding was that spermine synthase has evolved at least three times independently in eukaryotes, in the ancestor of metazoa and choanoflagellates, in the true yeasts (Saccharomycotina) but not in the rest of the fungi, and in flowering plants but not the rest of land plants and algae. In contrast, thermospermine synthase is present in all plants and algae and is also found in the Chromalveolata supergroup, most likely due to endosymbiotic gene transfer from the cyanobacterial ancestor of the chloroplast to the host cell that took up the chloroplast ancestor to form a red alga, and then from a red algal nucleus to the heterotrophic eukaryotic host nucleus that was the ancestral

host cell of the Chromalveolata (27). Thus, thermospermine synthase is found in nonplant, photosynthetic eukaryotes, such as diatoms and coccolithophores, and in cells that have lost the ability to photosynthesize, such as *Perkinsus* and *Phytophthora*.

2.3. The Carboxy(nor) Spermidine Pathway for Norspermidine and Spermidine Biosynthesis

1. Biosynthesis of norspermidine in *Vibrio alginolyticus* is dependent on the synthesis of diaminopropane from glutamate and aspartate β -semialdehyde, via a diaminobutyric acid intermediate (25). The diaminopropane is converted to norspermidine via the intermediate carboxynorspermidine. Although a diaminobutyrate decarboxylase activity had been reported in *V. alginolyticus*, the gene encoding the activity had not been identified. However, diaminobutyrate aminotransferase (DABA AT), which produces diaminobutyrate from glutamate and aspartate β -semialdehyde, and diaminobutyrate decarboxylase (DABA DC), which produces diaminopropane from diaminobutyrate, had been characterized and cloned from another γ -proteobacterium *Acinetobacter baumannii*. In the genome of *V. alginolyticus*, the DABA AT and DABA DC orthologs are present as a gene fusion (25). Conversion of carboxynorspermidine to norspermidine is achieved by another PLP-dependent enzyme, carboxynorspermidine decarboxylase (CANSDC), which had been identified originally in *V. alginolyticus*. The missing, unidentified gene in the norspermidine biosynthetic pathway was carboxynorspermidine synthase, which transfers an aspartate β -semialdehyde-derived carboxyaminopropyl group to diaminopropane to form the carboxynorspermidine intermediate. However, in *Vibrio* species, the DABA AT/DC fusion protein ORF is clustered together with the CANSDC ORF, with an ORF of unknown function juxtaposed between them. The genomic configuration of these three ORFs suggested that the ORF of unknown function might encode the missing carboxynorspermidine synthase enzyme. Using a combination of heterologous expression of the *V. cholerae* genomic cluster in *E. coli* and gene deletions strains of the corresponding genes of *V. cholerae*, it was functionally demonstrated that the ORF of unknown function was in fact the carboxyspermidine synthase, which was subsequently renamed carboxyspermidine dehydrogenase (CANSDH). This is an example of the “guilt by association” approach to identifying genes of unknown function.
2. Gene clusters around genes of interest can be visualized in genome sequences by using the gene ID/genome map facility provided with the BLASTP results output (Fig. 2). Outside of the Vibrionaceae, no other bacterial species have the entire

Pairwise sequence alignment from PBLAST

The figure illustrates the workflow for visualizing gene clusters from a BLAST search. It consists of three overlapping browser windows:

- Top Window:** Displays pairwise sequence alignment results from a PBLAST search. A blue arrow points from a specific alignment to the "Gene ID" label.
- Middle Window:** Shows the "Genome Map" for the gene cluster, with a blue arrow pointing from the "Genome Map" label to the map.
- Bottom Window:** Shows the "Gene clusters" map, with a blue arrow pointing from the "Gene clusters" label to the cluster visualization.

Fig. 2. Gene cluster maps from a BLASTP search. The genomic organization of local gene clusters can be graphically visualized by clicking on “Gene ID” hyperlink associated with each pairwise sequence alignment from the results of a BLASTP search. From the new page, clicking on “Genome Map” will provide the gene cluster graphical map.

norspermidine biosynthetic pathway clustered as an operon. The *V. cholerae* CANSDH/CANSDC pathway was also able to use putrescine, as well as diamino propane, to synthesize spermidine. It is important to note that most of the bacterial species that possess orthologs of CANSDH and CANSDC do not possess orthologs of DABA AT and DABA DC, strongly suggesting that the CANSDH/CANSDC pathway is used primarily to synthesize spermidine rather than *sym*-norspermidine.

2.4. Spermidine Hydroxycinnamoyl Transferases

1. Flowering plants often conjugate polyamines with hydroxycinnamic acids, secondary metabolites derived from phenylalanine. The tyramine *N*-hydroxycinnamoyl transferase has been identified in potato and tobacco and is a small acyltransferase belonging to the huge GNAT superfamily of acyltransferases. However, polyamine *N*-acyltransferases have been biochemically characterized from diverse plant species and the subunit size has been found to be about 55 kDa, roughly twice the size of the tyramine *N*-hydroxycinnamoyl transferase. This larger size corresponds to the monomer of another class of acyl transferases in plants, the BAHD family of transferases, which includes an agmatine *N*-hydroxycinnamoyl transferase. There are over 60 members of the BAHD family of genes in the model plant *Arabidopsis*. The main class of polyamine hydroxycinnamoyl conjugates in *Arabidopsis* are spermidine forms and particularly 5-hydroxyferuloyl and sinapoyl spermidine compounds.
2. To identify the genes encoding the enzymes responsible for spermidine hydroxycinnamoyl conjugate formation, a combination of bioinformatic analysis, recombinant enzyme characterization, and functional genomics was used (28). The main localization of the hydrophobic N^1, N^8 -disinapoyl spermidine conjugates was in seeds. Expression patterns of all BAHD family members were analyzed using the GENEVESTIGATOR microarray result database (29) and a gene expressed strongly in seeds was identified. The coding sequence of the gene (At2g23510) was cloned by PCR and expressed in *E. coli*. CoA-activated hydroxycinnamic substrates were synthesized and coumaroyl-CoA, caffeoyl-CoA, feruloyl-CoA, and sinapoyl-CoA were tested with putrescine, spermidine, *sym*-homospermidine, *sym*-norspermidine, and spermine as acyl acceptors. The enzyme encoded by At2g23510 was found to be specific for the acylation of spermidine by sinapoyl-CoA to form N^1, N^{10} -disinapoyl spermidine. Plants containing a homozygous transposon insertion mutant of the gene were found to completely lack disinapoyl spermidine. Other authors using a similar approach found another BAHD acyltransferase that was responsible for the formation of N^1, N^5, N^{10} -*tris*(feruloyl)spermidine in *Arabidopsis* anthers (30).

References

1. Wallace HM, Fraser AV, Hughes A (2003) A perspective of polyamine metabolism. *Biochem J* 376:1–14
2. Bacchi CJ, Yarlott N (2002) Polyamine metabolism as chemotherapeutic target in protozoan parasites. *Mini Rev Med Chem* 2:553–563
3. Ivanov IP, Atkins JF, Michael AJ (2010) A profusion of upstream open reading frame mechanisms in polyamine-responsive translational regulation. *Nucleic Acids Res* 38:353–359
4. Pegg AE, Michael AJ (2010) Spermine synthesis. *Cell Mol Life Sci* 67:113–121

5. Illingworth C, Mayer MJ, Elliott K, Hanfrey C, Walton NJ, Michael AJ (2003) The diverse bacterial origins of the Arabidopsis polyamine biosynthetic pathway. *FEBS Lett* 549:26–30
6. Adl SM, Simpson AG, Farmer MA, Andersen RA, Anderson OR, Barta JR, Bowser SS, Brugerolle G, Fensome RA, Fredericq S, James TY, Karpov S, Kugrens P, Krug J, Lane CE, Lewis LA, Lodge J, Lynn DH, Mann DG, McCourt RM, Mendoza L, Moestrup O, Mozley-Standridge SE, Nerad TA, Shearer CA, Smirnov AV, Spiegel FW, Taylor MF (2005) The new higher level classification of eukaryotes with emphasis on the taxonomy of protists. *J Eukaryot Microbiol* 52:399–451
7. Koonin EV, Wolf YI (2008) Genomics of bacteria and archaea: the emerging dynamic view of the prokaryotic world. *Nucleic Acids Res* 36:6688–6719
8. Fraser C, Alm EJ, Polz MF, Spratt BG, Hanage WP (2009) The bacterial species challenge: making sense of genetic and ecological diversity. *Science* 323:741–746
9. Chattopadhyay MK, Tabor CW, Tabor H (2009) Polyamines are not required for aerobic growth of *Escherichia coli*: preparation of a strain with deletions in all of the genes for polyamine biosynthesis. *J Bacteriol* 191:5549–5552
10. Momany C, Ernst S, Ghosh R, Chang NL, Hackert ML (1995) Crystallographic structure of a PLP-dependent ornithine decarboxylase from *Lactobacillus* 30a to 3.0 Å resolution. *J Mol Biol* 252:643–655
11. Bell E, Malmberg RL (1990) Analysis of a cDNA encoding arginine decarboxylase from oat reveals similarity to the *Escherichia coli* arginine decarboxylase and evidence of protein processing. *Mol Gen Genet* 224:431–436
12. Andrell J, Hicks MG, Palmer T, Carpenter EP, Iwata S, Maher MJ (2009) Crystal structure of the acid-induced arginine decarboxylase from *Escherichia coli*: reversible decamer assembly controls enzyme activity. *Biochemistry* 48:3915–3927
13. Kashiwagi K, Watanabe R, Igarashi K (1994) Involvement of ribonuclease III in the enhancement of expression of the speF-potE operon encoding inducible ornithine decarboxylase and polyamine transport protein. *Biochem Biophys Res Commun* 200:591–597
14. Igarashi K, Kashiwagi K, Hamasaki H, Miura A, Kakegawa T, Hirose S, Matsuzaki S (1986) Formation of a compensatory polyamine by *Escherichia coli* polyamine-requiring mutants during growth in the absence of polyamines. *J Bacteriol* 166:128–134
15. Nagano T, Kikuchi Y, Kamio Y (2000) High expression of the second lysine decarboxylase gene, ldc, in *Escherichia coli* WC196 due to the recognition of the stop codon (TAG), at a position which corresponds to the 33th amino acid residue of sigma38, as a serine residue by the amber suppressor, supD. *Biosci Biotechnol Biochem* 64:2012–2017
16. Hamana K, Matsuzaki S (1992) Polyamines as a chemotaxonomic marker in bacterial systematics. *Crit Rev Microbiol* 18:261–283
17. Lee J, Michael AJ, Martynowski D, Goldsmith EJ, Phillips MA (2007) Phylogenetic diversity and the structural basis of substrate specificity in the beta/alpha-barrel fold basic amino acid decarboxylases. *J Biol Chem* 282:27115–27125
18. Takatsuka Y, Yamaguchi Y, Ono M, Kamio Y (2000) Gene cloning and molecular characterization of lysine decarboxylase from *Selenomonas ruminantium* delineate its evolutionary relationship to ornithine decarboxylases from eukaryotes. *J Bacteriol* 182:6732–6741
19. Altschul SF, Gish W, Miller W, Myers EW, Lipman DJ (1990) Basic local alignment search tool. *J Mol Biol* 215:403–410
20. Thompson JD, Higgins DG, Gibson TJ (1994) CLUSTAL W: improving the sensitivity of progressive multiple sequence alignment through sequence weighting, position-specific gap penalties and weight matrix choice. *Nucleic Acids Res* 22:4673–4680
21. Wilgenbusch JC, Swofford D (2003) Inferring evolutionary trees with PAUP*. *Curr Protoc Bioinformatics*, Chapter 6, Unit 6 4
22. Kumar S, Tamura K, Nei M (1994) MEGA: molecular evolutionary genetics analysis software for microcomputers. *Comput Appl Biosci* 10:189–191
23. Hall BG (2008) *Phylogenetic trees made easy*, 3rd edn. Sinauer Associates, Sunderland, MA
24. Page RD (1996) TreeView: an application to display phylogenetic trees on personal computers. *Comput Appl Biosci* 12:357–358
25. Lee J, Sperandio V, Frantz DE, Longgood J, Camilli A, Phillips MA, Michael AJ (2009) An Alternative Polyamine Biosynthetic Pathway is Widespread in Bacteria and Essential for Biofilm Formation in *Vibrio Cholerae*. *J Biol Chem* 284:9899–9907
26. Wu H, Min J, Zeng H, McCloskey DE, Ikeguchi Y, Loppnau P, Michael AJ, Pegg AE, Plotnikov AN (2008) Crystal structure of human spermine synthase. *J Biol Chem* 283:16135–16146
27. Pegg AE, Michael AJ (2009) Spermine synthase. *Cell Mol Life Sci* 67:113–121
28. Luo J, Fuell C, Parr A, Hill L, Bailey P, Elliott K, Fairhurst SA, Martin C, Michael AJ (2009) A novel polyamine acyltransferase responsible

- for the accumulation of spermidine conjugates in Arabidopsis seed. *Plant Cell* 21:318–333
29. Zimmermann P, Hirsch-Hofmann M, Hennig L, Gruissem W (2004) GENEVESTIGATOR. Arabidopsis microarray database and analysis toolbox. *Plant Physiol* 136:2621–2632
30. Grienberger E, Besseau S, Geoffroy P, Debayle D, Heintz D, Lapierre C, Pollet B, Heitz T, Legrand M (2009) A BAHD acyltransferase is expressed in the tapetum of Arabidopsis anthers and is involved in the synthesis of hydroxycinnamoyl spermidines. *Plant J* 58:246–259

Chapter 3

Characterization of Genes for Polyamine Modulon

Kazuei Igarashi and Keiko Kashiwagi

Abstract

Polyamines are essential for normal cell growth and exist mainly as RNA-polyamine complexes in cells. Thus, effects of polyamines on protein synthesis have been studied. It was found that several kinds of protein synthesis, which are important for cell growth, were enhanced by polyamines at the level of translation. We proposed that a group of genes whose expression is enhanced by polyamines at the level of translation be referred to as a “polyamine modulon.” In *Escherichia coli*, most members of the polyamine modulon thus far identified were transcription factors. These transcription factors enhanced the synthesis of several kinds of mRNA and tRNA, and also rRNA. In this way, polyamines enhanced growth of *E. coli*. We also succeeded in identifying three kinds of “polyamine modulon” in mammalian cells. One of the mechanisms of polyamine stimulation at the molecular level was due to the stabilization of the bulged-out region of double-stranded RNA in mRNA. The procedures used to identify components of the polyamine modulon are described in this chapter.

Key words: Polyamine modulon, Protein synthesis, Polyamine-RNA interaction, Cell growth, Cell viability, Spermidine

1. Introduction

Polyamines are present at mM concentrations in both prokaryotes and eukaryotes and play important roles in cell growth and viability (1, 2). To study the effects of polyamines on cell growth, we first estimated their cellular distribution (3, 4). In *E. coli*, about 50% of putrescine and 90% of spermidine exist as polyamine-RNA complexes; in rat liver, about 80% of spermidine and 85% of spermine exist as polyamine-RNA complexes. Accordingly, the effects of polyamines on cell growth were mainly studied at the level of translation. It was found that several kinds of protein synthesis, which are important for cell growth, were enhanced by polyamines at the level of translation. We proposed that a group of genes whose expression is enhanced by polyamines at the level of translation

be referred to as a “polyamine modulon.” In *E. coli*, most members of the polyamine modulon thus far identified were transcription factors (see Note 1). These transcription factors enhanced the synthesis of several kinds of mRNA and tRNA, and also rRNA. In this way, polyamines enhanced cell growth of *E. coli*. We also succeeded in identifying three kinds of polyamine modulon in mammalian cells. One of the mechanisms of polyamine stimulation at the molecular level was due to the stabilization of the bulged-out region of double-stranded RNA in mRNA.

In this chapter, the procedure to identify proteins whose synthesis is enhanced by polyamines at the level of translation is described using *E. coli* and mammalian cells. Furthermore, procedures to investigate how polyamines stimulate protein synthesis at the molecular level are described.

2. Materials

2.1. Bacterial Strains, Plasmids, and Culture Conditions

1. *E. coli* MA261 (*speB spec gly leu thr thi*) (5), DR112 (*speA speC*) (6), and EWH 319 (*speA speB speC speED thr pro thi*) (7), polyamine-deficient mutants; MA261 *oppA::Km*, an *oppA*-deficient mutant derived from MA261 (8); and MA261 *lacZ::Km*, a *lacZ*-deficient mutant derived from MA261 (9).
2. pACYCoppA (pPI5.1), pMWoppA (pMW975), and pMWoppA (stem I+U) (10–12).
3. Luria-Bertani (LB) medium: consisting of 10 g of tryptone, 5 g of yeast extract, and 10 g of NaCl (per liter) was used for maintaining *E. coli* strains.
4. Medium A: dissolve 7 g of K_2HPO_4 , 3 g of KH_2PO_4 , 500 mg of sodium citrate, 1 g of $(NH_4)_2SO_4$, 100 mg of $MgSO_4/7H_2O$, 2 mg of thiamine, 10 mg of biotin, and 100 mg each of leucine, threonine, methionine, serine, glycine, and ornithine (per liter of water).
5. Medium B: dissolve 6 g of K_2HPO_4 , 3 g of KH_2PO_4 , 500 mg of NaCl, 1 g of NH_4Cl , 250 mg of $MgSO_4/7H_2O$, 13 mg of $CaCl_2/2H_2O$, 2 mg of thiamine, 1 g of arginine, 100 mg each of alanine, asparagine, aspartic acid, glutamic acid, glycine, methionine, proline, serine, and threonine, 50 mg each of cysteine, histidine, isoleucine, leucine, phenylalanine, tyrosine, and valine, and 5 mg of tryptophan (per liter of water).
6. 20% Glucose (1.1 M).
7. 50% Glutamic acid (3.5 M).
8. 100 mg/mL Putrescine dihydrochloride (0.6 M).
9. Buffer 1: 62 mM potassium phosphate, pH 7.0, 1.7 mM sodium citrate, 7.6 mM $(NH_4)_2SO_4$, and 0.41 mM $MgSO_4$.

2.2. Isolation of RNA and Dot Blotting

1. [α - ^{32}P]dCTP (111 GBq/mmol) and the BcaBEST labeling kit (Takara Shuzo Co.).
2. ECL direct nucleic acid labeling and detection system (GE Healthcare).
3. BAS-2000II imaging analyzer (Fuji Film).
4. LAS-1000 plus luminescent image analyzer (Fuji Film).

2.3. Preparation of Cell Lysate and Western Blotting

1. Buffer 2: 10 mM Tris-HCl, pH 7.5, and 20% sucrose.
2. 20 mg/mL lysozyme (Sigma).
3. Ultrasonic cell disruptor (Microson).
4. Immobilon transfer membrane (Millipore).
5. ECL Western blotting detection reagents (GE Healthcare).

2.4. Labeling of Cells with [^{35}S]Methionine, and Immunoprecipitation

1. [^{35}S]Methionine (3.15 TBq/mmol).
2. Buffer 3 (10 mM sodium phosphate, pH 7.4, 100 mM NaCl, 1% Triton X-100, and 0.1% sodium dodecyl sulfate).
3. French press (Aminco) or Multi-Beads Shocker (Yasui Kikai).

2.5. Construction of Plasmids Encoding a Gene for Polyamine Modulon Fused to a lacZ Gene and Site-Directed Mutagenesis

1. Plasmids pMC1871 (13) encoding a gene for β -galactosidase (*lacZ*) and a low copy number vector pMW119 (Nippon Gene).

2.6. Cell Culture of FM3A and Preparation of Cell Lysate

1. Mouse mammary carcinoma FM3A cells (Japan Health Science Foundation).
2. ES medium (Nissui Pharmaceutical Co., Tokyo).
3. DFMO (α -difluoromethylornithine), an irreversible inhibitor of ornithine decarboxylase.
4. Buffer 4 [25 mM Hepes-KOH, pH 7.8, 0.1 mM EDTA, 6 mM 2-mercaptoethanol, 5% (v/v) glycerol, and 20 μM FUT-175 (6-amino-2-naphthyl-4-guanidinobenzoate dihydrochloride), an inhibitor of serine protease].

2.7. Two-dimensional Gel Electrophoresis of Proteins and Identification of Proteins by Edman Degradation and Mass Spectrometry

1. Ready-PrepTM Sequential Extraction Kit (Bio-Rad Laboratories).
2. PROTEAN[®] IEF Cell using 17 cm (pH range 3–10) Ready StripTM IPG Strip gel (Bio-Rad Laboratories).
3. *Achromobacter* lysine-specific protease I (14).
4. Columns [DEAE-5PW (1 mm \times 20 mm or 0.5 mm \times 5 mm; Tosoh) and Inertsil ODS-3 (1 mm \times 100 mm or 0.5 mm \times 150 mm; GL Sciences Inc.)].

5. Model 1100 series liquid chromatography system (Agilent Technologies).
6. Solvent A: 0.09% (v/v) aqueous trifluoroacetic acid.
7. Solvent B: 0.075% (v/v) trifluoroacetic acid in 80% (v/v) acetonitrile.
8. Procise cLC protein sequencing system (Applied Biosystems).
9. Matrix-assisted laser desorption ionization time of flight mass spectrometry (MALDI-TOF MS) on a Reflex MALDI-TOF (Bruker-Franzen Analytik) in a reflector mode using α -cyano-4-hydroxycinnamic acid as a matrix.
10. Prematrix coated MALDI target plate (AnchorChip™ 600/384, Bruker Daltonics) using AccuSpot (Shimadzu).
11. Ultraflex mass spectrometer (Bruker Daltonics) using Fuzzy control system.

2.8. Western and Northern Blot Analysis and Measurement of Protein Synthesis for Mammalian Proteins

1. Quick Prep Total RNA Extraction Kit (GE Healthcare).
2. SuperScript™ II RNase H⁻ Reverse Transcriptase (Life Technologies).

3. Methods

To identify genes that constitute the polyamine modulon in *E. coli*, a polyamine-requiring mutant MA261 (or DR112, EWH319) was cultured in the presence and absence of putrescine, and the levels of mRNA and protein were measured by dot blotting and Western blotting. When the level of protein in cells cultured in the presence of putrescine was at least twofold higher than that in the absence of putrescine and the levels of mRNA were similar, the gene became a candidate member of the polyamine modulon. Synthesis of the protein in question was then measured by immunoprecipitation of [³⁵S]methionine-labeled protein. The mechanism of polyamine stimulation of the synthesis of the protein was examined using wild-type and mutated target gene fused to a *lacZ* gene in a low copy number plasmid. The plasmids were transformed into MA261*lacZ::Km* and the effect of putrescine was compared.

To identify genes belonging to the polyamine modulon in mammalian cells, FM3A cells were cultured in the presence of DFMO to make the cells polyamine-deficient. Proteins whose level was low in polyamine-deficient cells were isolated by two-dimensional electrophoresis and identified by Edman degradation and mass spectrometry. Then, synthesis of the protein was measured as described above.

3.1. Culture of *E. coli* Polyamine-Requiring Mutants

1. *E. coli* MA261 (or EWH319) was cultured in medium A with 0.4% glucose or 0.1% glucose plus 0.02% glutamate as an energy source in the presence and absence of 100 µg/mL putrescine at 37°C or 42°C. *E. coli* DR112 was similarly cultured in medium B instead of medium A.
2. Cells were harvested at logarithmic phase of cell growth by measuring absorbance at 540 nm, washed once with Buffer 1 and stored at -80°C.

3.2. Dot Blot Analysis of mRNAs

1. Total RNA was isolated from *E. coli* cells by the method of Emory and Belasco (15).
2. Dot blot analysis of mRNAs was performed according to the method of Sambrook et al. (16) using various amounts of total RNA.
3. PCR products of genes for candidates of polyamine modulon were labeled with [α -³²P]dCTP by the BcaBEST labeling kit or with ECL direct nucleic acid labeling and detection system and used as probes.
4. The radioactivity on the blot was quantified with a BAS2000II imaging analyzer or chemiluminescence was detected using a LAS-1000 plus luminescent image analyzer.

3.3. Western Blot Analysis

1. Cells were incubated in Buffer 2 with 100 µg/mL lysozyme at 25°C for 10 min and disrupted by sonication for 10 s 3 times with ultrasonic cell disruptor.
2. After centrifugation at 15,000 × *g* for 10 min, supernatant (cell lysate) was collected.
3. Protein concentration of cell lysate was determined by the method of Lowry et al. (17).
4. Proteins in cell lysate were separated by sodium dodecyl sulfate-polyacrylamide gel electrophoresis (SDS/PAGE) (18).
5. Proteins were transferred to Immobilon transfer membrane, and Western blot analysis was performed by the method of Nielsen et al. (19) using specific antibodies against candidate proteins and ECL Western blotting reagents.
6. The level of protein was quantified with a LAS-1000 plus luminescent image analyzer.

3.4. Measurement of Protein Synthesis by Immunoprecipitation of [³⁵S]Methionine-Labeled Proteins

1. *E. coli* MA261 was cultured in medium A as described in Subheading 3.1 in the absence of putrescine with 3 µg/mL methionine instead of 100 µg/mL.
2. When A₅₄₀ reached 0.15, the cells were divided into aliquots of 5 mL and grown in the presence and absence of 100 µg/mL putrescine for 10 min.
3. [³⁵S]Methionine (1 MBq) was added to each 5-mL aliquot, and the cells were allowed to grow for 20 min. They were harvested

after the addition of methionine at a final concentration of 20 mM.

4. Cells were resuspended in 1 mL of Buffer 3 and disrupted by French press at 20,000 p.s.i. or by grinding for 30 s at 2,500 rpm 6 times with Multi-Beads Shocker.
5. The supernatant (cell lysate) was collected by centrifugation at $15,000\times g$ for 10 min.
6. The amount of protein synthesized was determined using whole-cell lysate containing 1×10^6 cpm of [^{35}S]methionine-labeled proteins using specific antibodies according to the method of Philipson et al. (20).
7. Immunoprecipitates were separated by SDS/PAGE (18) and the radioactivity of labeled protein was quantified using BAS2000II imaging analyzer.

3.5. Analysis of the Mechanism of Polyamine Stimulation of Synthesis of the Protein Encoded by Polyamine Modulon (see Note 2)

1. pMWoppA (stem I+U) was prepared by site-directed mutagenesis using pMWoppA as template by overlap extension using PCR (21).
2. *E. coli* MA261 *oppA::Km* was transformed with pMWoppA or pMWoppA (stem I+U) and cultured in medium A with 0.1 mg/mL ampicillin and 0.05 mg/mL kanamycin in the presence and absence of 100 $\mu\text{g}/\text{mL}$ putrescine.
3. Effect of putrescine on the synthesis OppA protein in MA261 *oppA::Km/pMWoppA* or pMWoppA (stem I+U) was compared as described in Subheadings 3.3 and 3.4.
4. The nucleotides for 5'-UTR and N-terminal region of open reading frame of genes of the polyamine modulon were fused to the gene for β -galactosidase (*lacZ*) of pMC1871 and inserted into pMW119. Site-directed mutagenesis was performed by overlap extension using PCR (21).
5. The plasmids were transformed into MA261 *lacZ::Em* and effects of polyamines were examined using antibody against β -galactosidase (Sigma) as described in Subheadings 3.3 and 3.4.

3.6. Culture of FM3A Cells and Preparation of Cell Lysate

1. FM3A cells were cultured in ES medium, supplemented with 50 units/mL streptomycin, 100 units/mL penicillin G, and 2% heat-inactivated fetal calf serum at 37°C in an atmosphere of 5% CO_2 in air (22) in the presence and absence of 50 μM DFMO (see Note 3).
2. Cells (2×10^6 cells) were suspended in 0.1 mL of Buffer 4 and disrupted by repeated (3 times) freezing and thawing with intermittent mechanical mixing. The supernatant was obtained by centrifugation at $17,000\times g$ for 15 min and used as cell lysate. Protein content of the cell lysate was determined by the method of Lowry et al. (17).

3.7. Two-Dimensional Gel Electrophoresis of Proteins and Identification of Proteins by Edman Degradation and Mass Spectrometry

1. Cell lysate (200 μg of protein) for two-dimensional gel electrophoresis was prepared using Ready-Prep™ Sequential Extraction Kit.
2. The first-dimensional isoelectric focusing was performed in the PROTEAN® IEF Cell using 17 cm (pH range 3–10) Ready Strip™ IPG Strip gel.
3. The proteins on the first-dimensional Strip gel were further separated, in the second dimension, by SDS/PAGE on a 10.5% polyacrylamide gel (18). Proteins were stained with Coomassie Brilliant Blue R-250.
4. Coomassie-stained spots were excised and treated with 0.2 μg of *Achromobacter* lysine-specific protease I (14) at 37°C for 12 h in 0.1 M Tris–HCl (pH 9.0) containing 0.1% SDS.
5. For sequencing, peptides generated were extracted from the gel and separated on columns of DEAE-5PW (1 \times 20 mm) and Inertsil ODS-3 (1 \times 100 mm) connected in series with a model 1100 series liquid chromatography system. Peptides were eluted at a flow rate of 20 $\mu\text{L}/\text{min}$ using a linear gradient of 0–60% solvent B based on solvent A.
6. Selected peptides were subjected to Edman degradation using a Procise cLC protein sequencing system and to matrix-assisted laser desorption ionization time of flight mass spectrometry (MALDI-TOF MS) on a Reflex MALDI-TOF in a reflector mode using α -cyano-4-hydroxycinnamic acid as a matrix.
7. For LC-MS/MS analysis, peptide generated was separated on columns of DEAE-5PW (0.5 \times 5 mm) and Inertsil ODS-3 (0.5 \times 150 mm) with a model 1100 series liquid chromatography system. Peptide eluted at a flow rate 3 $\mu\text{L}/\text{min}$ was directly spotted onto a prematrix coated MALDI target plate using AccuSpot.
8. MS or MS/MS analysis was performed automatically on an Ultraflex mass spectrometer using Fuzzy control system. α -Cyano-4-hydroxycinnamic acid was used as a matrix.

3.8. Western and Northern Blot Analysis and Measurement of Protein Synthesis for Mammalian Proteins

1. Cell lysate (20 μg of protein) prepared as described in Subheading 3.6 was separated by SDS/PAGE (18), transferred on the Immobilon transfer membrane, and each protein was detected by using specific antibody, followed by ECL Western blotting detection reagents.
2. Concentration of polyacrylamide gel used was 10.5% for Hnrpl and Cct2, 12% for Pgam1 and Cct2-EGFP, and 13.5% for eIF5A.
3. The level of each protein was quantified by a LAS-1000 plus luminescent image analyzer.

4. Total RNA was isolated from 2.5×10^7 cells using the Quick Prep Total RNA Extraction Kit. Northern blot analysis was performed (16) using the ECL direct nucleic acid labeling and detection system with 10 μ g of total RNA.
5. The first-strand cDNA used for template DNA was prepared using SuperScript™ II RNase H⁻ Reverse Transcriptase.
6. Genes of the polyamine modulon in mammalian cells and eIF5A were amplified by PCR using the first-strand cDNA as template and specific primers. PCR products thus obtained were used as probes.
7. The level of mRNA was quantified with a LAS-1000 plus luminescent image analyzer.
8. A 10-mL cell suspension (6×10^5 /mL) in methionine-free ES medium was cultured with 11.1 MBq [³⁵S]methionine (25.5 nM) for 30 min at 37°C.
9. Cells were harvested in the presence of 2 mM methionine, and the cell lysate was prepared as described in Subheading 3.6. The amount of proteins synthesized was determined by immunoprecipitation using 1×10^7 cpm of [³⁵S]methionine-labeled total protein and specific antibodies.
10. Immunoprecipitates were separated by SDS/PAGE (18), and the radioactivity of the labeled protein was quantified using BAS2000II imaging analyzer.

4. Notes

1. Members of the polyamine modulon thus far identified in *E. coli* are shown in Fig. 1a. The mechanism of polyamine stimulation of synthesis of these proteins was classified into three groups. First, polyamine stimulation of protein synthesis can occur when a Shine-Dalgarno sequence in the mRNA is obscure or is distant from the AUG initiation codon. In this case, polyamines cause structural changes in a region of the Shine-Dalgarno sequence and the AUG initiation codon of the mRNA, facilitating formation of the initiation complex, and examples include OppA, a periplasmic substrate-binding protein of the oligopeptide uptake system (23); FecI σ factor (σ^{18}), for transcription of the iron transport operon (24); Fis, a global regulator of transcription of some growth-related genes, including those for rRNA and some tRNAs (24); RpoN σ factor (σ^{54}), for transcription of genes for nitrogen metabolisms (25); RpoE σ factor (σ^{24}), for transcription of a number of heat shock response genes (26); and H-NS/StpA, transcription factors of many kinds of mRNAs, including

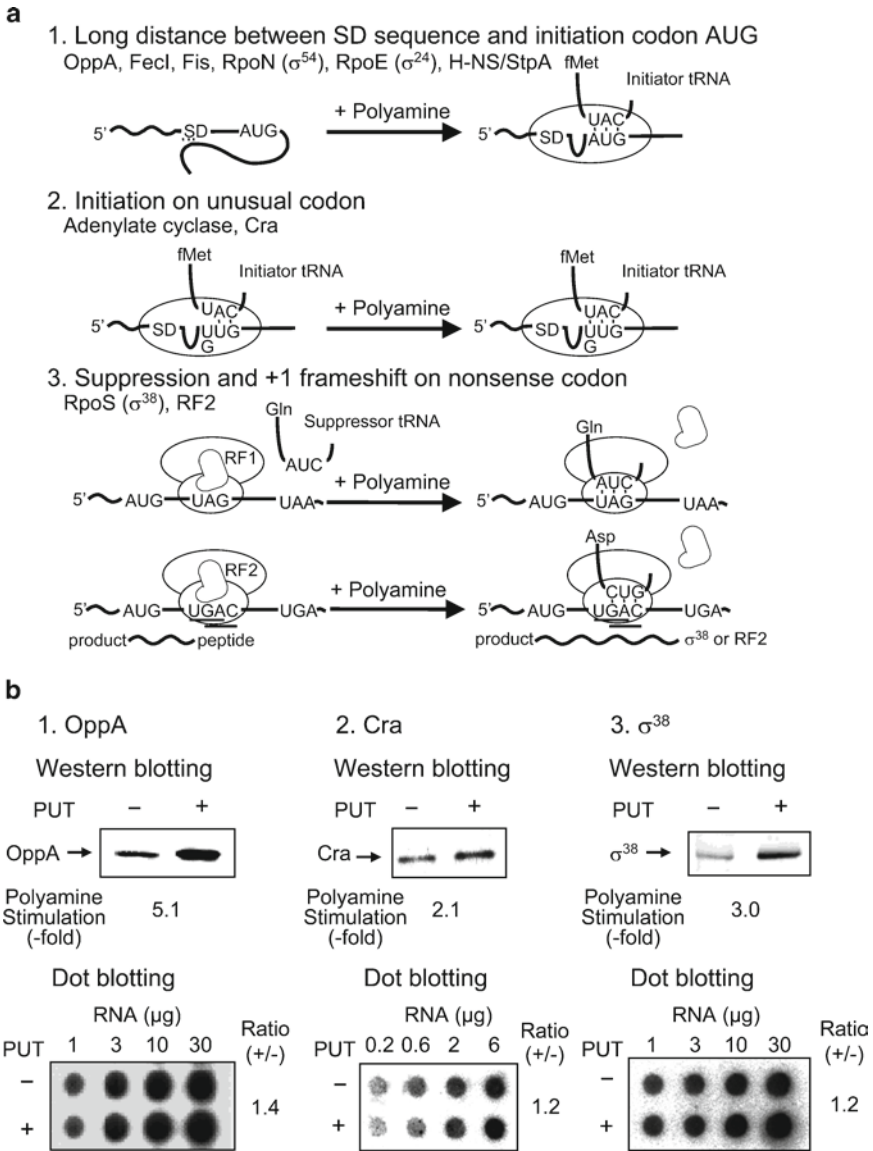


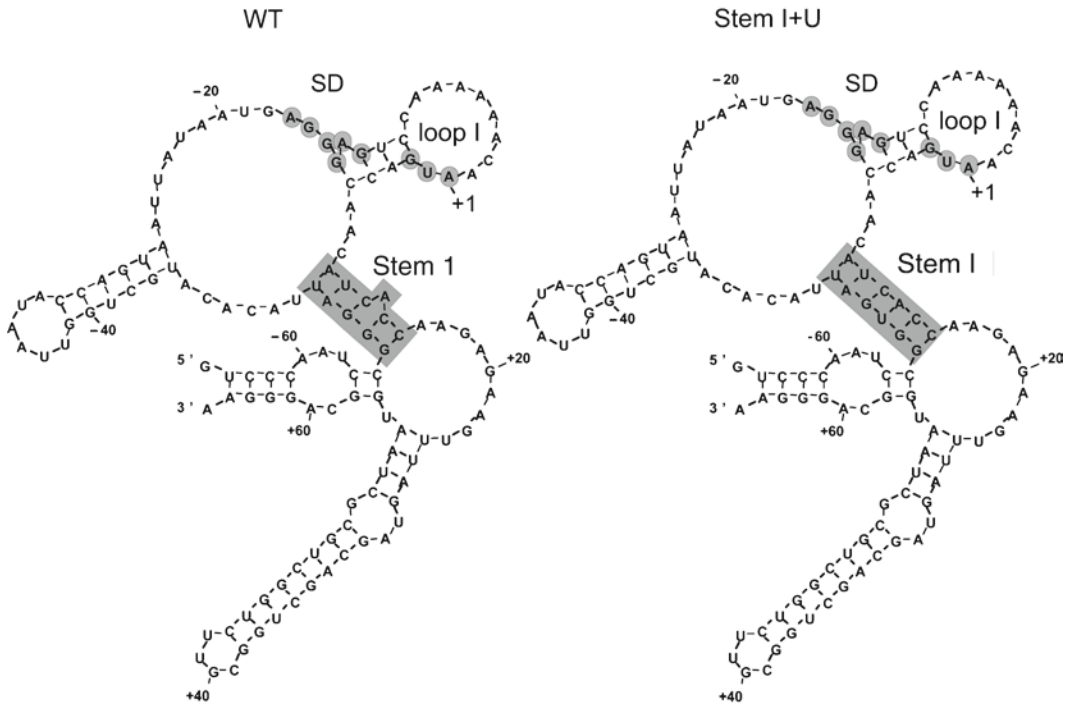
Fig. 1. Mechanism of polyamine stimulation of protein synthesis of polyamine modulon in *E. coli* (a) and effect of polyamines on the synthesis of OppA, Cra, and σ^{38} (RpoS) (b). (b) Western and dot blotting were performed as described in Subheadings 3.2 and 3.3. Figures are taken from Igarashi et al. (11), Terui et al. (25) and Yoshida et al. (28).

ribosomal protein mRNAs and flagellar protein mRNAs (25, 26). By a second mechanism, polyamines enhance the inefficient initiation codon UUG (or GUG)-dependent fMet-tRNA binding to Cya (or Cra) mRNA-ribosomes so that polyamines enhance the synthesis of Cya (adenylate cyclase) (27) and Cra (a global regulator of transcription of glycolysis and glycconeogenesis) (25). By a third mechanism, polyamines stimulate read-through of the amber codon

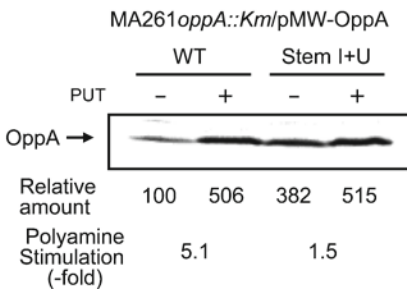
UAG-dependent Gln-tRNA^{supE} on ribosome-associated *rpoS* mRNA or stimulate a +1 frameshift at the 26th UGA codon of *prfB* mRNA, resulting in enhanced synthesis of RpoS σ factor (σ^{38}) for transcription of stationary-phase genes (28), and RF2 (polypeptide-releasing factor 2) (29). The effects of polyamines on the synthesis of OppA, Cra, and σ^{38} (RpoS) at the level of translation and transcription in *E. coli* MA261 cultured in the presence and absence of 100 $\mu\text{g}/\text{mL}$ putrescine are shown in Fig. 1b.

2. The mechanism of polyamine stimulation of OppA synthesis at the molecular level was studied because polyamine stimulation was most pronounced in OppA synthesis. It was previously suggested from the experimental results of the sensitivity of *oppA* mRNA against a single-stranded G-specific RNase T₁ and a double-stranded specific RNase V₁ that polyamines induce a structural change in the bulged-out region of double-stranded RNA (23). To study this further, the Stem I structure of *oppA* mRNA was modified to make intact double-stranded RNA (Stem I+U mRNA) (Fig. 2a). When *oppA* Stem I+U mRNA was used instead of wild-type mRNA, OppA synthesis in the absence of polyamines was enhanced, and the degree of polyamine stimulation was reduced from 5.1- to 1.5-fold (Fig. 2b). The results indicate that a structural change in the bulged-out region of double-stranded RNA by spermidine is important for spermidine-stimulation of OppA synthesis. Recently, we have shown a selective conformational change in the bases in the bulged-out region of double-stranded RNA by spermidine using U6-34, a model RNA of U6 small nuclear RNA by NMR (30).
3. To study the effects of polyamines on protein synthesis in mammalian cells, FM3A cells were treated with 50 μM DFMO to make the cells polyamine-deficient. Cell growth was gradually decreased together with a decrease in polyamine content. Under these conditions, spermidine and putrescine content became negligible and cell number decreased to approximately 25% of control on day 3. In contrast, the number of control cells increased from 1×10^4 to 7×10^5 cells on day 3. Proteins whose level is low in DFMO-treated cells were searched for by two-dimensional gel electrophoresis using cells cultured for 3 days. Enolase 1 was used as a control protein, because it was one of the major proteins in FM3A cells and its level was almost the same in control and DFMO-treated cells. It was confirmed that the level of active eIF5A, which contains hypusine [N^{ϵ} -(4-amino-2-hydroxybutyl) lysine] derived from spermidine, was decreased in DFMO-treated cells (31). It was also found that the level of three kinds of protein (termed P1, P2, and P3) decreased to less

a Possible secondary structure of the initiation region of *oppA* mRNA



b [³⁵S]Methionine-labeled OppA



c *oppA* mRNA

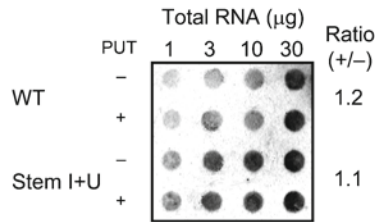


Fig. 2. Effect of polyamines on OppA synthesis in *E. coli* MA261. (a) Secondary structure of wild-type and Stem I + U *oppA* mRNA. Stem I + U; A uridine nucleotide was added to the Stem I structure to make intact double-stranded RNA. Optimal computer folding of mRNAs was performed by the method of Zuker (35). (b) Effect of polyamines on the synthesis of OppA. Immunoprecipitation of [³⁵S]methionine-labeled protein was performed as described in Subheading 3.4. (c) Dot blot analysis of *oppA* mRNA. This was performed as described in Subheading 3.3. SD, Shine-Dalgarno sequence; PUT, putrescine. Figures are taken from Higashi et al. (12).

than 50% of control. These three proteins were identified by Edman degradation and mass spectrometry (Fig. 3). Protein P1 was identified as Hnrpl (heterogenous nuclear ribonucleoprotein L) protein, which is a ribonucleoprotein affecting translation, mRNA stability, and splicing. Protein P2 was identified as Cct2 protein (T-complex protein 1, β-subunit),

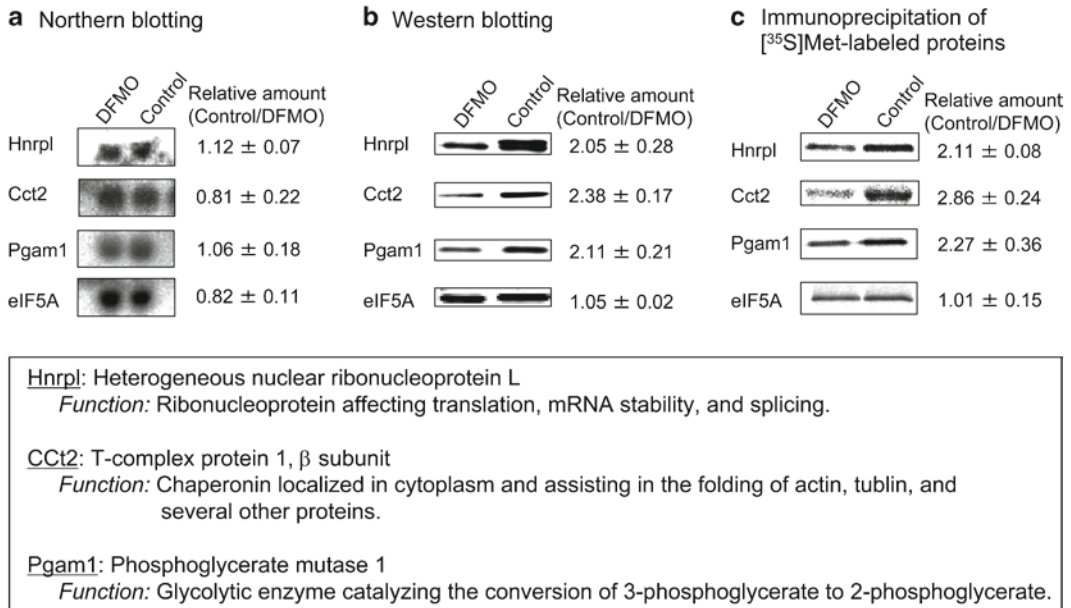


Fig. 3. Identification of genes for Hnrpl, Cct2, and Pgam1 as members of polyamine modulon in mammalian cells. Northern blotting (a), Western blotting (b), and protein synthesis (c) were examined as described in Subheading 3.8. eIF5A was used as a control. Description and function of Hnrpl, Cct2, and Pgam1 were represented in a *large box*. Figures are taken from Nishimura et al. (33).

which is a chaperonin located in cytoplasm and assisting in the folding of actin, tubulin, and several other proteins, and an essential protein of cell growth in yeast. Protein P3 was identified as Pgam1 protein (phosphoglycerate mutase 1), which is a glycolytic enzyme catalyzing the conversion of 3-phosphoglycerate to 2-phosphoglycerate and modulating cellular life span. Inhibition of cell growth by DFMO was reversed by the addition of 30 μ M spermidine or 3 μ M spermine in the presence of 1 mM aminoguanidine, an inhibitor of amine oxidase (32). Under these conditions, the levels of Hnrpl-, Cct2-, and Pgam1-proteins were similar to those in untreated cells. The results indicate that the reduced levels of these three proteins were mainly due to the decrease in polyamines in DFMO-treated cells. It was then examined whether synthesis of these three proteins was enhanced by polyamines at the level of translation. As shown in Fig. 3, the levels of Hnrpl-, Cct2-, Pgam1-, and eIF5A-mRNA in control cells were nearly equal to or slightly less than levels in polyamine-deficient cells. However, levels of Hnrpl-, Cct2-, and Pgam1-proteins were increased by polyamines: i.e., their levels were higher in control cells than in polyamine-deficient cells. With regard to eIF5A, the protein level was nearly equal, although the active hypusinated eIF5A level was low in

polyamine-deficient cells. Then, the synthesis of Hnrp1-, Cct2-, and Pgam1-proteins was determined by incorporation of pulse-labeled [³⁵S]methionine into each protein. On day 3, protein synthetic activity of polyamine-deficient cells was approximately 40% of control cells. The synthesis of these proteins in control and polyamine-deficient cells was compared using the same amount of [³⁵S]methionine-labeled proteins (1×10^7 cpm). The synthesis of Hnrp1-, Cct2-, and Pgam1-proteins was increased in control cells, but the synthesis of eIF5A did not change significantly between control and polyamine-deficient cells. These results indicate that synthesis of these three proteins was preferentially enhanced by polyamines at the level of translation (33). Since Cct2 was most strongly enhanced by polyamines among three proteins, the mechanism of polyamine stimulation of Cct2 synthesis was studied. Polyamines most likely enhanced ribosome shunting, which involved discontinuous scanning by 40S ribosomal subunits, on the 5'-UTR of Cct2 mRNA (34).

Acknowledgments

We are grateful to Drs. K. Williams and A. J. Michael for critical reading of the manuscript prior to submission. This study was supported in part by Grants-in-Aid for Scientific Research from the Ministry of Education, Culture, Sports, Science, and Technology, Japan.

References

1. Cohen SS (1998) A guide to polyamines. Oxford University Press, New York, pp 1–543
2. Igarashi K, Kashiwagi K (2000) Polyamines: mysterious modulators of cellular functions. *Biochem Biophys Res Commun* 271:559–564
3. Watanabe S, Kusama-Eguchi K, Kobayashi H, Igarashi K (1991) Estimation of polyamine binding to macromolecules and ATP in bovine lymphocytes and rat liver. *J Biol Chem* 266:20803–20809
4. Miyamoto S, Kashiwagi K, Ito K, Watanabe S, Igarashi K (1993) Estimation of polyamine distribution and polyamine stimulation of protein synthesis in *Escherichia coli*. *Arch Biochem Biophys* 300:63–68
5. Cunningham-Rundles S, Maas WK (1975) Isolation, characterization, and mapping of *Escherichia coli* mutants blocked in the synthesis of ornithine decarboxylase. *J Bacteriol* 124:791–799
6. Linderoth N, Morris DR (1983) Structural specificity of the triamines sym-homospermidine and aminopropylcadaverine in stimulating growth of spermidine auxotrophs of *Escherichia coli*. *Biochem Biophys Res Commun* 117:616–622
7. Hafner EW, Tabor CW, Tabor H (1979) Mutants of *Escherichia coli* that do not contain 1, 4-diaminobutane (putrescine) or spermidine. *J Biol Chem* 254:12419–12426
8. Kashiwagi K, Miyaji A, Ikeda S, Tobe T, Sasakawa C, Igarashi K (1992) Increase of sensitivity to aminoglycoside antibiotics by polyamine-induced protein (oligopeptide-binding protein) in *Escherichia coli*. *J Bacteriol* 174:4331–4337
9. Kashiwagi K, Watanabe R, Igarashi K (1994) Involvement of ribonuclease III in the enhancement of expression of the *speF-potE* operon encoding inducible ornithine decarboxylase

- and polyamine transport protein. *Biochem Biophys Res Commun* 200:591–597
10. Kashiwagi K, Yamaguchi Y, Sakai Y, Kobayashi H, Igarashi K (1990) Identification of the polyamine-induced protein as a periplasmic oligopeptide binding protein. *J Biol Chem* 265:8387–8391
 11. Igarashi K, Saisho T, Yuguchi M, Kashiwagi K (1997) Molecular mechanism of polyamine stimulation of the synthesis of oligopeptide-binding protein. *J Biol Chem* 272:4058–4064
 12. Higashi K, Terui Y, Suganami A, Tamura Y, Nishimura K, Kashiwagi K, Igarashi K (2008) Selective structural change by spermidine in the bulged-out region of double-stranded RNA and its effect on RNA function. *J Biol Chem* 283:32989–32994
 13. Shapira SK, Chou J, Richaud FV, Casadaban MJ (1983) New versatile plasmid vectors for expression of hybrid proteins coded by a cloned gene fused to *lacZ* gene sequences encoding an enzymatically active carboxy-terminal portion of β -galactosidase. *Gene* 25:71–82
 14. Masaki T, Tanabe M, Nakamura K, Soejima M (1981) Studies on a new proteolytic enzyme from *Achromobacter lyticus* M497-1. I. Purification and some enzymatic properties. *Biochim Biophys Acta* 660:44–50
 15. Emory SA, Belasco JG (1990) The *ompA* 5' untranslated RNA segment functions in *Escherichia coli* as a growth-rate-regulated mRNA stabilizer whose activity is unrelated to translational efficiency. *J Bacteriol* 172:4472–4481
 16. Sambrook J, Fritsch EF, Maniatis T (2001) Extraction, purification, and analysis of mRNA from eukaryotic cells, Chapter 7. In: Sambrook J, Russell DW (eds) *Molecular cloning: A Laboratory Manual*, 3rd edn. Cold Spring Harbor Laboratory, Cold Spring Harbor, New York
 17. Lowry OH, Rosebrough NJ, Farr AL, Randall RJ (1951) Protein measurement with the Folin phenol reagent. *J Biol Chem* 193:265–275
 18. Laemmli UK (1970) Cleavage of structural proteins during the assembly of the head of bacteriophage T4. *Nature (London)* 227:680–685
 19. Nielsen PJ, Manchester KL, Towbin H, Gordon J, Thomas G (1982) The phosphorylation of ribosomal protein S6 in rat tissues following cycloheximide injection, in diabetes, and after denervation of diaphragm. A simple immunological determination of the extent of S6 phosphorylation on protein blots. *J Biol Chem* 257:12316–12321
 20. Philipson L, Andersson P, Olshevsky U, Weinberg R, Baltimore D, Gesteland R (1978) Translation of MuLV and MSV RNAs in nuclease-treated reticulocyte extracts: enhancement of the gag-pol polypeptide with yeast suppressor tRNA. *Cell* 13:189–199
 21. Ho SN, Hunt HD, Horton RM, Pullen JK, Pease LR (1989) Site-directed mutagenesis by overlap extension using the polymerase chain reaction. *Gene* 77:51–59
 22. Ayusawa D, Iwata K, Seno T (1981) Alteration of ribonucleotide reductase in aphidicolin-resistant mutants of mouse FM3A cells with associated resistance to arabinosyladenine and arabinosylcytosine. *Somatic Cell Genet* 7:27–42
 23. Yoshida M, Meksuriyen D, Kashiwagi K, Kawai G, Igarashi K (1999) Polyamine stimulation of the synthesis of oligopeptide-binding protein (OppA). Involvement of a structural change of the Shine-Dalgarno sequence and the initiation codon AUG in OppA mRNA. *J Biol Chem* 274:22723–22728
 24. Yoshida M, Kashiwagi K, Shigemasa A, Taniguchi S, Yamamoto K, Makinoshima H, Ishihama A, Igarashi K (2004) A unifying model for the role of polyamines in bacterial cell growth, the polyamine modulon. *J Biol Chem* 279:46008–46013
 25. Terui Y, Higashi K, Taniguchi S, Shigemasa A, Nishimura K, Yamamoto K, Kashiwagi K, Ishihama A, Igarashi K (2007) Enhancement of the synthesis of RpoN, Cra and H-NS by polyamines at the level of translation in *Escherichia coli* cultured with glucose and glutamate. *J Bacteriol* 189:2359–2368
 26. Terui Y, Higashi K, Tabei Y, Tomitori H, Yamamoto K, Ishihama A, Igarashi K, Kashiwagi K (2009) Enhancement of the synthesis of RpoE and StpA by polyamines at the level of translation in *Escherichia coli* under heat shock conditions. *J Bacteriol* 191:5348–5357
 27. Yoshida M, Kashiwagi K, Kawai G, Ishihama A, Igarashi K (2001) Polyamine enhancement of the synthesis of adenylate cyclase at the translational level and cosequential stimulation of the synthesis of the RNA polymerase σ^{28} subunit. *J Biol Chem* 276:16289–16295
 28. Yoshida M, Kashiwagi K, Kawai G, Ishihama A, Igarashi K (2002) Polyamines enhance synthesis of the RNA polymerase σ^{38} subunit by suppression of an amber termination codon in the open reading frame. *J Biol Chem* 277:37139–37146
 29. Higashi K, Kashiwagi K, Taniguchi S, Terui Y, Yamamoto K, Ishihama A, Igarashi K (2006) Enhancement of +1 frameshift by polyamines during translation of polypeptide release factor 2 in *Escherichia coli*. *J Biol Chem* 281:9527–9537

30. Higashi K, Terui Y, Inomata E, Katagiri D, Nomura Y, Someya T, Nishimura K, Kashiwagi K, Kawai G, Igarashi K (2008) Selective structural change of bulged-out region of double-stranded RNA containing bulged nucleotides by spermidine. *Biochem Biophys Res Commun* 370:572–577
31. Nishimura K, Murozumi K, Shirahata A, Park MH, Kashiwagi K, Igarashi K (2005) Independent roles of eIF5A and polyamines in cell proliferation. *Biochem J* 385:779–785
32. Nishimura K, Nakatsu F, Kashiwagi K, Ohno H, Saito T, Igarashi K (2002) Essential role of *S*-adenosylmethionine decarboxylase in mouse embryonic development. *Genes Cells* 7:41–47
33. Nishimura K, Okudaira H, Ochiai E, Higashi K, Kaneko M, Ishii I, Nishimura T, Dohmae N, Kashiwagi K, Igarashi K (2009) Identification of proteins whose synthesis is preferentially enhanced by polyamines at the level of translation in mammalian cells. *Int J Biochem Cell Biol* 41:2251–2261
34. Chappell SA, Dresios J, Edelman GM, Mauro VP (2006) Ribosomal shunting mediated by a translational enhancer element that base pairs to 18S rRNA. *Proc Natl Acad Sci USA* 103:9488–9493
35. Zuker M (2003) Mfold web server for nucleic acid folding and hybridization prediction. *Nucleic Acids Res* 31:3406–3415

Chapter 4

Posttranscriptional Regulation of Gene Expression in Epithelial Cells by Polyamines

Lan Xiao and Jian-Ying Wang

Abstract

In addition to regulating gene transcription, polyamines also potently modulate gene expression posttranscriptionally. Posttranscriptional gene regulation, which includes processes such as mRNA transport, turnover, and translation, involves specific mRNA sequences (*cis*-element) that interact with *trans*-acting factors such as RNA-binding proteins (RBPs) and microRNAs. U- or AU-rich elements (ARE) are the best characterized *cis*-acting sequences located in the 3'-untranslated regions of many labile mRNAs. Several RBPs, including AUF1, BRF1, TTP, and KSRP, promote ARE-mRNA decay through the recruitment of the ARE-bearing mRNA to sites of mRNA degradation, whereas RBPs such as HuR, HuB, HuC, and HuD stabilize target mRNAs and stimulate their translation. HuR is one of the best-studied RBPs and has emerged as a key regulator of posttranscriptional control of gene expression and its activity is tightly regulated by cellular polyamines. Ribonucleoprotein immunoprecipitation assays and biotin pull-down assays are two major methods used extensively in experiments investigating the roles and mechanisms of cellular polyamines in the posttranscriptional regulation and are described in detail in this chapter.

Key words: RNA-binding proteins, mRNA stability, and translation, Posttranscriptional regulation, Ribonucleoprotein, 3'-Untranslated regions

1. Introduction

In response to stressful environmental conditions, mammalian cells elicit rapid changes in gene expression patterns to regulate their survival, adapt to stress, and maintain homeostasis (1). In addition to the stress-modulated gene transcription, changes in posttranscriptional regulation, particularly altered mRNA turnover and translation, also potently affect the steady-state levels of many transcripts and the levels of the encoded proteins (2, 3). Posttranscriptional fate of a given mRNA is primarily controlled

by the interaction of specific mRNA sequences (*cis*-elements) with specific *trans*acting factors such as RNA-binding proteins (RBPs) (3, 4) and microRNAs (5). Ribonucleoprotein (RNP) associations regulate the intracellular transport of the mRNA and its association with the translation and decay machineries (6). Many labile mRNAs contain relatively long 3'-untranslated regions (UTRs) bearing U- and AU-rich elements (AREs) that function as determinants of mRNA stability and translation (7–10). Among the RBPs that regulate specific subsets of mRNAs are several RBPs that modulate mRNA turnover (HuR, NF90, AUF1, BRF1, TTP, KSRP) and RBPs that modulate translation (HuR, TIAR, NF90, TIA-1), collectively known as *translation and turnover-regulatory* (TTR)-RBPs (11–13). In cells responding to proliferative, immune, and stress-causing stimuli, TTR-RBPs bind to the specific sequences in the 5'- and 3'-UTRs of collections of target mRNAs and govern their turnover and translation rates (1, 3).

Polyamines (putrescine, spermidine, and spermine) are ubiquitous polycationic molecules that are found in all eukaryotic cells and are implicated in many aspects of cellular physiology (14, 15). Besides regulating transcription, polyamines also potently modulate gene expression posttranscriptionally (16). For example, increased levels of cellular polyamines by ectopic ODC overexpression inhibit the expression of growth-inhibitory genes such as p53 (17, 18), nucleophosmin (NPM) (18, 19), JunD (18), activating transcription factor-2 (ATF2) (20), TGF- β (21), and XIAP (22) by increasing the degradation of their mRNAs, thus contributing to the stimulation of cell proliferation, while polyamine depletion increases these protein levels through stabilization of their gene transcripts, leading to growth arrest. RNP immunoprecipitation (IP) assays and biotin pull-down assays are two powerful methods used extensively in experiments investigating the roles and mechanisms of cellular polyamines in the posttranscriptional regulation of gene expression and they are to directly determine interactions of RBPs with given mRNAs *in vitro* as well as *in vivo*.

2. Materials

2.1. RNP-IP Assays

1. Polysome lysis buffer (PLB): 100 mM KCl, 5 mM MgCl₂, 10 mM Hepes (pH 7.0), 0.5% Nonidet P-40, 1 mM Dithiothreitol (DTT), 100 units/ml RNaseOUT (Invitrogen), Complete Protease Inhibitor Cocktail (Roche) (see Note 1).
2. Normal mouse IgG (Santa Cruz Biotechnology).

3. Anti-HuR antibody (Santa Cruz Biotechnology) and/or other antibodies against different RBPs, based on your interests.
4. Protein A-Sepharose (PAS beads) such as PAS beads from Sigma (P-3391). In a 50-ml tube, swell beads in 15 ml 5% BSA at 4°C overnight. Next day, discard excess BSA solution to make 50% (v/v) bead slurry and keep at 4°C. For long-term storage, add 0.1% Na-Azide.
5. NT-2 washing buffer: 50 mM Tris (pH 7.4), 150 mM NaCl, 1 mM MgCl₂, 0.05% Nonidet P-40.
6. Na-Azide.
7. 0.1 M DTT.
8. RNaseOUT or RNase inhibitor.
9. 0.5 M EDTA.
10. 10 mg/ml Proteinase K.
11. 10% SDS.
12. Phenol:Chloroform:Isoamylalcohol (25:24:1).
13. 3 M Sodium acetate.
14. 100% ETOH.
15. Glycogen.
16. 70% ETOH.
17. DNase I (Fermentas).
18. Chloroform.
19. Reverse Transcription System (Promega).
20. Agarose.

2.2. Biotin Pull-Down Assay

1. Polysome Extraction Buffer (PEB): 20 mM Tris-HCl (pH 7.5), 100 mM KCl, 0.3% Igepal CA-630, 5 mM MgCl₂, Complete Protease Inhibitor Cocktail (Roche) (see Note 2).
2. 2× TENT Binding buffer: 20 mM Tris-HCl (pH 8.0), 2 mM EDTA (pH 8.0), 500 mM NaCl, 1% (v/v) Triton X-100.
3. Solution A: 0.1 M NaOH, 0.05 M NaCl.
4. Solution B: 0.1 M NaCl.
5. Magnetic stand.
6. PBS.
7. Cycloheximide.
8. Gel and PCR Clean-up System (Promega).
9. 10 mM ATP, 10 mM GTP, 10 mM UTP, 10 mM CTP, 10 mM biotin-11-CTP.
10. Maxiscript T7 kit (Ambion).
11. NucAway Spin Columns (Ambion).

12. Dynabeads M-280 Streptavidin.
13. RNase inhibitor or RNaseOUT.
14. Anti-HuR antibody (Santa Cruz Biotechnology) and/or other anti-RBP antibody of interest.
15. Protein loading buffer.
16. Blocking buffer: 5% (w/v) nonfat dry milk in TBS-T.
17. TBS-T: 0.1% Tween-20 in 1× TBS.
18. Antibody stripping solution (Millipore).

3. Methods

3.1. RNP-IP

RNP-IP assays are often used to determine associations of endogenous mRNAs with endogenous RBPs. This is accomplished through the use of specific antibodies against RBPs under conditions that preserved RNP integrity (20, 23). The interactions of given mRNAs with specific RBPs such as HuR or TIAR are examined by isolating RNA from the IP material and subjecting it to reverse transcription (RT), followed by either conventional PCR or quantitative real-time (q)PCR analyses.

3.1.1. Preparation of mRNP Lysate from Cultured Cells

1. Grow cells in control medium or medium containing experimental agents such as 2-difluoromethylornithine (DFMO) in 15 cm dishes for certain times (usually 90–100% confluent). Rinse the cells with ice-cold PBS twice, scrape cells into chilled microcentrifuge tubes, and centrifuge the cells at 4°C, 2,000 rpm for 5 min (see Note 3).
2. After centrifugation, discard supernatant and loosen the cell pellets by gently flicking the bottom of the tubes and add an approximately equal pellet volume of ice-cold PLB buffer (freshly supplemented with RNaseOUT, DTT, and protease inhibitor) to the tubes. Pipette up and down the cells several times to mix and place the samples on ice for 10 min. Samples can be stored at –80°C or continue to the next step.
3. At the time of use, thaw the mRNP lysate on ice and centrifuge at 4°C, 14,000 rpm for 30 min. Transfer supernatants to chilled microcentrifuge tubes.
4. To preclear the supernatants, add 15 µg normal mouse IgG to each sample and incubate on a rotator at 4°C for 30 min. Then, add 50 µl PAS beads (without antibody coated) to the mixture and incubate on a rotator for another 30 min at 4°C.

5. Spin down the beads by brief centrifugation and save supernatants as precleared samples. Measure the protein concentration by Bradford methods (24) and the samples can be kept at -80°C . For optimal results, use 1.5–3 mg protein of each sample for precipitation assay.

3.1.2. Coating Protein A-Sepharose (PAS) Beads with Anti-HuR Antibody

1. Each assay will need 100 μl coated beads so we prepare 300 μl in total. Add 90 μg anti-HuR antibody (or other anti-RBP antibody of interest) and 300 μl NT-2 buffer to 300 μl PAS beads, mix, and incubate on a rotator overnight at 4°C (see Note 4).
2. Next day, spin down the beads by brief centrifugation and discard the supernatant without disturbing the beads. Wash the beads: add 1 ml ice-cold NT-2 buffer to the beads and vortex for 5 s, spin down the beads, and discard the supernatant. Repeat washing for a total of 5 times. After the last wash, resuspend the beads with NT-2 buffer to the final volume of 300 μl . The beads are now ready to be used. The beads can also be stored at 4°C with 0.1% Na-Azide.

3.1.3. Immunoprecipitation of mRNPs

1. Prepare three 1.5 ml microcentrifuge tubes that are labeled with “control,” “DFMO,” and “D+Put.” In each tube, mix 100 μl precoated beads with 500 μl NT-2 buffer. Then add following additives to each: 10 μl 0.1 M DTT, 10 μl RNaseOUT, 33 μl 0.5 M EDTA. After a brief vortex, add 100 μl lysate (or 1.5–3 mg) and more NT-2 buffer to a final volume of 1 ml for each precipitation reaction (see Note 5).
2. Incubate on a rotator for 2 h at room temperature. Spin down the beads and discard the supernatant (or save if analysis of binding efficiency is desired).
3. Wash the beads: add 1 ml ice-cold NT-2 buffer to the beads and vortex for 5 s, spin down the beads, and discard the supernatants. Repeat washing for a total of 5 times (see Note 6).
4. After last wash, add the following to the beads in each tube: 5 μl Proteinase K (10 mg/ml), 1 μl 10% SDS, and 100 μl NT-2. Incubate at 55°C , 700 rpm for 15–30 min on Thermomix.
5. After incubation, centrifuge the tubes at 4°C , 14,000 rpm for 2 min. Transfer the supernatant (about 100 μl /sample) to new prelabeled chilled tubes.
6. Add another 200 μl NT-2 buffer to the beads in each tube, vortex to mix and spin down the beads again at the same condition. Combine this new supernatant with the previous one to get a total of 300 μl supernatant (containing mRNP complex) for each sample. Discard the beads.

3.1.4. RNA Isolation and RT-PCR Analysis

1. Add 800 μl mixture of Phenol:Chloroform:Isoamylalcohol (25:24:1) to each 300 μl of supernatant and vortex for 1 min. Then centrifuge the samples at room temperature, 14,000 rpm for 1 min (see Note 7).
2. Carefully transfer the clear upper layer (about 300 μl /each) into new chilled microcentrifuge tubes and add 30 μl 3 M sodium acetate, 650 μl 100% ETOH, and 5 μl glycogen. Mix well and leave the samples at -20°C . You can stop here or continue the procedure after 1 h freezing.
3. Take out the samples and centrifuge directly at 4°C , 14,000 rpm for 30 min. You will see white solid pellet lying on the bottom of each tube after centrifugation (see Note 8). Discard supernatant carefully without disturbing the pellet.
4. Clean the pellet with 1 ml of ice-cold 70% ETOH, then spin down it at 4°C , 14,000 rpm for 2 min. Discard supernatant and air dry the pellet. Resuspend the pellet in 15 μl of RNase-free water at 65°C for 1–5 min.
5. Use DNase I for DNA removal: to each sample, add 2 μl of 10 \times reaction buffer, 1 μl water, 2 μl DNase I (Fermentas) for a total volume of 20 μl . Keep the reaction at 37°C for 30 min.
6. Add 80 μl of water and 100 μl of Phenol:Chloroform:Isoamylalcohol (25:24:1) to each reaction and vortex for 2 min. Then centrifuge the samples at 4°C , 14,000 rpm for 10 min. Carefully transfer the clear upper layer (about 100 μl /each) into new chilled microcentrifuge tubes.
7. Add equal volume of Chloroform to each sample and vortex vigorously for 20 s. Centrifuge at 4°C , 14,000 rpm for 10 min.
8. Carefully transfer the clear upper layer into new chilled microcentrifuge tubes and add 10 μl of 3 M sodium acetate, 250 μl of 100% ETOH, and 2.5 μl glycogen. Mix well and keep the samples in -20°C for 1 h or overnight if you need a stop here.
9. Take out the samples and centrifuge directly at 4°C , 14,000 rpm for 30 min. Discard supernatant carefully.
10. Wash pellet with 70% ice-cold ETOH and then spin down it at 4°C , 14,000 rpm for 5 min. Discard supernatant and air dry pellet. Resuspend the pellet in 15 μl of RNase-free water at 65°C for 1–5 min. You can store the RNA at -80°C or continue to do rt-PCR (see Note 9).
11. We use Reverse Transcription System (Promega A3500) for cDNA synthesis. You will need 3–5 μl of RNA for each reaction. Mix the RNA with 4 μl of 25 mM MgCl_2 , 2 μl of Reverse Transcription 10 \times Buffer, 2 μl of 10 mM dNTP Mixture, 0.5 μl of Recombinant RNasin[®] Ribonuclease Inhibitor, 15 unit of AMV Reverse Transcriptase, 0.5 μg of Oligo(dT)15 Primer, and add nuclease-free water to a final volume of 20 μl . Incubate

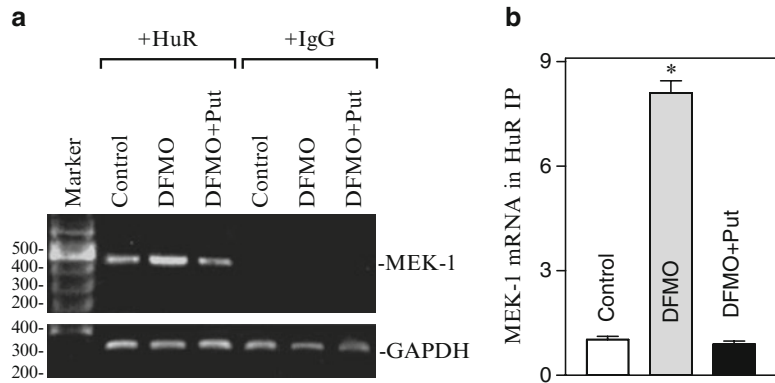


Fig. 1. Levels of association of endogenous HuR with endogenous MEK-1 mRNA in intestinal epithelial cells after polyamine depletion. IEC-6 cells were exposed to DFMO alone or DFMO plus putrescine for 6 days. After immunoprecipitation (IP) of RNA–protein complexes from cell lysates using either anti-HuR antibody (Ab) or control IgG1, RNA was isolated and used in RT reactions. (a) Representative RT-PCR products visualized in ethidium bromide-stained agarose gels; low-level amplification of GAPDH (housekeeping mRNA, which is not HuR targets) served as negative controls. (b) Fold differences in MEK-1 transcript abundance in HuR IP compared with IgG IP, as measured by quantitative real-time PCR analysis. Values were means \pm SE from triplicate samples. * $p < 0.05$ compared with controls and cells treated with DFMO plus Put.

the reaction at 42°C for 15 min and then heat the sample at 95°C for 5 min. Keep the reactions at 0–5°C for 5 min before keeping the first-strand cDNA at –20°C until use.

- For PCR amplification, follow the routine protocol in your lab and view the results in agarose gel. You can also do real-time PCR to analyze your results. We usually do both and GAPDH is one of the choices for loading control. An example of the results presented in Fig. 1 shows levels of association of endogenous HuR with endogenous MEK-1 mRNA after polyamine depletion in intestinal epithelial cells (IECs).

3.2. Biotin Pull-Down Assays

Biotin pull-down assays are commonly used to analyze RBPs bound to biotinylated RNAs *in vitro*. The synthesis of biotinylated transcripts and analysis of RBPs bound to biotinylated RNA are done as previously described (19, 20). Complementary DNA from cells is used as a template for PCR amplification of the coding regions (CR), 3'-UTR and 5'-UTR of given mRNAs, and PCR-amplified products are used as templates to transcribe biotinylated RNAs by using T7 RNA polymerase in the presence of biotin-cytidine 5'-triphosphate as described (19). For biotin pull-down assays, biotinylated transcripts are incubated with cytoplasmic lysate isolated from different groups of cells at room temperature. Complexes are isolated with paramagnetic streptavidin-conjugated Dynabeads and analyzed by Western blot analysis.

3.2.1. Preparation of Cytoplasmic Lysate from Cultured Cells

1. Grow IEC-6 cells in control, DFMO, and DFMO plus putrescine medium in 15 cm dishes for 6 days. Add fresh cycloheximide directly to the cell culture media to a final concentration of 0.1 mg/ml and keep the cells in incubator for another 5 min. At the same time, prepare 90 ml of ice-cold PBS by adding 9 mg cycloheximide for the next washing step.
2. Take out the dishes from the incubator and keep them on ice. Remove the cell media and wash the cells twice with ice-cold PBS (0.1 mg/ml cycloheximide added).
3. After washing, add 300 μ l of PEB to each plate and scrape cells off the plates. If you have more than one plate for each group, transfer the lysis buffer to the next plate and collect cells together.
4. Transfer the lysates to prechilled microcentrifuge tubes and incubate the lysates on ice for 10 min with occasional vortex.
5. Centrifuge the tubes at 4°C, 10,000 rpm for 10 min. Transfer the supernatants to fresh tubes. Measure the protein concentration by Bradford Assay and store the samples at -80°C (see Note 10).

3.2.2. Preparation of cDNA Probes

1. The pull-down probe is made from the PCR product of your interested RNA target beginning with T7 RNA polymerase promoter, so design the primer set with T7 promoter sequence 5'-CCAAGCTTCTAATACGACTCACTATAGGGAGA-3' in sense primer. For example: to amplify rat p53 3'UTR (untranslated region), we used the primers shown in the chart below (19):

Sense

CCAAGCTTCTAATACGACTCACTATAGGGAGA
TGACTCAGACTGACATTCTTCC

Antisense

TGGCAGCAAAGTTTTATTGTAAAATAAGAGATCG

2. For PCR amplification, follow the routine protocol in your lab and view the results in agarose gel (see Notes 11 and 12). Complementary DNA from IEC-6 cells is used as a template for PCR amplification.
3. Purification of PCR products. We use Promega Gel and PCR Clean-up System (A9282) to extract the cDNA. Please measure the probe concentration after extraction.

3.2.3. In Vitro Transcription Reaction of Biotinylated RNA Probe

1. Prepare biotin-11-CTP nuclear mixture in a fresh tube: 1 μ l of 10 mM ATP, 1 μ l of 10 mM GTP, 1 μ l of 10 mM UTP, 0.6 μ l of 10 mM CTP, 0.4 μ l of 10 mM biotin-11-CTP.
2. Perform in vitro transcription reaction (Maxiscript T7 kit from Ambion) in a fresh tube: 1 μ g of template cDNA (acquired

from step 2), 2 μl of 10 \times transcription buffer, 4 μl of biotin-11-CTP nuclear mixture, 2 μl of T7 RNA polymerase, and add nuclease-free water to a final volume of 20 μl . Mix well, centrifuge briefly, and incubate at 37°C for 60 min.

3. Add 1 μl of DNase I to the reaction and keep it incubated for another 15 min to remove the template.

3.2.4. Probe Purification by NucAway Spin Columns (Ambion)

1. Add 650 μl of 2 \times TENT buffer to the column and mix well. Keep it in room temperature for 15 min before centrifugation at 750 $\times g$ for 2 min. Discard flowthrough.
2. Add the biotinylated RNA probe you get from the last step into the column and centrifuge at 750 $\times g$ for 2 min. Collect the flowthrough (probe ready for pull-down) in a fresh tube and keep it in -80°C (see Note 13).

3.2.5. Pull-Down Assay

1. Preparation of pull-down beads. For each reaction, you will need 10 μl of beads with covalently bound streptavidin (Dynabeads M-280 Streptavidin). We use 30 μl for three reactions: control, DFMO, and DFMO plus putrescine. Before use, the beads need to be washed twice with 200 μl of Solution A and another twice with 200 μl of Solution B. Between each wash, keep the beads on magnetic stand long enough till particles are completely attached to the wall of the tube. After wash, restore the beads volume by adding 30 μl of 1 \times TENT buffer and keep them on ice.
2. Binding reaction. For each reaction, mix 40 μg of protein lysate with 4 μl of biotinylated probe, 25 μl of 2 \times TENT buffer, 25 units of RNase inhibitor or RNaseOUT, and water to a final volume of 50 μl (see Note 14). Incubate on a rotator with gentle mixing for 30 min at room temperature. Add 10 μl of prewashed beads to each reaction and continue incubation on rotator for another 30 min.
3. Spin down the beads and wash the beads twice with ice-cold PBS.
4. Add 10–30 μl of protein loading buffer to each reaction and boil the beads for 5 min.
5. Settle the beads on the magnetic stand.

3.2.6. SDS-Polyacrylamide Gel Electrophoresis (SDS-PAGE)

1. Use any gel system you feel comfortable with in your lab to separate the protein sample. We use Bio-Rad ready gel system.
2. Load equal amount of supernatant from each reaction into a well of 10% gel. Include one well for prestained molecular weight markers. Run the gel at 100 V in room temperature (less than 2 h) until the dye front reaches the bottom or the marker of 34 kDa (the weight of HuR) runs to desired position.

3.2.7. Western Immunoblotting Analysis

1. The samples that have been separated by SDS-PAGE are transferred to supported nitrocellulose electrophoretically. We use Mini Trans Blot tank system for transferring. Transfer can be accomplished at 100 V for 1 h.
2. Once the transfer is completed, carefully disassemble the cassette and take out the membrane.
3. Block the nitrocellulose with 10 ml 5% milk for 30 min to 1 h at room temperature on a rocking platform. Discard the blocking buffer and add 1:1,000 diluted anti-HuR antibody (or other antibody of your interest) in blocking buffer to the membrane. Keep the membrane in room temperature for 1 h or cold room overnight on a rocking platform.
4. Remove the primary antibody and wash the membrane 3 times for 10 min each with TBS-T.
5. The secondary antibody should be freshly made and added as 1:5,000-fold dilution in blocking buffer. Keep the membrane in room temperature for 1 h on a rocking platform.
6. Remove the secondary antibody and wash the membrane 3 times for 10 min each with TBS-T.

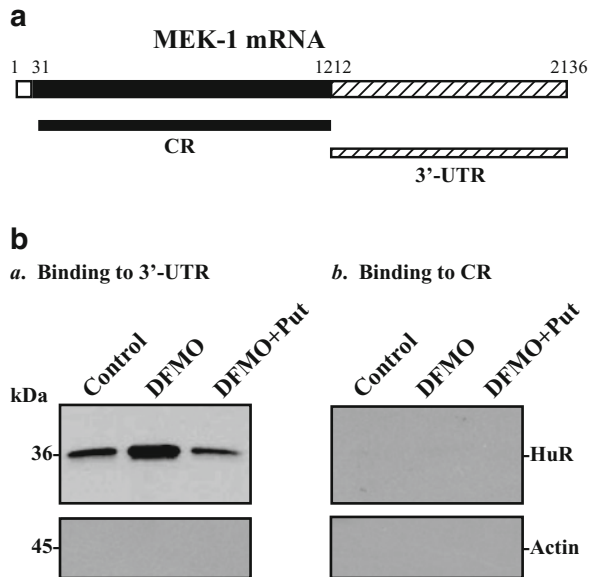


Fig. 2. HuR-binding to the 3'-UTR and coding region (CR) of MEK-1 mRNA after polyamine depletion. **(a)** Schematic representation of the MEK-1 biotinylated transcripts (CR and 3'-UTR) used in this study. **(b)** Representative HuR immunoblots using the pull-down materials by different fractions of MEK-1 mRNA after polyamine depletion: **(a)** HuR-binding to 3'-UTR; and **(b)** HuR-binding to CR. Cytoplasmic lysates prepared from control cells and cells exposed to DFMO alone or DFMO plus Put for 6 days were incubated with 6 μ g of biotinylated MEK-1 3'-UTR or CR for 30 min at 25°C, and the resulting RNP complexes were pulled down by using streptavidin-coated beads. The presence of HuR in the pull-down material was assayed by Western blotting. β -actin in the pull-down material was also examined and served as a negative control.

7. After last wash, add the mixed ECL reagents to the blot and place the membrane in an X-ray film cassette with film for a few seconds to 2 min.
8. Once a satisfactory exposure has been obtained, the membrane can be stripped of the signal and then re probed with other antibodies. Actin is usually used as a negative control. An example of the results presented in Fig. 2 shows representative HuR immunoblots using the pull-down materials by different fractions of MEK-1 mRNA in IECs after polyamine depletion.

4. Notes

1. It is better to add DTT, RNaseOUT, protease inhibitor freshly to the buffer before use. Otherwise, aliquot the complete buffer in small amount and store in -20°C .
2. Add protease inhibitor freshly to the buffer before use. Otherwise, aliquot the complete buffer in small amount and store at -20°C .
3. You may need two dishes for each sample if the protein yield is low in your system.
4. From this step, only use RNase-free microcentrifuge tubes and water through the whole experiment.
5. Do not add DTT to the pellet directly.
6. If high background is a problem in your result, try to add 1 M urea in NT-2 buffer and rinse the beads twice after last wash. We have never needed to use this step in our case.
7. You can always use commercial RNA isolation kit for this RNA extraction step, which can greatly save your time but costs more money (if you have had chemicals ready for traditional trizol isolation in your lab). However, according to our experience, you can get same quality result in either way. RNA isolation kit is available from a lot of companies like Qiagen, Invitrogen, etc. Follow the manufacturer's instruction if you use kit.
8. Sometimes the pellet can be very small and almost transparent. It may sit on the side of the tube rather than right on the bottom. However, you definitely should be able to see it. Otherwise, the RNA concentration may be too low to continue the experiment.
9. It is not necessary to measure OD260 of the RNA, because it may waste most of your sample.
10. The quality of the cytoplasm fraction can be checked by Western Blotting.

11. If the cDNA size has been confirmed first and there is no nonspecific PCR product, you can purify the PCR product directly without running a gel.
12. In order to get enough PCR products for probe preparation, you may need to run 5-20 reaction tubes and purify them together.
13. You can check the probe quality by running a RNA gel (optional).
14. 40 µg of protein lysate is a recommended starting amount, but the optimal amount may need to be empirically determined.

Acknowledgments

This work was supported by a Merit Review Grant (to J-Y Wang) from the Department of Veterans Affairs and by NIH Grants DK-57819, DK-61972, DK-68491 (to J-Y Wang). J-Y. Wang is a Research Career Scientist, Medical Research Service, US Department of Veterans Affairs.

References

1. Orphanides G, Reinberg D (2002) A unified theory of gene expression. *Cell* 108:439–451
2. Abdelmohsen K, Kuwano Y, Kim HH, Gorospe M (2008) Posttranscriptional gene regulation by RNA-binding proteins during oxidative stress: implications for cellular senescence. *Biol Chem* 389:243–255
3. Keene JD (2007) RNA regulons: coordination of post-transcriptional events. *Nat Rev Genet* 8:533–543
4. Wilusz CJ, Wilusz J (2004) Bringing the role of mRNA decay in the control of gene expression into focus. *Trends Genet* 20:491–497
5. Bhattacharyya SN, Habermacher R, Martine U, Closs EI, Filipowicz W (2006) Relief of microRNA-mediated translational repression in human cells subjected to stress. *Cell* 125:1111–1124
6. Moore MJ (2005) From birth to death: the complex lives of eukaryotic mRNAs. *Science* 309:1514–1518
7. Bakheet T, Frevel M, Williams BR, Greer W, Khabar KS (2001) ARED: human AU-rich element-containing mRNA database reveals an unexpectedly diverse functional repertoire of encoded proteins. *Nucleic Acids Res* 29:246–254
8. Chen CY, Shyu AB (1995) AU-rich elements: characterization and importance in mRNA degradation. *Trends Biochem Sci* 20:465–470
9. Espel E (2005) The role of the AU-rich elements of mRNAs in controlling translation. *Semin Cell Dev Biol* 16:59–67
10. Wilusz CJ, Wormington M, Peltz SW (2001) The cap-to-tail guide to mRNA turnover. *Nat Rev Mol Cell Biol* 2:237–246
11. Gherzi R, Lee KY, Briata P, Wegmuller D, Moroni C, Karin M, Chen CY (2004) A KH domain RNA binding protein, KSRP, promotes ARE-directed mRNA turnover by recruiting the degradation machinery. *Mol Cell* 14:571–583
12. Laroia G, Cuesta R, Brewer G, Schneider RJ (1999) Control of mRNA decay by heat shock-ubiquitin-proteasome pathway. *Science* 284:499–502
13. Stohr N, Lederer M, Reinke C, Meyer S, Hatzfeld M, Singer RH, Huttelmaier S (2006) ZBP1 regulates mRNA stability during cellular stress. *J Cell Biol* 175:527–534
14. Casero RA Jr, Marton LJ (2007) Targeting polyamine metabolism and function in cancer and other hyperproliferative diseases. *Nat Rev Drug Discov* 6:373–390

15. Seiler N, Raul F (2007) Polyamines and the intestinal tract. *Crit Rev Clin Lab Sci* 44:365–411
16. Wang JY (2007) Polyamines and mRNA stability in regulation of intestinal mucosal growth. *Amino Acids* 33:241–252
17. Kramer DJ, Chang BD, Chen Y, Diegelman P, Alm K, Black AR, Roninson IB, Porter CW (2001) Polyamine depletion in human melanoma cells leads to G1 arrest associated with induction of p21WAF1/CIP1/SDI1, changes in the expression of p21-regulated genes, and a senescence-like phenotype. *Cancer Res* 61:7754–7762
18. Zou T, Rao JN, Liu L, Marasa BS, Keledjian KM, Zhang AH, Xiao L, Bass BL, Wang JY (2005) Polyamine depletion induces nucleophosmin modulating stability and transcriptional activity of p53 in intestinal epithelial cells. *Am J Physiol Cell Physiol* 289:C686–C696
19. Zou T, Mazan-Mamczarz K, Rao JN, Liu L, Marasa BS, Zhang AH, Xiao L, Pullmann R, Gorospe M, Wang JY (2006) Polyamine depletion increases cytoplasmic levels of RNA-binding protein HuR leading to stabilization of nucleophosmin and p53 mRNAs. *J Biol Chem* 281:19387–19394
20. Xiao L, Rao JN, Zou T, Liu L, Marasa BS, Chen J, Turner DJ, Zhou H, Gorospe M, Wang JY (2007) Polyamines regulate the stability of activating transcription factor-2 mRNA through RNA-binding protein HuR in intestinal epithelial cells. *Mol Biol Cell* 18:4579–4590
21. Patel AR, Li J, Bass BL, Wang JY (1998) Expression of the transforming growth factor-beta gene during growth inhibition following polyamine depletion. *Am J Physiol Cell Physiol* 275:C590–C598
22. Zhang X, Zou T, Rao JN, Liu L, Xiao L, Wang PY, Cui YH, Gorospe M, Wang JY (2009) Stabilization of XIAP mRNA through the RNA binding protein HuR regulated by cellular polyamines. *Nucleic Acids Res* 37:7623–7637
23. Kuwano Y, Gorospe M (2008) Protecting the stress response, guarding the MKP-1 mRNA. *Cell Cycle* 7:2640–2642
24. Bradford MM (1976) A rapid and sensitive method for the quantitation of microgram quantities of protein utilizing the principle of protein-dye binding. *Anal Biochem* 72:248–254

Chapter 5

Identification, Chemical Synthesis, and Biological Functions of Unusual Polyamines Produced by Extreme Thermophiles

Tairo Oshima, Toshiyuki Moriya, and Yusuke Terui

Abstract

Unusual long polyamines such as caldopentamine and caldohexamine, and branched polyamines such as tetrakis(3-aminopropyl)ammonium and *N*³-aminopropylspermidine were often found in cells of extreme thermophiles and hyperthermophiles belonging to both Bacteria and Archaea domains. Some of these unusual polyamines are essential for life at extreme temperatures. In some cases, the unusual polyamines also exist in cells of nonthermophilic organisms and play important physiological roles under normal conditions. Methods for chromatographic analysis, isolation, and chemical syntheses of unusual polyamines as well as experimental methods for measuring their physiological roles are discussed. Especially, many newly improved methods for chemical syntheses are presented in this article.

Key words: Pentamine, Hexamine, Branched polyamine, Quaternary polyamine, Thermophiles, Protein synthesis, Depurination, Reverse genetics

1. Introduction

Most organisms, animals, plants, and microorganisms produce “the standard polyamines” which are putrescine, spermidine, and spermine; though some bacteria such as *Escherichia coli* cannot produce spermine (1). In addition to the standard polyamines, often cadaverine and agmatine are found in nature.

In contrast, extreme thermophiles (both (eu)bacterial and archaeal, including hyperthermophiles), which can grow at 75°C and higher temperatures, produce a variety of “unusual polyamines” (2–6), although moderate thermophiles such as *Geobacillus stearothermophilus* (bacteria) or *Thermoplasma acidophilum* (archaea) of which the highest growth temperature is in a range of 55–75°C, produce only standard polyamines. Unique polyamines found in extreme thermophiles are long polyamines such

as pentaamines and hexaamines, and branched polyamines such as tetrakis(3-aminopropyl)ammonium, a quaternary polyamine (5, 7–10). Systematic names and chemical structures of standard and unusual polyamines described in this article are listed in Table 1.

These unusual polyamines are more abundant if a thermophile is grown at higher temperatures; for instance, caldopentamine is

Table 1
Systematic names, trivial names, and chemical structures of polyamines described in this article

Systematic name	Trivial name	Chemical structure
1,3-Diaminopropane		$\text{NH}_2(\text{CH}_2)_3\text{NH}_2$
1,4-Diaminobutane	Putrescine	$\text{NH}_2(\text{CH}_2)_4\text{NH}_2$
1,5-Diaminopentane	Cadaverine	$\text{NH}_2(\text{CH}_2)_5\text{NH}_2$
<i>N</i> ¹ -Amino-4-guanidobutane	Agmatine	$(\text{NH}_2)(\text{NH})\text{CNH}(\text{CH}_2)_4\text{NH}_2$
1,7-Diamino-4-azaheptane	Norspermidine, caldine	$\text{NH}_2(\text{CH}_2)_3\text{NH}(\text{CH}_2)_3\text{NH}_2$
1,8-Diamino-4-azaoctane	Spermidine	$\text{NH}_2(\text{CH}_2)_3\text{NH}(\text{CH}_2)_4\text{NH}_2$
1,9-Diamino-5-azanonane	<i>sym</i> -Homospermidine	$\text{NH}_2(\text{CH}_2)_4\text{NH}(\text{CH}_2)_4\text{NH}_2$
<i>N</i> ⁸ -Guanido-1,8-diamino-4-azaoctane	Aminopropylagmatine	$(\text{NH}_2)(\text{NH})\text{CNH}(\text{CH}_2)_4\text{NH}(\text{CH}_2)_3\text{NH}_2$
1,11-Diamino-4,8-diazaundecane	Thermine	$\text{NH}_2(\text{CH}_2)_3\text{NH}(\text{CH}_2)_3\text{NH}(\text{CH}_2)_3\text{NH}_2$
1,12-Diamino-4,9-diazadodecane	Spermine	$\text{NH}_2(\text{CH}_2)_3\text{NH}(\text{CH}_2)_4\text{NH}(\text{CH}_2)_3\text{NH}_2$
1,12-Diamino-4,8-diazadodecane	Thermospermine	$\text{NH}_2(\text{CH}_2)_3\text{NH}(\text{CH}_2)_3\text{NH}(\text{CH}_2)_4\text{NH}_2$
1,13-Diamino-4,9-diazatridecane	Homospermine	$\text{NH}_2(\text{CH}_2)_3\text{NH}(\text{CH}_2)_4\text{NH}(\text{CH}_2)_4\text{NH}_2$
1,15-Diamino-4,8,12-triazapentadecane	Caldopentamine	$\text{NH}_2(\text{CH}_2)_3\text{NH}(\text{CH}_2)_3\text{NH}(\text{CH}_2)_3\text{NH}(\text{CH}_2)_3\text{NH}_2$
1,16-Diamino-4,8,12-triazahexadecane	Homocaldopentamine	$\text{NH}_2(\text{CH}_2)_3\text{NH}(\text{CH}_2)_3\text{NH}(\text{CH}_2)_3\text{NH}(\text{CH}_2)_4\text{NH}_2$
1,19-Diamino-4,8,12,16-tetraaza-nonadecane	Caldohexamine	$\text{NH}_2(\text{CH}_2)_3\text{NH}(\text{CH}_2)_3\text{NH}(\text{CH}_2)_3\text{NH}(\text{CH}_2)_3\text{NH}(\text{CH}_2)_3\text{NH}_2$
Tris(3-aminopropyl)amine	Mitsubishine	$[\text{NH}_2(\text{CH}_2)_3]_3\text{N}$
<i>N</i> ⁴ -Aminopropyl-1,8-diamino-4-azaoctane	<i>N</i> ⁴ -aminopropylspermidine	$[\text{NH}_2(\text{CH}_2)_3]_2\text{NH}(\text{CH}_2)_4\text{NH}_2$
Tetrakis(3-aminopropyl) ammonium		$[\text{NH}_2(\text{CH}_2)_3]_4\text{N}^+$

more abundant when *Thermus thermophilus* (ATCC 27634) (11) is grown at 78°C than grown at 65°C (6, 7, 9, 12). Knockout mutants of *T. thermophilus*, which cannot produce both long and branched polyamines, is unable to grow at 75°C or higher temperatures and the growth at higher temperatures can be restored by the addition of the unusual polyamines to the culture medium (Ohnuma et al. unpublished). These findings suggest that the unusual polyamines play important roles in life at high temperature extremes.

Unusual polyamines found in extreme thermophiles are also present in other microorganisms, plants, and lower animals. For instance, lobsters (13) and cockroaches synthesize thermine as the major cellular polyamine component; especially cockroaches produce long polyamines such as caldopentamine in addition to thermine (Oshima, unpublished). A branched polyamine, tetrakis(3-aminopropyl)ammonium was found in aquatic plants and in seeds of legumes (14, 15). A long polyamine, caldopentamine, was found in a mesophilic, halophilic archaeon (16).

Recently thermospermine, a structural isomer of spermine that was found for the first time in *T. thermophilus* (17) was detected in plants. In Arabidopsis, both thermospermine and spermine are biosynthesized by different enzymes, respectively, (18) and they have different physiological functions from each other; thermospermine is essential for plant vasculature and stem elongation (19, 20), whereas spermine is not essential for survival and plays a role in high salt stress (21, 22).

In this article, analysis, chemical synthesis, and biochemical functions of unusual polyamines are briefly dealt with.

2. Materials

2.1. Assay of Polyamines

1. CK-10S ion exchange column (8 mm diameter and 8 cm long). CK-10S is sulfonated polystyrene-divinylbenzene copolymer resin particles with average diameter of 11 μm , manufactured by Mitsubishi Chemical Co., and can be purchased from Nippon Rensui Co., Tokyo, Japan (see <http://www.rensui.co.jp/product/jushi.html>).
2. Other cation exchange resins used in automated amino acid analyzers can be used instead of CK-10S. A prepacked column for polyamine analysis is also available from Tosoh Co. (see <http://www.tosoh.com/Products/tcdsci2.htm#A11>). However, the commercial column uses fine resins (CK-10U; 5 μm diameter resin particles) and flow rate should be slower than 0.5 ml/min.
3. The standard elution buffer (Type 1 eluant) for CK-10S column is prepared as follows: dissolve 32.5 g of $\text{K}_3\text{C}_6\text{H}_5\text{O}_7\cdot\text{H}_2\text{O}$ (potassium citrate), 65 ml of 1M HCl, 150 g of KCl in about

800 ml purified water prepared by a Milli-Q water system (Millipore Corp.). After the salts are dissolved thoroughly, add 50 ml of 2-propanol and 10 ml of 30% Brij35 to the potassium citrate and potassium chloride solution and the final volume is adjusted to 1,000 ml. To remove invisible dust, the buffer solution is passed through a membrane filter with 0.2 μm pore size. For analysis of shorter polyamines than spermine, the KCl concentration is reduced to 125 g/l (Type 2 eluant).

4. The buffer for *o*-phthalaldehyde solution is prepared by dissolving 16.0 g of NaOH, 24.7 g of boric acid, and 20 ml of 30% Brij35 in Milli-Q water and final volume is adjusted to 1,000 ml.
5. Dissolve 10 g of *o*-phthalaldehyde in 100 ml of ethanol. The *o*-phthalaldehyde solution can be stored in a refrigerator for more than 3 months.
6. To an appropriate amount of the *o*-phthalaldehyde solution (for example, 3 ml for five samples), add 100 times volume of the borate buffer (300 ml), and then add one-fifth volume of 2-mercaptoethanol (0.6 ml) with stirring (see Notes 1 and 2). The final solution should be prepared immediately before use and should be used up within a day.
7. Trichloroacetic acid, 15%.

2.2. Chemical Syntheses of Unusual Polyamines Found in Thermophiles

2.2.1. One Pot Synthesis of Caldopentamine or Thermospermine

1. Norspermidine freebase and thermine freebase can be purchased from many reagent companies (One example is Tokyo Kasei, <http://www.tcieurope.eu/en/catalog/D0090.html>) (see Note 4)
2. 2-Propanol
3. Acrylonitrile
4. CoCl_2 (5% solution)
5. Acetic acid
6. NaBH_4 (10% solution)
7. Dowex 50W-X4.
8. 2M, 6M and 12M HCl
9. 3-Butenenitrile
10. 50% Ethanol

2.2.2. Alternative Procedure for Caldopentamine and Thermospermine or Synthesis of Sym-Homospermidine, and Homocaldopentamine

1. Reagents 1–10 as above
2. Putrescine
3. Thermine
4. *N*-(3-bromopropyl)phthalimide (Aldrich Chemical Company)
5. *N*-(4-Bromobutyl)phthalimide
6. Argon gas

2.2.3. *Synthesis
of Caldohexamine*

1. 1,3-Diaminopropane (freebase)
2. Benzaldehyde
3. Anhydrous magnesium sulfate
4. Methanol
5. Sodium borohydride
6. Ethyl acetate
7. *N*-(3-Bromopropyl)phthalimide
8. Acetonitrile
9. KF-celite
10. Anhydrous hydrazine
11. PtO₂
12. Silica gel column
13. Hexane
14. Chloroform
15. Ammonium hydroxide (25%)
16. Acetic acid
17. Ethanol
18. 12M HCl

2.2.4. *Synthesis
of Mitsubishiine
and Tetrakis(3-
Aminopropyl)Ammonium*

1. 3,3',3''-nitrilotris(propionamide)
2. Tetrahydrofuran
3. Lithium aluminum hydride
4. Argon gas
5. Dowex 50W-X4
6. Phthalic anhydride
7. Sodium acetate
8. Anhydrous magnesium sulfate
9. *N*-(3-Bromopropyl)phthalimide
10. Sodium iodide
11. Dioxane (see Note 5)
12. Hydrazine
13. Ethanol
14. 1M and 6M HCl
15. Ethyl acetate
16. Silica gel column
17. Hexane
18. Acetone (see Note 5)

2.2.5. Synthesis of
*N*⁴-Aminopropylspermidine

1. *N*-(4-aminobutyl)carbamic acid tert-butyl ester
2. *N*-(3-Bromopropyl)phthalimide
3. KF-celite
4. Acetonitrile
5. Conc. HCl
6. Hydrazine
7. Methanol
8. Chloroform
9. Ammonium hydroxide
10. Acetic acid
11. PtO₂
12. Ethanol

2.2.6. Synthesis of
Aminopropylagmatine

1. Putrescine (commercial name is 1,4-butanediamine)
2. Chloroformic acid phenyl ester
3. *N*-(3-bromopropyl)phthalimide
4. NaOH
5. KF-celite
6. Acetonitrile
7. Dowex 50W-X4
8. Dried ether
9. Hydrobromic acid (33%)
10. Acetic acid
11. Methanol
12. Ethanol
13. 1M, 6M and conc. HCl
14. 1-Guanyl-3,5-dimethylpyrazole hydrobromide prepared according to a literature (23)
15. Dowex 50W-X4
16. CD₃OH (for NMR measurement)
17. CDCl₃ (for NMR measurement)

2.3. Preparation of
Unusual Polyamines
from Cells
of *T. thermophilus*

1. Sucrose
2. Monosodium glutamate
3. K₂HPO₄
4. KH₂PO₄
5. (NH₄)₂SO₄

6. NaCl
7. $\text{MgCl}_2 \cdot 6\text{H}_2\text{O}$
8. $\text{CaCl}_2 \cdot 2\text{H}_2\text{O}$
9. Biotin
10. Thiamine
11. $\text{FeSO}_4 \cdot 7\text{H}_2\text{O}$
12. $\text{Na}_2\text{MoO}_4 \cdot 2\text{H}_2\text{O}$
13. VO_4
14. $\text{MnCl}_2 \cdot 4\text{H}_2\text{O}$
15. $\text{ZnSO}_4 \cdot 7\text{H}_2\text{O}$
16. $\text{CuSO}_4 \cdot 5\text{H}_2\text{O}$
17. $\text{CoCl}_2 \cdot 6\text{H}_2\text{O}$
18. $\text{NiCl}_2 \cdot 6\text{H}_2\text{O}$
19. Trichloroacetic acid
20. Dowex 50W-X4
21. CK-10S column
22. Potassium citrate buffer, 0.1M pH 6.0 containing 1.75M KCl
23. 1M NaOH
24. 1M, 2M and 6M HCl
25. Ethanol

**2.4. Determination
of Chemical Structure
of an Unknown
Polyamine**

1. Equipment for NMR analysis
2. D_2O

**2.5. Effects of Unusual
Polyamines on Cellular
Processes**

*2.5.1. Polyamine-Mediated
Protection of Nucleic Acid
Structures*

1. Prepacked column, Shideido Capcell Pak C18 UG 120 (<http://www.shiseido.co.jp/e/hplc/html/index.htm>).
2. KH_2PO_4 (20 mM).
3. 28-mer deoxyribo-oligonucleotides (commercially available from many suppliers).
4. SSC solution (0.15M NaCl, 0.015M sodium citrate, pH7.0).

*2.5.2. Polyamine-Mediated
Stimulation of In Vitro
Protein Synthesis*

1. S30 cell-free extract from *T. thermophilus*, or *T. thermophilus* ribosomes and S-100 extract
2. 20 mM Tris-HCl buffer, pH 7.5, containing 10 mM MgCl_2 , 50 mM ammonium chloride, and 6 mM 2-mercaptoethanol
3. DEAE-cellulose

4. [³H]Phenylalanyl-tRNA
5. ATP
6. GTP
7. *T. thermophilus* or *E. coli* tRNA
8. Poly(U) or phage MS2 RNA
9. 20 proteinaceous amino acids
10. Trichloroacetic acid

2.5.3. Reverse Genetics of Genes Involved in Polyamine Metabolism of T. thermophilus

1. Plasmid pBH_{TK}, which contains heat-stable kanamycin resistant gene H_{TK}, can be obtained from Prof. Seiki Kuramitsu of Osaka University, Department of Biology, 1-1 Yamadaoka, Suita, Osaka 565-0871, Japan.
2. Heat-stable hygromycin B resistant gene can be obtained from Prof. Akira Nakamura of Tsukuba University, Graduate School of Life and Environmental Sciences, 1-1 Tennodai, Ibaraki 305-8571, Japan.
3. Chromosomal DNA and genes (ORFs) of *T. thermophilus* can be obtained from Riken upon request (http://www.brc.riken.jp/lab/dna/en/thermus_en.html). The chromosomal DNA is also available from a commercial company (Takara Bio Inc., <http://www.takara-bio.co.jp/>).
4. Plasmids for construction of knockout mutants of about 50% of ORFs of the thermophile genome can also be provided from Riken, but unfortunately at present only *speDI* (putative activator for S-adenosylmethionine decarboxylase) depleted mutant is available among the genes involved in polyamine metabolism.
5. Wizard plus SV Minipreps DNA Purification System (Promega).
6. Takara Ligation Kit ver2 Solution 1.
7. Kanamycin. (50 mg/ml).
8. Hygromycin B.
9. Yeast extract.
10. Polypeptone.
11. Glucose.
12. NaCl.
13. CaCl₂ 2H₂O.
14. MgCl₂ 6H₂O.
15. Agar

3. Methods

3.1. Determination of Polyamine Composition Using HPLC

Cellular polyamines can be analyzed by using a high performance liquid chromatography (HPLC) (6–8), gas chromatography (GC) (24, 25), or thin-layer chromatography (TLC) (26). The most convenient way is HPLC with a column of cation exchange resin. Cell extracts can be directly applied on an HPLC column without any prior treatment and the same technique can be used for the isolation and purification of polyamines from living organisms. However, thermospermine cannot be separated from spermine on HPLC whereas, GC can be used for separation of these tetraamines. In contrast, GC requires derivatization of polyamines (for example, heptafluorobutylation) prior to the chromatographic analyses. Derivatized quaternary polyamines are unstable and degraded during the GC. Thus, each assay method has advantages and disadvantages over other methods. The method described below using CK-10S column chromatography has a sensitivity of around 20 pmol per 100 μ l sample.

1. Sample preparation. About 0.2–0.4 g wet weight cells are suspended in 2–4 ml respectively in water and polyamines are extracted by adding same volume of 15% trichloroacetic acid. After removal of cell debris by centrifugation, pass through a membrane filter with 0.2 μ m pore size. An aliquot of the filtrate should be diluted to appropriate concentration with Milli-Q water (usually around 10 times) and applied to the analytical column.
2. The original report for the method is in Ref. (8), but the method has been modified. The CK-10S column is located in a column oven of which temperature is regulated at 70°C and eluted with a single eluant containing potassium citrate and KCl using an HPLC pump at a constant rate of 2 ml/min. A stainless steel filter, SS Line Filter (GL Sciences, Tokyo) is added between 100 μ l autosampler and the CK-10S column to protect the column from fine dust and insoluble precipitates contaminated in the sample. The samples (100 μ l each) are applied to the column using an automatic sampler at a certain interval (normally every 30–60 min). It is not necessary to wash the column after each analysis (see Note 3).
3. The effluent from the column is mixed with *o*-phthalaldehyde solution supplied by the second pump at a rate of 1 ml/min. Then the mixed effluent is sent to a fluorescence detector made by Hitachi Co. (<http://www.hitachi-hitec.com/global/>), model L-2480. The signals from the detector are recorded on a pen recorder and/or stored in a data logger coupled with a computer. Figure 1 is a schematic illustration of the polyamine analyzer. An example of polyamine analysis is shown in Fig. 2.

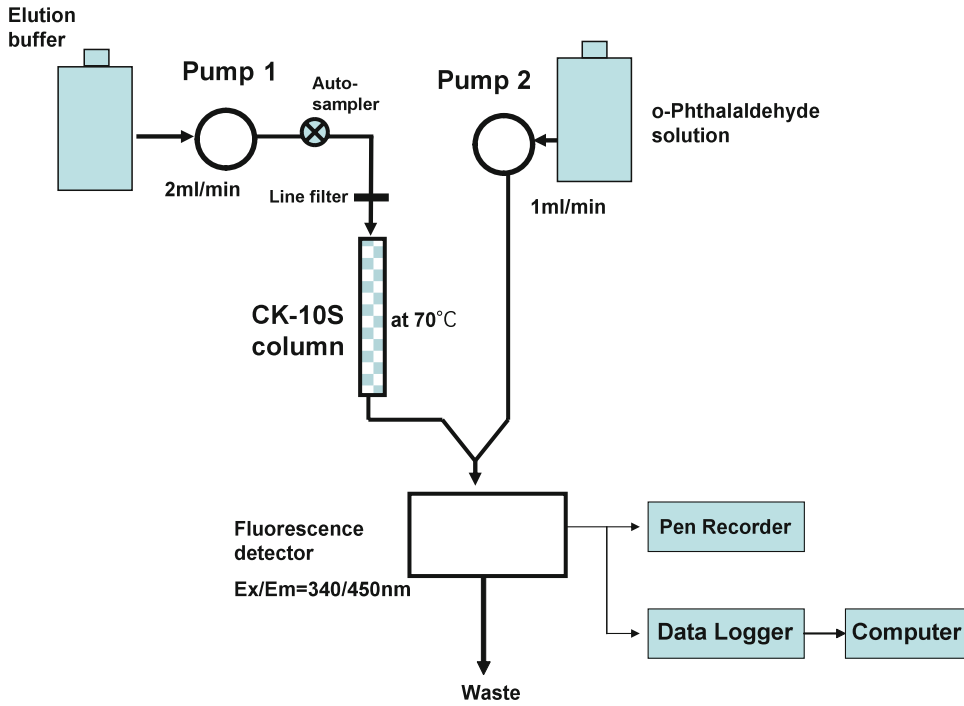


Fig. 1. Schematic diagram of polyamine analyzer.

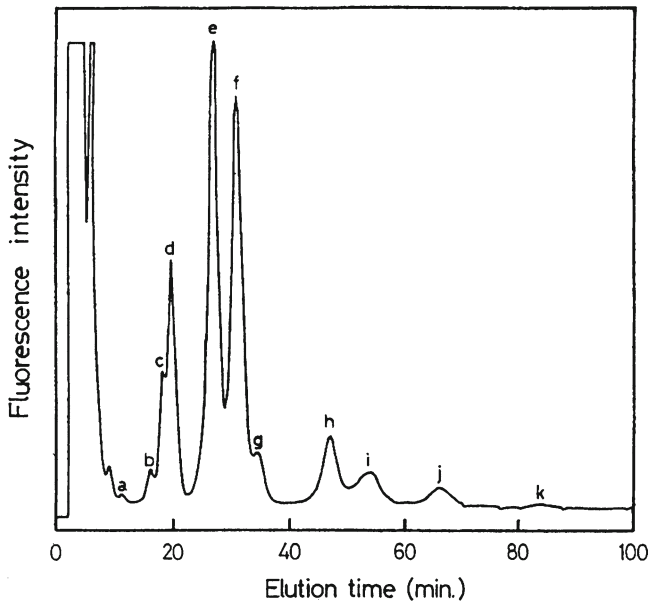


Fig. 2. An example of polyamine analysis of *T. thermophilus* cell extract. Polyamines are *a* putrescine; *b* caldine (norspermidine); *c* spermidine; *d* sym-homospermidine; *e* thermine; *f* spermine/thermospermine; *g* homospermine; *h* caldopentamine; *i* homocaldopentamine; *j* tetrakis(3-aminopropyl)ammonium; *k* unidentified.

3.2. Chemical Syntheses of Unusual Polyamines Found in Thermophiles

Most of unusual polyamines are not available from commercial companies and should be synthesized chemically or extracted from thermophile cells. Unusual linear polyamines can be synthesized by the addition of one or two aminopropyl or aminobutyl group(s) to the terminal primary amino nitrogen atoms of a shorter polyamine. For instance, caldopentamine can be synthesized by the addition of an aminopropyl group to either end of thermine. Caldohexamine can be obtained by the addition of aminopropyl groups to the both ends of thermine. Likewise, thermospermine and homocaldopentamine (27) can be synthesized by the addition of an aminobutyl group to an end of norspermidine and spermine, respectively. Chantrapromma et al. reported a sophisticated method for thermospermine synthesis (28).

Often these synthetic reactions can be completed in a single test tube and any sophisticated techniques are not required if the yield is not course of concern. In contrast, syntheses of branched polyamines need elaborated skills of organic chemistry. Especially quaternary polyamines are difficult to synthesize (10). Tertiary polyamines such as mitsubishine can be prepared from an intermediate in quaternary polyamine synthesis as shown below. In the following sections, ^{13}C - and ^1H -NMR spectra were measured in D_2O otherwise mentioned.

3.2.1. One Pot Synthesis of Caldopentamine or Thermospermine

1. The reactions for caldopentamine synthesis are illustrated in Fig. 3a. Dissolve 188 mg of thermine freebase (1) in 5 ml of 2-propanol in a Pyrex test tube. Add 53 mg of acrylonitrile to the test tube. After 16 h at room temperature, add 5 ml of 5% CoCl_2 solution. The pH of the mixture should be adjusted to six by dropwise addition of acetic acid and use of a pH test paper. Then add 5 ml of 10% NaBH_4 solution dropwise and pH should be adjusted to six during the addition of NaBH_4 . After the addition of the reducing agent, the mixture should be refluxed for 1 h. Caldopentamine (2) thus formed can be purified using a Dowex 50W-X4 column (H^+ -form, 1.8 cm diameter \times 22 cm long). The column was washed with water and then 2M HCl. The polyamine can be eluted with 6M HCl. The fractions containing caldopentamine were combined and evaporated to dryness under reduced pressure. If high purity is concerned, the synthesized polyamine can be purified by using CK-10S cation exchange column chromatography developed with the same buffer described in 2.1. The hydrochloride salt was crystallized from a hot 50% ethanol. The yield was 100 mg.

^1H -NMR; 2.1 (8H), 3.2 (16H) (for assignment, see Fig. 4)

^{13}C -NMR; 26.8, 28.0, 38.8, 46.4, 46.8

2. Likewise, thermospermine can be synthesized in the same way by using norspermidine and 3-butenenitrile ($\text{CH}_2=\text{CHCH}_2\text{CN}$) instead of acrylonitrile.

3.2.2. *Alternative Procedure for Synthesis of Caldopentamine, Thermospermine, Sym-Homospermidine, or Homocaldopentamine*

1. Caldopentamine can be synthesized by treating thermine freebase with equal molar amount of *N*-(3-bromopropyl)phthalimide as shown in Fig. 3b. Dissolve 2.3 g of thermine freebase (**1**) in 120 ml of 2-propanol. Add 4.00 g of *N*-(3-bromopropyl)phthalimide and the mixture was refluxed for 20 h under argon gas. Add about 5 ml of 12M HCl after cooling to room temperature. Reflux again for 10 h. Remove the solvent by evaporation under reduced pressure. Dissolve the residue in 10 ml water and remove the insoluble materials by filtration. Apply the filtrate on a Dowex 50W-4X column

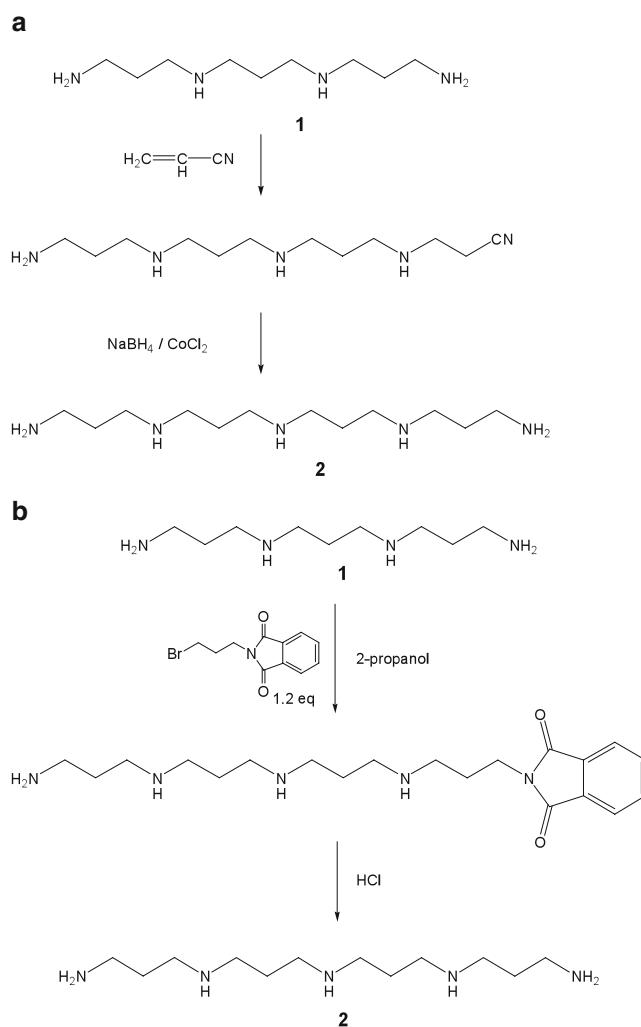


Fig. 3. Schemes for synthesis of polyamines found in thermophiles. (a) Synthesis of caldopentamine. (b) Synthesis of caldopentamine (alternative process).

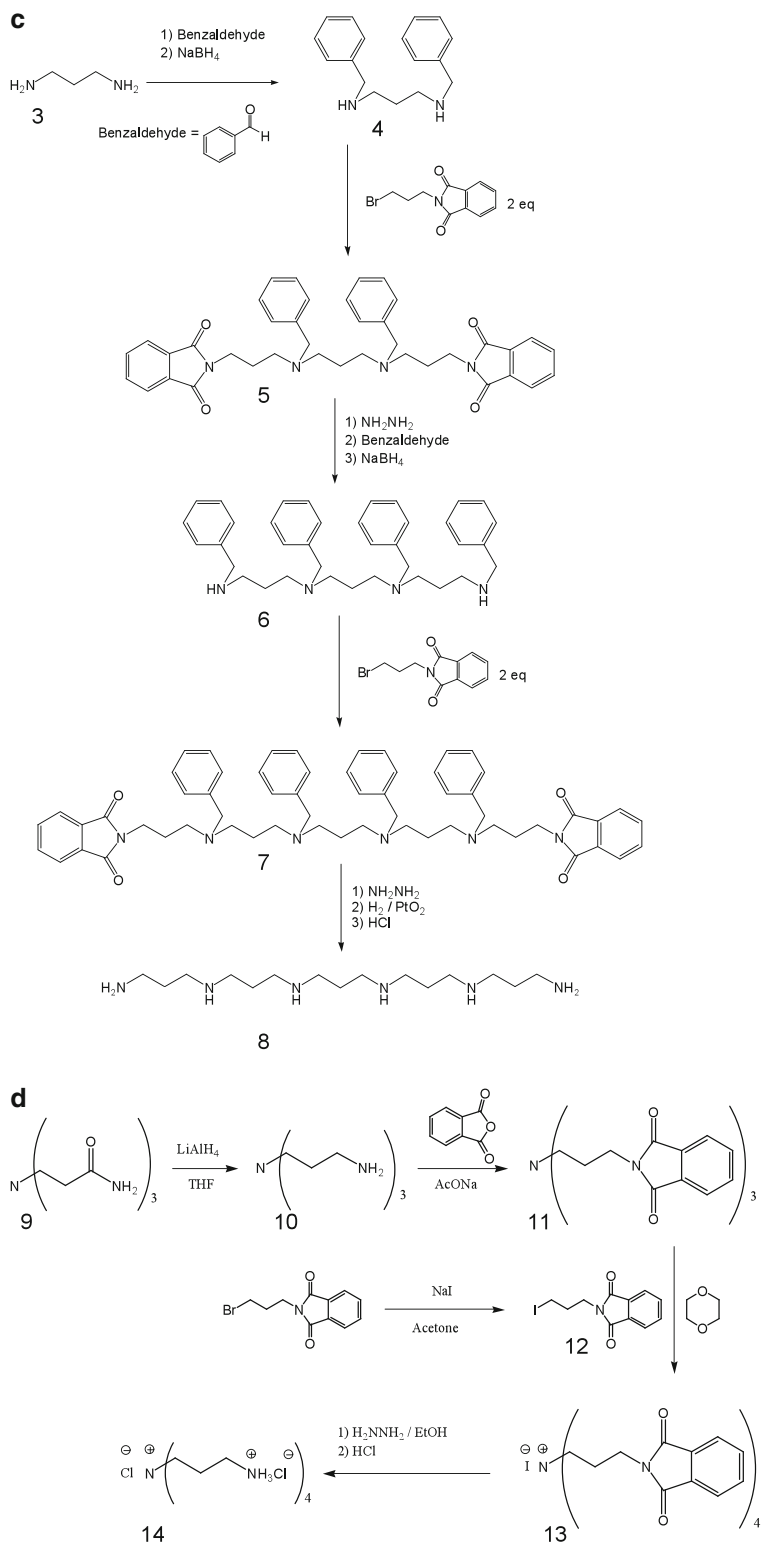


Fig. 3. (continued) (c) Synthesis of caldohexamine. (d) Synthesis of tetrakis(3-aminopropyl) ammonium.

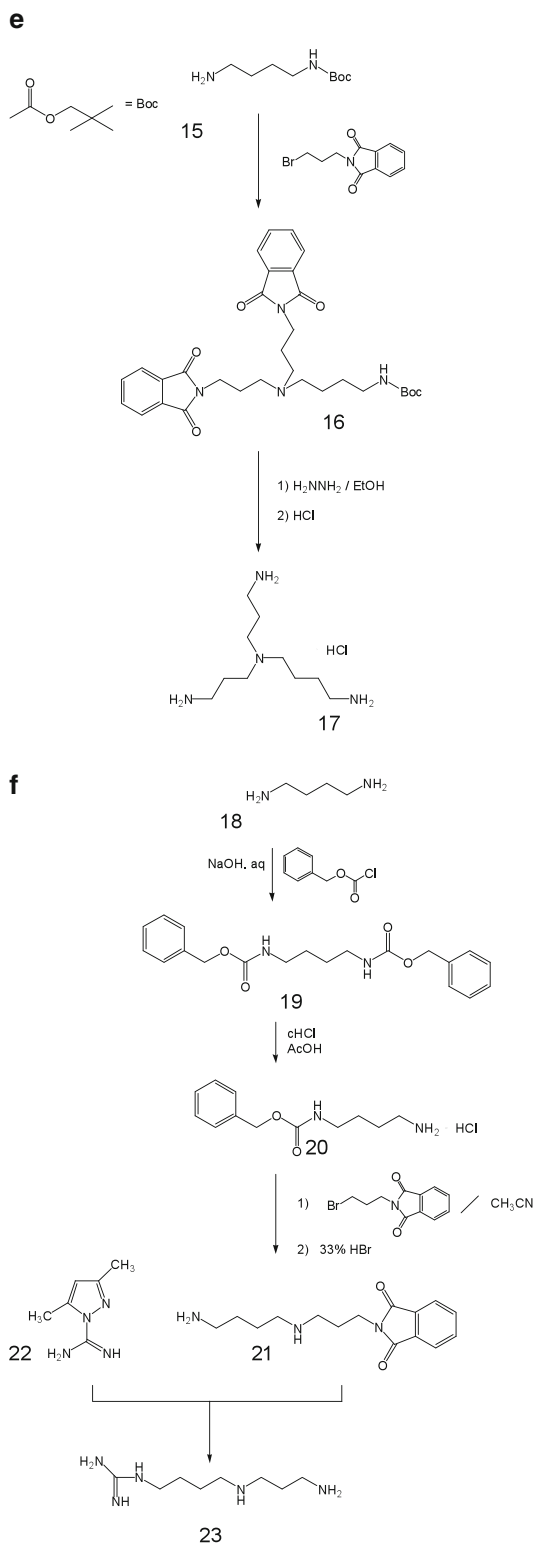
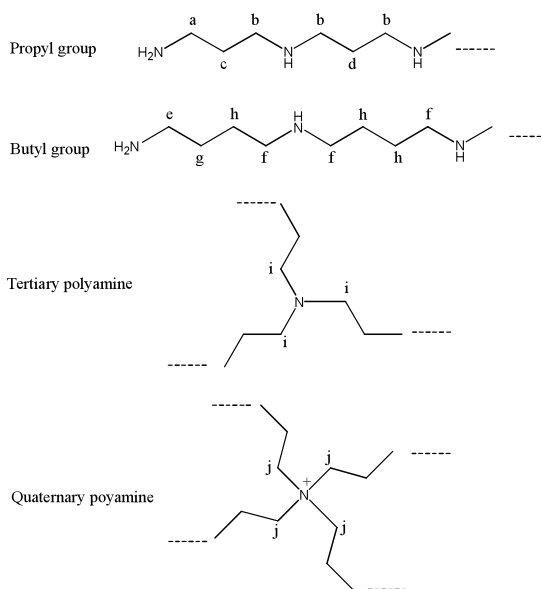


Fig. 3. (continued) (e) Synthesis of *N*⁴-aminopropylspermidine. (f) Synthesis of amino-propylagmatine.

Methylene group	$^1\text{H-NMR}$ δ (ppm)	$^{13}\text{C-NMR}$ δ (ppm)
a: adjacent to an aminopropyl terminal NH_2	3.2	37-39
b: adjacent to an NH group, in a propyl group		45-46
c: middle of an aminopropyl terminal	2.1	23-24
d: middle of a propyl group between two NH groups		24-25
e: adjacent to an aminobutyl terminal NH_2	3.2	37-39
f: adjacent to an NH group, in a butyl group		46-48
g: second methylene from an aminobutyl terminal NH_2	1.8	23-24
h: second methylene from an NH group, in a butyl group		22-23
i: adjacent to a tertiary amino nitrogen	3.5	52
j: adjacent to a quaternary amino nitrogen	3.6	57



NMR data for a polyamine isolated from *T. thermophilus*

$^1\text{H-NMR}$ δ (ppm)	1.8(1)*, 2.1(1)*, 3.2(3)*
$^{13}\text{C-NMR}$ δ (ppm)	23.5, 23.6, 24.6, 24.8, 37.4, 39.6 45.3, 45.5, 45.6, 47.9

*Figures in parenthesis are relative intensity.

Fig. 4. Empirical assignments of signals recorded on $^1\text{H-NMR}$ and $^{13}\text{C-NMR}$ spectra of polyamines.

(2.8 cm diameter 22 cm long, H^+ -form). The formed caldopentamine (2) should be purified by ion exchange column chromatography as described in Subheading 3.2.1, and the hydrochloride salt can be crystallized from 50% hot ethanol. The final yield was 15.1%.

$^1\text{H-NMR}$; 2.10 (8H, m), 3.19 (16H, t)

$^{13}\text{C-NMR}$; 22.64, 23.71, 36.50, 44.56, 44.71

2. *sym*-Homospermidine, thermospermine, and homocaldopentamine (27) can be prepared from putrescine, norspermidine, and thermine, respectively, using *N*-(4-bromobutyl)phthalimide instead of *N*-(3-bromopropyl)phthalimide in a similar manner.

3.2.3. Synthesis of Calдохexamine

The methods for linear polyamine syntheses described in Subheading 3.2.1 are simple and need no skill of organic synthesis. However, due to by-products formation, yields are often poor. To improve the yield, secondary amino nitrogen atoms of the starting polyamines should be protected. In this section, an improved method with protection of the secondary amino groups is described. As an example, calдохexamine synthesis is presented (see Fig. 3c, Terui et al. unpublished). Samejima and his colleagues (29) synthesized a variety of pentaamines (ten chemical species).

1. Dissolve 3.0 ml of 1,3-diaminopropane (freebase) (7), 9.06 ml of benzaldehyde, and 6.0 g of anhydrous magnesium sulfate in 40 ml of methanol. Stir for 1 h at room temperature.
2. Add 7.0 g of sodium borohydride carefully after the solution was cooled in an ice bath and diluted with 10 ml of additional methanol. Stir for 1 h and then evaporate the solvent under reduced pressure. The product was extracted with ethyl acetate 3 times, combine the extracts and evaporate to dryness under reduced pressure. Crude *N*¹,*N*⁴-dibenzyl-1,3-diaminopropane (3) (9.87 g, colorless oil) will be obtained.
3. Add 9.87 g of (3), 22.89 g of *N*-(3-bromopropyl)phthalimide and 10.0 g of KF-celite in 100 ml of acetonitrile and the suspension was refluxed for 19 h. Filtrate and evaporate to dryness under reduced pressure. The residue was purified by using a silica gel column chromatography developed with hexane-ethyl acetate (3:1 mixture).
4. The products in each fraction were analyzed by TLC and *N*⁴,*N*⁸-dibenzyl-*N*¹,*N*¹¹-diphtaloyl-4,8-diazaundecane (4) was obtained as white powder (2.76 g).
¹H-NMR; 1.83 (6H, m), 2.48 (8H, m), 3.53 (4H, s), 3.67 (4H, t), 7.16–7.19 (10H, m), 7.72 (4H, m), 7.81 (4H, m).
5. Dissolve 2.76 g of (4) in 40 ml of methanol containing 2 ml of anhydrous hydrazine, and reflux the solution for 3 h. After methanol was removed by evaporation under reduced pressure, the residue was shaken in a mixture of chloroform and 25% ammonium hydroxide solution for 30 min. The aqueous layer was separated and washed with chloroform 3 times. The chloroform extracts were combined and dried over anhydrous

magnesium sulfate. Evaporate the solvent under reduced pressure. The residue, 1.2 ml of benzaldehyde and 0.8 g of anhydrous magnesium sulfate were dissolved in 20 ml of methanol. Stir for 1 h at room temperature. Chill the solution in an ice bath, add 10 ml of methanol and 1.8 g of sodium borohydride carefully. Continue stirring on an ice bath for 1 h. Evaporate methanol under reduced pressure and suspend the residue in ethyl acetate. Extraction with ethyl acetate was repeated 3 times. Dry the ethyl acetate extract over anhydrous magnesium sulfate and evaporate under reduced pressure. Crude N^1, N^4, N^8, N^{11} -tetrabenzyl-4,8-diaza-1,11-diaminoundecane (**5**) was obtained as colorless oil (3.50 g).

- Suspend 3.50 g of (**5**), 3.76 g of *N*-(3-bromopropyl)phthalimide, and 5.0 g of KF-celite in 60 ml of acetonitrile and reflux the suspension for 18 h. Filtrate and evaporate the solvent to dryness under reduced pressure. The formed product was purified using a silica gel column chromatography developed with hexane-ethyl acetate mixture (1:1). N^4, N^8, N^{12}, N^{16} -tetrabenzyl- N^1, N^{19} -diphtaloyl-4,8,12,16-tetraazonadecane (**6**) was obtained as a white powder (2.53 g).

$^1\text{H-NMR}$; 1.62 (6H, m), 1.81 (4H, m), 2.39–2.49 (16H, m), 3.52 (8H, s), 3.66 (4H, t), 7.18–7.29 (20H, m), 7.70 (4H, m), 7.83 (4H, m).

- Dissolve 2.53 g of (**6**) in 40 ml of methanol containing 1.5 ml of anhydrous hydrazine. Reflux the solution for 5 h and remove methanol under reduced pressure. Add chloroform: ammonium hydroxide mixture 25% (1:1) to the residue and shake for 30 min. The ammonium layer was washed 3 times with chloroform after two layers had been separated. Chloroform extracts were combined and then the solvent was evaporated to dryness under reduced pressure. Add 20 ml of acetic acid and 1.0 g of PtO_2 to the residue and the mixture was stirred at 60°C in a reactor for hydrogenolysis until hydrogen absorption ceased. Filtrate through a Teflon Millipore membrane and then mix with 5 ml of concentrated HCl. Evaporate to dryness under reduced pressure at 40°C . Crystallize the product in 1:1 ethanol–methanol mixture. Caldohexamine hexahydrochloride salt (**8**) was obtained (0.493 g, yield 34.6%). $^1\text{H-NMR}$; 2.11 (10H, m), 3.08–3.22 (20H, m).

3.2.4. Synthesis of Mitsubishine and Tetrakis(3-Aminopropyl) Ammonium

The original method for the synthesis of tetrakis(3-aminopropyl) ammonium (**8**) was modified in order to improve the yield (Terui et al. unpublished). The chemical reactions for the improved synthesis are shown in Fig. 3d. As an intermediate of the process, mitsubishine (**10**) is also obtained.

1. Dissolve 6.0 g of 3,3',3''-nitrilotris(propionamide) (**9**) in 150 ml of tetrahydrofuran. Add 5.93 g of lithium aluminum hydride to the solution and reflux for 24 h under argon gas. Add water dropwise to the mixture and stir the resulted mixture for 2 h at 25°C. Remove the formed solid by filtration and wash the solid with ethanol several times. Add 1M HCl to the solid to dissolve the formed mitsubishine (**10**) and remove the solvent of the filtrate by evaporation under reduced pressure. The crude mitsubishine can be obtained as yellow oil (10.62 g) and this branched tertiary polyamine can be purified by using a Dowex-50W-X4 column.
2. Mix the obtained yellow oil (**10**) (10.6 g) with 45.8 g of phthalic anhydride and 12.7 g of sodium acetate, and keep the mixture at 170°C under argon for 2 h. Add 200 ml of water after cooling the mixture. Heat the water solution to boiling for 15 min and neutralize to pH 8 by adding sodium bicarbonate. Separate the formed tan solid by filtration, wash the solid with ethyl acetate, and dry over anhydrous magnesium sulfate. The formed compound should be purified by silica gel column chromatography eluted with hexane-ethyl acetate mixture. Tris(3-phthalimidopropyl)amine (**11**) is obtained as white powder (5.05 g, yield 33.5%).
 $^1\text{H-NMR}$; 1.80 (6H, m), 2.50 (6H, m), 3.74 (6H, m), 7.68 (6H, m), 7.80 (6H, m)
 $^{13}\text{C-NMR}$; 26.60, 36.78, 51.68, 123.51, 132.67, 134.11, 168.71
3. Add 1.0 g of *N*-(3-bromopropyl)phthalimide to solution of 2.8 g of sodium iodide in 20 ml of dry acetone (see Note 5). Reflux the solution for 2 h under argon. Add water after cooling, and extract with ethyl acetate 3 times. Dry over anhydrous magnesium sulfate and then remove the solvent by evaporation under reduced pressure. *N*-(3-iodopropyl)phthalimide (**12**) is obtained as yellow powder (1.3 g, almost 100% yield).
 $^1\text{H-NMR}$; 2.25 (2H, m), 3.17 (2H, t), 3.78 (2H, t), 7.73 (2H, m), 7.85 (2H, m). $^{13}\text{C-NMR}$; 1.12, 32.54, 38.63, 123.31, 131.98, 134.04, 168.21
4. Dissolve 2.74 g of tris(3-phthalimidopropyl)amine (**11**) and 1.79 g of *N*-(3-iodopropyl)phthalimide (**12**) in the minimum amount of dry dioxane (about 2.5 ml) (see Note 5). Stir the solution at 200°C for 3 h under argon. Separate the formed white precipitates by filtration and wash the precipitates with dry ethyl acetate. Combine the filtrate and the washings, and then evaporate the solvent under reduced pressure. Dissolve the residue in dry dioxane, reflux for 1 h, and remove the precipitates by filtration. Repeat several times. Combine all

precipitates of tetrakis(3-phthalimidopropyl)ammonium iodide (**13**), (3.23 g, 76.2% yield).

¹H-NMR; 1.92 (8H, m), 3.32 (8H, m), 3.58 (8H, t), 7.84 (16H, m)

¹³C-NMR; 20.96, 34.46, 56.07, 123.04, 131.64, 134.30, 167.84

5. Dissolve 0.30 g of tetrakis(3-phthalimidopropyl)ammonium (**13**) in 6 ml of ethanol and add 0.33 ml of hydrazine to the solution. Reflux the mixture for 2 h under argon. Add 1M HCl and remove the formed precipitates by filtration. Evaporate the solvent under reduced pressure and dissolve the residue in an appropriate amount of water and apply the solution on a Dowex 50W-X4 (H⁺ form). Wash the column with water and then with 1M HCl. Elute the quaternary polyamine with 6M HCl. Collect and combine the fractions containing the branched polyamine and dry up under reduced pressure at 40°C. Tetrakis(3-aminopropyl)ammonium (**14**) is obtained as slightly yellow powder (0.02 g, 12.4%).

¹H-NMR; 2.28 (8H, m), 3.21 (8H, t), 3.63 (8H, t)

¹³C-NMR; 20.20, 36.33, 56.56

3.2.5. Synthesis of *N*⁴-Aminopropylspermidine

This branched polyamine has been found as the major polyamine in some thermophiles (**3**, **4**). The method described below is similar to the reactions presented in Subheading 3.2.3 and the scheme is shown in Fig. 3e.

1. The procedures are same as the preparation of *N*⁴,*N*⁸-dibenzyl-*N*⁷,*N*¹¹-diphtaloyl-4,8-diazaundecane (**4**) except for use of *N*-(4-aminobutyl)carbamic acid tert-butyl ester (**15**) instead of (**3**). React (**15**) with twice molar equivalent of *N*-(3-bromopropyl)phthalimide in the presence of KF-celite in acetonitrile for 19 h under reflux.
2. The formed compound (**16**) was deprotected by treating with HCl as described in Subheading 3.2.1 for preparation of (**8**) from (**6**). *N*⁴-Aminopropylspermidine (**17**) can be obtained with a very good yield (35%) (Terui et al. unpublished).

¹H-NMR; 1.72–1.88 (4H, m), 2.10–2.21 (4H, m), 3.03–3.13 (6H, m), 3.27–3.36 (6H, m). ¹³C-NMR; 21.37, 22.48, 24.70, 37.33, 39.64, 50.83, 53.32

3.2.6. Synthesis of *Aminopropylagmatine*

The scheme is shown in Fig. 3f (**22**). This polyamine is an important intermediate in polyamine metabolism of *T. thermophilus* (**30**). We also found that this polyamine is present as a minor component in some extreme thermophiles (unpublished).

1. An intermediate, bis(benzoyloxycarbonyl)-1,4-butanediamine (**19**) can be synthesized by a method reported by Lawson et al.

(31) from putrescine and chloroformic acid phenyl ester (18), and converted to mono(benzyloxycarbonyl)-1,4-butanediamine hydrochloride (20) as described in (31). The yield was 32%.

$^1\text{H-NMR}$ (in CDCl_3); 7.26–7.35 (5H, m), 5.08 (3H, s), 3.16–3.23 (2H, m), 2.68–2.72 (2H, m), 1.44–1.56 (6H, m).

$^{13}\text{C-NMR}$ (in CDCl_3); 27.5, 30.9, 40.9, 41.8, 66.5, 76.6, 77.0, 77.4, 127.8, 128.2, 136.4, 156.1.

2. Dissolve 1.00 g of (20) and 1.04 g of *N*-(3-bromopropyl) phthalimide in 13 ml of acetonitrile and reflux the solution with stirring at 40°C for 19 h after adding 0.6 g of KF-celite. Filtrate the mixture and the precipitate was washed with ether and dried. Add 10 ml of 30–32% hydrobromic acid in acetic acid and keep at room temperature for 1 h. 1-Phthalimidopropyl-1,4-butanediamine dihydrobromide (21) can be obtained as precipitate by adding dry ether. Wash with dry ether and evaporate to dryness. The compound can be crystallized from methanol (0.90 g, 53% yield).

$^1\text{H-NMR}$ (in CD_3OH); 1.78–1.80 (4H, m), 2.07–2.13 (2H, m), 2.98–3.14 (6H, m), 3.79–3.84 (2H, t), 7.80–7.89 (4H, m).

3. 1-Guanyl-3,5-dimethylpyrazole hydrobromide (22) was prepared according to Bannard et al. (23) and crystallized by adding ether to ethanol solution of the reaction product. The yield was 68%.

$^1\text{H-NMR}$ (in CDCl_3); 2.26 (3H, s), 2.82 (3H, s), 6.15 (1H, s), 7.77 (2H, bs), 9.25 (2H, bs).

4. Dissolve 0.09 g of (21) and 0.045 g of (22) in 2 ml of dry ethanol. The solution was refluxed for 11 h in the presence of 0.025 g of NaOH. Remove sodium bromide formed by filtration. The reaction product was washed with ether and dried. The residue was added to 5 ml of concentrated hydrochloric acid and refluxed for 24 h. The product was applied on a Dowex 50W-X4 column after being appropriately diluted with water. The column was washed with water and then 1M HCl. *N*4-Aminopropylagmatine pentahydrochloride (24) was eluted with 6M HCl. The fractions containing the derivatized agmatine were combined and evaporated to dryness under reduced pressure at 40°C. The final product was pale yellow oil (0.06 g, 77% yield).

$^1\text{H-NMR}$; 1.69 (2H, m), 1.80 (2H, m), 2.13 (2H, m), 3.14 (6H, m), 3.25 (2H, t). $^{13}\text{C-NMR}$; 22.88, 23.78, 25.10, 36.60, 40.49, 44.52, 47.32, 156.77.

3.3. Preparation of Unusual Polyamines from Cells of *T. thermophilus*

Polyamines can be purified from the cells of the extreme thermophiles. As an example, isolation procedure for caldopentamine is described below. In most cases, chemical synthesis is much better than the extraction from thermophile cells for preparative purpose.

However, if a mutant accumulates a specific polyamine, the isolation from cells will be more convenient for biologists than the sophisticated chemical synthesis. One example is aminopropylagmatine; this metabolic intermediate is accumulated in cells of a *T. thermophilus* mutant, which lacks *speB* gene (coding for aminopropylagmatine ureohydrolase) (30), and the chemical synthesis of the aminopropylated polyamine is not easy for biochemists and molecular biologists. Likewise *sym*-homospermidine is accumulated in *T. thermophilus* mutants that lack either *speD2* (coding for S-adenosylmethionine decarboxylase) and/or *speE* (coding agmatine/triamine aminopropyltransferase) (to be published).

1. *T. thermophilus* and its mutants can be grown in a synthetic medium. The synthetic medium consists of 20 g of sucrose, 20 g of monosodium glutamate, 2 g of NaCl, 0.5 g of K_2HPO_4 , 0.25 g of KH_2PO_4 , 0.5 g of $(NH_4)_2SO_4$, 0.125 g of $MgCl_2 \cdot 6H_2O$, 0.025 g of $CaCl_2 \cdot 2H_2O$, 100 μ g of biotin and 1 mg of thiamine, 6 mg of $FeSO_4 \cdot 7H_2O$, 1.2 mg of $Na_2MoO_4 \cdot 2H_2O$, 0.1 mg of $VOSO_4$, 0.5 mg of $MnCl_2 \cdot 4H_2O$, 60 μ g of $ZnSO_4 \cdot 7H_2O$, 15 μ g of $CuSO_4 \cdot 5H_2O$, 0.8 mg of $CoCl_2 \cdot 6H_2O$, and 20 μ g of $NiCl_2 \cdot 6H_2O$ per liter. Trace metals can be added separately from stock solutions (1,000 times concentrated), but do not mix with others before adding to the culture medium. Adjust pH to 7.6 by adding 1M NaOH solution (see Note 6).
2. The cells should be harvested at the midlog phase since older cells contain only small amount of polyamines.
3. The cells grown at lower temperatures such as 65°C contains more triamines whereas the cells grown at higher temperatures such as 78 or 80°C contains more longer polyamines such as caldopentamine, and branched quaternary polyamine.
4. Suspend the cells harvested in twice amount (v/wet weight) of H_2O . Add same volume of 10% trichloroacetic acid to the suspension. Centrifuge to spin down the cell debris and wash the precipitates with 5% trichloroacetic acid once. The supernatant and wash are combined and diluted with the same volume of H_2O . Apply the diluted extract on a Dowex 50W-X4 column. For polyamines extracted from 10 g wet weight cells, 5 ml of column volume would be enough. Wash the column with 5 times column volume of H_2O and then with the same volume of 2M HCl. Elute polyamines with 6M HCl.
5. Analyze the polyamine content of each fraction by using the polyamine analyzer described in Subheadings 2.1 and 2.2. Combine the fractions that contain the desired polyamine. Remove HCl by evaporation under reduced pressure using a tap aspirator. Dissolve the crude preparation thus obtained in a suitable amount of H_2O and apply on a CK-10S column

- (9 mm diameter and 20 cm long) and elute polyamines with 0.1M potassium citrate buffer, pH 6.0, containing 1.75M KCl.
6. Combine the fractions that contain the desired polyamine, and dilute with four to five volume of water. Apply the diluted mixture on a small column of Dowex 50W-X4 (for example, 6 mm diameter and 8 cm long). Wash the column with 5 ml of water and then 2 ml of 1M HCl. Elute the polyamine from the column with 6M HCl. Combine fractions (0.5 ml per tube), which contain the polyamine.
 7. Evaporate the combined solution under reduced pressure using a tap aspirator. Dissolve the residue in the smallest volume of water and add an excess amount of cold ethanol. Collect the formed crystals (white precipitation) of hydrochloride salt by filtration and dried 60°C under reduced pressure. The final step (crystallization) cannot be applied for branched polyamines, which are extremely hygroscopic.

3.4. Determination of Chemical Structure of an Unknown Polyamine

Chemical structure of an unknown polyamine purified from cells or tissues can be determined by measuring their $^1\text{H-NMR}$, $^{13}\text{C-NMR}$, mass, and IR spectra. Finally, the structure should be confirmed by comparing the spectra of the chemically synthesized preparation.

1. As the first step, it is convenient to measure NMR spectra. Figure 4 summarizes the authors' empirical rules for the assignments of delta values (chemical shift) of $^1\text{H-NMR}$ and $^{13}\text{C-NMR}$ (polyamines were dissolved in D_2O). Using this data, chemical structure of an unknown polyamine isolated from living cells or tissues can be speculated. One example is shown in the lower part of Fig. 4, NMR data of an unknown polyamine isolated from *T. thermophilus*. The unknown compound showed $^1\text{H-NMR}$ signals at 1.8 ppm (internal two CH_2 groups of a butyl moiety) and at 2.1 ppm (internal CH_2 group in a propyl moiety). The intensities of these signals were 1:1 suggesting that the compound contains one butyl and two propyl groups or their integral multiples as carbon skeletons. Intensity of signal at 3.2 ppm is 3 times larger than the signals at 1.8 and 2.1 ppm indicating that the compound contains 6 CH_2 groups adjacent to NH_2 and NH groups. Thus, it can be speculated that the unknown compound consists of one aminobutyl and two aminopropyl groups (or their integral multiples), that is, spermine or most likely the structural isomer of spermine. $^{13}\text{C-NMR}$ gave 4 split signals around 23–24 ppm, 2 split signals at around 37–39 ppm, and 4 split signals at around 45–48 ppm suggesting asymmetric nature of the compound. In case of spermine, a symmetric molecule, $^{13}\text{C-NMR}$ signals should be less than five.

2. From the data shown in Fig. 4, structure $\text{NH}_2(\text{CH}_2)_3\text{NH}(\text{CH}_2)_3\text{NH}(\text{CH}_2)_4\text{NH}_2$ was proposed. The structure was confirmed by chemical synthesis and a new naturally occurring polyamine, thermospermine, was discovered (17).

3.5. Studies on Physiological Roles of Polyamines in Thermophiles

3.5.1. Polyamine-Mediated Protection of Nucleic Acid Structures

Polyamines interact with acidic biomolecules in a cell such as nucleic acid and membrane lipids and affect the biological activities such as nucleic acid and protein biosyntheses and cell proliferation. In this section, three different experiments concerning the physiology of unusual polyamines are described.

At high temperatures, DNAs and RNAs denature and lose their higher structures. Polyamines protect nucleic acids from thermal denaturations. T_m (thermal denaturation temperature) of DNA or RNA can be raised by the addition of a polyamine to the reaction mixture (7, 32–34).

In addition to the conformational changes, some covalent linkages are hydrolyzed at high temperature. In case of DNA, linkages between sugar moiety and purine bases are most sensitive to heat. Deamination of cytosine residues also takes place when DNA is heated. In case of RNAs, breakdown of phosphodiester linkages between adjacent nucleotides are most serious damages when heated. Polyamines may protect DNAs and RNAs from these thermal breakdown reactions. The authors confirmed that polyamines protect DNAs from thermal depurination (to be published).

1. Depurination of DNA has been measured using radio labeled DNA or fluorescent labeled DNA (35, 36). However, radio-labeled DNA should be handled in a specified area to avoid radiation hazard. Fluorescence labeling may affect the conformational stability of DNA, and thus may affect the rate of depurination at high temperature. The authors created a new method for determination of depurination rate of unlabeled DNA by measuring the liberated purine bases by HPLC.
2. HPLC analysis can be done using a reverse phase column developed with 20 mM KH_2PO_4 at 40°C at a flow rate of 1.0 ml/min. A sample solution (20 μl) is applied on a commercial prepacked column, Shiseido Capcell Pak C18 UG 120. A UV detector is connected to the column and absorption at 254 nm is recorded. This method can be used for the determination of base composition of DNA.
3. For precise comparison of depurination rates, a short oligomer of deoxyribonucleotide with defined base sequence should be used rather than DNA extracted from organisms (for instance, *E. coli* DNA). In the authors' laboratory, complementary 28-mers were used. Double-helical oligomers were prepared as follows: two single-stranded deoxyribo-

oligonucleotides which are complementary to each other, are dissolved in a $0.1 \times \text{SSC}$ solution, heated at 100°C for 3 min, and then gradually cooled to room temperature.

4. Polyamines are added in a concentration range of 0–125 μM . Since polyamines, especially long polyamines, induce the condensation of DNA and produce precipitates, polyamine concentration should be limited to 125 μM , which is about one-tenth of cellular concentration in bacterial cells at mid-log phase.
5. Incubate 200 μl of double stranded DNA solution containing appropriate concentration of a polyamine in a vial tube with a tight screw cap at 95°C for 24 h. After heating, apply 20 μl of the reaction mixture to the analytical column mentioned above to measure the loss of purine bases.
6. In the presence of 100 μM caldohexamine, depurination was suppressed to 75% of that without the addition of polyamine.

3.5.2. Polyamine-Mediated Stimulation of *In Vitro* Protein Synthesis

Polyamines enhance biopolymer syntheses such as DNA, RNA, and proteins (37, 38). Especially polyamines are essential for protein synthesis of *T. thermophilus* at the physiological temperature (39). No polypeptide synthesis was observed in the cell-free reaction directed by poly(U) as a messenger at 65°C or higher temperatures, though a considerable activity was detected when the reaction was carried out at the lower temperatures. The activity at 65°C was recovered by the addition of a tetraamine such as spermine or thermine.

The effect of polyamine is not to protect essential component(s) of the cell-free translation apparatus from thermal inactivation since the activity was restored immediately when a tetraamine such as spermine or thermine was added to the reaction mixture even after prolonged incubation at 65°C in the absence of polyamine. Detailed investigation revealed that polyamine is absolutely required for the formation of active initiation complex between 30S ribosomal subunit, the messenger, and aminoacyl-tRNA though the elongation step is also enhanced by the addition of polyamine. The addition of polyamine is not essential for the elongation step.

The reaction rate of the *in vitro* polypeptide synthesis catalyzed by *T. thermophilus* cell-free extract depends on the polyamine added. No activity was found in the presence of putrescine, and the activity is much lesser in the presence of a triamine compared with those in the presence of a tetraamine. The activity in the presence of thermine is about two-third of that in the presence of spermine. The optimum temperature also depends on the polyamine added (40).

A quaternary polyamine, tetrakis(3-aminopropyl)ammonium, supports the highest activity independent of the messenger used

(poly(U) and MS2 phage RNA were used) when phenylalanyl-tRNA is used instead of free phenylalanine to eliminate the effect of polyamine on aminoacyl-tRNA formation (see Note 7). However, this branched polyamine inhibits some of aminoacyl-tRNA formations including phenylalanyl-tRNA formation. The inhibition can be suppressed by the addition of linear polyamines such as tetraamines or pentaamines. Thus, the overall reaction is most active in the presence of both the branched polyamine and one of the linear polyamines (41).

1. S30 cell-free extract was prepared according to the original report (42) with slight modifications. The harvested cells were disintegrated by grinding with alumina in a cold room, and then subjected to centrifugation at 30,000 g for 30 min at 4°C.
2. The extract contains considerable amount of polyamines. Most of polyamines in the extract were bound to ribosomes (40). About two-third of the contaminated polyamines can be removed by dialysis for 3 days at 4°C against Buffer A. Pentamines and tetrakis(3-aminopropyl)ammonium were tightly bound to ribosomes. Polyamines in the extract can be removed completely by prolonged dialysis, however, the complete depletion results in inactivation of the extract.
3. S100 fraction was prepared by centrifugation at 100,000 g for 2.5 h according to a literature (42). The prepared S100 fraction was passed through a DEAE-cellulose column equilibrated with Buffer A. Precipitates formed with 80% saturation of ammonium sulfate, were dialyzed against the Tris buffer mentioned above. The final preparation contains only a small amount of polyamines.
4. Polypeptide synthesis was determined as follows: [³H]phenylalanyl-tRNA (70 pmoles) (see Note 7) was added to the reaction mixture (0.1 ml) consisting of 50 mM Tris-HCl buffer, pH 7.8, 100 mM ammonium chloride, 6 mM 2-mercaptoethanol, 15 mM magnesium acetate, 3.2 mM ATP, 0.4 mM GTP, 1 absorbance unit at 260 nm of *T. thermophilus* ribosomes plus 100 µg of S100 fraction or 3 absorbance units of S30 fraction, 81 µg of (either *E. coli* or *T. thermophilus*) tRNA, 10 µg of poly(U) or 40 µg of MS2 phage RNA, 2 nmol each of 19 other amino acids. Phenylalanyl-tRNA was prepared according to a literature (43). The activity was estimated by measuring the radioactivity in hot trichloroacetic acid-insoluble materials.
5. The highest activity was recorded when 1 mM tetrakis(3-aminopropyl)ammonium was added and the reaction was carried out at 75°C. Each component of translational apparatus such as ribosomal subunits, tRNAs and factors, and enzymes

in S100 fraction are exchangeable between *E. coli* and *T. thermophilus* as far as the reaction temperature is below 37°C.

3.5.3. Reverse Genetics of Genes Involved in Polyamine Metabolism of *T. thermophilus*

Knockout mutants are one of the most useful tools in the studies on metabolisms and physiology of polyamines *in vivo*. Genetic manipulation using *T. thermophilus* as a host is extremely easy (44). Two artificially, highly heat-stabilized antibiotic resistant genes; a heat-stable kanamycin resistant gene, HTK (45) and a heat-stable hygromycin B resistant gene (46) are available upon request from the experts (see Subheading 2.5.3) and can be used as markers.

The polyamine metabolic path was analyzed by using knockout mutants of homologous genes involved in polyamine metabolisms such as *speA*, *speB*, *speD1*, *speD2*, and *speE*, and a new metabolic path was proposed (30). To confirm the proposed pathway, each gene product was expressed in *E. coli*, and enzymatic properties of the expression product, especially the substrate specificities, were investigated. Table 2 summarizes the functions of *T. thermophilus speA*, *speB*, *speD1*, *speD2*, *speE*, and *dhs* genes.

Construction procedures of *speA*-deficient mutant are presented as an example in the following section. Outline of the genetic manipulation described below is illustrated in Fig. 5.

1. Prepare stock of plasmid pBHKT, which contains heat-stable kanamycin resistant gene, HTK.
2. Design a primer to amplify the upstream 500 bp fragment of *speA*. Add 5'-AAAGGGTACC to 5'-end of the forward

Table 2
Reverse genetics of polyamine biosynthetic genes in chromosomal DNA of *T. thermophilus*

Gene name	Function of the gene product in <i>T. thermophilus</i>	Major phenotype
<i>spe A</i>	Arginine decarboxylase	No growth at 75°C, poor growth at 70°C
<i>spe B</i>	Aminopropylglutaminase	No growth at 75°C, accumulation of aminopropylglutamine
<i>spe D1</i>	Putative SAM decarboxylase activator	No growth at 75°C
<i>spe D2</i>	SAM decarboxylase	No growth at 75°C, accumulation of sym-homospermidine
<i>spe E</i>	Agmatine/triamine aminopropyltransferase	No growth at 75°C, accumulation of sym-homospermidine
<i>dhs</i> ^a	Involved in sym-homospermidine biosynthesis	No change

^aHomologous gene to deoxyhypusine synthase

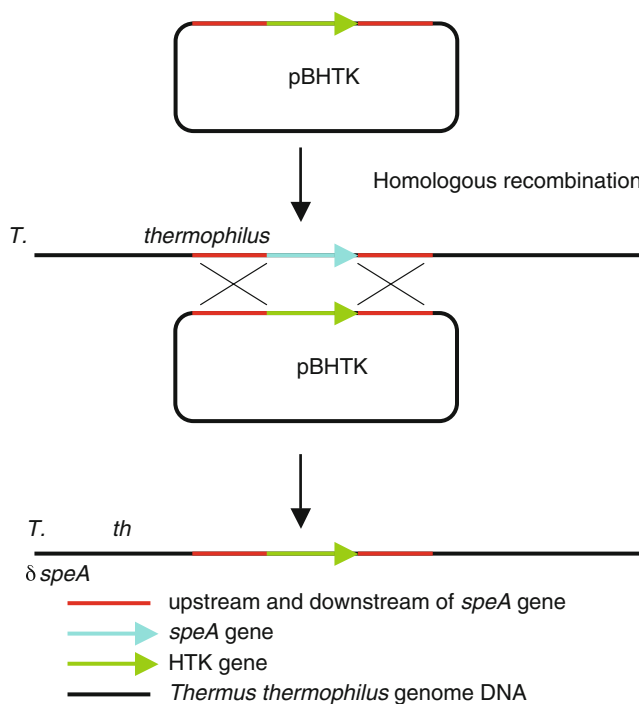


Fig. 5. Structure of the recombinant plasmid for construction of *speA*-mutant.

primer in order to induce a *KpnI* restriction site. Add 5'-CAGTATCGAT to 5'-terminal of the reverse primer to introduce *ClaI* site.

- Using these modified primers and *T. thermophilus* genome DNA as template, carry out PCR amplification. Purify the PCR product using Wizard plus SV Minipreps DNA Purification System (Promega) if necessary.
- Digest pBHTK and the PCR product with *KpnI* according to the instruction provided by the manufacturer. After 2 h, add ethanol to stop the reaction.
- Digest the ethanol precipitate with *ClaI* according to the instruction. Stop the reaction by adding ethanol after 2 h. The precipitate was dissolved in DNase-free MilliQ water and run on agarose gel electrophoresis. Prepare 1:1 mixture of the digested pBHTK and the upstream fragment, and dissolve the mixture in 5 μ l. Add 5 μ l of Takara Ligation Kit ver. 2 Solution 1 and incubate at 16°C for 30 min.
- Transform Chemical Competent Cell JM109 with the ligation solution. If transformation is failed, try again at 4°C overnight. Purify the fused plasmid using Wizard plus SV Minipreps DNA purification System (Promega).

7. Design primers for the downstream 500 bp fragment of *speA* gene, add 5'-TCTTGAATTC at the 5' terminal of the forward primer in order to produce an *EcoRI* site. Add 5'-CATATCTAGA to the 5' end of the reverse primer for *XbaI* digestion. Prepare downstream PCR product in a similar manner to upstream fragment.
8. Apply the product of step 6 and the downstream fragment on agarose gel electrophoresis. Prepare 1:1 mixture of these DNAs (in 5 μ l). Add 5 μ l of Takara Ligation Kit ver. 2 Solution 1 and incubate at 16°C for 30 min. Transform JM109 with the mixture and purify the plasmid in a similar manner to step 6.
9. Prepare a nutrient medium for *T. thermophilus* by dissolving 8 g of Bacto Peptone, 4 g of Bacto Yeast-extract 2 g glucose, and 2 g of NaCl in 1,000 ml of water. After autoclave, add 35 μ l of 1M CaCl₂ and 40 μ l of 1M MgCl₂. Also prepare 1.5% agar plates. Grow *T. thermophilus* HB8 or HB27 in 5 ml of the medium at 70°C (see Note 6).
10. Spread 200 μ l of the thermophile culture at the middle log phase on an agar plate. Drop the plasmid solution prepared at step 8 (10 μ g DNA per 100 μ l) on the plate. Mark the sites of the DNA drops, and incubate the marked plates at 70°C. The plates were tightly sealed with vinyl tape to prevent evaporation. Collect the cells grown at the marked sites, suspend and appropriately dilute with the growth medium.
11. Spread 20 μ l of 50 mg/ml kanamycin solution on each plates. Then spread the diluted cell suspension for colony isolation. After colony isolation, gene disruption should be confirmed by base sequencing of the genome DNA.

4. Notes

1. When *o*-phthalaldehyde-ethanol solution and 2-mercaptoethanol are measured, use mechanical pipettes for safety reasons.
2. When the fluorescent reagent solution is prepared, firstly place an appropriate amount of *o*-phthalaldehyde solution in a beaker and then pour the borate buffer into the beaker. Do not do vice versa. For unknown reasons this improves the background noise and baseline of the chromatographic chart.
3. It is essential to replace the eluant remained in lines and the column with Milli-Q water after the polyamine analyzer was used. The eluant contains a very high concentration of KCl, which is corrosive to metal joints and pumps. During wash with water, the flow rate of pump one should be reduced to 1 ml/min since the ion exchange resin particles bloat to larger

size in water and higher pressure is necessary to run water through the column of the bloated particles. In the authors' laboratory, both pumps run with water for about 2 h using an automatic shut down timer after polyamine assay was finished.

4. It is very important to note that the compound names used by companies are different from the systematic names and the trivial names listed in Table 1 and may differ from company to company. For instance, norspermidine is called "3,3'-diamino-dipropylamine" in Tokyo Kasei's catalog. Thermine freebase can be purchased from Aldrich Chemical Co., but the compound is listed with a different name, *N,N*-bis(3-aminopropyl)-1,3-propanediamine. The safest way to search polyamines and the raw materials for chemical syntheses is to use molecular formula index; for example, norspermidine is C₆H₁₇N₃.
5. The solvents acetone and dioxane should be dried by adding metallic sodium and purified by distillation before use.
6. Rinse the glassware used for the bacterial culture repeatedly and cautiously or use disposable tubes for growth since *T. thermophilus* is extremely sensitive to contaminated detergent.
7. The exogenous charged [³H]phenylalanyl-tRNA added to eliminate any possible influence of the polyamines on the aminoacylation reaction, was prepared by incubating *T. thermophilus* tRNAs prepared as described in reference (47) with L-[³H]phenylalanine and 19 other unlabeled amino acids in the S-100 cell-free extract of the thermophile according to reference (43).

Acknowledgements

Studies cited in this article were done by many former colleagues in our laboratories in University of Tokyo, Mitsubishi-Kasei Institute of Life Sciences, Tokyo Institute of Technology, Tokyo University of Pharmacy and Life Science, and the Institute of Environmental Microbiology, Kyowa-kako Company. Especially the authors are grateful to Drs. Mio Ohnuma, Taketoshi Uzawa, Yoshiko Ohno-Iwashita, and Nobuko Hamasaki-Katagiri.

References

1. Cohen SS (1998) A guide to the polyamines. Oxford University Press, USA
2. Oshima T (1978) Novel polyamines of extremely thermophilic bacteria. In: Friedman SM (ed) Biochemistry of thermophily. Academic, New York, pp 211–220
3. Hosoya R, Hamana K, Niitsu M, Itoh T (2004) Polyamine analysis for chemotaxonomy of thermophilic eubacteria: polyamine distribution profiles within the orders Aquificales, Thermotogales, Thermodesulfobacteriales, Thermales, Thermoanaerobacteriales, Clostridiales and Bacillales. J Gen Appl Microbiol 50:271–287

4. Hamana K, Hamana H, Niitsu M, Samejima K, Itoh T (1996) Polyamines of hyperthermophilic archaeobacteria, *Archaeoglobus*, *Thermococcus*, *Pyrobaculum* and *Sulfolobus*. *Microbes* 87:69–76
5. Kneifel H, Stetter KO, Andreesen JR, Wiegel J, König H, Schobeth SM (1986) Distribution of polyamines in representative species of archaeobacteria. *System Appl Microbiol* 7:241–245
6. Oshima T (1983) Novel polyamines in *Thermus thermophilus*: isolation, identification and chemical synthesis. *Meth Enzymol* 94:401–411
7. Oshima T (2007) Unique polyamines produced by an extreme thermophile, *Thermus thermophilus*. *Amino Acids* 33:367–372
8. Oshima T (1975) Thermine; a new polyamine from an extreme thermophile. *Biochem Biophys Res Commun* 63:1093–1098
9. Oshima T (1982) A pentaamine is present in an extreme thermophile. *J Biol Chem* 257:9913–9914
10. Oshima T, Hamasaki N, Senshu M, Kakinuma K, Kuwajima I (1987) A new naturally occurring polyamine containing a quaternary ammonium nitrogen. *J Biol Chem* 262:11979–11981
11. Oshima T, Imahori K (1999) Description of *Thermus thermophilus*, comb. nov., a nonsporulating thermophilic bacterium from a Japanese thermal spa. *Int J Syst Bacteriol* 24:102–112
12. Oshima T, Baba M (1981) Occurrence of sym-homospermidine in extremely thermophilic bacteria. *Biochem Biophys Res Commun* 103:156–160
13. Stillway LW, Walle T (1977) Identification of the unusual polyamines 3, 3'-diaminodipropylamine and *N*, *N'*-bis(3-aminopropyl)-1, 3-propanediamine in the white shrimp, *Penaeus estiferus*. *Biochem Biophys Res Commun* 77:1103–1107
14. Hamana K, Niitsu M, Samejima K (2000) Occurrence of tertiary branched tetraamines in two aquatic plants. *Can J Bot* 78:266–269
15. Hamana K, Matsuzaki S, Niitsu M, Samejima K (1992) Distribution of unusual polyamines in leguminous seeds. *Can J Bot* 70:1984–1990
16. Carteni-Farina M, Porcelli M, Cacciapouti G, DeRosa M, Gambacorta A, Grant WD, Ross HNM (1985) Polyamines in halophilic archaeobacteria. *FEMS Microbiol Lett* 28:323
17. Oshima T (1979) A new polyamine, thermospermine, 1, 12-diamino-4, 8-diazadodecane, from an extreme thermophile. *J Biol Chem* 254:8720–8722
18. Knott JM, Romer P, Sumper M (2007) Putative spermine synthases from *Thalassiosira pseudonana* and *Arabidopsis thaliana* synthesize thermospermine rather than spermine. *FEBS Lett* 581:3081–3086
19. Kakehi J, Kuwashiro Y, Niitsu M, Takahashi T (2008) Thermospermine is required for stem elongation in *Arabidopsis thaliana*. *Plant Cell Physiol* 49:1342–1349
20. Muniz L, Minguet EG, Singh SK, Pesquet E, Vera-Sirera F, Moreau-Courtois CL, Carbonell J, Blazquez MA, Touminen H (2008) ACAULIS5 controls *Arabidopsis* xylem specification through the prevention of premature cell death. *Development* 135:2573–2582
21. Imai A, Akiyama T, Kato T, Sato S, Tabata S, Yamamoto KT, Takahashi T (2004) Spermine is not essential for survival of *Arabidopsis*. *FEBS Lett* 556:148–152
22. Yamaguchi K, Takahashi Y, Berberich T, Imai A, Takahashi T, Michael AJ, Kusano T (2007) A protective role for the polyamine spermine against drought stress in *Arabidopsis*. *Biochem Biophys Res Commun* 352:486–490
23. Bannard RAB, Casselman AA, Cockburn WF, Brown GM (1958) Guanidine compounds II. Preparation of Mono- and *N*, *N*-dialkylguanidines. *Can J Chem* 36:1541–1549
24. Fernandes O, Ferreira MA (2000) Combined ion-pair extraction and gas chromatography-mass spectrometry for simultaneous determination of diamines, polyamines and aromatic amines in Port wine and grape juice. *J Chromatogr A* 886:183–195
25. Niitsu M, Samejima K, Matsuzaki S, Hamana K (1993) Systematic analysis of naturally occurring linear and branched polyamines by gas chromatography and gas chromatography-mass spectrometry. *J Chromatogr* 641:115–123
26. Shirahata A, Takeda Y, Kawase M, Samejima K (1983) detection of spermine and thermospermine by thin-layer chromatography. *J Chromatogr* 262:451–454
27. Oshima T, Kawahata S (1983) Homocaldopentamine: a new naturally occurring pentaamine. *J Biochem* 93:1455–1456
28. Chantrapromma K, McManis JS, Ganem B (1980) The chemistry of naturally occurring polyamines. A total synthesis of thermospermine. *Tetrahedron Lett* 21:2475–2476
29. Niitsu M, Samejima K (1986) Syntheses of a series of linear pentaamines with three and four methylene chain intervals. *Chem Pharm Bull* 34:1032–1038
30. Ohnuma M, Terui Y, Tamakoshi M, Mitome H, Niitsu M, Samejima K, Kawashima E, Oshima T (2005) *N'*-Aminopropylagmatine, a New Polyamine Produced as a Key

- Intermediate in Polyamine Biosynthesis of an Extreme Thermophile, *Thermus thermophilus*. J Biol Chem 280:30073–30082
31. Lawson WB, Leafer MD, Tewes A, Rao GJS (1968) Alkilation of serine at the active site of trypsin *Hoppe-Seyler's. Z Physiol Chem* 349:251–161
 32. Hayrapetyan A, Grosjean H, Helm M (2009) Effect of a quarternary pentamine on RNA stabilization and enzymatic methylation. *Biol Chem* 390:851–861
 33. Terui Y, Ohnuma M, Hiraga K, Kawashima E, Oshima T (2005) Stabilization of nucleic acids by unusual polyamines produced by an extreme thermophile, *Thermus thermophilus*. *Biochem J* 388:427–433
 34. Grosjean H, Oshima T (2007) How nucleic acids cope with high temperature. In: Gerday C, Glandsdorff N (eds) *Physiology and biochemistry of extremophiles*. ASM Press, Washington, pp 39–56
 35. Johnson NP, Macquet JP, Wiebers JL, Monsarrat B (1982) Structures of the adducts formed between [Pt(dien)Cl]Cl and DNA in vitro. *Nucleic Acids Res* 10:5255–5271
 36. Lindahl T, Nyberg B (1972) Rate of depurination of native deoxyribonucleic acid. *Biochemistry* 19:3610–3618
 37. Bachrach U (1970) Metabolism and function of spermine and related polyamines. *Ann Rev Microbiol* 24:109–134
 38. Tabor H, Tabor CH (1972) Biosynthesis and metabolism of 1, 4-diaminobutane, spermidine, spermine, and related amines. *Advan Enzymol* 36:203–268
 39. Ohno-Iwashita Y, Oshima T, Imahori K (1975) In vitro protein synthesis at elevated temperature by an extract of an extreme thermophile: effects of polyamines on the polyuridylic acid-directed reaction. *Arch Biochem Biophys* 171:490–499
 40. Uzawa T, Hamasaki N, Oshima T (1993) Effects of novel polyamines on cell-free polypeptide synthesis catalyzed by *Thermus thermophilus* HB8 extracts. *J Biochem* 114:478–486
 41. Uzawa T, Yamagishi A, Nishikawa K, Oshima T (1994) Effects of unusual polyamines on pheylalanyl-tRNA formation. *J Biochem* 115:830–832
 42. Nierenberg MW, Matthaei JH (1961) The dependence of cell-free protein synthesis in *E. coli* upon naturally occurring or synthetic polyribonucleotides. *Proc Natl Acad Sci USA* 47:1588–1602
 43. Conway TW, Lipmann F (1964) Characterization of a ribosome-linked guanosine triphosphate in *Escherichia coli* extracts. *Proc Natl Acad Sci USA* 52:1462–1469
 44. Tamakoshi M, Yaoi T, Oshima T, Yamagishi A (1999) An efficient gene replacement and deletion system for an extreme thermophile, *Thermus thermophilus*. *FEMS Microbiol Lett* 173:431–437
 45. Hoseki J, Yano T, Koyama Y, Kuramitsu S, Kagamiyama H (1999) Directed evolution of thermostable kanamycin-resistance gene: a convenient selection marker for *Thermus thermophilus*. *J Biochem* 126:951–956
 46. Nakamura A, Takakura Y, Kobayashi H, Hoshino T (2005) In vivo directed evolution for thermostabilization of *Escherichia coli* hygroycin B phosphotransferase and the use of the gene as a selection marker in the host-vector system of *Thermus thermophilus*. *J Biosci Bioeng* 100:158–163
 47. Zubay G (1962) The isolation and fractionation of soluble ribonucleic acid. *J Mol Biol* 4:347–356

Polyamine Block of Inwardly Rectifying Potassium Channels

Harley T. Kurata, Wayland W.L. Cheng, and Colin G. Nichols

Abstract

Polyamine blockade of inwardly rectifying potassium (Kir) channels underlies their steep voltage-dependence observed in native cells. The structural determinants of polyamine blockade and the structure-activity profile of endogenous polyamines requires specialized methodology for characterizing polyamine interactions with Kir channels. Recent identification and growing interest in the structure and function of prokaryotic Kir channels (KirBacs) has driven the development of new techniques for measuring ion channel activity. Several methods for measuring polyamine interactions with prokaryotic and eukaryotic Kir channels are discussed.

Key words: Inward rectifier, Potassium channel, Electrophysiology, Patch-clamp, Ion channel blockade

1. Introduction

Inwardly rectifying potassium (Kir) channels exhibit unique voltage-dependence *in vivo*, preferentially allowing inward conduction of potassium ions, a property commonly referred to as “inward rectification.” Kir channels influence diverse processes ranging from cardiac muscle contraction to insulin release from pancreatic β -cells (1–3), but perhaps the most obvious physiological role attributed to Kir channels is in excitable cells, where they play a fundamental role of regulating the resting membrane potential and action potential repolarization. In this milieu, the minimization of outward K^+ conductance of Kir channels is essential to permit action potentials to proceed (4, 5).

Interestingly, unlike the gating mechanisms that exemplify many other ion channel proteins, “inward rectification” is not an intrinsic property of Kir channels, but rather arises from

voltage-dependent channel blockade by cytoplasmic polycations, particularly polyamines (6). The prototypical inward-rectifiers are members of the Kir2 subfamily, but importantly, different Kir channel types exhibit different sensitivities to polyamine blockade, and consequently, different degrees of inward rectification are observed in vivo, these functional differences being related to the physiological role of a specific Kir channel type. The physical principles underlying the voltage-dependence of Kir channel polyamine block have stirred interest in diverse questions such as the identification of the structural determinants of high affinity and steeply voltage-dependent polyamine binding, and the interactions between blockers and permeating ions in ion channel pores (7, 8). Methods used for characterizing polyamine interactions with Kir channels continue to be applied to illuminate the detailed features of polyamine block and the physiological effects of mutations that disrupt this critical mechanism of Kir channel regulation.

Finally, recently identified prokaryotic Kir channels (“KirBacs”) have proven very useful for crystallographic determination of Kir channel structure, but the techniques for functional characterization of KirBac channels remain in development. Considerable effort has been invested in the development of methods for recording KirBac channel activity, which presents unique problems compared to their eukaryotic Kir channel counterparts (9, 10). In the long term, continued development of these methods will enable direct correlation of crystallographic data (11, 12) with measurable changes in ion channel function. In this chapter, we provide an overview of the electrophysiological techniques essential for characterization of polyamine interactions with eukaryotic Kir channels. In addition, methods for the purification, reconstitution, and functional characterization of prokaryotic KirBac ion channels are described.

2. Materials

2.1. KirBac Protein Purification

1. *Escherichia coli* strain BL21 Star (DE3) pLysS.
2. LB supplemented with antibiotic for selection (e.g., ampicillin or kanamycin).
3. 1 M IPTG (convenient in 1 mL aliquots).
4. Resuspension Buffer: 50 mM Tris-HCl pH 7.5, 150 mM KCl, 250 mM sucrose, 10 mM MgSO₄, one half EDTA-free mini protease inhibitor tablet per 20 mL resuspension buffer (i.e. 1/2 tablet per 1 L of bacteria) (Roche Diagnostics).
5. Wash Buffer A: 50 mM Tris-HCl pH 7.5, 150 mM KCl.
6. Wash Buffer B: 50 mM Tris-HCl pH 7.5, 150 mM KCl, 5 mM decyl maltoside, 10 mM imidazole.

7. Elution Buffer: 50 mM Tris-HCl pH 7.5, 150 mM KCl, 5 mM decyl maltoside, 500 mM imidazole.
8. Cobalt beads (Talon), and polystyrene columns (Pierce Chemical Co.).

2.2. Liposome Preparation for Electrophysiology

1. Lipids (e.g., POPE, POPG, Cardiolipin, Asolectin, PIP2).
2. 8 mL polystyrene columns (Thermo Fisher Scientific).
3. MOPS buffer: 150 mM KCl and 10 mM MOPS, pH 7.5.
4. Sephadex G-50 beads (Sigma), soaked in MOPS buffer overnight.
5. Glass coverslips incubated in polylysine.

2.3. ⁸⁶Rb⁺ Liposome Uptake Assay

1. Lipids (POPE, POPG, Cardiolipin, Asolectin, PIP2).
2. 170 mM CHAPS stock.
3. Sephadex G-50 beads, soaked in the desired buffer overnight.
4. Dowex 50 X-4-100 (H⁺ form) cation exchange matrix (Sigma).
5. Polystyrene columns (Pierce Chemical Co.).
6. Buffer B: 450 mM KCl, 10 mM HEPES, 4 mM NMDG, adjust pH to 7.5 with HEPES or NMDG. All buffers are sterile-filtered and stored at 4°C.
7. Buffer C: 400 mM sorbitol, 10 mM HEPES, 4 mM NMDG, 50 μM KCl, adjust pH to 7.5 with HEPES or NMDG.
8. Sorbitol solution (400 mM).
9. BSA (5 mg/mL) in sorbitol solution.
10. Valinomycin stock: 100 μg/mL in EtOH. Make 1 mL, and store at 4°C.

2.4. Eukaryotic Cell Culture

1. Dulbecco's modified eagle medium (DMEM)+10% FBS, supplemented with Pen/Strep antibiotic cocktail.
2. CosM6 cells.
3. Liposome-based transfection reagent (Fugene, Lipofectamine).
4. Sterile/flamed glass coverslips.

2.5. Patch-Clamp Electrophysiology

1. Thin-walled borosilicate glass (1.5 mm OD, 1.1 mm ID).
2. Buffered KCl recording solution, typical composition: 140 mM KCl, 1 mM K-EGTA, 1 mM K-EDTA, 4 mM K₂HPO₄, pH 7.3 (with KOH).
3. Standard patch-clamp equipment (electrode puller, patch-clamp acquisition electronics, microscope, manipulator, anti-vibration table).

3. Methods

3.1. Purification of KirBac Protein

1. Transform *E. coli* strain BL21 Star (DE3) pLysS (Invitrogen) with KirBac 1.1 DNA, and grow bacteria overnight on an LB-agar plate supplemented with an appropriate selection antibiotic. Optimal protein expression occurs only if the bacteria are newly transformed. Older bacterial stocks, even glycerol stocks, produce very low amounts of protein. Retransform every week or 2.
2. (DAY 1) Prepare a small (5 mL) seed culture of LB + selection antibiotic (e.g., ampicillin) with a single toothpick colony. Shake overnight at 37°C and 200–250 rpm.
3. (DAY 2) Inoculate 1 L of LB + selection antibiotic (e.g., ampicillin) with the 5 mL seed culture. Shake at 37°C and 250 rpm for 5 h (until $OD_{600} \sim 1.0$).
4. Induce with 1 mM IPTG (add 1 mL of 1 M IPTG aliquot to the 1 L bacterial culture) for 3 h at 37°C and 250 rpm.
5. Pellet cells by centrifugation ($4,000 \times g$) for 15 min. Pour off supernatant. (At this stage, pellets can be frozen for up to a few days, or the experiment can immediately proceed to the protein purification steps, which typically require ~4–5 h. If proceeding immediately, lysis of the pellets is achieved by rapid freeze–thaw, 10 min at -80°C .)
6. (DAY 3) Resuspend pellets with 20 mL of resuspension buffer (per 1 L of culture) in a 50 mL Falcon tube.
7. Add 30 mM decyl maltoside (30 μL of 1 M stock per mL of cell lysate) to the cell lysate and rock at 4°C for at least 2–3 h to solubilize the protein.
8. Centrifuge cell lysate for 30 min at 18,000 rpm ($40,000 \times g$).
9. While the cell lysate is centrifuging, prepare cobalt beads by washing a batch of beads with 5 bed volumes of Wash Buffer A. Use 0.2 mL (bed volume) of beads for each 1 L of culture.
10. Taking the centrifuged cell lysate, discard the pellet and put the washed beads into the supernatant. Rock at 4°C for 1 h to bind the protein to the beads.
11. Centrifuge the extract+beads at very low speed (100–200 rpm) for 5 min to collect the beads at the bottom. Pour off most of the supernatant and pipette the beads and remaining cell extract into the columns. Allow the extract to flow through.
12. Wash the beads with 40 bed volumes of Wash Buffer B.

13. Elute the protein with 4 bed volumes of Elution Buffer.
14. Store eluted protein at 4°C. WT KirBac1.1 is highly stable and remains active beyond 1 year of storage. Protein can be concentrated for future applications using Amicon columns, or other comparable products.

3.2. Storage of Lipids

1. Solubilize lipids in chloroform and aliquot the desired amount (2–4 mg of lipid) into glass culture tubes. Use a stream of nitrogen gas to dry the lipids.
2. Fill glass tubes containing dried lipids with nitrogen, and seal with parafilm. Store tubes in a container filled with nitrogen at –20°C.

3.3. Functional Assay for KirBac, ⁸⁶Rb⁺ Liposome Uptake Assay

1. Swell sephadex beads by incubating in buffer B or buffer C overnight at 4°C. One batch of beads should be swelled in each buffer.
2. Rinse polystyrene column bodies with double distilled water (ddH₂O), and push one polyethylene disk all the way to the end (with a Pasteur pipette). Rinse again with ddH₂O.
3. Fill each column about half-way with swollen Sephadex beads, and wash several times with the appropriate buffer (B or C). If storage is desired, apply 1–2 mL of buffer solution over beads to prevent drying, and cap the top and bottom of the column. (Capped columns can be stored at 4°C for weeks.)
4. Prepare lipids for the assay by resuspending stored lipids (in glass tubes, from Subheading 3.2) in buffer B and 35 mM CHAPS (for 4 mg of lipid, add 80 µL of 170 mM CHAPS stock and 320 µL of buffer B) to a concentration of 10 mg/mL. Use brief sonication of ~5–10 s and vortex to help with resuspension. Inspect the solution and re-sonicate if any dried lipids are visible in the bottom of the tube. Mix lipids to the desired composition (i.e., 3:1 POPE:POPG), and incubate for 2 h at room temperature. Allow 100 µL of lipid (10 mg/mL) per sample in the ⁸⁶Rb⁺ flux assay.
5. Dowex columns are prepared by placing ~0.5–1 mL of Dowex beads in serum separator columns. Wash the Dowex column with 1 mL of BSA–Sorbitol solution, and rinse with sorbitol solution (fill column). Next, wash the Dowex column with ~100 µg of lipid solution (resuspend 2 mg of POPG in 1 mL of sorbitol solution and add 50 µL) and rinse again with sorbitol solution.
6. Mix purified KirBac protein with each 100 µL sample of lipid solution, and incubate for 20 min. Protein:lipid ratios in the range of 6 µg KirBac per mg lipid are typical and may be adjusted depending on the activity of a particular protein prep.

7. Prespin a Sephadex column containing Buffer B by placing the column in a 15 mL conical tube and centrifuging in a Beckman TJ6 Centrifuge at maximum speed and stopping when 3,000 rpm ($\sim 1,000 \times g$) is reached.
8. Place the prespun column B in a glass collection tube (glass culture tubes work well for this purpose) and add lipid/protein mixture to the top of the column. One column is needed for each sample.
9. Recover liposomes by spinning the Sephadex column (with a collection tube) until the centrifuge reaches 2,500 rpm ($\sim 700 \times g$). Liposomes are contained in the flow-through, and a normal yield is $\sim 50 \mu\text{L}$ for each 100 μL loaded. Store the recovered liposomes at room temperature and use within 3 h (see Note 1).
10. Prespin a Sephadex column containing Buffer C as done previously with the Buffer B column.
11. Place the prespun column in a collection tube and add liposomes to the column.
12. Recover liposomes by spinning into the collection tube at 2,500 rpm ($\sim 700 \times g$) for 60 s. Use the recovered liposomes as soon as possible (at this point, liposomes are stable for hours, but dissipation of the gradient is noticeable within 20–30 min).
13. Mix recovered liposomes with 4–5 aliquot volumes (50 μL aliquots will be taken in subsequent steps) of Buffer C containing $^{86}\text{Rb}^+$ at a final specific activity of $\sim 1\text{--}1.5 \mu\text{Ci/mL}$, and start a timer (this is time = 0).
14. At each desired time point, remove a 50 μL aliquot from the mixture. Pipette the aliquot onto a Dowex column to remove extraliposomal $^{86}\text{Rb}^+$, and allow aliquot to enter beads. For KirBac1.1, useful time points are within the range of 15 s to 1 min, with uptake saturating in 2–4 min.
15. Elute liposomes with 1 mL of sorbitol solution. Allow the flow-through to drain into a scintillation vial. Elute a second time with another 1 mL of sorbitol solution.
16. Add scintillation fluid and count.
17. After all desired time points have been collected, add 1 μL of valinomycin stock, wait ~ 10 min, and process a final aliquot as above. Valinomycin is an ionophore that will allow $^{86}\text{Rb}^+$ to equilibrate inside and outside the liposomes. This provides an assessment of maximum possible uptake in the assay.
18. For characterization of polyamine interactions with KirBac channels (or mutant KirBac channels) using the ^{86}Rb uptake assay, several options are possible. The most straightforward is to include polyamines in $^{86}\text{Rb}^+$ -containing Buffer C during the $^{86}\text{Rb}^+$ uptake step of the assay (step 4). If the reconstituted

channel is polyamine-sensitive, uptake of $^{86}\text{Rb}^+$ into liposomes will be hindered (see Note 1). When interpreting this type of data (for polyamines or other blocker types), it is important to remember that reconstituted ion channels likely insert randomly into the liposome bilayer, so the “sidedness” of liposomes will not be uniform (see Note 2).

3.4. Reconstitution of KirBac Channels in Giant Liposomes for Patch-Clamp Electrophysiology

1. As in the preparation of liposomes for uptake assays, polystyrene columns (Thermo Fisher Scientific, 8 mL columns) are packed with Sephadex G-50 beads, soaked in the desired buffer overnight, and spun until reaching $1,500 \times g$ on a Beckman TJ6 Centrifuge (3,000 rpm). For KirBac electrophysiology, a MOPS buffer (150 mM KCl and 10 mM MOPS, pH 7.5) is typically used.
2. While the column is packing, mix KirBac protein with an appropriate lipid mixture (resuspend lipids as described above). A typical lipid mixture is 3:1 POPE:POPG (200–400 μL , 10 mg/mL in MOPS buffer with 35 mM CHAPS) with a small volume of the desired protein (depending on concentration). For KirBac1.1, 30–50 μg of protein per 1 mg of lipid can yield macroscopic currents, whereas 1–5 μg can be sufficient to observe single channel openings. The composition of lipids may change depending on the experimental question being addressed, but 3:1 POPE:POPG has proven generally reliable for the formation of giant liposomes suitable for patch-clamping. We have found no significant difference in recordings generated after reconstitution using Bio-Beads or Sephadex – both methods seem to effectively remove CHAPS detergent.
3. Spin the entire (~200–300 μL) protein–lipid solubilized mixture through the prespun sephadex column (step 1) until reaching $1,000 \times g$ (~2,500 rpm).
4. Collect the flow-through, and spin the liposome solution at $100,000 \times g$ for 1 h.
5. The key step for the formation of giant liposomes is to dry a high concentration of resuspended liposomes onto a glass slide. Thus, the pelleted liposomes should be resuspended in as small a volume as possible (usually ~3–8 μL of buffer depending on how much lipid was used). The quality of giant liposomes also depends on how much the liposome spots are spread out or smeared on the glass slide. By trial and error, one has to find the best balance here. Typically, 3–5 μL of liposome solution is applied onto the slide and smeared out slightly with the pipette tip. The spot of solution should be cloudy white and homogeneous.
6. Dry the liposomes in a petri dish containing a moderate amount of calcium sulfate desiccant for ~1–2 h at 4°C. Liposome spots have to be completely dried before moving

on to the next rehydration step, but it is best to rehydrate as soon as drying is complete.

7. Rehydrate each liposome spot with the same buffer used for liposome formation (e.g., 150 mM KCl, 10 mM MOPS, pH 7.5). A buffer with lower osmolarity may also work, but using a buffer with a higher osmolarity will lead to poorly formed liposomes. The volume used should simply be enough to cover the dehydrated spots.
8. Keep these rehydrated liposome spots at 4°C overnight – this stalls giant liposome formation.
9. The next day, put the liposomes in room temperature, after which there is a time window between ~1 and 3 h where they are best used for patch-clamp. After at least 1 h at room temperature, add an additional ~40–80 μ L of buffer (150 mM KCl, 10 mM MOPS, pH 7.5) to one of the spots, depending on the size of the spot. Pipette up and down to dislodge the liposomes from the glass, making a homogeneous-looking solution.
10. Place a shard of glass coverslip incubated in polylysine overnight at the bottom of the patch-clamp recording chamber. Pipette ~15 μ L of giant liposome solution onto the coated coverslip with no solution flow in the chamber, allow liposomes to settle for ~2–5 min (depending on the density of liposomes), and then start solution exchange to wash off any debris that is not adhering to the coverslip.
11. We have not identified any consistent rules for obtaining gigaohm seals with giant liposomes. Generally, best success seems to be achieved by sealing onto liposomes that are smaller and have a relatively thin membrane border (closer to being unilamellar). To obtain seals more easily, pipettes with a resistance of ~1–3 M Ω are typically used. Avoid adding EGTA/EDTA to solutions unless absolutely necessary because trace contaminating ions such as Ca²⁺ may help seals. Patch-clamp recording from liposomes is difficult, but with persistence and care, these recordings can be obtained routinely (see Subheading 3.6 for details on techniques for inside-out patch-clamp recordings).

3.5. Eukaryotic Cell Culture

1. CosM6 cells (see Note 3) are grown in standard T-25 (25 cm²) square tissue culture flasks. These cells are very adherent, and no measures are taken to maintain adherence. Flasks are passaged every 4–5 days, with standard tissue culture protocols, using trypsin/EDTA to dislodge cells from the bottom of the flask. We have not encountered problems with expression or reproducibility of ion channel function even at relatively high passage number (~50), but make it practice to discard cells after ~50 passages.

2. To prepare for experiments (DAY 1), cells are first split into 35 mm petri dishes or 6-well plates. A fairly high level of confluence is acceptable at this stage, to optimize transfection efficiency with liposomal transfection reagents (see manufacturer's instructions regarding the optimal confluence of cells for transfection with a particular reagent).
3. (DAY 2) Plated cells are transfected with plasmids containing the cDNA for the desired ion channel and any necessary auxiliary subunits. Standard liposome-based transfection reagents generally work well for this purpose. Some optimization may be necessary to maximize expression and efficiency. In addition, a plasmid encoding GFP or some other useful marker is also included in the transfection, to help assess efficiency and identify transfected cells while recording.
4. (DAY 3) Transfected cells are split and plated onto sterile glass coverslips, in 35 mm petri dishes (or a 6-well plate). Soaking coverslips in ethanol and flaming them is sufficient for sterilization. Trypsin/EDTA is used to dislodge cells from the bottom of tissue culture plates, and cells are gently triturated to break up clumps of cells. The density of plating may be varied according to the planned experiment. For characterizing the effects of polyamines, inside-out patch-clamp recordings are the typical method of choice. This recording configuration is sometimes easier at somewhat high levels of confluence (~50% on the day of recording), because cells tend to adhere better to the dish, making it easier to excise a membrane patch (other recording configurations, such as whole cell mode, require isolated individual cells). Lower and higher degrees of confluence are also tolerable, but not ideal. Typically, cells are useful for recording up to 3 days after plating onto cover slips.
5. (DAY 4–6) Electrophysiological recordings (see Sub-heading 3.6).

**3.6. Functional Assay:
Patch-Clamp
Electrophysiology**

High resolution characterization of polyamine effects on Kir channels necessitates the “inside-out” patch-clamp technique. In this technique, a giga-ohm seal is formed between a patch pipette and a cell or liposome, and a membrane patch is excised, thereby exposing the cytoplasmic membrane face to the bathing solution. This configuration allows the application of specific polyamines, at specific concentrations. The generation of high-quality inside-out patch-clamp recordings presents many challenges, especially with regard to polyamine interactions, and we will share some of the detailed methods we and others have used to overcome these experimental hurdles.

1. Patch-clamp pipettes are manufactured from thin-walled borosilicate glass, using a micropipette puller (e.g., Sutter P-97).

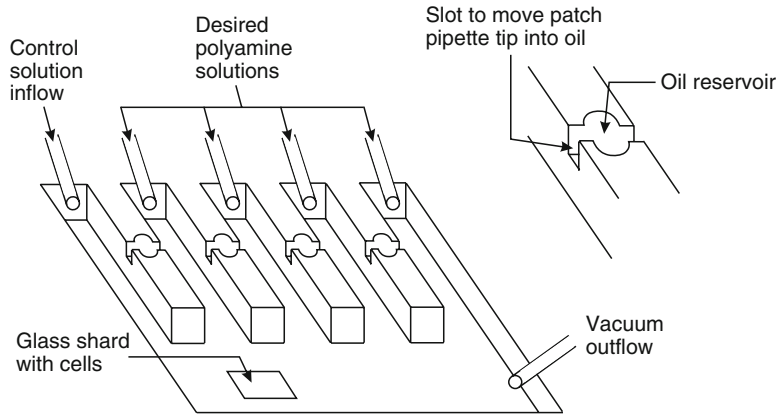


Fig. 1. Schematic diagram of patch-clamp recording chamber for studying polyamine interactions with inwardly rectifying potassium (K_{ir}) channels. Control (polyamine-free) and polyamine solutions flow into distinct lanes separated by physical barriers. The barriers are manufactured to contain small reservoirs that are filled with mineral oil. Small slots on either side of the reservoir are used to allow patch pipettes to be moved briefly into contact with oil. Solutions can be changed with relative ease by moving the chamber (on a translatable stage) relative to the patch pipette.

Using symmetrical 150 mM KCl solutions, the resistance of pipettes used is typically in the range of 0.5–1.5 M Ω . For measurement of kinetics of blockade, it may also be helpful to coat pipettes with Sylgard.

2. The recording chamber we employ is depicted in Fig. 1, although many possible configurations of recording chambers are used. This recording chamber is designed to accommodate up to five different solutions and enables relatively easy solution exchange, by moving the patch pipette between the lanes of the chamber (by moving the translatable microscope stage).
3. With solutions flowing in the recording chamber, glass coverslips plated with cells are broken into small shards, and a shard is transferred to the recording chamber using delicate forceps.
4. A transfected cell is selected for recording by green GFP fluorescence or some other marker of transfection.
5. Using a micromanipulator, a patch pipette is moved close to the vicinity of the cell, and fine adjustments are used to bring the pipette into contact with the cell. As the pipette contacts the cell, there is an increase in resistance across the tip of the pipette (patch-clamp acquisition programs have routines such as the “Seal Test” that monitor tip resistance to alert the operator that the pipette has contacted the cell). Application of a small amount of suction (using a syringe, or mouth) through a tube connected to the patch-clamp pipette holder will ideally result in a dramatic increase in resistance, and

- formation of a giga-ohm seal. Seal formation is not an easy task for a beginner, and requires practice.
6. Formation of an inside-out patch requires excision of a small patch of membrane from a cell. This is achieved by quickly moving the patch pipette away from the cell after formation of a giga-ohm seal. The best possible outcome is formation of a useful excised patch; however, this is not always the case. On occasion, the entire cell may lift from the bottom of the recording chamber, or alternatively, a vesicle may form in the tip of the patch pipette (by excess pieces of membrane sealing together). In these situations, a common approach is to briefly (<1 s) remove and return the patch pipette to the recording solution using the micromanipulator. This brief exposure to air sometimes ruptures the cell/vesicle and exposes the cytoplasmic face of the membrane patch to bathing solution. Another approach is to use a small bead of mineral oil in the recording chamber (as in Fig. 1). Brief exposure of a cell/vesicle to oil rapidly disintegrates cellular materials outside the patch, but typically leaves the excised patch (protected by the patch pipette) intact.
 7. Excised patches are perfused with control solution. During this time, polyamines diffuse away from the patch, until little rectification is apparent at positive voltages. It is often difficult to fully wash polyamines away from patches, and some residual polyamine block may be tolerable, depending on the goal of the experiment (see Note 4). Application of desired voltage-step or voltage-ramp protocols in the presence or absence of polyamines can be used to determine the voltage and dose-dependence of blockade for particular pairs of ion channels and polyamines.

4. Notes

1. Liposomes are formed in the presence of Buffer B, leading to liposomes with high internal KCl. For certain experimental questions, it may be desirable to switch the identity of the cation used during the formation of liposomes, to use a cation mixture, or to supplement the solution with a channel blocker/modifier such as a polyamine.

After the liposomes are exposed to Buffer C (400 mM Sorbitol, 0 KCl), permeant ions exit the liposomes via available conduction pathways (i.e., ion channels), generating a strong electrical gradient across the liposome membrane. In subsequent steps, when the liposomes are added to solutions that contain permeant ions, liposomes immediately begin to take up permeant ions.

2. It is important to recognize that many blockers interact with ion channels with specific “sidedness.” Polyamine blockade is far more potent from the intracellular side of the channel, and this is a complication that must be taken into account when analyzing $^{86}\text{Rb}^+$ uptake into liposomes and potentially patch-clamp recordings from giant liposomes. In the case of polyamine exposure during the $^{86}\text{Rb}^+$ uptake assay, we have observed that polyamine-sensitive mutants of KirBac1.1 exhibit a biphasic dose–response to spermine (Fig. 2). This likely corresponds to a 50:50 mix of ion channels oriented with their cytoplasmic side on either the outside or inside of the liposome (channels oriented outwards will exhibit a strong sensitivity to spermine, while channels with the cytoplasmic entrance inside the liposome will only be weakly sensitive to spermine). In the case of patch-clamp electrophysiology, we have used a variety of approaches to determine sidedness of channels in the liposome bilayer. One approach is to introduce a reactive cysteine (KirBac1.1 has no native cysteine) at a pore-lining position. This results in current reduction upon exposure to cysteine reactive compounds (e.g., MTSET), so long as the channel is oriented appropriately. A second approach (somewhat elegant in principle, but difficult in practice) is to use cysteine mutant channels in the KirBac “slide helix” region

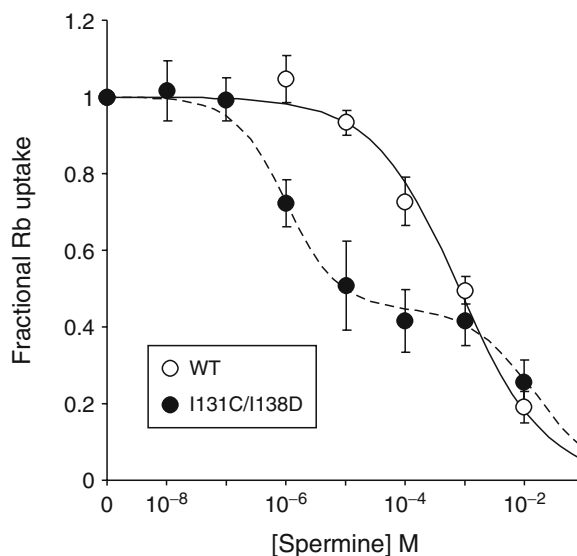


Fig. 2. Biphasic spermine dose–response relationship of KirBac1.1 channels in $^{86}\text{Rb}^+$ uptake assay. Plot of relative $^{86}\text{Rb}^+$ uptake of WT KirBac1.1 and KirBac1.1 I131C/I138D (a mutant that confers strong polyamine sensitivity) in liposomes at different concentrations of externally applied spermine, normalized to uptake without spermine ($n=9 \pm \text{SEM}$). The I131C/I138D data are fit with the sum of two Hill functions, and the WT data with a single Hill function. Most importantly, only 50% of $^{86}\text{Rb}^+$ uptake is inhibited with high affinity, because the I131C/I138D mutation generation of high affinity block only to internal/cytoplasmic spermine and channels are bidirectionally oriented.

which are inactive when unmodified, but become active after MTSET modification (9, 13). In this scenario, application of MTSET to the cytoplasmic face ensures that all recorded activity arises from channels with the same orientation.

3. Detailed characterization of polyamine interactions with eukaryotic Kir channels is most conveniently done in a heterologous expression system. The two basic options in this regard are immortalized mammalian cell lines or *Xenopus* oocytes, and the selection of an expression system will depend primarily on the relative expression of the ion channel of interest. In our own experiments, we have found that CosM6 cells (a mammalian cell line) work especially well for expression of KATP (Kir6.2 + SUR1), Kir2.1, and Kir4.1 channels – the model ion channels most frequently used in our experiments. We consistently achieve extremely high expression of all of these channels in CosM6 cells. In addition, this cell line has proven especially amenable to “inside-out” patch-clamp experiments, as CosM6 cells adhere very well to standard plastic tissue culture dishes. Other groups have successfully employed *Xenopus* oocytes for studies of similar channels.
4. A quantitative description of polyamine blockade requires reliable measurement of channel currents in the absence and presence of polyamines. In the inside-out patch configuration, it is certainly possible to wash away polyamines from patches, so that virtually no blockade/inward rectification is detectable in polyamine-free solutions. However, a hurdle that may be encountered is extremely slow washout of polyamines from patches. We envision that this issue arises due to formation of recessed patches in the tip of the patch pipette. To minimize this problem, we strive for “flat patches,” by using very little negative pressure during seal formation. When using cultured mammalian cell lines, it may help to experiment with different plating protocols (trypsinization time, cell density, etc.) to develop one that results in good seal formation with minimal negative pressure, but ultimately, patience, practice, and persistence are the prime requirements.

While much of this is viewed as simply good practice, other details are worth mentioning. Notably, spermine has proven to be especially “sticky” in our recording chambers and perfusion systems. Frequent replacement of plastic tubing and fastidious cleaning of the recording chamber will assist in the generation of cleanly washed patches. In addition, various impurities in commercially available HEPES buffer have proven to cause modest inward rectification and stand in the way of generating cleanly perfused patches. We and others have had greater success using phosphate-buffered solutions, together with EDTA (~1 mM), to ensure that no contaminating divalent cations contribute to rectification.

References

- Nichols CG (2006) KATP channels as molecular sensors of cellular metabolism. *Nature* 440:470–476
- Kane GC, Lam CF, O’Cochlain F, Hodgson DM, Reyes S, Liu XK, Miki T, Seino S, Katusic ZS, Terzic A (2006) Gene knockout of the KCNJ8-encoded Kir6.1 K(ATP) channel imparts fatal susceptibility to endotoxemia. *FASEB J* 20:2271–2280
- Bockenbauer D, Feather S, Stanescu HC, Bandulik S, Zdebek AA, Reichold M, Tobin J, Lieberer E, Sterner C, Landoure G, Arora R, Sirimanna T, Thompson D, Cross JH, van’t Hoff W, Al Masri O, Tullus K, Yeung S, Anikster Y, Klootwijk E, Hubank M, Dillon MJ, Heitzmann D, Arcos-Burgos M, Knepper MA, Dobbie A, Gahl WA, Warth R, Sheridan E, Kleta R (2009) Epilepsy, ataxia, sensorineural deafness, tubulopathy, and KCNJ10 mutations. *N Engl J Med* 360:1960–1970
- Nichols CG, Lopatin AN (1997) Inward rectifier potassium channels. *Annu Rev Physiol* 59:171–191
- Lu Z (2004) Mechanism of rectification in inward-rectifier K⁺ channels. *Annu Rev Physiol* 66:103–129
- Lopatin AN, Makhina EN, Nichols CG (1994) Potassium channel block by cytoplasmic polyamines as the mechanism of intrinsic rectification. *Nature* 372:366–369
- Shyng S, Ferrigni T, Nichols CG (1997) Control of rectification and gating of cloned KATP channels by the Kir6.2 subunit. *J Gen Physiol* 110:141–153
- Fujiwara Y, Kubo Y (2006) Functional roles of charged amino acid residues on the wall of the cytoplasmic pore of Kir2.1. *J Gen Physiol* 127:401–419
- Enkvetchakul D, Jeliaskova I, Nichols CG (2005) Direct modulation of Kir channel gating by membrane phosphatidylinositol 4,5-bisphosphate. *J Biol Chem* 280:35785–35788
- Enkvetchakul D, Bhattacharyya J, Jeliaskova I, Groesbeck DK, Cukras CA, Nichols CG (2004) Functional characterization of a prokaryotic Kir channel. *J Biol Chem* 279:47076–47080
- Kuo A, Gulbis JM, Antcliff JF, Rahman T, Lowe ED, Zimmer J, Cuthbertson J, Ashcroft FM, Ezaki T, Doyle DA (2003) Crystal structure of the potassium channel KirBac1.1 in the closed state. *Science* 300:1922–1926
- Kuo A, Domene C, Johnson LN, Doyle DA, Venien-Bryan C (2005) Two different conformational states of the KirBac3.1 potassium channel revealed by electron crystallography. *Structure* 13:1463–1472
- Cheng WW, Enkvetchakul D, Nichols CG (2009) KirBac1.1: it’s an inward rectifying potassium channel. *J Gen Physiol* 133:295–305

Part III

Transgenic Models for Study of Polyamine Function

Chapter 7

Carcinogenesis Studies in Mice with Genetically Engineered Alterations in Polyamine Metabolism

David J. Feith

Abstract

Polyamines are intimately linked to essential cellular processes that are required for cell growth and proliferation, and abundant evidence links polyamine metabolism to tumor susceptibility and progression. Intensive efforts over the past 2 decades have yielded numerous mouse models of cancer that utilize genetic manipulations to recapitulate the molecular alterations and cellular interactions that characterize human cancers. These models provide the ideal genetic context to examine the impact of altered polyamine content on tumor biology, with the goal of applying the knowledge acquired in mice to the prevention and treatment of human cancer. Transgenic and knockout mouse technologies allow the investigator to enhance or delete, respectively, the expression of a given polyamine metabolic enzyme or regulatory protein, and advanced models facilitate both temporal and spatial control of gene expression in the mouse. These methods can be utilized to modulate total polyamine content or relative polyamine ratios in specific cell populations *in vivo* and evaluate the impact of this manipulation on tumor appearance and progression. This chapter provides resources to identify existing mouse strains that exhibit increased susceptibility to tumor development as well as strains that were engineered for increased or decreased expression of polyamine regulatory proteins. A conceptual framework is then presented to combine these resources in order to successfully complete a carcinogenesis study in mice with altered polyamine metabolism.

Key words: Polyamine, Transgenic mice, Knockout mice, Conditional transgene, Conditional knockout, Carcinogenesis, Mouse models of cancer

1. Introduction

Cancer is a complicated process that involves uncontrolled cell growth, invasion of surrounding tissues, and eventually spread to noncontiguous sites in the body. To complete this process, cells must acquire numerous capabilities that are normally lacking or actively suppressed (1). Many of these capabilities are acquired through genetic alterations that lead to gain or loss of function in

particular genes during the evolution of a normal cell to an invasive and metastatic tumor cell. Evidence indicates that histologically similar human cancers can achieve this state through many distinct molecular alterations and mutations. Mutations in nearly 400 genes are casually linked to tumor development, and expression levels are altered for many other genes (2). Moreover, this cell autonomous molecular transformation occurs in the context of nonmutated cells of the same developmental lineage as well as heterotypic interactions with vascular cells, immune cells, and supporting fibroblasts. Many of these other cell types impart critical factors that contribute to cancer progression. Taken together, these observations suggest that *in vivo* systems with multiple defined genetic alterations are necessary to model the complexity of human cancer (1, 3).

A wealth of information on the genetics and developmental biology of the mouse has enabled the manipulation of preimplantation embryos to accomplish the gain or loss of gene function in the resulting mouse (4). This includes the microinjection of DNA into fertilized oocytes to generate transgenic mice that express a protein in a spatially restricted manner that is dictated by the promoter and enhancer elements that drive transgene transcription. Conversely, manipulation of murine embryonic stem cells allows for targeted disruption or replacement of endogenous genes to create knockout or knockin mice. Increasingly complex conditional systems enable temporal and spatial control of transgene expression through the use of small molecules to activate transgene transcription or protein location (5). Therefore, the levels of the transgene-derived protein can be turned on and off as needed and even titrated between these states. Moreover, the Cre/loxP system can catalyze targeted rearrangements of genomic DNA to effect conditional, but not reversible, gene knockout or activation of a latent knockin allele (5, 6). The advent and combination of these and other sophisticated methods (3, 7) now allow investigators to more accurately recapitulate the complex biology of cancer in mice. Critical factors to be considered in these models are tumor development within the relevant cell type; targeted genetic alterations that are important to human cancer; progression through sequential benign, malignant, and metastatic stages; and histology and gene expression signatures that are consistent with the human disease (3). Although there are some differences between the genetic networks and signaling pathways of mouse and human cells (8), sophisticated mouse models represent a far more accurate platform to examine tumorigenesis than the traditional subcutaneous human tumor xenograft model.

Polyamines participate in the macromolecular processes that are required for cell growth, such as DNA replication, gene transcription, and mRNA translation. Therefore, it is not surprising

that extensive genetic and pharmacological evidence links polyamine biosynthesis and catabolism with both normal and neoplastic growth (9, 10). This evidence includes studies with mice in which the polyamine metabolic pathway is modified by the overexpression or deletion of polyamine regulatory enzymes and proteins. The fundamental experimental paradigm is illustrated by representative carcinogenesis studies with alterations in ornithine decarboxylase (ODC) or spermidine/spermine N^1 -acetyltransferase (SSAT) activity (reviewed in (11–13)). Elevated activity was accomplished through tissue-specific promoters or increased gene copy number, and activity was suppressed via dominant negative ODC, antizyme (AZ) expression or heterozygous/homozygous gene knockout. These studies utilized two of the best-characterized mouse models of tumor initiation, promotion, and progression, namely DMBA/TPA chemical carcinogenesis of the skin (14) and the *Min*/+ mouse model of colorectal tumorigenesis (15).

The goal of this chapter is to stimulate the reader to conceive interesting and informative carcinogenesis studies that utilize mouse models of cancer in combination with genetically engineered alterations that modify polyamine metabolism and to provide a practical framework to successfully complete this type of study. Resources are presented to identify existing mouse strains that exhibit increased susceptibility to tumor development as well as those with altered polyamine metabolism. Looking forward, one can envision nearly infinite experimental models when considering target tissues and cell types, signaling pathways, oncogene activation, and tumor suppressor gene loss, as well as constitutive or stage-specific gene expression or deletion.

2. Materials

1. Oligonucleotide primers for polymerase chain reaction (PCR) amplification (see Table 1). Dissolve in 10 mM Tris-HCl pH 8 and store at -20°C .
2. REDExtract-N-AMP Tissue PCR Kit (XNAT), Sigma-Aldrich Co., St. Louis, MO.
3. Polytron homogenizer (PT 10-35) and generator (PTA 7), Kinematica-Inc., Bohemia, NY.
4. 5-Bromo-2 -deoxyuridine (BrdU, B5002), Sigma-Aldrich Co., St. Louis, MO. Dissolve in phosphate buffered saline at 10 mg/ml by heating at 37°C for 15–30 min. Stable for up to 6 months at -20°C . Sterile filter before use. Caution: BrdU is a known mutagen, avoid contact with powder or solution.

Table 1
Primer sequences to detect endogenous mouse genes or transgenes

	Primer sequences ^a	Product Size (bp) ^b
<i>Endogenous mouse genes</i>		
p53	Sense: 5'-TGAGTGCTAGCTAGGCTTAGAGGTGCAAGC-3' Antisense: 5'-AGTGGATGGTGGTATACTCAGAGCCGGCCT-3'	335
AZ	Sense: 5'-GACACTGCCTGTGAGGCCTG-3' Antisense: 5'-GCTGGGAGCTCGATGTAGAG-3'	520
<i>Transgenes</i>		
Neo	Sense: 5'-CTTGGGTGGAGAGGCTATTC-3' Antisense: 5'-AGGTGAGATGACAGGAGATC-3'	280
tTA or rtTA	Sense: 5'-CGCCAGAAAGCTAGGTGTAG-3' Antisense: 5'-GCTCCATCGCGATGACTTAG-3'	200
K5-AZ, K6-AZ, or tetO-AZ	Sense: 5'-GGCCTCGGTGGTGCTCCG-3' Antisense: 5'-GCTGGGAGCTCGATGTAGAG-3'	250
K6-SSAT	Sense: 5'-GCAGAAGGAGGGGACAATTATCAC-3' Antisense: 5'-TGGGCGGATCACGAATTTAGC-3'	400

^aThese primer sequences are used routinely in the author's laboratory for PCR-based identification of our transgenic and knockout mice. This is not a comprehensive list of transgenic and knockout mice with altered polyamine metabolism (reviewed in (11–13, 16)). Primers to detect an endogenous gene are included in each screening reaction in order to demonstrate successful PCR amplification in each genomic DNA sample. The AZ cDNA used to generate transgenic mice contains a single nucleotide deletion to eliminate the requirement for polyamine-stimulated frameshifting during translation of the transgene mRNA (24). The PCR primers are specific to this deletion, and therefore, may be used to detect any AZ transgenic mouse. Note that the AZ gene and transgene products share a common antisense primer

^bProduct sizes are approximate

3. Methods

The following methods provide the framework for a carcinogenesis study in mice with targeted genetic alterations. General principles are presented that apply to all carcinogenesis studies in mice, rather than specific details of a given protocol. Techniques to generate new transgenic and knockout models are provided elsewhere in extensive detail (4), and these services are available in core facilities at many large research institutions or through commercial vendors (see Note 1). It is essential that the specific activities in the investigator's laboratory must be reviewed and approved by the Institutional Animal Care and Use Committee (IACUC) or by an equivalent regulatory body.

3.1. Selection of Model Mouse System

1. Choose the tissue or tumor type of interest, determine the genes that play a critical role in tumorigenesis within that tissue, and investigate available mouse models. Table 2 lists some of the many resources and repositories that provide

Table 2
Internet resources for information on genetically engineered mice and mouse models of cancer

Source	Web address
Trans-NIH Mouse Initiatives	www.nih.gov/science/models/mouse/
NIH Knockout Mouse Project	www.komp.org/
International Knockout Mouse Consortium	www.knockoutmouse.org/
NIH Mutant Mouse Regional Resource Centers	www.mmrrc.org/index.html
NCI Mouse Models of Human Cancers Consortium	www.emice.nci.nih.gov/
Mouse Tumor Biology Database	www.tumor.informatics.jax.org/mtbwi/index.do
Cre Mouse Database	www.nagy.mshri.on.ca/cre/
Tet Mouse Database	www.zmg.uni-mainz.de/tetmouse/index.htm

mouse models to the research community, including well-characterized mouse models of cancer (Mouse Models of Human Cancer Consortium, MMHCC), pretargeted ES cell lines for the production of knockout mice (NIH Knockout Mouse Project, KOMP), strains with tissue-specific expression of tTA and rtTA proteins for tetracycline-regulated transgene systems (Tetmouse Base), and a database of resources for Cre recombinase-based genetic manipulation (Cre-X-Mice). Tumor induction or appearance must be reproducible within the chosen model without an excessively long latency. Tumors can be induced not only by genetic manipulation but also by chemical carcinogens, environmental factors such as UV radiation and dietary manipulation, or via protocols that combine several of these factors.

2. Choose a mouse model with the desired alteration in polyamine metabolism. A wide number of transgenic and knockout mice with altered polyamine metabolism have been published (reviewed in (11–13, 16)), and others that employ more advanced technology are undoubtedly under development. Alternatively, the investigator can design and create new lines of transgenic, knockout, regulated transgenic and conditional knockout mice (4). Consult the resources listed in Table 2 for available targeted ES cells and strains with tissue-specific tetracycline-regulated transcriptional activator (tTA or rtTA) or Cre expression to prevent expensive and time-consuming duplication of effort.

3. Acquire all of the necessary mouse strains and establish a colony within a specific pathogen free (SPF) animal facility to ensure that the animals are maintained in peak health. To identify animals with the desired genetic alteration, conduct PCR amplification on genomic DNA isolated from tail biopsies. The specificity of the PCR screen is determined by the design of the oligonucleotide primers (Table 1). Most transgenes are constructed such that the protein coding sequence is placed under the control of promoter and regulatory elements of an endogenous gene. Both the promoter and coding sequences are typically present in the mouse genome but not colocalized; therefore, an effective screening strategy is to design PCR primers that amplify the junction of the promoter and coding sequences. PCR primer design is very simple for transgenic and knockout animals that contain exogenous genes such as tTA or rtTA or Cre recombinase, primers are simply designed to amplify a region within this foreign DNA. Most targeting constructs for knockout mouse production contain the neomycin resistance gene (Neo) to facilitate the selection of embryonic stem cell clones with the desired targeting event, and a region of the Neo gene can be amplified to identify mice that carry the knockout allele. However, heterozygous animals are not differentiated from homozygous knockout mice by this method, and additional primer pairs are required to demonstrate the absence of the wild-type allele in homozygous knockout animals.
4. Collect tail biopsies according to methods recommended in the NIH “Guidelines for the genotyping of mice and rats” (<http://oacu.od.nih.gov/ARAC/>). Specifically, a sterile scalpel is used to excise an approximately 3 mm biopsy from the tip of the tail from mice less than 21 days of age. DNA is isolated from the tail biopsy and analyzed by PCR using the REDExtract-N-AMP Tissue PCR Kit according to the manufacturer’s instructions. Analyze PCR products by agarose gel electrophoresis (see Note 2).
5. When combining multiple transgenic or knockout mouse strains, all animals should ideally be maintained on the same homogeneous inbred genetic background. This can be accomplished prior to the carcinogenesis study by breeding the mouse with the targeted mutation with a wild-type mouse of the desired inbred strain for at least five generations. Transgenic or knockout offspring are identified by PCR screening and again crossed with a wild-type mouse of the inbred strain. Continued backcrossing in this manner results in a progressive increase in the percent of the genome that is contributed by the inbred strain. Alternatively, one can cross two mutant strains that are maintained on different genetic backgrounds

and analyze the F1 progeny of this cross in which 50% of the genome is derived from each strain (see Note 3).

3.2. Conduct of Carcinogenesis Experiments

1. Once the mouse strains have been acquired, expanded, and backcrossed if needed, establish a breeding scheme to generate animals of the desired genotype for the carcinogenesis study (see Note 4). The common breeding schemes outlined in Table 3 will yield progeny of the indicated genotype and frequency, assuming that mice of all genotypes are viable and all targeted alleles segregate independently. More complex schemes and multiple rounds of breeding are required to combine three or more targeted alleles. In addition, one can increase the frequency of useful progeny by producing homozygous transgenic animals. Maintain meticulous records to track all breeding pairs, resulting pups and their genotypes. Give a unique number or identifier to every mouse to facilitate unambiguous record keeping for both colony management and poststudy analysis of mouse tissues. A carefully designed spreadsheet is easily manipulated and works well for this purpose. See the following guide for additional guidance on breeding schemes and estimating yield based on expected genotype frequency, average pregnancy rates, and litter sizes in a given inbred strain background (http://transgenic.cwru.edu/docs/breeding_strategies_manual.pdf).
2. Assign animals to experimental groups for the carcinogenesis study (see Note 5). All groups should be composed of equal numbers of male and female animals to control for any

Table 3
Breeding schemes to combine transgene and knockout alleles

Parent 1 ^a	Parent 2 ^a	Offspring genotype and expected frequency (%)			
TgA/+	Wild type	Wild type (50)	TgA/+ (50)		
TgA/+	TgB/+	Wild type (25)	TgA/+ (25)	TgB/+ (25)	TgA/+, TgB/+(25)
TgA/+	+/-	Wild type (25)	TgA/+ (25)	+/- (25)	TgA/+, +/- (25)
+/-	-/-	+/- (50)	-/- (50)		
TgA/+, +/-	-/-	+/- (25)	TgA/+, +/- (25)	-/- (25)	TgA/+, -/- (25)

Offspring of each genotype are assumed to be 50% male and 50% female

Tg/+ hemizygous transgenic; ± heterozygous knockout; -/- homozygous knockout or null

^aTgA and TgB represent two different transgenes, and + or - represent wild type or knockout alleles, respectively, of an endogenous gene

sex-dependent differences in tumor response. When utilizing chemical carcinogens, treat all animals at the same age with a standard dose of carcinogen that is applied in a consistent and reproducible manner (see Note 6).

3. Monitor animals for tumor development weekly or at an appropriate frequency based on the established timing of tumor onset in the chosen protocol (see Note 7). The description provided here describes the analysis of solid tumors rather than hematological cancers. Techniques will vary depending on the tissue of interest and may include visual inspection (skin, oral cavity), palpation (mammary gland), or advanced imaging methodology (brain and other internal organs) (17). Collect age or time of tumor onset, tumor location, and tumor size for each experimental animal. Utilize technology for *in vivo* assessment of bioluminescence or fluorescence if the mouse model was designed to express one or more of these markers in association with the tumor-inducing genetic alteration (18, 19). In the absence of advanced imaging modalities to quantify tumor burden in internal organs on a weekly basis, assess tumor burden at a single endpoint upon euthanizing the experimental animals if the timing of tumor onset and growth is well established and reproducible in the carcinogenesis model. Collect tumor incidence, multiplicity, and size at this single time point for comparison between the groups.
 4. At the completion of the experiment, plot tumor-free survival vs. time, tumor multiplicity per mouse vs. time and tumor size for each experimental group. Consult with a statistician to determine the proper statistical methods for comparisons between the groups. Tumor-free survival is typically compared by Kaplan–Meier log-rank analysis of the curves, and tumor multiplicity and size are compared by a Student’s *t*-test.
 5. Terminate the study by euthanizing all experimental animals using accepted methods (<http://www.avma.org/resources/euthanasia.pdf>). Collect tissue samples for biochemical analysis and record terminal tumor measurements. This requires careful record keeping for each mouse and multiple sample collection tubes per animal. It is strongly recommended that a second tissue biopsy, not necessarily from the tail, be collected at this time in order to confirm the genotype of each animal.
1. Rapidly remove tissues from the animal, freeze in liquid nitrogen, and store at -80°C . Prepare tissue extracts by mechanical disruption of the tissue using a Polytron homogenizer in the appropriate assay buffer with the sample tube kept on ice to reduce sample heating. Assay polyamine metabolic enzyme activity and tissue polyamine content by standard methods ((20) and this volume) and protein content by Western blotting.

3.3. Analysis of Tissues Samples

Ideally, these measures should be done in both tumor tissue and surrounding normal tissue. If tumors are of sufficient size, complete the biochemical analyses and histology (see Subheading 3.3.2) on two pieces of tissue derived from the same tumor (see Note 8).

2. Collect specimens of tumor and adjacent normal tissue, fix 4 h to overnight in 10% neutral buffered formalin, embed in paraffin and section for histology and immunohistochemistry (IHC). The analysis should include a classification of tumor cell morphology in both control and PA-modulated samples and an assessment of tumor cell invasion into the surrounding normal tissue. Determine proliferation rate by BrdU IHC of S-phase cells or phospho-histone H3 IHC of mitotic cells and express the labeling index as (number of labeled cells/total number of cells) \times 100. Note that BrdU labeling of S phase cells requires that all animals be injected with the thymidine analog BrdU (100 mg/kg i.p.) 1–2 h prior to euthanasia. Identify apoptotic cells by terminal deoxynucleotidyl transferase dUTP nick end labeling (TUNEL) staining or cleaved caspase 3 IHC. Additional IHC assessment of differentiation markers as well as markers of tumor cell progression to a more malignant state is advised, but the specific markers depend on the tissue and tumor type under study.
3. Conduct Western blot or IHC analysis of relevant signaling pathways that regulate cell growth, cell cycle, or apoptosis to provide additional insight into the molecular mechanisms responsible for the observed phenotype. It is important to note that Western blot analysis of nuclear and membrane-associated phospho-proteins requires that whole cell lysates be prepared in buffer with phosphatase inhibitors.
4. Conduct a gene expression microarray or proteomic comparison of control and polyamine-modulated tumor tissue for an unbiased assessment of genes and proteins that are altered in response to the manipulation of polyamine levels.

4. Notes

1. All genetically altered mouse lines will require some initial characterization prior to their utilization in carcinogenesis studies. Transgenic animals produced by traditional methods exhibit random integration of the transgene DNA into the genome of the founder animal, usually with multiple copies arranged in head-to-tail arrays. This typically occurs at a single site, but one must consider the unlikely possibility of multiple independently segregating integration sites when breeding

founder animals. The transgene integration site and copy number will influence transgene expression, and the level of expression must be characterized in mice from each founder line. Tumorigenesis studies should be conducted with transgenic animals from multiple founder lines. If each of these independent founder lines exhibits an equivalent susceptibility to tumor development, then one can conclude with confidence that the phenotype is related to the expressed transgene rather than insertional mutagenesis of an endogenous gene or regulatory element.

Disruption or replacement of a mouse gene is accomplished through homologous recombination between a targeting construct and the endogenous gene locus in murine ES cells. Construct design and selection procedures enhance the isolation of clones with targeted rather than random integration events. Nevertheless, additional molecular analysis by Southern blotting with carefully chosen probe sequences must be conducted on DNA isolated from ES cells or knockout animals to confirm the desired integration event before converting to PCR screening to maintain a line with targeted gene disruption.

2. The high throughput and low cost of PCR analysis make this the preferred method to genotype genetically engineered mice. However, PCR is an enzymatic reaction that is extremely sensitive to both false positive and false negative results. Proper genotype discrimination by PCR is absolutely essential to every phase of the project from identification of the initial transgenic founder or targeted knockout to maintenance and expansion of the genetically altered line, to generation of the experimental animals. Therefore, the PCR screening protocol for each transgene or knockout allele should be extensively optimized to provide the utmost in both sensitivity and specificity. Parameters to be optimized include primer concentration, annealing temperature, cycle number, and cycle time. The investigator may eventually choose to design new primers if the initial set does not perform adequately. The reaction must produce a single, intense product of the expected size only in transgenic or knockout animals and must be sensitive enough to detect a single copy transgene in genomic DNA, which can be verified by established protocols (<http://www.med.umich.edu/tamc/spike.html>). Ideally, there should be no variability in product intensity since this will reduce confidence in the quantitative scoring of the PCR product and could lead to false positive results (scoring a wild-type mouse as transgenic/knockout). An additional source of false positive results is the carryover or cross-contamination of transgenic/knockout DNA during tail biopsy collection, genomic DNA isolation, or PCR reaction setup, all of which can be avoided by good molecular biology techniques. False negative

results (no product from the genomic DNA of a transgenic/knockout mouse) are typically derived from insufficient DNA extraction or technical errors in reaction setup. They can be identified and avoided by the inclusion of a second primer set in the PCR reaction that will amplify a region of endogenous genomic DNA in every sample. Therefore, this amplicon serves as a control to demonstrate that adequate genomic DNA, polymerase, and other components were included in the reaction to allow for PCR amplification of an endogenous genomic sequence (see Table 1).

3. Among the great strengths of mouse models of cancer are the wealth of available strains with targeted alterations and the ability to easily combine these alterations through straightforward breeding strategies. However, one must carefully consider the inbred strain background in a carcinogenesis study in order to properly interpret the experimental results and to conclusively demonstrate that the observed phenotype is related to the induced genetic alteration in a polyamine regulatory protein. The evolution of a tumor from a normal cell involves numerous genetic and epigenetic alterations (1, 2). Modifier genes either restrict or enhance this process, and functionally distinct alleles of the same gene may be present in two different inbred mouse strains (21). The unequal segregation of these modifier alleles can affect tumor incidence, multiplicity, and size in a carcinogenesis study, as demonstrated for the K6-ODC transgene (22). If steps are not taken to ensure genetic homogeneity of the experimental animals, experimental groups must include more animals to account for the expected heterogeneity in the tumor response and extensive endpoint analyses will be required to conclusively demonstrate that the expected alterations in polyamine metabolism correlate with the observed tumor phenotype.
4. One must consider the group sizes that are necessary to provide sufficient statistical power to detect an effect of the polyamine modifier on tumor development in the relevant carcinogenesis model. This is done in consultation with a statistician after careful analysis of the literature to determine the typical group sizes and tumor yield in the protocol of interest. Importantly, a mixed genetic background is very likely to increase the variability in tumor response and necessitate larger group sizes. In addition, consider the number of endpoint assays to be done on tumor tissue, the amount of tissue needed for each assay, and the expected yield and size of tumors when planning the number of experimental animals in each group.
5. In most cases, all progeny in a litter will be used for the carcinogenesis study because littermates represent the best

control animals due to their similar strain background, age, and environment. In experiments that combine multiple transgenes, knockout alleles or combinations thereof, the single transgene/knockout animals are necessary control groups that must be compared to the compound mutant animals. These strategies are greatly preferred over comparison to historical data due to the errors that can be introduced by variables such as differences in strain background, carcinogen stocks or observer. In conditional models where transgene expression is regulated by a small molecule in bitransgenic mice, additional control groups are required in order to demonstrate that any phenotype is not observed in bitransgenic mice in the absence of the inducing agent or in single transgenic animals treated with the small molecule inducer.

6. To conduct carcinogenesis studies that combine multiple transgenic and knockout alterations, the investigator must breed the relevant mouse strains and genotype the progeny to generate the experimental animals. Due to space constraints, limited breeder animals and practical limitations of massive weaning and genotyping efforts, these experiments are typically done with a rolling accrual process. Cohorts of experimental animals are generated, genotyped, and initiated into the study as they become available as opposed to the type of simultaneous study initiation that is feasible with commercially available mice that can be ordered in large volumes at a given age.
7. Frequent supervision of the experimental animals is required for any study that induces tumor development to ensure that the animals do not endure unnecessary pain and suffering. In addition, readily assessed criteria must be established at the onset to determine when an animal will be euthanized due to excessive tumor burden (23). Common criteria include large tumor mass, inability to ambulate, eat or drink, lethargic behavior, and/or ulcerated tumor mass.
8. The most comprehensive and informative dataset can be acquired by conducting all analyses (enzyme biochemistry, polyamine levels, IHC) on individual pieces of the same tumor. However, this is rarely feasible due to the small size of mice, the need to avoid excessive tumor burden in the experimental animals, and the requirement for different processing methods and buffers for each assay. An acceptable alternative is to conduct one assay per tumor or even pool individual small tumors to obtain sufficient tissue. Establish predetermined endpoints prior to initiating the experiment in order to guide group sizes (see Step 3.2.1 and Note 4) and sample collection methods to ensure an adequate supply of tumor tissue for the desired assays.

Acknowledgements

The author thanks Patricia Welsh for her outstanding technical expertise in the maintenance of mouse strains and utilization of mouse models of cancer in his laboratory.

References

- Hanahan D, Weinberg RA (2000) The hallmarks of cancer. *Cell* 100:57–70
- Stratton MR, Campbell PJ, Futreal PA (2009) The cancer genome. *Nature* 458:719–724
- Van Dyke T, Jacks T (2002) Cancer modeling in the modern era: progress and challenges. *Cell* 108:135–144
- Nagy A, Gertsenstein M, Vintersten K, Behringer R (2003) Manipulating the mouse embryo: a laboratory manual, 3rd edn. Cold Spring Harbor Laboratory Press, New York
- Lewandoski M (2001) Conditional control of gene expression in the mouse. *Nat Rev Genet* 2:743–755
- Nagy A (2000) Cre recombinase: the universal reagent for genome tailoring. *Genesis* 26:99–109
- Tuveson DA, Jacks T (2002) Technologically advanced cancer modeling in mice. *Curr Opin Genet Dev* 12:105–110
- Rangarajan A, Weinberg RA (2003) Opinion: comparative biology of mouse versus human cells: modelling human cancer in mice. *Nat Rev Cancer* 3:952–959
- Casero RA Jr, Marton LJ (2007) Targeting polyamine metabolism and function in cancer and other hyperproliferative diseases. *Nat Rev Drug Discov* 6:373–390
- Gerner EW, Meyskens FL Jr (2004) Polyamines and cancer: old molecules, new understanding. *Nat Rev Cancer* 4:781–792
- Gilmour SK (2007) Polyamines and nonmelanoma skin cancer. *Toxicol Appl Pharmacol* 224:249–256
- Janne J, Alhonen L, Pietila M, Keinänen TA, Uimari A, Hyvonen MT, Pirinen E, Jarvinen A (2006) Genetic manipulation of polyamine catabolism in rodents. *J Biochem* 139:155–160
- Pegg AE, Feith DJ (2007) Polyamines and neoplastic growth. *Biochem Soc Trans* 35:295–299
- Abel EL, Angel JM, Kiguchi K, DiGiovanni J (2009) Multi-stage chemical carcinogenesis in mouse skin: fundamentals and applications. *Nat Protoc* 4:1350–1362
- Shoemaker AR, Gould KA, Luongo C, Moser AR, Dove WF (1997) Studies of neoplasia in the Min mouse. *Biochim Biophys Acta* 1332:F25–F48
- Janne J, Alhonen L, Pietila M, Keinänen TA (2004) Genetic approaches to the cellular functions of polyamines in mammals. *Eur J Biochem* 271:877–894
- Lyons SK (2005) Advances in imaging mouse tumour models in vivo. *J Pathol* 205:194–205
- Zinn KR, Chaudhuri TR, Szafran AA, O'Quinn D, Weaver C, Dugger K, Lamar D, Kesterson RA, Wang X, Frank SJ (2008) Noninvasive bioluminescence imaging in small animals. *ILAR J* 49:103–115
- Hoffman RM (2005) The multiple uses of fluorescent proteins to visualize cancer in vivo. *Nat Rev Cancer* 5:796–806
- Morgan DML (ed) (1998) Polyamine protocols. In: *Methods in molecular biology*, vol 79. Humana Press, Totowa
- Balmain A (2002) Cancer as a complex genetic trait: tumor susceptibility in humans and mouse models. *Cell* 108:145–152
- George K, Iacobucci A, Uitto J, O'Brien TG (2005) Identification of an X-linked locus modifying mouse skin tumor susceptibility. *Mol Carcinog* 44:212–218
- Wallace J (2000) Humane endpoints and cancer research. *ILAR J* 41:87–93
- Matsufuji S, Matsufuji T, Miyazaki Y, Murakami Y, Atkins JF, Gesteland RF, Hayashi S (1995) Autoregulatory frameshifting in decoding mammalian ornithine decarboxylase antizyme. *Cell* 80:51–60

Transgenic Rodents with Altered SSAT Expression as Models of Pancreatitis and Altered Glucose and Lipid Metabolism

Anne Uimari, Mervi T. Hyvönen, Eija Pirinen, and Leena Alhonen

Abstract

Depletion of pancreatic acinar cell polyamines in response to activation of polyamine catabolism is associated with the development of acute pancreatitis in experimental rodent models. The disease is characterized by general hallmarks seen also in human pancreatitis, such as accumulation of intraperitoneal ascites, acinar cell necrosis, and pancreatic as well as remote organ edema and inflammation. Thus, these animals make useful models for the human disease. Determination of these hallmarks can be used to assess the severity of the disease and to evaluate the efficacy of any therapy applied. The metabolic changes seen in genetically modified mice with either accelerated or inactivated polyamine catabolism have revealed that polyamine catabolism is involved in the regulation of glucose and lipid metabolism. The simplest method to determine the metabolic phenotype of the animal is to assess the concentrations of blood metabolites. Fasting blood glucose level is an indicator of overall glucose homeostasis, whereas fasting insulin level is a useful marker of insulin sensitivity. A more detailed analysis of glucose homeostasis and insulin sensitivity can be obtained by intraperitoneal glucose and insulin tolerance tests. Blood lipid levels mainly reflect triglyceride, free fatty acid, and cholesterol metabolism. Altered blood glucose and/or lipid levels are associated with several diseases, e.g., diabetes, Cushing's syndrome, hyperthyroidism, atherosclerosis, pancreatitis, and dysfunction of the liver and kidneys.

Key words: Acute pancreatitis, Edema, Myeloperoxidase, Histological damage, Glucose metabolism, Insulin sensitivity, Glucose tolerance, Lipid metabolism, Lipoproteins, Cholesterol, Free fatty acids, Triglycerides

1. Introduction

Enhanced polyamine catabolism, due to overexpression of the key polyamine catabolic enzyme spermidine/spermine N^1 -acetyltransferase (SSAT), causes development of acute pancreatitis in rats and is associated with improved glucose, energy,

and lipid homeostasis in mice. In transgenic rats, the metallothionein promoter-driven SSAT gene expression is induced by a nontoxic dose of zinc. This leads to rapid depletion of spermidine and spermine, and results in a severe acute necrotizing pancreatitis within 24 h (1, 2). In transgenic mice, ubiquitous overexpression of SSAT causes reduced white adipose tissue (WAT) mass, high basal metabolic rate, improved glucose tolerance, high insulin sensitivity, and low circulating total cholesterol levels through activation of the key regulator of energy metabolism and bile acid synthesis, peroxisome proliferator activated receptor γ coactivator 1 α in WAT and liver (3, 4). By contrast, SSAT-KO mice develop insulin resistance upon aging, but they do not show any alterations in circulating lipid levels (5).

Pancreatitis, an inflammation of the pancreas, is a severe, life-threatening disease with many complications. Several rodent models of acute pancreatitis, induced by, e.g., L-arginine (6), caerulein (7), taurodeoxycholate (8), CDE-diet (9), or L-ornithine (10), have been developed to study the pathological features of the disease. All the models, including the MT-SSAT transgenic rat model, share many of the common characteristics in the pathogenesis of pancreatitis. In severe disease, macroscopic evaluation reveals accumulation of intraperitoneal ascites, pancreatic edema, fat necrosis of pancreas, and visceral fat as well as the signs of inflammation in other organs. Remote organ involvement can also be demonstrated by quantitating edema and leukocyte infiltration in these organs. Histological techniques show the destruction of pancreatic acini and acinar cell structures, invasion of inflammatory cells, and also any potential structural damage in remote organs.

The maintenance of blood glucose concentrations within a narrow physiological range is central for a continuous supply of glucose to the brain as a source of energy. Glucose homeostasis is accomplished through highly regulated mechanisms depending on three simultaneously ongoing processes involving insulin secretion by the pancreas, hepatic glucose output, and glucose uptake by splanchnic (liver and intestine) and peripheral tissues (skeletal muscle and WAT) (11). The main hormone regulating glucose homeostasis is insulin, the function of which is to reduce postprandial glucose levels by inhibiting hepatic glucose production and stimulating glucose uptake in peripheral tissues (11, 12). Skeletal muscle is the major site for insulin-stimulated glucose disposal whereas only 5–10% of disposal is accomplished by WAT (13). Glucose uptake in splanchnic tissues is stimulated only by glucose.

Lipids, derived either from the diet or from the synthesis in liver and WAT, are insoluble in the aqueous environment, in the blood, and they do not circulate in the free form (12). Free fatty acids (FFA) are bound to albumin and cholesterol; cholesterol esters, phospholipids, and triacylglycerides (TGs) are associated with apolipoproteins and transported in the circulation as

lipoproteins. The main function of lipoproteins is to facilitate the transport of lipids between various tissues where lipids are used, e.g., as energy source, sterols, and bile acid precursors or membrane components (12, 14). Dietary cholesterol and TGs absorbed from small intestine are transported to the liver by chylomicrons. Very low density lipoprotein (VLDL) particles transport TGs and cholesterol to the circulation where VLDL particles are converted to intermediate-density lipoprotein (IDL) and low density lipoprotein (LDL) particles. The function of LDL particles is then to deliver cholesterol to extrahepatic tissues. By contrast, high density lipoprotein (HDL) particles acquire lipids from peripheral tissues and transport them back to liver. In human, LDL cholesterol represents more than 50% of total cholesterol whereas HDL is the predominant plasma lipoprotein in mice (15). FFAs are the major source of energy for many tissues, and they are derived from WAT via lipolysis or hydrolysis of TGs in chylomicrons and VLDL particles. The important regulator of lipoprotein and FFA metabolism is insulin, which increases clearance of chylomicrons and VLDL from the circulation, reduces the hepatic synthesis of VLDL particles, and inhibits the release of FFAs via lipolysis in WAT.

Since insulin is a critical regulator of glucose and lipid homeostasis, alteration in insulin sensitivity often evokes substantial changes in the circulating concentrations of insulin, glucose, and lipid (FFA, TG and cholesterol) levels. Therefore, a simple method to evaluate glucose and lipid homeostasis in animals is to screen the concentrations of these blood metabolites. Insulin sensitivity can be evaluated in mice by performing intraperitoneal glucose and insulin tolerance tests.

2. Materials

2.1. Macroscopic Inspection of Pancreatitis

1. Equipment for animal euthanasia: CO₂ anesthesia, cervical dislocation, or decapitation.
2. Ethanol 70%.
3. 0.9% NaCl.
4. Scissors, forceps, and plastic film.

2.2. Tissue Edema

1. Microcentrifuge tubes.
2. A scale (precision at least 1 mg).
3. An oven heated to +80°C.

2.3. Myeloperoxidase Activity Assay

1. Buffer 1: 20 mM potassium phosphate buffer pH 7.4.
2. Buffer 2: 0.5% hexadecyl trimethylammoniumbromide (HTAB) in 50 mM potassium phosphate buffer pH 6.0. First

make 5% HTAB stock solution in water by dissolving 2.5 g in 50 ml and heating to $\sim 40^{\circ}\text{C}$.

3. Buffer 3: 500 μM *o*-dianisidine, 0.006% H_2O_2 in 50 mM potassium phosphate buffer pH 6.0. First dissolve *o*-dianisidine in distilled ultrapure H_2O , and then add potassium phosphate buffer and H_2O_2 .
4. Ultra Turrax or Potter homogenizer.
5. 8-Channel pipette.
6. ELISA 96-well plate reader at A (450 nm).

2.4. Basic Histology with Hematoxylin-Eosin (HE) Staining

1. Forceps.
2. Buffered formalin: Dissolve 16 g NaH_2PO_4 and 26 g Na_2HPO_4 in 3,600 ml of distilled water. Add 400 ml formalin (37–40% formaldehyde). Adjust pH to 7.0–7.2 with 5 M NaOH.
3. Histology cassettes.
4. Tissue processing system (Citadel, Shandon).
5. Ethanol 50, 80, 96, and 100%.
6. Xylene.
7. Paraffin granules (Algol).
8. Embedding system (Histocentre, Shandon).
9. Ethanol 100 and 96%.
10. Delafield's hematoxylin.
11. Acid ethanol: 5% HCl in 70% ethanol.
12. Eosin.
13. Xylene-based mounting medium (Depex, BDH 361254D).

2.5. Fasting Glucose, Insulin, and Lipid Samples

1. A restraining tube (e.g., 50 ml Falcon tube with holes in it).
2. Razor blades.
3. 21–25G needles.
4. Glass capillaries (e.g., Sarsted) or capillary tubes (e.g., Microvette) (see Note 1).
5. Eppendorf tubes (for blood, plasma, and/or serum).
6. Pipettes and tips.
7. Ice and dry ice.

2.6. Glucose and Insulin Tolerance Tests

1. An animal scale (precision 1 mg).
2. Clean cages.
3. Heparinized or EDTA coated capillaries or capillary tubes (e.g., Sarsted, Microvette).
4. Syringes (1 ml).
5. Scalpel blades.

6. 26–27G needles.
7. For *glucose tolerance test*: 20% d-glucose in sterile filtered physiological saline solution.
8. For *insulin tolerance test*: Human insulin (e.g., Actrapid, Novo Nordisk) in sterile filtered 0.1% BSA solution dissolved in physiological saline. Prepare shortly before use (see Note 2).
9. For *insulin tolerance test*: Sterile filtered 10% d-glucose solution in physiological saline solution.
10. Timer.
11. Ice and dry ice.
12. Pipettes and tips.
13. Eppendorf tubes (for plasma samples).

3. Methods

Macroscopic inspection of the abdomen and the central organs is an important part of the evaluation of the pathogenesis of pancreatitis. Depending on the model, the progression time and level of the signs vary; thus the time for euthanasia depends on the model. When the abdomen is opened, ascites, the extra fluid in peritoneal cavity, might be seen around the organs; and when the animal is turned a bit, the fluid accumulates against the abdominal wall. Inflamed pancreas is gray or yellow in color and is swollen or net-like because of the edema. Foci of steatonecrosis (fat necrosis) can be present in pancreatic tissue and in visceral fat.

Also the other organs, most often liver, kidney, and lungs can be affected. The changed color of the organs usually suggests inflammation. The extent of tissue edema can be easily quantified by measuring tissue wet and dry weights. Myeloperoxidase is an enzyme present at large amount in neutrophils. During acute inflammation, neutrophil proportion in the blood increases and they infiltrate to inflamed tissues. Thus, myeloperoxidase activity can be used as a measure of the extent of tissue inflammation.

For histological analysis, the tissue specimen is stained to visualize cellular structures. The tissue is fixed, paraffinated, and cut into thin sections. The standard staining consists of staining with hematoxylin, followed by eosin. After mounting, the stained slides are ready for microscopic inspection. The staining allows the distinction between nucleus and cytoplasm and reveals the appearance of inflammatory cells in the tissue. Edema can also be detected in the inspection of histology samples.

Mouse models are important tools for studying molecular mechanisms leading to metabolic disorders. Therefore, the ability to explore the hormonal and metabolic status of mouse strains and mutants is important. Analysis of circulating metabolites is an

initial step to evaluate glucose and lipid homeostasis in mice. Since feeding increases metabolite concentrations in the blood, they should be analyzed in the fasting state in order to reduce the variability of the results between animals. Fasting blood glucose level is the most commonly used indicator of overall glucose homeostasis whereas fasting insulin level is a useful marker of insulin sensitivity. An alteration in fasting insulin level is normally seen earlier than in fasting glucose level. Since blood TGs are associated with VLDL particles and chylomicrons, fasting TG level measures VLDL metabolism, as chylomicrons are cleared from the circulation during fasting. Circulating FFA level mainly reflects insulin sensitivity of adipose tissue and the rate of lipolysis. Total cholesterol level is a measure of LDL, IDL, and HDL cholesterol and therefore, it is more informative to analyze LDL and HDL cholesterol levels separately. Measurement of fasting glucose, insulin, and lipid values from plasma or serum samples can be performed using several methods (15). As the blood volume of mouse is limited, the parameters should be measurable using a very low amount of sample. Whole blood glucose levels can be measured using glucose meters (e.g., Roche Diagnostics, Abbot, Accu-Chek, and LifeScan) whereas enzymatic assays are suitable for analysis of plasma or serum samples. These enzymatic measurements can be carried out manually or with an automated laboratory work station. Insulin levels are usually analyzed using insulin ELISA kits (e.g., Crystal Chem Inc., Mercodia, and Linco research). Serum or plasma TG, total cholesterol, HDL cholesterol, LDL cholesterol, and FFA levels are measured using enzymatic colorimetric assays either manually or automatically. Nowadays, many of these measurements can also be performed using specific kits, which can be purchased for example from Sigma, Wako, or Roche Diagnostics.

If the initial screening shows abnormalities in fasting glucose and/or insulin levels, glucose and insulin tolerance tests described below can be used to investigate glucose homeostasis in more detail (16). Glucose tolerance test is used to measure a clearance rate of glucose from the blood after glucose administration. This test provides information about glucose-induced insulin secretion by pancreatic β -cells and insulin sensitivity in the liver and peripheral tissues. Glucose can be administered either by oral gavage or by injection into the intraperitoneal cavity. The advantage of oral gavage is that it takes into account the intestinal effects of glucose administration. The disadvantage is that it is more stressful to the animal, and therefore, intraperitoneal glucose tolerance test is more commonly used in mice. Blood is collected typically at least time points 0, 15, 30, 60, and 120 min for glucose and insulin measurements. Maximum size of experimental cohort is usually 12 mice. Intraperitoneal insulin tolerance test is commonly used

in mice to evaluate insulin sensitivity in peripheral tissues. The ability of an insulin load to reduce blood glucose levels is an index of insulin sensitivity. However, insulin tolerance test is sensitive to several confounding factors including effects of counterregulatory hormones (e.g., glucagons, catecholamines) and stress. A more reliable quantitative analysis is euglycemic hyperinsulinemic clamp technique, but this method is technically demanding due to need of catheterization of the mouse. Blood is collected for glucose measurements at several time points, e.g., 0, 20, 40, and 80 min. The number of animals that can be used in one test is from 12 to 16.

It should be noted that the animal experiments described here require approval by the local authorities (e.g., Institutional Animal Care and Use Committee).

3.1. Macroscopic Inspection of Pancreatitis

1. Sacrifice the animal with induced acute pancreatitis with the chosen method (see Note 3).
2. Spray the abdominal side with 70% ethanol.
3. Lift the abdominal skin up with the forceps and cut with scissors horizontally. Then continue the cutting vertically along the whole abdomen (see Note 4).
4. Cut the peritoneal membrane carefully and inspect the presence of ascites by turning the animal a little bit to its side. Figure 1a depicts abdomen of a healthy rat and Fig. 1b that of a rat with acute pancreatitis showing accumulation of ascites and pale, affected liver.
5. Inspect the presence of fat necrosis (chalky deposits) in visceral fat.
6. Pull up the pancreas by lifting the spleen with the forceps and inspect the color, structure, and appearance of the pancreas (see Note 5). Macroscopic views of a healthy and an edematous, hemorrhagic pancreas are shown in Fig. 1c.
7. Remove the pancreas by carefully cutting along the attached organs.
8. Place the pancreas on plastic film with some 0.9% NaCl on it and remove contaminating fat (white and light tissue) before analyses.
9. Inspect the color of the liver.
10. Inspect the appearance of kidneys.
11. Cut the ribs of the animal. While cutting, lift the chest up by holding from the xiphisternum with the forceps.
12. Inspect the appearance of the lungs and heart.
13. Excise extrapancreatic tissues for the analysis of edema and inflammation.

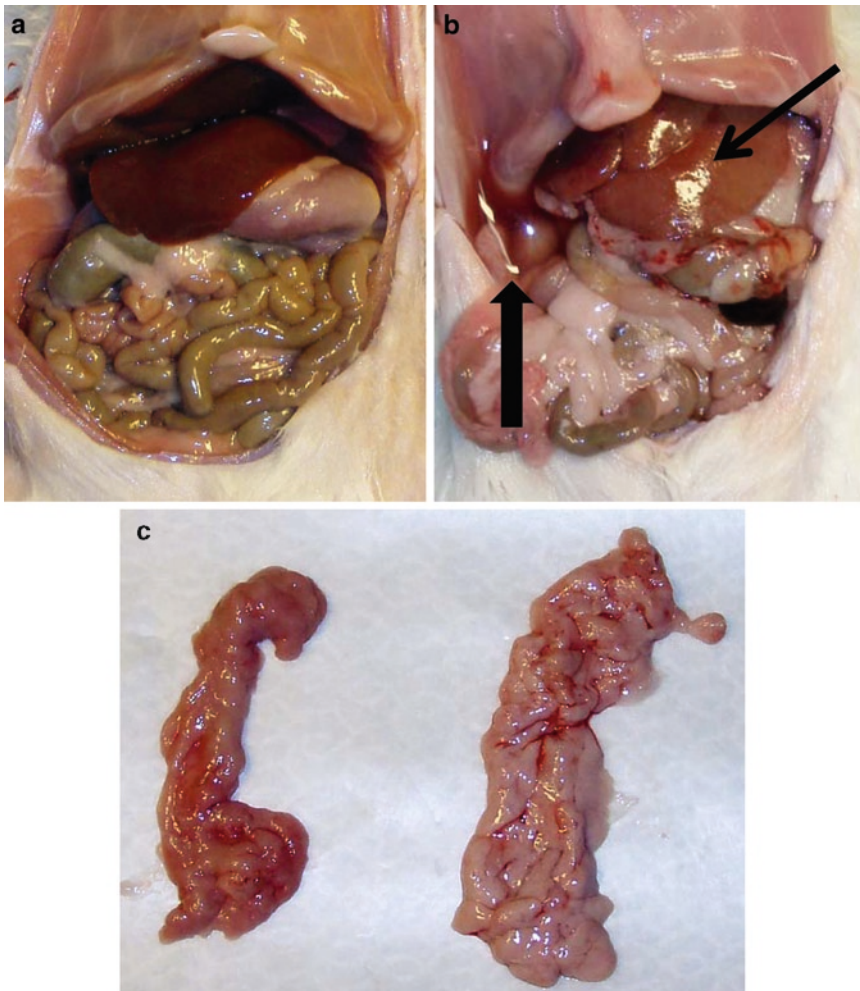


Fig. 1. Macroscopic abdominal findings 24 h after induction of acute pancreatitis in MT-SSAT transgenic rats. To induce pancreatitis, the rats were injected with ZnSO_4 (10 mg Zn^{2+}/kg i.p.) before sacrifice. In comparison with a healthy animal (a), accumulation of ascites (*thick arrow*) and paler liver (*thin arrow*) are seen in a transgenic rat with acute pancreatitis (b). Excised pancreas from a healthy rat [(c) left] and from a rat with acute pancreatitis showing edema and hemorrhage [(c) right].

3.2. Tissue Edema

1. Number and weigh empty microcentrifuge tubes (m_0).
2. Cut the tissue pieces to the size of ~100 mg and place them into the tubes.
3. Weigh the tubes (m_1).
4. Place the tubes with caps open into oven heated to $+80^\circ\text{C}$ and let the tissues dry for 48 h.
5. Weigh the tubes (m_2).
6. Calculate the percentage of water of total tissue weight with the following formula:

$$\text{water \%} = ((m_2 - m_0) / (m_1 - m_0)) \times 100\%.$$

7. Depending on the tissue investigated, the percentage of water should be around 60–80%. Higher percentage indicates the presence of edema.

3.3. Myeloperoxidase Activity Assay

1. Weigh a piece of fresh or frozen tissue (~100 mg).
2. Homogenate the tissue on ice in 10× vol of buffer 1 using Ultra Turrax or Potter homogenizer.
3. Transfer to round-bottomed 2 ml microcentrifuge tube and centrifuge at 10,000×*g* for 10 min at +4°C (see Note 6).
4. Resuspend the pellet to 3× vol of buffer 2 until homogenous (see Note 7).
5. Freeze in liquid nitrogen and thaw on +20°C water bath. Repeat 2 times.
6. Sonicate for 90 s.
7. Centrifuge at 12,000×*g* for 10 min at +4°C and transfer the supernatant to new tube.
8. During centrifugation, prepare fresh buffer 3.
9. Pipette samples to clear 96-well plates 10 µl/well in duplicate or triplicate (see Note 8).
10. Set ELISA plate reader ready at A (450 nm) with kinetic measurement at every 10 s for 10 min.
11. Pipette 200 µl of buffer 3 using 8-channel pipette and start the measurement.
12. Plot the absorbances (*y*) against time (*x*) and calculate the slope of each sample from the linear part of the curve.
13. Express the results as percentage or fold of control samples.

3.4. Basic Tissue Histology with Hematoxylin and Eosin (HE) Staining

1. Place a small, fresh specimen in a pencil-marked histology cassette and submerge in formalin solution (see Note 9). Keep in fixative for at least 24 h.
2. Check that the liquid reservoirs of the tissue processing system are filled to the line. Wash the histology cassette in running tap water for 15 min and place it in the processing basket (see Note 10). This process substitutes the tissue water content with paraffin. Run the processing according to the instruction manual (the run takes about 19 h). At the end of the program, the cassette is left in the paraffin reservoir.
3. Fill the reservoir of the embedding system with paraffin granules and switch the system on 2 h before use in order to melt the paraffin. Transfer the cassette from the processing system into the reservoir of the embedding system and open the cassette. Place the specimen with forceps in a preferred position in a steel mold filled with paraffin. Cool the mold on a cold plate and cap it with the base of the original cassette with

identification marks. Let cool for 30 min and remove the paraffin block from the mold.

4. Using disposable blades, cut the blocks to 4 μm sections with a rotary microtome (Microm) according to the instruction manual. Pick up the sections from the warm water bath on top of a microscope slide marked with a pencil to identify the sample. Let the slide dry in a vertical position overnight at room temperature.
5. Deparaffinize sections in xylene and rehydrate through graded ethanol series to water by immersing the slide twice in xylene for 5 min, twice in 100% ethanol for 2 min, and twice in 96% ethanol for 2 min. Rinse fast in distilled water.
6. Stain in Delafield's hematoxylin for 7 min (see Note 11). Wash in running tap water for 5 min (sections become blue again). Dip in acid ethanol until the color is as desired (4–5 times). Wash in running tap water for 5 min.
7. Stain in eosin for 2.5 min. Dehydrate through graded ethanol series and clear in xylene by immersing in 96% ethanol for 30 s, 96% ethanol for 1 min, twice in 100% ethanol for 2 min, and twice in xylene for 5 min.
8. Mount the slide using Depex or other xylene-based mounting medium and let dry overnight in the hood.
9. View the slide under light microscope using an appropriate magnification. Hematoxylin stains cell nuclei blue, while eosin stains cytoplasm and connective tissue pink or red. Eosin is strongly absorbed by red blood cells, coloring them bright red. Pancreatic histology of normal tissue and of tissue showing acute necrotizing pancreatitis is depicted in Fig. 2a, b, respectively.

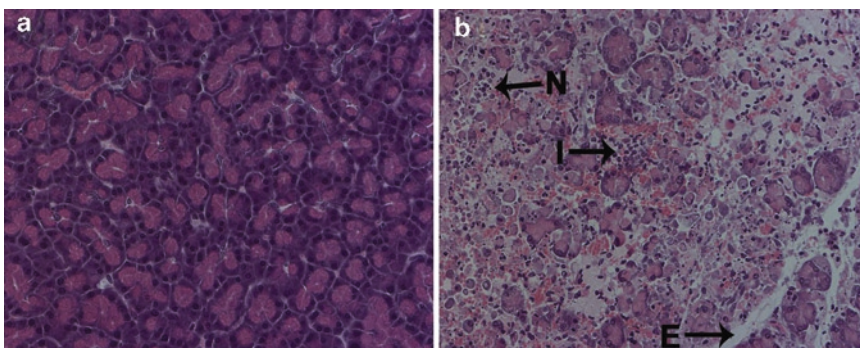


Fig. 2. Histology of pancreas 24 h after induction of acute pancreatitis in MT-SSAT transgenic rats. To induce pancreatitis, the rats were injected with ZnSO_4 (10 mg Zn^{2+} /kg i.p.) before sacrifice. (a) Pancreas from a healthy rat (not injected with Zn^{2+}), (b) pancreas from a rat with acute pancreatitis showing edema (E), acinar cell necrosis (N) and presence of inflammatory cells (I).

3.5. Fasting Glucose, Insulin, and Lipid Samples

1. Fast mice with water ad libitum (see Note 12).
2. Record the weight of each mouse.
3. Place a mouse into a restraining tube, head first.
4. In order to visualize the vein, remove hair from the caudal surface of the hind limb using razor blade or depilatory product.
5. Warming of the mouse will increase the blood flow. For example, keep the mouse under a lamp for a couple of minutes or place a lamp over the cage.
6. In order to distend the vein, apply pressure to the vein by pressing with a finger upstream the puncture site.
7. Puncture the saphenous vein with a 21–25G needle and release the pressure.
8. Collect blood drops using heparinized glass capillaries or capillary tubes (see Note 1). The maximum volume of blood to be collected at one time is 1% of body weight, e.g., 200 μ l from a 20 g mouse.
9. If blood is not flowing easily, apply pressure to the vein and release. Repeat several times (see Note 13).
10. In order to stop bleeding, apply pressure over the puncture site.
11. Return the mouse to its cage and ensure free access to food and water.
12. If glass capillaries are used, transfer blood into empty Eppendorf tubes kept on ice.
13. Centrifuge blood samples at 13,000 rpm for 1 min at +4°C.
14. Transfer plasma or serum into Eppendorf tubes and freeze samples quickly on dry ice. If multiple analyses will be made from the same sample, it is recommended to aliquot plasma or serum prior to freezing.
15. Determine glucose, insulin, and lipid levels using the methods of your choice.

3.6. Intraperitoneal Glucose and Insulin Tolerance Tests

1. Make sure that there is no other activity in the animal room while you are performing the test.
2. Fast mice with water ad libitum (see Note 12). Do so for insulin tolerance test only if the tested mice are not very sensitive to insulin (see Note 14).
3. Weigh the mice and mark their tails in the order in which you will handle them.
4. Place mice in clean cages without food (water ad libitum) (see Note 15). Mark the cages with the mouse number(s).
5. *Glucose tolerance test*: Calculate the volume of 20% glucose solution required by each mouse for a dose of 2 mg/g in an injection volume 5–10 μ l/g body weight.

6. *Insulin tolerance test*: Calculate the volume of insulin solution required by each mouse for the desired dose in an injection volume 5–10 $\mu\text{l/g}$ body weight (see Note 16).
7. Fill syringes with glucose or insulin solution, respectively, and remove air bubbles carefully.
8. Take fasting blood sample (time-point 0 min sample) of the first mouse. Use a scalpel blade to cut off a 1 mm piece of the tail tip and squeeze blood ($\sim 40\text{--}50\ \mu\text{l}$ for glucose tolerance test or $\sim 20\text{--}25\ \mu\text{l}$ for insulin tolerance test) (see Note 13) onto a capillary for glucose and insulin measurements in glucose tolerance test or just glucose level in insulin tolerance test (see Note 17).
9. Transfer blood from the capillary into an Eppendorf tube kept on ice.
10. Plasma is obtained after centrifugation at 13,000 rpm at $+4^\circ\text{C}$ for 1 min.
11. Transfer plasma into a clean Eppendorf tube and freeze the sample quickly on dry ice. *Glucose tolerance test*, it is recommended to aliquot plasma for glucose and insulin measurements prior to freezing.
12. After collecting time-point 0 min sample, inject the correct dose of glucose or insulin solution, respectively, intraperitoneally to the first mouse. When you do the injection, start the timer.
13. Take fasting blood samples from the other mice and inject glucose or insulin, respectively.
14. *Glucose tolerance test*: Take blood samples at the 15, 30, 60, and 120 min time points (see Note 18). Start with the first mouse injected and use the same interval as with the injections. Follow timing as accurately as possible. Recutting of tail tip is not needed, just remove the clot from the first incision.
15. *Insulin tolerance test*: Take blood samples at the 20, 40, and 80 min time points as described above. At the end of experiment, inject 10% glucose solution ($\sim 100\text{--}120\ \mu\text{l}$ for 20 g mouse) intraperitoneally in order to normalize blood glucose levels.
16. At the end of experiment, place mice into clean cages with food and water ad libitum.
17. *Glucose tolerance test*: The mean glucose and insulin values $\pm\text{SEM}$ for each group of mice are plotted vs. time as presented in Fig. 3a. Typically, the area under the glucose curve is also calculated using a trapezoidal method as described in (16).
18. *Insulin tolerance test*: For each mouse, glucose value is calculated as the percentage of the glucose value at time-point 0 min. The mean values $\pm\text{SEM}$ for each group are plotted vs. time as shown in Fig. 3b.

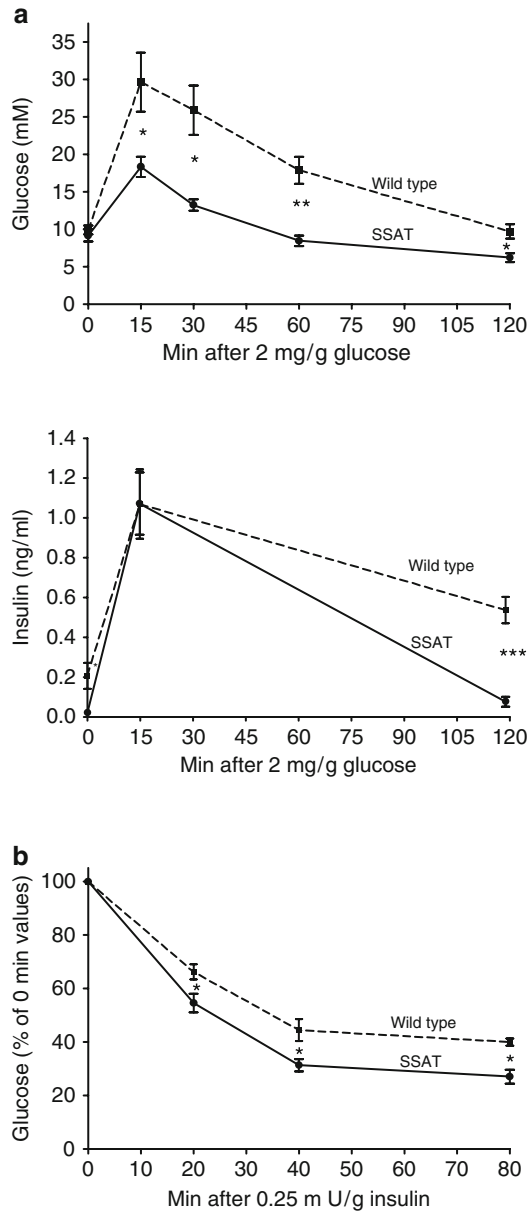


Fig. 3. Improved glucose tolerance and higher insulin sensitivity in SSAT mice. **(a)** Intrapерitoneal glucose tolerance test (2 mg/g glucose) was performed in fasted nonanesthetized female SSAT (*solid line*) and wild-type (*dashed line*) mice. SSAT mice had increased glucose clearance from the circulation showing improved glucose tolerance. Significantly lower insulin concentrations in SSAT mice indicated that they have increased insulin sensitivity. **(b)** Intrapерitoneal insulin tolerance test (0.25 mU/g insulin) was performed in fasted nonanesthetized female SSAT (*solid line*) and wild-type (*dashed line*) mice. The presence of higher insulin sensitivity in SSAT mice was evident as they had significantly decreased glucose concentrations after an insulin injection. Results are presented as means \pm SEM of six mice per group. *, $p < 0.05$, **, $p < 0.01$, and ***, $p < 0.001$.

4. Notes

1. Plasma samples can be collected using, e.g., heparinized glass capillaries (Sarsted) or potassium-EDTA or heparinized capillary tubes (Microvette). For serum samples, there are, e.g., serum-clotting activator coated capillary tubes (Microvette).
2. Insulin is dissolved in 0.1% BSA solution in order to avoid the binding of insulin to plastic walls of the tubes or syringes.
3. If you need to collect blood from the heart, sacrifice the animal with CO₂ and cut the chest at first. Collect the blood into suitable tubes (EDTA, heparin, etc.) by placing the tube under the right ventricle and cutting the tissue with the scissors.
4. Keep the scissors between the skin and the peritoneal membrane. That way you keep the peritoneal membrane intact and do not lose the abdominal fluid or break the organs.
5. Pancreas is a large loose organ, which attaches spleen and gastrointestinal tract (stomach and the guts) and sometimes visceral fats. Some experience is needed to recognize the whole organ.
6. This washing step removes the remaining hemoglobin that interferes with the reaction. If the samples have been perfused or otherwise do not contain hemoglobin, the samples can be homogenized directly to buffer 2 without the washing step.
7. Small Ultra Turrax can be used if resuspension with pipette is difficult.
8. The sample volume may be increased to 40 µl if the slopes of the reaction curves are too low. If nonlinear phase is obtained too quickly, the sample may be diluted to buffer 2.
9. The volume of fixative should be 10 times the volume of the specimen.
10. You can process several cassettes simultaneously.
11. Hematoxylin is replaced with fresh dye once a month: Replace half of the amount in the jar and leave the other half. Replace eosin every 2 or 3 weeks depending on the use. Ethanol, xylene, and acid ethanol are replaced after five uses: Discard the first jar of the two, replace it by the second and take a fresh one as the second. However, the first ethanol following eosin is replaced after every use.
12. The suitable fasting (e.g., 6–16 h) time may vary depending on a mouse model, e.g., 12–13 h fasting time should not be exceeded in transgenic mice overexpressing spermidine/spermine N¹-acetyltransferase (SSAT). Overnight fasting (~16 h) is most often used.

13. Avoid squeezing with too much force. It may cause hemolysis, which may interfere with certain measurements.
14. In order to avoid hypoglycemia, fed mice can be used if tested mice are very sensitive to insulin. If fasted mice are used, test suitable fasting time experimentally (e.g., 6–16 h).
15. Preferably, use individual caging especially for males. The maximum number of mice per cage is 2–3.
16. Depending on insulin sensitivity of mouse line and strain used, the dose may vary. Typically for conscious C57Bl/6 wild-type mice 0.25–0.50 mU/g of human insulin is optimal. If anesthesia is used, a higher insulin dose is needed.
17. Glucose measurement can also be done using a glucose meter. In that case, calibrate the meter before the first measurement and place a small drop of blood on the glucose test strip. Record this value. The use of a glucose meter as the only glucose assay method may be problematic during glucose tolerance test because glucose values at the 15 min time point maybe out of the range of the meter.
18. It is not absolutely necessary to measure insulin levels at time-points 30 and 60 min. If these time points are omitted, only a small volume of blood (~20 µl) is needed for glucose measurement.

Acknowledgements

The authors thank Riitta Sinervirta and Sisko Juutinen for technical assistance and Taina Roiha for the photography of material for Fig. 1. This work was supported by the Academy of Finland.

References

1. Alhonen L, Parkkinen JJ, Keinänen T, Sinervirta R, Herzig KH, Jänne J (2000) Activation of polyamine catabolism in transgenic rats induces acute pancreatitis. *Proc Natl Acad Sci U S A* 97:8290–8295
2. Hyvönen MT, Herzig KH, Sinervirta R, Albrecht E, Nordback I, Sand J, Keinänen TA, Vepsäläinen J, Grigorenko N, Khomutov AR, Krüger B, Jänne J, Alhonen L (2006) Activated polyamine catabolism in acute pancreatitis: alpha-methylated polyamine analogues prevent trypsinogen activation and pancreatitis-associated mortality. *Am J Pathol* 168:115–122
3. Pirinen E, Kuulasmaa T, Pietilä M, Heikkinen S, Tusa M, Itkonen P, Boman S, Skommer J, Virkamäki A, Hohtola E, Kettunen M, Fatrai S, Kansanen E, Koota S, Niiranen K, Parkkinen J, Levonen AL, Ylä-Herttua S, Hiltunen JK, Alhonen L, Smith U, Jänne J, Laakso M (2007) Enhanced polyamine catabolism alters homeostatic control of white adipose tissue mass, energy expenditure, and glucose metabolism. *Mol Cell Biol* 27:4953–4967
4. Pirinen E, Gylling H, Itkonen P, Yaluri N, Heikkinen S, Pietilä M, Kuulasmaa T, Tusa M, Cerrada-Gimenez M, Pihlajamäki J, Alhonen L, Jänne J, Miettinen T, Laakso M (2010) Activated polyamine catabolism leads to low cholesterol levels by enhancing bile acid synthesis. *Amino Acids* 38:549–560

5. Niiranen K, Keinänen TA, Pirinen E, Heikkinen S, Tusa M, Fatrai S, Suppola S, Pietilä M, Uimari A, Laakso M, Alhonen L, Jänne J (2006) Mice with targeted disruption of spermidine/spermine N1-acetyltransferase gene maintain nearly normal tissue polyamine homeostasis but show signs of insulin resistance upon aging. *J Cell Mol Med* 10:933–945
6. Tani S, Itoh H, Okabayashi Y, Nakamura T, Fujii M, Fujisawa T, Koide M, Otsuki M (1990) New model of acute necrotizing pancreatitis induced by excessive doses of arginine in rats. *Dig Dis Sci* 35:367–374
7. Niederau C, Niederau M, Luthen R, Strohmeyer G, Ferrell LD, Grendell JH (1990) Pancreatic exocrine secretion in acute experimental pancreatitis. *Gastroenterology* 99:1120–1127
8. Lankisch PG, Ihse I (1987) Bile-induced acute experimental pancreatitis. *Scand J Gastroenterol* 22:257–260
9. Lombardi B, Estes LW, Longnecker DS (1975) Acute hemorrhagic pancreatitis (massive necrosis) with fat necrosis induced in mice by DL-ethionine fed with a choline-deficient diet. *Am J Pathol* 79:465–480
10. Rakonczay Z Jr, Hegyi P, Dosa S, Ivanyi B, Jarmay K, Biczó G, Hracsko Z, Varga IS, Karg E, Kaszaki J, Varro A, Lonovics J, Boros I, Gukovsky I, Gukovskaya AS, Pandol SJ, Takacs T (2008) A new severe acute necrotizing pancreatitis model induced by L-ornithine in rats. *Crit Care Med* 36:2117–2127
11. Aronoff S, Berkowitz K, Shreiner B, Want L (2004) Glucose metabolism and regulation: beyond insulin and glucagon. *Diabetes Spectr* 17:183–190
12. Murray RK, Granner DK, Mayes PA, Rodwell VW (1993) *Harper's biochemistry*, 23rd edn. Prentice-Hall, Englewood Cliffs
13. DeFronzo RA (2004) Pathogenesis of type 2 diabetes mellitus. *Med Clin North Am* 88:787–835, ix
14. Taskinen MR (2003) Diabetic dyslipidaemia: from basic research to clinical practice. *Diabetologia* 46:733–749
15. Argmann, CA, Houten SM, Champy MF, Auwerx J (2006) Lipid and bile acid analysis. *Curr Protoc Mol Biol* Chapter 29:Unit 29B
16. Heikkinen S, Argmann CA, Champy MF, Auwerx J (2007) Evaluation of glucose homeostasis. *Curr Protoc Mol Biol* Chapter 29:Unit 29B

Use of (Gyro) Gy and Spermine Synthase Transgenic Mice to Study Functions of Spermine

Xiaojing Wang and Anthony E. Pegg

Abstract

The polyamines putrescine, spermidine, and spermine are essential for mammalian cell growth, differentiation, and cell death and have important physiological roles in all tissues. Many of the properties of polyamines that can be demonstrated *in vitro* are common to all three molecules with differences only in potency. Loss of any of the enzymes needed to make either putrescine or spermidine (which also prevent the production of spermine) is lethal, but male mice lacking spermine synthase (SpmS) due to a deletion of part of the X chromosome are viable on the B6C3H background. These mice are termed Gyro (Gy) due to their circling behavior. They have a variety of abnormalities including deafness, neurological problems, small size, and a tendency to early death. They can therefore be used to evaluate the physiological function(s) uniquely provided by spermine. They also provide a potential animal model for Snyder-Robinson syndrome (SRS), a rare human inherited disease due to a loss of SpmS activity. An essential control in experiments using Gy mice is to demonstrate that the abnormal phenotypes exhibited by these mice are abolished by providing replacement spermine and this can be accomplished by breeding with CAG-SMS mice that express SpmS from a ubiquitous promoter. Techniques for identifying, characterizing, and using these mouse strains and limitations of this approach are described in this chapter.

Key words: Spermine, Spermine synthase, Gy mice, CAG-SMS mice

1. Introduction

It is clear that polyamines play multiple and essential roles in mammalian physiology (see Chapter 1). However, the roles of each polyamine, putrescine, spermidine, and spermine are hard to assess individually. Although content of individual polyamines can be perturbed by use of inhibitors, their potential toxicity, lack of potency, and cellular compensatory mechanisms that increase both uptake and lead to compensatory changes in the activity of the biosynthesis/degradation pathways do not provide a clear system to determine their individual functions. Transgenic mice

with deletions of key genes potentially provide a useful system to answer this question, but genetic alterations abolishing either ornithine decarboxylase (1) or S-adenosylmethionine decarboxylase (2) activity are lethal. Attempts to generate mice with specific inactivation of the gene encoding SpmS (*SMS*) using standard gene targeting techniques with XY embryonic stem cells from strain 129/SvJ were not successful although ES cells lacking SpmS and containing no spermine were readily obtained (3). These cells were used to show that a lack of spermine had no effect on growth rate but did alter response to certain anticancer drugs (3). These results agreed with previous studies in which skin (4) and embryonic fibroblasts (5) were obtained from Gy mice that are described below. These Gy cells also have a total lack of spermine and showed no retardation of growth rate, but more detailed studies revealed altered responses to drugs, UV radiation, and oxidative stress (4–7). However, such cells have obvious limitations for more general attempts to study mammalian physiology.

Although the standard knock-out technique with strain 129/SvJ did not result in any viable mice with the *SMS* gene inactivated, a mouse strain lacking all SpmS activity had already been derived much earlier (8). This strain having an X-linked dominant mutation was isolated from a female offspring of an irradiated mouse and was termed gyro (Gy) based on a circling behavior pattern in affected males (8). Later studies using these mice have shown that they have a deletion of part of the X chromosome that inactivates *SMS* (9, 10). The lack of *SMS* causes a total absence of spermine (4, 5, 10, 11). These Gy mice have many abnormalities. These include a greatly reduced size (Fig. 1), deafness, sterility,

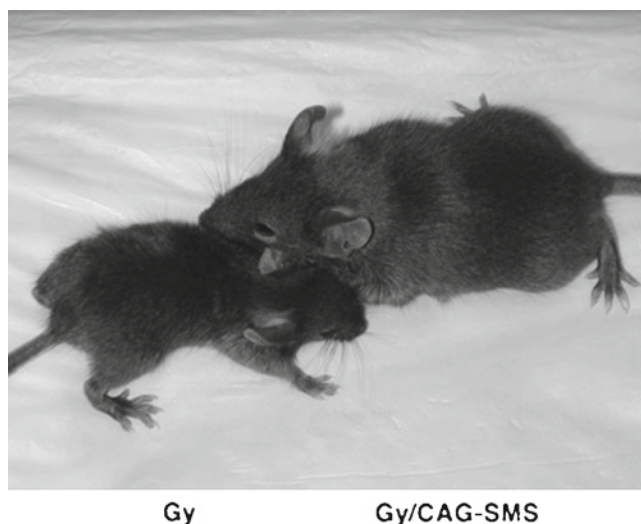


Fig. 1. Male Gy and CAG-SMS mice.

neurological abnormalities, and a short life span (5, 8, 10, 12, 13) (see Note 1). All of these changes are reversed when SpmS activity is restored by breeding with CAG-SMS mice, which, as described below, express SpmS from a general promoter (12, 13). Attempts to transfer the Gy mutation, which is on the mixed B6C3H strain, to other strains such as C57BL/6J by cross-breeding have not been successful in generating viable mice (14). This suggests that some genes present in B6C3H can modify the severity of the phenotype due to lack of spermine, and the absence of these genes may prevent the generation of viable mice with specific SMS gene activations in other strains including those normally used for gene-knockout technology such as 129/SvJ.

The X-chromosomal deletion in Gy mice not only inactivates SMS but also eliminates the product of the *Phex* gene (also called *Pex*), which is adjacent to SMS. The *Phex* gene product regulates phosphate metabolism, and its loss leads to hypophosphatemia in both Gy males and in XGy carrier females (since *Phex* loss imparts a dominant phenotype). Hence the Gy mice have significant defects in bone development and were originally proposed as a model of hypophosphatemic rickets (8). However, other mouse strains including those termed Hyp, which have deletions of *Phex* not extending into SMS (15), or specific inactivating point mutations in *Phex* (16) are better models for this purpose since they have normal polyamine levels and lack all of the phenotypic changes seen in the Gy mice that are described above. As expected, the hypophosphatemia in Gy mice is not abolished by breeding with CAG-SMS mice (12).

Normal mouse diets contain significant amounts of spermine, but this is clearly not available to provide spermine in the tissues since all tissues from Gy mice that have been examined so far have undetectable levels of spermine (5, 12). Even after increasing the spermine content in the diet or administration of spermine by injection of the maximally tolerated dose, there was only a very limited increase in the tissue content of spermine (13). Thus, at present the only feasible way to restore spermine is to provide the SpmS enzyme rather than its product.

CAG-SMS mice (see Note 2) were developed on the B6D2 background using standard transgenic techniques in which the human SpmS cDNA was inserted into a construct where it was under the control of a composite CMV-IE (cytomegalovirus immediate early gene enhancer-chicken beta-actin promoter) (17). This promoter was designed to provide ubiquitous expression of the transgene. Studies where it was used to drive production of green fluorescent protein confirmed that this was the case (18, 19). Assay of the increased SpmS activity and protein levels in some of the derived lines of CAG-SMS mice showed that SpmS was clearly elevated in all tissues examined, but the level of transgenic activity was much greater in some tissues than in others

with activities in heart and skeletal muscle being particularly high (17). Although the CAG-SMS mice had greatly elevated levels of SMS in some tissues and substantial increases in most others, there was only a small alteration in polyamine content with a small rise in the spermine:spermidine ratio. There was no adverse effect on any of the physiological parameters studied even when the mice were kept for more than a year. It is likely that the changes in polyamine levels are minimized by the lack of decarboxylated S-adenosylmethionine. The CAG-SMS mice do show a very severe phenotype if bred with transgenic mice overexpressing S-adenosylmethionine decarboxylase in the heart since this cross is embryonic lethal (17) and they can be used in experimental conditions where S-adenosylmethionine decarboxylase is more modestly increased to examine the effects of increased spermine content.

Four lines of CAG-SMS were derived; lines #5, #8, and #21 show generally similar levels of high SpmS expression in many organs including brain. Further studies were not carried out with line #5, but breeding of line #8 or #21 with the Gy mice reversed the defects in these mice as described above (12, 13). Line #8 was back-crossed for more than 15 generations to inbred B6 mice, and these mice can be used in many cases to avoid additional complications due to gene variations in the mixed B6D2 background. Line #18 gave lower levels of SpmS expression in some organs including brain and may express only in some cells with a mosaic pattern in some tissues such as heart. It did not reverse the Gy phenotype in all offspring.

The Gy mouse model has been used to investigate the role of spermine in hearing (13), in general growth (12), fertility (12), and in cardiac functions leading to sudden death (12, 20). It can clearly be exploited to study these effects in more detail using isolated cells and other tissue extracts. The intact mice can be used to study the behavioral/neurological and metabolic aspects of the absence of spermine. They also provide an animal model, albeit an imperfect one, for Snyder-Robinson syndrome (SRS). This is a very rare human inherited disease characterized by mental retardation and other abnormalities caused by mutations in the human *SMS* gene that greatly reduce the SpmS activity (21–24). Studies with cultured lymphoblastoid and fibroblast cells from these patients show that they have a reduced spermine content and an elevated spermidine level. Cells and tissues from Gy mice have an elevated spermidine but have no detectable spermine and although their behavioral phenotype suggests significant neurological impairment, it is not closely related to that of SRS.

When SpmS activity is abolished, earlier steps in the biosynthetic pathway are activated and this leads to a substantial increase in spermidine in Gy mice (5, 12, 20). Total polyamine content also increases since the rise in spermidine is greater than the decrease in spermine. There is also a huge rise in the content of

dcAdoMet due to an increase in its synthesis and lack of conversion into spermine. It is possible that the rise in dcAdoMet or spermidine affects the phenotype in spermine deficiency.

We describe below methods for screening and characterizing the Gy and CAG-SMS mice. In addition to these methods, standard assays for determination of polyamines (25–27) should be used to assess the tissue spermine concentration, and the SpmsS activity can be determined using tissue extracts as described (5, 28, 29).

2. Materials

2.1. Mice

1. CAG-SMS mice line #8 (see Note 2) on B6D2 or B6 background obtainable from our laboratory (contact apegg@psu.edu).
2. Gy mice obtainable as breeding pairs with an XGy female carrier and a normal male on the B6C3H background from The Jackson Laboratory (Bar Harbor, ME).
3. Offspring of crosses of XGy females with male CAG-SMS mice.

2.2. DNA Extraction, PCR Amplification, and Gel Electrophoresis of PCR Products

1. REDExtract-N-Amp™ Tissue PCR Kit (Sigma). Store at -20°C .
2. PTC-0220 DNA Engine Dyad Peltier Thermal Cycler (MJ Research, Inc., MA 02451).
3. UltraPure™ Agarose (Invitrogen, Carlsbad CA 92008).
4. 0.5 M Ethylenediaminetetraacetic acid disodium salt dihydrate (EDTA): 93.06 g of EDTA dissolve in 400 mL distilled water and adjust the pH to 8.0 with NaOH. Top up the solution to a final volume of 500 mL.
5. TAE (50X) 242 g Tris base is dissolved in approximately 750 mL distilled water. Carefully add 57.1 mL glacial acetic acid and 100 mL of 0.5 M EDTA (pH 8.0) and adjust the solution to a final volume of 1 L. Filter and store at room temperature (RT).
6. Oligodeoxyribonucleotides obtainable from many commercial suppliers.

2.3. Phosphate Assay

1. Anesthesia: Ketamine (Ketaset®, NDC 0856-2013-01, 100 mg/mL), Xylazine (VEDCO, NDC 50989-113-09, 20 mg/mL).
2. Heparinized microcentrifuge tubes (BD Microtainer®).
3. Drummond Microcaps Disposable Micropipettes.
4. PYREX® Disposable Culture Tube (Corning Inc, NY).

5. AK-POLY-BAC™ Ophthalmic Ointment (Akorn, Inc, NDC 17478-238-35).
6. Beckman Coulter DU 800 UV/Vis Spectrophotometer (Beckman Coulter, CA 92834).
7. 6N H₂SO₄.
8. 2.5% (w/v) ammonium molybdate.
9. 10% ascorbic acid.
10. 10% trichloroacetic acid (TCA) (6.12M).

3. Methods

3.1. Generation and Identification of Gy Male Mice

1. Heterozygous Gy (XGy) mice are bred with B6C3H males.
2. Female offspring are retained, and the heterozygous females are required for further breeding distinguished from homozygous wild-type females. Since these mice have one copy of *SMS* from the unaffected X chromosome, they cannot be identified by PCR but they can be recognized by assay of plasma phosphate content (see Note 3). The XGy female carriers have plasma phosphate levels below 1.4 mM, and all control littermates have plasma phosphate levels above 1.4 mM (Fig. 2). The XY Gy status can then be confirmed by breeding with a normal male, which gives offspring that include Gy males, which can readily be identified by PCR.

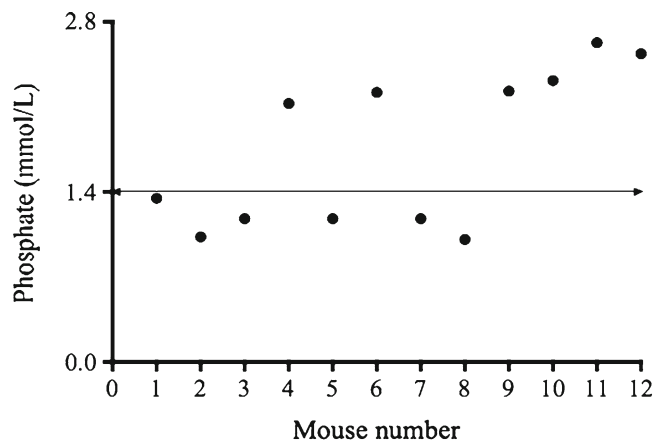


Fig. 2. Plasma phosphate concentrations for XGy and XX female mice. Results are shown for heterozygous XGy females (numbers 1, 2, 3, 5, 7, and 8), which have a mean plasma phosphate of $1.15 \text{ mM} \pm 0.05$ (SE), and wild type XX females (numbers 4, 6, 9, 10, 11, and 12), which have a mean of $2.35 \text{ mM} \pm 0.08$ (SE). The line indicates 1.4 mM, and all mice with plasma phosphate values below this value are used as breeders to generate Gy male mice.

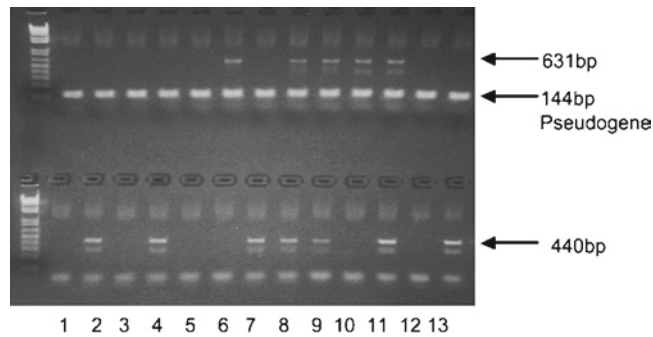


Fig. 3. PCR products from screening of Gy and CAG-SMS mice. The *upper* panel shows PCR amplification of part of the endogenous *SMS* gene. The 631-bp product is derived from intron 3 and the 144-bp product is derived from a pseudogene. The *lower* panel shows PCR amplification of the transgene in CAG-SMS mice, which is positive only in these transgenic mice. Sample mouse numbers 1, 3, 5, and 12 are Gy mice showing absence of the 631-bp product from *SMS* and no band in the *bottom* panel. Sample mouse numbers 2, 4, 7, and 13 show the absence of 631-bp product from *SMS* and the presence of 440-bp product from CAG-SMS indicating they are Gy/CAG-SMS. Sample mouse numbers 6 and 10 show the 631-bp band and no band in the *bottom* panel indicating they are control wild-type mice. Sample mouse numbers 8, 9, and 11 show bands at 631 bp in the *upper* panel and 440 bp in the *lower* panel indicating they are CAG-SMS. Note that all 13 samples show the 144-bp band.

3. The Gy males resulting from the breeding of XGy mice with B6C3H males are identified by PCR using genomic DNA isolated from the tails as described in Subheading 3.3. The 5' sense primer used is 5'-GGTGTTGCTGGACCTTCAGA-3', and the 3' antisense primer is 5'-CCCAGTACTGTCTTGACTCA-3'. These primers amplify a 631-bp product from *SMS*, and this product is absent in the male Gy mice (Fig. 3). Fortunately, they also amplify a 144-bp band, which is the size expected from a pseudogene. Since this pseudogene is present in both normal and Gy males, it provides a control that the PCR is successful and the absence of the 631-bp product indicates a Gy mouse (5, 10). Approximately 15% of the offspring from mating of XGy females and normal males after weaning are Gy males (see Note 4).

3.2. Generation and Identification of CAG-SMS Mice

1. The CAG-SMS mice were generated by DNA microinjection of fertilized B6D2F2 oocytes using a 3.5-kb fragment released by *Sal* I and *Bam* HI digestion from plasmid pCAG-hSpm-Syn, which was constructed by replacing the insert encoding GFP in plasmid pCX-EGFP with the human spermine synthase cDNA (17, 18, 30).
2. Genomic DNA, which was isolated as described in Subheading 3.3, is subjected to PCR analysis in order to identify mice bearing the transgene. For identification of the

CAG-SMS mice, the 5' sense primer used is 5'-TTCGGCTTCTGGCGTGTGAC-3', which corresponds to a sequence in the actin promoter region and the 3' antisense primer is 5'-CCAGTACTGTCCTGACTC-3', which corresponds to nucleotides 300–317 in the SpmS coding sequence. As shown in Fig. 3, a 440-bp fragment is produced from the transgene (17) (see Notes 2 and 4).

3.3. DNA Isolation

1. DNA is isolated from tail biopsies taken before 3 weeks of age. Specifically, mice aged 10–21 days are used and local anesthesia achieved by immersion of the tail in ice-cold ethanol for 10 s. The distal 3 mm of the tail is removed using a sterile scalpel. It is important to rinse the scalpel in 95% ethanol and distilled water prior to use and between different samples to prevent any contamination. The fresh tail samples can be used directly for extractions or stored at -80°C for later use.
2. DNA extraction is carried out using the REExtract-N-Amp™ Tissue PCR kit according to the kit instructions. Make the extraction and tissue preparation mix in a ratio of 4:1, add 125 μL of the mix to each tail sample, incubate at the RT for 10 min, followed by incubation at 95°C for 3 min, then add 100 μL of neutralization solution B to sample, and mix by vortexing. The DNA can be used immediately or stored at 4°C .

3.4. PCR Amplification

1. Add the following reagents to the microcentrifuge tube: water, PCR grade, 5.2 μL ; REExtract-N-Amp PCR Reaction Mix, 10 μL ; sense primer, 0.4 μL ; antisense primer, 0.4 μL ; tissue extract, 4 μL so that total volume is 20 μL . If less than 4 μL of tissue extract is used, a 1:1 mixture of extraction:neutralization B solution is added to bring the volume of tissue extract up to 4 μL .
2. PCR for Gy males is performed using the following cycling parameters: initial denaturation at 95°C for 1 min; 40 cycles of denaturation 92°C for 30 s increasing by 2 s every cycle, annealing at 63°C for 30 s, extension at 74°C for 30 s; final extension at 74°C for 5 min and indefinite hold at 4°C . Lid Control Mode is kept constant at 100°C .
3. PCR for CAG-SMS mice is performed using the following cycling parameters: initial denaturation at 95°C for 1 min; 40 cycles of denaturation 92°C for 30 s, annealing at 58°C for 30 s, extension at 74°C for 30 s; final extension at 74°C for 5 min and indefinite hold at 4°C . Lid Control Mode is kept constant at 105°C .
4. The amplified DNA is loaded onto 2% agarose gels after the PCR is completed. An example of the results produced is shown in Fig. 3.

3.5. Plasma Phosphate Assays to Identify XGy Carrier Female Mice

1. Female mice (6–8 weeks old) are anesthetized with ketamine (100 mg/kg ip) and Xylazine (10 mg/kg ip).
2. Blood (50–60 μ l) from a retro-orbital bleed is collected in heparinized microcentrifuge tubes, spun at 14,000 rpm (15,000 $\times g$) for 15 min, and then plasma is used for analysis.
3. Add 20 μ L of plasma or 20 μ L of standard phosphate solution (1, 2, 3, and 4 mM) to 1.35 mL 10% TCA in Eppendorf tube.
4. Vortex samples and spin at 14,000 rpm (15,000 $\times g$) for 10 min.
5. Take 1 mL of supernatant and add to 2.0 mL reagent mix in glass disposable culture Tube.
6. Vortex and then incubate at 37°C for 90 min.
7. Cool for 10 min.
8. Read in spectrophotometer at 820 nm.
9. Use standard solution samples to construct standard curve and read off plasma phosphate level.
10. Typical results for XX and XGy female mice are shown in Fig. 2.

3.6. Immunochemical Detection of SpmS Expression

1. The expression of the SpmS in tissues from CAG-SMS mice and from Gy/CAG-SMS mice can be assessed by Western blotting or immunohistochemistry.
2. The only antiserum, which we have found to be satisfactory for this purpose, is that which we raised in rabbits in our laboratory to human SpmS and purified by affinity chromatography using a column of immobilized human SpmS (7, 23). Commercially available antisera that we have tested had inadequate specificity and/or sensitivity.
3. Even with the purified antiserum, it is difficult to see any band of SpmS in the control mouse tissues (Fig. 4) (see Note 5) and, therefore, this is not a viable method of distinguishing male Gy mice from controls. The high level of expression of the transgene from the CAG-SMS mice not only allows ready confirmation of the status by Western blotting (Fig. 4) but also permits immunohistochemistry to investigate cell specific expression.

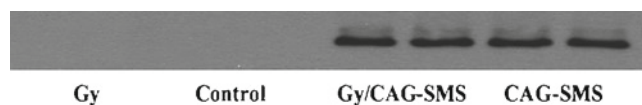


Fig. 4. Western blotting using anti-SpmS of heart tissue extracts from Gy, normal, Gy/CAG-SMS, and CAG-SMS mice.

4. Notes

1. Studies on Gy mice present a number of challenges: (a) The very small size of the Gy mice renders some procedures difficult and also makes it hard to decide on the most appropriate normal control since normal male littermates and Gy/CAG-SMS mice of the same age are much larger. (b) The propensity of Gy mice to sudden death makes it necessary to breed excess mice to ensure that there are relevant numbers for an experiment. As described in Note 4, only 10–15% of the litters are male Gy mice instead of the expected 25%, and this number decreases steadily over the next 3 months. (c) Since Gy mice are only viable on the mixed B6C3H background, greater individual experimental variation is to be expected and the genetic background of crosses with CAG-SMS mice on the B6D2 background is also variable. The survival and fertility of male Gy/CAG-SMS mice after such breeding do also provide an opportunity to identify the gene(s) that are present in the B6C3H strain that allow the male Gy spermine synthase mice to survive even in the absence of spermine by further breeding. (d) While it is clear that the poor bone development in Gy mice is related to the loss of the *Phex* gene product, there is evidence from a number of other sources including the phenotype of the SRS patients (21, 24) that spermine may also be involved in bone metabolism. Comparisons of the femoral abnormalities in males and females carriers of the Gy and Hyp mutations are also consistent with this (14). Thus, spermine may also exert effects on bone metabolism, but this is not readily studied without a model in which Phex activity is maintained.
2. There are four available lines of CAG-SMS mice. Lines #8, #21, and #5 show widespread overexpression of Spms in many organs including brain. Breeding of line #8 or #21 with the Gy mice reverses the changes due to the absence of spermine. It is likely that breeding with line #5 would also be effective, but this has not been tested. Breeding with line #18, which gives a lower expression of spermine synthase, did not reverse the phenotype.
3. XGy female carrier mice have only one X chromosome in which the *SMS* and *Phex* locus has been deleted. Therefore, they cannot be identified by PCR. However, since the loss of even one copy of *Phex* alters phosphate metabolism leading to hypophosphatemia, they can be distinguished from normal females by measurement of the plasma phosphate level.

4. Although 25% of the offspring from XGy females should have the Gy genotype, and this is the case with late-stage embryos (5), only 10–15% of the Gy males survive past weaning.
5. It is possible that the antiserum, which was raised to human SpmS, does not react well with mouse SpmS. This seems unlikely since it is a polyclonal antibody and there are only 16 differences in the 301 amino acids of SpmS between the two species, but has not been ruled out directly.

Acknowledgements

This work was supported by grant 3R01GM026290-29S1 from the NIH using funds from the NIH Recovery Act.

References

1. Pendeville H, Carpino N, Marine JC, Takahashi Y, Muller M, Martial JA, Cleveland JL (2001) The ornithine decarboxylase gene is essential for cell survival during early murine development. *Mol Cell Biol* 21:6459–6558
2. Nishimura K, Nakatsu F, Kashiwagi K, Ohno H, Saito H, Saito T, Igarashi K (2002) Essential role of *S*-adenosylmethionine decarboxylase in mouse embryonic development. *Genes Cells* 7:41–47
3. Korhonen V-P, Niranen K, Halmekyto M, Pietilä M, Diegelman P, Parkkinen JJ, Eloranta T, Porter CW, Alhonen L, Jänne J (2001) Spermine deficiency resulting from targeted disruption of the spermine synthase gene in embryonic stem cells leads to enhanced sensitivity to antiproliferative drugs. *Mol Pharmacol* 59:231–238
4. Nilsson J, Gritli-Linde A, Heby O (2000) Skin fibroblasts from spermine synthase-deficient hemizygous gyro male (Gy/Y) mice overproduce spermidine and exhibit increased resistance to oxidative stress but decreased resistance to UV irradiation. *Biochem J* 352:381–387
5. Mackintosh CA, Pegg AE (2000) Effect of spermine synthase deficiency on polyamine biosynthesis and content in mice and embryonic fibroblasts and the sensitivity of fibroblasts to 1,3-bis(2-chloroethyl)-*N*-nitrosourea. *Biochem J* 351:439–447
6. Rider JE, Hacker A, Mackintosh CA, Pegg AE, Woster PM, Casero RA Jr (2007) Spermine and spermidine mediate protection against oxidative damage caused by hydrogen peroxide. *Amino Acids* 33:231–240
7. Ikeguchi Y, Mackintosh CA, McCloskey DE, Pegg AE (2003) Effect of spermine synthase on the sensitivity of cells to antitumor agents. *Biochem J* 373:885–892
8. Lyon MF, Scriver CR, Baker LR, Tenenhouse HS, Kronick J, Mandla S (1986) The Gy mutation: another cause of X-linked hypophosphatemia in mouse. *Proc Natl Acad Sci USA* 83(13):4899–4903
9. Grieff M, Whyte MP, Thakker RV, Mazzarella R (1997) Sequence analysis of 139 kb in Xp22.1 containing spermine synthase and 5' region of PEX. *Genomics* 44:227–231
10. Meyer RA Jr, Henley CM, Meyer MH, Morgan PL, McDonald AG, Mills C, Price DK (1998) Partial deletion of both the spermine synthase gene and the *Pex* gene in the x-linked hypophosphatemic, Gyro (Gy) mouse. *Genomics* 48:289–295
11. Lorenz B, Francis F, Gempel J, Böddrich AJM, Schmahl W, Schmidt J (1998) Spermine deficiency in Gy mice caused by deletion of the spermine synthase gene. *Hum Mol Genet* 7:541–547
12. Wang X, Ikeguchi Y, McCloskey DE, Nelson P, Pegg AE (2004) Spermine synthesis is required for normal viability, growth and fertility in the mouse. *J Biol Chem* 279:51370–51375
13. Wang X, Levic S, Gratton MA, Doyle KJ, Yamoah EN, Pegg AE (2009) Spermine synthase deficiency leads to deafness and a profound sensitivity to alpha-difluoromethylornithine. *J Biol Chem* 284:930–937
14. Meyer RA Jr, Meyer MH, Gray RW, Bruns ME (1995) Femoral abnormalities and vitamin D

- metabolism in X-linked hypophosphatemic (*Hyp* and *Gy*) mice. *J Orthop Res* 13:30–40
15. Strom T, Francis F, Lorenz B, Böddrich A, Econs M, Lehrach H, Meitinger T (1997) *Pex* gene deletions in *Gy* and *Hyp* mice provide mouse models for X-linked hypophosphatemia. *Hum Mol Genet* 6:165–171
 16. Carpinelli MR, Wicks IP, Sims NA, O'Donnell K, Hanzinikolas K, Burt R, Foote SJ, Bahlo M, Alexander WS, Hilton DJ (2002) An ethyl-nitrosourea-induced point mutation in *phex* causes exon skipping, x-linked hypophosphatemia, and rickets. *Am J Pathol* 161:1925–1933
 17. Ikeguchi Y, Wang X, McCloskey DE, Coleman CS, Nelson P, Hu G, Shantz LM, Pegg AE (2004) Characterization of transgenic mice with widespread overexpression of spermine synthase. *Biochem J* 381:701–707
 18. Okabe M, Ikawa M, Kominami K, Nakanishi T, Nishimune Y (1997) Green mice as a source of ubiquitous green cells. *FEBS Lett* 407:313–319
 19. Kato M, Yamanouchi K, Ikawa M, Okabe M, Naito K, Tojo H (1999) Efficient selection of transgenic mouse embryos using EGFP as a marker gene. *Mol Reprod Dev* 54:43–48
 20. Pegg AE, Wang X (2009) Mouse models to investigate the function of spermine. *Commun Integr Biol* 2:271–274
 21. Cason AL, Ikeguchi Y, Skinner C, Wood TC, Lubs HA, Martinez F, Simensen RJ, Stevenson RE, Pegg AE, Schwartz CE (2003) X-Linked spermine synthase gene (*SMS*) defect: the first polyamine deficiency syndrome. *Eur J Hum Genet* 11:937–944
 22. de Alencastro G, McCloskey DE, Kliemann SE, Maranduba CM, Pegg AE, Wang X, Bertola DR, Schwartz CE, Passos-Bueno MR, Sertie AL (2008) New *SMS* mutation leads to a striking reduction in spermine synthase protein function and a severe form of Snyder-Robinson X-linked recessive mental retardation syndrome. *J Med Genet* 45:539–543
 23. Becerra-Solano LE, Butler J, Castañeda-Cisneros G, McCloskey DE, Wang X, Pegg AE, Schwartz CE, Sánchez-Corona J, Garcia-Ortiz JE (2009) A missense mutation, p. V132G, in the X-linked spermine synthase gene (*SMS*) causes Snyder-Robinson syndrome. *Am J Med Genet A* 149A:328–335
 24. Schwartz C, Pegg AE (2010) Methods in molecular biology. In: Pegg AE, Casero RA Jr (eds) *Polyamine protocols*. Humana Press, Totowa
 25. Seiler N, Knödgen B (1985) Determination of polyamines and related compounds by reversed-phase high-performance liquid chromatography: improved separation systems. *J Chromatogr* 339:45–57
 26. Kabra PM, Lee HK, Lubich WP, Marton LW (1986) Solid-phase extraction and determination of dansyl derivatives of unconjugated and acetylated polyamines by reversed-phase liquid chromatography; improved separation systems for polyamines in cerebrospinal fluid, urine and tissue. *J Chromatogr Biomed Appl* 380:19–32
 27. Häkkinen MR (2010) Polyamine analysis by LC-MS. In: Pegg AE, Casero RA Jr (eds) *Methods in molecular biology. Polyamine protocols*. Totowa, Humana Press
 28. Wiest L, Pegg AE (1998) Assay of spermidine and spermine synthase. In: Morgan DML (ed) *Methods in molecular biology. Polyamine protocols*, vol 79. Humana Press, Totowa, pp 51–58
 29. Schwartz CE, Stevenson RE, Wang X, Pegg AE (2010) Spermine synthase deficiency resulting in X-linked intellectual disability (Snyder-Robinson syndrome). In: Pegg AE, Casero RA Jr (eds) *Methods in molecular biology. Polyamine protocols*. Totowa, Humana Press
 30. Sawicki JA, Morris RJ, Monks B, Sakai K, Miyazaki J-I (1998) A composite CMV-IE enhancer/ β -actin promoter is ubiquitously expressed in mouse cutaneous epithelium. *Exp Cell Res* 244:367–369

Part IV

Enzymes Involved in Polyamine Catabolism and Posttranslational Protein Modification

Chapter 10

A Simple Assay for Mammalian Spermine Oxidase: A Polyamine Catabolic Enzyme Implicated in Drug Response and Disease

**Andrew C. Goodwin, Tracy R. Murray-Stewart,
and Robert A. Casero, Jr.**

Abstract

Spermine oxidase (SMO), the most recently characterized polyamine metabolic enzyme, catalyzes the direct back-conversion of spermine to spermidine in an FAD-dependent reaction that also yields the byproducts hydrogen peroxide (H_2O_2) and 3-aminopropanal. These metabolites, particularly H_2O_2 , have been implicated in cytotoxic cellular responses to specific antitumor polyamine analogs, as well as in the inflammation-associated generation of DNA damage. This chapter describes a rapid, sensitive, and inexpensive method for the chemiluminescent measurement of SMO (or alternatively, *N*¹-acetyl polyamine oxidase, APAO) enzyme activity in cultured cell lysates, without the need for radioactive reagents or the use of high performance liquid chromatography (HPLC). Specifically, H_2O_2 production by SMO is coupled to chemiluminescence generated by the horseradish peroxidase-catalyzed oxidation of luminol. Detailed protocols for preparation of reagents, harvesting cell lysates, generation of a standard curve, assaying of samples, and calculation of SMO enzyme activity are presented.

Key words: Spermine oxidase, Polyamine catabolism, Hydrogen peroxide, Chemiluminescence

1. Introduction

While the enzymatic biosynthesis of polyamines is irreversible, a group of tightly regulated, complementary enzymes facilitate the back-conversion of the higher polyamines spermine and spermidine to spermidine and putrescine, respectively (1). The first pathway involves acetylation of spermine or spermidine to *N*¹-acetylspermine or *N*¹-acetylspermidine by spermidine/spermine *N*¹-acetyltransferase (SSAT) (2). The acetylated polyamine then undergoes oxidation to spermidine or putrescine by acetyl polyamine oxidase (APAO), with generation of hydrogen peroxide

(H_2O_2) as a byproduct (3, 4). Alternatively, spermine oxidase (SMO), the most recently characterized polyamine catabolic enzyme (5, 6), catalyzes the direct back-conversion of spermine to spermidine, 3-aminopropanal, and H_2O_2 , without an acetylated intermediate. This stoichiometric production of H_2O_2 by SMO facilitates quantification of SMO enzyme activity by the chemiluminescent method described in this chapter.

The production of H_2O_2 by SMO and APAO activity has been associated with downstream oxidative damage and has important implications in the etiology and treatment of human diseases (7–9). The cytotoxic effect of numerous polyamine analogs under investigation as chemotherapeutic agents has been ascribed to the generation of reactive oxygen species, resulting from massive upregulation of polyamine catabolism through the SSAT/APAO pathway (10–12). Recent studies, however, suggest that SMO is the more critical source of H_2O_2 with respect to analog-induced cell death (13, 14). Furthermore, oxidative damage following modest upregulation of SMO in epithelial tissues by inflammatory stimuli is hypothesized to contribute to inflammation-associated carcinogenesis (reviewed by (1)). The following protocol, based on a method originally reported by Fernandez et al. (15), has been altered to provide greater sensitivity, allows for real-time analysis of polyamine oxidase activity (SMO or APAO) (16, 17), and provides the potential for modification to high-throughput applications, such as the screening of potential antitumorigenic compounds for induction of oxidase activity in cancer cell lysates.

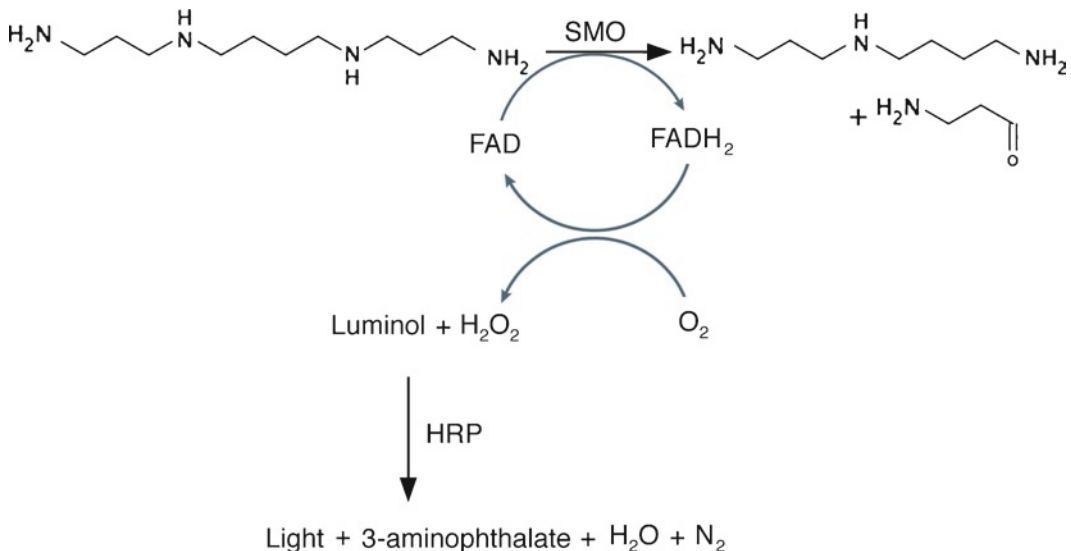


Fig. 1. Schematic illustrating the coupled enzyme reactions that comprise the enzyme activity assay described in this chapter. First, spermine oxidase (SMO) catalyzes the FAD-dependent oxidation of spermine to spermidine, 3-aminopropanal, and H_2O_2 . Second, in the presence of this H_2O_2 , luminol is oxidized by horseradish peroxidase (HRP), resulting in production of chemiluminescence.

In preparation for the measurement of SMO activity, cells are harvested in glycine buffer and lysed by freezing at -80°C . The assay reaction mix contains cell lysate, horseradish peroxidase (HRP), luminol, pargyline (monoamine oxidase inhibitor), and aminoguanidine (diamine oxidase inhibitor), in a glycine buffer at pH 8.0. This reaction is incubated briefly at 37°C , followed by addition of spermine (substrate for SMO) and integration of chemiluminescence. The slightly basic pH (8.0) permits the HRP to catalyze the oxidation of luminol in a reaction coupled to the production of H_2O_2 by SMO. Upon oxidation of luminol, a light-emitting molecule (excited 3-aminophthalate ion) is produced (Fig. 1). The amount of chemiluminescence measured in a sample corresponds to the relative oxidation of spermine by SMO in the cell lysate.

2. Materials

2.1. Reagents That May Be Prepared in Advance and Stored at -20°C

1. Aminoguanidine (Sigma #A7009; FW: 123.1 g/mol). Dissolve 123.1 mg/10 mL HPLC-grade water to yield 100 mM stock solution; aliquot in 1.5 mL tubes and store at -20°C .
2. Luminol (3-aminophthalhydrazide; Fluka Biochemika #09253; FW: 177.16 g/mol). Dissolve 177.2 mg/10 mL dimethyl sulfoxide (DMSO) to yield 100 mM stock solution; aliquot in light-protected 1.5 mL tubes and store at -20°C .
3. Pargyline (*N*-methyl-*N*-(2-propynyl)benzylamine hydrochloride; Sigma #P8013). Dissolve in HPLC-grade water to yield 2.3 mg/mL stock solution; aliquot in 1.5 mL tubes and store at -20°C .
4. Spermine tetrachloride (see Note 1) (Sigma #S2846; FW: 348.19 g/mol). Dissolve 52.2 mg/10 mL HPLC-grade water to yield 15 mM stock solution; aliquot in 1.5 mL tubes and store at -20°C . On the day of the assay, dilute to a 1.5 mM working stock with HPLC-grade water.

2.2. Reagents That Must Be Prepared Fresh for Each Assay

1. Glycine buffer (J.T. Baker# 4059-02; FW: 75.07 g/mol). Dissolve 375.4 mg/10 mL HPLC-grade water to yield 0.5 M stock solution and adjust pH to 8.0 with NaOH. Make a further dilution to 0.083 M (1 part 0.5 M glycine, pH 8.0 plus 5 parts HPLC-grade water) for harvesting cells and enzyme assay blank (see Note 2).
2. HRP (Roche #10814407001, EIA grade, lyophilized). Dissolve in HPLC-grade water to yield a 0.4 mg/mL solution (see Note 3).
3. H_2O_2 (3% w/v solution) (see Note 4).

2.3. Common Laboratory Reagents and Disposables

1. Bradford protein assay reagent (Bio-Rad #500-0006).
2. Cell lifters (Fisher #08-773-1).
3. Dimethyl sulfoxide (DMSO; Sigma #D1435).
4. HPLC-grade water (J.T. Baker #4218-03).
5. Light-shielded (1.5, 15, 50 mL) and standard microcentrifuge tubes (1.5 mL).
6. Luminometer cuvettes (12×75 mm; BD Biosciences #556862).

3. Methods

3.1. Harvesting of Adherent Cells and Preparation of Cell Lysates

1. Remove culture media, rinse adherent cells with ice-cold 1× PBS, aspirate PBS.
2. Cover cells with 0.083 M glycine buffer, pH 8.0 (approximately 300 μ L/well of 6-well dish or 700 μ L/25 cm² flask), and place in -80°C freezer to lyse cells (see Note 5).
3. On day of assay, thaw flasks or dishes on ice, scrape cells with disposable cell lifters, transfer lysates to 1.5 mL tubes, and vortex 10s.
4. Centrifuge cell lysates (10 min, $>12,000\times g$, 4°C) and keep lysates on ice at all times during assay.

3.2. Prepare Assay Master Mix and Determine Hydrogen Peroxide Standard Curve

1. Preheat water bath containing a rack suitable for holding luminometer cuvettes to 37°C .
2. Thaw spermine, aminoguanidine, and pargyline on ice and thaw luminol at room temperature.
3. In a light-shielded conical tube on ice, prepare the assay reaction mix according to the chart in Table 1 for the desired number of reactions (see Notes 3 and 6) and mix by vortexing.
4. In light-shielded 15 mL tubes, serially dilute H_2O_2 in HPLC-grade water:
 - Dilution A: add 100 μ L H_2O_2 (3% w/v solution, 0.882 M) to 8.72 mL HPLC-grade water to yield a 10 mM solution. Mix gently by inversion (see Note 7).
 - Dilution B: add 100 μ L Dilution A to 10 mL HPLC-grade water to yield a 100 μ M solution, and mix gently by inversion.
 - Dilution C: add 100 μ L Dilution B to 10 mL HPLC-grade water to yield a 1 μ M solution, and mix gently by inversion.

Table 1
SMO enzyme activity assay setup and workflow

Reagent	Stock concentration	Final concentration	Per reaction (μL)	Per 100 reactions
Glycine, pH 8.0	0.5 M	0.083 M	50	5 mL
Aminoguanidine	100 mM	1 mM	3	300 μL
Pargyline	2.3 mg/mL	0.019 mg/mL	2.5	250 μL
Luminol	100 mM	0.017 mM	0.05	5 μL
HPLC-grade water			94.5	9.45 mL
Horseshoe peroxidase	0.4 mg/mL	0.067 mg/mL	50	5 mL
Reaction mix			200	
Cell lysate or 0.083 M glycine blank			50	
<i>Vortex cuvette briefly and incubate for 2 min in 37°C water bath</i>				
Spermine	1.5 mM	0.25 mM	50	
Final reaction volume			300	
<i>Inject substrate and integrate luminescence for 40 s</i>				

The necessary assay reagents are indicated above as well as calculations for preparing a master mix for 100 reactions (see Subheading 2 for preparation instructions). The general assay scheme is also summarized (see Subheading 3 for detailed protocol)

- Prepare a series of solutions containing increasing concentrations of H₂O₂ (0–100 pmol/100 μL) for production of a standard curve relating H₂O₂ concentration to RLU, in a total volume of 300 μL:
 - 0 pmol: 1,000 μL HPLC-grade water.
 - 20 pmol: 800 μL HPLC-grade water + 200 μL Dilution C from step 3.2.4.
 - 40 pmol: 600 μL HPLC-grade water + 400 μL Dilution C.
 - 60 pmol: 400 μL HPLC-grade water + 600 μL Dilution C.
 - 80 pmol: 200 μL HPLC-grade water + 800 μL Dilution C.
 - 100 pmol: 1,000 μL Dilution C.
- Pipette 200 μL reaction mix into a luminometer cuvette and incubate for 2 min in 37°C water bath.
- Remove cuvette from water bath, remove condensation with Kimwipe, pipette 100 μL of the “0 pmol” solution into the reaction mix, and immediately read the luminescence for a 20 s integration time (see Note 8).
- Repeat steps 3.2.6 and 3.2.7 to generate a standard curve with triplicate measurements of reactions containing 0, 20, 40, 60, 80, and 100 pmol H₂O₂ (18 total reactions) (see Note 9).

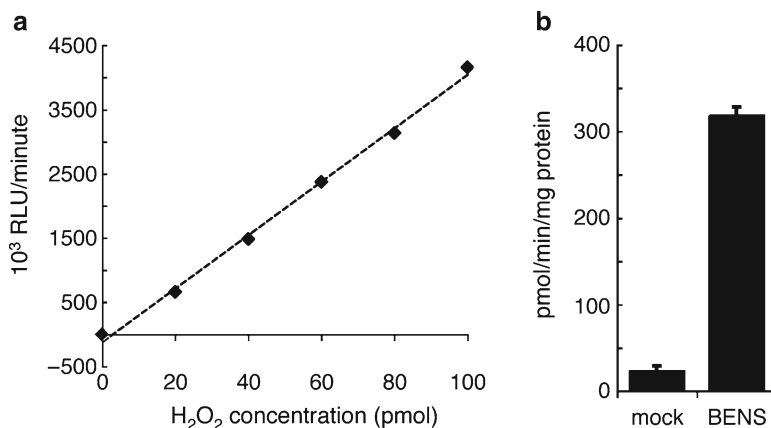


Fig. 2. (a) Representative plot of H₂O₂ standard curve displaying H₂O₂ concentration (0–100 pmol in 300 μ L reaction; x-axis) versus 10³ RLU/min (y-axis). A best-fit line is also plotted ($r^2 > 0.99$). (b) Representative data. A549 lung adenocarcinoma cells were treated for 24 h with or without 10 μ M of the SMO-inducing polyamine analog, bis(ethyl)norspermine (BENS). Cell lysate was harvested and SMO enzyme activity measured as described in this chapter.

- Using Microsoft Excel or other preferred method, fit a trend line to the standard curve data and calculate the r^2 value to validate the assay reaction mix (Fig. 2a) and for interpolation of raw sample RLU data.

3.3. Determination of SMO Enzyme Activity from Cell Lysates

- If luminometer is equipped with an autoinjector, load and prime with 1.5 mM spermine substrate solution. Set the luminometer program to inject 50 μ L/sample, followed by a 10 s delay and a 40 s integration of luminescence. Alternatively, the substrate can be manually pipetted into each cuvette as in step 3.2.3.
- For blank, pipette 200 μ L reaction mix into a luminometer cuvette, add 50 μ L 0.083 M glycine buffer, pH 8.0, vortex briefly, and incubate 2 min in a 37°C water bath.
- Remove cuvette from water bath, remove condensation with Kimwipe, and read luminescence as described in step 3.3.1.
- Repeat steps 2 and 3 as necessary to measure blank and each cell lysate (50 μ L supernatant from step 4) in triplicate. Alternatively, this protocol may be amended to assay enzyme kinetics of purified, recombinant SMO (see Note 10; Fig. 3).
- Determine total protein concentration in each cell lysate supernatant using Bradford or other preferred method.
- Calculate SMO activity as pmol H₂O₂ per min per mg protein, based on interpolation on the H₂O₂ standard curve (Fig. 2b).

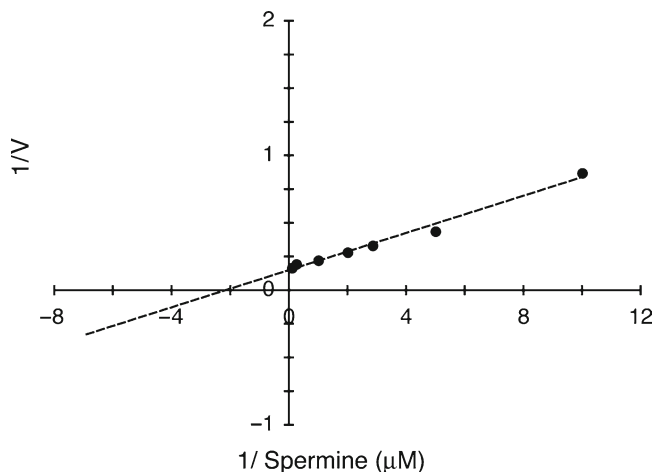


Fig. 3. Data generated using alterations to the described protocol, as described in Note 10. Purified, recombinant spermine oxidase protein was used with the current protocol for the determination of kinetic properties. Plot depicts Lineweaver–Burk transformation ($r^2 > 0.99$) of SMO/PAOh1, assayed in the presence of increasing concentrations of spermine (0–250 μM).

4. Notes

1. Alternatively, to measure the enzyme activity of APAO instead of SMO, use N^1 -acetylspermine (Fluka Biochemika #01467; FW: 353.76 g/mol) as the substrate.
2. 0.083 M Glycine buffer may be stored at 4°C for several weeks exclusively for use in harvesting cells. However, for optimal results, the 0.5 M glycine to be used in the reaction mix should be made fresh on each assay date.
3. Prepare the HRP solution only after all other components have been added to the assay reaction mix, immediately prior to proceeding with the assay protocol. Working quickly, dissolve HRP in HPLC-grade water to yield a 0.4 mg/mL solution, add the appropriate amount to the assay reaction mix on ice, and proceed with assay.
4. While 30% w/v H_2O_2 solutions are available from chemical vendors (i.e., Sigma-Aldrich #216763), we have found 3% w/v solutions sold in supermarkets and drug stores to be preferable. These solutions are significantly less expensive, yield equivalent results, and can be replaced with a fresh bottle after several uses.
5. Alternatively, following trypsinization of adherent cells, or for suspension cells, cells can be centrifuged, washed in ice-cold

- 1× PBS, resuspended in 0.083 M glycine, and then lysed at -80°C . In this case, thaw tubes containing cell lysates on ice and proceed with the protocol at step 3.1.4. Note: due to the presence of divalent metal cations in tissue homogenates, this assay protocol is not suitable for the measurement of oxidase activity in tissue samples.
6. All samples should be assayed in triplicate; allow at least 18 reactions for the standard curve, 3 reactions for the blank, and three times the number of cell lysates to be assayed.
 7. Whenever working with H_2O_2 solutions, it is critical to work quickly and minimize the amount of time that the tubes containing H_2O_2 are open and exposed to air.
 8. It is imperative to develop efficient and consistent timing and actions when adding the H_2O_2 to the reaction mix. For best results, we recommend placing the cuvette containing the 200 μL reaction mix into the luminometer, then pipetting the 100 μL H_2O_2 solution directly into the reaction mix (not down the side of the cuvette), and immediately starting the luminescence measurement. If this technique is followed, it is not necessary or advantageous to vortex the reaction mix + H_2O_2 mixture before reading.
 9. After becoming comfortable with the mechanics of the assay technique, it is possible to process samples (for both the standard curve and experimental cell lysates) more quickly using a staggered strategy. After starting the first 2-min incubation, wait about 45 s and then start preparing the second sample.
 10. For assay of purified SMO (or APAO) enzyme, the MAO and DAO inhibitors (pargyline and aminoguanidine) can be omitted and replaced with H_2O . Purified enzyme is diluted to 2 $\text{ng}/\mu\text{L}$ in 0.083 M glycine buffer, pH 8.0, then 50 μL is added to the reaction mix for each reaction, incubated 2 min at 37°C , substrate is added, and chemiluminescence is integrated over 20 s (16, 17).

References

1. Casero RA, Pegg AE (2009) Polyamine catabolism and disease. *Biochem J* 421:323–338
2. Casero RA Jr, Pegg AE (1993) Spermidine/spermine N1-acetyltransferase – the turning point in polyamine metabolism. *FASEB J* 7:653–661
3. Vujcic S, Liang P, Diegelman P, Kramer DL, Porter CW (2003) Genomic identification and biochemical characterization of the mammalian polyamine oxidase involved in polyamine back-conversion. *Biochem J* 370:19–28
4. Wu T, Yankovskaya V, McIntire WS (2003) Cloning, sequencing, and heterologous expression of the murine peroxisomal flavoprotein, n1-acetylated polyamine oxidase. *J Biol Chem* 278:20514–20525
5. Wang Y, Devereux W, Woster P, Stewart T, Hacker A, Casero R Jr (2001) Cloning and characterization of a human polyamine oxidase that is inducible by polyamine analogue exposure. *Cancer Res* 61:5370–5373
6. Vujcic S, Diegelman P, Bacchi CJ, Kramer DL, Porter CW (2002) Identification and

- characterization of a novel flavin-containing spermine oxidase of mammalian cell origin. *Biochem J* 367:665–675
7. Chaturvedi R, Cheng Y, Asim M, Bussiere FI, Xu H, Gobert AP, Hacker A, Casero RA Jr, Wilson KT (2004) Induction of polyamine oxidase 1 by *Helicobacter pylori* causes macrophage apoptosis by hydrogen peroxide release and mitochondrial membrane depolarization. *J Biol Chem* 279:40161–40173
 8. Xu H, Chaturvedi R, Cheng Y, Bussiere FI, Asim M, Yao MD, Potosky D, Meltzer SJ, Rhee JG, Kim SS, Moss SF, Hacker A, Wang Y, Casero RA Jr, Wilson KT (2004) Spermine oxidation induced by *Helicobacter pylori* results in apoptosis and DNA damage: implications for gastric carcinogenesis. *Cancer Res* 64:8521–8525
 9. Goodwin AC, Jadallah S, Toubaji A, Lecksell K, Hicks JL, Kowalski J, Bova GS, De Marzo AM, Netto GJ, Casero RA Jr (2008) Increased spermine oxidase expression in human prostate cancer and prostatic intraepithelial neoplasia tissues. *Prostate* 68:766–772
 10. Ha HC, Woster PM, Yager JD, Casero RA Jr (1997) The role of polyamine catabolism in polyamine analogue-induced programmed cell death. *Proc Natl Acad Sci U S A* 94:11557–11562
 11. Chen Y, Kramer DL, Diegelman P, Vujcic S, Porter CW (2001) Apoptotic signaling in polyamine analogue-treated SK-MEL-28 human melanoma cells. *Cancer Res* 61:6437–6444
 12. Devereux W, Wang Y, Stewart TM, Hacker A, Smith R, Frydman B, Valasinas AL, Reddy VK, Marton LJ, Ward TD, Woster PM, Casero RA (2003) Induction of the PAOh1/SMO polyamine oxidase by polyamine analogues in human lung carcinoma cells. *Cancer Chemother Pharmacol* 52:383–390
 13. Pledgie A, Huang Y, Hacker A, Zhang Z, Woster PM, Davidson NE, Casero RA Jr (2005) Spermine oxidase SMO(PAOh1), Not N1-acetylpolyamine oxidase PAO, is the primary source of cytotoxic H₂O₂ in polyamine analogue-treated human breast cancer cell lines. *J Biol Chem* 280:39843–39851
 14. Pledgie-Tracy A, Billam M, Hacker A, Sobolewski MD, Woster PM, Zhang Z, Casero RA, Davidson NE (2010) The role of the polyamine catabolic enzymes SSAT and SMO in the synergistic effects of standard chemotherapeutic agents with a polyamine analogue in human breast cancer cell lines. *Cancer Chemother Pharmacol* 65(6):1067–1081
 15. Fernandez C, Sharrard RM, Talbot M, Reed BD, Monks N (1995) Evaluation of the significance of polyamines and their oxidases in the aetiology of human cervical carcinoma. *Br J Cancer* 72:1194–1199
 16. Wang Y, Murray-Stewart T, Devereux W, Hacker A, Frydman B, Woster P, Casero R Jr (2003) Properties of purified recombinant human polyamine oxidase, PAOh1/SMO. *Biochem Biophys Res Commun* 304:605–611
 17. Murray-Stewart T, Wang Y, Goodwin A, Hacker A, Meeker A, Casero RA Jr (2008) Nuclear localization of human spermine oxidase isoforms – possible implications in drug response and disease etiology. *FEBS J* 275:2795–2806

Chapter 11

Characterization, Assay, and Substrate Specificity of Plant Polyamine Oxidases

Panagiotis N. Moschou and Kalliopi A. Roubelakis-Angelakis

Abstract

Polyamine oxidation is the main catabolic process of polyamines. This process is crucial because not only it participates in the regulation of the endogenous titers of polyamines but also it generates hydrogen peroxide, which can act as a signaling molecule. The recent identification of polyamine oxidases that differ in substrate specificity and mode of action in plants necessitates the use of additional techniques for their characterization based on the determination of the end-product. Herein, we describe the most widely used techniques as well as new techniques that can be used for analysis of the newly identified polyamine oxidases.

Key words: Diamine oxidases, Polyamine oxidases, Oxidation, Polyamine back-conversion, Interconversion, Hydrogen peroxide, Flavin adenine dinucleotide, Peroxisomes

1. Introduction

Oxidation is the main catabolic pathway of polyamines (PAs). Recent data on PA oxidation in plants have proposed potential roles that could be exerted by this pathway (reviewed in ref. (1)). In mammals, PA oxidation is mediated by multiple enzymatic activities. PA oxidase (PAO; EC 1.5.3.11) is mainly localized to peroxisomes and converts Spm to Put, via Spd, producing hydrogen peroxide (H_2O_2 ; (2)). The best substrates for this back-conversion process are the acetyl-derivatives of Spd and Spm (2). On the contrary, in plants, PA oxidation is exerted by both the apoplasmic and the peroxisomal PAOs. The apoplasmic oxidation pathway is oxidizing Put, Spm, and Spd to 1,3-diaminopropane, H_2O_2 , and the corresponding aldehyde, while the latter pathway is converting Spm to Put, via the intermediate Spd, as in mammals, thus being responsible for the interconversion of PAs (3–5).

Biochemical evidence for the existence of a back-conversion pathway in plants was presented by Del Duca et al. (6) and Tassoni

et al. (7), who reported that exogenously supplied Spd to *Helianthus tuberosus* chloroplasts and *Arabidopsis* plants, respectively, was converted to Put, but the enzymatic activity(ies) responsible for this conversion could not be determined at that time; it was hypothesized that an enzyme similar to the animal PAO enzyme responsible for this pathway should exist in plants. Recently, Tavladoraki et al. (8) and Moschou et al. (5) identified two *Arabidopsis thaliana* genes, *AtPAO1* and *AtPAO3*, respectively, as PAOs able to convert Spm to Spd, and to Put, thus being functionally similar to their mammalian counterparts, giving new insights into the plant PA catabolism and thus reinforcing the view that additional PAOs, similar to animal PAOs, do exist in plants.

There are two main types of plant amine oxidases: the copper-containing amine oxidases (Cu-AOs), commonly known as diamine oxidases (DAOs; EC 1.4.3.6), and the flavin-containing amine oxidases (FAD-AOs), generically known as polyamine oxidases (PAOs; EC 1.5.3.11). All PAOs characterized so far contain a FAD molecule (5) and produce H₂O₂ upon PAs oxidation, features which seem to be conserved in all organisms.

PAO genes can be identified in silico, expressed in heterologous systems, and the synthesized proteins can be easily purified to high degree. Thus, in vitro assay can be performed to identify the substrates, as well as the inhibitors of these enzymes. PAO proteins are relatively stable, which facilitates their purification.

2. Materials

2.1. Constructs

1. pDONR 207 is from the GATEWAY series vectors (Invitrogen, Carlsbad, CA, USA) with a resistance gene against gentamycin.
2. pDEST-TH1 is a modified pMAL plasmid that can be used for in vitro recombination reactions (9).

2.2. Cell Culture, Protein Expression Induction, and Lysis

1. BL21/BL21 Codon Plus (Stratagene, La Jolla, CA, USA) *Escherichia coli* cells stored as glycerol stab at -80°C (see Note 1).
2. Luria-Bertani medium (LB) supplemented with 100 µg/mL Ampicillin (see Note 2).
3. Isopropyl β-D-thiogalactopyranoside (IPTG, Sigma-Aldrich, St. Louis, Mo, USA) dissolved in water. Store aliquots at -20°C.
4. Maltose binding buffer (MBP) which contains 20 mM Tris-HCl, pH 7.4, 400 mM NaCl, and 1 mM ethylenediamine tetraacetic acid (EDTA). The buffer is sterilized and stored at 4°C.
5. Phenylmethylsulfonyl fluoride (PMSF; Sigma-Aldrich, St. Louis, Mo, USA) dissolved in methanol (as a 200 mM stock solution) and stored at 4°C (see Note 3).

6. Sonicator Fischer 550 Sonic Dismembrator setting with 4.5 with microtip.
7. Eppendorf centrifuge 5417R set at 4°C.

2.3. Purification of MBP Fusions

1. Maltose binding buffer (MBP) contains 20 Tris-HCl, pH 7.4, 400 mM NaCl and 1 mM EDTA, supplemented with 10 mM Maltose. This buffer is prepared fresh.
2. Amylose resin (New England Biolabs, County Road Ipswich, MA, USA).
3. Plastic column 9×2 cm for gravity flow.

2.4. Enzymatic Assays

1. The hydrochloride forms of Putrescine, Spermidine and Spermine, *N*¹-Acetyl-spermine (Sigma-Aldrich, St. Louis, Mo, USA) are dissolved in ddH₂O as 1 M stock solutions and stored at -20°C.
2. Assay buffer: 200 mM Na₂HPO₄/NaH₂PO₄ prepared from stock solutions of 1 M Na₂HPO₄ and 1 M NaH₂PO₄ by mixing them to prepare the desired pH solution. The final solution is dissolved 5 times to give the 200 mM solution.
3. 4-Amino-antipyrin (Sigma-Aldrich, St. Louis, Mo, USA) freshly prepared, dissolved in ddH₂O as 0.1 mM stock solution.
4. 3,5-Dichloro-2-hydroxybenzosulfonic acid, sodium salt (Sigma-Aldrich, St. Louis, Mo, USA) freshly prepared, dissolved in ddH₂O as 1 mM stock solution.
5. Horseradish peroxidase (0.8 mg/mL) (Sigma-Aldrich, St. Louis, Mo, USA) dissolved in 10 mM K₂HPO₄/KH₂PO₄ pH 7.2.
6. Lumination buffer: 10 mM Tris, pH 7.0, 1 mM CaCl₂, 0.1 mM KCl supplemented with 100 μL 2.5 mg mL⁻¹ luminol (Sigma-Aldrich, St. Louis, Mo, USA), and 10 μL of 0.1 U mL⁻¹ peroxidase.
7. Scintillation liquid: The scintillation liquid is prepared by mixing 0.5% (w/v) 2,5-diphenyloxazole (Sigma-Aldrich, St. Louis, Mo, USA) and 0.05% (w/v) 1,4-bis(5-phenyloxazolyl)benzene (Sigma-Aldrich, St. Louis, Mo, USA) dissolved in toluene (Sigma-Aldrich, St. Louis, Mo, USA). The solution is agitated using a magnetic stirrer.
8. Hydrogen peroxide standard curve preparation: Hydrogen Peroxide (H₂O₂) stock solution (Sigma-Aldrich, St. Louis, Mo, USA) stored at 4°C.
9. Counts are estimated using a Beckman Scintillation Counter (Beckman, South Kraemer Boulevard Brea, CA, USA).
10. 96-well Elisa plates (Titertek, Flow Laboratories, Mountain View, CA, USA) with flat bottom wells 1.0×0.6 cm approximately (Cat. No. 76-008-05).

**2.5. PA Extraction,
Qualitative and
Quantitative Analysis**

1. Polymerase chain reaction (PCR) tubes (strips) 1 × 8, 0.2 mL thin walled (Greiner Bio-one, Palm Springs, CA, USA).
2. Extraction solution: Perchloric acid (PCA; Sigma-Aldrich, St. Louis, Mo, USA) 5% (v/v), prepared in ddH₂O.
3. Derivatizing agent: Benzoylchloride (Sigma-Aldrich, St. Louis, Mo, USA). Store at RT in a dark place.
4. Stop solution: Saturate ddH₂O with NaCl.
5. Equilibration solution: 2 N NaOH prepared in ddH₂O.
6. Diethyl ether (Sigma-Aldrich, St. Louis, MO, USA) stabilized with 2,6-di-tert-butyl-4-methylphenol (see Note 4).
7. Dissolving solution: 63% (v/v) methanol, prepared in ddH₂O.
8. HPLC analysis solutions: Solution A: ddH₂O and Solution B: Methanol HPLC grade (Sigma-Aldrich, St. Louis, Mo, USA).
9. Analytical column: C-18 narrow-bore 2.1 × 200 mm column with 5 μm particle size (Hypersyl, Hewlett-Packard, Palo Alto, CA, USA).
10. Dansylation: Dansyl chloride (Sigma-Aldrich, St. Louis, Mo; 5 mg/mL in acetone, prepared fresh) and a stock solution of 100 mg/mL proline (stop solution).
11. Benzene, chloroform, and triethylamine (Sigma-Aldrich, St. Louis, Mo, USA).

3. Methods

Purification of PAOs from their source is rather laborious, since in dicotyledonous species like *Arabidopsis*, their abundance is rather low. Moreover, the peroxisomal ones cannot be analyzed using proteomics, due to their low cellular content (5, 10). Heterologous expression seems to be a very promising alternative method. The method relies on the efficient expression and purification of the protein in an active state. The use of rather large affinity tags simplifies the procedure, since no further solubilization step of the proteins is required. Thus, high amounts of soluble purified protein can be obtained.

These proteins exhibit high reactivity with the corresponding substrate, while an addition of FAD in the cell culture at the time of protein synthesis induction is not necessary for maintaining the activity. PAOs are stable for rather long time in buffered solutions, and subsequent enzymatic reactions can be carried out immediately after purification. More importantly, the tags used, although not appropriate for further structural analysis of the protein by crystallography for example, they do not interfere with the activity of the enzyme. Analysis of the reaction products of the recombinant expressed PAOs can be performed using a simple and reliable HPLC analysis (see data figures later).

3.1. Protein Synthesis Induction Conditions

1. A transformed *E. coli* colony BL21 (Codon Plus) with the corresponding cDNA subcloned into pDEST-TH1 vector (or any similar vector) is grown overnight in LB supplemented with 100 µg/mL Ampicillin, and is inoculated (1 mL) in 1 L LB (in a 2 L flask) supplemented with 100 µg/mL Ampicillin, on a rotary shaker (agitation rate 250 rpm) at 37°C, until OD₆₀₀ reaches 0.6–0.7 (see Note 5).
2. Induction of protein production: The culture is let to reach RT and subsequently is supplemented with 0.5 mM IPTG and placed on a rotary shaker (250 rpm) at 22°C (see Note 6). The culture is incubated overnight.

3.2. Cell Lysis Conditions

1. Cells are pelleted at 6,000 × *g* and 4°C and the supernatant is discarded. Cells are incubated at –80°C for at least 3 h and subsequently resuspended in 5 mL MBP buffer.
2. The resuspended cells are placed in a prechilled 50 mL falcon tube kept into ice. In addition, 0.5 mM of PMSF is added as protease inhibitors.
3. Cells are lysed by sonication: 4–10 × 20 s with 20 s rest time, setting 4.5 with microtip. The microtip is placed just above the bottom of the falcon tube.
4. Lysed cells are pelleted at 16,000 × *g* and 4°C for 30 min to 1 h, and the supernatant is filtrated through two layers of miracloth. The volume is approximately 7 mL and is brought to 50 mL by the addition of MBP buffer supplemented with 0.5 mM PMSF.

3.3. Purification of MBP:PAO Proteins by Affinity Chromatography

1. Three milliliters Amylose resin is added in the plastic column prepared for gravity flow. Amylose resin is dissolved by the manufacturer in ethanol, which is removed by the addition to the amylose resin of 10 volumes chilled MBP buffer.
2. Equilibration of the resin: 12 volumes (36 mL) of MBP buffer are added on top of the resin to equilibrate it.
3. Loading of the sample: All the volume of the supernatant of the lysed cells is loaded on top of the resin.
4. By the time all the volume has passed through the resin, the resin color should change to yellow due to the FAD cofactor of the PAO protein.
5. Washings: To remove other proteins showing affinity with amylose, at least 10 volumes of MBP buffer should be loaded on top of the amylose resin.
6. Protein elution: MBP:PAO is eluted using 2 mL of MBP buffer supplemented with 10 mM Maltose. Fractions of 200 µL are received (normally 10 fractions), and the fractions 3–6 usually are yellowish. The other fractions are discarded.

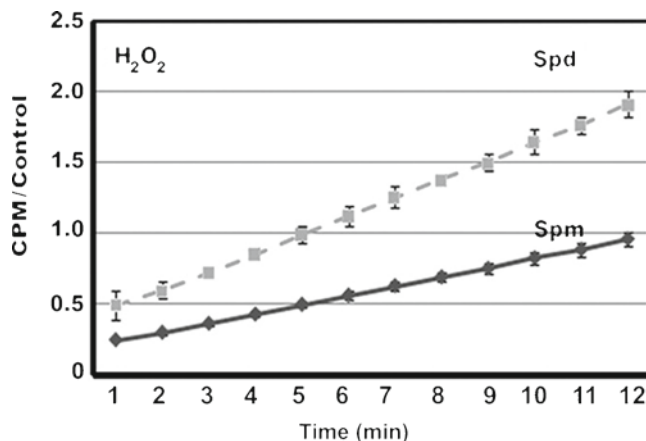


Fig. 1. Relative H₂O₂ production (CPM, counts per minute normalized to controls) using Spd and Spm as substrates (10 mM each) by the *Arabidopsis* AtPAO3 (modified from Moschou et al. (5)).

3.4. Assay for Determination of Hydrogen Peroxide Production by MBP:PAO

1. The concentration of the purified enzyme is determined using SDS-PAGE and the Lowry et al. (11) method. Ten microliters of the purified enzyme is enough for precise determination of the concentration. Normally, more than 1 mg/mL should be purified, depending also on the protein. An example of the result produced is shown in Fig. 1.
2. Aliquots of 2 μg of the enzyme are placed into a scintillation vial containing 690-μL H₂O₂ lumination buffer (10 mM Tris, pH 7.0, 1 mM CaCl₂, 0.1 mM KCl) supplemented with 100 μL 2.5 mg mL⁻¹ luminol, 10 μL of 0.1 U mL⁻¹ peroxidase, and 1–10 mM final concentration of Put 2HCl, Spd 3HCl, or Spm 4HCl.
3. A standard curve of H₂O₂ concentration is prepared by adding known amounts of H₂O₂ in lumination buffer (10 mM Tris, pH 7.0, 1 mM CaCl₂, 0.1 mM KCl) supplemented with 100 μL 2.5 mg mL⁻¹ luminol, 10 μL of 0.1 U mL⁻¹ peroxidase. Concentrations may vary between 0 and 1 mM.
4. Counts are measured in a scintillation counter (Beckman) for 10 min, and values are taken in the linear part of the assay.

3.5. Assay for Determination of Kinetic Parameters of MBP:PAO

1. For the determination of kinetic parameters, the method of the oxidation of 4-aminopterine is used (8).
2. In a 96-well Elisa plate, 100 μL of 200 mM N-P buffer is added supplemented with 0.1 mM 4-aminopterine and 1 mM 3,5-Dichloro-2-hydroxybenzosulfonic acid, and horseradish peroxidase (0.08 mg/mL), with the corresponding concentration of PA. For each reaction, 2 μg of protein is added.
3. The pink color produced by the oxidation of 4-aminoantipyrin is red at 511 nm in an Elisa plate reader (Synergy HT,

Bio-TEK, Winooski, VT, USA). The extinction coefficient is $2.63 \times 10^4 \text{ M}^{-1} \text{ cm}^{-1}$. A standard curve is additionally prepared by omitting the enzyme but using known concentrations of H_2O_2 solution.

3.6. Reaction Products Analysis of MBP:PAO

1. Analysis of PAOs oxidation products is performed by incubating saturating amounts of substrate with $4 \mu\text{g}$ of purified protein, in a final volume of $200 \mu\text{L}$, buffered with 100 mM

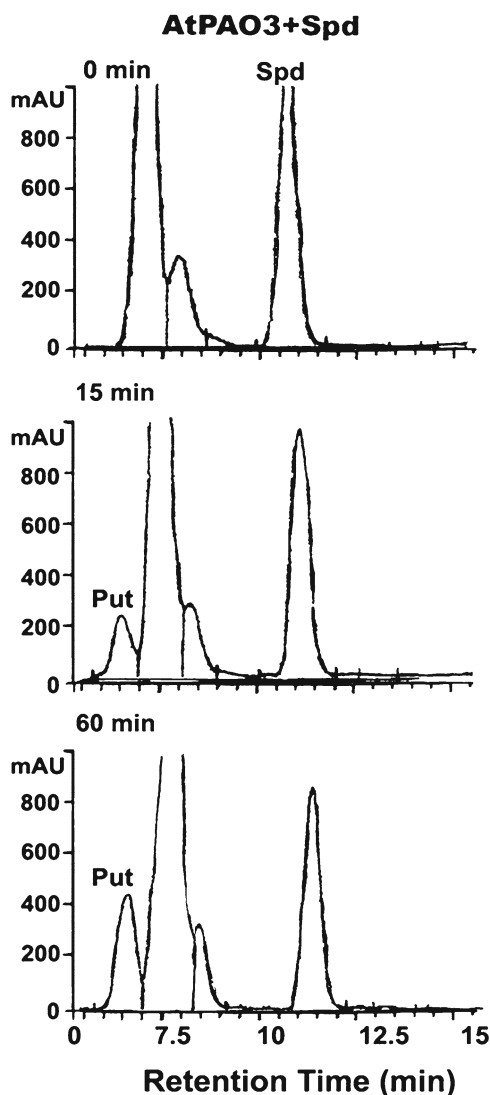


Fig. 2. HPLC analysis of the AtPAO3-dependent Spd conversion to Put. A total 1 mM substrate was used and $2 \mu\text{g}$ of AtPAO3 enzyme. The peaks with retention time varying between approximately $7\text{--}8 \text{ min}$ correspond to traces of benzoyl chloride used as derivatization reagent (modified from Moschou et al. (5)).

- Tris, pH 7.5. It is recommended to use PCR strips for the reactions. An example of the result produced is shown in Fig. 2.
2. Reaction is stopped by the addition of equal volume of 5% (v/v) PCA and the samples are centrifuged for 20 min at $12,000 \times g$ and 4°C .
 3. Derivatization: The supernatant is derivatized by adding 10 μL of benzoylchloride, followed by incubation for 20 min at RT.
 4. Stop reaction: The derivatization is terminated by the addition of 2 mL of saturated NaCl solution. Samples are vortexed for 20 s.
 5. Polyamine extraction: PAs are extracted from the aqueous phase by the addition of 2 mL diethyl-ether. Samples are vortexed for 20 s to mix the two phases. Samples are centrifuged at $3,000 \times g$ for 5 min and the ether phase is evaporated in a water bath at 60°C .
 6. Resuspension: Benzoyl-PAs are redissolved in 100 μL of 63% (v/v) methanol. The samples are vortexed for 30 s. 20–100 μL of the sample is injected into the HPLC preferably using an autosampler.
 7. Analysis is performed using a Hewlett-Packard 1100 HPLC, equipped with a C-18 narrow bore column (2.1×200 mm, 5 μm particle size, Hypersyl; Hewlett-Packard). Separation temperature is kept at 25°C . Flow rate is $200 \mu\text{L min}^{-1}$. Regression curves are used for quantification of PAs. The lower detection limit is 5 pmol, equal to that of the dansylated derivatization. To ensure appropriate separation of Put from Cad, a gradient elution should be used. The most appropriate separation is achieved when using 55% methanol at the onset to 84% methanol at 23 min and 84% from 23 to 26 min. Residual benzoyl-chloride appeared at a retention time of 8.3 min, between Cad and Spd. The HPLC standards are Put, 6.6 min; Cad, 7.5 min; Spd, 10.5 min; Spm, 13.9 min; Agm, 23.9 min. In addition, in each sample a known amount of internal standard should be added after the extraction of the PAs, such as Cad.

3.7. Detection of Reaction Products by Radiometric Assay

1. Additionally, reaction products are estimated using radio-labeled Spm by a modification of the radiometric method of Paschalidis and Roubelakis-Angelakis (12), using $[1,4\text{-}^{14}\text{C}]\text{Put}$, $[1,4\text{-}^{14}\text{C}]\text{Spd}$, $[1,4\text{-}^{14}\text{C}]\text{Spm}$ (Amersham, Buckinghamshire, UK; specific activities, $4.37 \text{ GBq mmol}^{-1}$) as labeled substrates and 4 μg of AtPAO3 enzyme (see Note 7). The assay mixture contains 0.2 mL of Tris, pH 7.5, 1 mM unlabeled Put, Spd, and Spm and 3.7 KBq of $[1,4\text{-}^{14}\text{C}]\text{Put}$, $[1,4\text{-}^{14}\text{C}]\text{Spd}$, $[1,4\text{-}^{14}\text{C}]\text{Spm}$. After incubation

- on a shaker at 37°C for 60 min, the reaction is terminated by adding 150 μ L of saturated sodium carbonate.
2. Dansylation: In 200 μ L of the sample 400 μ L of dansyl chloride (5 mg/mL in acetone, prepared fresh). After brief vortexing, the mixture is incubated in darkness at room temperature overnight. Excess dansyl reagent is removed by the addition of 100 mg/mL proline and incubation for 30 min. Dansylpolyamines are extracted in 0.5 mL benzene and vortexed for 30 s. Organic phase is transferred.
 3. Products are separated on a thin layer chromatography plate using as a mobile phase chloroform/triethylamine 4:1 (v/v). The plate is dried out for 10 min at 60°C, the radioactivity is estimated after scraping off the spots from the plate, and the powder from each spot was measured using a scintillation counter (Beckman).
 4. To identify the retention time of each spot, 1 mM standards of PAs are also used and were visualized under UV light following dansylation as described by Flores and Galston (13).
 5. The powder from each spot is placed into scintillation liquid, incubated at RT in 1 mL scintillation liquid (0.5% (w/v) 2,5-diphenyloxazole and 0.05% (w/v) 1,4-bis[5-phenyloxazolyl]benzene in toluene) for 1 h, and centrifuged at 16,000 $\times g$ for 5 min. Five hundred microliters from the supernatant is put into a scintillation vial containing 3.5 mL of scintillation liquid and are counted in an LS 6000SE (Beckman, Fullerton, CA, USA) scintillation counter. Additionally, radiolabeled products are also dansylated to maintain the Rr accuracy.

3.8. Radiometric Estimation of Δ^1 -Pyrroline

1. Some PAOs, especially those involved in the terminal catabolism of PAs, are producing Δ^1 -pyrroline. Pyrroline production can be estimated by a modification of the radiometric method of Biondi et al. (14), using [1,4- 14 C]Put and [1,4- 14 C]Spd (Amersham, Buckinghamshire, UK; specific activities 4.37 GBq mmol $^{-1}$) as labeled substrates.
2. The assay mixture contained 0.5 mL of the extract, 1 mM unlabeled Put or Spd, and 3.7 KBq of [1,4- 14 C]Put or [1,4- 14 C]Spd. After incubation on a shaker at 37°C for 60 min, the reaction is terminated by adding 150 μ L of saturated sodium carbonate (15). Δ^1 -[14 C]pyrroline from [1,4- 14 C]putrescine (4.03 TBq mol $^{-1}$, Amersham Pharmacia Biotech, Italy) during a 30 min incubation at 37°C (16).
3. Labeled Δ^1 -pyrroline is extracted immediately in 1 mL toluene. The 0.5-mL aliquots are placed in scintillation liquid (0.5% (w/v) 2,5-diphenyloxazole and 0.05% (w/v) 1,4-bis[5-phenyloxazolyl]benzene in toluene) and counted in an LS 6000SE

3.9. Colorimetric Estimation of Δ^1 -Pyrroline

(Beckman, Fullerton, CA) scintillation counter. One unit of enzyme (U) represents the amount of enzyme catalyzing the formation of 1 μmol of Δ^1 -[^{14}C]pyrroline/min.

1. A spectrophotometric assay can also be used for the determination of Δ^1 -pyrroline, according to Holnsted et al. (17) and Federico et al. (18). The principle of the method is that Δ^1 -pyrroline formed by the enzymatic oxidation of Spd can react with *o*-aminobenzaldehyde to produce a yellowish-colored dihydroquinazolinium derivative.
2. The extraction buffer for pyrroline determination is different from the one described above. The reaction mixture contains the extract, 12 μL Put or Spd 0.1 M, for DAO and PAO respectively, and up to 1 mL 0.1 M K-phosphate, pH 6.5.
3. Reactions are carried out for 1 h at 37°C, and the reaction is terminated by the addition of 0.125 μL of 10% (w/v) TCA followed by 12.5 μL *o*-aminobenzaldehyde (10 mg mL $^{-1}$) dissolved in ethanol. Under these conditions, Δ^1 -pyrroline forms a yellowish complex. After a centrifugation step at 12,000 $\times g$ at 4°C to remove proteins, the complex absorbance is red at 430 nm ($\epsilon = 1.86 \cdot 10^3 \text{ mol}^{-1} \text{ cm}^{-1}$). One unit represents the amount of enzyme catalyzing the formation of 1 μmol of Δ^1 -pyrroline/min.

3.10. Identification of the FAD Molecule and Stoichiometric Analysis

1. The in silico analysis of the PAO protein may reveal the existence of an N terminus domain responsible for the binding of a FAD molecule. For motif and domain scan, the Simple Modular Architecture Research Tool database can be used

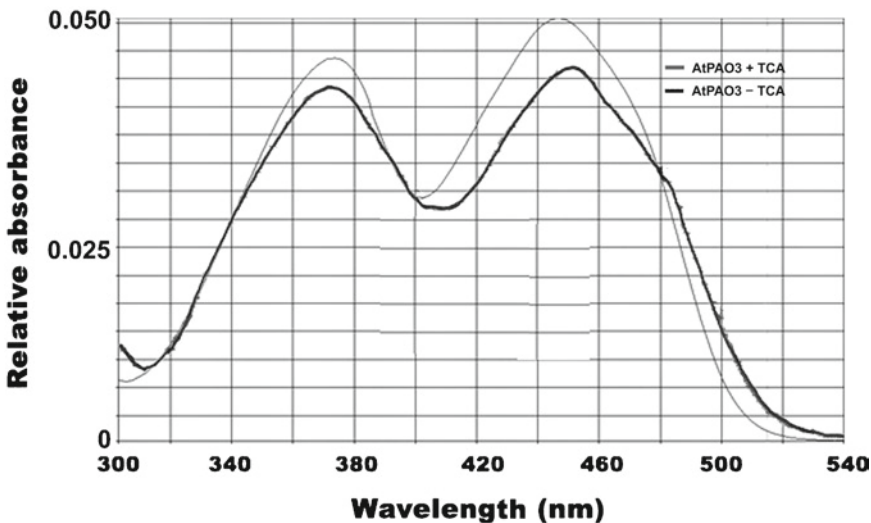


Fig. 3. Determination of PAO cofactor. As an example, the absorption spectrum of the AtPAO3 purified protein between wavelengths 300–540 from TCA-treated or nontreated protein is presented. AtPAO3 exhibits the characteristic absorbance of FAD-containing enzymes with two maxima (modified from Moschou et al. (5)).

(<http://smart.embl.de>) to identify such domains. An example result is shown in Fig. 3.

2. To test whether the PAO protein is able to bind to FAD molecule(s) in vitro, the noncovalent bonds should be disrupted through the addition of 5% TCA to the purified protein, which is subsequently precipitated by centrifugation at $12,000 \times g$ at 4°C . Supernatant absorbance is measured in a spectrophotometer. Should the protein exhibit the characteristic two-curve spectrum, typical for FAD-containing proteins, it contains a FAD molecule (absorption maxima at 380 and 460 nm).
3. A similar spectrum is obtained without disrupting the bonds between the FAD and the PAO, while slight differences observed are most probably due to the protein microenvironment that surrounds the FAD molecule, which alters its absorbance characteristics. No significant differences are observed between the tagged and nontagged PAO proteins absorbance, suggesting that MBP protein does not affect the absorbance features of protein.
4. The molecular ratio PAO:FAD can be determined by estimating the amount of the protein and the amount of FAD. FAD extinction coefficient is $11,300 \text{ M}^{-1} \text{ cm}^{-1}$.

4. Notes

1. *E. coli* BL21 Codon Plus contain an enriched tRNA pool. In some cases, BL21 cells were insufficient in expressing some PAO proteins.
2. Ampicillin should be filter-sterilized to avoid any biogenic contaminants or even Ampicillin resistant bacterial cells.
3. PMSF is a very toxic substance and should be handled as such. Avoid any contact with skin. In case of contact with clothes discard them.
4. Diethyl-ether is highly volatile and flammable. It should always be used in a fume hood.
5. The appropriate OD_{600} may vary upon protein of interest. Above OD 0.7 in some cases PAO proteins are sufficiently expressed as well.
6. The appropriate IPTG concentration may vary upon protein of interest. Pilot experiments with concentrations varying between 0.01 and 1 mM should be performed.
7. Radioactive material should be treated with care. Always take all necessary precautions depending also on the type of the isotope and the specific activity used.

References

1. Kusano T, Berberich T, Tateda C, Takahashi Y (2008) Polyamines: essential factors for growth and survival. *Planta* 228:367–381
2. Schrader M, Fahimi DH (2004) Mammalian peroxisomes and reactive oxygen species. *Histochem Cell Biol* 122:383–393
3. Rea G, de Pinto MC, Tavazza R, Biondi S, Gobbi V, Ferrante P, De Gara L, Federico R, Angelini R, Tavladoraki P (2004) Ectopic expression of maize polyamine oxidase and pea copper amine oxidase in the cell wall of tobacco plants. *Plant Physiol* 134:1414–1426
4. Cona A, Rea G, Angelini R, Federico R, Tavladoraki P (2006) Functions of amine oxidases in plant development and defence. *Trends Plant Sci* 11:80–88
5. Moschou PN, Sanmartin M, Andriopoulou AH, Rojo E, Sanchez-Serrano JJ, Roubelakis-Angelakis KA (2008) Bridging the gap between plant and mammalian polyamine catabolism: a novel peroxisomal polyamine oxidase responsible for a full back-conversion pathway in *Arabidopsis*. *Plant Physiol* 147:1845–1857
6. Del Duca S, Beninati S, Serafini-Fracassini D (1995) Polyamines in chloroplasts: identification of their glutamyl and acetyl derivatives. *Biochem J* 305:233–237
7. Tassoni A, Van Buuren M, Franceschetti M, Fornale IS, Bagni N (2000) Polyamine content and metabolism in *Arabidopsis thaliana* and effect of spermidine on plant development. *Plant Physiol Biochem* 38:383–393
8. Tavladoraki P, Rossi MN, Saccuti G, Perez-Amador MA, Polticelli F, Angelini R, Federico R (2006) Heterologous expression and biochemical characterization of a polyamine oxidase from *Arabidopsis* involved in polyamine back conversion. *Plant Physiol* 149:1519–1532
9. Hammarstrom M, Hellgren N, Van der Berg S, Berglund H, Hard T (2002) Rapid screening for improved solubility of small human proteins produced as fusion proteins in *Escherichia coli*. *Protein Sci* 11:313–321
10. Reumann S, Ma C, Lemke S, Babujee L (2004) AraPerox. A database of putative Arabidopsis proteins from plant peroxisomes. *Plant Physiol* 136:2587–2608
11. Lowry OH, Rosebrough NJ, Farr AL, Randall RJ (1951) Protein measurement with the Folin-Phenol reagents. *J Biol Chem* 193:265–275
12. Paschalidis KA, Roubelakis-Angelakis KA (2005) Sites and regulation of polyamine catabolism in the tobacco plant. Correlations with cell division/expansion, cell cycle progression, and vascular development. *Plant Physiol* 138:2174–2184
13. Flores EH, Galston AW (1984) Osmotic stress-induced polyamine accumulation in cereal leaves: II. Relation to amino acid pools. *Plant Physiol* 75:110–113
14. Biondi S, Scaramagli S, Capitani F, Maddalena M, Patrizia A, Torrigiani P (2001) Methyl jasmonate upregulates biosynthetic gene expression, oxidation and conjugation of polyamines, and inhibits shoot formation in tobacco thin layers. *J Exp Bot* 52:231–242
15. Bhatnagar P, Glasheen BM, Bains SK, Long SL, Minocha R, Walter C, Minocha SC (2001) Transgenic manipulation of the metabolism of polyamines in poplar cells. *Plant Physiol* 125:2139–2153
16. Scaramagli S, Biondi S, Torrigiani P (1999) Methylglyoxal (bis-guanyldrazone) inhibition of organogenesis is not due to S-adenosylmethionine decarboxylase inhibition/polyamine depletion in tobacco thin layers. *Physiol Plant* 107:353–360
17. Federico R, Angelini R (1988) Distribution of polyamines and their related catabolic enzymes in etiolated and light-grown *Leguminosae* seedlings. *Planta* 173:317–321
18. Holmsted B, Larsson L, Tham R (1961) Further studies on spectrophotometric method for the determination of amine oxidase activity. *Biochim Biophys Acta* 48:182–186

Assay of Deoxyhypusine Synthase Activity

Edith C. Wolff, Seung Bum Lee, and Myung Hee Park

Abstract

Deoxyhypusine synthase catalyzes an unusual protein modification reaction. A portion of spermidine is covalently added to one specific lysine residue of one eukaryotic protein, eIF5A (eukaryotic initiation factor 5A) to form a deoxyhypusine residue. The assay measures the incorporation of radioactivity from [1,8-³H]spermidine into the eIF5A protein. The enzyme is specific for the eIF5A precursor protein and does not work on short peptides (<50 amino acids). Optimum conditions for the reaction and four detection methods for the product, deoxyhypusine-containing eIF5A, are described in this chapter. The first, and most specific, method is the measurement of the amount of [³H]deoxyhypusine in the protein hydrolysate after its separation by ion exchange chromatography. However, this method requires some specialized equipment. The second method is counting the radioactivity in TCA-precipitated protein after thorough washing. The third method involves determining the radioactivity in the band of [³H]deoxyhypusine-containing eIF5A after separation by SDS-PAGE. The fourth method is a filter-binding assay. It is important to minimize nonspecific binding of [³H]spermidine to proteins in the assay mixture, especially for methods 2 and 4, as illustrated in a comparison figure in the chapter.

Key words: Polyamine, Spermidine, Deoxyhypusine synthase, Deoxyhypusine, Hypusine, eIF5A, Posttranslational modification

1. Introduction

Deoxyhypusine synthase (DHS) (EC 2.5.1.46) is an essential protein found in all eukaryotes. It catalyzes the synthesis of deoxyhypusine [*N*^ε-(4-aminobutyl)-lysine], the first step in the post-translational synthesis of an unusual amino acid hypusine [*N*^ε-(4-amino-2-hydroxybutyl)-lysine] (see a recent review (1)). This enzyme uses two substrates, spermidine (butylamine donor) and eIF5A precursor (butylamine acceptor) and requires a cofactor, NAD (2–5). It catalyzes a NAD-dependent cleavage between N4 and C5 of spermidine and the transfer of the butylamine moiety to the ε-amino group of a specific lysine residue of the eIF5A precursor, eIF5A(Lys), to form the deoxyhypusine residue

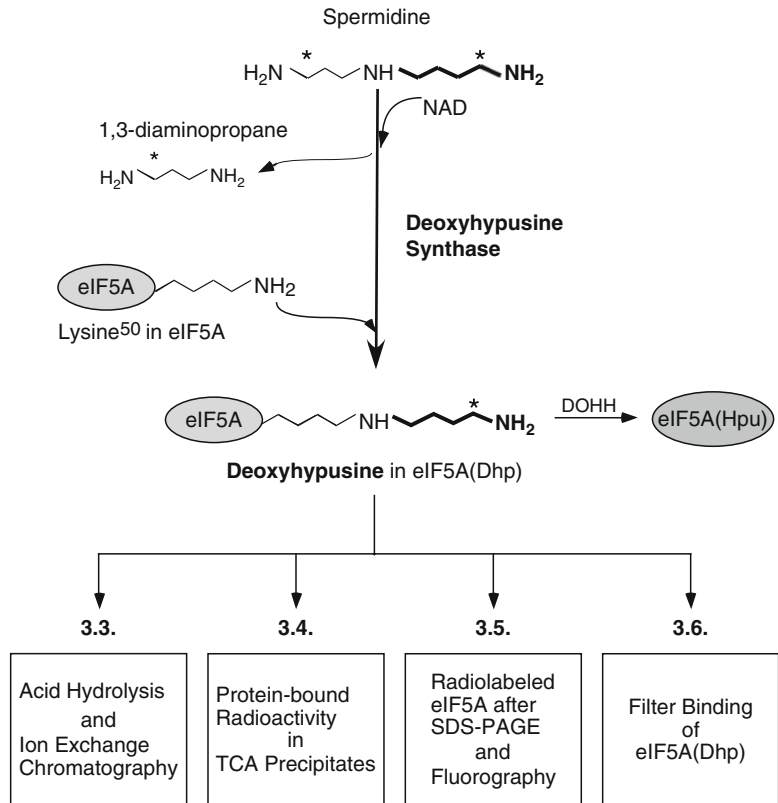


Fig. 1. Biosynthesis of deoxyhypusine from the polyamine spermidine and detection methods for deoxyhypusine-containing eIF5A, eIF5A(Dhp). Deoxyhypusine synthase catalyzes the cleavage of spermidine and conjugation of its 4-aminobutyl moiety (in *bold*) to the ϵ -amino group of a specific lysine residue of eIF5A precursor to form a deoxyhypusine residue. [1,8-³H]spermidine is used in the assay and the positions of radioactivity in spermidine, 1,3-diaminopropane and deoxyhypusine are indicated by *asterisk*. The aminobutyl moiety derived from spermidine is indicated in *bold*. Four different methods for detection of radiolabeled eIF5A(Dhp) are presented in *boxes*.

(Fig. 1). 1,3-Diaminopropane is released as a byproduct from spermidine cleavage. This protein modification is strictly specific for one single lysine residue of one cellular protein, eukaryotic initiation factor 5A (eIF5A) (6). DHS also exhibits a remarkable specificity toward its amine substrate, spermidine (7).

Cultured cells or tissues normally contain the mature hypusine-containing form of eIF5A, but little or no eIF5A precursor, eIF5A(Lys) (8, 9). Cells or tissues can serve as a source of deoxyhypusine synthase, but eIF5A(Lys) must be added as a substrate (4). The DHS assay protocol can be designed either for detection of the enzyme or of eIF5A(Lys) (4, 5, 10). The cDNAs for both eIF5A (11) and DHS (12) have been cloned and recombinant proteins can be purified by simple methods (12–14). Since the *in vitro* assay uses a low concentration of [1,8-³H]spermidine, it is critical to use a high pH buffer (pH 9.2–9.5) (2) (since the percentage of the properly charged spermidine substrate (15) with the unprotonated secondary

amino group is highest at this pH range (16)). Because only a very small portion of [1,8-³H]spermidine in the assay is converted to deoxyhypusine and because spermidine tightly adheres to proteins in the assay mixture, it is most critical to remove all the unreacted radiolabeled spermidine from the labeled protein product.

Typical reaction conditions for deoxyhypusine synthesis are described under Subheading 3.2. The [³H]deoxyhypusine formed in eIF5A can be measured by four different methods (Fig. 1, Subheading 3.3–3.6): (1) determination of radioactive deoxyhypusine after its ion exchange chromatographic separation (4, 5, 17, 18), (2) determination of protein-bound radioactivity by TCA precipitation after repeated washing, (3) determination of radioactivity in eIF5A after SDS-PAGE (3, 10, 15, 19), (4) filter binding assay of radiolabeled eIF5A (20). The first method (Subheading 3.3) gives the most accurate estimate of the amount of [³H]deoxyhypusine formed, since it is measured after its complete separation from [1,8-³H]spermidine. However, it requires an amino acid analyzer (or HPLC system) with an ion exchange column with specific buffers. For those who do not have access to such a separation system, one of the other methods can be employed for an estimation of enzyme activity. The sensitivity (signal) and the background of the DHS assay are compared for the four detection methods (Fig. 2).

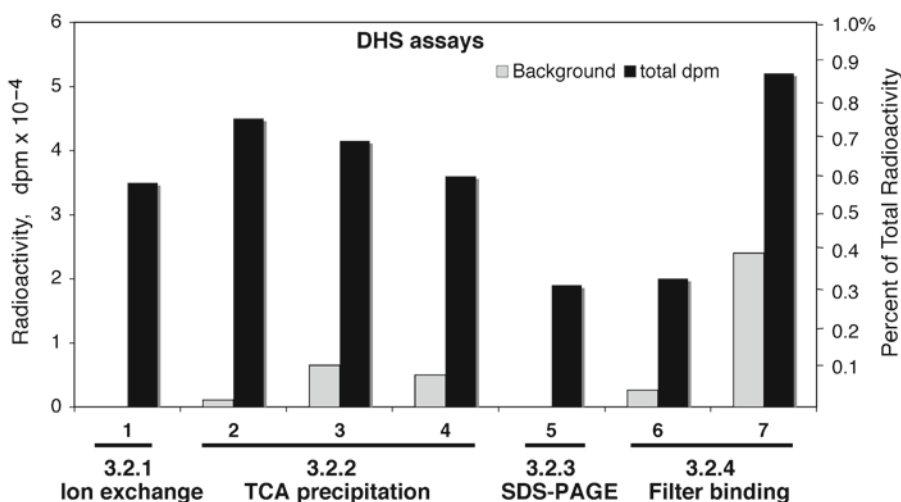


Fig. 2. Comparison of different methods of measurement of deoxyhypusine formed. Approximately 2.5 units of purified DHS (lanes 1, 2, 5–7) or 50 μ g of total HeLa cell protein (lanes 3 and 4) was used as enzyme source. Purified eIF5A(Lys) (2.5 μ g) was used in each case. 1, Measurement of [³H]deoxyhypusine after its separation by ion exchange chromatography, accurate estimate with no background. 2–4, Estimation of TCA precipitable radioactivity after thorough TCA wash. The background is low when pure DHS and eIF5A(Lys) were used with no carrier BSA in the reaction mix (lane 2). However, when crude HeLa extract was used as an enzyme source, the amount of [1,8-³H]spermidine noncovalently bound to proteins increases (lanes 3 and 4). This background binding was estimated when DHS is completely inhibited in the presence of 0.1 mM of a DHS inhibitor, *N*-guanyl-1,7-diaminoheptane (GC7). 5, Radioactivity in the 18 kDa eIF5A after its separation by SDS-PAGE. 6, A filter-binding assay with purified DHS and eIF5A(Lys) without BSA. 7, A filter-binding assay that contained BSA in the reaction mix shows high background level of [1,8-³H]spermidine binding to the filter. Total dpm per assay is indicated on the *left axis*, and the percent of the total radioactivity in the reaction mix is shown on the *right axis*.

2. Materials

Those required for a specific protocol are indicated by the method number.

2.1. Equipment

1. Plastic Eppendorf tubes (1.5 ml size) with screw caps, resistant to heating at 110°C (Subheading 3.3).
2. Dry heating block (108°C) for acid hydrolysis (Subheading 3.3).
3. SpeedVac concentrator (e.g., Savant) with a NaOH trap (Subheading 3.3).
4. An amino acid analyzer with an ion exchange column (e.g., 0.4 × 7.5 cm, DC-6A cation exchange resin) (Subheading 3.3) (see Note 1).
5. Liquid scintillation fluid that tolerates high salt buffers (Optiphase High Safe 3 from PerkinElmer works well) (Subheading 3.3).
6. Whatman 3 MM filter discs (2.4 cm diameter) (Subheading 3.6).

2.2. Reagent Stock Solutions

1. Use deionized or ultrapure water for preparation of all solutions.
2. Buffer A: 50 mM Tris-HCl buffer (pH 7.5) and 1 mM DTT.
3. Glycine/NaOH buffer: 1 M, pH 9.2 buffer. Dissolve 7.5 g of glycine in 50 ml of water, and adjust pH to 9.2 by adding NaOH solution (2 N), adjust the final volume to 100 ml with water and store at 4°C.
4. eIF5A(Lys) solution (5 mg/ml) (see Note 2 for pure recombinant protein or alternate source of eIF5A precursor). Store aliquots of solutions in 50 mM Tris-HCl pH 7.5, 0.3 M KCl, 1 mM DTT buffer in a -70°C freezer.
5. 20 mM NAD: Dissolve 13.7 mg/ml of NAD sodium salt in water and store at -20°C in aliquots.
6. DTT (100 mM): the solution of 100 mM DTT (15.4 mg/ml) in water is stored frozen at -20°C in aliquots.
7. BSA (50 mg/ml in water), Store frozen at -20°C in aliquots.
8. [1,8-³H]spermidine (16–20 Ci/mmol) from PerkinElmer Life Sciences is stored at 4°C.
9. TCA polyamine solution (10% trichloroacetic acid (TCA) containing 1 mM each of putrescine, spermidine, and spermine), Store at 4°C.
10. 0.1 N NaOH containing 1 mM each of putrescine, spermidine, and spermine.

11. 6 N HCl solution (Subheading 3.2).
12. PA buffer B: 13.2 mM sodium citrate buffer, 1.5 N NaCl, pH 5.55, 0.1% Phenol.
13. PA buffer C: 53 mM sodium citrate buffer, 3.0 N NaCl, pH 5.55, 0.1% Phenol. Buffers filtered and stored at room temperature; Brij is added (to 0.1%) just before use (Subheading 3.3).
14. SDS-PAGE buffers, sample buffer and running buffers from Invitrogen (Subheading 3.5).
15. Coomassie-Blue staining solution: 10% acetic acid, 50% methanol, 1.25 g/l Brilliant Blue R dye.
16. Destaining solution: 10% acetic acid, 10% methanol (Subheading 3.5).
17. Amplify (GE Healthcare) for soaking gels prior to fluorography (Subheading 3.5).
18. PCA polyamine solution: 4% perchloric acid solution containing 1 mM each of putrescine, spermidine, and spermine (Subheading 3.6).

3. Methods

3.1. Preparation of Enzyme Extract from Cultured Cells or Tissues

For preparation of a crude enzyme extract, sonicate freshly harvested cell pellets or homogenize fresh tissues in Buffer A containing protease inhibitor cocktail (0.2 ml buffer for 10^7 cells, or 1 ml per 1 g wet tissue). Centrifuge the lysates in a refrigerated microfuge (at $15,000 \times g$) for 20 min and take the supernatants for protein determination and enzyme assays (see Note 3). Use 20–100 μg of total protein per assay as an enzyme source.

3.2. DHS Assay for Measurement of DHS Activity (see Note 4)

1. Just before the assay, make a master mixture by multiplying each volume by the sample number (n) and keep on ice in an Eppendorf tube.

Stock solution volume per assay final concentration

1. 1 M Glycine NaOH buffer pH 9.2	4 μL	0.2 M
2. 100 mM DTT	0.2 μL	1 mM
3. 20 mM NAD	1 μL	1 mM
4. 50 mg/ml BSA (optional, see Note 5)	1 μL	2.5 mg/ml
5. [1,8- ^3H]spermidine (see Note 6)	3 μL (~150 pmol)	7.5 μM
6. 6 mg/ml eIF5A(Lys)	0.5 μL	9.0 μM
7. H_2O	5.3 μL	
8. Volume of master mix per tube	15 μL	
9. Enzyme solution/lysate	5 μL	
10. Total volume	20 μL	

2. Set up screw cap plastic Eppendorf tubes and number them. Add an enzyme sample in 5 μ l to each. Use 5 μ l of Buffer A as a negative control and 2–10 units of purified DHS (if available) as a positive control (see Note 7).
3. Start the reaction by adding 15 μ l of the master mix to each tube. Mix gently and cap each tube.
4. Incubate the reaction mixtures in a 37°C water bath for 60 min.

**3.3. Determination
of Deoxyhypusine
Formed After Ion
Exchange
Chromatographic
Separation**

1. Stop the reaction by adding 5 μ l of spermidine (0.1 M), 5 μ l (250 μ g) of carrier BSA to each tube. Immediately add 1 ml of ice-cold 10% TCA polyamine solution. Gently mix and keep on ice for 30 min.
2. Centrifuge the TCA precipitated samples in a refrigerated microfuge (4°C) at 15,000 $\times g$ for 5 min and remove all the supernatant by careful suction using a fine 10 μ l tip.
3. Add 1 ml of the TCA polyamine solution to each sample. Resuspend the pellet by pipetting up and down using 200 μ l tips and centrifuge again to remove all the supernatant.
4. Dissolve the TCA pellet in 0.1 ml 0.1 N NaOH containing 1 mM each of polyamines. Immediately add 1 ml of the TCA polyamine solution and keep on ice for 30 min to precipitate the proteins. Repeat this step if needed, until the radioactivity in the 0.1 ml of the final wash is sufficiently low (<200 dpm) (see Note 8).
5. After removing all the TCA supernatant, resuspend the pellet in 0.4 ml of 6 N HCl, tighten the cap and place in a heating block at 108°C overnight.
6. Dry the hydrolyzed samples using a SpeedVac concentrator set up with a NaOH trap.
7. Add 0.1 ml of water to each tube to dissolve dried residues. Count a 5 μ l aliquot and apply an aliquot containing up to 50,000 dpm to the amino acid analyzer (see Note 9).
8. Separate deoxyhypusine by running 13 min of PA Buffer B at the speed of 0.75 ml per min. Collect 13 tubes of 1 min fractions and count the total radioactivity in a liquid scintillation counter. In our machine, the elution peak time for deoxyhypusine is approximately 10 min (fractions 9–11 contain deoxyhypusine). After running five samples, the column should be washed with PA buffer C for 30 min and reequilibrated with PA buffer B (20 min) for the next cycle of five samples (see Note 10).
9. Sum the radioactivity of the deoxyhypusine peak (usually in four fractions, 9–12), after subtraction of background radioactivity in the negative control, and multiply the number by a

factor (100/volume injected) to estimate the total amount of deoxyhypusine formed in each reaction (see Note 11).

3.4. Determination of Protein-Bound Radioactivity by TCA Precipitation

If an amino acid analyzer or HPLC system is not available, one can follow the Subheading 3.3, steps 1–4 described above and count radioactivity in the TCA precipitates (see Note 12).

Dissolve the TCA precipitates (from Subheading 3.3, step 4) in 0.1 ml of 0.1 N NaOH and count the radioactivity of the dissolved proteins.

3.5. Determination of Radiolabeled eIF5A(Dhp) After SDS-PAGE (see Note 13)

1. Mix 10 μ l of each reaction sample with 10 μ l of SDS sample buffer (2 \times) and separate proteins by PAGE on 4–12 % gradient NuPAGE Bis-Tris gel and MES electrophoresis buffer.
2. Stain for 1 h, destain the gel for 20 h with two changes of destaining solution, and identify the eIF5A band (18 kDa) (see Note 14). Scan the stained gel for a record.
3. Cut out the stained eIF5A band and add to a screw cap Eppendorf tube. Add 0.5 ml of 30% hydrogen peroxide solution and incubate at 70°C overnight. After the gel pieces dissolve, count the radioactivity by liquid scintillation counting.
4. The radioactivity incorporated into eIF5A can also be determined by fluorography. Wash the destained gel with deionized water for 15 min and soak it in Amplify (GE Healthcare) for 30 min. Expose the gel to X-Ray film (BioMax XAR film) at –70°C. Develop the film after 2–20 days (see Note 15) of exposure and scan the intensity of the labeled eIF5A band using a densitometer.

3.6. Filter Binding Assay of Radiolabeled eIF5A(Dhp) Formed

1. Set up the reaction as in Subheading 3.2, but with omission of BSA (see Note 16). Stop the reaction by adding 5 μ l of 100 mM spermidine.
2. Spot 10 μ l of the reaction mixtures on Whatman 3 MM filter paper discs in duplicate. Mark numbers on the discs with a pencil.
3. Let the filters dry for 5 min, then wash the filters in the PCA polyamine solution (50 ml per ten filters in a beaker, heated at 90°C) for 5 min.
4. Wash the filters in fresh hot PCA polyamine solution and heat for 5 min. Repeat washing, if necessary, until the radioactivity in the wash is sufficiently low (see Note 17).
5. Rinse the filters briefly in 0.2 N HCl and in ethanol. Count radioactivity of the filters after letting the filters sit in the liquid scintillation fluid for 20 h at room temperature (see Note 18).

4. Notes

1. We use a Dionex D-400 analyzer using a column (0.4×7.5 cm) of cation exchange resin, DC-6A (17, 18). Elution conditions on our analyzer are temperature 66°C , flow rate 0.75 ml/min, and we collect 0.5 or 1 min fractions directly into 7 ml glass scintillation vials. An amino acid analyzer or HPLC system can be modified to separate basic compounds (e.g., hypusine, deoxyhypusine, spermidine, and 1,3-diaminopropane (17, 18)) using the high salt PA buffers given in step 12 in Subheading 2.2.
2. The human recombinant protein substrate is purified from BL21(DE3) cells transformed with pET11a/heIF5A as described in ref. (14). Crude extracts prepared from mammalian cells, that are depleted of spermidine and thereby have accumulated eIF5A(Lys), can be used as a source of substrate protein (2–4).
3. Crude extracts from cells or tissues contain spermidine (~ 10 nmol per mg protein) and will dilute the specific activity of $[1,8\text{-}^3\text{H}]$ spermidine added to the assay. This dilution has to be calibrated for accurate estimation of DHS activity. Crude extract from fresh HeLa cells contain ~ 1 unit of activity per 10 μg of total proteins. If not used immediately, the crude extracts should be frozen on dry ice and stored at -80°C .
4. The assay can be set up for detection of DHS activity (as in Subheading 3.2) or for detection of substrate, eIF5A(Lys) (4, 10, 14, 15, 19, 21). In the latter case, add 10 units of DHS per assay (if purified enzyme is available) instead of eIF5A(Lys) in the master mix and samples containing eIF5A(Lys) in 5 μl is assayed by addition of master mix containing DHS. If a crude cell lysates sample containing both eIF5A(Lys) and DHS are assayed (2–4, 19), the master mix lacking both protein substrate and enzyme can be used. If accurate quantitative measurement is required, set up the samples in duplicate and/or in larger volume (40–100 μl per assay).
5. Addition of carrier BSA (25 μg per assay) prevents loss of eIF5A(Lys) and DHS by their adsorption to the plastic tubes, and increases the yield of products. If the product is separated from radioactive spermidine by ion exchange chromatographic separation (Subheading 3.3) or SDS-PAGE (Subheading 3.3, step 3), it is better to include carrier BSA in the reaction mix. Since BSA binds $[1,8\text{-}^3\text{H}]$ spermidine tightly and markedly increases the background (Fig. 2), its addition is not recommended when counting TCA precipitable radioactivity (Subheading 3.4) or the filter-binding assay (Subheading 3.6).

6. One could use [^{14}C]spermidine (100–124 mCi/mmol) instead of [$1,8\text{-}^3\text{H}$]spermidine. However, its specific activity is ~200 times lower than that of [$1,8\text{-}^3\text{H}$]spermidine and is much more costly. The concentration of [$1,8\text{-}^3\text{H}$]spermidine is based on a batch with specific activity of 20 Ci/mmol. The amount added can be adjusted if another batch with a different specific activity is used.
7. 1 unit of activity is defined as that generating 1 pmol of deoxyhypusine in 1 h at 37°C (22). Human recombinant DHS freshly prepared from BL21(DE3) cells has ~1 unit per 1 ng of enzyme (12), but its activity gradually decays upon storage at 70°C.
8. If one removes the wash supernatant completely, one repeat is sufficient, but it is useful to count the wash supernatant (0.1 ml) at each step of washing.
9. By estimating total radioactivity in 100 μl of hydrolyzed sample, one can calculate the volume of sample to apply to the column. It is recommended *not* to overload the column with too high radioactivity (>50,000 dpm) to avoid machine contamination and carry-over to the next run.
10. In our system, spermidine elutes at ~67 min in PA buffer B. Therefore, after a cycle of five runs of 13 min each with B buffer, the column should be washed with a high salt buffer (PA buffer C) (30 min) and reequilibrated with buffer B (20–25 min) to elute all the radioactive spermidine accumulated in the previous runs.
11. The radioactivity in deoxyhypusine fraction in dpm can be converted to pmol as follows. For a batch of [$1,8\text{-}^3\text{H}$]spermidine with 20 Ci/mmol specific activity, 1 pmol of spermidine is 4×10^4 dpm. Since only the aminobutyl side of [$1,8\text{-}^3\text{H}$]spermidine is incorporated into deoxyhypusine, the specific activity of [^3H]deoxyhypusine is 2×10^4 dpm per pmol.
12. [$1,8\text{-}^3\text{H}$]spermidine binds very tightly to BSA or other cell proteins, and it is impossible to remove completely the [$1,8\text{-}^3\text{H}$]spermidine noncovalently bound to TCA precipitates. One can minimize this background by following the wash protocol in Subheading 3.2, step 1, point 8.
13. It is convenient to use precast NuPAGE gels (4–12%) from Invitrogen and ready-made electrophoresis buffers. However, any other SDS-PAGE system that resolves eIF5A (18 kDa) will work. When the radioactive reaction mix is applied to the SDS gel, the buffer, staining and destaining solutions all contain radioactive spermidine and need to be disposed of properly.
14. eIF5A(18 kDa) can be easily identified on a stained gel, if purified DHS and eIF5A are used. If crude eIF5A or DHS preparations are used, the eIF5A band can be identified after fluorography.

15. The period required to detect the labeled eIF5A band depends on the amount of radioactivity. The radiolabeled band with >2,000 dpm of ³H-labeled protein of a SDS gel treated with Amplify is visible after 3-day exposure to X-ray film at -80°C.
16. As shown in Fig. 1, this assay works well when purified enzyme and eIF5A(Lys) are used, for example, for screening of DHS inhibitors. However, in assays containing a large amount of crude proteins or BSA carrier which traps [1,8-³H]spermidine, the background filter binding is quite high, regardless of wash methods. So it is appropriate only when a large enzyme activity is used (high signal/noise ratio) or when purified enzyme and substrate proteins are used.
17. Count 0.1 ml of the second and third wash until the radioactivity in the wash is low (<100 dpm) and constant.
18. Since ³H is low energy beta emitter, its counting efficiency on the filter bound form is low. However, after sitting in the liquid scintillation fluid for 18 h, a stable level of radioactivity is obtained, probably due to the release of radiolabeled protein into the liquid phase.

Acknowledgement

This research was supported by the Intramural Research Program of the NIDCR, National Institutes of Health.

References

1. Park MH (2006) The post-translational synthesis of a polyamine-derived amino acid, hypusine, in the eukaryotic translation initiation factor 5A (eIF5A). *J Biochem* 139: 161–169
2. Murphey RJ, Gerner EW (1987) Hypusine formation in protein by a two-step process in cell lysates. *J Biol Chem* 262:15033–15036
3. Chen KY, Dou QP (1988) NAD⁺ stimulated the spermidine-dependent hypusine formation on the 18 kDa protein in cytosolic lysates derived from NB-15 mouse neuroblastoma cells. *FEBS Lett* 229:325–328
4. Park MH, Wolff EC (1988) Cell-free synthesis of deoxyhypusine. Separation of protein substrate and enzyme and identification of 1, 3-diaminopropane as a product of spermidine cleavage. *J Biol Chem* 263:15264–15269
5. Wolff EC, Park MH, Folk JE (1990) Cleavage of spermidine as the first step in deoxyhypusine synthesis. The role of NAD. *J Biol Chem* 265:4793–4799
6. Wolff EC, Kang KR, Kim YS, Park MH (2007) Posttranslational synthesis of hypusine: evolutionary progression and specificity of the hypusine modification. *Amino Acids* 33: 341–350
7. Jakus J, Wolff EC, Park MH, Folk JE (1993) Features of the spermidine-binding site of deoxyhypusine synthase as derived from inhibition studies Effective inhibition by bis- and mono- guanylated diamines and polyamines. *J Biol Chem* 268:13151–13159
8. Duncan RF, Hershey JW (1986) Changes in eIF-4D hypusine modification or abundance are not correlated with translational repression in HeLa cells. *J Biol Chem* 261:12903–12906
9. Park MH (1987) Regulation of biosynthesis of hypusine in Chinese hamster ovary cells.

- Evidence for eIF-4D precursor polypeptides. *J Biol Chem* 262:12730–12734
10. Byers TL, Wiest L, Wechter RS, Pegg AE (1993) Effects of chronic 5'-[(Z)-4-amino-2-butenyl]methylamino)-5'-deoxy-adenosine (AbeAdo) treatment on polyamine and eIF-5A metabolism in AbeAdo-sensitive and -resistant L1210 murine leukaemia cells. *Biochem J* 290:115–121
 11. Smit-McBride Z, Dever TE, Hershey JW, Merrick WC (1989) Sequence determination and cDNA cloning of eukaryotic initiation factor 4D, the hypusine-containing protein. *J Biol Chem* 264:1578–1583
 12. Joe YA, Wolff EC, Park MH (1995) Cloning and expression of human deoxyhypusine synthase cDNA Structure- function studies with the recombinant enzyme and mutant proteins. *J Biol Chem* 270:22386–22392
 13. Smit-McBride Z, Schnier J, Kaufman RJ, Hershey JW (1989) Protein synthesis initiation factor eIF-4D Functional comparison of native and unhyposinated forms of the protein. *J Biol Chem* 264:18527–18530
 14. Joe YA, Park MH (1994) Structural features of the eIF-5A precursor required for post-translational synthesis of deoxyhypusine. *J Biol Chem* 269:25916–25921
 15. Dou QP, Chen KY (1990) Characterization and reconstitution of a cell free system for NAD(+)-dependent deoxyhypusine formation on the 18 kDa eIF-4D precursor. *Biochim Biophys Acta* 1036:128–137
 16. Lee YB, Joe YA, Wolff EC, Dimitriadis EK, Park MH (1999) Complex formation between deoxyhypusine synthase and its protein substrate, the eukaryotic translation initiation factor 5A (eIF5A) precursor. *Biochem J* 340:273–281
 17. Folk JE, Park MH, Chung SI, Schrode J, Lester EP, Cooper HL (1980) Polyamines as physiological substrates for transglutaminases. *J Biol Chem* 255:3695–3700
 18. Park MH, Cooper HL, Folk JE (1983) Chromatographic identification of hypusine [Ne-(4-amino-2-hydroxyl)lysine] and deoxyhypusine [Ne-(4-aminobutyl)lysine]. *Methods Enzymol* 94:458–462
 19. Byers TL, Ganem B, Pegg AE (1992) Cytostasis induced in L1210 murine leukemia cells by the S-adenosyl-L-methionine decarboxylase inhibitor 5'-[(Z)-4-amino-2-butenyl]methylamino)-5'-deoxyadenosine may be due to hypusine depletion. *Biochem J* 287(Pt 3):717–724
 20. Sasaki K, Abid MR, Miyazaki M (1996) Deoxyhypusine synthase gene is essential for cell viability in the yeast *Saccharomyces cerevisiae*. *FEBS Lett* 384:151–154
 21. Byers TL, Lakanen JR, Coward JK, Pegg AE (1994) The role of hypusine depletion in cytoskeleton induced by S-adenosyl-L-methionine decarboxylase inhibition: new evidence provided by 1-methylspermidine and 1, 12-dimethylspermine. *Biochem J* 303(Pt 2): 363–368
 22. Wolff EC, Lee YB, Chung SI, Folk JE, Park MH (1995) Deoxyhypusine synthase from rat testis: purification and characterization. *J Biol Chem* 270:8660–8666

Assay of Deoxyhypusine Hydroxylase Activity

Jong Hwan Park, Edith C. Wolff, and Myung Hee Park

Abstract

The eukaryotic translation initiation factor 5A (eIF5A) is the only cellular protein that contains an unusual amino acid, hypusine [*N*^ε-(4-amino-2-hydroxybutyl)-lysine]. eIF5A and its hypusine/deoxyhypusine modification are vital for eukaryotic cell proliferation. Hypusine is formed posttranslationally by two enzymatic steps catalyzed by deoxyhypusine synthase and deoxyhypusine hydroxylase. Deoxyhypusine hydroxylase catalyzes a stereo-specific hydroxylation of the deoxyhypusine residue in the eIF5A intermediate protein, eIF5A(Dhp). The enzyme is totally specific for this protein and does not act on short peptides (<50 amino acids). The assay measures the conversion of the radiolabeled deoxyhypusine residue to a hypusine residue in eIF5A. Optimum conditions for the reaction and two detection methods for the product, hypusine-containing eIF5A, are described in this chapter. The first, and most reliable, method is the measurement of the amount of [³H]hypusine in the protein hydrolysate after its separation from [³H]deoxyhypusine, by ion exchange chromatography. This method does not require specialized equipment. The second method is based on counting the total TCA soluble radioactivity after sodium periodate oxidation of the reaction mixture, since the radiolabeled 4-amino-2-hydroxy butyl moiety of the hypusine residue is cleaved and is released from protein as radiolabeled β-proprionaldehyde and formaldehyde by periodate oxidation.

Key words: Polyamine, Spermidine, Deoxyhypusine hydroxylase, Deoxyhypusine, Hypusine, Monooxygenase, eIF5A, Posttranslational modification, Protein hydroxylation

1. Introduction

Deoxyhypusine hydroxylase (deoxyhypusine monooxygenase, DOHH) (EC. 1.14.99.29) catalyzes the final step in the posttranslational synthesis of an unusual amino acid, hypusine [*N*^ε-(4-amino-2-hydroxybutyl)-lysine] (see a recent review (1)). This enzyme converts the deoxyhypusine-containing eIF5A intermediate, eIF5A(Dhp), to the mature hypusine-containing form, eIF5A(Hpu), by stereo-specific hydroxylation at the C2 of the aminobutyl side chain of the deoxyhypusine residue ((2, 3), Scheme 1). DOHH exhibits a strict substrate specificity toward its protein substrate (4, 5).

DOHH is a non-heme diiron enzyme that is inhibited by iron chelators (6). It is a HEAT-repeat protein consisting of eight tandem α -helical hairpin structures (3). It has a structure and mechanism distinct from those of other 2-oxoacid and iron-dependent dioxygenases, such as prolyl or lysyl hydroxylases. Rather, DOHH resembles the monooxygenases with a diiron active center, such as methane monooxygenase (7). Cultured cells or tissues normally contain DOHH enzyme, but little or no substrate protein, deoxyhypusine-containing eIF5A intermediate, eIF5A(Dhp). Thus, radiolabeled eIF5A(Dhp) must be prepared and added as a substrate to measure the enzyme activity. The cDNAs for eIF5A (8), DHS (9), and DOHH (3) have been cloned, and recombinant proteins can be purified by simple methods (3, 9–11). Radiolabeled eIF5A(Dhp) can be prepared by an *in vitro* DHS reaction using purified recombinant eIF5A(Lys) and DHS (12).

Typical reaction conditions for deoxyhypusine hydroxylase are described, and two methods are presented for measurement of the hypusine formed (Fig. 1). The [^3H]hypusine formed in

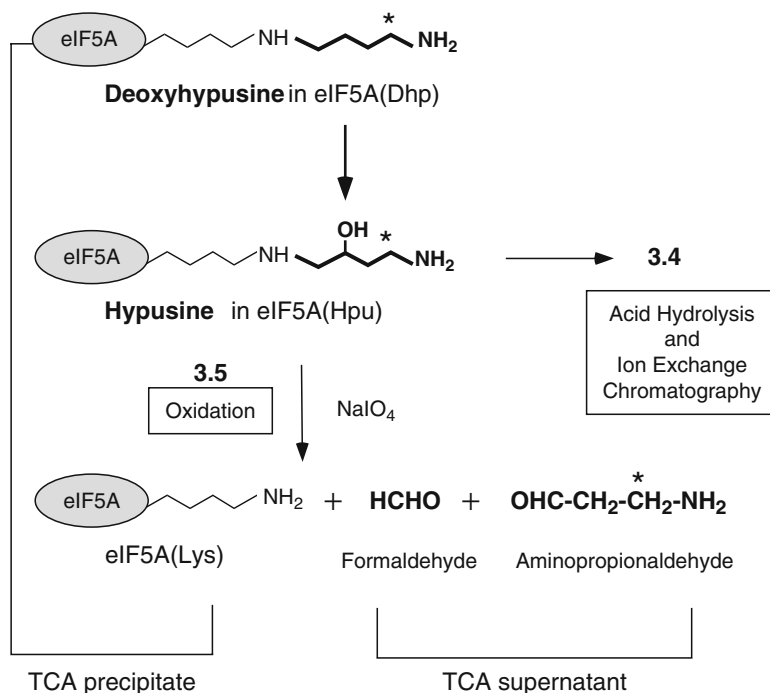


Fig. 1. Biosynthesis of hypusine by two enzymatic steps and degradation of hypusine residue by periodate oxidation. Deoxyhypusine hydroxylase catalyzes hydroxylation of the deoxyhypusine residue at C2 of its aminobutyl side chain. Sodium (meta) periodate causes oxidative cleavages (due to vicinal amino hydroxyl groups) of the hypusine side chain to release β -propionaldehyde, which is measured as the radioactivity in the TCA supernatant, whereas the unreacted substrate protein eIF5A(^3H)Dhp) is precipitated with TCA. The *asterisk* indicates the position of radioactivity derived from [$1,8\text{-}^3\text{H}$]spermidine.

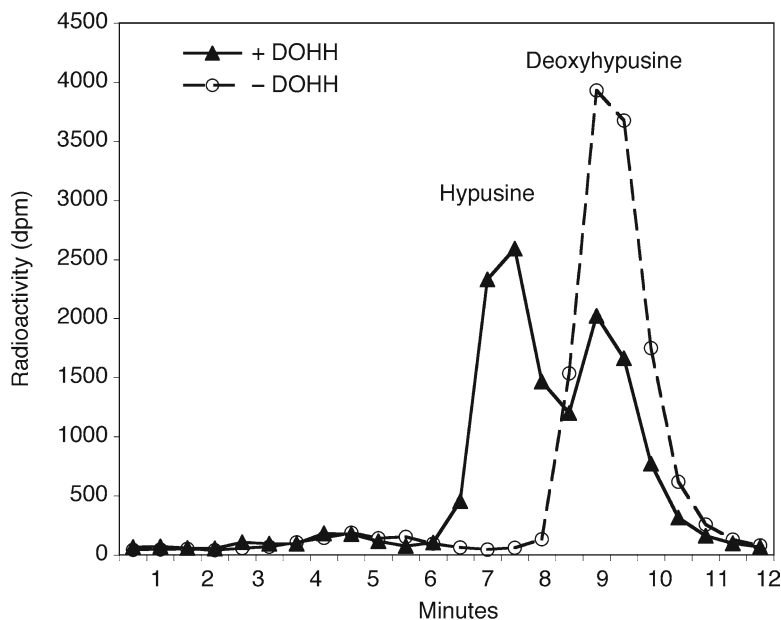


Fig. 2. Ion exchange chromatographic separation of deoxyhypusine and hypusine. The proteins in the DOHH reaction mixture were precipitated with TCA and hydrolyzed in 6 N HCl. The amino acids in the hydrolyzed proteins were separated by ion exchange chromatography on DC6A column using PA Buffer B. Hypusine is eluted from the column 2 min earlier than deoxyhypusine.

eIF5A can be measured after acid hydrolysis of the proteins and its separation from [^3H]deoxyhypusine by ion exchange chromatographic separation (Fig. 2) (6, 13). This first method gives the most accurate estimate of the amount of [^3H]hypusine formed. However, it requires an amino acid analyzer (or HPLC system) with a high resolution ion exchange column (14) to separate two similar amino acids, hypusine and deoxyhypusine. For those who do not have access to such a separation system, an oxidation method can be employed for an estimation of DOHH activity. Unlike deoxyhypusine, hypusine contains a vicinal amino (secondary) and hydroxyl group, which can be cleaved by periodate oxidation (15–17). Thus, the radiolabeled 4-amino-2-hydroxybutyl side chain of the hypusine residue of the reaction product, eIF5A(Hpu), is cleaved to radiolabeled β -propionaldehyde and formaldehyde by periodate oxidation (Fig. 1), whereas the deoxyhypusine-containing substrate protein is not cleaved. The radiolabeled β -propionaldehyde released from the hydroxylated protein, eIF5A(Hpu), is soluble in TCA and can be measured after its separation from proteins by TCA precipitation.

2. Materials

2.1. Equipment

1. Plastic Eppendorf tubes (1.5 ml size) with screw caps, resistant to heating at 110°C.
2. Dry heating block (108°C) for acid hydrolysis.
3. SpeedVac concentrator (e.g., Savant) with a NaOH trap.
4. An amino acid analyzer with an ion exchange column (e.g., 0.4 × 7.5 cm, DC-6A cation exchange resin) (see Note 1).
5. Liquid scintillation fluid that tolerates high salt buffers (Optiphase High Safe 3 from PerkinElmer works well).

2.2. Reagent Stock Solutions

1. Use deionized or ultrapure water for preparation of all solutions.
2. Buffer A (50 mM Tris-HCl buffer pH 7.5, 1 mM DTT).
3. Mammalian protease inhibitor cocktail not containing EDTA (Sigma or Roche).
4. M Tris-HCl buffer (pH 7.5).
5. PBS (phosphate buffered saline).
6. Spermidine (100 mM), store frozen at -20°C in aliquots.
7. eIF5A(Dhp) substrate (2 μM, 40,000 dpm/μl, if the specific activity of [1,8-³H]spermidine used is 20 Ci/mmol). Store aliquots of solutions in 50 mM Tris-HCl pH 7.5, 1 mM DTT, 1 mg/ml of BSA at -20°C.
8. DTT (100 mM), the solution of 100 mM DTT (15.4 mg/ml in water) is stored frozen at -20°C in aliquots.
9. BSA (50 mg/ml in water), store frozen at -20°C in aliquots.
10. TCA solution (10% trichloroacetic acid). Store at 4°C.
11. 6 N HCl solution made by 1:1 dilution of concentrated HCl (Subheading 3.3, step 1).
12. Buffer B (13.2 mM sodium citrate buffer, 1.5 N NaCl, pH 5.55, 0.1% Phenol) and PA buffer C (53 mM sodium citrate buffer, 3.0 N NaCl, pH 5.55, 0.1% Phenol). Buffer is stored at room temperature and filtered, and Brij (0.1%) is added before use.
13. 0.2 M Na₂HPO₄, 45 mM Citric acid buffer pH 6.4.
14. 0.3 M Sodium (meta)periodate, NaIO₄. Make fresh solution just before use.

3. Methods

**3.1. Preparation
of eIF5A([³H] Dhp)
Substrate Protein
(High Specific Activity)
by In Vitro DHS
Reaction
(see Note 2)**

1. Set up a large scale DHS reactions in a mixture (2 ml) containing 0.2 M Glycine NaOH pH 9.2 buffer, 1 mM DTT, 1 mM NAD, 35 μ M eIF5A(Lys) (1.2 mg, 70 nmol), 37.5 μ M [1,8-³H]spermidine (75 nmol, 1.5 mCi, if the specific activity is 20 Ci/mmol), and 1×10^5 units of DHS (~0.1 mg of freshly prepared human recombinant enzyme) and incubate at 37°C for 3 h.
2. Take 20 μ l of reaction mixture to estimate the amount of radiolabeled eIF5A in the TCA precipitate after thorough washing in TCA containing 1 mM polyamines, to calculate the total yield from the large scale reaction (see Note 3).
3. The unreacted [1,8-³H]spermidine is removed from the labeled protein substrate by repeated ammonium sulfate precipitation as follows. To the reaction mixture (2 ml), add 0.55 g (45% saturation) of finely ground ammonium sulfate, mix well until all the ammonium sulfate dissolves, and keep on ice for 20 min. Remove the precipitated proteins by centrifugation in a microfuge at 15,000 $\times g$, at 4°C for 20 min. Add ammonium sulfate to the supernatant to 80% saturation to precipitate eIF5A. After centrifugation, remove the supernatant completely and dissolve the precipitate in 2 ml of Buffer A containing 1 mM unlabeled spermidine. This sample is precipitated again with ammonium sulfate (80% saturation), and this step is repeated three more times to remove all the unreacted [1,8-³H]spermidine.
4. Dissolve the proteins from the fourth ammonium sulfate precipitation in 2 ml of Buffer A and dialyze against ice-cold Buffer A for 3 h to remove the salts and unreacted radioactive spermidine.
5. To 5 μ l of the dialyzed sample and add 250 μ g of carrier BSA and 0.1 ml of 10% TCA. Keep on ice for 10 min and centrifuge the precipitate in microfuge (15,000 $\times g$ at 4°C, 10 min).
6. Separate the supernatant and dissolve the pellet in 0.1 ml of 0.1 N NaOH solution.
7. Count radioactivity in the supernatant and in the pellet to determine the radiopurity of the substrate protein (see Note 4).
8. If the substrate protein is sufficiently pure (>98% TCA precipitable), dilute the substrate to 2 μ M and add carrier BSA to 1 mg/ml and store in aliquots at -20°C.

3.2. Preparation of the Enzyme Extract from Cultured Cells or Tissues

1. For preparation of a crude enzyme extract, sonicate freshly harvested cell pellets in Buffer A (50 mM Tris-HCl buffer (pH 7.5), 1 mM DTT) containing protease inhibitor cocktail not containing EDTA, (0.2 ml buffer for 10^7 cells), or homogenize tissues in the same buffer (1 ml per 1 g wet tissue).
2. Centrifuge the lysates in a refrigerated microfuge (at $15000\times g$) for 20 min and take supernatants for protein determination and enzyme assays. Use 100–500 μg of total protein per assay as an enzyme source (see Note 5).

3.3. Deoxyhypusine Hydroxylase Assay

1. Just before the assay, make a master mixture by multiplying each volume by the sample number (n) and keep on ice in an Eppendorf tube.

Stock solution volume per assay final concentration

1 M Tris-HCl pH 7.5	0.8 μl	20 mM
100 mM DTT	2.4 μl	6 mM
50 mg/ml BSA	0.8 μl	1 mg/ml
eIF5A(^3H)-Dhp) (2 μM)	2 μl	0.1 μM
H ₂ O	14 μl	
Volume of master mix per tube	20 μl	
Enzyme solution/lysate (see Note 6)	20 μl	
Total volume	40 μl	

2. Set up screw cap plastic Eppendorf tubes and number them. Add an enzyme sample in 20 μl to each tube on ice. Use 20 μl of Buffer A as a negative control and 2–10 units of purified DOHH (if available) as a positive control (see Note 7).
3. Start the reaction by adding 20 μl of the master mix to each tube. Mix gently and cap each tube.
4. Incubate the reaction mixtures in a 37°C water bath for 2 h.

3.4. Determination of Hypusine Formed after Ion Exchange Chromatographic Separation

1. Stop the reaction by adding 5 μl (250 μg) of carrier BSA and 0.2 ml of ice-cold 10% TCA solution. Gently mix and keep on ice for 20 min.
2. Centrifuge the TCA precipitated samples in a refrigerated microfuge (4°C) at $15,000\times g$ for 5 min and remove the supernatant and count radioactivity in the supernatant (see Note 8).
3. After removing all the TCA supernatant, add 0.4 ml of 6 N HCl to the pellet, tighten the cap and place in a heating block at 108°C overnight.
4. Dry the hydrolyzed samples using a SpeedVac concentrator set up with a NaOH trap.

5. Add 0.1 ml of water to each tube to dissolve dried residues. Count a 5 μ l aliquot and apply an aliquot containing up to 50,000 dpm to the amino acid analyzer (see Note 9).
6. Separate hypusine from deoxyhypusine by running 13 min of PA Buffer B at the speed of 0.75 ml per min. Collect 26 tubes of 0.5 min fractions and count the total radioactivity in a liquid scintillation counter. In our system, the elution peak time for hypusine is 7.25 min and deoxyhypusine is approximately 9.25 min (Fig. 2) (see Note 10).
7. Sum the radioactivity of the hypusine peak (usually in 4–5 fractions) after subtraction of background radioactivity in the negative control, and multiply the number by a factor (100/volume injected) to estimate the total amount of hypusine formed in each reaction (see Note 11). Sum the radioactivity in both hypusine and deoxyhypusine peaks to estimate % conversion.

**3.5. Determination
of Protein-Bound
Hypusine by Periodate
Oxidation**

If an amino acid analyzer or HPLC system is not available and steps 3 and 4 cannot be used, one can estimate hypusine formed by periodate oxidation of the reaction mixture (see Note 12).

1. To half of the reaction mixture (use 20 μ l), add 5 μ l (250 μ g) of carrier BSA and 100 μ l of 10% TCA. Keep on ice for 20 min, spin and measure the radioactivity in the TCA supernatant (see Note 8).
2. To the other half of the reaction mixture (20 μ l), add 40 μ l of Sodium phosphate/citrate buffer.
3. Add 15 μ l of sodium (meta)periodate (0.3 M) solution and mix well and keep at RT for 1 h.
4. Add 5 μ l (250 μ g) of carrier BSA and add 0.2 ml of 10% TCA and keep on ice for 20 min.
5. Centrifuge the precipitates in the microfuge at 4°C at 15,000 $\times g$ for 5 min.
6. Take all the supernatant and count the radioactivity in the supernatant. Subtract the radioactivity in the TCA supernatant of unoxidized sample from that of the oxidized sample to calculate the hypusine formed (see Note 13).

4. Notes

1. We use a Dionex D-400 analyzer with a column (0.4 \times 7.5 cm) of cation exchange resin, DC-6A (13, 14). The resin has hydrophobic as well as ionic interactions with amino acids and polyamines. Since hypusine is less hydrophobic than deoxyhypusine due to a hydroxyl group addition, it is eluted 2 min

earlier than deoxyhypusine under our separation conditions. Elution conditions on our analyzer are temperature 66°C, flow rate 0.75 ml/min, and we collect 0.5 min fractions directly into 7 ml glass scintillation vials.

2. Alternatively, the deoxyhypusine containing eIF5A(Dhp) can be prepared from mammalian cells cultured in the presence of (1,8-³H)spermidine and metal chelating inhibitors of DOHH (2, 16). However, the yield of radiolabeled eIF5A(³H)Dhp) is very low, compared to that from the *in vitro* DHS reaction. Endogenous spermidine in cells (~10 nmol per mg protein) dilutes the specific activity of (1,8-³H)spermidine added to the medium. This dilution has to be taken into consideration in estimation of specific activity of radiolabeled substrate protein prepared from cells.
3. Under this reaction condition, approximately 15% of eIF5A(Lys) is converted to the deoxyhypusine protein and a total of 10 nmol (2×10^8 dpm, if the specific activity of (1,8-³H)spermidine used is 20 Ci/mmol) is obtained. Since unreacted eIF5A(Lys) does not interfere with the DOHH reaction (4), it is not necessary to separate the labeled eIF5A(Dhp) from the eIF5A(Lys) protein.
4. It is critical to get rid of all unreacted (1,8-³H)spermidine (to a level not more than 1–2% of total radioactivity in the substrate preparation) by repeated ammonium sulfate precipitation and dialysis. It is important to keep the background radioactivity in the TCA supernatant low especially when the oxidation method is used for estimation of hypusine.
5. Fresh cultured cells or tissues contain approximately 1–10 units of DOHH activity per mg protein (2). 1 unit of DOHH activity is defined as that converting 1 pmol of eIF5A(³H)Dhp) to eIF5A(³H)Hpu) in 2 h at 37°C.
6. The protein concentration of cell or tissue crude extracts should be high (10–25 mg/ml) to test activity of lysates containing up to 200–500 µg protein in 20 µl. To test the activity of less than 20 µl of extract, dilute it with buffer A to 20 µl.
7. The recombinant human DOHH or yeast DOHH can be purified from BL21(DE3) cells transformed with pGEX-4T-3/hDOHH or pGEX-4T-3/yDOHH plasmids (3).
8. The radioactivity in the TCA supernatant would be either due to (1,8-³H)spermidine contaminant in the substrate preparation or due to proteolytic degradation of eIF5A(³H)Dhp). If the cell or tissue extract contains the protease inhibitor cocktail, the level of proteolytic degradation is usually quite low. If the extract is prepared from tissues or cells highly overexpressing DHS, one may observe the release of radioactivity due to reversal of deoxyhypusine synthesis (12).

However, with normal cells or tissues, the reversal is negligible. One may include one control with a DOHH inhibitor (0.1 mM ciclopirox olamine) to obtain a value for DOHH-mediated release of radioactivity.

9. By estimating the total radioactivity in 100 μ l of a hydrolyzed sample, one can calculate the volume of sample to apply to the column. It is recommended not to overload the column with too high radioactivity (>50,000 dpm) to avoid machine contamination from sample overloading and carry-over to the next run.
10. The radioactive impurity in the substrate preparation (mainly [1,8-³H]spermidine, should be <2% of total radioactivity of the substrate) can be removed by TCA precipitation after DOHH reaction. Thus, as many as 20 samples can be analyzed in sequence in PA Buffer B without much interference due to spermidine contaminant. However, if the background level of radioactivity in collected fractions increases, a 30 min wash with PA Buffer C and reequilibration (20 min) with PA Buffer B is recommended.
11. The radioactivity in the hypusine fraction in dpm can be converted to pmol as follows. For a batch of [1,8-³H]spermidine with 20 Ci/mmol specific activity, 1 pmol of spermidine is 4×10^4 dpm. Since only the aminobutyl side of [1,8-³H]spermidine is incorporated into deoxyhypusine, the specific activity of [³H]deoxyhypusine is 2×10^4 dpm per pmol.
12. In Subheading 3.3, step 2, one only need to count TCA soluble radioactivity released by periodate oxidation. This works when the radiolabeled substrate protein is highly pure and contain a minimum level (<2% of total radioactivity in the substrate preparation) of [1,8-³H]spermidine. If the substrate protein is contaminated with a significant amount of [1,8-³H]spermidine, this will cause a high background radioactivity in the TCA supernatant. In this case, it is necessary to distinguish between the radioactivity in the β -propionaldehyde from that of [1,8-³H]spermidine. A method employing reaction of aldehydes with dimedone (5,5-dimethyl-1,3-cyclohexanedione) and extraction of the aldehyde/dimedone adducts with toluene was reported (17). However, the method in Subheading 3.3, step 2 is simple and more accurate than the dimedone method, if the radiolabeled protein substrate is highly pure.
13. Under this condition, periodate oxidation completely cleaves the hypusine residue without causing any degradation of the deoxyhypusine residue or the eIF5A protein. The difference between the radioactivity in the TCA supernatant of the oxidized reaction mixture (step 6) and that of the oxidized sample in step 10 is the radioactivity of hypusine formed.

Acknowledgements

This research was supported by the Intramural Research Program of the NIDCR, National Institutes of Health.

References

1. Park MH (2006) The post-translational synthesis of a polyamine-derived amino acid, hypusine, in the eukaryotic translation initiation factor 5A (eIF5A). *J Biochem* 139:161–169
2. Abbruzzese A, Park MH, Folk JE (1986) Deoxyhypusine hydroxylase from rat testis. Partial purification and characterization. *J Biol Chem* 261:3085–3089
3. Park JH, Aravind L, Wolff EC, Kaevel J, Kim YS, Park MH (2006) Molecular cloning, expression, and structural prediction of deoxyhypusine hydroxylase: a HEAT-repeat-containing metalloenzyme. *Proc Natl Acad Sci USA* 103:51–56
4. Kang KR, Kim YS, Wolff EC, Park MH (2007) Specificity of the deoxyhypusine hydroxylase-eukaryotic translation initiation factor (eIF5A) interaction: identification of amino acid residues of the enzyme required for binding of its substrate, deoxyhypusine-containing eIF5A. *J Biol Chem* 282:8300–8308
5. Jakus J, Wolff EC, Park MH, Folk JE (1993) Features of the spermidine-binding site of deoxyhypusine synthase as derived from inhibition studies. Effective inhibition by bis- and mono-guanylated diamines and polyamines. *J Biol Chem* 268:13151–13159
6. Park MH, Cooper HL, Folk JE (1982) The biosynthesis of protein-bound hypusine (N^ε-(4-amino-2-hydroxybutyl)lysine). Lysine as the amino acid precursor and the intermediate role of deoxyhypusine (N^ε-(4-aminobutyl)lysine). *J Biol Chem* 257:7217–7222
7. Vu VV, Emerson JP, Martinho M, Kim YS, Munck E, Park MH, Que L Jr (2009) Human deoxyhypusine hydroxylase, an enzyme involved in regulating cell growth, activates O₂ with a nonheme diiron center. *Proc Natl Acad Sci USA* 106:14814–14819
8. Smit-McBride Z, Dever TE, Hershey JW, Merrick WC (1989) Sequence determination and cDNA cloning of eukaryotic initiation factor 4D, the hypusine-containing protein. *J Biol Chem* 264:1578–1583
9. Joe YA, Wolff EC, Park MH (1995) Cloning and expression of human deoxyhypusine synthase cDNA. Structure function studies recombinant enzyme mutant proteins. *J Biol Chem* 270:22386–22392
10. Smit-McBride Z, Schnier J, Kaufman RJ, Hershey JW (1989) Protein synthesis initiation factor eIF-4D. Functional comparison native unhyposinated forms protein. *J Biol Chem* 264:18527–18530
11. Joe YA, Park MH (1994) Structural features of the eIF-5A precursor required for post-translational synthesis of deoxyhypusine. *J Biol Chem* 269:25916–25921
12. Park JH, Wolff EC, Folk JE, Park MH (2003) Reversal of the deoxyhypusine synthesis reaction. Generation spermidine or homospermidine deoxyhypusine by deoxyhypusine synthase. *J Biol Chem* 278:32683–32691
13. Park MH, Cooper HL, Folk JE (1983) Chromatographic identification of hypusine (N^ε-(4-amino-2-hydroxy)lysine) and deoxyhypusine (N^ε-(4-aminobutyl)lysine). *Meth Enzymol* 94:458–462
14. Folk JE, Park MH, Chung SI, Schrode J, Lester EP, Cooper HL (1980) Polyamines as physiological substrates for transglutaminases. *J Biol Chem* 255:3695–3700
15. Park MH, Cooper HL, Folk JE (1981) Identification of hypusine, an unusual amino acid, in a protein from human lymphocytes and of spermidine as its biosynthetic precursor. *Proc Natl Acad Sci USA* 78:2869–2873
16. Abbruzzese A, Park MH, Folk JE (1986) Indirect assays for deoxyhypusine hydroxylase using dual-label ratio changes and oxidative release of radioactivity. *Anal Biochem* 154:664–670
17. Csonga R, Ettmayer P, Auer M, Eckerskorn C, Eder J, Klier H (1996) Evaluation of the metal ion requirement of the human deoxyhypusine hydroxylase from HeLa cells using a novel enzyme assay. *FEBS Lett* 380:209–214

Part V

Regulation of Polyamine Content

Identification and Assay of Allosteric Regulators of S-Adenosylmethionine Decarboxylase

Erin K. Willert, Lisa N. Kinch, and Margaret A. Phillips

Abstract

Polyamine biosynthesis is extensively regulated in cells by multiple mechanisms, including regulation of enzyme activity posttranslationally. The identified regulatory factors include both small molecules and regulatory proteins, and the mechanisms vary in different species across the evolutionary tree. Based on this diversity of mechanism, it is likely that regulatory factors of the pathway remain unidentified in many species. This article focuses on methods for identifying novel regulatory factors of polyamine biosynthesis as illustrated by the discovery of a novel protein activator of the key biosynthetic enzyme S-adenosylmethionine decarboxylase in the protozoan trypanosomatid parasites.

Key words: Trypanosoma, Prozyme, Polyamines, Spermidine, Putrescine, Ornithine decarboxylase, S-adenosylmethionine decarboxylase

1. Introduction

Polyamines are organic cations that are found in all organisms and are essential for growth in eukaryotic cells (1) (Fig. 1). Polyamines are synthesized from L-ornithine and S-adenosylmethionine, and the rate-limiting steps in the pathway are catalyzed by ornithine decarboxylase (ODC) and S-adenosylmethionine decarboxylase (AdoMetDC). Enzymes in this pathway have been extensively targeted for the identification of inhibitors with therapeutic potential against infectious diseases, cancer, and other proliferative disorders (2, 3). A suicide inhibitor of ODC, eflornithine, is currently the front-line therapy for the treatment of late-stage African sleeping sickness and remains the only clinically approved inhibitor to arise from these efforts (4). Maintenance of polyamine homeostasis is important for normal cellular function, and the biosynthetic and catabolic enzymes in this pathway are highly

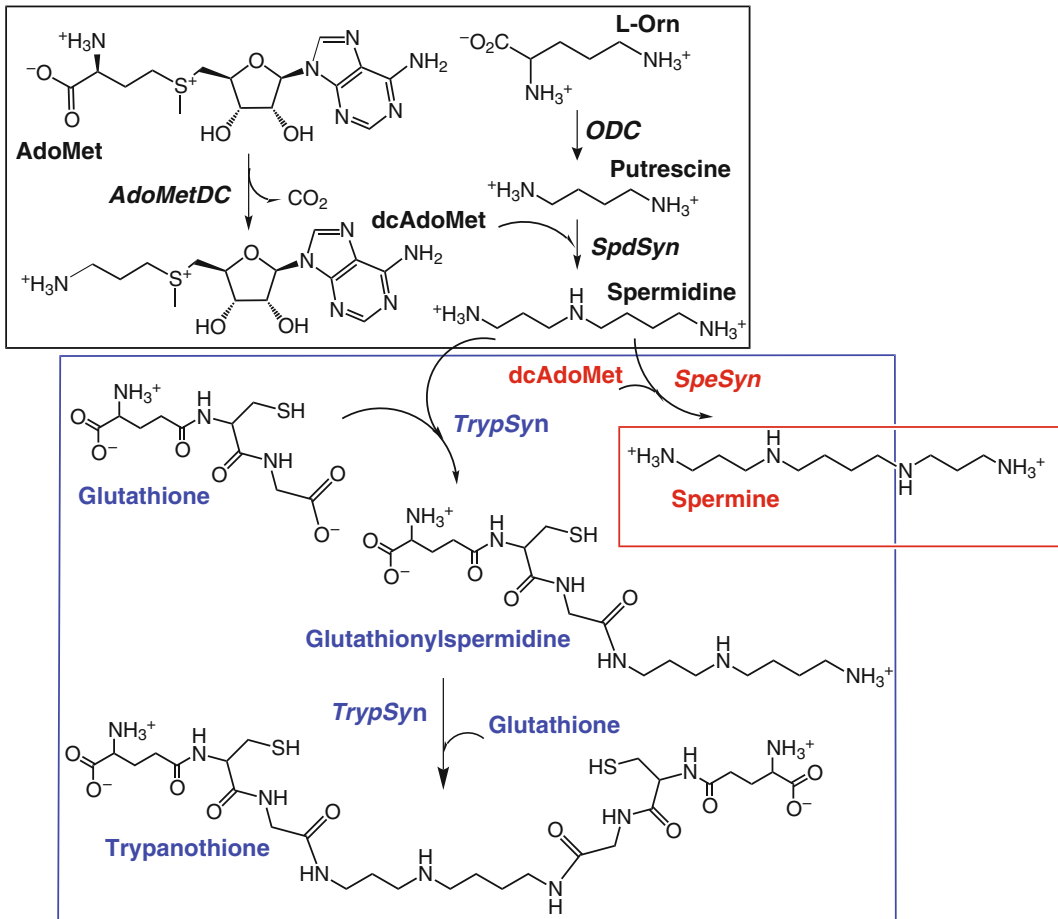


Fig. 1. The polyamine biosynthetic pathway. Reaction steps in the upper box are common between mammals and trypanosomatids, the SpeSyn reaction is found in mammals and not in trypanosomatids, and those in the lower box are specific to trypanosomatids. ODC ornithine decarboxylase; AdoMetDC S-adenosylmethionine decarboxylase; SpdSyn spermidine synthetase; SpeSyn spermine synthase; TrypSyn trypanothione synthetase.

regulated at multiple levels, which include transcriptional, translational, and posttranslational mechanisms (5). The posttranslational regulatory mechanisms include polyamine-mediated regulation of the degradation of ODC and AdoMetDC, as well as control of enzyme activity by protein or small molecules acting either as activators or as inhibitors.

AdoMetDC is a pyruvoyl-dependent enzyme that catalyzes the decarboxylation of S-adenosylmethionine (AdoMet) to produce the aminopropyl donor for the formation of the longer chain polyamines, spermidine, and spermine. While spermine is the end product of polyamine metabolism in mammalian cells, in the trypanosomatid parasites, spermidine is conjugated to glutathione, yielding the novel cofactor trypanothione, which is used to

maintain reduced thiol pools in the cell (Fig. 1). The pyruvate cofactor is derived from a serine residue by autocatalytic processing that results in cleavage of the precursor AdoMetDC polypeptide into two chains, a smaller β -chain and a larger α -chain containing the N-terminal pyruvate (1). The $\alpha\beta$ chains remain tightly associated after processing and are structurally interwoven. The active form of AdoMetDC varies in oligomerization state between enzymes from different species. Plant AdoMetDC is active as a monomer ($\alpha\beta$) (6) while the human enzyme is a homodimer ($\alpha\beta$)₂ (7–9).

AdoMetDC protein levels are controlled by transcriptional, translational, and posttranslational mechanisms (1), the latter of which includes control by allosteric regulatory molecules. The allosteric regulatory mechanisms are not conserved in the enzymes from different species. Monomeric plant AdoMetDC has no known allosteric effectors (6), while human AdoMetDC is activated by putrescine (1). Putrescine accelerates both the processing reaction to generate the pyruvyl cofactor and the catalytic efficiency of the enzyme. The putrescine binding-site is found in a buried pocket containing acidic residues that are near the dimer interface, but distant from the active site (7, 9). Structural studies of site-directed mutants in the putrescine binding-site suggest that putrescine influences the orientation of essential catalytic residues through electrostatic interactions, thus promoting the catalytically competent active site configuration.

Uniquely in the trypanosomatid parasites, the active form of AdoMetDC is a heterodimer formed from two gene products: the direct homolog of the eukaryotic AdoMetDC containing the processed $\alpha\beta$ chains and an inactive and unprocessed paralog termed prozyme (10, 11). Prozyme arose through gene duplication and mutational drift of the ancestral enzyme (Fig. 2). The heterodimeric *T. brucei* AdoMetDC/prozyme complex has a catalytic efficiency that is 3,500-fold greater than the homodimeric ($\alpha\beta$) enzyme (Table 1). Putrescine stimulates the activity of the homodimeric *T. brucei* enzyme by 10-fold, but it has no effect on the activity of the AdoMetDC/prozyme heterodimer. Species differences are however observed even within the trypanosomatids as the *T. cruzi* heterodimer is stimulated 5-fold by the addition of putrescine (11). Further, putrescine does not influence the autocatalytic processing reaction (12). Unlike in mammalian cells, *T. brucei* AdoMetDC expression does not appear to be regulated, but instead prozyme protein levels are regulated most likely at the level of translation, providing a mechanism to control pathway flux in the parasite (13). Interestingly, human spermine synthase contains a domain with structural similarity to AdoMetDC, and this domain, which is inactive as an AdoMetDC, has been shown to be required for spermine synthase activity (14).

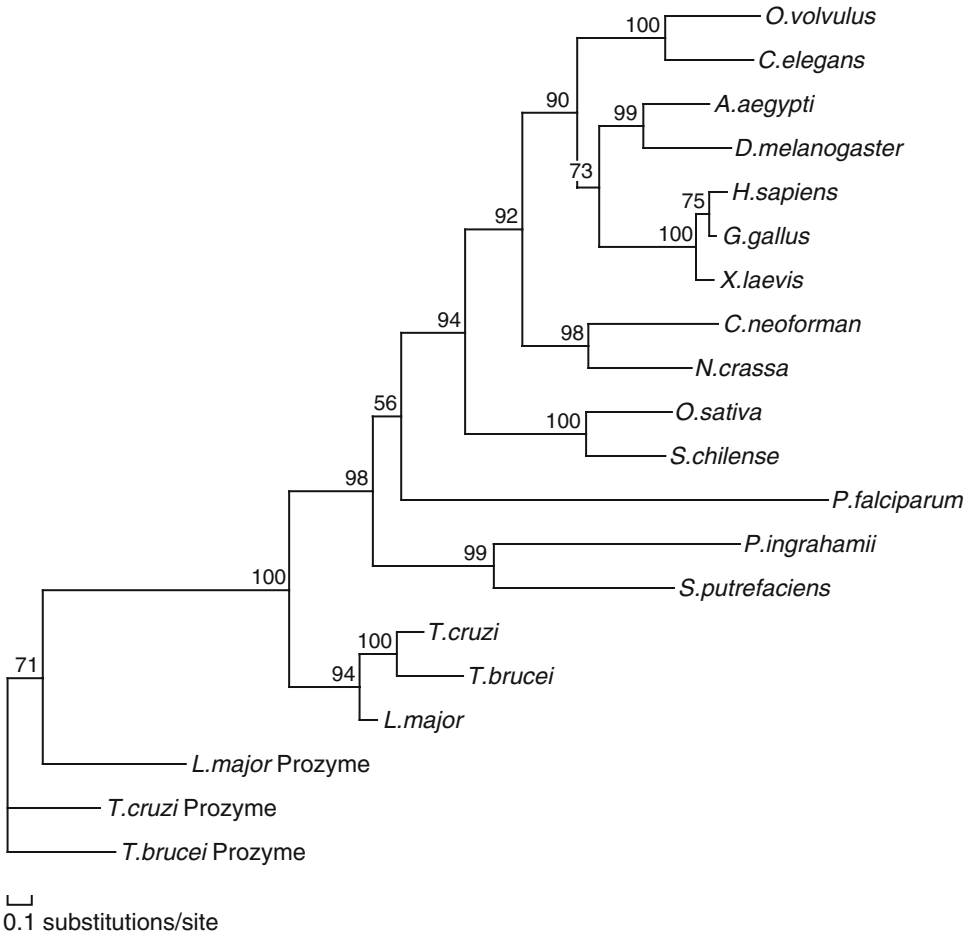


Fig. 2. Maximum likelihood phylogenetic tree of AdoMetDC sequences in representative eukaryotic and prokaryotic organisms. Prozyme arose by gene duplication from the ancestral enzyme and is found only in the trypanosomatids.

Together, these data demonstrate that the allosteric regulation of AdoMetDC is an important mechanism for controlling enzyme activity and polyamine homeostasis. Given the diversity of polyamine function and the discovery of alternative routes for polyamine biosynthesis in different species (e.g., alternative biosynthetic pathways have been described in bacteria (15)), it is likely that key regulatory mechanisms remain undiscovered. As the regulatory control mechanisms are not conserved across different species, the identification of novel regulatory factors cannot rely on evolutionary analysis alone. In this article, we describe the methods used to identify the *T. brucei* AdoMetDC regulatory subunit prozyme. These methods are appropriate for application to other cell types for the discovery of novel regulators of protein function.

Table 1
Comparison of the catalytic efficiency of trypanosomatid AdoMetDC
in the presence of prozyme or putrescine activators

Catalytic efficiency k_{cat}/K_m ($M^{-1}s^{-1}$)	AdoMetDC homodimer			AdoMetDC/prozyme heterodimer		
	No putrescine	5 mM putrescine	Putrescine activation	No putrescine	5 mM putrescine	Putrescine activation
Human ¹¹	2.5×10^{4a}	4.4×10^{4a}	1.8-fold ^a	N/A	N/A	
<i>T. brucei</i> ⁸ Prozyme activation	3.4	35	10-fold	1.2×10^4 3,500-fold	1.1×10^4 310-fold	0.92-fold
<i>T. cruzi</i> ¹² Prozyme activation	8.7	130	15-fold	1,100 130-fold	5,100 39-fold	4.6-fold

Catalytic efficiency (given as $M^{-1}s^{-1}$) of AdoMetDCs is stimulated by putrescine and prozyme

^aHuman AdoMetDC was determined to be half bound by putrescine prior to the assay (no putrescine), indicating that the putrescine stimulation of human AdoMetDC may be greater than 1.8 fold

2. Materials

2.1. Expression and Protein Purification of AdoMetDC

1. pET 15b (Novagen, San Diego, CA) and pT7-Flag1 (Sigma, St. Louis, MO) expression vectors.
2. BL21/DE3 *Escherichia coli* cells are grown in Luria Broth (LB, Sigma).
3. Isopropyl β -D-1-thiogalactopyranoside (IPTG) (Lab Scientific).
4. Lysis buffer: 0.05 M HEPES (pH 8), 0.3 M NaCl, 2 mM β -mercaptoethanol (β -Me), protease inhibitors: 1 μ g/ml leupeptin, 2 μ g/ml antipain, 10 μ g/ml benzamidin, 1 μ g/ml pepstatin, 1 μ g/ml chymostatin, and 2 mM phenylmethylsulfonyl fluoride (PMSF). A dash of DNase and 1 mg/ml egg-white lysozyme are added after resuspension of the pellet. All components are purchased from Sigma.
5. SDS-PAGE: Resolving phase: 12% of 30:0.8 acrylamide:bisacrylamide in 0.375 M Tris-HCL (pH 8.8), 0.1% SDS, 0.05% Ammonium persulfate, 0.01% TEMED. Stacking phase: 4% of 30:0.8 acrylamide:bisacrylamide in 0.125 M Tris-HCL (pH 8.8), 0.1% SDS, 0.05% Ammonium persulfate, 0.01% TEMED.
6. Charged nickel resin: Ni-NTA agarose (Qiagen, Valencia, CA). Resin can be stripped and reused according to manufacturer's

manual. Buffer exchange is carried out with the HiPrep 26/10 desalting column (Amersham, Piscataway, NJ) and anion exchange chromatography with the MonoQ 50 Gl column (Amersham).

7. Nickel (Ni^{2+}) chromatography Buffer A: 0.05 M HEPES (pH 8.0), 0.3 M NaCl, 5 mM β -Me. 8. Nickel (Ni^{2+}) chromatography Buffer B: 0.05 M HEPES (pH 8.0), 0.3 M NaCl, 5 mM β -Me, 0.2 M imidazole.
8. Desalting (buffer exchange) and anion exchange (AE) chromatography: Buffer C: 0.05 M HEPES (pH 8.0), 0.05 M NaCl, 1 mM DTT. Buffer D: 0.05 M HEPES (pH 8), 0.5 M NaCl, 1 mM DTT. Buffers used on the FPLC are filtered before use (0.22 μm pore size).
9. Sample concentration: YM centriprep centrifugal filtration system (Millipore, Billerica, MA). Extinction coefficient: Expasy ProtParam (<http://www.expasy.ch/tools/protparam.html>). Beer's Law: $A = \epsilon bc$ (A = Absorbance at 280 nm (Abs_{280}); ϵ = extinction coefficient at 280 nm; b = path length; c = concentration).

2.2. Molecular Weight Analysis of Purified Proteins: Determination of the Oligomeric State

1. Gel filtration buffer F: 0.05 M HEPES (pH 8.0), 0.15 M NaCl.
2. Gel filtration column: Superdex 200 HR 10/30 (Amersham).
3. Calibration standards of molecular weight markers from 1.35 to 670 kDa (BioRad, Hercules, CA).
4. Sedimentation equilibrium analysis is performed on the XLI analytical ultracentrifuge (Beckman) with an AN60 Ti rotor with six-sector equilibrium centerpieces. Radial step size of 0.001 cm is used for collecting equilibrium data, and Abs_{280} at 42,000 rpm is used as the baseline. Buffer H: 0.05 M HEPES (pH 8.0), 0.05 M NaCl, 1 mM β -Me.

2.3. Isolation of Polyamines Bound to Purified Recombinant AdoMetDC

1. Polyamines are labeled by conjugation to the AccQ-tag reagent (6-aminoquinolyl-n-hydroxysuccinimidyl in acetonitrile, Waters, Milford, MA) and separated on an AccQtag (3.9 \times 150 mm) column (Waters) using a SystemGold HPLC (Beckman, Fullerton, CA) and detected with a Dynamax Fluorescence detector (Ranin) with an excitation wavelength of 250 nm and emission wavelength of 394 nm.
2. HPLC Buffer E: 0.14 M $\text{NaC}_2\text{H}_3\text{O}_2$, 0.017 M triethylamine, 0.01% NaN_3 , pH to 4.95 with H_3PO_4 . Buffer F: 60% Acetonitrile, 0.01% NaN_3 . Buffers must be filtered through a nylon membrane.

2.4. Steady-State Kinetic Analysis of AdoMetDC

1. Buffer I: 0.1 M HEPES (pH 8), 0.05 M NaCl, 5 mM DTT. Substrates: [*carboxy*- ^{14}C]AdoMet (Amersham) and unlabeled AdoMet (Sigma).

2. Michaelis-Menten equation of steady-state kinetics: $v_o = V_{\max} [S]/(K_m + [S])$ where v_o = velocity, V_{\max} = maximum rate, $[S]$ = substrate concentration, and K_m = the Michaelis constant (substrate concentration at half-maximal velocity). The catalytic constant or turnover number of the enzyme is $k_{\text{cat}} = V_{\max}/[\text{enzyme}]$. Catalytic efficiency is reported as k_{cat}/K_m .
3. Irreversible (time-dependant) inhibition equations where $[I]$ is inhibitor concentration:

$$v_i / v_o = e^{(-k_{\text{obs}}t)} \quad \text{and} \quad k_{\text{obs}} = k_{\text{inact}}[I] / (K_i^{\text{app}} + [I]).$$

4. Nonlinear regression analysis is performed using Prism 5.0 (Graphpad).
5. Buffer J: 0.05 M HEPES (pH 8.0), 0.1 M NaCl, 5 mM β -Me, 1 $\mu\text{g}/\text{ml}$ leupeptin, 2 $\mu\text{g}/\text{ml}$ antipain, 10 $\mu\text{g}/\text{ml}$ benzamidine, 1 $\mu\text{g}/\text{ml}$ pepstatin, 1 $\mu\text{g}/\text{ml}$ chymostatin, and 2 mM PMSE.

2.5. Identification of Allosteric Regulators of AdoMetDC by Genome Analysis

2.5.1. Western Analysis of AdoMetDC in Cell Lysates

1. Buffer K: 5% nonfat milk in Tris-buffered saline (TBS: 20 mM Tris-HCl pH 7.6, 137 mM NaCl).
2. Polyvinylidene difluoride (PVDF) membrane (Hybond-P, Amersham).
3. Horseradish peroxidase-(HRP) linked donkey antirabbit secondary antibodies (Amersham Biosciences).
4. ECL chemiluminescent HRP substrate reagents (Amersham).

2.5.2. Blast Analysis: Sequence Similarity Searches

1. National Center for Biotechnology Information (NCBI) BLAST: <http://blast.ncbi.nlm.nih.gov/Blast.cgi>.
2. PROMALS3D: <http://prodata.swmed.edu/promals3d/promals3d.php>.
3. MOLPHY: http://bioweb.pasteur.fr/seqanal/interfaces/prot_nucml.html.

3. Methods

3.1. Expression and Protein Purification of AdoMetDC

Recombinant AdoMetDC is purified by column chromatography after expression in *E. coli*. Purification is facilitated by the inclusion of a six histidine tag (His_6) or FLAG tag on the amino (N) terminus of the protein (10). Placement of the tag on the carboxy (C) terminus attenuates activity of the enzyme. His_6 tagged proteins bind with high affinity to Ni^{+2} -agarose resin and are then eluted from the column with buffer containing imidazole, resulting in significant purification. An additional anion exchange column enhances the purity of the enzyme preparation. For modifications

associated with the purification of heterodimeric AdoMetDC complexes, see Note 1. Samples are analyzed by SDS-PAGE and Coomassie blue staining (see Note 2). Purification of AdoMetDC enzymes has been described (10, 12, 16).

1. The AdoMetDC coding sequence is PCR amplified from cDNA or genomic DNA (trypanosome species do not contain introns in most of their genes) and cloned into the bacterial expression vector pET22b to create an N-terminal His₆ fusion protein. The constructs are verified by Sanger sequencing of the insert encoding the open reading frame.
2. The AdoMetDC expression vector is transformed into chemically competent BL21/DE3 *E. coli* cells by heat shock, and grown in LB with appropriate antibiotics to retain the plasmid. A single colony from the selection plate is used to inoculate a 200-ml starter culture and grown overnight. A portion of this culture (25 ml) is added to 1 L of LB and cells are grown at 37°C with shaking at 240 rpm until an optical density at 600 nm (OD₆₀₀) of 0.6 is reached. (Typically 6 L of culture produces sufficient enzyme for kinetic analysis.) IPTG is added to each culture at a final concentration of 0.2 mM to induce recombinant protein expression and the temperature is reduced. Cells continue to shake at 240 rpm and can be grown at room temperature (RT) for 3–5 h or overnight at 16°C. Cells are harvested by centrifugation at 4,000 rpm for 10 min and the supernatant is discarded. The pellets are resuspended in 200 ml lysis buffer with a dash of DNase and 1 mg/ml lysozyme. The lysate is incubated at RT for 5 min, frozen in N₂, and stored at –80°C (the freeze/thaw facilitates cell lysis in the next step).
3. Frozen lysate is thawed on ice or at 4°C with stirring. Thawed lysate is sonicated with a 3 s pulse, 80% amplitude for 2 min, and then centrifuged at 16,000 rpm for 30 min at 4°C. The lysate is filtered through cheesecloth and stored at 4°C. All remaining steps are carried out at 4°C. Ni-NTA resin (10–15 ml slurry in 50% ethanol) is packed into a column and equilibrated with 5–10 column volumes of buffer A. This chromatographic step can be performed by gravity but is faster with controlled pressure (i.e., an FPLC). The lysate is loaded onto the column and washed with 80% buffer A/20% buffer B. The column flow through is monitored at Abs₂₈₀, and washing is continued until the Abs₂₈₀ returns to baseline levels. The protein is eluted into fractions using a linear gradient from 20 to 100% buffer B. Fractions are analyzed by SDS-PAGE and Coomassie blue staining. Fractions that contain AdoMetDC are pooled and stored overnight at 4 °C (see Note 3).

4. Anion exchange chromatography on a Pharmacia Mono Q column is performed at 4°C by FPLC. First, the buffer is exchanged to buffer C with a desalting column to reduce salt concentration. The anion exchange column is equilibrated with buffer C, protein is loaded and washed with buffer C, and then protein is eluted from the column using a linear gradient of 0–100% buffer D (increased salt). Fractions are monitored by Abs₂₈₀ and SDS-PAGE and Coomassie blue staining. The purified protein is then desalted into buffer C and concentrated by centrifugation through a filtration unit.
5. The extinction coefficient of the protein can be estimated by protein prediction programs, and the purified protein preparation is quantified by measuring the Abs₂₈₀. Concentrated protein is stored at –80°C.

3.2. Molecular Weight Analysis of Purified Proteins: Determination of the Oligomeric State

In order to determine the oligomerization state of the protein, gel filtration (size exclusion) chromatography and/or analytical ultracentrifugation (AUC) can be utilized. AUC has the advantage that it can also allow determination of the binding constants for sub-unit association. This method was used to demonstrate that the heterodimer of trypanosomatid AdoMetDC/prozyme formed at higher affinity than the homodimeric AdoMetDC (10, 11).

3.2.1. Gel Filtration Chromatography

The size-exclusion column was equilibrated with buffer G and calibrated with standards using a flow rate of 0.5 ml/min. Purified protein (50 μM) was loaded on to the column and eluted using a constant flow rate of 0.5 ml/min of buffer G. The apparent molecular weight is estimated from the standard curve from molecular weight markers used to calibrate the column. This method can be used for individually, copurified or separately purified, mixed protein preparations (10).

3.2.2. Analytical Ultracentrifugation

Purified protein is prepared in buffer H and loaded into the sedimentation equilibrium setup on the AUC. Samples are equilibrated at 15,000 and 20,000 rpm, and Abs₂₈₀ is recorded after equilibration is reached at each speed. Data are analyzed by published equations describing single ideal species and complex species (17). To determine the association of two proteins or a protein and a small molecule, the samples are mixed prior to loading onto the AUC, and the same procedure is followed.

3.3. Isolation of Polyamines Bound to Purified Recombinant AdoMetDC

The identification of potential small molecule activators of AdoMetDC can be facilitated if the activator is tightly bound to the protein of interest. For example, putrescine is tightly bound to the human AdoMetDC, and can be found in complex with the protein even when the purification steps are carried out in the absence of putrescine. The bound small molecule can be isolated

after denaturation of the protein both for the purposes of identification and quantitation. For known polyamines, HPLC analysis can be used for both identification and quantitation as described below. The identification of small molecules of unknown identity is discussed in Subheading 3.5.

1. For estimation of bound polyamines, purified protein is boiled for 10 min to denature the enzyme and release small molecules and is then precipitated with 9% trichloroacetic acid and removed from solution by centrifugation. The primary and secondary amines (as found in polyamines) in the sample (mol/mol equivalent to 100 pmol protein) are analyzed by conjugation to the fluorescent AccQ-tag reagent (6-aminoquinolyl-*n*-hydroxysuccinimidyl in acetonitrile) followed by separation on a Waters AccQtag (3.9 x 150 mm) column using a Beckman System Gold HPLC with a Ranin Dynamax Fluorescence detector. HPLC buffers and gradients have been previously described (12, 18). Polyamine content is determined using a standard curve of known concentrations. The HPLC column is equilibrated and samples loaded in buffer E, and polyamines are separated with the buffer F mobile phase.

3.4. Steady-State Kinetic Analysis of AdoMetDC

Steady-state kinetic properties of AdoMetDC are measured by a radioactive assay that monitors the release of $^{14}\text{CO}_2$ (see Note 4). This assay can be used to characterize the unmodified protein, to determine allosteric stimulation by small molecules or proteins, and to characterize reversible or irreversible inhibitors of the enzyme. Additionally, this assay can be used to measure AdoMetDC activity in crude whole cell lysates (10, 12, 16).

1. The activity of the purified protein is monitored by the release of $^{14}\text{CO}_2$ from [^{14}C]AdoMet in buffer I. Labeled (25 μM) and unlabeled (0–975 μM) AdoMet are added to buffer I in a test tube on ice. The reaction (100 μl total volume) is initiated by the addition of enzyme (25–400 nM, based on monomer concentration), and filter paper soaked in saturated barium hydroxide is hung inside of the test tube, which is then capped with a rubber stopper. Tubes are incubated at 37°C in a water bath for 2.5–10 min (see Note 5). The assay is stopped by the addition of 200 μl 6 M HCl. The quenched reaction is incubated at 37°C for 30 min to allow for evolution of the CO_2 from solution. The filter paper is removed and placed in a scintillation vial with 5 ml of scintillation fluid and counted. Total cpm of the samples is converted to μmol product formed per unit time using the specific activity of the radiolabeled substrate yielding initial rates (v_i). Data points are collected in triplicate, and the data is fitted to the Michaelis–Menten equation by nonlinear regression analysis using Prism 5.0

(Graphpad) or similar graphing program. The kinetic parameters k_{cat} , K_m , and the catalytic efficiency, k_{cat}/K_m , can be determined by this analysis (19). In order to ensure that the kinetic data has been properly obtained, data must be collected during the initial rates phase of the reaction when the relationship between product formed and time is in the linear part of the curve. Furthermore, the measured reaction rate must be determined to be proportional to the AdoMetDC concentration such that a change in enzyme concentration must result in an equal change in reaction rate.

2. AdoMetDC activity can also be determined from cell lysates by initiating the reaction with cell lysate instead of purified protein. The cultivation of trypanosomes and preparation of cell lysates for the assay of AdoMetDC have been described (10, 13). Lysates are prepared at 4°C and cells are harvested by centrifugation, washed in PBS (pH 7.4) and resuspended in buffer J; lysates can be stored at -80°C (see Note 6). The radioactive AdoMetDC activity assay is performed as described above.
3. *Allosteric activation.* To determine the contribution of a known or putative allosteric activator, the molecule of interest is added to the reaction mix prior to addition of the enzyme. The radioactive assay described above is performed, and for small molecule activators the substrate concentration is held constant while the activator concentration is varied. Using a modified Michaelis–Menten kinetic analysis, the half-maximal activation constant (K_{act}) can be determined. The contribution of the allosteric activator can be reported as the fold-change of catalytic efficiency (k_{cat}/K_m) in the presence of saturating activator over value obtained for the unstimulated enzyme.
4. *Reversible inhibition.* Known or putative inhibitors are added to the reaction mixture prior to addition of the enzyme. A dose response curve of inhibitor concentration is performed, and either the IC_{50} (the inhibitor concentration required for half-maximal inhibition) value is determined, or by evaluating the inhibition at a range of substrate concentrations, the mechanism of inhibition can be determined (competitive, noncompetitive, uncompetitive) and a K_i calculated (19).
5. *Irreversible inhibition.* Compounds that are irreversible inhibitors will show time-dependent inhibition kinetics. In order to evaluate the kinetics of this inhibition, inhibitors are incubated at various concentrations with the enzyme in buffer I for a range of time. At various time points, the enzyme-inhibitor mix is diluted into the assay reaction mixture to determine the remaining enzyme activity. The dilution factor needs to be sufficiently large to effectively stop further

inactivation of the enzyme by the inhibitor during the time frame of the subsequent assay ($\sim 1/100$ -fold). The remaining enzyme activity (velocity in the presence of inhibitor (v_i)) is determined relative to the uninhibited velocity (v_o , the velocity of the enzyme incubated for the same time without inhibitor prior to addition to the reaction mix). The observed rate constant (k_{obs}), inactivation rate constant (k_{inact}), and the apparent inactivation constant (K_i^{app}) are determined using the equation in Subheading 2.4, and data are reported as the inactivation efficiency ($k_{\text{inact}}/K_i^{\text{app}}$), which has the equivalent meaning to k_{cat}/K_m (catalytic efficiency) for steady-state kinetic analysis of the substrate (19).

3.5. Identification of Allosteric Regulators of AdoMetDC

The physiologically relevant allosteric activators of AdoMetDC that have been described to date include the polyamines putrescine and cadaverine and the protein activator of the trypanosomatid enzymes prozyme (10, 12, 16, 20). While the known modulators are all activators, it is possible that protein inhibitors of AdoMetDC or other negative regulators may be discovered. To assess the potential for regulatory molecules to contribute to the physiological AdoMetDC activity, comparative kinetic analysis of the reaction rates should be performed for the purified recombinant enzyme and the protein as expressed in the extracts of the cell or organism under study. Additionally, enzyme orthologs from different species tend to have similar catalytic efficiency; therefore, if the activity of the recombinant AdoMetDC under study differs significantly from the other published homologs, this may be a hint that an allosteric regulator could be involved. Indeed this was observed for the trypanosomatid AdoMetDCs, where the activity of the recombinant homodimers was found to be ~ 500 -fold lower than that observed for the recombinant mammalian and plant homologs (10, 12, 16, 21, 22).

Identification of prozyme regulation of *T. brucei* AdoMetDC followed the observation that the activity of AdoMetDC expressed in *T. brucei* cell lysates was significantly higher than that for the recombinant enzyme, and in fact similar in level to that described for the mammalian and plant enzymes. The key experimental strategy that led to this finding was the determination of the concentration of AdoMetDC in cell lysates using active site titration with a suicide inhibitor (described below). Genome wide Blast analysis of the completed *T. brucei* genome then led to the discovery of a novel gene duplication of AdoMetDC in the trypanosomatids, leading to the hypothesis and experimental demonstration that both gene products were required to form the fully active enzyme (10). The identification of small molecule activators of AdoMetDC enzymes will require biochemical isolation and characterization (see Note 7).

3.5.1. Determination of AdoMetDC Concentration in Cell Lysates by Titration of AdoMetDC Active Sites Using a Suicide Inhibitor

The suicide inhibitor MDL 73811 (Fig. 3a) is a mechanism-based irreversible inhibitor of AdoMetDC and can be used to determine the concentration of active enzyme in a cell lysate or purified protein preparation (10). The approach is to determine how much inhibitor is required to fully inactivate the AdoMetDC activity in the lysate, and this value gives an estimation of the enzyme concentration. Cell lysates (as prepared in Subheading 3.3) are incubated with various amounts of MDL 73811 at 37°C for 0.5–2 h (allowing for complete enzyme inactivation to occur) in buffer I. The time required for complete inactivation must be determined first. For a given inhibitor concentration, several incubation times should be tried in order to choose a time that is sufficiently long that further incubation does not result in additional inactivation. Control incubations in the absence of inhibitor need to be included to rule out loss of enzyme activity from nonspecific denaturation or proteolysis in the extract. If the enzyme concentration in the extract is greater than the amount of MDL 73811 added to the mixture, residual activity will remain at the end of the incubation and this is monitored using the standard ^{14}C -AdoMet (40 μM) assay as described above. The ratio of

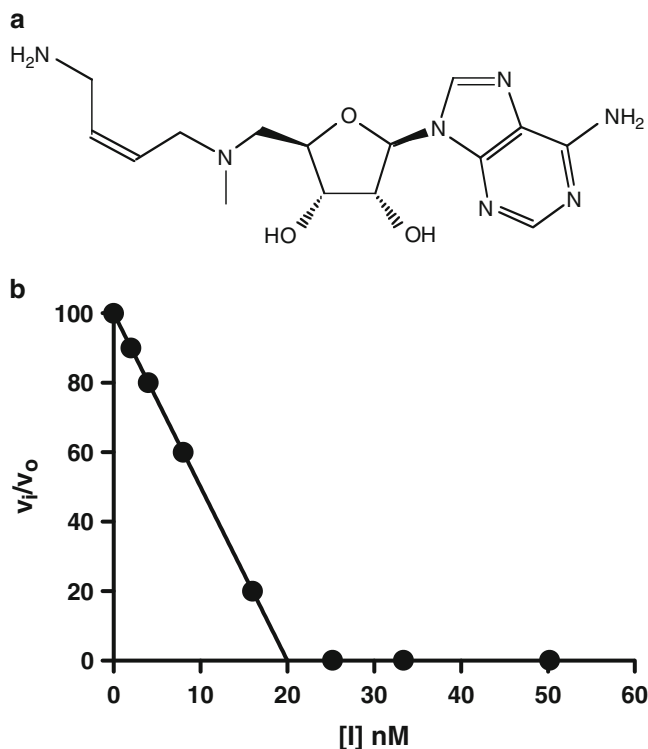


Fig. 3. Active site titration to determine enzyme concentration using a suicide inhibitor (MDL 73811) of AdoMetDC. (a) Structure of MDL 73811. (b) Hypothetical analysis of the effects of increasing inhibitor concentration on enzyme activity where v_i is the inhibited velocity and v_0 is the velocity in the absence of inhibitor. In this example, enzyme concentration was assumed to be 20 nM.

remaining activity (v_i) over uninhibited velocity (v_o ; the AdoMetDC activity of the lysate in the absence of inhibitor) is plotted as a function of MDL 73811 concentration. The molar concentration of active AdoMetDC can be estimated as the extrapolated x -intercept of the graph (Fig. 3b). Once the concentration of AdoMetDC present in the lysate has been determined, the specific activity of pure enzyme can be estimated by dividing v_o ($\mu\text{molAdoMet formed}/\text{min}$) with the determined AdoMetDC amount in the same volume of lysate (μmoles). The specific activity of AdoMetDC from the lysate is then compared to the activity measured for the purified recombinant enzyme. A significant difference between the two suggests that the recombinant protein does not reflect the state of the enzyme in the cell. If activity of the enzyme expressed in the cell of interest is higher than for the recombinant enzyme, this result suggests several possibilities, including the presence of an allosteric activator in the cell lysates or some type of covalent modification of the enzyme that results in higher activity. The allosteric activator could potentially be either a small molecule or a protein regulator as was observed for the trypanosomatid AdoMetDCs. If the recombinant enzyme is significantly more active than the enzyme in the lysate, this may suggest the presence of an endogenous inhibitor or that the enzyme has been inactivated by some type of nonspecific mechanism (denaturation, proteolysis, etc.).

3.5.2. Determination of AdoMetDC Concentration by Western Analysis

1. As an alternative method, the concentration of AdoMetDC in the cell lysate can be estimated by Western Analysis provided an antibody to the protein under study is available. In this method, the intensity of the band observed in the cell lysate is quantitated by comparison to that for a standard curve generated using known amounts of recombinant protein. For *T. brucei* AdoMetDC, determination of the AdoMetDC levels by Western gave very similar results to that observed for the MDL 73811 titration (10).

3.5.3. Candidate Screening of Potential Allosteric Regulators

1. Putrescine is a known activator of human AdoMetDC. Potentially, AdoMetDC from other species may be regulated by other polyamines or divalent cations that are present in that organism. Indeed, some bacteria produce alternative polyamines such as carboxynorspermidine and norspermidine (15). To determine if these molecules are activators of the enzyme, the compound is added to the reaction mix (buffer I) as described in Subheading 3.3. A sufficiently large range of potential activator concentration should be tested to determine how much is required to saturate the response. Analysis of polyamine stimulation of the *T. cruzi* AdoMetDC homodimer indicated that several other polyamines (e.g., cadaverine) could stimulate activity to a similar level as putrescine (12),

though as noted this stimulation is over two orders of magnitude less effective than activation by prozyme (10).

3.5.4. Phylogenetic Analysis

1. Proteins with similarity to AdoMetDC can be identified by BLAST analysis of the target genome. For the identification of prozyme in the trypanosomatid genomes, AdoMetDC sequences were identified by PSI-BLAST (23) against the nonredundant protein sequence database with default parameters (*E*-value cutoff 0.005) starting from the *T. brucei* AdoMetDC sequence (GI|146345538). Representative sequences were aligned using the program PROMALS3D (24) with default parameters and manual adjustments. Columns with mostly gaps were removed for generating the tree. Maximum likelihood phylogenetic trees were constructed using local rearrangement search of initial tree topologies (-R option) from the MOLPHY package (25). Distances were estimated by the JTT matrix, and initial tree topologies were built with Njdist. The reliability was assessed by the resampling of estimated log-likelihood (RELL) method of MOLPHY.

4. Notes

1. In the case of heterodimeric AdoMetDC complexes (i.e., AdoMetDC/prozyme), proteins can be individually purified or can be copurified together from bacteria containing the individual constructs, or can be coexpressed in the same plasmid and purified (10, 11). Both AdoMetDC and prozyme can accept N-terminal tags. His₆-tagged AdoMetDC mixed with Flag tagged or untagged prozyme can be purified by Ni²⁺ and AE chromatography as described in Subheading 3.1.
2. Samples should be collected for SDS-PAGE analysis during protein purification at the following stages: during *E. coli* growth before and after induction with IPTG; after lysis and filtration; during Ni²⁺-agarose column loading and wash; Ni²⁺-agarose column elution fractions; during desalting; during AE loading and wash; AE elution fractions; and after final desalting.
3. Ni²⁺ column fractions should not be concentrated before storing overnight, since increased salt concentration can precipitate the protein out of solution.
4. Spectrophotometric assays, such as those used to study ornithine decarboxylase kinetics (26), have not yet been described for AdoMetDC.

5. A range of enzyme concentration and time are used to ensure that the assay is conducted in the linear range. Concentrations and times given were used for kinetic analysis of the AdoMetDC/prozyme heterodimer from *T. brucei*; conditions for the assay of other AdoMetDCs may have to be optimized.
6. Cell lysis has been described for *T. brucei* AdoMeDC; sample preparation from other species may have to be optimized.
7. Identification of tightly associated small molecules may be facilitated by a modification of the process described to determine the mole fraction of polyamines bound to the enzyme (Subheading 3.3). After denaturation and TCA precipitation of the purified protein, the sample can be submitted for mass spec analysis to identify small molecules. Additionally, immunoprecipitated AdoMetDC from cell lysates could be used as the starting material. In this case, the identification of associated proteins could also be identified.

References

1. Pegg AE (2009) Mammalian polyamine metabolism and function. *IUBMB Life* 61:880–894
2. Casero RA Jr, Marton LJ (2007) Targeting polyamine metabolism and function in cancer and other hyperproliferative diseases. *Nat Rev Drug Discov* 6:373–390
3. Heby O, Persson L, Rentala M (2007) Targeting the polyamine biosynthetic enzymes: a promising approach to therapy of African sleeping sickness Chagas' disease, and leishmaniasis. *Amino Acids* 33:359–366
4. Priotto G, Kasparian S, Mutombo W, Ngouama D, Ghorashian S, Arnold U, Ghabri S, Baudin E, Buard V, Kazadi-Kyanza S, Ilunga M, Mutangala W, Pohlig G, Schmid C, Karunakara U, Torrele E, Kande V (2009) Nifurtimox-eflornithine combination therapy for second-stage African *Trypanosoma brucei* gambiense trypanosomiasis: a multicentre, randomised, phase III, non-inferiority trial. *Lancet* 374:56–64
5. Casero RA, Pegg AE (2009) Polyamine catabolism and disease. *Biochem J* 421:323–338
6. Bennett EM, Ekstrom JL, Pegg AE, Ealick SE (2002) Monomeric S-adenosylmethionine decarboxylase from plants provides an alternative to putrescine stimulation. *Biochemistry* 41:14509–14517
7. Bale S, Lopez MM, Makhatadze GI, Fang Q, Pegg AE, Ealick SE (2008) Structural basis for putrescine activation of human S-adenosylmethionine decarboxylase. *Biochemistry* 47:13404–13417
8. Ekstrom JL, Mathews II, Stanley BA, Pegg AE, Ealick SE (1999) The crystal structure of human S-adenosylmethionine decarboxylase at 2.25 Å resolution reveals a novel fold. *Structure* 7:583–595
9. Ekstrom JL, Tolbert WD, Xiong H, Pegg AE, Ealick SE (2001) Structure of a human S-adenosylmethionine decarboxylase self-processing ester intermediate and mechanism of putrescine stimulation of processing as revealed by the H243A mutant. *Biochemistry* 40:9495–9504
10. Willert EK, Fitzpatrick R, Phillips MA (2007) Allosteric regulation of an essential trypanosome polyamine biosynthetic enzyme by a catalytically dead homolog. *Proc Natl Acad Sci U S A* 104:8275–8280
11. Willert EK, Phillips MA (2009) Cross-species activation of trypanosome S-adenosylmethionine decarboxylase by the regulatory subunit prozyme. *Mol Biochem Parasitol* 168:1–6
12. Beswick TC, Willert EK, Phillips MA (2006) Mechanisms of allosteric regulation of *Trypanosoma cruzi* S-adenosylmethionine decarboxylase. *Biochemistry* 45:7797–7807
13. Willert EK, Phillips MA (2008) Regulated expression of an essential allosteric activator of polyamine biosynthesis in African trypanosomes. *PLoS Pathog* 4:e1000183

14. Wu H, Min J, Zeng H, McCloskey DE, Ikeguchi Y, Loppnau P, Michael AJ, Pegg AE, Plotnikov AN (2008) Crystal structure of human spermine synthase: implications of substrate binding and catalytic mechanism. *J Biol Chem* 283:16135–16146
15. Lee J, Sperandio V, Frantz DE, Longgood J, Camilli A, Phillips MA, Michael AJ (2009) An alternative polyamine biosynthetic pathway is widespread in bacteria and essential for biofilm formation in *Vibrio cholerae*. *J Biol Chem* 284:9899–9907
16. Kinch LN, Scott JR, Ullman B, Phillips MA (1999) Cloning and kinetic characterization of the *Trypanosoma cruzi* S-adenosylmethionine decarboxylase. *Mol Biochem Parasitol* 101:1–11
17. Lebowitz J, Lewis MS, Schuck P (2002) Modern analytical ultracentrifugation in protein science: a tutorial review. *Protein Sci* 11:2067–2079
18. Osterman AL, Brooks HB, Jackson L, Abbott JJ, Phillips MA (1999) Lysine-69 plays a key role in catalysis by ornithine decarboxylase through acceleration of the Schiff base formation, decarboxylation, and product release steps. *Biochemistry* 38:11814–11826
19. Copeland R (1996) *Enzymes: a practical introduction to structure, mechanism, and data analysis*. Wiley, New York
20. Stanley BA, Pegg AE (1991) Amino acid residues necessary for putrescine stimulation of human S-adenosylmethionine decarboxylase proenzyme processing and catalytic activity. *J Biol Chem* 266:18502–18506
21. Persson K, Aslund L, Grahn B, Hanke J, Heby O (1998) *Trypanosoma cruzi* has not lost its S-adenosylmethionine decarboxylase: characterization of the gene and the encoded enzyme. *Biochem J* 333:527–537
22. Roberts S, Scott J, Gasteier J, Jiang Y, Brooks B, Jardim A, Carter N, Heby O, Ullman B (2002) S-adenosylmethionine decarboxylase from *Leishmania donovani*: molecular, genetic and biochemical characterization of null mutants and overproducers. *J Biol Chem* 277:5902–5909
23. Altschul SF, Madden TL, Schaffer AA, Zhang J, Zhang Z, Miller W, Lipman DJ (1997) Gapped BLAST and PSI-BLAST: a new generation of protein database search programs. *Nucleic Acids Res* 25:3389–3402
24. Pei J, Kim BH, Grishin NV (2008) PROMALS3D: a tool for multiple protein sequence and structure alignments. *Nucleic Acids Res* 36:2295–2300
25. Adachi J, Hasegawa M (1992) *Molphy: programs for molecular phylogenetics based on maximum likelihood*. Computer Science Monographs, Tokyo, Institute of Statistical Mathematics.
26. Osterman A, Grishin NV, Kinch LN, Phillips MA (1994) Formation of functional cross-species heterodimers of ornithine decarboxylase. *Biochemistry* 33:13662–13667

Chapter 15

Protocols for Studying Antizyme Expression and Function

Noriyuki Murai, Yasuko Murakami, and Senya Matsufuji

Abstract

Antizyme (AZ) is a key molecule in feedback regulation of cellular polyamines. It is induced by polyamines through stimulation of ribosomal frameshifting during its translation. In mammals, AZ is diverged into three paralogs, AZ1–3. Tissue and subcellular distribution are different among the paralogs, as determined by immunochemical methods or expression of fluorescent-tagged proteins. Only AZ2 is known to be phosphorylated. AZ regulates cellular polyamine levels through multiple mechanisms. It binds to ornithine decarboxylase (ODC) to form an inactive complex and to trigger degradation of ODC by 26S proteasomes. The AZ activity to promote ODC degradation can be measured both *in vitro* and in cells. AZ also inhibits cellular uptake of polyamines. This chapter comprises seven subchapters describing methods for studying expression and function of AZ.

Key words: Antizyme, Ornithine decarboxylase, Antizyme inhibitor, Translational frameshifting, Antibody, Immunochemistry, Localization, Phosphorylation, Protein degradation, Polyamine transport

1. Introduction

Antizyme (AZ) is a polyamine-induced protein that negatively regulates polyamine synthesis and uptake (1, 2). It is conserved among a wide range of eukaryotes, from yeast to vertebrates, but is not found in plants (3). In mammals, the AZ family consists of three members, namely ubiquitously expressed AZ1 and AZ2, and male germ cell-specific AZ3. All AZs are synthesized by the translational frameshift mechanism that is stimulated by polyamines (4). AZ1 binds to a subunit of ornithine decarboxylase (ODC), inhibits the enzyme activity, and accelerates the degradation of ODC protein by the 26S proteasome without *polyubiquitination* (5). AZ2 essentially shares these activities, except that AZ2 stimulates ODC degradation only in the cells, but not in cell-free systems. In addition, AZ2 has some properties that differ from AZ1.

2. Materials

2.1. Assay for Translational Frameshifting of Antizyme In Vitro

1. Solutions of wild-type and in-frame mRNAs prepared by in vitro transcription with T7 RNA polymerase on linearized plasmids of pGEM4Z-NE and pGEM4Z- Δ T205, respectively (4) (see Note 1). Transcripts are purified by phenol–chloroform extraction and dissolved in RNase-free water at 0.2 μ g/ μ L.
2. Rabbit reticulocyte lysate, nuclease treated (Promega).
3. Amino acid mixture, containing 19 amino acids except methionine at 1 mM each, attached with the rabbit reticulocyte lysate.
4. L-[³⁵S]Methionine (37 TBq/mmol, 555 MBq/mL, translation grade).
5. RNase A solution, 1 mg/mL pancreatic RNase A in 5 mM EDTA.
6. RNase-free water.
7. RNase inhibitor (40 units/ μ L, Promega).
8. Polyamine solution. One each of putrescine dihydrochloride, spermidine trihydrochloride, and spermine trihydrochloride is dissolved in appropriate volumes of nuclease-free water and the pH adjusted to 7.0–7.2 with KOH. We prepare putrescine solution of 150 mM, spermidine solution of 15 mM, and spermine solution of 3.75 mM. Aliquots are stored at -80°C .

2.2. Immunochemical Detection of Antizyme

2.2.1. Cell Culture and Western Blotting

1. Human pancreatic adenocarcinoma AsPC-1 cells (Dainippon Sumitomo Pharma, Osaka, Japan).
2. Six-well culture plates.
3. RPMI 1640 medium supplemented with 10% fetal bovine serum (FBS).
4. Phosphate-buffered saline (PBS): 137 mM NaCl, 2.7 mM KCl, 10 mM Na₂HPO₄, 1.8 mM KH₂PO₄.
5. 0.05% Trypsin/EDTA (GIBCO).
6. Serum-free DMEM/F10 medium (a 1:1 mixture of Dulbecco's modified Eagle's medium (DMEM, GIBCO) and Nutrient Mixture Ham's F-10 (GIBCO)) containing 17.5 mM glucose and 1% BSA.
7. Lysis buffer: 1% NP-40, 0.1% SDS, 0.5% sodium deoxycholate and protease inhibitors, (Complete, Mini, Roche Diagnostics).
8. Hybond-P PVDF membrane (GE Healthcare).
9. Chromatography Paper 3MM CHR (Whatman).
10. Running buffer: 25 mM Tris, 0.19 M glycine, 0.1% SDS, pH8.3.
11. Transfer buffer: 48 mM Tris, 39 mM glycine, 0.037% SDS, 20% methanol.

12. ECL Advance Western Blotting Detection Kit (GE Healthcare).
13. TBS-T: 10 mM Tris-HCl, 150 mM NaCl, pH 7.5, 0.05% Tween20.
14. Blocking solution: TBS-T containing 2% Advanced Blocking Agent (Supplied with ECL Advance Western Blotting Detection Kit, GE Healthcare).
15. Rabbit polyclonal antirat AZ (IgG fraction, 20 mg protein/ml. Dilute 1:3,000 in blocking solution) (6).
16. A peroxidase-conjugated secondary antibody (Histofine, Nichirei, Japan, diluted 1:100,000 in blocking solution) (see Note 2).

2.2.2. Immunocytochemistry

1. Phosphate-buffered saline (PBS): 137 mM NaCl, 2.7 mM KCl, 10 mM Na₂HPO₄, 1.8 mM KH₂PO₄.
2. 4% Paraformaldehyde.
3. 0.3% Triton X-100 in PBS.
4. 3% BSA/PBS.
5. Primary antibody: rabbit polyclonal antirat AZ1 antibody (IgG fraction, 20 mg protein/ml, diluted 1:2,000 in 3% BSA/PBS) (6).
6. Secondary antibody-nuclear stain mixture: 1:300 dilution of Alexa Fluoro 488-conjugated antirabbit IgG (Highly cross-adsorbed, Molecular Probes) and 1:150 dilution of TO-PRO-3 iodide (642/661)-1 mM solution in DMSO (Molecular Probes) in 3% BSA/PBS. This mixture should be prepared immediately before use.
7. Glass coverslips (11 mm).
8. 24-Well plates.
9. 0.01% of poly-L-lysine (Sigma). Store at 4°C.
10. Rotary mixer for microfuge tubes.

2.3. Detection of Phosphorylated Antizyme 2

2.3.1. Cell Culture

1. FreeStyle 293-F cells (Invitrogen).
2. FreeStyle 293 Expression Medium (Invitrogen).
3. 125 mL polycarbonate sterile vented cap Erlenmeyer flask (CORNING).
4. CO₂ incubator with a humidified atmosphere of 5% CO₂ in air.
5. Compact rotary shaker with flask holders that work in the CO₂ incubator at 120–135 rpm.

2.3.2. Transfection of 293-F Cells

1. Suspension FreeStyle™ 293-F cells.
2. 293fectin™ Transfection Reagent (Invitrogen).
3. Opti-MEM I (Invitrogen).
4. Three 125-mL polycarbonate sterile vented cap Erlenmeyer flask (CORNING).

5. pCMV-HA-AZ2 (in-frame mutant forms of mouse AZ2) (7) (see Note 1).
6. p3×FLAG-ODC (7). FLAG-ODC serves as a ligand in the pull-down assay of AZ2.

2.3.3. Immunoprecipitation and Immunoblot Analyses

1. Anti-HA antibody (C29F4) (Cell Signaling technology).
2. Anti-P-S186. A polyclonal antibody from rabbits immunized with a synthesized AZ2 peptide corresponding to the C-terminal 12 amino acid residues with phosphoserine (pS) at residue 186, CYPLDQNL(pS)DED. The antibody was absorbed by a nonphosphorylated AZ2 peptide column and purified with a protein A-Sepharose column.
3. Anti-FLAG M2 Affinity Agarose Gel (Sigma).
4. Antirabbit IgG-conjugated horseradish peroxidase (GE Healthcare).
5. Hybond-P PVDF membrane (GE Healthcare).
6. ECL Plus Western Blotting Detection System (GE Healthcare).
7. Membrane blocking agent (GE Healthcare).
8. Proteinase inhibitor cocktail Set III EDTA-Free (Calbiochem).
9. M-PER mammalian protein extraction reagent (Pierce).
10. ImmunoPure Gentle Elution Buffer (Pierce).
11. Chromatography paper 3MM CHR (Whatman).
12. Transfer buffer: 48 mM Tris, 39 mM glycine, 0.037% SDS, 20% methanol.
13. TBS-T: 10 mM Tris-HCl, 150 mM NaCl, pH 7.5, 0.05% Tween20.

2.4. Ornithine Decarboxylase-Inhibitory Activity of Antizyme

2.4.1. Preparation of Mouse Kidney ODC

1. Testosterone enanthate, 250 mg/mL in Sesami oil.
2. Homogenizing buffer: 25 mM Tris-HCl, pH 7.5, 1 mM dithiothreitol (DTT), 0.01% Tween 80.

2.4.2. Preparation of Recombinant Antizyme Inhibitor 1 (AIn1)

1. *Escherichia coli* BL21 competent cells.
2. pGEX-4T-3-AIn1: Rat AIn1 cDNA lacking the first 14 nucleotides of the coding region was cloned in pGEX-4T-3 bacterial expression vector (GE Healthcare).
3. LB medium containing 50 mg/L ampicillin.
4. 1 M Isopropyl-1-thio-β-D-galactopyranoside (IPTG). Store at -20°C.

5. PBS: 137 mM NaCl, 2.7 mM KCl, 10 mM Na₂HPO₄, 1.8 mM KH₂PO₄. pH is adjusted to 7.4 with HCl if necessary.
6. 10 mg/mL lysozyme (Sigma).
7. Glutathione-Sepharose 4B (GE Healthcare).
8. Poly-Prep Chromatography Column, Bio-Rad.
9. Column buffer: 50 mM Tris-HCl, pH 8.0.
10. 10 mM glutathione in column buffer.
11. Dialyzing buffer: 25 mM Tris-HCl, pH 7.5, 1 mM DTT, 0.01% Tween 80, 20% glycerol.

2.4.3. Preparation of Samples for Assay of AZ Activity and ODC-AZ Complex

1. Homogenizing buffer: 25 mM Tris-HCl, pH 7.5, 1 mM DTT, 0.01% Tween 80.
2. PBS.
3. Protease inhibitor cocktail (Complete Mini, Roche).

2.4.4. Assay of AZ Activity and ODC-AZ Complex

1. Buffer mixture: 0.5 M Tris-HCl, pH 7.5, 25 mM DTT, 0.125% Tween 80, 0.5 mM pyridoxal phosphate. Store in suitable aliquots at -20°C.
2. [¹⁴C]ornithine solution: 46.25 kBq/mL L-[1-¹⁴C]ornithine, 1 mM L-ornithine. It is made by mixing L-[1-¹⁴C] ornithine (specific activity 1.85–2.22 GBq/mmol, Moravek) and unlabeled L-ornithine solution. Gloves should be worn and containment precautions taken when handling radioactive materials. Store at 4°C.
3. Mouse kidney ODC.
4. AZ sample. Store at -80°C.
5. Recombinant AIn1.
6. 10% KOH.
7. 6 M HCl.
8. Toluene-based scintillation fluid.
9. Glass scintillation vials.

2.5. In Vitro Assay for Ornithine Decarboxylase Degradation-Promoting Activity of Antizyme

2.5.1. Preparation of Labeled ODC

1. In vitro translation and transcription system (TNT T7 Coupled Reticulocyte Lysate System, Promega).
2. L-[³⁵S]Methionine (>37 TBq/mmol, 370 MBq/mL, Easy Tag, PerkinElmer).
3. Linear DNA of plasmid p9T7ODC71 (0.5 µg/µL). The plasmid carries 71-bp 5'-untranslated region (UTR), 1,386-bp coding region, and 552-bp 3'-UTR of rat ODC under the control of the T7 RNA polymerase promoter (8). The plasmid is digested with *Eco*RI and purified with phenol-chloroform extraction followed by ethanol precipitation.

4. RNase inhibitor (40 units/ μ L, Promega).
5. Nuclease-free water.

2.5.2. Preparation of Recombinant Antizyme

1. *E. coli* BL21(DE3) competent cells.
2. Plasmid DNA pET-AZ1 expressing N-terminal His-tagged in-frame mutants of rat AZ1. It is prepared by insertion of the coding sequence of pGEM4Z/ Δ T205 (4) at the *Nde*I-*Xho*I sites of pET-15b vector (Novagen) (see Note 1).
3. LB medium containing 50 mg/L ampicillin.
4. 1 M IPTG. Store at -20°C .
5. Buffer A: 50 mM Sodium-phosphate buffer pH 7.5 containing 0.3 M NaCl.
6. 10 mg/mL lysozyme (Sigma).
7. NuPAGE LDS Sample Buffer (4 \times) (Invitrogen).
8. Buffer A containing 10, 20, 30, and 250 mg/mL imidazole (Sigma)
9. Ni-NTA Agarose (QIAGEN).
10. Chromatography columns (Poly-Prep Chromatography column, Bio-Rad).
11. Dialysis buffer: 50 mM Tris-HCl, pH 7.5, 1 mM DTT.

2.5.3. Preparation of a Cell Extract for ODC Degradation

1. Rat hepatoma tissue culture (HTC) cells (9).
2. Culture medium: Dulbecco's modified Eagle's medium (DMEM, GIBCO) supplemented with 2% fetal bovine serum, 4% newborn-calf serum, and antibiotics.
3. PBS: 137 mM NaCl, 2.7 mM KCl, 10 mM Na_2HPO_4 , 1.8 mM KH_2PO_4 . pH is adjusted to 7.4 with HCl if necessary.
4. Homogenizing buffer: 25 mM Tris-HCl, pH 7.5, 1 mM DTT, 0.01% Tween 80. Store at 4°C . Stable for up to 7 days.

2.5.4. ODC Degradation Assay

1. 0.1 M ATP, pH adjusted to 7 with 2 M NaOH. Store at -80°C .
2. 125 mM DTT. Store at -80°C .
3. 0.5 M MgCl_2 .
4. 1.5 M Tris-HCl, pH 7.5.
5. 1 M phosphocreatine. Store at -80°C .
6. 10 mg/mL creatine kinase. Store at -80°C .
7. HTC cell extract.
8. Recombinant His-tagged AZ.
9. ^{35}S -labeled ODC.

10. Sample buffer (4×): 0.2 M Tris/HCl, pH 6.8, containing 4% SDS, 4% mercaptoethanol, 0.4% bromophenol blue, and 80% glycerol. Store at 4°C.

2.6. Cell Culture Assay for Ornithine Decarboxylase Degradation-Promoting Activity of Antizyme

2.6.1. Cell Culture

11. Materials for SDS-PAGE.
 1. FreeStyle 293-F cells (Invitrogen).
 2. FreeStyle 293 Expression Medium (Invitrogen).
 3. 125 mL polycarbonate sterile vented cap Erlenmeyer flask (CORNING).
 4. CO₂ incubator with a humidified atmosphere of 5% CO₂ in air.
 5. Compact rotary shaker with flask holders that work in the CO₂ incubator at 120–135 rpm.

2.6.2. Transfection of 293-F Cells

1. Suspension FreeStyle™ 293-F cells.
2. 293fectin™ Transfection Reagent (Invitrogen).
3. Opti-MEM I (Invitrogen).
4. Three 125-mL polycarbonate sterile vented cap Erlenmeyer flask (CORNING).
5. pCMV-HA-AZ1 (in-frame mutant forms of rat AZ1) (7) (see Note 1).
6. pCMV-HA-AZ2 (in-frame mutant forms of mouse AZ2) (7).
7. pCMV-HA-ODC.

2.6.3. ODC Degradation Assay

1. 10 mg/mL cycloheximide (Sigma). Store at –20°C.

2.6.4. Immunoprecipitation and Immunoblot Analyses

1. ProFound Mammalian HA Tag IP/Co-IP Kit (Pierce).
2. Bradford reagent (BioRad).
3. Anti-HA antibody (C29F4) (Cell signaling technology).
4. Antirabbit IgG-conjugated horseradish peroxidase (GE Healthcare).
5. Hybond-P PVDF membrane (GE Healthcare).
6. ECL Plus Western Blotting Detection System (GE Healthcare).
7. Membrane blocking agent (GE Healthcare).
8. Proteinase inhibitor cocktail Set III EDTA-Free (Calbiochem).
9. Chromatography Paper 3MM CHR(Whatman).
10. Transfer buffer: 48 mM Tris, 39 mM glycine, 0.037% SDS, 20% methanol.
11. TBS-T: 10 mM Tris–HCl, 150 mM NaCl, pH 7.5, 0.05% Tween20.
12. 1 M Dithiothreitol (DTT).

2.7. Inhibition of Polyamine Transport by Antizyme

2.7.1. Cell Culture

1. FreeStyle 293-F cells (Invitrogen).
2. FreeStyle 293 Expression Medium (Invitrogen).
3. 125 mL polycarbonate sterile vented cap Erlenmeyer flask (CORNING).
4. CO₂ incubator with a humidified atmosphere of 5% CO₂ in air.
5. Compact rotary shaker with flask holders that work in the CO₂ incubator at 120–135 rpm.

2.7.2. Transfection of 293-F Cells

1. Suspension FreeStyle™ 293-F cells.
2. 293fectin Transfection Reagent (Invitrogen).
3. Opti-MEM I (Invitrogen).
4. Three 125-mL polycarbonate sterile vented cap Erlenmeyer flask (CORNING).
5. pd2EGFP-N1 vector (Clontech) (control).
6. pCMV-HA-AZ1 (in-frame mutant forms of rat AZ1ΔT) (7) (see Note 1).
7. pCMV-HA-AZ2 (in-frame mutant forms of mouse AZ2ΔT) (7).

2.7.3. Assay of Spermidine Uptake

1. [¹⁴C]Spermidine trihydrochloride (4.11 GBq/mmol, 1.85 MBq/mL) (GE Healthcare).
2. 60 mm Plastic dishes.
3. PBS: 137 mM NaCl, 2.7 mM KCl, 10 mM Na₂HPO₄, 1.8 mM KH₂PO₄. pH is adjusted to 7.4 with HCl if necessary.
4. 0.1% SDS.
5. Toluene-based scintillation fluid.

3. Methods

3.1. Translational Frameshifting of Antizyme In Vitro

A most remarkable feature of the expression of AZ is translational frameshifting (4). Frameshift efficiency is stimulated by polyamines (putrescine, spermidine, and spermine) and thus it serves as a polyamine sensor in the feedback regulation of cellular polyamine concentrations. The translational frameshifting is directed by a set of sequences of AZ mRNA, the frameshift site, a downstream structure, and an upstream stimulatory signal. Frameshift events can be assayed more easily using reporter systems either in vitro or in vivo (10, 11). This protocol describes frameshift assay in rabbit reticulocyte lysates of native rat AZ1 mRNA generated in vitro.

1. Dilute polyamine solutions according to experimental plan. Maximal concentrations for dose-dependent frameshift stimulation are approximately 10 mM for putrescine, 1 mM for spermidine, and 0.25 mM for spermine (see Note 3).

2. Prepare a premixture with following.
 - Rabbit reticulocyte lysate 10.5 μL per tube.
 - Amino acid mixture without methionine 0.3 μL per tube.
 - L-(^{35}S)Methionine 1.0 μL per tube.
 - RNase inhibitor 0.2 μL per tube.

Dispense 13 μL of the premixture into the bottom of 1.5-mL microfuge tubes placed on ice.
3. Add 1 μL of polyamine solution and 1 μL of the RNA solution. If the polyamine concentration is fixed, it can be included in the premixture.
4. Mix the solution with a vortex mixer with precaution not to introduce air bubbles. Incubate at 30°C for 45 min.
5. Stop the reaction by adding 1 μL of 1 mg/mL RNaseA-5 mM EDTA. Incubate at room temperature for 10 min.
6. Mix an aliquot of solution with sample buffer and subject to SDS-PAGE of 15% acrylamide gel (see Note 4).
7. The gel is processed for autoradiography or fluorography. The wild-type and in-frame rat AZ1 mRNAs give approximately 29 and 23 kDa products, respectively, the latter of which is synthesized by the initiation at the second AUG codon (4). Determine the intensity of product bands. Frameshift efficiency is calculated as a ratio of product from the wild-type mRNA to that from in-frame mRNA under the same reaction condition (see Note 5).

3.2. Immunochemical Detection of Antizyme

There are a number of reports of immunochemical detection of AZ. However, detection of AZ, particularly in animal tissues, is often difficult due mainly to its small contents (up to several ng per mg total protein). Most of mammalian tissues contain both AZ1 and AZ2, but there is no established antibody that can distinguish the two AZ species with a satisfactory sensitivity. In this subchapter, we describe an experiment where endogenous AZ1 is detected by western blotting and fluorescent immunocytochemistry (12). In addition, a list of representative antibodies against mammalian AZs and their application from literature is supplied (Table 1).

3.2.1. Cell Culture and Western Blotting

1. AsPC-1 cells are maintained in RPMI 1640 with 10% FBS. Plate the cells at a density of 1×10^6 cells/well in a 6-well culture plate and incubate overnight at 37°C in a CO₂ incubator with a humidified atmosphere of 5% CO₂ in air.
2. To induce differentiation, the cells were washed with 0.5 mL PBS 3 times and treated with trypsin/EDTA at room temperature for 30–60 s with care not to detach the cells from the dishes, followed by culturing in serum-free DMEM/F10 for designated time. The cells will grow forming clusters, which attach to the plate loosely.

Table 1
Antibodies against mammalian antizymes and their applications.

Name	Preparation (antigen)	Specificity						AZ3	AZ2	AZ1	Human	Application
		Rat	Mouse	Human	AZ1	AZ2	AZ3					
<i>Polyclonal antibodies</i>												
Anti-AZ	Matsufuji (28) (recombinant rat AZ1)	+	+	+	+	+	+	+	+	+	IP, W	Matsufuji (6)
											IP, W	Kanamoto (20)
											IH	Kilpelainen (29)
											W	Levillain (30)
											W	Hoshino (31)
											W	Liao (32)
											W, IC	Suzuki (12)
Anti-AZ	Mitchell (25) (GST-AZ1)	+	+	+	+	+	+	+	+	+	W	Mitchell (25)
											W	Mitchell (33)
											W	Mitchell (34)
											W ^b	Tsuji (35)
											W, IP	Newman (36)
											W, IC	Mangold (37)
Anti-AZ	Mamroud-Kidron (19) (recombinant mouse AZ1)	+	+	+	+	+	+	+	+	+	IP	Mamroud-Kidron (21)
Anti-AZ1	Kankare (38) (His-AZ1 ^c)										W, ELISA	Kankare (38)
Anti-AZ	Gritli-Linde (39) (His-AZ)										W, IH	Gritli-Linde (39)
Anti-AZ											IC	Schipper (40)
Anti-AZ	Feith (41) (His-AZ1)										W	Feith (41)
Anti-AZ											IH	Feith (42)
Anti-AZ											IH	Wang (43)

Anti-AZ	Biomol (PW8885) (AZ1)	+	+	+	+	+	+	+	IP, W		
Anti-AZ	Sigma (HPA009291) (AZ1 peptide)				+				IH		
Anti-AZ	Abcam (ab85221) (human AZ1 N-terminal region)				+				W, ELISA		
Anti-AZ2	Murakami et al (AZ2-peptide) ^a				+		+	-	W ^a		
Anti-AZ2	Sigma (SAB2104401) (AZ2 peptide)				+				W		
Anti-AZ2	Santa Cruz Biotechnology (sc-163720) (human AZ2 internal region)				+				IP, W, ELISA		
Anti-AZ2	Santa Cruz Biotechnology (sc-163719) (human AZ2 C-terminal region)				+				W, ELISA		
Anti-AZ3	Tosaka (44) (recombinant mouse AZ3)				+			+	W, IH	Tosaka (44)	
<i>Monoclonal antibodies</i>											
HZ-3H1	Matsufuji (45) (rat liver AZ)				+			+	- ^a	IP, W	Matsufuji (45)
HZ-1B3	Matsufuji (45) (rat liver AZ)				+			+	- ^a	IP, W	Matsufuji (45)
HZ-1C5	Matsufuji (45) (rat liver AZ)				+			+	- ^a	IP, W	Matsufuji (45)
HZ-2E9	Matsufuji (45) (rat liver AZ)				+			+	- ^a	IP	Matsufuji (45)
Anti-AZ	Gandre (46) (rat AZ ^d)							+		IC	Murakami (46)
					+			+		W, IH	Murakami (47)
					+			+		W	Gandre (48)
					+			+		W, IC	Gandre (49)

IP: immunoprecipitation; W: western blotting; IC: immunocytochemistry; IH: immunohistochemistry; ELISA: enzyme-linked immunosorbent assay

^a Unpublished results by Murakami et al.

^b Hamster

^c ORF1- and ORF2- specific antibodies were separated from each other by immunoaffinity.

^d Part of ORF2

3. Transfer the cells to a microfuge tube.
4. Wash the cells with 0.5 mL cold PBS twice.
5. Add lysis buffer to the cells.
6. Keep on ice for 30 min.
7. Sonicate the lysate for 10 s.
8. Centrifuge the lysate at $14,000 \times g$ at 4°C for 10 min.
9. Heat the supernatant in SDS-PAGE sample buffer at 95°C for 5 min.
10. Load the sample (100 μg protein) on SDS-PAGE gel (10%, 8×9 cm).
11. Transfer to PVDF membrane.
12. Soak the membrane with TBS-T briefly and incubate in blocking solution for 1 h.
13. Wash the membrane with 15 mL of TBS-T for 5 min.
14. Incubate the membrane and anti-AZ antibody with gentle agitation overnight at 4°C .
15. Wash the membrane with 15 mL of TBS-T 3 times for 5 min each.
16. Detect AZ protein by using ECL Advance Western Blotting Detection Kit.

3.2.2. Immunocytochemistry

1. The cells induced for differentiation (Subheading 3.2.1, step 2) are transferred to a microfuge tube.
2. Wash the cells with 0.5 mL cold PBS 3 times.
3. Fix the cells with 0.3 mL 4% paraformaldehyde at room temperature for 30 min.
4. Wash the cells with 0.5 mL PBS 3 times. Remove the PBS completely.
5. Permeabilize the cells with 0.3% Triton X-100 (0.3 mL) at room temperature for 5 min.
6. Wash the cells with 0.5 mL PBS at room temperature 3 times.
7. Block the cells with 0.3 mL 3% BSA in PBS at room temperature for 30 min.
8. Remove the blocking buffer and wash the cells with 0.5 mL PBS once.
9. Add the diluted primary antibody (0.2 mL) to the cells and incubate with mixing on a rotary mixer at 4°C overnight.
10. Wash the cells with 0.5 mL PBS at room temperature 3 times.
11. Add secondary antibody-nuclear stain mixture (0.2 mL) to the cells and incubate with mixing on a rotary mixer at room temperature for 20 min.

12. Wash the cells with 0.5 mL PBS at room temperature 3 times.
13. Place glass coverslips in 24-well plates and immerse the coverslips in 0.3 mL poly-L-lysine for 15 min. Remove the poly-L-lysine by aspiration. Wash the coverslips with 0.5 mL PBS at room temperature 3 times.
14. Suspend the stained AsPC-1 cells from step 12 in 150 μ L PBS and transfer onto the coverslip. The cells will loosely attach on the surface.
15. Pick up the coverslip with forceps and blot excess buffer off with Kimwipe. Mount the coverslips on slide. The slides should be kept in the dark.
16. The stained cells were observed with a confocal laser microscope (Fluoview, FV1000, Olympus, Tokyo, Japan). A typical result is shown in Fig. 1.

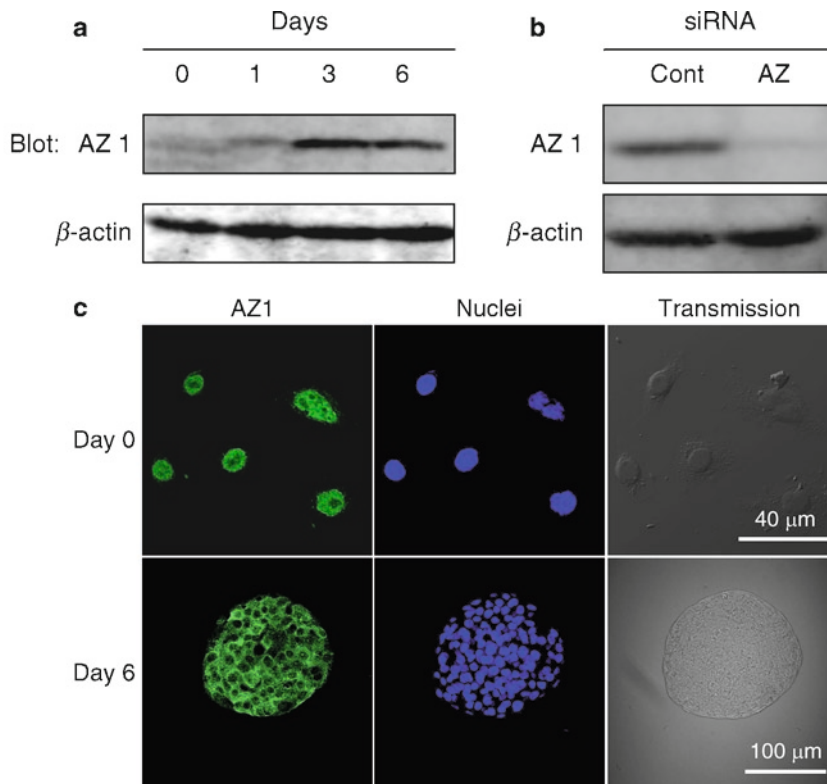


Fig. 1. The expression and intracellular localization of AZ1 in pancreatic tumor cells. **(a)** Western blot analysis of AZ1. Cell extracts from AsPC-1 cells on days 0, 1, 3, and 6 in serum-free culture were analyzed by Western blotting with polyclonal anti-AZ1 and anti- β -actin antibodies. **(b)** The effect of AZ1 siRNA. AsPC-1 cells were transfected with AZ1 siRNA or control siRNA (150 nM) for 2 days and then induced for differentiation in serum-free medium in the presence of the same siRNA for 4 days. Western blot analysis of AZ1 protein was performed on AsPC-1 cells 6 days after the first transfection with AZ1 siRNA (Cont). **(c)** Cellular localization of AZ1. Cells were stained with polyclonal anti-AZ1 antibody and TO-PRO-3 iodide (nuclear staining) on day 0 (*the upper panels*) and day 6 in culture (*the lower panels*). Images were taken with a confocal laser microscope. Scale bars: 40 μ m (*upper*) and 100 μ m (*lower*) (reproduced from ref. (12) with modifications).

3.3. Detection of Phosphorylated Antizyme 2

We have reported that mouse AZ2 expressed in NIH3T3 or 293-F cells is phosphorylated at Ser-186 residue and that AZ2 is phosphorylated in vitro by protein kinase CK2. AZ1 is not phosphorylated under the same condition. In this protocol, we describe a detection of AZ2 phosphorylation using ODC pull-down assay and immunoblotting with anti-P-S186 antibody (7).

3.3.1. Cell Culture

1. Suspension 293-F cells are maintained in a 125-mL polycarbonate sterile vented cap Erlenmeyer flask containing 10 mL of prewarmed FreeStyle 293 Expression Medium at 37°C with rotary shaking in a CO₂ incubator with a humidified atmosphere of 5% CO₂ in air.
2. Transfer aliquot of suspension to an Erlenmeyer flask. Grow the cells until the viable cell number reaches 3 × 10⁶/mL.
3. On the day of transfection, check the cell viability using the trypan blue dye exclusion method. The cell viability must be over 90%. In addition, most of the cell should be suspended singly, not forming clumps.

3.3.2. Transfection

1. The 293-F cells are diluted to 1 × 10⁶/mL. A 10-mL culture is dispensed in a 125-mL Erlenmeyer flask.
2. Dispense each 5 μg of p3×FLAG-ODC and pCMV-HA-AZ2 in a microfuge tube.
3. Add Opti-MEM I to the tube to make a total volume 333 μL. Mix gently.
4. Dilute 40 μL of 293fectin™ with 960 μL Opti-MEM I. Mix gently and incubate at room temperature for 5 min.
5. Add 333 μL of the diluted 293fectin™ to the diluted DNA solutions. Mix gently.
6. Incubate the mixture at room temperature for 20–30 min to form DNA-293fectin™ complex (see Note 6).
7. Transfer 660 μL solution of plasmid DNA-293fectin™ complex to the shaker flask containing the 293-F cell suspension.
8. Incubate the cells in the CO₂ with rotary shaking for 24 h.

3.3.3. Immunoprecipitation and Immunoblot Analyses

1. Add 0.3 mL of M-PER mammalian protein extraction reagent supplemented with 1% protease inhibitor cocktail to the cell pellets. Suspend the cells with pipetting gently.
2. Gently shake the cell suspension at room temperature for 15 min.
3. Gently resuspend the cells with pipetting.

4. Remove cell debris by centrifugation at $2,000 \times g$ at 4°C for 25 min.
5. Transfer the supernatants (cell lysates) to microfuge tubes (rocked type).
6. Resuspend the anti-FLAG agarose by inverting the vial several times before dispensing (see Note 7).
7. Dispense 30 μL of anti-FLAG agarose slurry into each microfuge tube containing cell lysate.
8. Incubate with gentle rotating at 4°C for 2 h to overnight.
9. Centrifuge the tube at 5,000 rpm for 3 min.
10. Remove the supernatant and add 0.5 mL of TBS-T to the tube.
11. Centrifuge the tube at 5,000 rpm for 3 min.
12. Repeat steps 11–12 twice more.
13. Remove the supernatant and add 40 μL of ImmunoPure Gentle Elution Buffer and tap the tube to mix.
14. Place the tube at room temperature for 5 min and centrifuge at 5,000 rpm. Transfer the supernatant (eluate) to a new microfuge tube.
15. A portion of the eluate is treated with bacterial alkaline phosphatase for 75 min at 37°C .
16. Both bacterial alkaline phosphatase-treated and untreated eluates are mixed with SDS-PAGE sample buffer and subject to SDS-PAGE (12.5% gel) (see Note 8).
17. After electroblotting, HA-AZ2 and its phosphorylated form are detected with anti-HA (at 1:2,000 dilution) and anti-P-S186 antibodies (at 1:5,000 dilution), respectively. The secondary antibody, antirabbit IgG-conjugated horseradish peroxidase, is used at 1:20,000 dilution (Fig. 2).

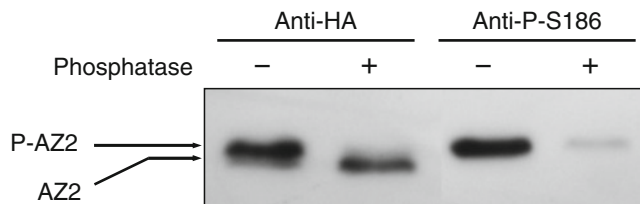
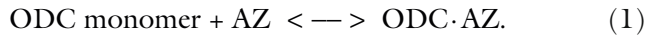
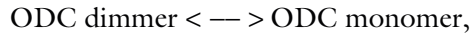


Fig. 2. Separation of phosphorylated and unphosphorylated AZ2 proteins. Suspension 293-F cells were cotransfected with 3 \times FLAG-ODC and HA-AZ2. After 24 h, cell extracts were prepared and immunoprecipitated with anti-FLAG (M2) antibody-conjugated agarose. A portion of the immunoprecipitate was treated with bacterial alkaline phosphatase. After SDS-PAGE and blotting, HA-AZ2 and its phosphorylated derivative were detected with anti-HA and anti-P-S186 antibodies, respectively. P-AZ2 denotes phosphorylated AZ2. Reproduced from ref. (7).

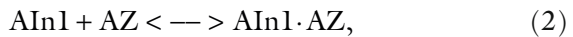
3.4. Ornithine Decarboxylase-Inhibitory Activity of Antizyme

The activity of AZ is measured primarily by its inhibition of ODC in vitro. AZ stoichiometrically binds to ODC forming inactive ODC–AZ complex (13–15).



The equilibrium constant of AZ binding to ODC is estimated to be as high as 1.4×10^{-11} M (15).

Another regulatory protein, antizyme inhibitor 1 (AIn1, formerly AIn), binds to AZ with a higher affinity than that of ODC. When added to ODC–AZ complex, AIn1 replaces ODC, releasing active ODC from ODC–AZ complex (14, 16).



Most tissue and cell extracts contain free ODC, AIn1·AZ complex, ODC–AZ complex, and free AIn1. Some complexes may be formed during tissue homogenization. Free AZ is present under limited conditions such as after addition of exogenous polyamines.

Only free AZ and ODC–AZ complex are determined as ODC inhibitory activity (shown as (1)) and an increase in ODC activity after an addition of excess amounts of AIn1, respectively (14, 17) (see Note 9). Total AZ activity (a sum of free AZ, ODC–AZ complex, and AIn1·AZ complex) cannot be precisely determined without separating AZ from ODC or AIn1 (17).

3.4.1. Preparation of Mouse Kidney ODC

1. ODC is induced in mice kidney by single subcutaneous injection of testosterone enanthate (25 mg/animal) (see Note 10). Five days later, the mice are sacrificed under appropriate anesthesia and the kidneys are removed. All the following procedures are performed at 0–4°C.
2. The kidneys are homogenized with three volumes of homogenizing buffer in a Dounce-type all-glass homogenizer.
3. The homogenate is centrifuged at $100,000 \times g_{\text{max}}$ for 60 min (see Note 11).
4. The supernatant is saved and determine ODC activity as described in Subheading 3.4. Store in single use aliquots at –80°C.

3.4.2. Preparation of Recombinant Antizyme Inhibitor 1 (18)

1. *E. coli* BL21 competent cells are transformed with pGEX-4T-3-AIn1.
2. A colony of transformant is picked up and grown in 10 mL of LB with ampicillin at 37°C overnight with shaking.

3. Dilute the overnight culture 1:10 in fresh LB with ampicillin (100 mL) and grow at 37°C for 1 h with shaking.
4. Add 1 M IPTG to a final concentration of 1 mM and continue to shake for 2 h.
5. Chill the culture on ice, centrifuge it at 5,000 rpm for 20 min at 4°C, and discard the supernatant. The cell pellet can be stored at -20°C.
6. Resuspend the pellet in 9 mL PBS. Add 1 mL of 10 mg/mL lysozyme, mix by swirling, and incubate the suspension on ice for 60 min.
7. Sonicate the suspension for 30 s with cooling on ice. Repeat sonication 4 times with a 60-s interval.
8. Centrifuge the lysate at 10,000 rpm at 4°C for 20 min. Save clear supernatant.
9. Load the supernatant to a Glutathione-Sepharose 4B column (0.5 mL bed) that has been washed with 4 mL of column buffer. Column operation is carried out in a holder tube placed on ice.
10. Wash the column with column buffer until UV absorbance at 280 nm becomes less than 0.02.
11. Elute AIn1 fusion protein with 10 mM glutathione in column buffer. Collect five fractions of 0.75 mL. The fusion protein is usually eluted within the first three fractions and easily detected by UV absorbance at 280 nm.
12. AIn1 fractions are combined, dialyzed in cold dialyzing buffer overnight. Measure the protein concentration and store in aliquots at -20°C. A fraction with UV absorbance at 280 nm to be 1 approximately corresponds to 1 µg/µL AIn1 and 1 µg of this preparation can release at least 130 units of ODC activity from ODC-AZ complex (see Note 12).

3.4.3. Preparation of Samples for Assay of AZ Activity and ODC-AZ Complex

3.4.3.1. From Cultured Cells

1. Cells attached on a dish are washed with cold PBS 3 times and disrupted by three freeze-thaw cycles.
2. Cold homogenizing buffer is added to the dish (~250 µL/35-mm dish). The cells are collected with a rubber scraper and transferred to a microfuge tube.
3. Sonicate the cell suspension for 20 s with cooling on ice.
4. Centrifuge the tubes at 18,000 × *g* for 20 min at 4°C. Store the supernatant at -20°C.

3.4.3.2. From Animal Tissues

1. Tissue is homogenized in three volume of cold homogenizing buffer containing 1% protease inhibitor cocktail (Complete, Mini, Roche).

2. Centrifuge the homogenate at $10,000 \times g$ for 10 min at 4°C . The supernatant is then ultracentrifuged at $100,000 \times g$ for 1 h at 4°C .
3. Dialyze the supernatant against homogenizing buffer at 4°C overnight. Store at -20°C (see Note 9).

3.4.4. Determination of ODC Inhibiting Activity of AZ

Reaction tubes and all assay solutions are kept on ice until starting reaction.

1. Reaction is carried out in a 2.0-mL Eppendorf tube with a 3MM filter disk (diameter of 9.0 mm) attached to the inside of the cap.
2. (a) Standard assays contain 10 μL of buffer mixture, 0.8–2.0 units of ODC (see Note 13), 20–50 μL of sample (cell or tissue extract), 50 μL of [^{14}C]ornithine solution, and deionized water in a total volume of 125 μL (see Note 14).
(b) Control assay should be included in duplicate where AZ sample is substituted by homogenizing buffer.
(c) Blank assay should be included in duplicate where both ODC and AZ sample are substituted by homogenizing buffer (see Note 15).
3. Put 10 μL KOH to the filter disk inside the cap of each tube.
4. Close the caps and start the reaction by putting the tubes into a 37°C water bath. Incubate the tubes for 60–90 min with shaking.
5. After the reaction, cool the tubes by placing on melting ice. Open the cap, quickly add 50 μL of HCl to the solution, and immediately cap again.
6. Incubate the tubes at 37°C for more than 15 min.
7. In a radioactive fume hood, transfer the filter disks to mini scintillation vial containing 4 mL scintillation fluid with forceps.
8. The vials are shaken and kept at room temperature for 30 min before counting radioactivity with a scintillation counter.
9. AZ activity is calculated as $2 \cdot (b) - 2 \cdot (a)$ (see Note 13).

3.4.5. Determination of ODC–AZ Complex Activity

Reaction tubes and all assay solutions are kept on ice until starting reaction.

1. Reaction is carried out in a 2.0-mL Eppendorf tube with 3MM filter disk (diameter of 9.0 mm) attached to the inside of the cap.
(a) AIn1(+) assays contain 10 μL of buffer mixture, 20–50 μL of sample (cell or tissue extract), recombinant AIn1 (0.1 μg), [^{14}C]ornithine solution, and deionized water in a total volume of 125 μL .

- (b) AIn1(-) assays contain all the components of AIn1(+) assays except recombinant AIn1, which is substituted by homogenizing buffer.
 - (c) Blank assay should be included in duplicate where both sample and recombinant AIn1 are substituted by homogenizing buffer (see Note 15).
2. Put 10 μL of KOH to the filter disk inside the cap of each tube.
 3. Close the caps and start the reaction by putting the tubes into a 37°C water bath. Incubate the tubes for 60–90 min with shaking.
 4. After the reaction, cool the tubes by placing on melting ice. Open the cap, quickly add 50 μL of HCl to the solution, and immediately cap again.
 5. Incubate the tubes at 37°C for more than 15 min.
 6. In a radioactive fume hood, transfer the filter papers to mini scintillation vial containing 4 mL scintillation fluid with forceps.
 7. The vials are kept at room temperature for 30 min with occasional shaking before counting radioactivity with a scintillation counter.
 8. ODC–AZ complex activity is calculated as 2. (a) – 2. (b) (see Note 13).

3.5. In Vitro Assay for Ornithine Decarboxylase Degradation-Promoting Activity of Antizyme

An increase in cellular polyamines induces rapid decay of ODC. AZ plays a key role in the regulation; it is induced by polyamines, binds to ODC subunit to form inactive complex, and triggers ubiquitin-independent degradation of ODC by the 26S proteasome (5). Besides ubiquitin, AZ is the first and most established molecule that signals the degradation target to the 26S proteasome. The in vitro ODC degradation assay has largely contributed to this discovery.

A reaction mixture for in vitro ODC degradation assay contains a source of the 26S proteasomes, labeled ODC, and an ATP-regenerating system. Degradation is usually determined by a decrease in intensity of the ODC band on SDS-PAGE (see Note 16). Although several ODC degradation assay methods have been reported (5, 19–22), we show here methods using a cell extract as the 26S proteasome source, which is suitable to observe effects of AZ on ODC degradation (see Note 17).

3.5.1. Preparation of Labeled ODC

1. Mix the following components in a 1.5-mL microfuge tube placed on ice.
 - (a) 25 μL of TNT Rabbit Reticulocyte Lysate (supplied with the Kit)

- (b) 2 μL of TNT Reaction Buffer (supplied with the Kit)
 - (c) 1 μL of T7 TNT RNA Polymerase (supplied with the Kit)
 - (d) 1 μL of Amino Acid Mixture minus methionine (supplied with the Kit)
 - (e) 2 μL of L-[^{35}S]methionine
 - (f) 1 μL of RNase inhibitor
 - (g) 2 μL of 0.5 $\mu\text{g}/\mu\text{L}$ linear DNA of p9T7ODC71.
 - (h) 16 μL of nuclease-free water (total volume 50 μL).
2. Gently mix the content by pipetting.
 3. Incubate at 30°C for 90 min.
 4. The mixture is used as ^{35}S -labeled ODC. It can be stored at -80°C for 1 week.

3.5.2. Preparation of Recombinant AZ

1. *E. coli* BL21 (DE3) competent cells are transformed with pET-AZ1.
2. A colony of transformant is picked up and grown in 10 mL of LB with ampicillin at 37°C overnight with shaking.
3. Dilute the overnight culture 1:10 in fresh LB with ampicillin (100 mL) and grow at 37°C for 1 h with shaking.
4. Add 1 M IPTG to a final concentration of 1 mM and continue to shake at 37°C for 4 h (see Note 18).
5. Chill the culture on ice, centrifuge it at 6,000 rpm for 15 min at 4°C, and discard the supernatant. The cell pellet can be stored at -20°C.
6. Resuspend the pellet in 10 mL of Buffer A containing 10 mM imidazole. Add 10 mg lysozyme (1 mg/mL), dissolve by swirling, and incubate the suspension on ice for 60 min.
7. Sonicate the suspension for 30 s with cooling on ice. Repeat sonication 4 times with a 60 s interval.
8. Centrifuge the lysate at 100,000 $\times g$ at 4°C for 30 min.
9. Load the supernatant to a Ni-NTA Agarose column (0.5 mL bed), which has been equilibrated with Buffer A containing 10 mM imidazole.
10. Wash the column with 10 bed volumes of Buffer A containing 20 mM imidazole.
11. Wash the column with 10 bed volumes of Buffer A containing 30 mM imidazole.
12. Elute His-tagged AZ1 protein in four fractions each with 0.5 mL of Buffer A containing 250 mM imidazole.

13. Check the yield and purity of each fraction by SDS-PAGE.
14. Fractions with His-tagged recombinant AZ1 are combined and dialyzed in cold dialysis buffer overnight. Measure the protein concentration and store in aliquots at -20°C .

3.5.3. Preparation of a Cell Extract for ODC Degradation

1. HTC cells are grown to subconfluence in culture medium in 100 mm dishes. *Do not overgrow the cells.*
2. Replace the medium with a fresh medium and incubate the cells for 2.5 h. This step reduces the endogenous level of AZ in the cells.
3. Wash the cells twice with ice-cold PBS. Place the dishes on ice and drain the PBS completely.
4. Disrupt the cells by three cycles of freeze–thawing. One cycle of freeze–thawing is done by placing the drained dishes in -20°C freezer for 5 min, place on a bench (room temperature) briefly until the cells are thawed, and place them back on ice.
5. Add 0.2 mL of ice-cold homogenizing buffer per 100 mm dish.
6. Using a cell scraper and a micropipette, collect the cells into a microfuge tube.
7. Centrifuge the tube at $14,000\times g_{\text{max}}$ for 20 min.
8. Collect the supernatants as a cell extract.
9. Determine the protein concentration.
10. The cell extract should be prepared fresh for each experiment.

3.5.4. ODC Degradation Assay

1. Assay mixture contains 1 μL of 0.1 M ATP, 1 μL of 125 mM DTT, 1 μL of 0.5 M MgCl_2 , 1 μL of 1.5 M Tris–HCl, pH 7.5, 1 μL of 1 M phosphocreatine, 1 μL of 10 mg/mL creatine kinase, HTC cell extract containing 20–30 μg protein, 0.8 μL ^{35}S -labeled ODC, and up to 15 ng of recombinant AZ in a total volume of 50 μL .
2. 15 μL aliquots of the assay mixture are incubated at 37°C for 30 or 60 min. Save an aliquot without incubation (time zero sample).
3. After the incubation, add 5 μL of sample buffer (4 \times) to the tube.
4. Heat the tube at 100°C for 5 min.
5. Centrifuge the mixture at 15,000 rpm for 30 s and the whole supernatant is subjected to SDS-PAGE using 11% separating gel and 3% stacking gel.
6. After electrophoresis, the gel is fixed and dried using a gel dryer.

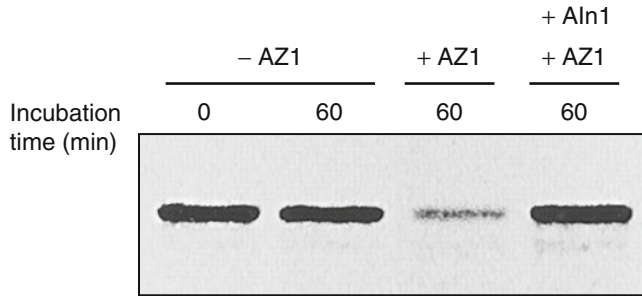


Fig. 3. Antizyme-dependent degradation of ODC by cell extracts. [^{35}S]Methionine-labeled ODC was incubated with an HTC cell extract supplemented with ATP-regenerating system in the absence (*lane 2*) or the presence (*lane 3*) of recombinant AZ1, or in the presence of both AZ and AIn1 (*lane 4*) at 37°C for 60 min. The reaction mixtures were subjected to SDS-PAGE, and labeled ODC on the dried gel was visualized with a FLA 2000 image analyzer. *Lane 1* is a time zero control. In this experiment, nontagged product from a partial-length rat AZ1 cDNA was immunoaffinity purified and used as the recombinant AZ1, instead of His-tagged AZ1 described in the text. Modified from ref. (18).

- The labeled ODC protein is detected and quantified using a FLA-2000 image analyzer (Fujifilm).
- Figure 3 shows a typical result of an experiment to determine effects of AZ1 on ODC degradation. Antizyme inhibitor 1 (AIn1) is used to confirm that the ODC degradation is caused by AZ (see Note 19).

3.6. Cell Culture Assay for Ornithine Decarboxylase Degradation-Promoting Activity of Antizyme

This subchapter describes an assay of AZ activity to promote degradation of ODC in suspension 293-F cells cotransfected with AZ and ODC. This method is nonradioisotopic. Use of suspension culture has advantage over adherent cells as it allows us to take samples at several time points from the same culture. This method is also useful to investigate candidates for degradation targets of AZ other than ODC.

3.6.1. Cell Culture

- Suspension 293-F cells are maintained in a 125-mL polycarbonate sterile vented cap Erlenmeyer flask containing 10 mL of prewarmed FreeStyle 293 Expression Medium at 37°C with rotary shaking in a CO₂ incubator with a humidified atmosphere of 5% CO₂ in air.
- Transfer aliquot of suspension to a 125-mL Erlenmeyer flask. Grow the cells until the viable cell number reaches 3×10^6 /mL.
- On the day of transfection, check the cell viability using the trypan blue dye exclusion method. The cell viability must be over 90%. In addition, most of the cell should be suspended singly, not forming clumps.

3.6.2. *Transfection*

1. The 293-F cells are diluted to 1×10^6 /mL and divided into three 10-mL cultures in 125 mL Erlenmeyer flasks.
2. Dispense in three microfuge tubes the following plasmid DNA(s).
 - (a) 5 μ g of pCMV-HA-ODC (control) DNA
 - (b) 5 μ g each of pCMV-HA-ODC and pCMV-HA-AZ1
 - (c) 5 μ g each of pCMV-HA-ODC and pCMV-HA-AZ2
3. Add Opti-MEM I to each tube to make a total volume 333 μ L. Mix gently.
4. Dilute 40 μ L of 293fectin™ with 960 μ L Opti-MEM I. Mix gently and incubate at room temperature for 5 min.
5. Add 333 μ L of the diluted 293fectin™ to each of three diluted DNA solutions. Mix gently.
6. Incubate the mixtures at room temperature for 20–30 min to form DNA-293fectin™ complex (see Note 6).
7. Transfer 660 μ L solution of plasmid DNA-293fectin™ complex to each shaker flask containing the 293-F cell suspension.
8. Incubate the cells in 5% CO₂ with rotary shaking for 24 h.

3.6.3. *ODC Degradation Assay*

1. Twenty-four hour after transfection, cycloheximide is added to the culture at a final concentration 50 μ g/mL. Cells are incubated in the CO₂ incubator with rotary shaking.
2. At designated time points (0, 15, 30, 45 min or 0, 30, 60, 90 min), each 2 mL of cells are transferred to microfuge tubes and centrifuged at 1,800 rpm for 3 min.
3. Remove the supernatant and the tubes with the cell pellets are placed on ice until sampling has finished. The samples can be stored at –80°C.

3.6.4. *Immunoprecipitation and Immunoblot Analyses*

1. Add 300 μ L of M-PER mammalian protein extraction reagent (supplied with ProFound Mammalian HA Tag IP/Co-IP Kit) to the cell pellets and gently suspend the cells with pipetting.
2. Gently shake the samples at room temperature for 15 min.
3. Gently pipette the cells again.
4. Centrifuge the tubes at $2,000 \times g$ at 4°C for 25 min to remove cell debris.
5. Transfer the supernatants (cell lysates) to new microfuge tubes. Determine protein concentration of cell lysates with the Bradford assay using bovine serum albumin as standard.
6. Attach the bottom plugs on the Handee Mini-Spin Columns (supplied with the kit). Add appropriate amount of cell lysate containing 500–800 μ g protein to the spin column.
7. Resuspend the anti-HA agarose (supplied with the kit) by inverting the vial several times (do not vortex) (see Note 20).

8. Dispense 6 μ L of anti-HA agarose slurry (containing 10 mg anti-HA antibody) into each spin column using wide-bore pipette tip. Screw on the cap.
9. Incubate with gentle rotating for 2 h to overnight at 4°C.
10. Loosen the top cap on the column and then remove bottom plug. Place a collection tube under the column and centrifuge at 5,000 rpm for 10 s. Discard the flow-through.
11. Add 0.5 mL of TBS-T to each column and screw on the cap. Invert the column 2–3 times.
12. Repeat step 10.
13. Repeat step 11–12 twice more.
14. Place the spin column on a new collection tube. Add 25 μ L of 2 \times Nonreducing Sample Buffer (prepare from ImmunoPure Lane Maker Nonreducing Sample Buffer (5 \times), supplied with the kit) to the column. Screw on the cap and gently tap the tube to mix.
15. Heat the spin column with the collection tube at 95°C on heat block for 5 min. Centrifuge the column with the collection tube at 5,000 rpm for 10 s (see Note 21).
16. Add 2–3 μ L of 1 M DTT to the 25 μ L sample for SDS-PAGE.
17. Apply the immunoprecipitated samples to 12.5% SDS-PAGE gel.
18. After electrophoresis, proteins are electroblotted to a PVDF membrane with transfer buffer by a semidry blotting apparatus (Constant current: 2 mA/cm², 90 min).
19. Detect the ODC band using ECL Plus Western Blotting Detection System. Dilution of the primary antibody (Anti-HA) is 1:2,000 and the secondary antibody (Antirabbit IgG-conjugated horseradish peroxidase) is 1: 20,000. See ECL Plus Western Blotting Detection manual for details.
20. A result is shown in Fig. 4.

3.7. Inhibition of Polyamine Transport by Antizyme

Uptake of extracellular polyamines by mammalian cells is under negative feedback regulation of cellular polyamines (23) and inhibited by overexpressed AZ (24, 25). However, no mammalian polyamine transporter that is regulated by AZs has been discovered to date. In this chapter, we describe an experiment to quickly test the activity of transfected AZ on spermidine uptake in FreeStyle 293-F cells using [¹⁴C]spermidine.

3.7.1. Cell Culture

1. Suspended 293-F cells are maintained in a 125-mL polycarbonate sterile vented cap Erlenmeyer flask containing 10 mL of prewarmed FreeStyle 293 Expression Medium at 37°C with rotary shaking in a CO₂ incubator with a humidified atmosphere of 5% CO₂ in air.

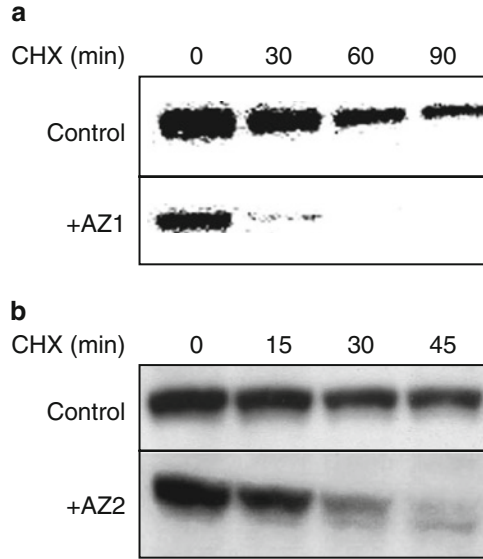


Fig. 4. Stimulation of ODC degradation by antizyme in transfected cultured cells. Suspension 293-F cells were transfected with pCMV-HA-ODC alone or together with either pCMV-HA-AZ1 (a) or pCMV-HA-AZ2 (b). Cycloheximide (CHX) was added to the medium 24 h after transfection and cells were collected at the indicated times. ODC protein was detected on immunoblotting with anti-HA antibody.

3.7.2. Transfection of 293-F Cells

2. Transfer aliquot of suspension to three Erlenmeyer flasks. Grow the cells until the viable cell number reaches 3×10^6 /mL.
 3. On the day of transfection, check the cell viability using the trypan blue dye exclusion method. The cell viability must be over 90%. In addition, most of the cell should be suspended singly, not forming clumps.
1. The 293-F cells are diluted to 1×10^6 /mL and divided into three 5-mL cultures in Erlenmeyer flasks.
 2. Dispense in three microfuge tubes the following plasmid DNA(s).
 - (a) 5 μ g of pd2EGFP-N1 (control) DNA
 - (b) 5 μ g of pCMV-HA-AZ1
 - (c) 5 μ g of pCMV-HA-AZ2
 3. Add Opti-MEM I to each tube to make a total volume 166 μ L. Mix gently.
 4. Dilute 20 μ L of 293fectin™ with 480 μ L Opti-MEM I. Mix gently and incubate at room temperature for 5 min.
 5. Add 166 μ L of the diluted 293fectin to each of three diluted DNA solutions. Mix gently.
 6. Incubate the mixtures at room temperature for 20–30 min to form DNA-293fectin complex (see Note 22).

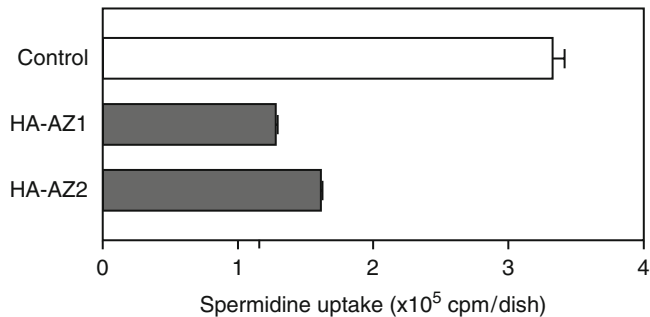


Fig. 5. Inhibition of polyamine uptake by AZs. Suspension 293-F cells were transfected with pd2EGFP-N1 (control), pCMV-HA-AZ1, or pCMV-HA-AZ2. Twenty-four hours later, aliquots of the cells were transferred to dishes and [¹⁴C]spermidine was added. After incubation at 37°C for 30 min, cells were washed with cold PBS, lysed with 0.1% SDS, and counted for radioactivity. Transport activities were expressed as cpm/dish.

7. Transfer 330 μ L solution of plasmid DNA-293fectin complex to each shaker flask containing the 293-F cell suspension.
8. Incubate the cells at 37°C in the CO₂ incubator with rotary shaking for 24 h.

3.7.3. Assay of Spermidine Uptake

1. Twenty-four hours after transfection, 2 mL of suspension cells in flask is transferred to 60 mm dishes in duplicate.
2. Add 18.5 kBq of [¹⁴C]spermidine to the medium. The final concentration of total spermidine in the medium becomes 2.25 μ M.
3. Place the dish at 37°C in a CO₂ incubator with a humidified atmosphere of 5% CO₂ in air for 30 min.
4. Harvest the cells by centrifugation at 1,800 rpm, 4°C for 3 min (see Note 23).
5. Wash the cells with ice-cold PBS 5 times. Polyamine uptake is terminated by this washing.
6. Cells are lysed with 0.1 mL/dish of 0.1% SDS and whole amount of lysate is mixed with 4 mL of toluene-based scintillation fluid.
7. Radioactivity is determined in a scintillation counter. Uptake activity is designated as cpm/dish (Fig. 5).

4. Notes

1. The in-frame construct is a mutant lacking the T-base of the TGA (UGA in RNA) triplet at the frameshift site. It serves as a size marker of the frameshift product and as a control to

- estimate frameshift efficiency. When introduced into cells, an in-frame AZ construct is expressed constitutively, i.e., regardless of the cellular polyamine levels.
2. If the sensitivity of Western blot analysis is insufficient, AZ can be concentrated with immunoprecipitation. However, AZ comigrates with immunoglobulin light chain on SDS-PAGE. To avoid interference, it is recommended to use commercially available horseradish peroxidase-conjugated secondary antibody that does not detect reduced and denatured immunoglobulin in the blot (TrueBlot, eBioscience).
 3. Commercially available rabbit reticulocyte lysate contains variable concentrations of polyamines ranging 0–0.1 mM putrescine, 0.3–0.7 mM spermidine, and 0–0.05 mM spermine. Dose dependency of frameshift stimulation is thereby variable. The sensitivity to polyamines can be increased by removal of polyamines from the lysate with gel-filtration (26).
 4. Alternatively, the products can be concentrated by immunoprecipitation with a specific antibody before SDS-PAGE (4).
 5. Nonframeshift products are too small (less than 7 kDa) to be detected on SDS-PAGE. If detection of both frameshift and nonframeshift products is desired, another gene (such as the coat protein of brome mosaic virus or rabbit β -globin) is fused to the 5' of AZ1 gene (4).
 6. Longer incubation may result in a decreased activity.
 7. Anti-FLAG M2 affinity resin must be equilibrated with TBS-T before use. See instructions of Anti-FLAG M2 Affinity Agarose Gel (Sigma).
 8. Phosphorylated AZ2 migrates slightly slowly than unphosphorylated AZ2. If running time of SDS-PAGE is prolonged by 50%, the two products may be separated on a mini gel.
 9. ODC activity is affected by various substances in extracts. AZ samples are preferably dialyzed or gel-filtered before assay to remove possible interfering substances, such as salts (>0.1 M), ornithine and arginine (27). It is also recommended that in order to conclude that an ODC inhibiting activity is AZ, several criteria for AZ activity are confirmed. For example, AZ activity is stoichiometric (showing a linear dose-inhibition curve), time-independent, heat-labile, and sensitive to AIn1 and protease. In addition, AZ in biological sources should be induced by polyamines (13, 14).
 10. Renal ODC activities in male mice exhibited strain-dependent variation (28). We have successfully obtained kidney extracts with ODC activity of >5 units/ μ L from male ICR and C57BL/6J mice with this protocol. Kidney extracts from untreated, regularly fed male mice have ODC activity of 1–5 units/ μ L and may be used for the same purpose.

11. ODC is labile in kidney homogenate, but stable in postmitochondrial supernatants for up to 5 years at -80°C .
12. His-tagged AIn1 proteins work as well as the GST-AIn1 fusion protein.
13. Unit definitions: One unit of ODC activity is the amount producing 1 nmol of CO_2/h at 37°C under the specified conditions. One unit of AZ activity is the amount inhibiting 1 unit of ODC. One unit of ODC-AZ complex activity is the amount causing an increase of 1 unit of ODC activity upon addition of AIn1.
14. The amount of AZ added to the assay should be kept low enough to cause less than 75% inhibition since the dose-inhibition curve beyond this range is not linear.
15. Background radioactivity is usually 30–50 cpm. A high background may be lowered by heating [^{14}C]ornithine solution at 95°C for 5 min in a radioactive fume hood.
16. Using purified labeled ODC, degradation can also be monitored by a decrease in a TCA-insoluble radioactivity or an increase in released TCA-soluble radioactivity (5, 20).
17. The ODC degradation rate correlates well with AZ/ODC ratio in cultured cells, animal tissues, and in vitro degradation system (19). Some proteasome or ODC sources, such as fresh rabbit reticulocyte lysate, contain a high level of endogenous AZ and therefore are not suitable for measuring effects of exogenous AZ (22).
18. When this method is applied to AZ2, it is recommended to perform the induction culture at 25°C for 8 h or at 18°C overnight since 6×His-tagged AZ2 expressed in *E. coli* tends to form insoluble aggregates at 37°C .
19. To confirm that the stimulation of ODC degradation is caused by AZ, pretreatment of the extract or reticulocyte lysate with an anti-AZ antibody is also useful (20).
20. If immunoprecipitation is carried out with a standard protocol, it is recommended to use a secondary antibody specific to the native disulfide-form of IgG (Rabbit TrueBlot™ Horseradish Peroxidase antirabbit IgG, eBioscience).
21. The use of 2× Nonreducing Sample Buffer eliminates coeluting antibody. This step is important to detect ODC protein because the molecular weight of ODC is close to that of immunoglobulin heavy chain.
22. Longer incubation may result in decreased activity.
23. Parallel incubation at 0°C (on ice) is often used as a control (23), but background radioactivity under this condition is almost negligible.

Acknowledgment

The authors thank Dr. Jun-ichi Suzuki for providing detailed protocols.

References

- Hayashi S, Murakami Y, Matsufuji S (1996) Ornithine decarboxylase antizyme: a novel type of regulatory protein. *Trends Biochem Sci* 21:27–30
- Coffino P (2001) Regulation of cellular polyamines by antizyme. *Nat Rev Mol Cell Biol* 2:188–194
- Ivanov IP, Atkins JF (2007) Ribosomal frameshifting in decoding antizyme mRNAs from yeast and protists to humans: close to 300 cases reveal remarkable diversity despite underlying conservation. *Nucleic Acids Res* 35:1842–1858
- Matsufuji S, Matsufuji T, Miyazaki Y, Murakami Y, Atkins JF, Gesteland RF, Hayashi S (1995) Autoregulatory frameshifting in decoding mammalian ornithine decarboxylase antizyme. *Cell* 80:51–60
- Murakami Y, Matsufuji S, Kameji T, Hayashi S, Igarashi K, Tamura T, Tanaka K, Ichihara A (1992) Ornithine decarboxylase is degraded by the 26S proteasome without ubiquitination. *Nature* 360:597–599
- Matsufuji S, Miyazaki Y, Kanamoto R, Kameji T, Murakami Y, Baby TG, Fujita K, Ohno T, Hayashi S (1990) Analyses of ornithine decarboxylase antizyme mRNA with a cDNA cloned from rat liver. *J Biochem* 108:365–371
- Murai N, Shimizu A, Murakami Y, Matsufuji S (2009) Subcellular localization and phosphorylation of antizyme 2. *J Cell Biochem* 108:1012–1021
- Van Steeg H, Van Oostrom CT, Hodemaekers HM, Peters L, Thomas AA (1991) The translation in vitro of rat ornithine decarboxylase mRNA is blocked by its 5' untranslated region in a polyamine-independent way. *Biochem J* 274:521–526
- Granner D, Chase LR, Aurbach GD, Tomkins GM (1968) Tyrosine aminotransferase: enzyme induction independent of adenosine 3', 5'-monophosphate. *Science* 162:1018–1020
- Howard MT, Shirts BH, Zhou J, Carlson CL, Matsufuji S, Gesteland RF, Weeks RS, Atkins JF (2001) Cell culture analysis of the regulatory frameshift event required for the expression of mammalian antizymes. *Genes Cells* 6:931–941
- Petros LM, Howard MT, Gesteland RF, Atkins JF (2005) Polyamine sensing during antizyme mRNA programmed frameshifting. *Biochem Biophys Res Commun* 338:1478–1489
- Suzuki J, Murakami Y, Samejima K, Kohda K, Ohtani M, Oka T (2009) Antizyme is necessary for conversion of pancreatic tumor cells into glucagon-producing differentiated cells. *Endocr Relat Cancer* 16:649–659
- Heller JS, Fong WF, Canellakis ES (1976) Induction of a protein inhibitor to ornithine decarboxylase by the end products of its reaction. *Proc Natl Acad Sci USA* 73:1858–1862
- Hayashi S, Fujita K (1983) Antizyme and antizyme inhibitor of ornithine decarboxylase (rat liver). *Methods Enzymol* 94:185–193
- Kitani T, Fujisawa H (1984) Purification and some properties of a protein inhibitor (antizyme) of ornithine decarboxylase from rat liver. *J Biol Chem* 259:10036–10040
- Fujita K, Murakami Y, Hayashi S (1982) A macromolecular inhibitor of the antizyme to ornithine decarboxylase. *Biochem J* 204:647–652
- Murakami Y, Matsufuji S, Nishiyama M, Hayashi S (1989) Properties and fluctuations in vivo of rat liver antizyme inhibitor. *Biochem J* 259:839–845
- Murakami Y, Ichiba T, Matsufuji S, Hayashi S (1992) Cloning of antizyme inhibitor, a highly homologous protein to ornithine decarboxylase. *J Biol Chem* 271:3340–3342
- Murakami Y, Tanaka K, Matsufuji S, Miyazaki Y, Hayashi S (1992) Antizyme, a protein induced by polyamines, accelerates the degradation of ornithine decarboxylase in Chinese-hamster ovary-cell extracts. *Biochem J* 283:661–664
- Kanamoto R, Kameji T, Iwashita S, Igarashi K, Hayashi S (1993) Spermidine-induced destabilization of ornithine decarboxylase (ODC) is mediated by accumulation of antizyme in ODC-overproducing variant cells. *J Biol Chem* 268:9393–9399
- Mamroud-Kidron E, Omer-Itscovich M, Bercovich Z, Tobias KE, Rom E, Kahana C (1994) A unified pathway for the degradation of ornithine decarboxylase in reticulocyte lysate requires interaction with the

- polyamine-induced protein, ornithine decarboxylase antizyme. *Eur J Biochem* 226:547–554
22. Murakami Y, Matsufuji S, Tanaka K, Ichihara A, Hayashi S (1993) Involvement of the proteasome and antizyme in ornithine decarboxylase degradation by a reticulocyte lysate. *Biochem J* 295:305–308
 23. Lessard M, Zhao C, Singh SM, Poulin R (1995) Hormonal and feedback regulation of putrescine and spermidine transport in human breast cancer cells. *J Biol Chem* 270:1685–1694
 24. Suzuki T, He Y, Kashiwagi K, Murakami Y, Hayashi S, Igarashi K (1994) Antizyme protects against abnormal accumulation and toxicity of polyamines in ornithine decarboxylase-overproducing cells. *Proc Natl Acad Sci USA* 91:8930–8934
 25. Mitchell JL, Judd GG, Bareyal-Leyser A, Ling SY (1994) Feedback repression of polyamine transport is mediated by antizyme in mammalian tissue-culture cells. *Biochem J* 299:19–22
 26. Ohnishi R, Nagami R, Hirose S, Igarashi K (1985) Methylglyoxal bis(guanylhydrazone) elimination of polyamine effects on protein synthesis. *Arch Biochem Biophys* 242:263–268
 27. Obenrader MF, Prouty WF (1977) Production of monospecific antibodies to rat liver ornithine decarboxylase and their use in turnover studies. *J Biol Chem* 252:2866–2872
 28. Melanitou E, Cohn DA, Bardin CW, Jänne OA (1987) Genetic variation in androgen regulation of ornithine decarboxylase gene expression in inbred strains of mice. *Mol Endocrinol* 1:266–273
 29. Kilpeläinen P, Rybnikova E, Hietala O, Pelto-Huikko M (2000) Expression of ODC and its regulatory protein antizyme in the adult rat brain. *J Neurosci Res* 62:675–685
 30. Levillain O, Greco A, Diaz JJ, Augier R, Didier A, Kindbeiter K, Catez F, Cayre M (2003) Influence of testosterone on regulation of ODC, antizyme, and N^1 -SSAT gene expression in mouse kidney. *Am J Physiol Renal Physiol* 285:F498–F506
 31. Hoshino K, Momiyama E, Yoshida K, Nishimura K, Sakai S, Toida T, Kashiwagi K, Igarashi K (2005) Polyamine transport by mammalian cells and mitochondria: role of antizyme and glycosaminoglycans. *J Biol Chem* 280:42801–42808
 32. Liao CP, Lasbury ME, Wang SH, Zhang C, Durant PJ, Murakami Y, Matsufuji S, Lee CH (2009) *Pneumocystis* mediates overexpression of antizyme inhibitor resulting in increased polyamine levels and apoptosis in alveolar macrophages. *J Biol Chem* 284:8174–8184
 33. Mitchell JL, Choe CY, Judd GG, Daghfal DJ, Kurzeja RJ, Leyser A (1996) Overproduction of stable ornithine decarboxylase and antizyme in the difluoromethylornithine-resistant cell line DH23b. *Biochem J* 317:811–816
 34. Mitchell JL, Judd GG, Leyser A, Choe C (1998) Osmotic stress induces variation in cellular levels of ornithine decarboxylase-antizyme. *Biochem J* 329:453–459
 35. Tsuji T, Usui S, Aida T, Tachikawa T, Hu GF, Sasaki A, Matsumura T, Todd R, Wong DT (2001) Induction of epithelial differentiation and DNA demethylation in hamster malignant oral keratinocyte by ornithine decarboxylase antizyme. *Oncogene* 20:24–33
 36. Newman RM, Mobascher A, Mangold U, Koike C, Diah S, Schmidt M, Finley D, Zetter BR (2004) Antizyme targets cyclin D1 for degradation. A novel mechanism for cell growth repression. *J Biol Chem* 279:41504–41511
 37. Mangold U, Hayakawa H, Coughlin M, Mürnger K, Zetter BR (2008) Antizyme, a mediator of ubiquitin-independent proteasomal degradation and its inhibitor localize to centrosomes and modulate centriole amplification. *Oncogene* 27:604–613
 38. Kankare K, Uusi-Oukari M, Jänne OA (1997) Structure, organization and expression of the mouse ornithine decarboxylase antizyme gene. *Biochem J* 324:807–813
 39. Gritli-Linde A, Nilsson J, Bohlooly-Y M, Heby O, Linde A (2001) Nuclear translocation of antizyme and expression of ornithine decarboxylase and antizyme are developmentally regulated. *Dev Dyn* 220:259–275
 40. Schipper RG, Cuijpers VM, De Groot LH, Thio M, Verhofstad AA (2004) Intracellular localization of ornithine decarboxylase and its regulatory protein, antizyme-1. *Histochem Cytochem* 52:1259–1266
 41. Feith DJ, Shantz LM, Pegg AE (2001) Targeted antizyme expression in the skin of transgenic mice reduces tumor promoter induction of ornithine decarboxylase and decreases sensitivity to chemical carcinogenesis. *Cancer Res* 61:6073–6081
 42. Feith DJ, Origanti S, Shoop PL, Sass-Kuhn S, Shantz LM (2006) Tumor suppressor activity of ODC antizyme in MEK-driven skin tumorigenesis. *Carcinogenesis* 27:1090–1098
 43. Wang X, Feith DJ, Welsh P, Coleman CS, Lopez C, Woster PM, O'Brien TG, Pegg AE (2007) Studies of the mechanism by which increased spermidine/spermine N^1 -acetyltransferase activity increases susceptibility to skin carcinogenesis. *Carcinogenesis* 28:2404–2411

44. Tosaka Y, Tanaka H, Yano Y, Masai K, Nozaki M, Yomogida K, Otani S, Nojima H, Nishimune Y (2000) Identification and characterization of testis specific ornithine decarboxylase antizyme (OAZ-t) gene: expression in haploid germ cells and polyamine-induced frameshifting. *Genes Cells* 5:265–276
45. Matsufuji S, Kanamoto R, Murakami Y, Hayashi S (1990) Monoclonal antibody studies on the properties and regulation of murine ornithine decarboxylase antizymes. *J Biochem* 107:87–91
46. Murakami Y, Suzuki J, Samejima K, Kikuchi K, Hasilowicz T, Murai N, Matsufuji S, Oka T (2009) The change of antizyme inhibitor expression and its possible role during mammalian cell cycle. *Exp Cell Res* 315:2301–2311
47. Murakami Y, Suzuki J, Samejima K, Oka T (2010) Developmental alterations in expression and subcellular localization of antizyme and antizyme inhibitor and their functional importance in the murine mammary gland. *Amino Acids* 38:591–601
48. Gandre S, Bercovich Z, Kahana C (2002) Ornithine decarboxylase-antizyme is rapidly degraded through a mechanism that requires functional ubiquitin-dependent proteolytic activity. *Eur J Biochem* 269:1316–1322
49. Gandre S, Bercovich Z, Kahana C (2003) Mitochondrial localization of antizyme is determined by context-dependent alternative utilization of two AUG initiation codons. *Mitochondrion* 2:245–256

Identification, Assay, and Functional Analysis of the Antizyme Inhibitor Family

Chaim Kahana

Abstract

Polyamines are small aliphatic polycations present in all living cells. Polyamines are involved in regulating fundamental cellular functions and are absolutely essential for the process of cellular proliferation. Because they fulfill essential cellular functions, their intracellular concentration is tightly regulated via a unique autoregulatory circuit that responds to the intracellular concentration of polyamines. In the heart of this circuit is a small protein called antizyme (Az), whose synthesis is stimulated by polyamines. Az inactivates Ornithine decarboxylase [(ODC), the first key enzyme in the polyamine biosynthetic pathway] and marks it for ubiquitin-independent degradation by the 26S proteasome. In addition, Az inhibits uptake of polyamines via a yet unresolved mechanism. Az itself is subjected to regulation by an ODC-related protein termed antizyme inhibitor (AzI). AzI is highly homologous to ODC, but it lacks ornithine decarboxylating activity. Since its affinity to Az is greater than the affinity Az has for ODC, it rescues ODC from degradation and enables polyamines uptake into the cell.

Key words: Ornithine decarboxylase, Antizyme, Antizyme inhibitor, Polyamines

1. Introduction

The polyamines spermidine and spermine, and their precursor, putrescine, are positively charged aliphatic amines. Polyamines are implicated in regulating a variety of cellular processes including ion channel function, DNA folding and replication, transcription, translation and apoptosis, and most notably, they are essential for the process of cellular proliferation (1–4). All cells have the ability to synthesize polyamines, and most cells can also absorb polyamines from their environment by transporting them across the plasma membrane. L-Ornithine decarboxylase (ODC) is the first rate-limiting enzyme in the biosynthesis pathway of polyamines. ODC is a highly regulated enzyme whose activity is induced by

growth promoting stimuli. ODC, which is one of the most rapidly degraded mammalian proteins, is degraded without requiring ubiquitination (5, 6). Instead, a small polyamine-induced protein termed antizyme binds to transient ODC monomeric subunits, preventing their reassociation to form active homodimer and targets them to proteasomal degradation. Antizyme (Az) reduces cellular polyamine pools not only by stimulating ODC degradation but also by interfering with the uptake of external polyamines via a yet unknown mechanism (7–9). Interestingly, an ODC-related protein termed antizyme-inhibitor (AzI) acts as an additional regulator of this pathway, as it negates these two activities of Az. This protein, that lacks ornithine decarboxylating activity, binds Az with higher affinity than ODC, thus saving ODC from degradation (10). Methods for the detection and for assaying Az and AzI activities and for the detection of target proteins affected by these activities are described here.

2. Materials

2.1. Cell Culture Conditions

1. Dulbaco's Modified Eagle's medium (DMEM, Gibco/BRL), supplemented with 10% fetal bovine serum (Sigma).
2. RIPA buffer for cell lysis prior to electrophoretic fractionation: 150 mM NaCl, 0.5% sodium deoxycholate, 0.1% SDS, 50 mM Tris-HCl, pH 8.0, and protease inhibitors cocktail (Sigma) (see Note 1).

2.2. SDS-Polyacrylamide Gel Electrophoresis (SDS-PAGE)

1. Lower (separating) buffer (4×): 1.5 M Tris-HCl pH 8.8, 0.4% SDS. Adjust pH with HCl.
2. Upper (stacking) buffer (4×): 0.5 M Tris-HCl pH 6.8, 0.4% SDS. Adjust pH with HCl.
3. 30% Acrylamide/0.8% Bis Acrylamide (37.5:1): Dissolve 150 g Acrylamide and 4 g Bis-Acrylamide in water (final volume 500 ml) (see Note 2).
4. *N,N,N,N*'-Tetramethyl-ethylenediamine (TEMED) (see Note 3).
5. 10% ammonium persulfate in water (see Note 4).
6. Running buffer (10×): 250 mM Tris-HCl, 1.92 M glycine, 1% SDS.
7. Sample buffer (2×): 125 mM Tris-HCl pH 6.8, 4% w/v SDS, 1.4 M β-mercaptoethanol, 20% v/v Glycerol, a pinch of Bromophenol blue.

2.3. Western Blot Analysis

1. Transfer buffer: 25 mM Tris-HCl, 192 mM glycine, 20% methanol (see Note 5).

2. Nitrocellulose membrane 0.45 μm , Whatman GmbH.
3. Blocking buffer: 10% low fat (1%) milk, 0.1% tween-20 in 1 \times phosphate buffered saline (PBS).

2.4. Degradation Reaction

1. Reticulocyte lysate (Promega biotech)
2. 1 M Tris-HCl pH 7.5
3. 50 mM DTT (kept frozen)
4. 100 mM MgCl_2
5. 10 mM ATP (kept frozen)
6. 500 mM creatine phosphate
7. 40 mg/ml Creatine phosphokinase

2.5. Ornithine Decarboxylase Activity Assay

1. 1 M Tris-HCl pH 7.5
2. 0.1 M DTT
3. 0.2 M EDTA
4. 20 mM pyridoxal phosphate (PLP)
5. 10 mM L-ornithine
6. ^{14}C -ornithine

2.6. Polyamine Uptake Assay

1. Hank's Buffered Salt Solution (HBSS)
2. MHBSS: 10 mM HEPES in HBSS. pH adjusted to 7.4 with NaOH
3. 10 mM spermidine
4. Radioactive 100 μM spermidine stock: 25 μl [^3H]spermidine (36 Ci/mmol), 50 μl 10 mM spermidine, 4,925 μl MHBSS

3. Methods

The ability of Az and AzI to stimulate protein degradation can be determined both *in vitro* (in a degradation reactions) and *in vivo* in intact cells, while their ability to affect polyamine transport across the plasma membrane can be monitored only in intact cells. The two experimental systems enable not only monitoring the ability of Az and AzI to affect ODC degradation but also enable assessing their effect on the degradation of other proteins that like ODC may be targeted to degradation by Az.

3.1. Preparation of Expression Plasmids and Expression of Proteins

1. The first step in performing the degradation assay is the preparation of the tested substrates and regulators. For reasons of convenience and rapidity, we prefer preparing Az, AzI, and the potential substrates by translation *in vitro* in reticulocyte lysate, although bacterially expressed proteins can be used as well.

2. DNA encoding Az, AzI, and the tested substrate proteins are cloned into a plasmid downstream to a promoter that is suitable for in vitro transcription reaction. Usually, we use plasmid containing the T7 promoter, but plasmids containing other promoters such as SP6 or T3 promoters can be used as well.
3. The corresponding proteins are expressed either in a coupled transcription/translation system [a TNT reaction mix (Promega) in the presence of [³⁵S]methionine] or in a standard rabbit reticulocyte system programmed with RNA that was synthesized in vitro using RNA polymerase compatible to the promoter used. The TNT reaction mix is clearly more convenient as the plasmid DNA is added directly without requiring preparation of RNA in a separate reaction. The translation reaction is set up according to the manufacturers' protocol.
4. The successful synthesis of the required proteins is verified by SDS-PAGE followed by visualization using autoradiography or a bioimager.

3.2. SDS-PAGE

1. The provided instructions relate to the use of a Bio-Rad mini gel.
2. Assemble clean glass plates with 1.5-mm thick spacers and prepare a 10% gel (although we usually use a 10% gel, other gel concentrations can be prepared to fit the size of the fractionated proteins).
3. Mix 2.5 ml of 4× lower buffer, with 4.0 ml water, 0.2 ml 50% glycerol, 3.3 ml acrylamide/bis solution, 150 μl ammonium persulfate solution, and 25 μl TEMED.
4. Pour the gel, leaving space for the stacking gel, and overly with water-saturated isobutanol.
5. Prepare the stacking gel by mixing 1.25 ml upper buffer, 0.5 ml acrylamide/bis, 3.25 ml water, 50 μl ammonium persulfate, and 50 μl TEMED.
6. After polymerization of the lower gel, rinse the top of the gel with water, pour the stacking gel and insert the comb.
7. After polymerization of the stacking gel, assemble the gel into the running apparatus and fill the upper and lower chambers with 1× running buffer.
8. Mix equal amount of the protein sample with 5× sample buffer to bring it to 1× sample buffer. Adjust the volumes and load the samples into the individual slots under the running buffer. One slot should be reserved for running molecular weight markers.

3.3. In Vitro Degradation Reaction

1. Aliquots of the ³⁵S-labeled substrate(s) and of Az, AzI, or both are added to a degradation reaction (typically 50 μl reaction) containing 40 mM Tris-HCl, pH 7.5, 5 mM MgCl₂, 2 mM DTT, 0.5 mM ATP, 10 mM phosphocreatine, 1.6 mg/ml creatine phosphokinase, 6 μl of reticulocyte lysate (Promega), and incubated at 37°C for various times. Based on our experience, more than one substrate can be tested simultaneously in the same reaction yielding the relative effect of Az and AzI on each of them.
2. In order to introduce the substrates and the regulators in the desired molar ratio, the radioactivity present in the relevant bands is determined after their translation and divided by the number of their methionine residues. At the end of the degradation reaction, the proteins are resolved by SDS-PAGE, and the radioactivity present in individual bands is determined using a bioimager and used to calculate the degradation rate.
3. Figure 1 demonstrates the ability of Az to stimulate ODC degradation in a reticulocyte lysate-based degradation mix, and the ability of AzI to negate this activity. Figure 2 demonstrates the testing of a potential Az target in comparison to its known substrate ODC in a degradation reaction performed in the presence of Az.

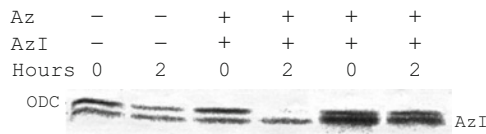


Fig. 1. ODC, Az, and AzI were synthesized in vitro in the presence of ³⁵[S]. ODC was incubated in a reticulocyte lysate-based degradation mix either alone or together with Az or Az+AzI. Following 2 h of incubation at 37°C, the material was fractionated by SDS-PAGE, the gel was dried, and the individual bands were visualized and quantified using a bioimager.

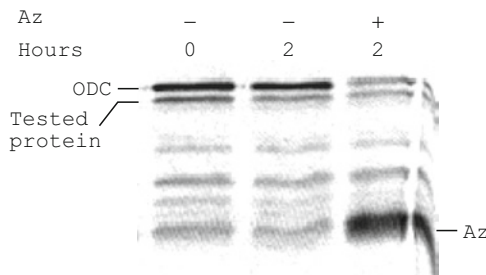


Fig. 2. ODC and another putative substrate protein (tested protein) were synthesized in vitro and incubated in a reticulocyte lysate-based degradation mix in the absence or presence of in vitro synthesized Az. Following 2 h of incubation at 37°C, the material was resolved by SDS-PAGE and individual bands visualized using a bioimager. As can be seen, unlike the degradation of ODC that is stimulated by Az, the degradation of the tested putative substrate was practically unaffected.

3.4. Degradation in Cells

1. DNA encoding Az, AzI, and the tested substrate proteins (ODC or other proteins) are cloned into an expression vector downstream to mammalian promoter (CMV or another promoter). We routinely use a bicistronic vector in which the DNA of interest is cloned as the first open reading frame (ORF), while the second ORF encodes a selectable marker (11). Such a vector enables performing transient transfections as well as selection of stable transfectants.
2. Usually we test Az and AzI activity in 293T or in NIH3T3 cells. DNA is transfected into 293T cells using the calcium phosphate method, while NIH3T3 cells are transfected using the jetPEI™ reagent following the manufacturer's instructions (other transfection reagents can be used). Cells are cotransfected with a vector encoding the tested protein (ODC or another protein) together with vector encoding Az or AzI or both. We usually keep a 1:1 ratio between the effectors and the substrates. The effect of Az or AzI on the degradation rate of the tested protein can be determined by monitoring the level of the tested protein at a given time after transfection (using western blot analysis), or by monitoring the effect of the coexpressed Az or AzI or both on the degradation rate. The rate of degradation can be monitored either by adding cycloheximide (20 µg/ml) to the growth medium and subjecting cellular extracts prepared at various times thereafter to western blot analysis or by performing pulse-chase analysis. As in the case of the *in vitro* degradation reactions, the effect of Az and AzI on the degradation of a tested protein can be evaluated when this protein is cotransfected together with Az or AzI, or both. However, it would be advisable to include also ODC in the transfection mix to provide an internal control of a protein whose degradation is affected by Az and AzI.

Figure 3 demonstrates the testing of the degradation of a potential Az target in comparison to ODC in 293T cells cotransfected with these three proteins.

3.5. Ca-Phosphate-Mediated Transfection

1. Twenty four h before transfection, split cells to a density of 5×10^5 in a 90-mm dish.
2. Add 5–20 mg plasmid DNA (one or a mixture of plasmids) into a 15-ml snap-cap tube, and adjust the volume with H₂O to 455 µl.
3. Add 45 µl of 2.5 M CaCl₂.
4. Add drop-by-drop 500 µl of 2× HBS with frequent mixing.
5. After 1–10 min when the solution became cloudy, add it to the plate and mix into the medium by gentle agitation.

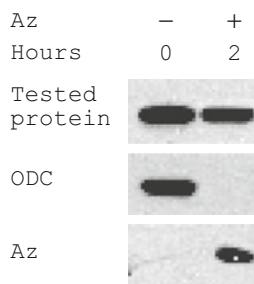


Fig. 3. 293T cells were cotransfected with expression vectors encoding flag-tagged ODC, another putative substrate (tested protein), and Az. Two-days post transfection, cells were harvested, cellular extracts prepared, fractionated by SDS-PAGE, and subjected to western blot analysis using antFLAG antibodies. As is clearly seen, while ODC was completely eliminated, the level of the tested protein suspected as a potential target of Az was practically not affected.

3.6. Western Blot Analysis

1. Cellular extracts are prepared by harvesting cells at various times after the addition of cycloheximide to their growth medium. The cells are washed 3 times with PBS, scrapped into PBS and collected by centrifugation. After aspirating PBS, the cell pellet can be frozen or processed directly.
2. The cell pellet is resuspended and lysed in RIPA buffer for 20 min at 4°C and cellular debris removed by centrifugation. The protein concentration in the supernatant is determined by the Bradford method (using a protein assay kit from Bio-Rad). Aliquots containing 10–100 µg of proteins are fractionated by SDS-PAGE.
3. Soak gel, nitrocellulose filter and six pieces of 3MM paper (cut to the size of the gel), and two sponges in blot buffer for 10 min.
4. Place sponge and three pieces of 3MM on the cathode plate. On top of it place the gel, filter, three additional pieces of 3MM, sponge and the anode plate.
5. Run for 20 min at 10 mA/cm². During the blotting process, the temperature should be kept low (5–10°C). This can be achieved by blotting in a cold room or by placing the blotting tank in ice.
6. Disassemble the running cassette and incubate the filter in blocking buffer on a shaker for 1–16 h at 4°C.
7. The blocking buffer is replaced by a fresh one containing the desired primary antibodies (see Note 6). The dilution at which the antibodies should be used is determined empirically (usually we use dilution of 1:500 up to 1:2,000). The blot is incubated with the antibody for 1 h at room temperature or 16 h at 4°C.

8. The primary antibodies are removed, and the membrane is washed 3 times with PBS-T.
9. Secondary antibody (HRP-conjugated anti-IgG) at a dilution of 1:10,000 is added in blocking buffer and incubated with the membrane for 60 min at room temperature.
10. The secondary antibody is removed, and the membrane is washed 5 times with PBS-T.
11. The blot is developed using an ECL reagent following the manufacturers instructions.

3.7. ODC Activity Assay

Although the most convenient and convincing way to demonstrate induction of Az or AzI activity is by demonstrating their effect on the stability of the ODC protein, frequently the extremely low level of the endogenous ODC protein does not permit its direct detection using western blot analysis. In such a case, it is advisable to follow ODC by monitoring ODC activity.

1. Place plates on ice.
2. Harvest cells into 50 ml tubes, wash 3 times with PBS, transfer into Eppendorf tubes and pellet cells.
3. Resuspend cells in 100–200 μ l ODC activity buffer.
4. Lyse cells by three cycles of freeze/thaw, spin and transfer the supernatant to fresh tube.
5. Determine the amount of protein using the Bradford method.
6. Add 0.5 mg protein to wells of a 96-well microtiter plates. Add 1 μ l 20 mM PLP, 1 μ l [14 C]ornithine (50 mCi/ml: 57 mCi/mmol), and bring with ODC buffer to 100 μ l.
7. Soak a 3MM filter paper and cut to the size of the microtiter plate in freshly prepared saturated solution of BaOH.
8. Dry the paper to a level it remains wet, and cover it with the plate. Place on top of it two more pieces of 3MM and tightly close with the plate cover.
9. Incubate 2–3 h at 37°C.
10. Wash the wet 3MM paper with acetone, air dry, and monitor the trapped [14 C]CO₂ using a bioimager.

3.8. Pulse-Chase Analysis

1. Half an hour before labeling, replace medium to DMEM lacking methionine.
2. Reduce the volume of the medium to the minimal amount that covers the cells and add [35 S]methionine (100 μ Ci/ml) for 10–30 min.
3. Remove the labeling medium, wash with fresh medium and chase with DMEM containing 2% unlabeled methionine.

4. Harvest cells at the desired time points, add sample buffer, incubate 5 min at 90°C, and fractionate by SDS-PAGE.
5. Fix the gel in 10% acetic, dry and visualize protein bands using a bioimager.

3.9. Polyamine Uptake

As in the case of monitoring degradation, cells are transfected with expression vector encoding Az, AzI, or induced to express Az. Uptake activity is then compared between these cells and uninduced cells or cells transfected with empty vector.

1. Plate 10^4 cells in 200 μ l of medium in wells of a 96-well microtiter plate.
2. Fill outer wells with 200 μ l PBS and leave some empty wells for generating protein standard curve.
3. After 24 h, aspirate medium and wash each well with 170 μ l of MHBSS prewarmed to 37°C.
4. Add to each well 50 μ l of the radioactive spermidine stock.
5. Transfer the microtiter plate to a CO₂ incubator and incubate for 5–15 min.
6. At the end of the incubation period, place the microtiter plate on ice, aspirate the radioactive spermidine, and wash 5 times with cold PBS (100 μ l each time).
7. Determine protein concentration by performing a Bradford assay directly on the cells. Use the empty wells to construct a standard curve.
8. Add 100 μ l formic acid to each of the tested wells and to two wells of the standard curve whose protein concentration is close to that of the real samples.
9. Incubate for 10 min at room temperature.
10. Transfer the content of the wells to a scintillation vials. Wash each well with 100 μ l water and add it to the same vials. Add 10 μ l of the radioactive polyamine solution to the two vials containing the Bradford standards.
11. Add to each vial 3 ml scintillation fluid and read radioactivity in a β -counter.

4. Notes

1. All solutions are prepared in double distilled water.
2. Premade Acrylamide-Bis (37.5:1) 30% (w/v) can be obtained.
3. We order small amounts and store it at 4°C.

4. Prepare freshly or store frozen in small aliquots to avoid repeated freezing and thawing.
5. The transfer buffer should be kept cold during the transfer process. The transfer is therefore performed either in a cold room or on ice.
6. The primary antibody can be stored at 4°C in the presence of 0.02% sodium azide and used several times until the signal obtained with a control protein becomes unsatisfactory.

References

1. Childs AC, Mehta DJ, Gerner EW (2003) Polyamine-dependent gene expression. *Cell Mol Life Sci* 60:1394–1406
2. Marton LJ, Pegg AE (1995) Polyamines as targets for therapeutic intervention. *Annu Rev Pharmacol Toxicol* 35:55–91
3. Pegg AE, Feith DJ (2007) Polyamines and neoplastic growth. *Biochem Soc Trans* 35:295–299
4. Pegg AE, Feith DJ, Fong LY, Coleman CS, O'Brien TG, Shantz LM (2003) Transgenic mouse models for studies of the role of polyamines in normal, hypertrophic and neoplastic growth. *Biochem Soc Trans* 31:356–360
5. Bercovich Z, Rosenberg-Hasson Y, Ciechanover A, Kahana C (1989) Degradation of ornithine decarboxylase in reticulocyte lysate is ATP-dependent but ubiquitin-independent. *J Biol Chem* 264:15949–15952
6. Rosenberg-Hasson Y, Bercovich Z, Ciechanover A, Kahana C (1989) Degradation of ornithine decarboxylase in mammalian cells is ATP dependent but ubiquitin independent. *Eur J Biochem* 185:469–474
7. Hoshino K, Momiyama E, Yoshida K, Nishimura K, Sakai S, Toida T, Kashiwagi K, Igarashi K (2005) Polyamine transport by mammalian cells and mitochondria: role of antizyme and glycosaminoglycans. *J Biol Chem* 280:42801–42808
8. Mitchell JL, Judd GG, Bareyal-Leyser A, Ling SY (1994) Feedback repression of polyamine transport is mediated by antizyme in mammalian tissue-culture cells. *Biochem J* 299:19–22
9. Suzuki T, He Y, Kashiwagi K, Murakami Y, Hayashi S, Igarashi K (1994) Antizyme protects against abnormal accumulation and toxicity of polyamines in ornithine decarboxylase-overproducing cells. *Proc Natl Acad Sci U S A* 91:8930–8934
10. Fujita K, Murakami Y, Hayashi S (1982) A macromolecular inhibitor of the antizyme to ornithine decarboxylase. *Biochem J* 204:647–652
11. Hobbs S, Jitrapakdee S, Wallace JC (1998) Development of a bicistronic vector driven by the human polypeptide chain elongation factor 1alpha promoter for creation of stable mammalian cell lines that express very high levels of recombinant proteins. *Biochem Biophys Res Commun* 252:368–372

Chapter 17

Posttranscriptional Regulation of Ornithine Decarboxylase

Shannon L. Nowotarski, Sofia Origanti, and Lisa M. Shantz

Abstract

Activity of the polyamine biosynthetic enzyme ornithine decarboxylase (ODC) and intracellular levels of ODC protein are controlled very tightly. Numerous studies have described ODC regulation at the levels of transcription, translation, and protein degradation in normal cells and dysregulation of these processes in response to oncogenic stimuli. Although posttranscriptional regulation of ODC has been well documented, the RNA binding proteins (RBPs) that interact with ODC mRNA and control synthesis of the ODC protein have not been defined. Using Ras-transformed rat intestinal epithelial cells (Ras12V cells) as a model, we have begun identifying the RBPs that associate with the ODC transcript. Binding of RBPs could potentially regulate ODC synthesis by either changing mRNA stability or rate of mRNA translation. Techniques for measuring RBP binding and translation initiation are described here. Targeting control of ODC translation or mRNA decay could be a valuable method of limiting polyamine accumulation and subsequent tumor development in a variety of cancers.

Key words: Ornithine decarboxylase, Polyamines, RNA stability, Protein synthesis, Translational regulation, Polysome profiles, mRNP assay, AU-rich region, HuR

1. Introduction

Ornithine decarboxylase (ODC) is the first rate-limiting enzyme in the polyamine biosynthetic pathway, converting the amino acid ornithine to the diamine putrescine, which is subsequently used to synthesize the higher polyamines spermidine and spermine (1). Polyamine content, as well as ODC enzyme activity, is tightly regulated in the cell, and ODC is regulated at the levels of transcription, translation, and degradation (1–6). It has been shown that ODC enzyme activity is induced in numerous epithelial cancers, including skin, breast, and colon (7–10). Understanding how ODC synthesis is controlled is crucial in defining the role of high ODC levels in maintaining the transformed phenotype. Our recent studies have used a Ras-transformed rat epithelial cell line (Ras12V cells) to

study posttranscriptional regulation of the ODC mRNA (11). These cells will be used as a model in the methods described here.

Cap-dependent translational regulation of ODC through its long, structured 5'-untranslated region (5'UTR) has been well established, and ODC activity and translation are induced in eIF4E-overexpressing cells (4E-P2 cells) (12, 13). It has also been shown that the presence of the ODC 3'UTR results in decreased synthesis of the ODC protein (14–16). Interestingly, despite extensive study, the RNA-binding proteins (RBPs) that control either ODC translation or stability of the ODC transcript have yet to be described. However, Wang and colleagues have reported a link between changes in intracellular polyamines and posttranscriptional regulation of a variety of mRNAs. It has been found that the RBP human antigen R (HuR) binds to and stabilizes several mRNAs encoding proteins essential for growth control, including p53 and ATF-2, in response to polyamine depletion (17, 18). RBPs generally regulate labile mRNA transcripts by binding to adenosine and uridine-rich elements defined as AREs. These sequences are typically located within the 3'UTR of mRNA (19). One of the best-characterized RBP families is the Hu/ELAV family of proteins, including the ubiquitously expressed HuR protein. HuR binding generally leads to stabilization of its target mRNAs (20). Binding of a second class of proteins, including the zinc finger protein tristetraprolin (TTP) and TIA-1, promotes instability of target messages (20, 21). A third class of RBPs, for example AUF1, can play a role in both stabilization and destabilization (19). In addition to the control of mRNA decay, several RBPs, including HuR and TIA-1, have been shown to modify translation efficiency of their target RNAs as well (22, 23).

Given the extensive posttranscriptional regulation of ODC and the response of RBPs to changes in polyamines, we have undertaken experiments to determine whether RBPs interact with the ODC mRNA itself, and the consequences of this interaction. In order to assay for endogenous binding of RBPs to the ODC transcript, we conduct mRNP assays, in which RBPs are immunoprecipitated under conditions that preserve their association with target mRNAs (17). To examine changes in translation initiation of the ODC mRNA brought about by RBP binding, polysome profiles are performed (24). Examples of results obtained using both of these techniques in Ras12V cells are shown.

2. Materials

2.1. Cell Culture and Cell Extract Preparation

1. 1× phosphate buffer: 14 mM NaCl, 2.7 mM KCl, 10 mM Na₂HPO₄, 1.8 mM KH₂PO₄, pH buffer to 7.4, and sterilize by autoclaving. Store at 4°C.

2. Cycloheximide stock: Dissolve 100 mg cycloheximide (Calbiochem, San Diego, CA) in 1 ml 100% ethanol; Store at -20°C .
3. Heparin stock: Dissolve 50 mg Heparin (Grade I, Sigma, St. Louis, MO) in 1 ml RNase-free water; Store at 4°C .
4. mRNP lysis buffer (RLB): 100 mM KCl, 5 mM MgCl_2 , 10 mM Hepes, pH 7.0, 0.5% Nonidet P-40a; additions to be added at time of use: 1 mM dithiothreitol (DTT), 100 U/ml RNase OUT (Invitrogen), and 1 \times complete protease inhibitor cocktail (Roche, Nutley, NJ) (store in aliquots at -20°C).
5. Polysome lysis buffer (PLB): Make before each use at the following final concentrations in 0.2 μ -filtered, RNase-free water: 15 mM Tris-HCl pH 7.6, 15 mM MgCl_2 , 0.3 M NaCl, 1% Triton X-100, 0.1 mg/ml Cycloheximide, and 1 mg/ml Heparin.

2.2. mRNP Immunoprecipitation

1. Mouse IgG1 antibody (Invitrogen, Carlsbad, CA).
2. HuR antibody (Santa Cruz Biotechnology, Inc., Santa Cruz, CA).
3. Protein A Sepharose (PAS) beads (Sigma).
4. Bovine serum albumin (BSA): 5% (w/v) in RNase free water (Invitrogen).
5. NT2 buffer: 50 mM Tris, pH 7.4, 150 mM NaCl, 1 mM MgCl_2 , 0.05% Nonidet P-40. Store at 4°C .
6. RNA OUT (Invitrogen).
7. Proteinase K (New England BioLabs, Ipswich, MA).
8. Phenol:chloroform:isoamylalcohol (25:24:1) (VWR, West Chester, PA).
9. Dnase, 10 \times Dnase reaction buffer (Ambion, Austin, TX).
10. Chloroform (J.T. Baker Chemical Company, Phillipsburg, NJ).
11. Glycoblue (Qiagen, Valencia, CA).

2.3. Polysome Gradient Analysis

1. 20% (w/w) Sucrose (step 1 for sucrose gradient): Combine the following: 21.6 g ultra-pure sucrose; 10 ml 3 M NaCl; 3 ml 500 mM MgCl_2 ; 1.5 ml 1 M Tris-HCl, pH 7.6; 100 μ l 100 mg/ml cycloheximide; 2 ml 50 mg/ml Heparin. Bring to 100 ml final volume with RNase-free water and filter through a 0.2 μ filter. Store at 4°C .
2. 47% (w/w) Sucrose (step 9 for sucrose gradient): Combine the following: 57 g ultra-pure sucrose; 10 ml 3 M NaCl; 3 ml 500 mM MgCl_2 ; 1.5 ml 1 M Tris-HCl, pH 7.6; 100 μ l 100 mg/ml cycloheximide; 2 ml 50 mg/ml Heparin. Bring to 100 ml final volume with RNase-free water and filter through a 0.2 μ filter. Store at 4°C .

3. 8 M Guanidine-HCl made with RNase-free water (solution will be very cold; if problems in dissolving occur, leave at 4°C for 1 h). Store at room temperature.
4. 3 M Sodium acetate made with RNase-free water; adjust pH to 5.2 with glacial acetic acid. Store at room temperature.
5. TE, pH 8.0: 10 mM Tris-HCl, pH 8.0 and 0.1 mM EDTA in RNase-free water. Store at 4°C.

2.4. Northern Blot Analysis

1. Hybod N+ membrane (GE Healthcare, Piscataway, NJ).
2. Hybridization buffer: 0.5 M NaH₂PO₄, pH 7.2, 7% SDS, 1 mM EDTA, and 1% BSA in RNase-free water; store at -20°C in aliquots.
3. 20× SSPE: Combine the following: 175.3 g NaCl; 27.6 g NaH₂PO₄; 7.4 g EDTA; bring to a final volume of 1,000 ml with 0.2 μ-filtered, RNase-free water, adjust pH to 7.4 with NaOH, sterilize by autoclaving, and store at room temperature.
4. 10× MOPS: Combine the following: 46.3 g MOPS – Na salt; 6.8 g sodium acetate; 3.4 g EDTA; bring to a final volume of 1,000 ml with 0.2 μ-filtered, RNase-free water, adjust pH to 7.0 with glacial acetic acid, sterilize by autoclaving, and store at room temperature.
5. 20× SSC: Combine the following: 175.3 g NaCl; 88.2 g sodium citrate; bring to a final volume of 1,000 ml with 0.2 μ-filtered, RNase-free water, adjust pH to 7.0 with NaOH, sterilize by autoclaving, and store at room temperature.

3. Methods

3.1. Preparation of mRNP Lysates from Cell Culture

1. Grow and harvest tissue culture cells at confluence by washing 2 times with ice-cold PBS followed by trypsinizing cells according to the standard protocol for the cell line used. Once the cells detach from the plates, add PBS to each plate in order to dilute the trypsin. The cells are transferred to a 50 ml Falcon tube and pelleted by centrifugation at 3,000 rpm for 5 min at 4°C.
2. The supernatant is discarded and the pellet is loosened by gently flicking the bottom of the Falcon tube.
3. One pellet volume of RLB buffer that has been fully supplemented with RNase, DTT, and protease inhibitor is added to the pellet. The cells are resuspended by pipetting, *not* by vortexing.
4. Place the resuspended pellet/RLB mixture on ice for 10 min.
5. Freeze in liquid nitrogen and store in -80°C until use.

3.2. Preparing the Protein A Sepharose Beads for mRNP Assay

1. In order to prepare the beads for use, swell the beads in a 50 ml Falcon tube overnight in 5% BSA solution at 4°C. Extra solution is added to the 15 ml mark of the Falcon tube.
2. The next morning, pour off the excess solution so that the beads are in a 50% (v/v) slurry.
3. Add 0.1% sodium azide to the bead slurry and place at 4°C for long-term storage.

3.3. Coating Protein A Sepharose Beads with Antibody for mRNP Assay

1. Place a 100 µl volume of PAS beads into a clean, RNase-free 1.5 ml microfuge tube.
2. Add 30 µg of antibody, in our case HuR, to the beads. Make a separate tube with beads plus the appropriate IgG control antibody (see Note 2). Add between 100 and 200 µl more NT-2 buffer to each tube.
3. Allow the antibody to bind to the beads overnight by placing the tubes in a tabletop, end-over-end rotator on medium speed at 4°C.
4. The next morning, centrifuge the beads at 18,000 × *g* for 5 min at 4°C. Remove the supernatant.
5. Wash the beads with 1 ml of NT-2 buffer, vortex the tubes for 10 s, and centrifuge at 18,000 × *g* for 5 min at 4°C.
6. Remove the supernatant, and repeat step 8 for a total of 5 times.
7. After the fifth wash, remove the NT-2 buffer. The beads are now ready to be used for the pulldown (proceed immediately to Subheading 3.4).

3.4. Preclearing the mRNP Lysate (see Note 3)

1. Thaw the mRNP lysate (step 7, Subheading 3.1) and centrifuge for 18,000 × *g* for 30 min at 4°C. Transfer the supernatant to a clean, RNase-free 1.5 ml tube.
2. Preclear the lysate by adding 15 µg IgG1 antibody (see Note 4) to the lysate and allowing it to incubate for 30 min on ice.
3. Add 50 µl noncoated PAS beads to the lysate (step 2), and incubate the mixture on a tabletop, end-over-end rotator on medium speed for 30 min at 4°C.
4. Centrifuge the PAS beads/lysate mix (step 3) at 18,000 × *g* for 1 min at 4°C.
5. Place the supernatant into a clean, RNase-free 1.5 ml microfuge tube. This is the precleared lysate.
6. Conduct a protein assay to determine the protein concentration. We use the method of Bradford (25). The precleared lysate can be stored at -80°C or can subsequently be used for the immunoprecipitation step (see Note 5).

3.5. Immuno-precipitation of mRNPs

1. Add 700 μ l NT-2 buffer to the precoated PAS/antibody beads (from Subheading 3.3). Subsequently, add 10 μ l 100 mM DTT (see Note 6), 10 μ l RNase OUT, and 33 μ l 0.5 M EDTA. Vortex the tubes briefly for 5–10 s.
2. Add precleared lysate (from Subheading 3.4). Typically, we use enough cells to obtain 2–3 mg of lysate for each immunoprecipitation reaction.
3. Bring the total volume of each tube to 1 ml with NT-2 buffer.
4. Mix the contents of the tube by flicking the bottom of the 1.5 ml tube.
5. Incubate the tube for 2 h at room temperature on a table top, end-over-end rotator.
6. Centrifuge the tubes at 18,000 $\times g$ for 5 min at 4°C.
7. Remove the supernatant and wash the pellet with 1 ml ice-cold NT-2 buffer. Vortex the tube for 5 s, and then centrifuge at 18,000 $\times g$ for 5 min at 4°C.
8. Repeat step 7 four additional times.
9. After the final wash, discard the supernatant. Add the following to the pellet: 2.5 μ l of Proteinase K (10 mg/ml), 1 μ l of 10% SDS, and 100 μ l of NT-2 buffer.
10. Incubate the tubes at 55°C for 30 min in a Thermomix (Eppendorf, Westbury, NY) set at 700 rpm.
11. Centrifuge the tubes at 18,000 $\times g$ for 2 min at 4°C.
12. Collect the supernatant (approximately 100 μ l) and place into a clean, RNase-free 1.5 ml microfuge tube.
13. Add 200 μ l NT-2 buffer to the beads and vortex the tubes for 5 s.
14. Centrifuge the tubes at 18,000 $\times g$ for 2 min at 4°C.
15. Collect the supernatant from step 14 (approximately 200 μ l) and combine with the supernatant collected in step 12. A total of 300 μ l should now be in a 1.5 ml tube. The beads can now be discarded.
16. Add 800 μ l phenol:chloroform:isoamylalcohol (25:24:1) to the 300 μ l supernatant (see Note 7).
17. Vortex the tubes for 1 min.
18. Centrifuge the tubes at 18,000 $\times g$ for 1 min at room temperature.
19. Collect the upper phase (approximately 300 μ l) and add 30 μ l of 3 M sodium acetate, 650 μ l 100 % ethanol, and 5 μ l glyco-blue to each tube. Mix the contents of the tube well and store overnight at –20°C.
20. The next day, spin the tubes at 18,000 $\times g$ for 30 min at 4°C.
21. Discard the supernatant.

22. Add 1 ml ice-cold 70% ethanol to the pellet and mix by inversion.
23. Centrifuge the tubes at $18,000 \times g$ for 2 min at 4°C .
24. Discard the supernatant.
25. Centrifuge the pellet at $18,000 \times g$ for 1 min at 4°C .
26. Remove any residual ethanol from the pellet carefully with a pipette.
27. Allow the pellet to air dry for 5 min at room temperature.
28. Resuspend the pellet in 20 μl of water that has been heated to 65°C . Place the tubes at 65°C for 5 min.
29. Add 2 μl $10\times$ DNase reaction buffer and 1 μl DNase I to each tube.
30. Mix the contents of the tube and incubate the tubes at 37°C for 30 min.
31. Add 80 μl of RNase-free water and 100 μl phenol:chloroform:isoamylalcohol to the tubes and vortex for 2 min.
32. Centrifuge the tubes at $18,000 \times g$ for 10 min at 4°C .
33. Place the upper phase into a clean, RNase-free 1.5 ml microfuge tube.
34. To the upper phase (from step 33), add 100 μl chloroform and vortex for 20 s.
35. Centrifuge the tubes at $18,000 \times g$ for 10 min at 4°C .
36. Remove the upper phase and place into a clean, RNase-free 1.5 ml microfuge tube.
37. To the upper phase (from step 36), add 10 μl of 3 M sodium acetate, 250 μl 100% ethanol, and 2.5 μl glycoblue.
38. Mix the contents of the tube well and place at -20°C for at least 1 h.
39. Centrifuge the tubes at $18,000 \times g$ for 30 min at 4°C .
40. Discard the supernatant.
41. Wash the pellet with 70% ice-cold ethanol.
42. Centrifuge the tubes at $18,000 \times g$ for 5 min at 4°C .
43. Discard the supernatant.
44. Centrifuge the tubes at $18,000 \times g$ for 1 min at 4°C .
45. Remove any residual ethanol from the pellet.
46. Allow the pellet to air dry for 5 min at room temperature.
47. Resuspend the pellet in 15 μl of water that has been heated to 65°C .
48. Incubate the tubes at 65°C for 5 min.
49. This is your pulldown RNA. cDNA can be made for RT PCR analysis or qRT-PCR analysis using one of several commercially

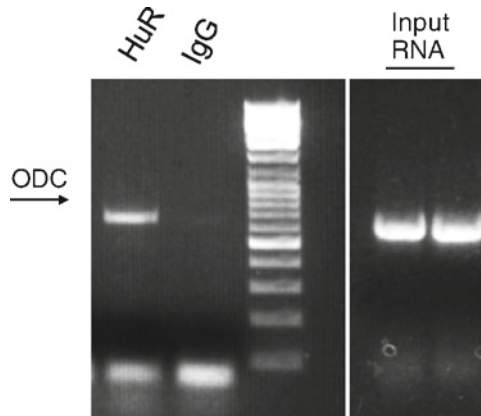


Fig. 1. mRNP assay of Ras12V cell lysate to measure endogenous RBP binding to ODC RNA. To determine endogenous binding of HuR to the ODC transcript, HuR was immunoprecipitated from Ras12V cells as described in the Methods. Cell lysates isolated in RLB were incubated with a 50% (v/v) suspension of Protein A-sepharose beads precoated with either IgG1 or anti-HuR (Santa Cruz Biotech). After washing in NP40-based buffer, beads were treated with RNase-free DNase I and proteinase K, then RNA was extracted and reverse transcribed to obtain cDNA. The presence of ODC was analyzed by conventional PCR using primer pairs corresponding to a 635 bp region within the ODC transcript (see Note 8). Lanes labeled “Input RNA” represent duplicate PCR reactions performed with the same ODC primers on cDNA prepared from cell lysate without immunoprecipitation, indicating the presence of ODC RNA in the lysate.

available kits. We use the TranscripT^{er} first Strand cDNA Synthesis Kit (Roche). PCR primers to detect ODC RNA bound to HuR are listed in Note 8. Typical results are shown in Fig. 1.

3.6. Pouring Sucrose Step Gradients for Polysome Analysis

1. Use step 1 (20% sucrose) and step 9 (47% sucrose) solutions prepared as described in Subheading 2; all other steps are combinations of these two.
2. Pouring gradients: First make steps as follows:

40 ml Step 1 +	40 ml Step 9 =	80 ml Step 5
20 ml Step 1 +	20 ml Step 5 =	40 ml Step 3
10 ml Step 1 +	10 ml Step 3 =	20 ml Step 2
10 ml Step 3 +	10 ml Step 5 =	20 ml Step 4
20 ml Step 5 +	20 ml Step 9 =	40 ml Step 7
10 ml Step 5 +	10 ml Step 7 =	20 ml Step 6
10 ml Step 7 +	10 ml Step 9 =	20 ml Step 8

3. Layering gradients:
 - Start with step 9 and end with step 1.
 - Add 1.25 ml of step 9 into a disposable ultracentrifuge tube (we use Beckman polyallomer tubes cat #344059).

- After adding step 9, freeze in liquid nitrogen, then continue with each additional step (add 1.25 ml step 8, freeze, etc. until step 1 is added to the top).
- Store step gradients at -80°C until use.
- Thaw gradients overnight at 4°C the day before your experiment (once gradients are thawed be very careful when moving the tubes).

3.7. Preparation of Cell Lysates for Polysome Analysis

1. Treat cells as desired for experiment. We use about 1×10^7 cells per gradient.
2. For extraction, aspirate medium, add 5 ml prewarmed PBS containing 0.1 mg/ml cycloheximide to each plate, and incubate for 5 min at 37°C .
3. Aspirate and wash 2 times with ice cold PBS/cycloheximide (100 $\mu\text{g}/\text{ml}$). Be sure to remove all traces of PBS when aspirating.
4. Scrape cells into 600 μl total volume PLB (300 μl twice) into a sterile microfuge tube on ice.
5. Rock samples gently for 10 min at 4°C .
6. Centrifuge samples at $3,000 \times g$ for 15 min at 4°C .
7. Load 600 μl supernatant directly onto the top of a 20–47% sucrose gradient prepared as described in Subheading 3.7. Layer gently, so the gradient is not disturbed. Balance tubes if necessary with PLB.
8. Cool centrifuge and rotor at least 1 h prior to use. Centrifuge gradients at 34,000 rpm for 160 min at 4°C using a Beckman SW41Ti rotor (Beckman Coulter, Fullerton, CA) in a L90K Beckman ultracentrifuge or equivalent.

3.8. Collection of Fractions and RNA Isolation (see Note 9)

1. Gradients are fractionated immediately after removing from the centrifuge.
2. The entire gradient can be split into many fractions. We split it into 11 fractions every 30 s.
3. Each fraction is collected directly into 2.5 ml of 8 M guanidine-HCl plus 250 μl RNase-free water.
4. Shake each fraction vigorously, add $2 \times$ volume of 100% ethanol, and precipitate overnight at -20°C .
5. Next day (after at least 16 h), centrifuge fractions at $10,000 \times g$ and 4°C for 20 min to pellet RNA.
6. Aspirate supernatant, wash pellet with 75% ethanol (made with RNase-free water) and centrifuge at $10,000 \times g$ and 4°C for 10 min.
7. Dissolve pellet in 400 μl TE, pH 8.0.
8. Add 50 μl 3 M sodium acetate, pH 5.2 and 1 ml 100% ethanol. Precipitate overnight at -20°C .

9. Next day, centrifuge at $10,000 \times g$ for 20 min at 4°C .
10. Remove supernatant and wash pellet one time with 75% ethanol. Centrifuge at $10,000 \times g$ for 10 min at 4°C .
11. Remove supernatant and dry pellet at room temperature for 5 min.
12. Add 15 μl nuclease-free water. If pellets do not dissolve, wait 3–5 min and carefully resuspend using a pipette.
13. Measure concentration using a spectrophotometer at 260 nm. Store at -80°C until use.

3.9. Northern Blot Analysis of Polysome Gradient Fractions

1. For each fraction, use 15 μg RNA in 6 μl nuclease-free water. Fractions may need to be concentrated by lyophilizing before use.
2. To each sample add: 12.5 μl formamide, 2.5 μl 10 \times MOPS, 4.0 μl formaldehyde (37% solution).
3. Incubate at 65°C for 5 min, then chill on ice.
4. Add 3 μl of 50% glycerol (in nuclease-free water) containing 0.1% bromphenol blue and 1 mM EDTA to each sample.
5. Prepare a 1.2% Formaldehyde gel as follows (prepare in fume hood): Combine 1.8 g agarose, 15 ml 10 \times MOPS, and 109.5 ml water. Dissolve agarose by heating in a microwave (do not allow the solution to boil). Cool to 50°C . Add 25.5 ml of Formaldehyde (37% solution). Mix and pour immediately (volumes may need to be adjusted depending on the gel apparatus used). Allow gel to polymerize at room temperature.
6. For each fraction, load the entire sample onto the gel. Run gel in 1 \times MOPS overnight at 20 V.
7. Before transfer, soak gel in 100 ml nuclease-free water containing 4 μl of 10 mg/ml ethidium bromide (Caution: Mutagen. Wear appropriate protection) for 20 min, then destain 1 h in water to visualize 18S and 28S bands.
8. Transfer to Hybond N+ membrane for 4.5 h in 20 \times SSPE using a Turboblotter (Whatman Schleicher and Schuell, St. Louis, MO) or similar apparatus, following the instructions of the manufacturer.
9. Wash membrane in 5 \times SSPE for 5 min, then remove from wash and place membrane on a piece of filter paper or paper towel.
10. Crosslink RNA to membrane using a Stratalinker (Agilent Technologies Stratagene, La Jolla, CA) or similar apparatus at a setting of 120,000 $\mu\text{J}/\text{cm}^2$ (“auto-crosslink” on the Stratalinker).

11. Prehybridize membrane for 1–2 h at 65°C in 5 ml hybridization buffer.
12. Probe preparation requires a DNA template. For ODC we use pGEM-ODC (26). The entire ODC coding region is removed by restriction digest as follows:

pGEM-ODC	10 µg
BamHI (Invitrogen)	10 U
EcoRI (Invitrogen)	10 U
100×BSA (Invitrogen)	1 µl
Invitrogen React 2 Buffer	10 µl
Nuclease-free water	To a final volume of 100 µl

13. Allow reaction to proceed at 37°C for 1 h.
14. Run reaction mix on 0.8% agarose gel containing 1 µg/ml ethidium bromide. Visualize the bands by placing the gel on a Transilluminator box and cut the 1.8 Kb insert from the gel with a scalpel.
15. Purify DNA from the agarose using Quick-spin columns (Sigma) according to the manufacturer's instructions.
16. Several commercial kits are available for probe preparation. We use 25 ng of the purified insert as a template to make the [32-P]-labeled probe with the Ladderman kit (Takara Bio, Inc., Shiga, Japan), following the manufacturer's instructions exactly (see Note 10).
17. After probe synthesis, add 20 µl of probe to a sterile 1.2 ml microfuge tube, and place in a boiling water bath for 5 min.
18. Add 1 µl boiled probe per ml of hybridization buffer (we generally use 5 ml hybridization buffer).
19. Hybridize overnight at 65°C.
20. Next day, wash membrane once with 1× SSC+0.1% SDS at room temperature for 10 min.
21. Wash membrane 3 times with 0.5× SSC+0.1% SDS at 65°C for 10 min.
22. Expose membrane (wrapped in plastic) to Autoradiography film (e.g., HyBlot, Denville Scientific, Metuchen, NJ) in a cassette placed at –80°C overnight.
23. Next day, process film to reveal bands corresponding to ODC mRNA in each polysome fraction. Exposure time may need to be adjusted to get an optimal signal. Typical results of both agarose gel staining with ethidium bromide and polysome profile of ODC mRNA are shown in Fig. 2.

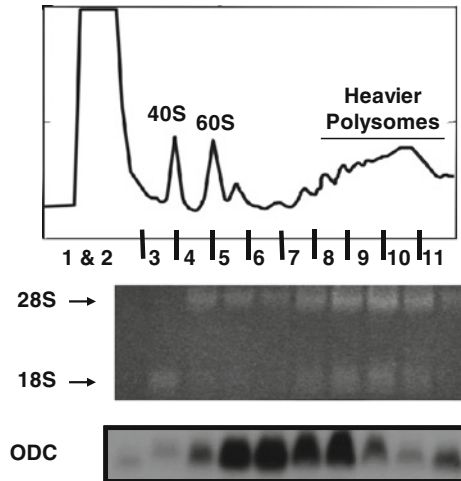


Fig. 2. Analysis of polysomal RNA integrity and polysomal association of ODC RNA in Ras12V cells. Sucrose gradient centrifugation and polysome analysis of Ras12V cells were carried out as described in Methods. Eleven gradient fractions were collected, and RNA was isolated from each fraction and analyzed on a 1.2% formaldehyde-MOPS agarose gel stained with ethidium bromide. Equal volumes of total RNA were loaded for each fraction, and the agarose gel image shows total RNA corresponding to each fraction. *Arrows* indicate the position of 18S rRNA and 28S rRNA. Fractions 1 and 2 do not show any detectable levels of RNA as they represent the nonpolysomal fraction. Only 18S rRNA is visible in fraction 3, suggesting that it consists predominantly of the 40S ribosomal subunit. Fraction 4 represents the 60S ribosomal subunit that consists mostly of 28S rRNA. Fractions 5 and 6 represent the 80S and disome fractions showing mostly 28S rRNA and faint levels of 18S rRNA. Fractions 7 through 11 represent the polysomal peak, displaying similar levels of 18S rRNA in comparison to 28S rRNA. To visualize ODC RNA in each fraction, the gel was destained and northern blot analysis was performed. The membrane was probed with a [32 P] radiolabeled cDNA complementary to the full length ODC open reading frame. The polysome profile shows that ODC RNA is associated mostly with the disome and small polysome fractions, indicating ODC is poorly translated in these cells.

4. Notes

1. For all of these procedures, it is important to use RNase-free pipette tips, RNase-free water, RNase-free microfuge tubes, and to wear gloves.
2. For each antibody used, an IgG control must be added. For example, the HuR antibody is anti-mouse and thus for each cell line used we have a mouse IgG negative control.
3. This step can be completed the day before the mRNP is conducted or can be completed while the coated beads are being washed.
4. Make sure the IgG preclear is for the correct species. For example, the HuR antibody is anti-mouse; therefore, we use a mouse IgG to preclear the supernatant.

5. Clearing of the lysate can be accomplished before the beads are coated and the mRNP is conducted. If you preclear the lysate before you are able to move forward with the experiment, store the precleared lysates in -80°C .
6. Do not add DTT directly to the pellet. This reduces antibody efficiency.
7. Make sure that the phenol chloroform solution is mixed well prior to use.
8. The following primers are used for ODC PCR following the mRNP assay (Note that these primers are to the mouse ODC sequence and may need to be altered for other species): Sense: 5'-CGAGAACCATGAGCAGCTTTAC-3', Antisense: 5'-CTACACATTGATCCTAGCAGCC-3'.
9. This step requires a fractionator (such as an ISCO sucrose gradient absorbance profile analyzer, Teledyne Isco, Lincoln, NE) and UV detector at 254 nm. Parameters we use while collecting: Flow rate 2 ml/min, chart speed 150 cm/h, sensitivity 0.5. This must be determined experimentally for the fractionator used.
10. The Ladderman kit is designed for use with [α - ^{32}P], [^{-35}S], or [^3H] dCTP labels. Generally, a probe with specific activity of >109 dpm/ μg DNA will be obtained with [α - ^{32}P] dCTP ($\sim 3,000$ Ci/mmol). Although kits designed for nonradioactive probe labeling are also available (e.g., Biotin-labeling kits), it is our experience that [^{32}P]-labeled probes give better-quality results.

Acknowledgements

The authors would like to thank Suzanne Sass-Kuhn for excellent technical assistance. This work was supported by R01 CA82768 and R03 CA142051 (to LMS).

References

1. Pegg AE (2006) Regulation of ornithine decarboxylase. *J Biol Chem* 281:4529–14532
2. Zhao B, Butler AP (2001) Core promoter involvement in the induction of rat ornithine decarboxylase by phorbol esters. *Mol Carcinog* 32:92–99
3. Li R, Abrahamsen MS, Johnson RR, Morris DR (1994) Complex interactions at a GC-rich domain regulate cell type-dependent activity of the ornithine decarboxylase promoter. *J Biol Chem* 269:7941–7949
4. Wallon UM, Persson L, Heby O (1995) Regulation of ornithine decarboxylase during cell growth. Changes in the stability and translatability of the mRNA, and in the turnover of the protein. *Mol Cell Biochem* 146:39–44
5. Shantz LM (2004) Transcriptional and translational control of ornithine decarboxylase during Ras transformation. *Biochem J* 377: 257–264
6. Shantz LM, Pegg AE (1999) Translational regulation of ornithine decarboxylase and

- other enzymes of the polyamine pathway. *Int J Biochem Cell Biol* 31:107–122
7. Huang Y, Pledgie A, Casero RA Jr, Davidson NE (2005) Molecular mechanisms of polyamine analogs in cancer cells. *Anticancer Drugs* 16:229–241
 8. Gerner EW, Meyskens FL Jr (2004) Polyamines and cancer: old molecules, new understanding. *Nat Rev Cancer* 4:781–792
 9. O'Brien TG, Megosh LC, Gilliard G, Peralta Soler A (1997) Ornithine decarboxylase overexpression is a sufficient condition for tumor promotion in mouse skin. *Cancer Res* 57:2630–2637
 10. O'Brien TG (1976) The induction of ornithine decarboxylase is an early, possibly obligatory event in mouse skin carcinogenesis. *Cancer Res* 36:2644–2653
 11. Origanti S, Shantz LM (2007) Ras transformation of RIE-1 cells activates cap-independent translation of ornithine decarboxylase: regulation by the Raf/MEK/ERK and phosphatidylinositol 3-kinase pathways. *Cancer Res* 67:4834–4842
 12. Shantz LM, Pegg AE (1994) Overproduction of ornithine decarboxylase caused by relief of translational repression is associated with neoplastic transformation. *Cancer Res* 54:2313–2316
 13. Rousseau D, Kaspar R, Rosenwald I, Gehrke L, Sonenberg N (1996) Translation initiation of ornithine decarboxylase and nucleocytoplasmic transport of cyclin D1 mRNA are increased in cells overexpressing eukaryotic initiation factor 4E. *Proc Natl Acad Sci USA* 93:1065–1070
 14. Grens A, Scheffler IE (1990) The 5'- and 3'-untranslated regions of ornithine decarboxylase mRNA affect the translational efficiency. *J Biol Chem* 265:11810–11816
 15. Lorenzini EC, Scheffler IE (1997) Co-operation of the 5' and 3' untranslated regions of ornithine decarboxylase mRNA and inhibitory role of its 3' untranslated region in regulating the translational efficiency of hybrid RNA species via cellular factors. *Biochem J* 326:361–367
 16. Lökvist-Wallstrom E, Stjernborg-Ulvbäck L, Scheffler IE, Persson L (1995) Regulation of mammalian ornithine decarboxylase. Studies on the induction of the enzyme by hypotonic stress. *Eur J Biochem* 231:40–44
 17. Zou T, Mazan-Mamczarz K, Rao JN, Liu L, Marasa BS, Zhang AH, Xiao L, Pullmann R, Gorospe M, Wang JY (2006) Polyamine depletion increases cytoplasmic levels of RNA-binding protein HuR leading to stabilization of nucleophosmin and p53 mRNAs. *J Biol Chem* 281:19387–19394
 18. Xiao L, Rao JN, Zou T, Liu L, Marasa BS, Chen J, Turner DJ, Zhou H, Gorospe M, Wang JY (2007) Polyamines regulate the stability of activating transcription factor-2 mRNA through RNA-binding protein HuR in intestinal epithelial cells. *Mol Biol Cell* 18:4579–4590
 19. Garneau NL, Wilusz J, Wilusz CJ (2007) The highways and byways of mRNA decay. *Nat Rev Mol Cell Biol* 8:113–126
 20. Barreau C, Paillard L, Osborne HB (2005) AU-rich elements and associated factors: are there unifying principles? *Nucleic Acids Res* 33:7138–7150
 21. Hau HH, Walsh RJ, Ogilvie RL, Williams DA, Reilly CS, Bohjanen PR (2007) Tristetraprolin recruits functional mRNA decay complexes to ARE sequences. *J Cell Biochem* 100:1477–1492
 22. Parker R, Sheth U (2007) P bodies and the control of mRNA translation and degradation. *Mol Cell* 25:635–646
 23. Eulalio A, Behm-Ansmant I, Izaurralde E (2007) P bodies: at the crossroads of post-transcriptional pathways. *Nat Rev Mol Cell Biol* 8:9–22
 24. Johannes G, Carter MS, Eisen MB, Brown PO, Sarnow P (1999) Identification of eukaryotic mRNAs that are translated at reduced cap binding complex eIF4F concentrations using a cDNA microarray. *Proc Natl Acad Sci USA* 96:13118–13123
 25. Bradford M (1976) A rapid sensitive method for the quantitation of microgram quantities of protein utilizing the principle of protein-dye binding. *Anal Biochem* 72:248–254
 26. Lu L, Stanley BA, Pegg AE (1991) Identification of residues in ornithine decarboxylase essential for enzymatic activity and for rapid protein turnover. *Biochem J* 277:671–675

Part VI

Polyamine Transport and Uptake

Identification and Assays of Polyamine Transport Systems in *Escherichia coli* and *Saccharomyces cerevisiae*

Keiko Kashiwagi and Kazuei Igarashi

Abstract

Polyamine content in cells is regulated by biosynthesis, degradation, and transport. With regard to transport, uptake and excretion proteins exist in *Escherichia coli* and *Saccharomyces cerevisiae*. In *E. coli*, the uptake systems comprise a spermidine-preferential uptake system consisting of the PotA, B, C, and D proteins, and a putrescine-specific uptake system consisting of the PotF, G, H, and I proteins. Two other proteins, PotE and CadB, each containing 12 transmembrane segments, function as antiporters (putrescine-ornithine and cadaverine-lysine) and are important for cell growth at acidic pH. MdtJI was identified as a spermidine excretion system. When putrescine was used as energy source, PuuP functioned as a putrescine transporter. In *S. cerevisiae*, DUR3 and SAM3, containing 16 or 12 transmembrane segments, are the major polyamine uptake proteins, whereas TPO1 and TPO5, containing 12 transmembrane segments, are the major polyamine excretion proteins, and UGA4 is a putrescine transporter on the vacuolar membrane. The activities of DUR3 and TPO1 are regulated by phosphorylation of serine/threonine residues. The identification and assay procedures of these transporters are described in this chapter.

Key words: Polyamines, Putrescine, Spermidine, Spermine, Uptake, Excretion, Antiporter

1. Introduction

Polyamines are essential for normal cell growth (1, 2). Levels of polyamines in cells are elaborately maintained at an optimal level by biosynthesis, degradation, and transport. With regard to transport, the genes for several polyamine transport proteins have been identified and the properties of the polyamine transport proteins have been clarified in *Escherichia coli* and *Saccharomyces cerevisiae* (3–7). Most of them are polyamine-specific or polyamine-preferential transport proteins, suggesting that polyamines play important roles in cell growth and viability. In *E. coli*, there are two

ATP binding cassette transporters – a spermidine-preferential uptake system consisting of the PotA, B, C, and D proteins and a putrescine-specific uptake system consisting of the PotF, G, H, and I proteins (see Note 1 and Fig. 1). PotE and CadB, containing 12 transmembrane segments, are antiporters (putrescine-ornithine and cadaverine-lysine), which are important for cell growth at acidic pH (see Note 2 and Fig. 1). MdtJI was identified as a spermidine excretion system (see Note 3 and Fig. 1). When putrescine was used as an energy source, PuuP functioned as a putrescine transporter. In *S. cerevisiae*, DUR3 and SAM3, containing 16 or 12 transmembrane segments, are major polyamine uptake proteins (see Note 4 and Figs. 2 and 3). TPO1 and TPO5, containing 12 transmembrane segments, were identified as major polyamine excretion proteins (see Note 5 and Fig. 2).

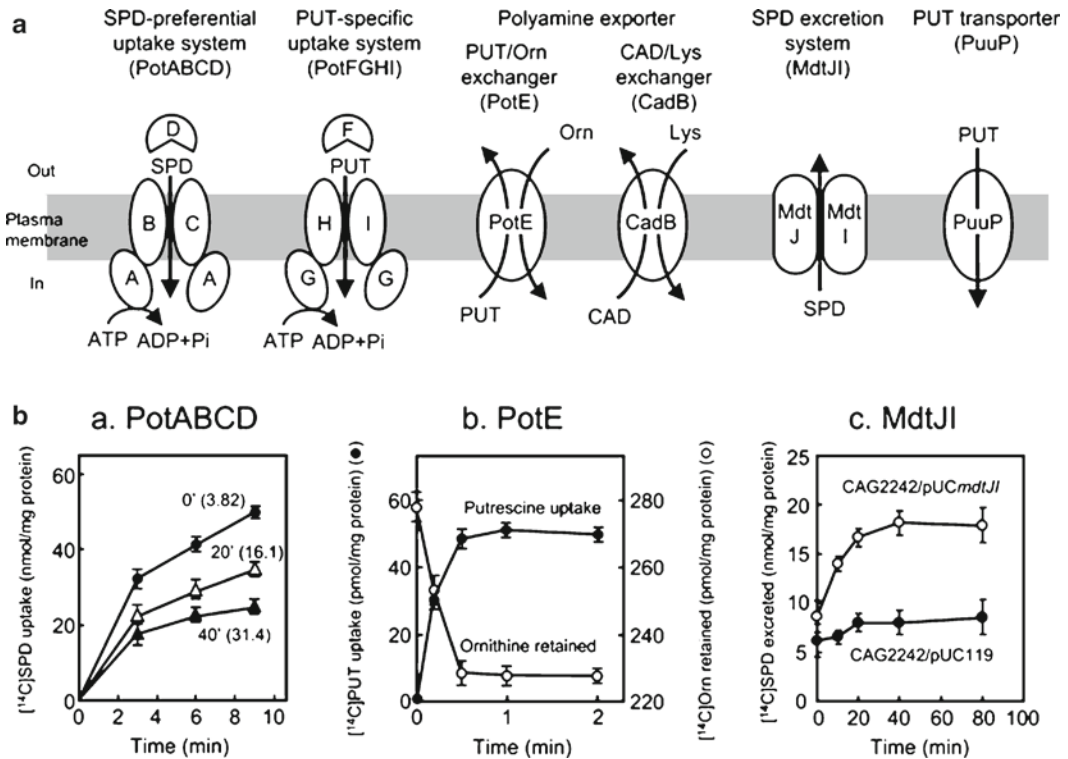


Fig. 1. Polyamine transport systems and polyamine transport activities in *E. coli*. (a) Polyamine transport systems in *E. coli* are schematically depicted. (ba) Spermidine uptake activity by PotABCD is shown. MA261/pPT104 cells were cultured in Medium A until $A_{540} = 0.25$, and 100 μM spermidine was added, and incubated for 0 min (closed bullet), 20 min (open triangle), and 40 min (filled triangle). Cells were harvested and spermidine uptake activity was measured as described in Subheading 3.2. Spermidine content (nmol/mg protein) in cells was shown in parentheses. (bb) Putrescine-ornithine antiporter activity by PotE is shown. The activity was measured as described in Subheading 3.3. (bc) Spermidine excretion activity by MdtJI is shown. Spermidine excretion activity was measured as described in Subheading 3.4. Figures are taken from Kashiwagi et al. (20, 27) and Higashi et al. (7).

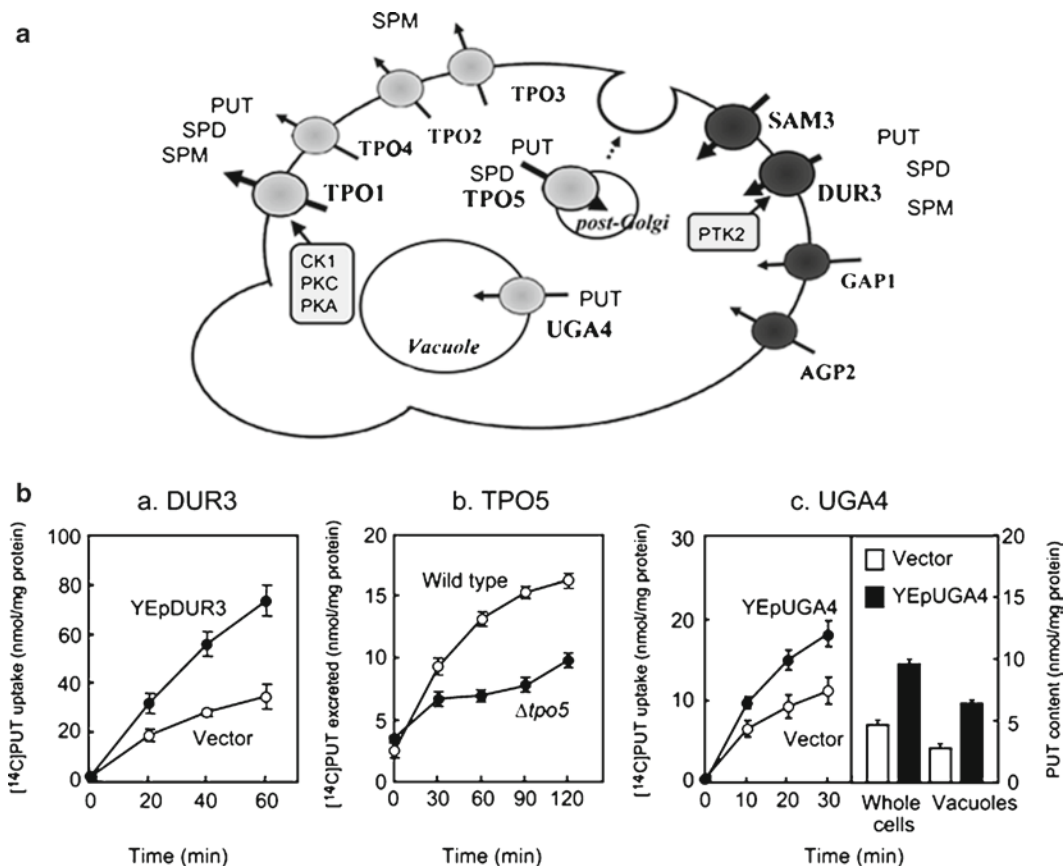


Fig. 2. Polyamine transport systems and polyamine transport activities in *S. cerevisiae*. (a). Polyamine transport systems and their cellular localization are schematically depicted. (ba). Putrescine uptake activity by DUR3 is shown. YPH499/YEpDUR3 and YPH499/YEp352 (vector) were cultured, and putrescine uptake activity was measured as described in Subheading 3.5. (bb) Putrescine excretion activity by TPO5 is shown. Putrescine excretion activity by YPH499 and YPH499 $\Delta tpo5$ cells was measured as described in Subheading 3.5. (bc) Putrescine uptake by UGA4 in vacuoles and putrescine accumulation in whole cells and vacuoles by UGA4 are shown. Putrescine uptake activity by YTM22-8/YEpUGA4 and YTM22-8/YEp352 (vector) and polyamine content in whole cells and vacuoles were measured as described in Subheading 3.5. Figures are taken from Uemura et al. (6, 13) and Tachihara et al. (5).

UGA4 is a putrescine transporter on vacuolar membrane. The activities of DUR3 and TPO1 are regulated by phosphorylation of serine/threonine residues (Fig. 2 and 3).

In this chapter, the identification and assay procedures of polyamine transporters are described using normal and polyamine-deficient cells transformed with plasmids encoding the polyamine transport proteins, polyamine transport gene-disrupted cells, and inside-out membrane vesicles. The assays were performed using ^{14}C -labeled polyamines as substrates.

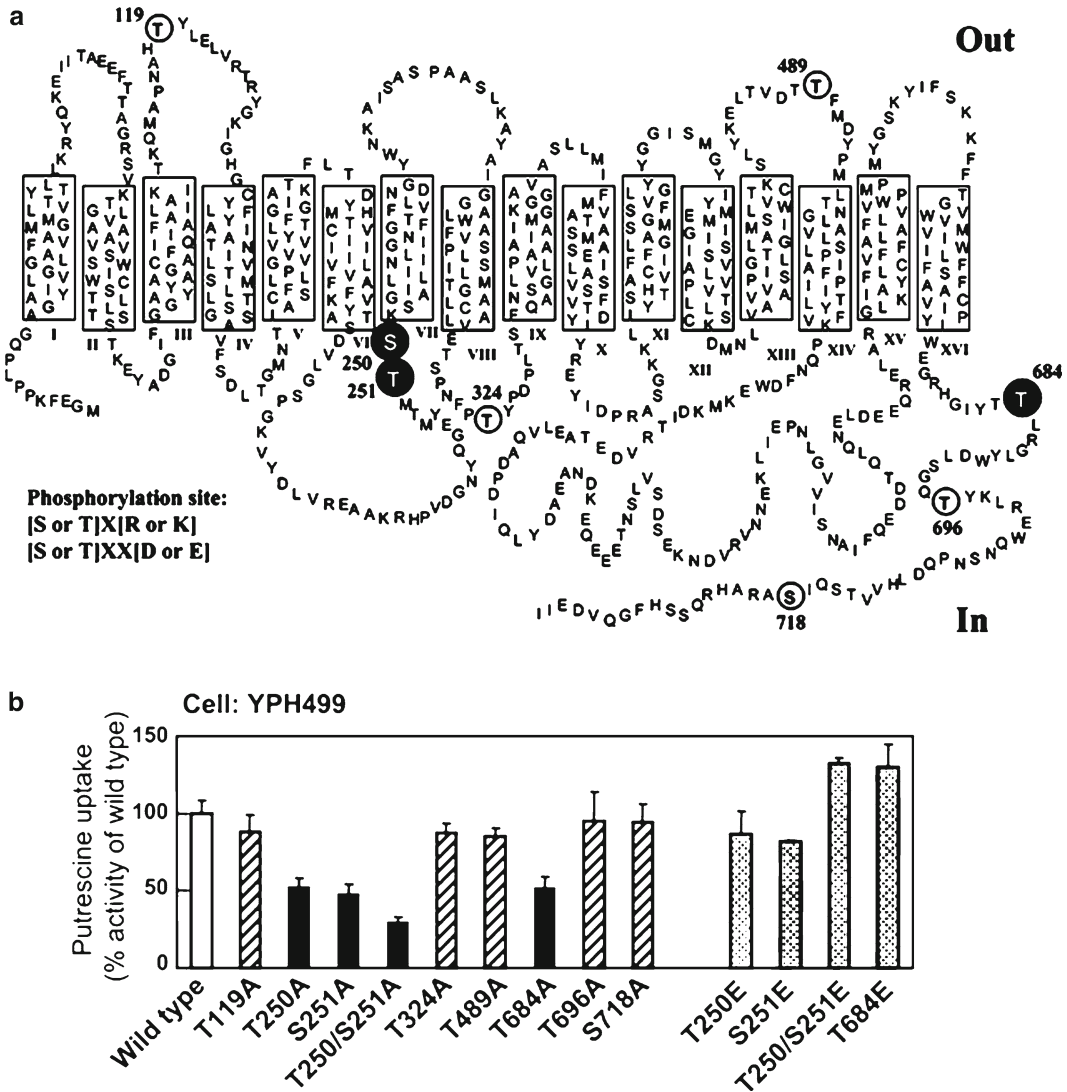


Fig. 3. Model of the secondary structure (a) and serine/threonine residues involved in the activities of DUR3 (b). (a) A model of the secondary structure of protein was constructed according to the average hydropathy profiles obtained with a hydrophilicity/hydrophobicity Plot (GENETYX-MAC version 10). Putative transmembrane segments are shown in *large boxes*. Candidate phosphorylation sites are shown by *white* and *black circles*. (b) Candidate phosphorylation sites of Ser and Thr were replaced by Ala or Glu, and putrescine uptake activities of the mutants were measured. Data shown are the mean \pm S. E. of triplicate determinations. The 100% value of putrescine uptake by DUR3 was 0.87 ± 0.04 nmol/min/mg protein. Phosphorylation sites by PTK2 are shown by *black circles* with white lettering in (a). Figures are taken from Uemura et al. (6).

2. Materials

2.1. Bacterial Strains and Culture Medium

1. *E. coli* MA261 (*speB speC serA thr leu thi*) (8) and DR112 (*speA speB thi*) (9), polyamine-deficient mutants, NH1596, a polyamine transport-deficient mutant isolated from MA261

(10), and CAG2242 (*speG putE hsdR thi thr lacYI tonA2I*), a spermidine acetyltransferase-deficient mutant (11), were used.

2. Luria-Bertani (LB) medium for maintaining *E. coli* strains: 10 g of tryptone, 5 g of yeast extract, and 10 g of NaCl per liter.
3. Medium A: 4 g of glucose, 7 g of K_2HPO_4 , 3 g of KH_2PO_4 , 500 mg of sodium citrate, 1 g of $(NH_4)_2SO_4$, 100 mg of $MgSO_4/7H_2O$, 2 mg of thiamine, 10 mg of biotin, and 100 mg each of leucine, threonine, methionine, serine, glycine, and ornithine per liter of water.
4. Medium B: 4 g of glucose, 6 g of K_2HPO_4 , 3 g of KH_2PO_4 , 500 mg of NaCl, 1 g of NH_4Cl , 250 mg of $MgSO_4/7H_2O$, 13 mg of $CaCl_2/2H_2O$, 2 mg of thiamine, 1 g of arginine, 100 mg each of alanine, asparagine, aspartic acid, glutamic acid, glycine, methionine, proline, serine, and threonine, 50 mg each of cysteine, histidine, isoleucine, leucine, phenylalanine, tyrosine, and valine, and 5 mg of tryptophan per liter of water.

2.2. Cloning of the Genes for Polyamine Transport Systems in *E. coli*

1. Plasmid pACYC184, a medium copy number vector, carrying the genes for tetracycline- and chloramphenicol-resistance.
2. Total chromosomal DNA of DR112 was partially digested by *Sau3A*I. 7–14 kb DNA fragments were isolated from agarose gel after separating by electrophoresis.
3. Agar plates composed of medium A, 1.5% agar, and 0.03 mg/mL of chloramphenicol.
4. 10 μ M [^{14}C]spermidine (1.85 GBq/mmol) and 10 μ M [^{14}C]putrescine (1.85 GBq/mmol).

2.3. Polyamine Transport Assay by Intact Cells in *E. coli*

1. Buffer 1: 0.4% glucose, 62 mM potassium phosphate, pH 7.0, 1.7 mM sodium citrate, 7.6 mM $(NH_4)_2SO_4$, and 0.41 mM $MgSO_4$.
2. 0.25 mM [^{14}C]spermidine (370 MBq/mmol) and 0.25 mM [^{14}C]putrescine (370 MBq/mmol).
3. Cellulose acetate membrane filters (type EH, 0.5 μ m, 25 mm diameter; Millipore Corp.).

2.4. Preparation of Inside-Out Membrane Vesicles and Assay for Antiport

1. Buffer 2: 100 mM potassium phosphate buffer, pH 6.6, 10 mM EDTA, and 2.5 mM ornithine.
2. Buffer 3: 10 mM Tris-HCl, pH 8.0, 0.14 M KCl, 2 mM 2-mercaptoethanol, and 10% glycerol.
3. Buffer 4: 10 mM Tris-HCl, pH 8.0, 10 mM potassium phosphate buffer, pH 8.0, and 0.14 M KCl.
4. 1 mM [^{14}C]putrescine (1.48 GBq/mmol).

5. 1 mM [¹⁴C]ornithine (1.48 GBq/mmol) in Buffer 4.
6. Cellulose nitrate membrane filters (0.45 μm, 25 mm diameter; Advantec Toyo, Tokyo).

2.5. Yeast Strains, Plasmids, and Culture Medium

1. *S. cerevisiae* YPH499 (*MATa ade2-101 his3-Δ200 leu2-Δ1 lys2-801 trp1-Δ63 ura3-52*), YTM22-8 (*MATa, spt1 trp1 ura3-52 leu-2-3, 112*), a polyamine-transport deficient strain (12), and YPH499Δ*tpo5* (*MATa ade2-101 his3-Δ200 leu2-Δ1 lys2-801 trp1-Δ63 ura3-52 ykl174c::TRP*) (see Note 5) (5).
2. Plasmids, YEp351 and YEp352, vectors, YEpDUR3 encoding the gene for DUR3 (6), YEpUGA4 encoding the gene for UGA4 (13), and YEpTPO1 encoding the gene for TPO1.
3. Mg²⁺-limited (50 μM) complete synthetic medium containing glucose (Mg²⁺-limited CSD): 20 g of glucose, 850 mg of KH₂PO₄, 150 mg of K₂HPO₄, 12.3 mg of MgSO₄/7H₂O, 3.5 g of (NH₄)₂SO₄, 0.5 mg of H₃BO₃, 0.4 mg of MnCl₂/4H₂O, 0.4 mg of Zn(CH₃COO)₂/H₂O, 0.2 mg of FeCl₃/H₂O and Na₂MoO₄/2H₂O, 0.1 mg of KI, 0.02 mg of CuSO₄, 10 mg of inositol, 2 mg of D-pantothenic acid calcium salt, 0.4 mg of nicotinic acid, pyridoxine hydrochloride and thiamine hydrochloride, 0.2 mg of *p*-aminobenzoic acid and riboflavin, 0.1 mg of folic acid, 1.5 g of asparagine, 400 mg of serine, 220 mg of threonine, 150 mg of valine, 100 mg of glutamic acid-HCl, 80 mg of aspartic acid, 50 mg of phenylalanine, 40 mg of methionine, 30 mg of tyrosine, isoleucine, histidine and lysine-HCl, and 20 mg of arginine and tryptophan per liter of water (14).

2.6. Assays for Spermidine or Putrescine Uptake, Putrescine Excretion and Putrescine Uptake in Vacuoles, and Measurement of Polyamines in *S. cerevisiae*

1. Buffer 5: 20 mM Na/MES buffer, pH 5.0, and 10 mM glucose.
2. Cellulose acetate membrane filters (type EH, 0.5 μm, 25 mm diameter; Millipore Corp.).
3. Buffer 6: 0.35 M citric acid buffer, pH 5.35, 2 M NaCl, and 20% methanol.
4. *o*-Phthalaldehyde solution; 0.06% *o*-phthalaldehyde, 0.4 M boric buffer (pH 10.4), 0.1% Brij35, and 37 mM 2-mercaptoethano.

2.7. Determination of the Effect of Phosphorylation on Transport Activities

1. QuickChange site-directed mutagenesis kit (Stratagene).

3. Method

Polyamine transport genes in *E. coli* were identified by cloning the genes that restored polyamine transport activity in a polyamine transport-deficient mutant NH1596. The putrescine-ornithine antiport activity was determined by measuring [^{14}C]putrescine uptake into ornithine-loaded inside-out membrane vesicles, and by measuring [^{14}C]ornithine retained in [^{14}C]ornithine-loaded inside-out membrane vesicles following the addition of putrescine. The spermidine excretion system was identified by the relief of cell toxicity caused by overaccumulated spermidine in CAG2242, which is deficient in spermidine acetyltransferase. In *S. cerevisiae*, candidate genes, which show homology to bacterial polyamine transport systems, were cloned into a multicopy vector, and the polyamine transport activity of transformants was measured. Putrescine excretion activity was identified by measuring [^{14}C]putrescine excretion from cells preloaded with [^{14}C]putrescine using gene-disrupted cells. The effects of phosphorylation on transport activities were examined by site-directed mutagenesis of serine/threonine residues that can be phosphorylated by protein kinases.

3.1. Identification of Polyamine Transport Systems in *E. coli*

1. 7–14 kb DNA fragments of DR112 was inserted into the BamHI site of pACYC184.
2. *E. coli* polyamine transport-deficient mutant NH1596 was transformed with the above plasmids according to the standard method (15).
3. 100–200 transformants were spread on to an agar plate as described in Subheading 2.2. After incubation at 37°C for 24 h, two replica plates were prepared, and the replica plates were incubated at 37°C for 24 h.
4. One replica plate was sprayed with 0.7 mL of 10 μM [^{14}C]spermidine and the other with 0.7 mL of 10 μM [^{14}C]putrescine. These plates were incubated at 37°C for 30 min, and the colonies on each plate were transferred to a filter paper (No. 1, 82 mm diameter, Advantec Toyo, Tokyo). After drying, the paper was exposed to Kodak XAR-5 film for 3 days.
5. Dark colonies revealed by autoradiography were isolated, and three independent clones containing polyamine transport genes were identified by measuring the polyamine uptake activity of the transformants. These were named pPT104, pPT79, and pPT71.

3.2. Assays for Spermidine and Putrescine Uptake by Intact *E. coli* Cells (see Note 1)

1. Plasmids pPT104 encoding *potABCD* operon, pPT79 encoding *potFGHI* operon, and pPT71 encoding *speF-potE* operon were transformed into MA261 or NH1596.
2. Transformed cells were cultured in 20 mL of Medium A containing 0.03 mg/mL chloramphenicol at 37°C until $A_{540} = 0.3$.
3. Cells were harvested by centrifugation at $12,000 \times g$ for 10 min, washed with Buffer 1, and suspended in the same buffer to yield a protein concentration of 0.1 mg/mL. Protein was measured by the method of Lowry et al. (16) after trichloroacetic acid precipitation of cells.
4. The cell suspension (0.48 mL) was preincubated at 30°C for 5 min, and the reaction was started by the addition of 0.02 mL of 0.25 mM [^{14}C]spermidine or [^{14}C]putrescine. After incubation at 30°C, the cells were collected on cellulose acetate membrane filters, and the filters were washed 3 times at room temperature with a total of 6 mL of Buffer 1. The radioactivity on the filter was assayed with a liquid scintillation spectrometer.

3.3. Preparation of Inside-Out Membrane Vesicles and Assay for Putrescine-Ornithine Antiport (see Note 2)

1. *E. coli* DR112/pPT71 was cultured in 1,000 mL of Medium B until $A_{540} = 0.5$.
2. Cells were washed with Buffer 2 without ornithine and suspended in Buffer 2. Inside-out membrane vesicles were prepared by French press treatment (10,000 p.s.i.) of the cells. After removal of unbroken cells and cell debris, membrane vesicles were collected by ultracentrifugation ($170,000 \times g$, 1 h).
3. Membrane vesicles were washed with Buffer 3, collected by ultracentrifugation, and suspended in the same buffer at the protein concentration of 5–10 mg/mL.
4. The reaction mixture (final 0.1 mL) for putrescine uptake by inside-out membrane vesicles contained 50 μg of inside-out membrane vesicle protein in Buffer 4. The reaction mixture was incubated at 22°C for 5 min, and the reaction was started by the addition of 5 μL of 1 mM [^{14}C]putrescine at a final concentration of 50 μM . After incubation at 22°C for 10 s to 2 min, membrane vesicles were collected on cellulose nitrate membrane filters and washed with Buffer 4, and their radioactivities were measured with a liquid scintillation spectrometer.
5. For the assay for ornithine excretion by inside-out membrane vesicles, preloading of inside-out membranes with ornithine (the reaction mixture, 0.02 mL) was performed by incubating inside-out membrane vesicles (0.1 mg of protein) in the presence of 0.5 mM [^{14}C]ornithine in Buffer 4 at 37°C for 1 h.

The excretion assay was started by tenfold dilution of the above membrane vesicle solution with Buffer 4 containing 50 μ M nonlabeled putrescine.

3.4. Identification of Spermidine Excretion System (*MdtJI*) and Assay for Spermidine Excretion (see Note 3)

1. *E. coli* CAG2242 was transformed with genes of 33 putative drug exporters in pUC119, a multicopy vector, and cell viability was measured by culturing the transformants on LB-1.5% agar plates containing 2 mM spermidine, which causes cell death due to the overaccumulation of spermidine. The transformant with pUC*mdtJI* restored the cell viability (7).
2. CAG2242/pUC*mdtJI* or pUC119 was cultured in 100 mL of LB-medium containing 100 μ g/mL ampicillin and harvested at $A_{540}=0.5$. After cells were washed with Buffer 1, [14 C]spermidine was preloaded by the incubation of cells (0.2 mg protein/mL Buffer 1) with 1 mM [14 C]spermidine (37 MBq/mmol) for 90 min. After cells were washed with Buffer 1, spermidine excretion from cells was measured by incubating cells (0.2 mg/mL Buffer 1) at 37°C for the designated times. The cells were then removed by centrifugation at 17,000 $\times g$ for 5 min, and the radioactivity of the supernatant (0.5 mL) was counted by a liquid scintillation counter.

3.5. Assays for Spermidine or Putrescine Uptake, Putrescine Excretion and Putrescine Uptake in Vacuoles, and Measurement of Polyamines in *S. cerevisiae* (see Note 4–6)

1. Transformation of *S. cerevisiae* cells with plasmids was performed by the lithium acetate method of Ito et al. (17).
2. For the assay of spermidine or putrescine uptake, YPH499/YEpDUR3 was cultured in 100 mL of Mg²⁺-limited CSD medium and harvested at $A_{540}=0.5$. Cells were washed 3 times with Buffer 5, suspended at 0.2 mg protein/mL in the same buffer, and incubated at 30°C for 5 min. The measurement of spermidine or putrescine uptake was started by the addition of [14 C]spermidine (37 MBq/mmol) or [14 C]putrescine (37 MBq/mmol) at the final concentration of 0.1 or 0.5 mM, respectively. After incubation for 20, 40, or 60 min, 0.5 mL aliquot of reactions was filtered through a cellulose acetate membrane filter and washed twice with 2 mL of Buffer 5 containing tenfold concentrations of nonlabeled spermidine or putrescine. The radioactivity on the filter was counted in a liquid scintillation counter.
3. For the assay of putrescine excretion by YPH499 and YPH499 Δ *tpo5* cells, [14 C]putrescine was preloaded by the incubation of cells (0.2 mg/mL) with 2.0 mM [14 C]putrescine (18.5 MBq/mmol) at pH 8.0 for 90 min. After the cells were washed with Buffer 5, [14 C]putrescine loaded cells were incubated in the same buffer. After incubation for 30, 60, 90, or 120 min at 30°C, a 0.5-mL aliquot of the reaction mixture was centrifuged (17,000 $\times g$ for 5 min at 4°C),

and the radioactivity of the supernatant was counted in a liquid scintillation counter.

4. For the assay of putrescine uptake in vacuoles, [^{14}C]putrescine uptake activity of YTM22-8/YEpUGA4 or YEp352 was measured as described in Subheading 3.5.2 (13). To confirm the accumulation of putrescine in vacuoles, YTM22-8/YEpUGA4 or YEp352 cells were also cultured in the presence of 0.5 mM nonlabeled putrescine, and harvested at $A_{540}=0.5$. Subcellular fractionation into cytosol and vacuoles was performed by the method of Joho et al. (18). Polyamines in whole cells and vacuoles were extracted by the treatment with 10% (w/v) trichloroacetic acid at 37°C for 1 h. The polyamines in 10 μL of the trichloroacetic acid supernatant were measured by a Tosoh HPLC system on which a TSK gel IEX215 column (4 by 80 mm) heated to 50°C was mounted (19). The flow rate of Buffer 6 was 0.35 mL/min. Detection of the polyamines was by fluorescence intensity after reaction of the column effluent at 50°C with the *o*-phthalaldehyde solution. The flow rate of the *o*-phthalaldehyde solution was 0.8 mL/min, and fluorescence was measured at an excitation wavelength of 388 nm and an emission wavelength of 410 nm. The retention times for putrescine, spermidine, and spermine were 9, 15, and 27 min, respectively.

3.6. Effect of Phosphorylation on Transport Activities

1. Site-directed mutagenesis of serine/threonine residues of transporters encoded in YEpDUR3 or YEpTPO1 was performed by QuickChange site-directed mutagenesis kit.
2. Mutated plasmids were transformed into YPH499 or YTM22-8, and transport activities of transformants were measured as described in Subheading 3.5.

4. Notes

1. A schematic that summarizes the polyamine transport systems in *E. coli* is shown in Fig. 1a. There are two polyamine uptake systems – a spermidine-preferential uptake system consisting of PotA, B, C, and D proteins and a putrescine-specific uptake system consisting of PotF, G, H, and I proteins. As an example, the activity of spermidine uptake by pPT104 encoding *potA-BCD* is shown in Fig. 1b. Since the copy number of the vector pACYC184 is approximately 20, the spermidine uptake activity of *E. coli* cells is estimated to be approximately 500 pmol/min/mg protein, if spermidine is present at more than 1 μM in the medium ($K_m=0.10 \mu\text{M}$). Spermidine uptake activity is reduced by accumulation of spermidine in cells, due to inhibition of

- PotA ATPase activity by spermidine (20) and transcriptional inhibition of the *potABCD* operon by PotD-spermidine complex (21). The K_m value for the putrescine uptake by PotFGHI was 0.5 μM , indicating that putrescine is also effectively influxed to *E. coli* (10). When putrescine was the only energy source, PuuP functioned as a putrescine transporter (22).
2. With regard to antiporters that are important for cell growth at acidic pH, PotE (a putrescine-ornithine antiporter) and CadB (a cadaverine-lysine antiporter) were identified. For the expression of these genes, high concentrations of ornithine and lysine (0.5–1 mM) are necessary in the acidic medium. Thus, CadB probably plays a more important role than PotE in the cell growth at acidic pH. The antiporter activity of PotE is shown in Fig. 1b. PotE and CadB contain 12 transmembrane segments, and key amino acids involved in the function of both antiporters were identified (23, 24). The *potE* gene makes an operon with the inducible ornithine decarboxylase (*speF*) gene, as does the *cadB* gene with the inducible lysine decarboxylase (*cadA*) gene. Thus, PotE and CadB contribute to neutralize the pH of medium by excreting putrescine or cadaverine, and inducible ornithine decarboxylase (or inducible lysine decarboxylase) synthesizes putrescine (or cadaverine), generates a pH gradient by consumption of a cytoplasmic proton, and produces CO_2 . A pH gradient contributes the uptake of nutrients, and CO_2 is used for the synthesis of ATP.
 3. Overaccumulation of spermidine inhibits cell growth of *E. coli*. Overaccumulation of spermidine is relieved by spermidine acetyltransferase (11) or induction of L-glycerol 3-phosphate (25). Acetylated spermidine cannot interact with RNA, and thus does not inhibit protein synthesis and cell growth. Similarly, L-glycerol 3-phosphate makes a complex with spermidine, which prevents spermidine binding to RNA. A third mechanism to decrease the concentration of active or free spermidine in cells is the excretion of spermidine by MdtJI (Fig. 1b). The MdtJ and MdtI proteins each contain four transmembrane segments, and the level of *mdtJI* mRNA is increased by spermidine (7). Functional amino acids involved in spermidine excretion by MdtJ and MdtI have been identified (7).
 4. Regarding polyamine uptake protein in *S. cerevisiae*, DUR3 and SAM3 were identified as preferential polyamine uptake proteins (Fig. 2a). Putrescine uptake by DUR3 is shown in Fig. 2b. Polyamine uptake activity in yeast is relatively low compared with that in *E. coli*. The K_m values at DUR3 for putrescine and spermidine were 479 and 21.2 μM , respectively. The K_m values of SAM3 for putrescine and spermidine were 433 and 20.7 μM , respectively. DUR3 catalyzes the uptake of urea together with polyamines, and SAM3 catalyzes the

uptake of glutamine, lysine, and *S*-adenosylmethionine together with polyamines. Thus, DUR3 with 16 transmembrane segments is the most important polyamine uptake protein in yeast (Fig. 3a). The polyamine uptake in yeast is regulated by PTK2 (polyamine transport protein kinase 2), a serine/threonine protein kinase (26), and the polyamine uptake by DUR3 is regulated by PTK2 through the phosphorylation of Thr²⁵⁰, Ser²⁵¹, and Thr⁶⁸⁴ (Fig. 3b) (6). PTK2 enhancement of polyamine uptake by DUR3 was confirmed using YTM22-8, which is deficient in PTK2.

5. Spermidine/spermine *N*¹-acetyltransferase does not exist in yeast, but there are a number of polyamine excretion proteins (TPO1 to TPO5) (Fig. 2a). Among them, TPO1 and TPO5 are the most important excretion proteins. Since TPO5 is a specific polyamine excretion protein, the excretion activity of preloaded [¹⁴C]putrescine in wild-type cells was compared with that in *TPO5*-disrupted cells. The excretion activity of wild-type cells was much higher than that of $\Delta tpo5$ cells (Fig. 2b). TPO5 was located on Golgi or post-Golgi secretory vesicles, and excretion of putrescine and spermidine by TPO5 was regulated by the secretory or endocytic pathways. TPO1 was located mainly on the plasma membrane. The activity of TPO1 was enhanced through phosphorylation at Ser¹⁹ by protein kinase C and at Thr⁵² by casein kinase I, and sorting of TPO1 from the endoplasmic reticulum to the plasma membrane was enhanced through phosphorylation at Ser³⁴² by cAMP-dependent protein kinases1 and 2 (Fig. 2a) (4).
6. UGA4 on the vacuolar membrane, confirmed by immunofluorescence microscopy, catalyzed the uptake of putrescine as well as GABA (γ -aminobutyric acid). Although putrescine uptake activity of UGA4 was measured using YTM22-8, which is deficient in the DUR3-dependent polyamine transport activity, i.e., deficient in PTK2, the *K_m* value (0.69 mM) for putrescine may not directly reflect the property of UGA4 on vacuoles. The putrescine uptake activity in YTM22-8 cells was stimulated by UGA4, and accumulation of putrescine in vacuoles was confirmed (Fig. 2b). However, it remains to be clarified whether polyamines play important roles in vacuoles or excess amounts of polyamines are stored in vacuoles.

Acknowledgements

We are grateful to Drs. A. J. Michael and K. Williams for critical reading of the manuscript prior to submission. This study was supported in part by Grants-in-Aid for Scientific Research from the Ministry of Education, Culture, Sports, Science, and Technology, Japan.

References

- Cohen SS (1998) A guide to polyamines. Oxford University Press, New York, pp 1–543
- Igarashi K, Kashiwagi K (2000) Polyamines: mysterious modulators of cellular functions. *Biochem Biophys Res Commun* 271:559–564
- Igarashi K, Kashiwagi K (1999) Polyamine transport in bacteria and yeast. *Biochem J* 344:633–642
- Uemura T, Tachihara K, Tomitori H, Kashiwagi K, Igarashi K (2005) Characteristics of the polyamine transporter TPO1 and regulation of its activity and cellular localization by phosphorylation. *J Biol Chem* 280:9646–9652
- Tachihara K, Uemura T, Kashiwagi K, Igarashi K (2005) Excretion of putrescine and spermidine by the protein encoded by YKL174c (TPO5) in *Saccharomyces cerevisiae*. *J Biol Chem* 280:12637–12642
- Uemura T, Kashiwagi K, Igarashi K (2007) Polyamine uptake by DUR3 and SAM3 in *Saccharomyces cerevisiae*. *J Biol Chem* 282:7733–7741
- Higashi K, Ishigure H, Demizu R, Uemura T, Nishino K, Yamaguchi A, Kashiwagi K, Igarashi K (2008) Identification of a spermidine excretion protein complex (MdtJI) in *Escherichia coli*. *J Bacteriol* 190:872–878
- Cunningham-Rundles S, Maas WK (1975) Isolation, characterization, and mapping of *Escherichia coli* mutants blocked in the synthesis of ornithine decarboxylase. *J Bacteriol* 124:791–799
- Linderoth N, Morris DR (1983) Structural specificity of the triamines sym-homospermidine and aminopropylcadaverine in stimulating growth of spermidine auxotrophs of *Escherichia coli*. *Biochem Biophys Res Commun* 117:616–622
- Kashiwagi K, Hosokawa N, Furuchi T, Kobayashi H, Sasakawa C, Yoshikawa M, Igarashi K (1990) Isolation of polyamine transport-deficient mutants of *Escherichia coli* and cloning of the genes for polyamine transport proteins. *J Biol Chem* 265:20893–20897
- Fukuchi J, Kashiwagi K, Yamagishi M, Ishihama A, Igarashi K (1995) Decrease in cell viability due to the accumulation of spermidine in spermidine acetyltransferase-deficient mutant of *Escherichia coli*. *J Biol Chem* 270:18831–18835
- Kakinuma Y, Maruyama T, Nozaki T, Wada Y, Ohsumi Y, Igarashi K (1995) Cloning of the gene encoding a putative serine/threonine protein kinase which enhances spermine uptake in *Saccharomyces cerevisiae*. *Biochem Biophys Res Commun* 216:985–992
- Uemura T, Tomonari Y, Kashiwagi K, Igarashi K (2004) Uptake of GABA and putrescine by UGA4 on the vacuolar membrane in *Saccharomyces cerevisiae*. *Biochem Biophys Res Commun* 315:1082–1087
- Kaiser C, Michaelis S, Mitchell A (1994) *Methods in yeast genetics: a cold harbor laboratory course manual*. Cold Spring Harbor Laboratory, Cold Spring Harbor
- Maniatis T, Fritsch EF, Sambrook J (1982) Transformation of the calcium chloride procedure. In: Maniatis T, Fritsch EF, Sambrook J (eds) *Molecular cloning: a laboratory manual*. Cold Spring Harbor Laboratory, Cold Spring Harbor, pp 250–251
- Lowry OH, Rosebrough NJ, Farr AL, Randall RJ (1951) Protein measurement with the Folin phenol reagent. *J Biol Chem* 193:265–275
- Ito H, Fukuda Y, Murata K, Kimura A (1983) Transformation of intact yeast cells treated with alkali cations. *J Bacteriol* 153:163–168
- Joho M, Ishikawa Y, Kunikane M, Inouhe M, Tohoyama H, Murayama T (1992) The subcellular distribution of nickel in Ni-sensitive and Ni-resistant strains of *Saccharomyces cerevisiae*. *Microbios* 71:149–159
- Igarashi K, Kashiwagi K, Hamasaki H, Miura A, Kakegawa T, Hirose S, Matsuzaki S (1986) Formation of a compensatory polyamine by *Escherichia coli* polyamine-requiring mutants during growth in the absence of polyamines. *J Bacteriol* 166:128–134
- Kashiwagi K, Innami A, Zenda R, Tomitori H, Igarashi K (2002) The ATPase activity and the functional domain of PotA, a component of the spermidine-preferential uptake system in *Escherichia coli*. *J Biol Chem* 277:24212–24219
- Antognoni F, Del Duca S, Kuraishi A, Kawabe E, Fukuchi-Shimogori T, Kashiwagi K, Igarashi K (1999) Transcriptional inhibition of the operon for the spermidine uptake system by the substrate-binding protein PotD. *J Biol Chem* 274:1942–1948
- Kurihara S, Oda S, Kato K, Kim HG, Koyanagi T, Kumagai H, Suzuki H (2005) A novel putrescine utilization pathway involves γ -glutamylated intermediates of *Escherichia coli* K-12. *J Biol Chem* 280:4602–4608
- Kashiwagi K, Kuraishi A, Tomitori H, Igarashi K, Nishimura K, Shirahata A, Igarashi K (2000) Identification of the putrescine recognition site on polyamine transport protein PotE. *J Biol Chem* 275:36007–36012
- Soksawatmaekhin W, Uemura T, Fukiwaki N, Kashiwagi K, Igarashi K (2006) Identification of the cadaverine recognition site on the

- cadaverine-lysine antiporter CadB. *J Biol Chem* 281:29213–29220
25. RajVS, Tomitori H, Yoshida M, Apirakaramwong A, Kashiwagi K, Takio K, Ishihama A, Igarashi K (2001) Properties of a revertant of *Escherichia coli* viable in the presence of spermidine accumulation: increase in L-glycerol 3-phosphate. *J Bacteriol* 183:4493–4498
26. Nozaki T, Nishimura K, Michael AJ, Maruyama T, Kakinuma Y, Igarashi K (1996) A second gene encoding a putative serine/threonine protein kinase which enhances spermine uptake in *Saccharomyces cerevisiae*. *Biochem Biophys Res Commun* 228:452–458
27. Kashiwagi K, Miyamoto S, Suzuki F, Kobayashi H, Igarashi K (1992) Excretion of putrescine by the putrescine-ornithine antiporter encoded by the *potE* gene of *Escherichia coli*. *Proc Natl Acad Sci USA* 89:4529–4533

Chapter 19

Genetic and Biochemical Analysis of Protozoal Polyamine Transporters

Marie-Pierre Hasne and Buddy Ullman

Abstract

Polyamines are aliphatic polycations that function in key cellular processes such as growth, differentiation, and macromolecular biosynthesis. Intracellular polyamines pools are maintained from de novo synthesis and from transport of polyamines from the extracellular milieu. This acquisition of exogenous polyamines is mediated by cell surface transporter proteins. Protozoan parasites are the etiologic agents of a plethora of devastating and often fatal diseases in humans and their domestic animals. These pathogens accommodate de novo and/or salvage mechanisms for polyamine acquisition. Because of its therapeutic relevance, the polyamine biosynthetic pathway has been thoroughly investigated in many genera of protozoan parasites, but the polyamine permeation pathways have generally been ignored. Our group has now identified at the molecular level polyamine transporters from two species of protozoan parasites, *Leishmania major* and *Trypanosoma cruzi*, characterized these polytopic proteins with respect to ligand specificities and affinities, and determined the subcellular environments in which these transporters reside.

Key words: Polyamines, Diamines, Transporters, Parasites, *Leishmania*, *Trypanosoma cruzi*, Localization, Confocal microscopy

1. Introduction

Polyamines are ubiquitous aliphatic cations that play essential roles in cellular homeostasis. Mammalian cells and most organisms, including prokaryotes, acquire polyamines by two routes: de novo via synthesis from basic amino acids and through the transport of extracellular polyamines, a process that is mediated by polyamine transporters or permeases. The polyamine biosynthetic pathway in protozoan parasites has stimulated considerable interest among scientists and clinicians alike because it has been targeted successfully by a novel and currently employed chemotherapy for African trypanosomiasis. D, L- α -Difluoromethylornithine,

an irreversible inactivator of ornithine decarboxylase (1), the first enzyme in the polyamine biosynthesis pathway, can eliminate *Trypanosoma brucei* infections in both mice and humans with late stage African sleeping sickness (2–5). Inhibitors of another polyamine enzyme, S-adenosylmethionine decarboxylase, are also effective antitrypanosomal agents (6–9).

Leishmania spp. and *Trypanosoma cruzi*, parasites that are phylogenetically related to *T. brucei*, are the etiologic agents of leishmaniasis and Chagas' disease, respectively. *Leishmania* can synthesize polyamines from arginine and ornithine (2, 10), whereas *T. cruzi* cannot (11, 12), and both pathogens have the capacity to translocate extracellular polyamines into the cell. Because the polyamine transporters of *T. cruzi* serve an essential nutritional function, they are valid targets for chemotherapeutic intervention. Our laboratory has identified and characterized the polyamine transporters of *L. major* and *T. cruzi* using straightforward molecular, biochemical, and cellular biological approaches. Immunofluorescence microscopy enabled the localization of these polyamine permeases to assorted subcellular milieus.

The methods described in this chapter have been implemented to measure polyamine transport in *Leishmania*, *T. cruzi*, and *Xenopus laevis* oocytes and can also be adapted to *Saccharomyces cerevisiae* or any cell type that can grow in suspension culture. In particular, we report on the overexpression of polyamine transporters in homologous systems, a method that has demonstrable advantages when transporters localize to specialized internal structures absent in organisms classically used for heterologous expression (e.g., *S. cerevisiae* or *Xenopus* oocytes). In order to measure transport on whole cells, the expression of the transporter at the cell surface is compulsory, and for that purpose, we have found it useful to conduct localization and transport studies simultaneously. The *X. laevis* expression system, also presented in this chapter, is a well-established expression system that has been used to characterize a variety of transporters (13–15). Although oocyte expression can be very robust (16), some transporters are difficult to express in *Xenopus* oocytes. The main drawbacks are in the production of intact cRNA, variability among batches of oocytes that can impair the collection of reliable data, and intracellular localization of some transporters that preclude contact with extracellular ligand.

2. Materials

2.1. Protozoan Parasites

2.1.1. Parasite Cell Culture

1. *Leishmania major* culture medium: one pouch of M199 powder base (Gibco/BRL, Bethesda, MD), 5.96 g HEPES, 10 g NaHCO₃, 0.6 g penicillin, 0.1 g streptomycin, 1 mM glutamine, 10 ml 100× RPMI vitamin mixture (Gibco/BRL),

100 μ M folic acid, 100 μ M adenosine, 5 mg hemin, and 10% fetal bovine serum (HyClone, Ogden, UT) in 1 L water.

2. SDM-79 growth medium for *T. cruzi* epimastigotes and *T. brucei* procyclic forms: 7.0 g MEM (Earl's) powder (Gibco/BRL), 2.0 g M199 powder (Gibco/BRL), 8 ml 50 \times MEM essential amino acids, 6 ml 100 \times MEM nonessential amino acids, 1.0 g glucose (anhydrous), 8.0 g HEPES (sodium salt), 5.0 g MOPS (free acid), 2.0 g NaHCO₃, 0.1 g sodium pyruvate, 200 mg DL-alanine, 100 mg L-arginine, 300 mg L-glutamine, 70 mg DL-methionine, 80 mg L-phenylalanine, 600 mg L-proline, 60 mg DL-serine, 160 mg taurine, 350 mg DL-threonine, 100 mg L-tyrosine, 10 mg guanosine, 4 mg folic acid, 50 mg D(+)-glucosamine-HCl, 2 mg *p*-aminobenzoic acid, 0.2 mg biotin, and 10% fetal bovine serum (HyClone) in 1 L water.
3. LIT growth medium used for culturing *T. cruzi* epimastigotes: 4 g NaCl, 0.4 g KCl, 12.1 g Na₂HPO₄ (anhydrous), 2 g glucose, 5 g tryptone, 5 g liver-infused-broth powder, and 50 mg hemin in 1 L water.

2.1.2. Parasite Transfection

1. Vectors: *Leishmania* pXG series and pXG-GFP+ expression vectors (17); pHD309 *T. brucei* expression vector (18); *T. cruzi* pTEX (19) or pTEX-GFP (20) expression plasmids, the latter a vector in which the green fluorescent protein (GFP) gene is ligated to the expressed DNA insert.
2. Parasite polyamine transporter genes: *LmPOT1.1* from *L. major*, and *TcPOT1.1*, and *TcPOT1.2* from *T. cruzi*.
3. Column-purified DNA: 2–5 μ g/transfection for *Leishmania*, 5–10 μ g/transfection for *T. brucei*, and 80–100 μ g/transfection for *T. cruzi*.
4. Cells: *Leishmania* promastigotes, *T. brucei* procyclic forms, and *T. cruzi* epimastigotes from early- to mid-exponential phase cultures.
5. Electroporation buffers: For *Leishmania* and *T. brucei* use cytomix: 120 mM KCl, 0.15 mM CaCl₂, 10 mM K₂HPO₄, 25 mM HEPES, 2 mM EDTA, and 5 mM MgCl₂, pH 7.6. For *T. cruzi* use HBS buffer: 21 mM HEPES, 137 mM NaCl, 5 mM KCl, 0.7 mM Na₂HPO₄, and 6 mM glucose, pH 7.5.
6. Electroporator: Gene Pulser Xcell (Bio-Rad Laboratories, Hercules, CA).
7. Electroporation cuvettes: 4 mm gap cuvettes for *Leishmania* and *T. brucei*, 2 mm gap cuvettes for *T. cruzi*.

2.1.3. Microscopy

1. Poly-L-Lysine diluted 1/10 (v/v) in deionized water.
2. Lab-Tek® II Chambered #1.5 German cover glass system (Nunc, Rochester, NY).

3. Fluorescence microscope, e.g., a Zeiss Axiovert 200 M deconvolution microscope (Carl Zeiss, Inc., Thornwood, NY).

2.1.4. Transport Assay

1. Cells: Transgenic strains of *Leishmania*, *Trypanosoma brucei*, or *T. cruzi* (see Note 1). Two transgenic parasite lines of each species are required. One cell line (experimental cell line) carries a recombinant plasmid that overexpresses the gene of interest, e.g., the polyamine transporter, and the other contains a nonrecombinant episome lacking the gene of interest or a chimeric plasmid expressing an unrelated gene (control cell line). The experimental and control cell lines are grown to the same specific cell density prior to transport experiments (see Note 2).
2. Phosphate buffered saline-glucose (PBSG) or CBSS buffers: PBSG buffer consists of 137 mM NaCl, 2.7 mM KCl, 10 mM Na₂HPO₄, and 2 mM KH₂PO₄, pH 7.4. If sterilized, PBSG can be stored for months at room temperature. PBSG should be supplemented with 10 mM glucose just prior to the start of the experiment. CBSS buffer is composed of 25 mM HEPES, 120 mM NaCl, 5.4 mM KCl, 0.55 mM CaCl₂, 0.4 mM MgSO₄, 5.6 mM Na₂HPO₄, and 11.1 mM D-glucose, pH 7.4. Filter sterilize and store at 4°C for up to a month. PBSG and CBSS buffers are equivalent for transport measurements (see Note 3).
3. 1-Bromododecane, a chemically inert oil (Sigma Aldrich, St. Louis, MO).
4. Radiolabeled polyamines: [2,3-³H]Putrescine dihydrochloride (60 Ci/mmol) in 0.01 N HCl (American Radiolabeled Chemicals, Inc., St. Louis, MO), [³H(N)] spermidine trihydrochloride (19.1 Ci/mmol) in 0.01 N HCl (PerkinElmer, San Jose, CA), [³H]spermine tetrahydrochloride (60 Ci/mmol) in 90% ethanol (American Radiolabeled Chemicals, Inc.), and [1,5-¹⁴C]cadaverine dihydrochloride (15.8 mCi/mmol) in aqueous solution containing 2% ethanol (Sigma-Aldrich) (see Note 4). All diamines and polyamines are stored between 0 and 5°C, and the rate of decomposition under these conditions is <1% per month.
5. Liquid nitrogen (see Note 5) or an ethanol/dry-ice mixture.
6. A nail clipper for dogs (allows uncomplicated excision of the tip of microcentrifuge tubes into a scintillation vial).
7. A repeater[®] plus pipette (Brinkman Instruments, Inc., Westbury, NY).
8. Scintillation vials (see Note 6).
9. 1% Triton X-100: Mix 1 ml of Triton X-100 with 100 ml of H₂O. This solution can be stored at room temperature for months.

10. Scintillation liquid: CytoScint (Research Products Division, Irvine, CA) (see Note 7).
11. Scintillation counter: LS6500 liquid scintillation counter (Beckman Coulter, Fullerton, CA).

2.2. *X. laevis* Oocytes

2.2.1. Preparation of cRNA for Microinjection

1. DNA template: The open reading frame of the putative transporter should be cloned into an oocyte expression vector, e.g., pL2.5 (21), in order to provide DNA template for the cRNA synthesis reaction. The oocyte expression vector must contain a T7, T3, or SP6 RNA polymerase promoter site upstream of the gene insert in order to enable transcription and a multiple cloning site flanked by *X. laevis* DNA sequences, e.g., the 5' UTR and 3' UTR of the endogenous β -globin gene. A unique restriction site must be available downstream of the 3' UTR in order to linearize the plasmid prior to injection.
2. ~20 units/mg proteinase K.
3. Phenol:chloroform:isoamyl alcohol (25:24:1) in Tris-HCl buffer, pH 7.9. Store in 50 ml aliquots at -20°C for up to 6 months.
4. 3.0 M sodium acetate, pH 5.2.
5. RNase-free water.
6. RNA decontamination solution (RNaseZap[®], Ambion[®] Applied Biosystems, Austin, TX).
7. mMessage mMachine[®] Kit corresponding to the RNA polymerase promoter site present in the oocyte expression vector (T7, T3, or SP6) (Ambion[®] Applied Biosystems).
8. 10 \times MOPS: 0.4 M MOPS [(3-(*N*-morpholino)-propanesulfonic acid)] pH 7.0, 0.1 M sodium acetate, and 0.01 M EDTA in RNase-free water (10 \times MOPS can also be purchased from Ambion[®] Applied Biosystems).
9. 12.3 M formaldehyde.
10. Formaldehyde loading dye.
11. RNA ladder.

2.2.2. *Xenopus* Oocytes Harvest, cRNA injection, and Transport Assay

1. cRNA stored at -80°C .
2. Oocytes positive tested female *X. laevis* (*Xenopus* express).
3. Curved extra-fine point watchmaker's forceps (Bio-Bridge Science, Oak Brook, IL), a scalpel, a set of forceps (#78313-00B and #78317-2, Electron Microscopy Sciences, Hatfield, PA), and fine point scissors (#72940, Electron Microscopy Sciences).

4. A nonhumidified incubator set at 16°C.
5. Plastic Pasteur pipettes with tips excised to enlarge the opening (~4 mm).
6. A 60×15 mm Petri dish lined with woven mesh filter (SpectraMesh, Rancho Dominguez, CA) (see Note 8).
7. Capillary needles: 3.5 nl glass replacement needles (World Precision Instruments, Sarasota, FL).
8. Micropipette puller (World Precision Instruments).
9. Micropipette beveller (World Precision Instruments).
10. Nanoliter injector (World Precision Instruments).
11. Mineral oil.
12. ND-96 buffer: 96 mM NaCl, 2 mM KCl, 1.8 mM CaCl₂, 1 mM MgCl₂, 5 mM HEPES, pH 7.5. ND-96 buffer should be filter sterilized. For convenience, a 10× filter sterilized ND-96 stock solution can be prepared in advance and stored at 4°C (see Note 9).
13. Complete ND-96 buffer: To 1× ND-96 buffer, add sodium pyruvate, gentamycin, and fetal bovine serum to final concentrations of 2.5 mM, 50 µg/ml, and 1–3% FBS, respectively, just prior to use. The pyruvate serves as an additional energy, and fetal bovine serum provides an additional source of nutrients for the oocytes.
14. OR-2: 82.5 mM NaCl, 2 mM KCl, 1 mM MgCl₂·6H₂O, 5 mM HEPES, pH, 7–7.5.
15. Collagenase solution: 2 mg/ml collagenase A (F. Hoffman La Roche AG, Basel, Switzerland) in OR-2. Filter sterilize and store at –20°C in 30 ml aliquots.
16. *X. laevis* anesthetic: Prepare anesthetic by dissolving 2 g of 3-aminobenzoic acid ethyl ester and 4 g NaHCO₃ in 2 L H₂O. Pour into a large bucket with a tight lid to keep the frog from jumping out. This anesthetic solution can be maintained at room temperature and reused until it becomes murky in color.
17. Radiolabeled polyamines: Same polyamine stocks used in transport experiments in Subheading 2.1.4.
18. 1% Triton X-100: Mix 1 ml of Triton X-100 with 100 ml of H₂O. This solution can be kept at room temperature for months.
19. Scintillation liquid: CytoScint (Research Products Division, Irvine, CA) (see Note 5).
20. Scintillation counter: LS6500 liquid scintillation counter (Beckman Coulter, Fullerton, CA).

3. Methods

3.1. Protozoan Parasites

3.1.1. Parasite Transfection

1. Harvest parasites from mid-log phase cultures by centrifugation ($1,500\times g$, 10–15 min, 4°C).
2. Wash the pellet once with 25 ml electroporation buffer.
3. Resuspend the cell pellet in electroporation buffer at a cell density of $1\text{--}3\times 10^8$ cells/ml. Use 450 μl of cell suspension per transfection reaction. It is important to have an additional no DNA control (buffer only) transfection to ensure that the selective agent in the experimental samples is killing non-transfected parasites.
4. Add the plasmid DNA (see Note 10) in a volume of $50\text{--}450\ \mu\text{l}$ of cell suspension. Mix the DNA and parasites gently by pipetting up and down 3–5 times. Transfer the mixture to electroporation cuvettes, and place the cuvettes on ice.
5. Electroporate cells using the electroporation conditions appropriate to the parasite to be transfected. For *Leishmania* and *T. brucei*, use two pulses, 10 s apart at 1.5 kV and 25 μF . For *T. cruzi*, use just one pulse at 1.5 kV and 50 μF .
6. Transfer the cells from the electroporation cuvette to a vented cell culture flask and resuspend in 5 ml of appropriate culture medium. Place flask in a humidified CO_2 incubator. Transfected *T. cruzi* epimastigotes, *T. brucei* procyclic forms, and *Leishmania* promastigotes are cultured in a humidified 5% CO_2 incubator in their respective growth media at 26°C.
7. Add the selective agent 24 h after electroporation. The choice of selective agent, e.g., G418 or hygromycin, needs to be appropriate for the drug resistance cassette employed in the transfection. The initial drug concentrations employed to select for transfectants are 20 $\mu\text{g}/\text{ml}$ G418 or 30–50 $\mu\text{g}/\text{ml}$ hygromycin for *Leishmania* promastigotes, 15 $\mu\text{g}/\text{ml}$ G418 or 25–50 $\mu\text{g}/\text{ml}$ hygromycin for *T. brucei* procyclic forms, and 50–200 $\mu\text{g}/\text{ml}$ G418 for *T. cruzi* epimastigotes.
8. Monitor the cultures for cell growth of parasites transfected with plasmid DNA and for cell death in mock-transfected control cultures. Only transfectants that proliferate robustly are employed for microscopy and for transport studies. If the transporter of interest has been fused to a fluorescent tag, localization experiments can also be carried out as described below.

3.1.2. Microscopy

1. Using a chambered #1.5 German cover glass system, add poly-L-lysine to cover the chambers and incubate at room temperature for 5 min.
2. Remove the poly-L-lysine from the chambers, and dry the glass slide.

3. Add transfected parasites to the slide and wait 15 min.
4. Remove the culture medium, and add phosphate buffered saline (PBS) to cover the bottom of the chambers. The exact volume of PBS will correspond to the volume of chamber employed in the experiments.
5. Observe the fluorescence distribution under a fluorescence microscope using a filter fitting the excitation and emission criteria of the fluorophore used (see Note 11).

3.1.3. Transport Assay

1. Enumerate cells with a hemocytometer. All cell lines, both parasites transfected with a polyamine transporter gene and control parasites, should be at equivalent densities.
2. All transport assays are performed in triplicate. Prepare three microfuge tubes per condition. Conditions will vary in terms of ligand concentration, time of incubation, and whether a putative transport antagonist is added to the transport medium.
3. Add 100 μ l 1-bromododecane oil to the bottom of each microfuge tube (Fig. 1).
4. Prepare a mixture of radiolabeled and nonradiolabeled polyamine in CBSS or PBSG to twice the final concentration desired. Overlay 100 μ l of that mixture onto the 100 μ l of 1-bromododecane already present in the microfuge tubes (see Note 12). Centrifuge the tubes for 30 s at maximum speed in a microcentrifuge ($\sim 16,000 \times g$). This step will ensure complete separation of the inert oil layer (at the bottom) and the radioactive mixture (at the top) prior to cell addition (Fig. 1).
5. Prepare scintillation vials in advance. The number of scintillation vials required should correspond to the number of

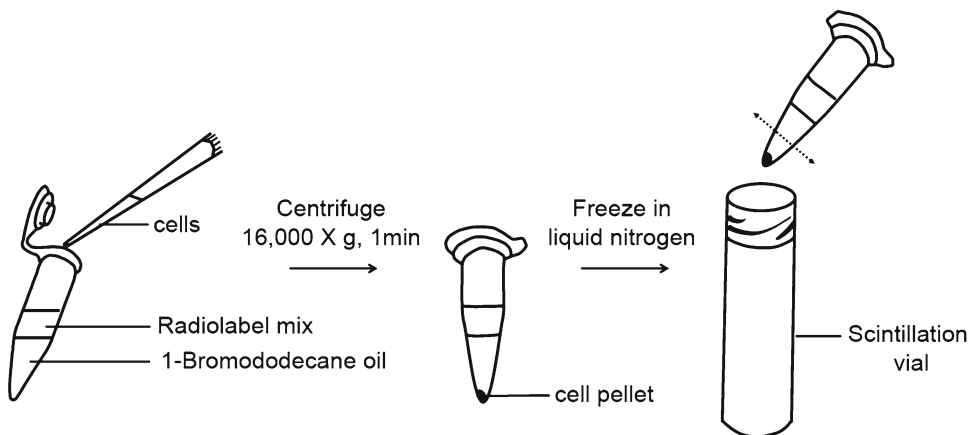


Fig. 1. Schematic diagram of transport assay using protozoan parasites.

- microfuge tubes employed in the transport experiment. Prepare an additional scintillation vial in order to assess the number of counts in the radiolabeled transport cocktail.
6. Pellet parasites by centrifugation at $1,500 \times g$ for 10–15 min at 4°C . Remove supernatant and resuspend sedimented cells in 50 ml PBSG or CBSS buffer.
 7. Repeat previous washing step two more times. Then resuspend the cell pellet from the last wash at $\sim 1.0 \times 10^8$ cells/ml in PBSG or CBSS.
 8. Place microfuge tubes containing radiolabeled buffer overlaying the 1-bromododecane into the rotor of a benchtop microfuge with caps open. Pipette 100 μl of cell suspension (10^7 cells) into the aqueous layer of each tube using a multichannel pipette (see Fig. 1). Quickly close the caps and the centrifuge lids. At fixed intervals, as determined by a timer that is started at the initiation of the experiment, the cells are sedimented at $16,000 \times g$ through the inert 1-bromododecane oil layer for 60 s. This centrifugation step pellets the cells and separates them from the less dense aqueous layer containing the nonincorporated radiolabel, a process that terminates the transport assay.
 9. At the end of each 60 s centrifugation, the parasite pellet should be clearly visible at the bottom of the microfuge tube. Without delay, flash freeze the microfuge tubes with either liquid nitrogen or ethanol/dry-ice (see Note 5).
 10. Repeat steps 8 and 9 until all experimental and control samples are processed.
 11. Sever the tip of the frozen microfuge tube containing the cell pellet with a dog nail clipper and drop the tip into a scintillation vial (Fig. 1). It is straightforward to discern the frozen pellet through the microfuge tube, and the excision should be made just above the pellet but below the nonincorporated radioactive mixture to avoid contamination of the cell pellets postexperimentally. Keeping the microfuge tubes frozen throughout the processing of the pelleted cells is essential to avoid spillage of thawed contents into the scintillation vial.
 12. Add 200 μl of 1% Triton X-100 to each scintillation vial to solubilize the cell pellets. Vortex at maximal speed for ~ 30 s.
 13. Add 3–4 ml of scintillation fluid to each vial, and again vortex at maximum speed. Quantify radiolabel incorporated by the parasites using a liquid scintillation counter (Beckman LS6500). Each sample is counted for 1 min.
 14. In order to experimentally calculate the specific activity of the radiolabel in the experiment, an aliquot of the radiolabeled mixture used in the assay is added to an extra scintillation vial containing 200 μl 1% Triton X-100 and 3–4 ml scintillation fluid.

This sample is treated identically to those containing cell pellets; the sample is mixed by vortexing and enumerated by liquid scintillation spectrometry as described above.

3.1.4. Data Analysis

3.1.4.1. Determining Ligand Specificity of Permeases

Determining the ligand specificity of a putative transporter can be problematic. If you are having problems, consider the following points.

1. First check that the transporter is expressed and that it localizes to the surface of the parasite by fluorescence microscopy.
2. Measure ligand uptake at different ligand concentrations. A transport cocktail containing only radiolabeled substrate will provide maximum sensitivity and should be tried initially. Adding nonradiolabeled substrate to the uptake mix decreases the specific activity of the transport assay mixture but will also increase transport flux and allows assessment of transporter affinities, i.e., K_m values. It is often most useful to characterize transporters at ligand concentrations that are close to or just below the K_m value.
3. Consider varying experimental parameters, e.g., pH buffer, temperature, and/or the presence or absence of Na^+ (to date, no Na^+ -dependent transporters in protozoan parasites have been identified).
4. Consider the possibility that the permease of interest may be an antiporter, perhaps requiring preloading of the parasites.

3.1.4.2. Calculations

1. Liquid scintillation counters can be set up to report data in disintegrations per min (dpm) or counts per min (cpm). If the liquid scintillation counter displays results as cpm, these numbers will need to be converted first into dpm using the equation $\text{dpm} = \text{cpm} \times \text{counting efficiency}$. The counting efficiency will vary with radionuclide and instrument. This information can be obtained from the manufacturer and can also be determined experimentally by counting an aliquot of the transport cocktail of known specific activity.
2. Transport data should then be converted from dpm to molecules of product formed per unit time per unit number of cells. For example, to transform data from dpm into $\text{pmol/s}/10^8$ cells, use the following formula.

$$V(10^8) / A \cdot N$$

Where:

V = initial rate of transport (dpm/s)

A = specific activity of radiolabel in transport cocktail (dpm/pmol)

N = number of cells added to each transport measurement

3. Subtract background values of transport measured in control cell lines from those obtained with parasites overexpressing the transporter of interest.

3.1.4.3. Data Collection and Representation

1. For any transporter, initial rates of uptake are the first data to be collected, since it is imperative to determine that the time course over which the rate of uptake is determined is linear with time. Initial rates are usually obtained by measuring the transport or uptake rates over very short time intervals, e.g., every 5 s over the first 30 s of the experiment. The data are then fitted to a straight line by linear regression analysis. Only transport measurements exhibiting rates with a regression coefficient (r) >0.95 should be considered linear rates.
2. To determine the basic kinetic parameters of a transporter, uptake measurements must be collected over a range of ligand concentrations. These data can then be fit to the Michaelis–Menten equation from which the typical kinetic constants of K_m and V_{max} can be deduced. Nonlinear regressions fitting Michaelis–Menten equation are available through software like GraFit (Erithacus Software Limited) or Prism (GraphPad Software).

3.2. *X. laevis* Oocytes

3.2.1. cRNA synthesis

1. Linearize >20 μg template DNA by restriction endonuclease digestion using an enzyme that cuts the plasmid downstream from the transporter gene open reading frame. The restriction reaction should be accomplished in a large volume, i.e., 500 μl , using an excess amount of enzyme and for several hours to ensure complete digestion. Fractionate an aliquot of the mixture on an agarose gel, and check for complete digestion by ethidium bromide staining.
2. Treat DNA sample with 100–200 $\mu\text{g}/\text{ml}$ proteinase K for 30 min at 50°C .
3. Add an equal volume of phenol:chloroform:isoamyl alcohol, i.e., 500 μl , to the aqueous DNA sample, and vortex for 2 min.
4. Centrifuge at $16,000 \times g$ for 2 min and meticulously transfer the aqueous (top) phase into a new microfuge tube carefully, avoiding transfer of interface material.
5. To precipitate the linearized plasmid DNA, add 1/10 volume of 3.0 M sodium acetate (pH 5.2) to the aqueous phase followed by 3 volumes of 100% ethanol. Mix thoroughly. Place the mixture in the freezer at -20°C for 20–30 min to precipitate the DNA. Centrifuge the precipitated DNA at $16,000 \times g$ for 10 min. The linearized plasmid DNA will be visible as a pellet at the bottom of the tube.
6. Carefully remove the liquid and wash the DNA pellet with 1 ml 70% ethanol at room temperature to remove the salt.
7. Allow the DNA pellet to air dry and resuspend at 1 $\mu\text{g}/\mu\text{l}$ of RNase-free water. Store the linearized DNA template at -20°C until oocyte injection. The DNA is stable for several months after preparation.

8. Preparation of reagents: To prepare reagents for the synthesis of capped RNA, place the RNA polymerase and the 2× NTP/CAP from the mMessage mMachine® kit on ice, but maintain the 10× reaction buffer at room temperature. Make sure that the 2× NTP/CAP and 10× reaction buffer are in solution (if not, vortex). All reagents should be spun briefly in a microfuge just prior to use.
9. Assembly of transcription reaction: In an RNase-free microfuge tube at room temperature, add 10 µl 2× NTP/CAP, 2 µl 10× Reaction buffer, 0.1–1 µg linear template DNA, and 2 µl of Enzyme mix to RNase-free water to bring the final reaction volume to 20 µl. Gently blend the contents of the solution, and spin the tube in a microcentrifuge at maximum speed to collect all of the reaction ingredients at the bottom of the tube in order to ensure complete mixture.
10. Incubate at 37°C for 1 h. Increasing incubation time to 2 h can occasionally increase cRNA yield.
11. Add 1 µl of TURBO DNase mix and incubate at 37°C for an additional 15 min (see Note 13).
12. The cRNA can be recovered by lithium chloride precipitation, phenol:chloroform extraction, or using the MEGAclean™ kit from Ambion. Resuspend cRNA in a small volume of RNase-free H₂O. Determine cRNA yield by measuring absorbance of a 1/100 dilution of the resuspended cRNA at 260 nm. Dilute cRNA to a final concentration of 1 µg/µl in RNase-free H₂O and store at –80°C.
13. cRNA integrity is verified by running an aliquot on a formaldehyde denaturing gel. To prepare a 100 ml denaturing gel, melt 1 g of agarose in 72 ml of water. In a chemical fume hood, add 10 ml of 10× MOPS and 18 ml of 12.3 M formaldehyde (see Note 14).
14. Pour gel in a fume hood in order to minimize formaldehyde exposure. Solidify the gel at room temperature and remove the comb.
15. To make 1× MOPS running buffer, dilute the 10× MOPS stock solution with 9 volumes of RNase-free water. Submerge the solidified gel in the running buffer.
16. Mix the cRNA sample with 3 volumes of formaldehyde loading dye and incubate the samples for 15 min at 65°C. Do the same for the molecular size standards.
17. Centrifuge samples at 16,000 × *g* for 30 s to sediment samples and place tubes on ice.
18. Load cRNA samples in the wells of the denaturing gel and electrophorese at ~5 V/cm. Final voltage (commonly 50–60 V) is estimated by measuring the distance between the two electrodes of the gel apparatus.

19. At the end of the electrophoresis procedure, add ethidium bromide to a final concentration of 0.5 $\mu\text{g}/\text{ml}$ into $1\times$ MOPS, and allow staining to proceed for 20 min. Visualize cRNA under ultraviolet light.

3.2.2. Oocyte Harvest

1. Place a female *X. laevis* in the anesthetic mix for 15–20 min (depending on the size of the animal). Complete anesthesia is confirmed by lack of mobility (see Note 15).
2. Wet a paper towel, and place it on top of an ice bucket. Place the anesthetized *X. laevis* on its back on the paper towel.
3. Make a small incision on the ventral and lateral portion of the abdomen (see Note 16).
4. The oocyte lobes can then be excised using forceps and placed in a Petri dish filled with OR-2 buffer (Ca^{2+} -free) (see Note 17).
5. Gently tease the oocyte lobes apart with watchmakers' forceps to generate smaller clusters of ~ 50 oocytes, and transfer all clusters into 50 ml conical tubes containing OR-2 buffer.
6. Wash oocytes 3 times with 50 ml OR-2 buffer by gently inverting the tube 2 or 3 times. Rinsing the oocytes in this fashion will ensure a low concentration of Ca^{2+} , a divalent cation that inhibits the collagenase enzyme employed in the next step of the procedure.
7. Incubate the oocytes in 20 mg/ml collagenase in the conical tube placed on a rotisserie-type shaker at room temperature for ~ 1 h. This collagenase treatment will separate oocyte clusters into individual oocytes. Because oocyte batches can vary from harvest to harvest, the collagenase treatment should be monitored closely to avoid damaging the oocyte surface membrane, thereby compromising the integrity and survival of the oocyte.
8. Discard the collagenase solution by pouring the oocyte supernatant into a sink and quickly filling the 50 ml conical tube to the top with ND-96 buffer at room temperature. Gently shake the tube to rinse the oocytes of residual collagenase. Allow the oocytes to settle to the bottom of the tube and discard the supernatant, and repeat rinsing procedure at least 5 more times.
9. Place the oocytes in a Petri dish in ND-96 at room temperature, and sort out stage V and VI oocytes under a dissecting microscope. Stage V and VI oocytes can be distinguished by their unmistakable light and dark poles and a well-defined margin separating the two poles and should be homogeneous in size and appearance. Discard misshapen and discolored oocytes. The time involved in sorting is variable and depends greatly on the batch and the number of oocytes required for the experiment.

10. Store sorted oocytes overnight at 16°C in complete-ND-96 in Petri dishes. Rotate Petri dishes slowly during the overnight storage.

3.2.3. *cRNA Injection*

1. During the entire cRNA microinjection protocol, keep all materials and reagents free from RNase contamination.
2. Make capillary needles for oocyte injection employing a micropipette puller and micropipette beveller.
3. Attach a 27 gauge needle to a syringe (usually 3 cc) and load syringe with mineral oil. Fill the glass micropipette with the mineral oil, and install the micropipette onto the nanoliter injector.
4. Incubate cRNA samples at 65°C for 10 min, and centrifuge the tube briefly.
5. Pipette the cRNA onto the paper-side of a piece of parafilm (paper must be removed) and load the micropipette with the cRNA at 1 µg/µl using the loading function of the microinjector.
6. Set the microinjector to the desired injection volume, typically 5–20 nl.
7. Add a few (5–15) oocytes to a small Petri dish lined with woven mesh filter (SpectraMesh) and filled with ND-96 buffer. Place Petri dish under the dissecting microscope.
8. Inject cRNA into the light pole of the oocytes. Avoid accidentally injecting cRNA into the nucleus. The nucleus is located within the dark pole of the oocyte.
9. Inject H₂O into the same number of oocytes that were injected with cRNA. These water-injected oocytes serve as background controls and are preferable to control oocytes that have not been H₂O-injected.
10. After microinjection, incubate oocytes in complete ND-96 buffer and place at 16°C on a rotator set at low speed.
11. Change complete ND-96 buffer daily and remove any damaged oocytes.
12. Transport activity may be observed after 24 h, but 3–5 days post injection is a more common time frame to measure transport. The highest level of transport protein expression will have to be experimentally determined for every transporter.

3.2.4. *Transport Assay*

Oocyte transport assays are performed in 24-well plates.

1. Rinse oocytes twice in ND-96 buffer, and keep at room temperature for at least 30 min prior to the initiation of the transport measurements.

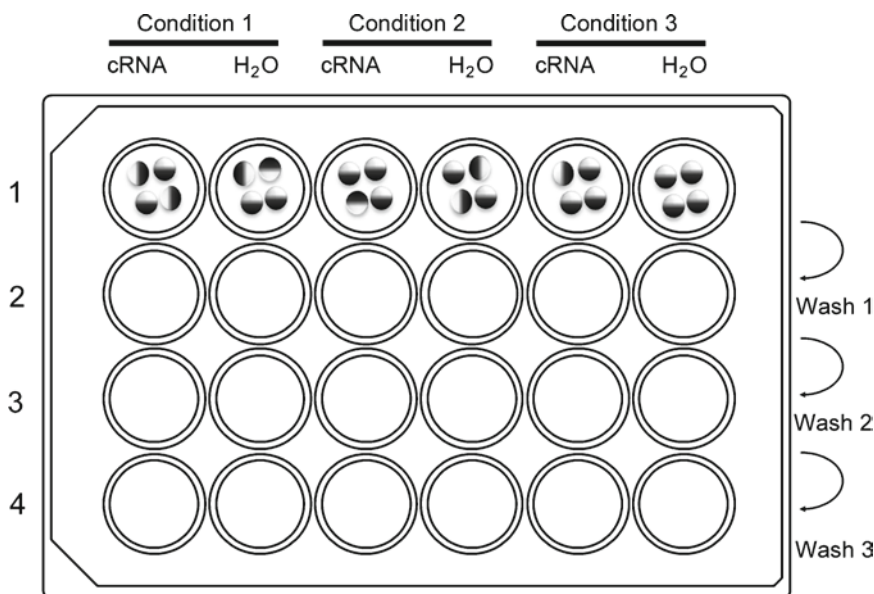


Fig. 2. Organization of a transport experiment using *Xenopus laevis* oocytes.

2. Add 250 μ l of ND-96 buffer to each well of the top row of the 24-well plate (row 1 in Fig. 2). This top row will be used for the transport assays. The three remaining rows in the 24-well plates will be used for successive washing steps.
3. Prepare a transport cocktail of radiolabeled polyamine in ND-96 buffer at twice the final concentration desired.
4. Carefully add 3–6 cRNA-injected oocytes and 3–6 water-injected control oocytes to adjacent wells using a plastic Pasteur pipette (see Note 18) (row 1 in Fig. 2).
5. The transport experiment is initiated when 250 μ l of the 2 \times transport cocktail is added to each oocyte-containing well.
6. The transport assay is terminated by transferring the 24-well plates to ice and the addition of 500 μ l of ice-cold ND-96 buffer to the oocyte-containing wells (row 1 in Fig. 2).
7. Using a Repeater[®] plus pipette, quickly add 500 μ l of ice cold ND-96 to rows 2–4 of the 24-well plate (Fig. 2) and keep 24-well plates on ice. The wells in rows 2–4 are used to wash the oocytes free of exogenous radiolabel.
8. Transfer the 3–6 oocytes serially into the rinsing wells (rows 2–4 in Fig. 2) containing ice-cold ND-96 buffer (see Note 19).
9. Remove washed oocytes from row 4 of the 24-well plates and deposit oocytes into scintillation vials containing 200 μ l 1% Triton-X 100. Rupture the oocytes using a 200 μ l micropipette until a homogenous cell extract is obtained.

10. Add 3–4 ml of scintillation fluid to each vial and vortex.
11. Measure the amount of radioactivity present in each sample for 1 min using liquid scintillation spectrometry (Beckman LS6500). Also count an aliquot of the radiolabel transport cocktail.
12. Data analysis is essentially the same as for the transport measurements in protozoan parasite (see Subheading 3.1.4). Uptake assays should be repeated a minimum of 3 times because of variability in oocyte transport experiments. Due to this unpredictability among oocyte batches, it is often problematic to combine data from independent experiments. Therefore, oocyte transport data are often not averaged between or among independent experiments, and data are depicted from a “representative experiment.”

4. Notes

1. All experimental manipulations with intact *Leishmania* spp., *T. brucei*, and *T. cruzi* must be carried out under Biosafety Level Class II safety guidelines.
2. It is important to reproduce transport experiments on parasites harvested at the same growth stage.
3. PBSG and CBSS buffers are effectively equivalent for transport measurements.
4. Stock [^3H]polyamine reagents have higher specific activities than [^{14}C]polyamine stock reagents, so if available, it is preferable to employ polyamines labeled with ^3H in the uptake assays.
5. Liquid nitrogen and ethanol/dry-ice can cause severe burns if in contact with skin or eyes. Use appropriate protection, especially goggles for eye protection.
6. The preference is for plastic scintillation vials over glass to minimize the risk of breakage.
7. This scintillation cocktail will accommodate a maximum of 15% (v/v) of aqueous sample. Typically, the aqueous component of a scintillation mix to be counted is <10% (v/v).
8. Place a piece of SpectraMesh inside the Petri dish. Fuse the mesh to the Petri dish using a few drops of chloroform. The SpectraMesh provides resistance that facilitates the micro injection process and also effectively retains the oocytes in place during the injection process.
9. ND-96 complete buffer is used for oocytes storage, and ND-96 incomplete buffer is used for transport measurements. These buffers should be prepared meticulously as osmolarity

- is critical to maintain oocyte viability. It is imperative during the oocyte experiments to ensure that all liquid containers are thoroughly washed free of residual traces of dish washing detergent, which can harm the integrity of the oocytes.
10. For transfection in *T. brucei*, the plasmid to be transfected must be first linearized by restriction endonuclease digestion for integration into the parasite genome. *T. brucei* does not stably maintain episomes.
 11. Microscopy is a rapid and facile method that can be employed prior to the labor-intensive transport assays in order to assess if the expressed transporter is located at the parasite cell surface. Although the parasites are attached to the bottom of the chamber slide, they remain viable and relatively motile. If parasite movement hampers image recording, the parasites can also be fixed with 4% formaldehyde for 15–30 min followed by rinsing in PBS. These fixation conditions, however, can also decrease the intensity of fluorescence. A more in depth microscopic analysis, beyond the scope of this chapter, will have to be undertaken to localize the transporter of interest within the complex intracellular milieu of the parasite.
 12. Aerosol filter tips should be used to protect pipettes from aerosol contamination of radioactive or/and infectious material.
 13. This step removes the DNA template.
 14. Formaldehyde is volatile, irritating to mucous membranes, and toxic.
 15. Coordinating oocyte experiments among laboratories minimizes *X. laevis* use.
 16. The incision can either be stitched and the frog kept alive or the frog is euthanized according to institutional guidelines.
 17. To prevent damage, oocytes must be continuously submerged in buffer.
 18. Allow the oocytes to drop by gravity to the tip of the Pasteur pipette to ensure a negligible amount of buffer is added to the well.
 19. This step should be performed carefully and rapidly in order to avoid damaging the oocytes. This procedure takes practice.

Acknowledgements

This work was supported in part by Grant-in-Aid #0950095G provided by the American Heart Association and by Grant AI41622 from the National Institute of Allergy and Infectious Disease.

References

- Pegg AE, McGovern KA, Wiest L (1987) Decarboxylation of alpha-difluoromethylornithine by ornithine decarboxylase. *Biochem J* 241:305–307
- Bacchi CJ, McCann PP (1987) Parasitic protozoa and polyamines. In: McCann PP, Pegg AE, Sjoerdsma A (eds) *Inhibition of polyamine metabolism: biological significance and basis for new therapies*. Academic, Orlando, FL, pp 317–344
- Burri C, Brun R (2003) Eflornithine for the treatment of human African trypanosomiasis. *Parasitol Res* 90(Suppl 1):S49–S52
- Pepin J, Milord F (1994) The treatment of human African trypanosomiasis. *Adv Parasitol* 33:1–47
- Van Nieuwenhove S, Schechter PJ, Declercq J, Bone G, Burke J, Sjoerdsma A (1985) Treatment of gambiense sleeping sickness in the Sudan with oral DFMO (DL-alpha-difluoromethylornithine), an inhibitor of ornithine decarboxylase; first field trial. *Trans R Soc Trop Med Hyg* 79:692–698
- Bacchi CJ, Nathan HC, Yarlett N, Goldberg B, McCann PP, Bitonti AJ, Sjoerdsma A (1992) Cure of murine *Trypanosoma brucei* rhodesiense infections with an S-adenosylmethionine decarboxylase inhibitor. *Antimicrob Agents Chemother* 36:2736–2740
- Bitonti AJ, Byers TL, Bush TL, Casara PJ, Bacchi CJ, Clarkson AB Jr, McCann PP, Sjoerdsma A (1990) Cure of *Trypanosoma brucei* brucei and *Trypanosoma brucei* rhodesiense infections in mice with an irreversible inhibitor of S-adenosylmethionine decarboxylase. *Antimicrob Agents Chemother* 34:1485–1490
- Bitonti AJ, Dumont JA, McCann PP (1986) Characterization of *Trypanosoma brucei* brucei S-adenosyl-L-methionine decarboxylase and its inhibition by Berenil, pentamidine and methylglyoxal bis(guanylhydrazone). *Biochem J* 237:685–689
- Danzin C, Marchal P, Casara P (1990) Irreversible inhibition of rat S-adenosylmethionine decarboxylase by 5'-([Z]-4-amino-2-butenyl)methylamino)-5'-deoxyadenosine. *Biochem Pharmacol* 40:1499–1503
- Balana-Fouce R, Escribano MI, Alunda JM (1991) Leishmania infantum: polyamine biosynthesis and levels during the growth of promastigotes. *Int J Biochem* 23:1213–1217
- Ariyanayagam MR, Fairlamb AH (1997) Diamine auxotrophy may be a universal feature of *Trypanosoma cruzi* epimastigotes. *Mol Biochem Parasitol* 84:111–121
- Carrillo C, Cejas S, Gonzalez NS, Algranati ID (1999) *Trypanosoma cruzi* epimastigotes lack ornithine decarboxylase but can express a foreign gene encoding this enzyme. *FEBS Lett* 454:192–196
- Magagnin S, Bertran J, Werner A, Markovich D, Biber J, Palacin M, Murer H (1992) Poly(A)⁺ RNA from rabbit intestinal mucosa induces b_{0,+} and y⁺ amino acid transport activities in *Xenopus laevis* oocytes. *J Biol Chem* 267:15384–15390
- Sanchez MA, Tryon R, Green J, Boor I, Landfear SM (2002) Six related nucleoside/nucleobase transporters from *Trypanosoma brucei* exhibit distinct biochemical functions. *J Biol Chem* 277:21499–21504
- Hasne MP, Ullman B (2005) Identification and characterization of a polyamine permease from the protozoan parasite *Leishmania major*. *J Biol Chem* 280:15188–15194
- Nishimura H, Pallardo FV, Seidner GA, Vannucci S, Simpson IA, Birnbaum MJ (1993) Kinetics of GLUT1 and GLUT4 glucose transporters expressed in *Xenopus* oocytes. *J Biol Chem* 268:8514–8520
- Ha DS, Schwarz JK, Turco SJ, Beverley SM (1996) Use of the green fluorescent protein as a marker in transfected *Leishmania*. *Mol Biochem Parasitol* 77:57–64
- Wirtz E, Hartmann C, Clayton C (1994) Gene expression mediated by bacteriophage T3 and T7 RNA polymerases in transgenic trypanosomes. *Nucleic Acids Res* 22:3887–3894
- Kelly JM, Ward HM, Miles MA, Kendall G (1992) A shuttle vector which facilitates the expression of transfected genes in *Trypanosoma cruzi* and *Leishmania*. *Nucleic Acids Res* 20:3963–3969
- Montalvetti A, Rohloff P, Docampo R (2004) A functional aquaporin co-localizes with the vacuolar proton pyrophosphatase to acidocalcisomes and the contractile vacuole complex of *Trypanosoma cruzi*. *J Biol Chem* 279:38673–38682
- Arriza JL, Kavanaugh MP, Fairman WA, Wu YN, Murdoch GH, North RA, Amara SG (1993) Cloning and expression of a human neutral amino acid transporter with structural similarity to the glutamate transporter gene family. *J Biol Chem* 268:15329–15332

Chapter 20

Heparan Sulfate Proteoglycan-Mediated Polyamine Uptake

Johanna Welch, Katrin Svensson, Paulina Kucharzewska,
and Mattias Belting

Abstract

The polyamines are polycationic compounds essential for cellular proliferation and transformation. In addition to a well-defined biosynthesis pathway, polyamines are internalized into cells by as yet incompletely defined mechanisms. Numerous reports have shown that efficient polyamine uptake depends on the presence of polyanionic, cell surface-associated heparan sulfate proteoglycans (HSPGs). In this chapter, we provide protocols for studying HSPG-mediated uptake of polyamines in various cell lines, and provide instructions for the use of two different genetic models of HSPG deficiency. We describe the enzymatic reduction of cell surface HSPG through Heparinase III lyase treatment as well as the use of phage display-derived single chain variable fragment (scFv) anti-HS antibodies to block HSPGs at the cell surface. Finally, we provide a protocol for the quantitative verification of loss or reduction of cell surface HSPGs and a detailed description of polyamine uptake measurement.

Key words: HSPG, Polyamine uptake, Flow cytometry analysis, CHO-cells, Anti-HS antibodies, Heparinase III lyase treatment, EXT-1 knock-out cells

1. Introduction

The polyamines (putrescine, spermidine, and spermine) are essential for cellular proliferation (1). There is mounting evidence for their involvement in transformation and cancer disease; overexpression of ornithine decarboxylase (ODC), the rate-limiting enzyme in the biosynthesis of the polyamines, leads to cellular transformation in vitro (2) and to increased susceptibility for tumor formation in transgenic mice (3). As such, the polyamine pathway is an attractive target for anticancer therapy, and numerous inhibitors of the polyamine biosynthetic system have been developed. However, due to compensatory increase in cellular uptake of polyamines in vivo, clinical studies have overall proved disappointing (4). This points at the importance of a

detailed understanding of the polyamine uptake mechanism, and furthermore, shows that antitumor therapy directed at the polyamine system requires simultaneous targeting of *de novo* biosynthesis as well as uptake.

The internalization mechanism for polyamines has been well characterized in bacteria and yeast (5). As of yet, no plasma membrane transporter has been isolated and cloned in mammalian cells, but an energy-dependent, carrier-mediated and saturable transport system has been suggested (6). During the last 15 years, various reports have elucidated the dependence on the presence of cell surface-associated heparan sulfate proteoglycans (HSPGs) for efficient uptake of polycationic polyamines (7–10). HSPGs comprise a family of polysaccharide-substituted proteins present on the cell surface and in the extracellular matrix (11). They are pivotal binding partners for several growth factors and viruses (11) as well as DNA/peptide complexes (12, 13) with implication for cancer, viral infections, and drug delivery. HS constitutes a polysaccharide chain of repetitive glucuronic acid/*N*-acetylglucosamine disaccharide units. A series of modifications, e.g., epimerization of glucuronic acid into iduronic acid and sulfation at various positions along the chain result in an extremely complex and highly negatively charged structure (11). Removal of HS from the cell surface with heparinase III lyase treatment (7) or blockage of HSPG activity with phage display–derived single chain variable fragment (scFv) anti-HS antibodies (10) resulted in an approximately 60% reduction of spermine uptake, indicating the existence of an HSPG-dependent transport pathway as well as a pathway independent of HSPGs. The kinetics of polyamine uptake (6) is consistent with electrostatic interactions between the polyanionic HS chains and the positively charged polyamines, and the role of cell surface HSPGs in this process might be two-fold: (1) to attract and present the polyamines to their true transporter or (2) to be an integral part of the transport machinery.

In this chapter, we provide protocols to study the role of cell surface-associated HSPGs in the uptake of polyamines. Firstly, we describe the use of two different genetic models for HSPG deficiency; wild-type and HSPG-deficient (pgsD-677) Chinese hamster ovary (CHO) cell lines (14) and adenoviral vector-mediated knockout of EXT-1 in endothelial-like cells derived from an EXT-1/loxP mouse (15). Secondly, we depict an enzymatic method employing heparinase III lyase treatment to remove cell surface HSPGs. Thirdly, we suggest the use of recently developed phage display–derived scFv anti-HS antibodies (16) to block HSPGs on the cell surface (10). To verify a reduction of cell surface HSPG levels, we describe a quantitative method based on anti-HS antibody labeling of HSPGs and subsequent fluorescence-assisted cell sorting (FACS) analysis. Finally, a detailed protocol for polyamine uptake is provided.

2. Materials

2.1. Alternative Strategies to Reduce the Level or Activity of Cell Surface HSPGs

2.1.1. Wild-Type and HSPG-Deficient Chinese Hamster Ovary Cells

1. Wild-type CHO cells, CHO-K1 (ATCC).
2. HS-deficient CHO cells, pgsD-677 (ATCC).
3. F12K medium (Fisher Scientific) supplemented with 2 mM L-glutamine, penicillin–streptomycin (100 IU/ml and 100 µg/ml, respectively) and 10% fetal bovine serum (FBS), pH 7.4.
4. Dulbecco's Phosphate buffered saline (D-PBS, Fisher Scientific): 137 mM NaCl, 2.7 mM KCl, 10 mM Na₂HPO₄, 1.8 mM KH₂PO₄; pH 7.4.
5. Solution of trypsin (0.25%) and ethylenediamine tetraacetic acid (EDTA) (1 mM) (Sigma).
6. Twenty-four-well cell culture plates (Nunc).

2.1.2. Heparinase III Lyase Treatment

1. HeLa cells (ATCC).
2. Dulbecco's modified Eagle medium (DMEM, Fisher Scientific) supplemented with 2 mM L-glutamine, penicillin–streptomycin (100 IU/ml and 100 µg/ml, respectively) and 10% FBS, pH 7.4.
3. D-PBS (Fisher Scientific): 137 mM NaCl, 2.7 mM KCl, 10 mM Na₂HPO₄, 1.8 mM KH₂PO₄; pH 7.4.
4. Solution of trypsin (0.25%) and EDTA (1 mM).
5. Twenty-four-well cell culture plates (Nunc).
6. Digestion buffer: DMEM supplemented with 20 mM Hepes (pH 7.0) and 0.5% bovine serum albumin.
7. Heparinase III lyase (E.C. 4.2.2.8, Sigma). Powder can be reconstituted in 20 mM Tris–HCl (pH 7.5) containing 0.1 mg/ml BSA and 4 mM CaCl₂. The solution is stable for a week at –20°C.
8. Chondroitinase ABC (E.C. 4.2.2.4, Sigma). Store at –20°C. Lyophilized powder should be reconstituted in distilled water containing 0.01% BSA. Subsequent dilutions can be made with a buffer containing 50 mM Tris (pH 8.0), 60 mM sodium acetate, and 0.02% BSA. Solutions should be prepared fresh.

2.1.3. Blocking of Cell Surface-Associated HSPGs with Anti-HS Antibodies

1. HeLa cells (ATCC).
2. DMEM (Fisher Scientific) supplemented with 2 mM L-glutamine, penicillin–streptomycin (100 IU/ml and 100 µg/ml, respectively) and 10% FBS, pH 7.4.
3. D-PBS (Fisher Scientific): 137 mM NaCl, 2.7 mM KCl, 10 mM Na₂HPO₄, 1.8 mM KH₂PO₄; pH 7.4.
4. Solution of trypsin (0.25%) and EDTA (1 mM).

5. VSV-tagged phage display–derived scFv antiheparan sulfate antibody RB4EA12 (kindly provided by Prof. van Kuppevelt, Radboud University Nijmegen Medical Center, The Netherlands).
6. VSV-tagged phage display–derived scFv antichondroitin sulfate antibody IO3HIO3 (kindly provided by Prof. van Kuppevelt).
7. Twenty-four-well cell culture plates (Nunc).

2.1.4. Transduction of Wild-Type and EXT-1/loxP Cells with Cre-Expressing Adenoviral Vector

1. Endothelial-like cells derived from lungs of wild-type (WT) mice (C57BL/6).
2. Endothelial-like cells derived from lungs of EXT-1/loxP mice (C57BL/6).
3. D-PBS (Fisher Scientific): 137 mM NaCl, 2.7 mM KCl, 10 mM Na₂HPO₄, 1.8 mM KH₂PO₄; pH 7.4.
4. Solution of trypsin (0.25%) and EDTA (1 mM).
5. Endothelial cell medium (ECM): MCDB 131 (Sigma) supplemented with 10% heat inactivated (see Note 1) FBS, 2 mM L-glutamine, penicillin–streptomycin (100 IU/ml and 100 µg/ml, respectively), 10 ng/ml epidermal growth factor (EGF, R&D Systems), 1 µg/ml hydrocortisone (Sigma), pH 7.4.
6. Transduction medium: MCDB 131 (Sigma) supplemented with 1% heat inactivated FBS (Sigma), 2 mM L-glutamine, penicillin–streptomycin (100 IU/ml and 100 µg/ml, respectively), pH 7.4.
7. *p*-Adeno-X-CRE-IRES-GFP adenoviral vector – recombinant adenoviral vector expressing CRE recombinase and reporter green fluorescent protein (GFP) constructed using the Adeno-X™ Expression System I (Clontech Laboratories, Inc.) (see Note 2).
8. Gelatin from bovine skin, type B: prepare a 0.3% (w/v) solution in water (Milli-Q) and sterilize by filtration. Store at 4°C.
9. Twenty-four-well cell culture plates (Nunc).
10. Filter-plugged tips (Sarstedt).

2.2. Verification of Deficiency/Reduction of Cell Surface HSPGs by Staining with Anti-HS Antibody and Subsequent FACS Analysis

1. HeLa cells (ATCC).
2. DMEM (Fisher Scientific) supplemented with 2 mM L-glutamine, penicillin–streptomycin (100 IU/ml and 100 µg/ml, respectively), and 10% FBS, pH 7.4.
3. D-PBS (Fisher Scientific): 137 mM NaCl, 2.7 mM KCl, 10 mM Na₂HPO₄, 1.8 mM KH₂PO₄; pH 7.4.
4. D-PBS supplemented with EDTA (1 mM).
5. D-PBS supplemented with 1% (w/v) bovine serum albumin.
6. Twenty-four-well cell culture plates (Nunc).

7. VSV-tagged phage display–derived scFv antiheparan sulfate antibody RB4EA12 (kindly provided by Prof. van Kuppevelt).
8. Mouse anti-vsv antibody (P5D4) (Sigma).
9. Alexa Fluor 488-conjugated goat anti-mouse antibody (Invitrogen).
10. FACS tubes (BD Biosciences).
11. Flow cytometer equipped with a 488-nm argon laser and FITC filter, e.g., FACSCalibur (BD Biosciences).

2.3. Polyamine Uptake

1. Spermine, spermidine, or putrescine (Sigma) dissolved at 1 mM in medium. The solutions can be stored at 4°C for up to 1 week.
2. Radiolabeled 20 μ M polyamine solutions with final specific activity of 31 Ci/mol: prepare a solution of one of the polyamines [¹⁴C]-spermine, [¹⁴C]-spermidine, or [¹⁴C]-putrescine (Amersham) (stock concentration 113 Ci/mol, 50 μ Ci/ml) by mixing with corresponding nonradiolabeled polyamine diluted in serum-free medium (Fisher Scientific) (see Note 3). The solutions can be stored at 4°C for up to 1 week.
3. Working solution of radiolabeled polyamine: dilute 20 μ M radiolabeled polyamine solution in serum-free medium to a final concentration of 5 μ M. Working solution can be stored at 4°C for up to 1 week.
4. 0.5 M NaOH for cell lysis (see Note 4).
5. 0.5 M HCl solution.
6. Scintillation vials (Beckman Coulter).
7. Scintillation liquid (Beckman Coulter).
8. Scintillation Counter (Beckman Coulter LS 6500).

3. Methods

Manipulation of cell surface HSPG expression for the study of HSPG-mediated polyamine uptake can be achieved by several approaches, as summarized in Fig. 1. Pharmacological interventions interfering with the glycosaminoglycan (GAG) chain synthesis (β -D-xylosides) (17) or modification (chlorate) (18) as well as enzymatic degradation of the GAG chains (GAG lyases) (19) are traditional methods often used. Treatment of cells with xylosides or chlorate targets the PG pool as a whole whereas the use of different GAG lyases offers the possibility of specific HSPG targeting. Disruption of HSPG can also be achieved at the genetic level; mutant CHO cells deficient in various enzymes involved in

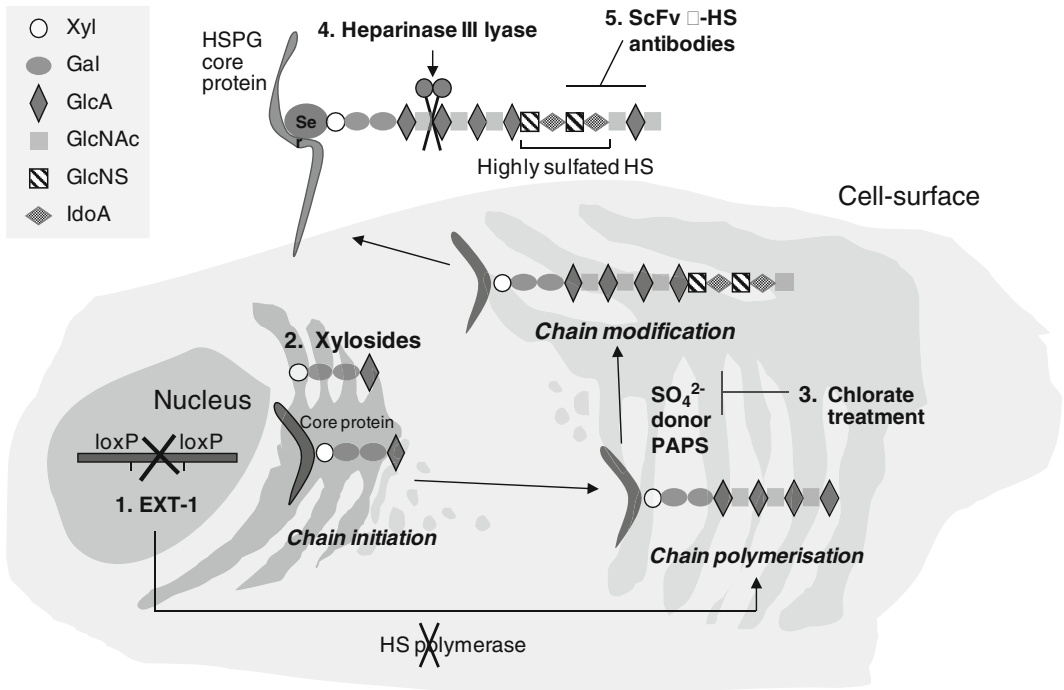


Fig. 1. Strategies to interfere with HSPG biosynthesis and function. 1. Recombination of loxP-flanked EXT-1 locus by Cre recombinase shuts down HS polymerase, resulting in deficient HS polymerization. 2. Xylosides act as false substrates for HS chain initiation, resulting in competitive inhibition of HS link region formation onto the natural substrate, i.e., the HSPG core protein. 3. Chlorate inhibits the formation of 3'-phosphoadenosine 5'-phosphosulfate (PAPS), i.e., the sulfate donor for sulfation of the HS polymer, resulting in less modified HS chains. 4. Heparinase III lyase cleaves cell surface HS chains at the indicated position, resulting in depolymerization into oligosaccharide fragments. 5. Epitope specific, phage-derived single chain variable fragment (scFv) anti-HS antibodies block polyamine-binding regions of HS chains. *Xyl* xylose; *Gal* galactose; *GlcA* glucuronic acid; *GlcNAc* *N*-acetyl-glucosamine; *GlcNS* *N*-sulfoglucosamine; *IdoA* iduronic acid.

PG biosynthesis (*pgsA*, *pgsB*, *pgsD* and *pgsG*) (20) are well-established tools in the HSPG field and have been shown to display decreased polyamine uptake in comparison to wild-type CHO-K1 cells (8). In this chapter, we propose the use of one of the CHO mutant cell lines, *pgsD*-677, which lacks the active EXT-1 enzyme (HS polymerase) required for the polymerization of HS chains.

The generation of knockout animals lacking functional genes of the various enzymes of the HSPG biosynthetic pathway has allowed the expansion of the HSPG field into *in vivo* models. So far, knockout mouse strains for EXT-1, two different *N*-deacetylase/*N*-sulfotransferase (NDST) isoforms, HS epimerase and a number of HS sulfotransferases have been described (21). Depending on the targeted gene, the change in HS structure is more or less extensive, e.g., disruption of EXT-1 leads to complete abrogation of HS polymerization and early embryonic death. In case of NDST knockout animals, the polysaccharide chain is

formed but remains low sulfated, whereas lack of *O*-sulfotransferases changes the fine structure of the HS chain. Cell lines derived from these models provide a unique opportunity to study effects of HSPG modifications on polyamine uptake (Fig. 1). We provide a protocol for the study of HSPG-dependent polyamine uptake in a murine endothelial-like cell line isolated from conditional EXT-1 knockout mice (15). EXT-1 is flanked by loxP-sites, and can thus be excised from the cell genome through the transduction of the cells with a CRE-expressing adenoviral vector.

As of yet, little is known about the specific epitope requirements for polyamine interaction with HSPGs. Polyamine deprivation with α -difluoromethylornithine (DFMO) was associated with structural alterations of the HS chain and a subsequent increase in affinity for spermine (7). This would suggest the necessity of certain modification patterns in the HS chain, and not only electrostatic interaction, for efficient polyamine binding to HSPGs. The phage display-derived epitope-specific scFv anti-HS antibodies produced by the van Kuppevelt group (16) are excellent tools to study the importance of specific HS domain structures for the binding and uptake of polyamines (Fig. 1). The antibodies recognize domains with varying degrees of sulfation, and potentially they could be used for the mapping of the “polyamine specific” HS epitope. We describe a protocol for the use of one of the antibodies, RB4EA12, which was shown to efficiently reduce polyamine uptake in human cancer cells (10).

Irrespective of the method used to deprive cells of functional HSPGs, it is important to quantitatively verify their loss or reduction. Owing to the extensive sulfation of HS chains, radio labeling through incubation of cells with [³⁵S]-sulfate in sulfate-depleted medium is relatively specific, and the polyanionic properties of the PGs enable isolation and purification by anion exchange chromatography (22). The [³⁵S]-sulfate is almost exclusively incorporated into the GAG, and the [³⁵S]-radioactivity can be used as a quantitative tool to monitor PG levels. As an alternative to the rather time consuming biochemical methods for PG labeling and purification, we propose the labeling of cell surface HSPGs with scFv anti-HS antibodies followed by FACS analysis as a reliable and quantitative tool to verify loss or reduction of cell surface HSPGs (10).

3.1. Alternative Strategies to Reduce the Level or Activity of Cell Surface HSPGs

3.1.1. Preparation of Wild-Type and HSPG-Deficient CHO Cells

1. Seed 100,000 cells/well of the respective cell type in a 24-well culture plate in F12K medium with 10% FBS 24 h prior to analysis (see Note 5).
2. For verification of deficiency of cell surface HSPGs, follow the procedure under Subheading 3.2.
3. For polyamine uptake analysis of wild-type and HS-deficient CHO cells, follow the procedure under Subheading 3.3.

3.1.2. Heparinase III Lyase Treatment

1. Seed 70,000 cells/well in a 24-well culture plate in DMEM with 10% FBS 24 h prior to heparinase III lyase treatment (see Note 5).
2. Wash the cells twice with digestion buffer.
3. Incubate the cells in 0.5 ml of digestion buffer containing 5 mIU heparinase III lyase or, as a control, 225 mIU of chondroitinase ABC for 3 h at 37°C (see Note 6).
4. Aspirate the digestion buffer containing the liberated cell surface HS and wash the cells twice with D-PBS.
5. For verification of removal of HSPGs from the cell surface, follow the procedure under Subheading 3.2.
6. For polyamine uptake analysis of heparinase III lyase treated cells, follow the procedure under Subheading 3.3.

3.1.3. Blocking of Cell Surface-Associated HSPGs with Anti-HS Antibodies

1. Seed 70,000 cells/well in a 24-well culture plate in DMEM with 10% FBS 24 h prior to antibody incubation (see Note 5).
2. Wash the cells three times with D-PBS and add serum-free DMEM.
3. Follow the procedure described under Subheading 3.3; in addition to adding polyamine solution, add the anti-HS antibody RB4EA12 prepared at the appropriate dilution in DMEM. As a negative control, use the anti-CS antibody IO3HIO3 (see Note 7).

3.1.4. Transduction of Wild-Type and EXT-1/loxP Cells with Cre-Expressing Adenoviral Vector

1. Coat wells of a 24-well plate with 0.3% gelatin solution (0.25 ml/well) for 1 h at 37°C.
2. Remove gelatin solution and wash wells once with D-PBS.
3. Seed WT and EXT-1/loxP endothelial-like cells at 3.5×10^4 cells/well in a 24-well cell culture plate in ECM to reach 80–90% confluency after 12–24 h.
4. The next day, dilute the adenoviral vector in transduction medium (see Note 8) to achieve 500 multiplicity of infection (M.O.I.) (see Note 9).
5. Wash the cells twice with D-PBS and add 0.25 ml of adenoviral vector-containing transduction medium to each well without touching the monolayer (see Note 10). Rock the plate to spread the virus evenly.
6. Incubate the cells at 37°C for 4 h to allow the virus to infect the cells.
7. Fill up with ECM to regular volume (e.g., 0.5 ml/well of 24-well cell culture plate).
8. Incubate cells at 37°C for 48 h.

9. For verification of removal of HSPGs from the cell surface of WT and EXT-1/loxP cells transduced with CRE-expressing adenoviral vector, follow the procedure under Subheading 3.2 (see Note 11).
10. For polyamine uptake analysis in WT and EXT-1/loxP cells transduced with CRE-expressing adenoviral vector, follow the procedure under Subheading 3.3.

3.2. Verification of Deficiency/Reduction of Cell Surface HSPGs by Staining with Anti-HS Antibody and Subsequent FACS Analysis

1. Remove growth medium and rinse cells with 0.5 ml of D-PBS.
2. Prepare tertiary antibody complexes by incubating primary scFv anti-HS antibody (1:20), secondary anti-mouse antibody P5D4 (1:500), and tertiary goat anti-mouse antibody conjugated to Alexa Fluor 488 (1:200). Complexes should be prepared in serum-free medium at room temperature and protected from light (see Note 12).
3. Preincubate antibody complexes at room temperature for 30 min.
4. Put cells on ice and remove culture media. Rinse the cells with ice-cold serum-free medium.
5. Add 200 μ l of precooled antibody complexes to each well and incubate for 30 min at 4°C on ice (see Note 13).
6. Remove solutions and rinse cells with 500 μ l of D-PBS per well.
7. Add 100 μ l of ice-cold D-PBS/EDTA to detach cells without removing antibody bound to the cell surface.
8. Resuspend cells in ice-cold serum-free medium and wash twice with 2 ml of ice-cold D-PBS supplemented with 1% BSA.
9. Resuspend the cell pellet in 300 μ l of ice-cold D-PBS supplemented with 1% BSA and keep on ice until analysis with FACSCalibur.

3.3. Polyamine Uptake

1. Remove medium and rinse the cells carefully with 1 ml of serum-free medium.
2. Add 250 μ l of polyamine working solution (5 μ M) per well and incubate for 30 min at 37°C (see Note 14).
3. Place the cells on ice, remove and discard the polyamine solution (discard radioactive material into a hazardous radioactivity waste container).
4. Wash with 1 ml of ice-cold serum-free medium, followed by washing three times with 1 ml of 1 mM nonradiolabeled polyamine solution diluted in serum-free medium (see Note 15).

5. Wash with 1 ml of ice-cold serum-free medium; make sure to remove all remaining medium from the well (see Note 16). After washing, use a microscope to check that the cell monolayer is intact.
6. Lyse cells in 500 μ l of 0.5 M NaOH for 1 h at 37°C.
7. Suspend the cell lysate and transfer 400 μ l of the solution to a scintillation vial.
8. Neutralize lysate by adding 400 μ l of 0.5 M HCl to the scintillation vial.
9. Add 10 ml of scintillation liquid to a scintillation vial, put on a vial cap and mix samples by vortexing.
10. Measure the radioactivity in a scintillation counter (Beckman Coulter LS 6500). The amount of radioactivity (DPM) per sample corresponds to the amount of polyamines taken up by the cells. Also include a blank (scintillation liquid) and an aliquot (e.g., 2.5 μ l) of 5 μ M working polyamine solution in order to measure the total amount of radioactive polyamine added to the cells (see Note 17).

4. Notes

1. Preheat the serum to a temperature of 56°C, then heat inactivate for 30 min.
2. Production and gene transfer applications of adenoviral vectors require a Biosafety Level 2 facility.
3. Calculation example: 1 ml of the 20 μ M stock solution with specific activity of 31 Ci/mol corresponds to 6.2×10^{-7} Ci in total. Hence, 12.4 μ l of the stock solution (113 Ci/mol, 50 μ Ci/ml) will be mixed with nonradiolabeled polyamine. The number of moles provided by the radioactive solution (5.5 nmol) is then subtracted from the total number in the 20 μ M 1 ml solution. For example, if the nonradiolabeled polyamine solution has a concentration of 500 μ M, the volume to add to the final solution is 29.0 μ l. Add serum-free medium up to 1 ml to get a final concentration of 20 μ M.
4. NaOH is dissolved in distilled water at 1 M concentration and stored at room temperature in 50 ml plastic tubes.
5. When seeding cells, include wells for your test samples as well as for verification of reduction of cell surface-associated HS.
6. Heparinase III lyase recognizes HS as its primary substrate whereas chondroitinase ABC degrades chondroitin and dermatan sulfate.

7. We recommend dilutions from 1:5 to 1:40 for effect on polyamine uptake in HeLa cells, but the protocol might need to be optimized depending on cell line used.
8. Adenoviral vector stocks should be aliquoted and stored with 10% glycerol at -80°C . Repeated freezing and thawing of aliquots should be avoided as it will cause a loss of vector titer. Adenoviral vector preparations should be kept on ice during transduction preparations. Sterile filter-plugged tips should always be used for pipetting of vector suspension.
9. The viral titer is a quantitative measurement of the biological activity of the recombinant virus and is expressed as plaque forming units (PFU) per milliliter. M.O.I. is a quantitative measure of conditions of virus infection, which is simply the average number of PFUs per cell utilized in the original infection. An M.O.I. of 1 means 1 PFU/cell, so if 10^6 cells were infected at an M.O.I. of 10, one would need to add 10^7 PFUs of virus.
10. To infect the maximum number of cells, use the smallest volume needed to cover the cells. This will help to keep the viral particles in the close proximity to cells.
11. Adenoviral vector transduction results in gene delivery to the majority of infected cells. However, if a population of 100% transduced cells is desired, one could make use of GFP that is expressed together with CRE recombinase in the vector and collect GFP-positive cells using a cell sorter (e.g., BD FACSAria Flow Cytometer).
12. As negative control, use secondary and tertiary antibody complexes at the same concentrations and conditions as for other samples.
13. In order to restrict the antibody complexes to the cell surface and to preclude antibody internalization, it is important to have cells and all solutions at 4°C during the whole staining procedure.
14. Since polyamine uptake is a temperature-dependent process, it is essential that the polyamine uptake at 4°C is subtracted from corresponding values at 37°C to obtain a measure of specific polyamine uptake.
15. An excess of nonlabeled polyamine solution will compete for polyamine binding sites, resulting in reduced background signal from unspecific binding of radioactive polyamine to the plastic of the wells.
16. It is recommended to use vacuum suction to remove all solution on the sides of the wells when rinsing cells.
17. This sample is included to enable calculation of number of mole/DPM. After normalization to cell number and incubation time, it is possible to recalculate the actual uptake of polyamines from DPM to, e.g., nmol/ 10^6 cells/h.

Acknowledgement

This work was supported by grants from The Swedish Cancer Fund; The Swedish Research Council; The Swedish Society of Medicine; The Physiographic Society, Lund; The Crafoordska, Gunnar Nilsson, and Kamprad Foundations; and the Lund University Hospital (ALF).

References

1. Gerner EW, Meyskens FL Jr (2004) Polyamines and cancer: old molecules, new understanding. *Nat Rev Cancer* 4:781–792
2. Auvinen M, Paasinen A, Andersson LC, Hölttä E (1992) Ornithine decarboxylase activity is critical for cell transformation. *Nature* 360:355–358
3. Clifford A, Morgan D, Yuspa SH, Soler AP, Gilmour S (1995) Role of ornithine decarboxylase in epidermal tumorigenesis. *Cancer Res* 55:1680–1686
4. Wallace HM, Fraser AV (2004) Inhibitors of polyamine metabolism. *Amino Acids* 26: 353–365
5. Igarashi K, Kashiwagi K (1999) Polyamine transport in bacteria and yeast. *Biochem J* 344:633–642
6. Seiler N, Delcros JG, Moulinoux JP (1996) Polyamine transport in mammalian cells. An update. *Int J Biochem Cell Biol* 28:843–861
7. Belting M, Persson S, Fransson LA (1999) Proteoglycan involvement in polyamine uptake. *Biochem J* 338:317–323
8. Belting M, Borsig L, Fuster MM, Brown JR, Persson L, Fransson LA, Esko JD (2002) Tumor attenuation by combined heparan sulfate and polyamine depletion. *Proc Natl Acad Sci U S A* 99:371–376
9. Belting M, Mani K, Jönsson M, Cheng F, Sandgren S, Jonsson S, Ding K, Delcros JG, Fransson LA (2003) Glypican-1 is a vehicle for polyamine uptake in mammalian cells: a pivotal role for nitrosothiol-derived nitric oxide. *J Biol Chem* 278:47181–47189
10. Welch JE, Bengtson P, Svensson K, Wittrup A, Jenniskens GJ, Ten Dam GB, van Kuppevelt TH, Belting M (2008) Single chain fragment anti-heparan sulfate antibody targets the polyamine transport system and attenuates polyamine-dependent cell proliferation. *Int J Oncol* 32:749–756
11. Whitelock JM, Iozzo RV (2005) Heparan sulfate: a complex polymer charged with biological activity. *Chem Rev* 105:2745–2764
12. Sandgren S, Cheng F, Belting M (2002) Nuclear targeting of macromolecular polyanions by an HIV-TAT derived peptide. Role for cell-surface proteoglycans. *J Biol Chem* 277:38877–38883
13. Wittrup A, Sandgren S, Lilja J, Bratt C, Gustavsson N, Mörgelin M, Belting M (2007) Identification of proteins released by mammalian cells that mediate DNA internalization through proteoglycan-dependent macropinocytosis. *J Biol Chem* 282:27897–27904
14. Lidholt K, Weinke JL, Kiser CS, Lugenwa FN, Bame KJ, Cheifetz S, Massagué J, Lindahl U, Esko JD (1992) A single mutation affects both *N*-acetylglucosaminyltransferase and glucuronosyltransferase activities in a Chinese hamster ovary cell mutant defective in heparan sulfate biosynthesis. *Proc Natl Acad Sci U S A* 89:2267–2271
15. Inatani M, Irie F, Plump AS, Tessie-Lavigne M, Yamaguchi Y (2003) Mammalian brain morphogenesis and midline axon guidance require heparan sulfate. *Science* 302:1044–1046
16. Dennissens MA, Jenniskens GJ, Pieffers M, Versteeg EM, Petitou M, Veerkamp JH, van Kuppevelt TH (2002) Large, tissue-regulated domain diversity of heparan sulfates demonstrated by phage display antibodies. *J Biol Chem* 277:10982–10986
17. Fritz TA, Esko JD (2001) Proteoglycans protocols. Humana, Totowa, NJ
18. Humphries DE, Silbert JE (1988) Chlorate: a reversible inhibitor of proteoglycan sulfation. *Biochem Biophys Res Commun* 154:365–371
19. Fransson LA (1985) Mammalian glycosaminoglycans. Academic, New York
20. Bai X, Crawford B, Esko JD (2001) Proteoglycan protocols. Humana, Totowa, NJ
21. Forsberg E, Kjellén L (2001) Heparan sulfate: lessons from knockout mice. *J Clin Invest* 108:175–180
22. Whitelock JM, Iozzo RV (2002) Isolation and purification of proteoglycans. *Methods Cell Biol* 69:53–67

Polyamine Transport Systems in Mammalian Cells and Tissues

Takeshi Uemura and Eugene W. Gerner

Abstract

Polyamine transport plays an important role in the homeostatic regulation of the polyamine levels. In animals, dietary polyamines are absorbed efficiently in the intestinal tract. In the colon, luminal bacterial derived polyamines are important contributors to cellular polyamine contents. Polyamine transport involves unique uptake and export mechanisms. The amino acid transporter SLC3A2 acts as a polyamine exporter in colon cancer-derived cells. Polyamine uptake is mediated by caveolin-1 dependent endocytosis. The K-RAS oncogene signals increased polyamine uptake and decreased polyamine export. Here, we describe the methods of polyamine transport analysis in the colon and the small intestine using membrane vesicles, culture cells, and mouse models.

Key words: Polyamine, Putrescine, Spermidine, Spermine, Plasma membrane vesicles, Culture cells, Mouse tissues, Transport, Colon, Small intestine

1. Introduction

Cellular polyamines are derived from intracellular biosynthesis and uptake from extracellular sources. The major sources of exogenous polyamines come from the diet and luminal bacteria (1). It has been shown that dietary polyamines were taken up by the intestinal tract and enter the systemic circulation (2–4). Treatment with antibiotics to remove microbial flora activity (5) or a polyamine-free diet (6) increases the polyamine depleting effect of the polyamine biosynthetic enzyme inhibitor α -difluoromethylornithine (DFMO). The export of polyamines from cells is also important for the maintenance of cellular polyamine levels.

Recently, we identified the amino acid transporter SLC3A2 as a polyamine export protein in colon cancer-derived cells (7). SLC3A2 catalyzes the export of acetylated polyamines by a

polyamine/arginine exchange reaction. We and others have reported that polyamine uptake is mediated by caveolae-dependent endocytosis in colon cancer-derived cells (8, 9). Knocking down caveolin-1 (CAV-1) using antisense RNA increases polyamine uptake activity in colon cancer-derived HCT116 cells. Since CAV-1 inhibits caveolar endocytosis, these results suggest that polyamine uptake occurs via a caveolar endocytotic pathway.

Polyamine transport is well characterized in *Escherichia coli* and *Saccharomyces cerevisiae* (10–14). There are several polyamine transport protein families including ATP-binding cassette transporters and proton potential-dependent solute carriers. In animals, the molecular mechanisms of polyamine transport appear to be somewhat different from those in simpler organisms.

In this chapter, we describe the methods for polyamine transport analysis in the gastrointestinal system using mouse models, cultured cells, and plasma membrane-derived vesicles.

2. Materials

2.1. Cell Culture

1. Dulbecco's Modified Eagle's Medium (DMEM) and Modified Essential Medium (MEM) (Gibco/BRL, Bethesda, MD) supplemented with 10% fetal bovine serum (FBS, PAA Laboratories).
2. Saline: 0.91% NaCl, autoclaved (see Note 1).
3. Puromycin Ready Made Solution (10 mg/mL, Sigma).
4. Trypsin solution (Mediatech, Manassas, VA).

2.2. Animals

1. Wild-type B6129SF2/J and CAV-1 knockout STOCK *Cav1^{tm1Mts}/J* mice were obtained from the Jackson Laboratory (Bar Harbor, ME) and bred in the University of Arizona's Animal Care Facility in accordance with The University of Arizona Institutional Animal Care and Use Committee guidelines.
2. Defined synthetic diet AIN93G (Harlan Teklad, Indianapolis, IN).
3. One percent putrescine prepared in water (see Note 2).
4. Phosphate buffered saline (PBS): 137 mM NaCl, 2.7 mM KCl, 10 mM Sodium Phosphate dibasic, and 2 mM potassium phosphate monobasic, pH 7.4.

2.3. Preparation of Inside-Out Membrane Vesicles

1. Putrescine · 2HCl (Calbiochem).
2. EDTA-PBS: 1 mM ethylenediaminetetraacetic acid (EDTA) in PBS.

3. Hypotonic buffer: 0.5 mM sodium phosphate, pH 7.0, 0.1 mM ethyleneglycol bis(2-aminoethyl ether)-tetraacetic acid (EGTA). Add 0.1 mM phenylmethylsulfonyl fluoride (PMSF) before use. Stored at 4°C.
4. TS buffer: 10 mM Tris-HCl, pH 7.4, 250 mM sucrose, 50 mM NaCl. Stored at 4°C.
5. Thirty-eight percent sucrose.
6. Fifteen-milliliters Potter-Elvehjem homogenizer.
7. Beckman 50.2 Ti fixed-angle rotor (Beckman Coulter).
8. Beckman SW28 swinging bucket rotor (Beckman Coulter).
9. Twenty-seven-gauge needle with a syringe.
10. BCA Protein Assay Kit (Pierce).

**2.4. Putrescine Uptake
by Inside-Out
Membrane Vesicles**

1. Assay buffer: 1 mM ATP, 10 mM MgCl₂, 0.2 mM CaCl₂, 10 mM dithiothreitol, 10 mM creatine phosphate, 100 µg/mL creatine kinase, 250 mM sucrose, 10 mM Tris-HCl, pH 7.4. Prepared before use.
2. Stop buffer: 250 mM sucrose, 150 mM NaCl, 10 mM MES-NaOH, pH 5.5. Stored at 4°C.
3. [H³]putrescine·2HCl (GE Healthcare).
4. Millipore HAWP 0.45-µm filter (Millipore).
5. Sampling manifold (Millipore).
6. CytoScint (MP, Irvine, CA).
7. Liquid scintillation counter LS 5000 TD (Beckman Coulter).

**2.5. Polyamine
Transport Assay
in Cells**

1. Assay buffer: 5 mM HEPES-NaOH, pH 7.4, 145 mM NaCl, 3 mM KCl, 1 mM CaCl₂, 0.5 mM MgCl₂, 5 mM glucose. Stored at 4°C.
2. Plastic container large enough to place 6-well plate in it.
3. Trichloric acid (TCA) solution (5% in water).
4. NaOH solution (0.5 N in water).

**2.6. Polyamine
Determination
by HPLC**

1. Perchloric acid (PCA) solution (0.2 N in water).
2. Teflon pestle (Daigger, Vernon Hills, IL).
3. Buffer A: 0.1 M sodium acetate, 10 mM octane sulfonate. Adjust to pH 4.5 with HPLC grade glacial acetate. Filter before use.
4. HPLC grade acetonitrile.
5. OPA buffer stock: 24.7 g/L boric acid, 20 g/L KOH, 0.1% Brij-35.
6. *o*-phthalaldehyde (OPA).

7. β -mercaptoethanol.
8. Methanol.
9. Standard solution: 2.5 μ M each of putrescine, spermidine, spermine, and diaminoheptane in 0.2 N PCA solution.
10. Diaminoheptane solution for internal standard (250 μ M).
11. μ Bondapak C18 10 μ m 125A 3.9 \times 300 mm column (Waters, Milford, MA).
12. Waters HPLC system with Multi λ Fluorescence Detector (Waters).

3. Methods

Polyamine transport activity can be measured in membrane vesicles, culture cells, and animal model systems. Plasma membrane vesicles are used for short time transport analysis, on the order of seconds to minutes. This system is suitable for the direct measurement of polyamine transport activity of the plasma membrane. Other factors influencing polyamine transport activity, such as metabolism and binding to the macromolecules, are eliminated in this system. The limitation to this system is that long-term transport activity cannot be measured since polyamine uptake into the vesicles is saturated within 1 h. In addition, a large amount of cells (10^9 cells) is required for the preparation of membrane vesicles.

The culture cell system is used for relatively short to long term (minutes to days) of polyamine transport activity. The polyamine transport activity can be measured in a relatively small amount of cells. This system represents many physiological features of cells. Polyamine metabolism and binding to the cellular components should be considered. The results are the sum of uptake and export.

We analyze the polyamine transport *in vivo* by measuring the polyamine contents in tissues after oral administration of polyamines. The results represent all physiological activities including uptake and export, metabolism, circulation, and distribution between organs. The use of genetically engineered mouse (GEM) models can provide insight regarding specific mechanisms.

3.1. Preparation of Inside-Out Membrane Vesicles

1. Putrescine tolerant and normal CHO cells are cultured in MEM. For maintenance, supply 15 mM putrescine in putrescine-tolerant CHO cell culture media. Prepare 30 of 100-mm culture dishes for preculture. Trypsinize cells and combine when cultures reach 70–80% confluent. Inoculate cells in

- six roller bottles and culture for 3 days (see Note 3). Supply 30 mM putrescine in the culture of putrescine tolerant cells and 10 mM putrescine in normal cells.
2. Place 50.2 Ti rotor and SW28 rotor in cold room on the day before harvest of cells. Check rotors are in good status. Apply grease if needed.
 3. Weigh an empty 500-mL centrifuge tube. Collect cells by treating cells with EDTA-PBS at 37°C for 10 min to detach cells and centrifugation at $2,000 \times g$ for 5 min at 4°C. Discard the supernatant and the cell pellet with 100 mL of saline. Collect cells by centrifugation at $2,000 \times g$ for 5 min at 4°C and discard the supernatant. Determine the wet weight of cells.
 4. Suspend cells in 15 volumes of ice-cold hypotonic buffer. Stir slowly at 4°C for 16 h (see Note 4).
 5. Remove unbroken cells by centrifugation at $3,500 \times g$ for 5 min at 4°C. Transfer supernatant to a 30 mL ultracentrifuge tube (see Note 5) and centrifuge at $100,000 \times g$ (37,500 rpm in 50.2 Ti rotor) for 45 min at 4°C.
 6. Collect white fluffy material around the yellowish pellet into 10 mL of hypotonic buffer. Homogenize with 20 strokes in a 15 mL Potter-Elvehjem homogenizer on ice.
 7. Layer the homogenate onto 14 mL of 38% sucrose and centrifuge at $100,000 \times g$ (25,000 rpm in SW28 rotor) for 45 min at 4°C. Use hypotonic buffer for balancing tubes (see Note 6).
 8. Collect the turbid layer at the interface between the sample and the sucrose into 17 mL of TS buffer (see Note 7). Pass the suspension through a 27-gauge needle with a syringe. Centrifuge at $100,000 \times g$ (37,500 rpm in 50.2 Ti rotor) for 45 min at 4°C. Remove the supernatant.
 9. Suspend the pellet in 50 μ L of TS buffer. Determine the protein amount by the BCA Protein Assay Kit according to the manufacturer's protocol. Membrane vesicles can be stored at -80°C until use.

3.2. Putrescine Uptake by Inside-Out Membrane Vesicles

1. Prepare the stop buffer and substrate mixture. The substrate mixture contains 10 μ M [H^3]putrescine (37 MBq/mmol) in the assay buffer (see Note 8). Place stop buffer on ice.
2. Set the temperature of water bath to 37°C. Place Millipore 0.45- μ m filters in a 100-mm culture dish with assay buffer.
3. Construct the assay mixture containing membrane vesicles (100 μ g of protein in 90 μ L assay buffer) in a glass test tube on ice. Prepare one tube for each time point.
4. Set up filters in the sampling manifold (see Note 9).

5. Incubate the assay mixture at 37°C for 5 min. Start transport reaction by adding 10 μ L of the substrate mixture.
6. After incubation for 5, 10, 20, 30, and 40 min, terminate reaction by placing the reaction mixture on ice and diluting with 1 mL of ice-cold stop buffer. Collect vesicles by rapid filtration through premoistened Millipore 0.45- μ m filter using the sampling manifold. Wash the filter three times with ice-cold stop buffer (see Note 10).
7. Dry filters and place in scintillation vials with 4 mL of CytoScint. Count the radioactivity on the filter in a liquid scintillation counter LS 5000 TD (see Note 11).

3.3. Putrescine Transport Assay in Cells

1. HCT116 cells stably transfected with mock or caveolin-1 antisense siRNA expressing vector are maintained in DMEM supplemented with 0.5 μ g/mL of puromycin. Seed one million cells per well of 6-well plates. Cells reach 80–90% confluent after 2 days (see Note 12). Each well corresponds to one time point.
2. Prepare assay buffer, substrate mixture, and wash buffer. Substrate mixture contains 2 mM [H^3]putrescine (37 MBq/mmol) in assay buffer. Wash buffer contains 20 mM cold putrescine in assay buffer. Place wash buffer on ice.
3. Set the temperature of water bath to 37°C. Place the plastic container with water-wet paper in the water bath. Place assay buffer and substrate mixture in water bath.
4. Place 6-well plate that cells were inoculated in the plastic container.
5. Aspirate culture medium. Wash cells twice with 1 mL of assay buffer (see Note 13).
6. Start transport reaction by applying 1 mL of substrate mixture.
7. After incubation for 5, 10, 15, 20, and 25 min, aspirate substrate mixture and wash cells twice with ice-cold wash buffer.
8. Treat cells with 0.2 mL of 5% TCA solution at room temperature for 30 min with gentle shaking. Add 0.2 mL of 0.5 N NaOH and incubate at room temperature with gentle shaking until cell lysate becomes clear.
9. Take 30 μ L of cell lysate and determine the protein amount by the BCA Protein Assay Kit according to the manufacturer's protocol.
10. Transfer 300 μ L of cell lysate to the scintillation vial containing 4 mL CytoScint, vortex and count the incorporated radioactivity by a liquid scintillation counter.

3.4. Measuring Putrescine Transport in Small Intestine and Colon in Mice

1. Wild-type B6129SF2/J, CAV-1 knockout STOCK *CAV1^{tm1Mls}/J* are raised in cages under nonsterile microisolator conditions and fed with AIN-93G diet.
2. Supply 1% putrescine in drinking water for 2 weeks (see Note 14).
3. After 2 weeks of treatment, sacrifice mice by CO₂ inhalation and spine displacement.
4. Remove intestinal tract, open and flush with PBS. Take approximately 2.5 cm portion of small intestine and colon (see Note 15). Tissues are rapidly frozen in liquid nitrogen and stored at -30°C.
5. Take 20 mg of tissues and cut into small pieces. Transfer tissues to microcentrifuge tubes and homogenize in 0.35 mL of 0.2 N PCA solution using a teflon pestle. Mix homogenates by vortexing and stand at room temperature for 1 min. Repeat five times. Stand homogenates at 4°C for 16 h.
6. Centrifuge the homogenate at 14,000 rpm for 10 min.
7. Remove supernatant and store at 4°C for polyamine determination by HPLC.
8. Suspend pellet in 0.5 mL of NaOH and stand at room temperature for overnight.
9. Centrifuge 14,000 rpm for 10 min. Determine the protein amount in the supernatant by the BCA Protein Assay Kit according to the manufacturer's protocol.

3.5. Polyamine Determination by HPLC

1. Prepare buffer A. Add 27.2 g of sodium acetate and 4.32 g of octane sulfonate to 550 mL of water. Stir until dissolved. Adjust pH to 4.5 with HPLC grade glacial acetic acid (less than 15 mL). Bring volume to 2 L with water. Filter before use.
2. Prepare buffer B. Mix 1 L of buffer A with 282 mL of HPLC grade acetonitrile just before use. Filter.
3. Prepare OPA buffer. In a 15 mL conical tube, add 0.56 g of OPA and 10 mL methanol. Vortex until OPA is completely dissolved. Add 2 mL of β-mercaptoethanol and OPA solution to 1 L of OPA buffer stock. Stir and filtrate before use. Use brown bottle or aluminum foil to protect from light.
4. Set up HPLC system. Place buffer A, buffer B, and OPA buffer, and flush to remove air bubbles in all tubes (see Note 16). Set flow rates for buffer A and OPA buffer to 1.5 mL/min. The pump for buffer B is stopped. The buffer A went through the column is mixed with OPA buffer and fluorescence is detected using Multi λ Fluorescence detector. Excitation and emission were performed at 340 and 455 nm, respectively.

5. Prepare samples for HPLC injection. Add 2 μL of 250 μM diaminoheptane solution to 198 μL of sample.
6. Equilibrate $\mu\text{Bondapak}$ column with buffer A until the base line becomes stable. It usually takes up to 1 h.
7. Perform the run with 200 μL injection of 0.2 N PCA without any amines to see the base line is stable (see Note 17). The program starts with 20 min of 100% buffer A at 1.5 mL/min followed by a gradual increase of buffer B from 0 to 100% for 30 min. The program is finished with 5 min of 100% buffer A.
8. Inject and run 200 μL of standard mixture under the same condition. Standard solution contains 500 pmol of each amine in 200 μL .
9. Run samples. Perform the standard run after every five sample runs.
10. Calculate polyamine contents (see Note 18).

4. Notes

1. Unless stated otherwise, all solutions should be prepared in Milli-Q generated water. This is referred to as “water” in this chapter.
2. Food coloring dye can be used for putrescine solution. This may avoid using the wrong solution.
3. This procedure is modified from the methods described by Schaub et al. (15) and Saxena and Henderson (16). This protocol can be adopted for other cell culture systems including suspension-growing cells.
4. It is important that cells are completely separated from each other. Cells can be suspended in a small volume of hypotonic buffer by repeated pipetting and the rest of buffer is added.
5. The supernatant can be easily transferred using a 10 mL pipette, and prevent the contamination of unbroken cells.
6. The homogenate can be layered using 200 μL Pipettman tip. Contact the tip with the surface of sucrose and slowly push the homogenate.
7. To collect the turbid layer, take out upper TS buffer layer first using 1 mL Pipettman tip. It is important to take out upper layer carefully and slowly.
8. The substrate mixture contains tenfold putrescine of final concentration of reaction mixture.
9. Make sure that there are no holes and leaks in all filters. Leaks can be tested by applying 1 mL of assay buffer onto filters.

- Under optimal vacuum condition, 1 mL assay buffer goes through the filter in approximately 2 s.
10. For washing, apply ice-cold assay buffer to the same test tube and pour onto the filter. This ensures all vesicles go through the filter.
 11. It is necessary to count the radioactivity in the substrate mixture to calculate the amount of transported putrescine. The portion of substrate mixture can be directly added to CytoScint in scintillation vial.
 12. The CAV-1 protein level in antisense transfected cells is decreased to less than 10% of mock transfected cells after 2 days.
 13. It is important to remove and apply assay buffer carefully. The rough operation causes detachment of cells. The poly-l-lysine coated plate can be used for more strong attachment of cells.
 14. Sometimes mice do not drink the putrescine solution as much as normal water. Supplementation of 2% sugar may increase consumption.
 15. It is important to take the same portion of tissues in every mouse.
 16. To remove air bubbles, place all buffers lower than the pump, flush at the maximum speed and flick tubes. Flushing all tube systems with methanol before set up buffers makes it easier to remove air bubbles.
 17. Air bubbles and trace amount of contaminated amines and ions make the baseline unstable. Connecting the column in a reverse direction may help to stabilize the base line. Sometimes making new buffer is a faster way to stabilize the baseline.
 18. Correct the variability of injection volume between samples using the signal of diaminoheptane as an internal standard.

Acknowledgements

We would like to thank Dr. Kirk E. Pastorian, Dr. Leo Hawel III, and Dr. Craig V. Byus, Department of Biomedical Sciences, University of California, Riverside, for development of the putrescine tolerant CHO cells. We thank Dr. B. Sloane and Dr. D. Cadavello-Medved, Department of Pharmacology, Barbara Karmanos Cancer Institute, Wayne State University, School of Medicine, for providing HCT116/Mock and HCT116/Cav-1 A. S. cells. This work was supported, in whole or in part, by National Institutes of Health Grants CA123065, and CA095060.

References

1. Larqué E, Sabater-Molina M, Zamora S (2007) Biological significance of dietary polyamines. *Nutrition* 23:87–95
2. Bardocz S, White A, Grant G, Brown DS, Duguid TG, Puzstai A (1996) Uptake and bioavailability of dietary polyamines. *Biochem Soc Trans* 24:226S
3. Nakaike S, Kashiwagi K, Terao K, Iio K, Igarashi K (1988) Combined use of alpha-difluoromethylornithine and an inhibitor of S-adenosylmethionine decarboxylase in mice bearing P388 leukemia or Lewis lung carcinoma. *Jpn J Cancer Res* 79:501–508
4. Wery I, Kaouass M, Deloyer P, Buts JP, Barbason H, Dandrifosse G (1996) Exogenous spermine induces maturation of the liver in suckling rats. *Hepatology* 24:1206–1210
5. Hessels J, Kingma AW, Ferwerda H, Keij J, van den Berg GA, Muskiet FA (1989) Microbial flora in the gastrointestinal tract abolishes cytostatic effects of alpha-difluoromethylornithine in vivo. *Int J Cancer* 43:1155–1164
6. Quemener V, Moulinoux JP, Havouis R, Seiler N (1992) Polyamine deprivation enhances antitumoral efficacy of chemotherapy. *Anticancer Res* 12:1447–1453
7. Uemura T, Yerushalmi HF, Tsapraillis G, Stringer DE, Pastorian KE, Hawel L, Byus CV, Gerner EW (2008) Identification and characterization of a diamine exporter in colon epithelial cells. *J Biol Chem* 283:26428–26435
8. Belting M, Mani K, Jonsson M, Cheng F, Sandgren S, Jonsson S, Ding K, Delcros JG, Fransson LA (2003) Glypican-1 is a vehicle for polyamine uptake in mammalian cells: a pivotal role for nitrosothiol-derived nitric oxide. *J Biol Chem* 278:47181–47189
9. Roy UK, Rial NS, Kachel KL, Gerner EW (2008) Activated K-RAS increases polyamine uptake in human colon cancer cells through modulation of caveolar endocytosis. *Mol Carcinog* 47:538–553
10. Igarashi K, Ito K, Kashiwagi K (2001) Polyamine uptake systems in *Escherichia coli*. *Res Microbiol* 152:271–278
11. Uemura T, Kashiwagi K, Igarashi K (2005) Uptake of putrescine and spermidine by Gap1p on the plasma membrane in *Saccharomyces cerevisiae*. *Biochem Biophys Res Commun* 328:1028–1033
12. Uemura T, Kashiwagi K, Igarashi K (2007) Polyamine uptake by DUR3 and SAM3 in *Saccharomyces cerevisiae*. *J Biol Chem* 282:7733–7741
13. Uemura T, Tachihara K, Tomitori H, Kashiwagi K, Igarashi K (2005) Characteristics of the polyamine transporter TPO1 and regulation of its activity and cellular localization by phosphorylation. *J Biol Chem* 280:9646–9652
14. Uemura T, Tomonari Y, Kashiwagi K, Igarashi K (2004) Uptake of GABA and putrescine by UGA4 on the vacuolar membrane in *Saccharomyces cerevisiae*. *Biochem Biophys Res Commun* 315:1082–1087
15. Schaub T, Ishikawa T, Keppler D (1991) ATP-dependent leukotriene export from mastocytoma cells. *FEBS Lett* 279:83–86
16. Saxena M, Henderson GB (1995) ATP-dependent efflux of 2, 4-dinitrophenyl-S-glutathione. Properties of two distinct transport systems in inside-out vesicles from L1210 cells and a variant subline with altered efflux of methotrexate and cholate. *J Biol Chem* 270:5312–5319

Procedures to Evaluate the Importance of Dietary Polyamines

Paul Acheampong, Mary J. Macleod, and Heather M. Wallace

Abstract

Polyamines not only play vital physiological functions including modulating transcription and translation of genetic material, cell proliferation and growth, ion channel regulation and cell signaling, but have also been cited in the pathogenesis of diseases. Many plant and animal sources used as food contain high amounts of polyamines. Knowledge of the content of polyamines in food as a source of these growth factors is therefore critical. A 2-step perchloric acid precipitation method to obtain acid soluble extracts from food that are subsequently taken through a dansylation process to produce dansyl polyamine derivatives for HPLC measurement is described. Examples are provided to illustrate mathematical correction factors

Key words: Polyamine, Food, Diet, Dansylation, Perchloric acid

1. Introduction

1.1. Dietary Polyamines and Their Absorption After Ingestion

Many plant and animal species have been used as sources of nutrition and supplements for man. The total polyamine content varies significantly between different nutritional sources. The amounts of the naturally occurring polyamines – putrescine, spermidine, and spermine – together with some of their metabolites have been analyzed from many food sources. The amount of these polyamines varies significantly between different foods (1–5).

Across many plant sources of food, putrescine is usually the polyamine found at the highest concentration compared with spermidine and spermine. Citrus fruits such as orange and mandarins have particularly high levels exceeding >1,500 nmol/ml, in some instances (3). On the contrary, putrescine content in animal sources of food is relatively low. Spermine is reported as the predominant polyamine in many meat products compared to

putrescine and spermidine. These reciprocal variations in the amounts of putrescine and spermine have been well demonstrated by Kalac and Krausová (2). Furthermore, polyamine content in the same food source may vary significantly between fresh and cooked products (2). For instance, the amount of putrescine in potatoes was more than doubled when cooked (3).

Using data from the British National Food Survey, Bardocz et al. (6) reported the average adult intake of polyamine to be between 350 and 500 $\mu\text{mol}/\text{person}/\text{day}$. For individuals, the daily intake may vary depending on what is consumed and in what quantities. Changes in eating habits, and the growing availability of transcontinental dishes, may significantly affect the levels of polyamine ingested as varied plant and animal sources of food becomes readily available.

Through ingested food, a high polyamine load is delivered to the gut (4) and together with other sources of intestinal luminal polyamines derived from bacterial activity, epithelial slough and pancreatic/bile secretion, they serve as an extracellular source of polyamines for cellular activity. However, ingested diet remains the most abundant source of exogenous polyamine with the others providing a significantly smaller contribution (2, 7).

Upon intake of food, there is a rapid decline of intestinal lumen polyamine concentration to fasting levels within 120 min (4). This decline is attributed to absorption – which predominantly occurs in the duodenum and proximal jejunum, intraepithelial usage and intraluminal enzymatic metabolic activities leading to polyamine and nonpolyamine derivatives (8, 9). The most predominant of the catabolic enzymes involved in the metabolism of polyamines are polyamine oxidase and diamine oxidase (10, 11). Due to the effects of the catabolic enzymes, polyamine metabolites may end up in systemic circulation. This is supported by evidence that an infusion of putrescine into the gut results in alteration in systemic levels of *N*-acetyl-putrescine, spermidine, and spermine (all of which could be produced from putrescine), and that the amount of polyamines absorbed from the gut lumen bears a linear relationship with the amount present or ingested (12).

Polyamines have many important physiological functions including modulating transcription and translation of genetic material, cell proliferation and growth, ion channel regulation and cell signaling. Dietary means of supply of these vital polycations may be crucial for survival and significant research has been undertaken to evaluate the levels of polyamines in food. In the following subheadings, we describe a reliable method for the measurement of dietary polyamines.

1.2. Measurement of Polyamines

Several methods have been used to quantify polyamine content. Principal among these have been biological and chemical methods employed to measure polyamines and their acetyl derivatives.

Most of these are reliable in measuring the naturally occurring polyamines such as putrescine, spermidine, and spermine but significant limitations exist in the application of some of these in the measurement of the acetyl derivatives.

The biological approaches have involved enzymatic but principally, immunoassays using ELISA and RIA. Although the immunoassay techniques provide a rapid and highly sensitive method with the ability to carry out multiple sample analysis and no need for derivatization, they are of low specificity. There are also issues of cross reactivity among the polyamines (13). RIA methods are also associated with the additional problem of the handling of radioactive materials.

The chemical methods involve electrophoretic and chromatographic techniques. The main electrophoretic methods are paper, high voltage, and capillary electrophoresis. Paper and high voltage electrophoresis are simple to carry out but less used in polyamine measurements due to their low sensitivity and specificity although attempts have been made to improve these (14–17). Capillary electrophoresis, compared to the other electrophoretic methods, provides a better analytic resolution but remains less sensitive compared to the widely used chromatographic methods (13).

Chromatographic methods such as paper, thin layer, gas, and high performance liquid chromatography (HPLC) have been used most often in polyamine determinations. Although simple to use, thin layer chromatography is semiquantitative, less specific, and precise. Despite considerable efforts at improving the use of gas chromatography in polyamine analysis since its introduction in the 1960s, it remains less favorable compared to HPLC because of poor sensitivity and difficulties with obtaining derivatizable salt-free extracts from body fluids (13).

HPLC was first introduced into polyamine analysis over three decades ago (18). Since then there have been great improvements in the processing time, resolution, and sensitivity. It is presently the method of choice for polyamine assay due to its high reproducibility and sensitivity as well as its suitability for automation (13). Some of the improvements have entailed the production of polyamine derivatives, obtained by conjugating polyamine molecules with detectable chemical moieties, either pre- or postcolumn, for fluorescent or spectrophotometric detection.

Precolumn derivatization occurs before the constituents of the mixture to be analyzed reaches the chromatographic column where the components in a mixture are separated by virtue of their partitioning between the stationary and mobile phases. Precolumn derivatization is usually part of the processing of samples before they are injected into the HPLC set-up. Postcolumn derivatization occurs after separation of the constituents of the sample to be analyzed.

Precolumn derivatisation with dansyl chloride, fluorescamine, and *o*-phthalaldehyde generates fluorescence-producing derivatives (19) while benzoyl chloride, dabsyl chloride, and tosyl chloride have been used to produce postcolumn derivatives for spectrophotometric detection. Compared with spectrophotometric methods, fluorimetry produces a better detection limit for polyamines (13). Wang et al. have reported a limit of detection of 0.05 nmol/ml of RBC for putrescine, spermidine, spermine, and their acetyl derivatives with the use of dansyl chloride to obtain derivatives for HPLC (20).

The fluorimetry-based technique has a higher sensitivity and specificity as the reagents used react with primary and secondary amines. The dansyl chloride may also react with imidazole nitrogen, hydroxyls, and some alcohols to form fluorescent derivatives (14, 21, 22). In spite of all the advantages of using fluorimetry, there are setbacks such as prolonged time for derivatization, unstable derivatives leading to broad peaks in chromatograms, and dilution of samples but attempts are being made to improve the method further. Attempts have been made to combine gas chromatography and HPLC with mass spectrometry in order to couple the great separation capabilities of these chromatographic methods with the specificity and sensitivity of mass spectrometry (13).

2. Materials

1. Perchloric acid: dissolved in distilled water at 1.2 M and 0.2 M and stored at 4°C.
2. Putrescine hydrochloride: 5 mM (Sigma Aldrich, St Louis MO, USA) dissolved in 0.2 M perchloric acid and stored in aliquots of 1 ml at -20°C.
3. Spermidine hydrochloride: 5 mM (Sigma Aldrich, St Louis MO, USA) dissolved in 0.2 M perchloric acid and stored in aliquots of 1 ml at -20°C.
4. Spermine hydrochloride: 5 mM (Sigma Aldrich, St Louis MO, USA) dissolved in 0.2 M perchloric acid stored in aliquots of 1 ml at -20°C.
5. Dansyl chloride: 15 mg/ml (Sigma Aldrich, St Louis MO USA) dissolved in either HPLC grade acetonitrile or methanol. Make fresh, protect from light.
6. 1,7 - diaminoheptane: 2 mM (Sigma Aldrich, St Louis MO USA) dissolved in 0.2 M perchloric acid and stored at -20°C. Dilute with 0.2 M perchloric acid to obtain 1 in 20 dilution.

7. Sodium carbonate decahydrate: 0.75 g/ml (BDH Laboratory Supplies, Poole England) dissolved in distilled water and adjusted to pH 10.5 with 5 M HCl.
8. L-Proline: 10 mg/ml (Sigma Aldrich, St Louis MO USA) dissolved in distilled water. Make fresh.
9. HPLC grade acetonitrile (Fischer Scientific UK Ltd, Leicestershire UK).
10. HPLC grade methanol.
11. Toluene (Rathburn Chemicals, Walkerburn Scotland).
12. Nitrogen gas (industrial suppliers).
13. Autosampler/injector (Gilson 234 sampling injector).
14. Pumps (Two Gilson 306 pumps).
15. HPLC stationary phase (Hichrom HIRPB-6527 or H2922, 150×4.6 mm).
16. Fluorescence monitor/detector (Shimadzu (Cynkotek) RF1002 Fluorescence HPLC Monitor).

3. Methods

The perchloric acid precipitation method is used to obtain acid soluble extracts from food. Similar methods have been used by other research groups (3, 23) and the method described here has been adapted for our laboratory practice. These acid soluble extracts and standards are then processed using a modified version of the dansylation method described by Seiler and Knödgen (19). This method has been used extensively in our laboratory and has undergone significant improvement in its precision characteristics. We have adopted it for use in measuring only the naturally occurring polyamines putrescine, spermidine, and spermine.

3.1. Preparing Liquefied Extracts of Solid Food

Homogenization is the principal method employed in obtaining liquefied extracts from nonliquid food sources. Both distilled water and perchloric acid have been used either independently or in sequence to obtain the liquefied extracts. We recommend the use of distilled water from practical experience. In general, concentrations of 7.5–30% w/v have typically been used and a maximum volume of 20 ml is advised. The normal handheld kitchen blender have been used for food samples up to 30 g and the Janke-Kunkel homogenizer has been used for samples as low as 1 g. Homogenization speeds of up to 3,000 revolutions per min for 10 min and 20,000–23,000 revolutions per min (rpm) for 1 min have been used in the application of the kitchen blender

and Janke-Kunkel homogenizations, respectively (3, 23). A balance between speed and duration of homogenization is necessary. A 2-step liquefying process is recommended to get as much of the polyamine content as possible into the liquefied extract.

Step 1:

1. About half of the required volume of the diluent (preferably distilled water) to make the needed concentration is added to a predetermined weight of the food substance and homogenized at the required speed and time duration to achieve a smooth homogenate.
2. At the end of the initial homogenization, the homogenate should be centrifuged at $1,000 \times g$ for 10 min. Paper filtration may be an alternative.
3. Decant the supernatant into a clean receptacle.

Step 2: To the residue from step 1 '3',

1. Rehomogenize with the remainder of the diluent (distilled water) under same conditions as in step 1 '1'.
2. At the end of this second homogenization, centrifuge the homogenate at centrifuge $1,000 \times g$ for another 10 min. Paper filtration may be used as an alternative.

Then decant and add the supernatant to that from step 1 '3' (see Note 1).

3.2. Determination of the Appropriate Dilution of Liquefied Supernatant of Solid Food or Nonsolid Food to Use for Perchloric Acid Precipitation

In order to achieve the best possible results, it is imperative to obtain the best possible acid soluble extract for polyamine quantification. This can be achieved by identifying the dilution of the liquefied food or non solid food that yields the best possible acid soluble extract.

This is done by preparing a series of dilutions of the liquefied food extract and subjecting them to the two-stage perchloric acid (PCA) precipitation as described below. The target concentration of PCA in the final mixture should be 0.2 M.

1. To a series of 2-ml Eppendorf tubes containing 1 ml of liquefied food each, add 100 μ l of 1.2 M PCA and vortex mix for 2 min.
2. Keep the resultant solution from step 1 on ice for 15 min and then centrifuge at $3,000 \times g_{av}$ for 5 min to produce an acid soluble supernatant.
3. Add another 100 μ l of 1.2 M PCA to the resultant solutions from step 2, vortex mix for 2 min bringing the final concentration of PCA in the mixture to 0.2 M and repeat step 2.
4. From the results of step 3 in the two-stage precipitation protocol, choose the lowest dilution that produces the best PCA precipitation for subsequent polyamine analysis. This

provides the highest possible concentration of polyamines to be measured in the best acid soluble extract.

- For the determination of polyamine concentrations in liquefied solid food sources, different concentrations of the homogenized food may need to be analyzed to obtain the best dilution that yields the best PCA precipitation results.

3.3. Preparation of a Working Polyamine Stock Solution Containing Putrescine, Spermidine, and Spermine

- Prepare a working stock of 25 μM polyamine mixture solution by the addition of 100 μl each of 5 mM of putrescine, spermidine, and spermine to 19.7 ml of 0.2 M PCA. Prepare just enough of this polyamine mixture for each experiment.
- Prepare standard solutions containing 0, 0.5, 1.0, 2.0, 3.0, and 4.0 nmol of all three polyamines in 200 μl of 0.2 M PCA. This is achieved by the addition of a required volume of PCA to a predetermined volume of the 25 μM polyamine stock solution in a 1-ml Eppendorf tube. In all cases, the total volume of the standard polyamine solutions ready for use in the dansylation process is 200 μl as indicated in Table 1 below.

3.4. Processing of Acid Soluble Extracts and Standards for Polyamine Quantification

3.4.1. Processing of Acid Soluble Extracts and Standards by Dansylation

- To 200 μl of acid soluble extracts (from the 2-stage precipitation method of the predetermined dilution of the liquefied food or non solid food which has the best yield of acid soluble extract) and standards in different Eppendorf tubes, add 10 μl of 1:20 dilution of 2 mM 1, 7-diaminoheptane (internal standard).
- To the solutions from step 1, add 50 μl of sodium carbonate decahydrate (1 g/ml) and vortex mix thoroughly.

Table 1
Preparation of standard concentrations of polyamine for HPLC

Standard polyamine concentration (nmol/200 μl)	Volume of 25 μM polyamine stock (μl)	Volume of 0.2 M PCA (μl)
0	0	200
0.5	20	180
1.0	40	160
2.0	80	120
3.0	120	80
4.0	160	40

The stock solution of polyamines contain putrescine, spermidine, and spermine at concentrations of 25 μM

3. Then add 500 μl of dansyl chloride (15 mg/ml in acetonitrile) to each of the solutions from step 2 and vortex mix thoroughly.
4. Incubate the resultant solutions from step 3 in a shaking water bath in the dark at 25–37°C overnight (for 8–10 h).
 - (a) In the course of the incubation, mix the samples on two occasions to ensure that the dansyl chloride remains well mixed with the rest of the solution.
 - (b) After each vortex mixing, centrifuge the Eppendorf tubes very briefly (up to 5 s) at 1,500–3,000 $\times g$ to cause gravitation of solution trapped in the cap. This will remove any solution trapped in the cap of the Eppendorf tube and will avoid trapped solution in the cap later staining the toluene extract which may interfere with the purity of the chromatograms.
5. At the end of the incubation period, add 125 μl of L-proline (10 mg/ml) to each Eppendorf tube from step 4 and vortex mix intermittently (2–4 times for up to 5 s each) to neutralize excess dansyl chloride. Leave the resultant solution to stand for 15–30 min or until the solution turns pale yellow or colorless (see Note 2).

3.4.2. Toluene Extraction of Dansylated Polyamines and Internal Standard

1. Add 500 μl of toluene to each of the Eppendorf tubes from step 5 in Subheading 3.4.1 and vortex mix (2–3 times for 15 s each).
2. Centrifuge the solutions in the Eppendorf tubes from step 1 at 3,000 $\times g$ in a microcentrifuge for 2–3 min.
3. Decant the upper toluene layer (which contains the dansylated polyamines) from each Eppendorf tube from step 2 into a new 5–10 ml plastic test tube.
4. Evaporate the contents of the tubes from step 3 to dryness using nitrogen gas in a laminar flow chamber.
5. Direct the nitrogen gas into the plastic tubes with the aid of Pasteur tubes (see Notes 3–6).

3.4.3. Reconstitution of Polyamines in Acetonitrile for HPLC analysis

1. Add 200 μl of HPLC grade acetonitrile to each plastic tube to reconstitute the dried polyamine and internal standard residue from step 4 in Subheading 3.4.2. Allow the plastic tubes to stand for 1–2 min and then vortex mix intermittently (2–3 times for 5–10 s each).
2. Transfer the reconstituted samples from step 1 into new Eppendorf tubes and then centrifuge these at 3,000 $\times g$ for 2–3 min in a microcentrifuge (see Note 7).
3. Pipette 50 μl of reconstituted samples from step 2 into HPLC vials with cover for subsequent HPLC analysis.

3.5. High Performance Liquid Chromatography (HPLC) Set-up

1. An automated reverse-phase Gilson HPLC system consisting of a 234 autosampler, two 306 pumps, an 805 manometric module and an 811C dynamic mixer is used. Detection and quantification of separated dansyl polyamine derivatives is performed using a Cynkotek RF1002 fluorescence monitor. Mobile phase gradient and data acquisition and integration are carried out using Gilson 715 software. The set-up is illustrated below in Fig. 1.
2. 10 μl of sample is injected onto a Hichrom RPB (5 μm) column (150 \times 4.6 mm) at room temperature.
3. The dansylated polyamines elute from the chromatographic column after the application of gradient elution which is generated by a combination of varying proportions of two mobile phases (both mobile phases are degassed with nitrogen before use) – A and B, at a flow rate of 1 ml/min. Mobile phase A is 40% acetonitrile in water and mobile phase B is 100% acetonitrile. The elution gradient is as follows: 0–5 min 0% B, 5–20 min 0–100% B, 20–22 min 100% B, 22–22.01 min 100–0% B, 22.01–27 min 0% B.
4. Fluorescence detection is achieved by excitation at 320 nm and emission at 523 nm. The result of the chromatographic process is the production of a chromatogram for each sample. An example of a typical chromatogram is shown below in Fig. 2.
5. The areas of the peaks from the standard solution are used to produce a standard curve from which the polyamine concentration of unknown solutions is determined. The use of the peak of 1, 7-diaminoheptane to derive ratios of the areas of the polyamine peaks serves as an internal standardization of the method.

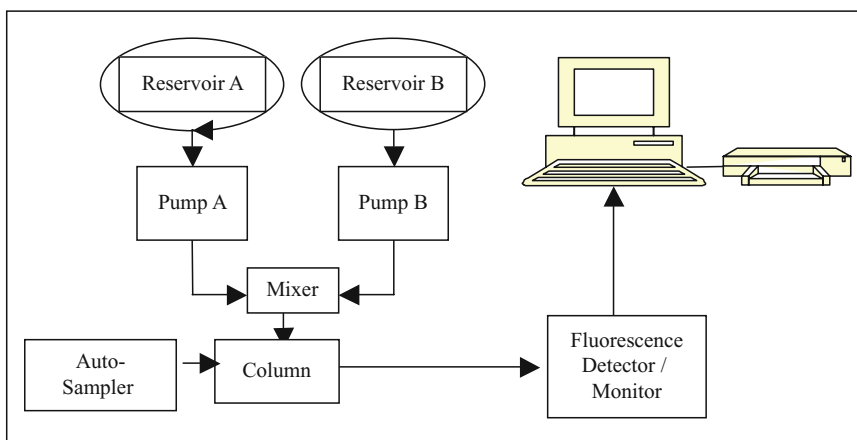


Fig. 1. Illustration of an automated HPLC set-up.

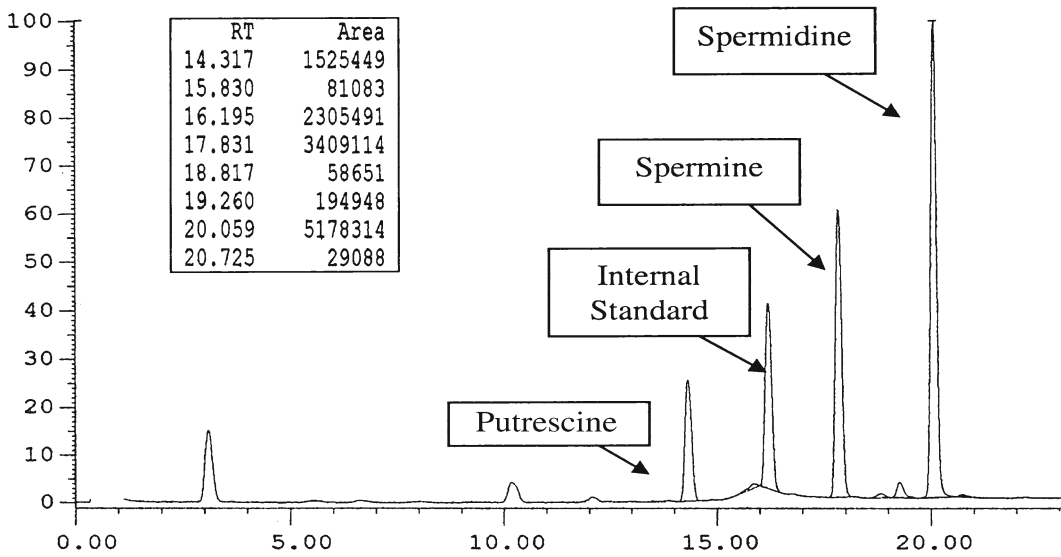


Fig. 2. Chromatogram of an HPLC run of natural polyamines with an internal standard. The retention or run times (RT) for putrescine, internal standard, spermine, and spermidine are about 14, 16, 18, and 20 s, respectively and the areas of their respective peaks are indicated against the RT.

6. Methanol can be used as a substitute for acetonitrile, which has been subject to supply difficulties (see Note 8). Methanol may be cheaper as a solvent, and the run time per sample on the HPLC set-up is shorter compared to the acetonitrile method.

3.6. Determination of Polyamine Concentration after an HPLC Run

To determine the polyamine concentration of a food extract, an HPLC run of the extract together with known polyamine standards as described in Subheading 3 is imperative. The chromatograms of the standard polyamine solutions are used to derive a standard curve, and from this the polyamine concentrations in the food extract can be determined.

1. Plot individual standard curves for the three polyamines – putrescine, spermidine, and spermidine. This is obtained by plotting the area ratios (area of polyamine/area of the internal standard) of the different concentrations on the y -axis against their known respective concentrations on the x -axis for each of the polyamines as illustrated in Fig. 3. Linear regression equations should then be determined for each of the standard curves. This is easily obtained from many statistical softwares including Microsoft Excel.
2. The polyamine concentration in the acid soluble dietary extract is determined by extrapolation from the linear regression equations derived from the standard curves.

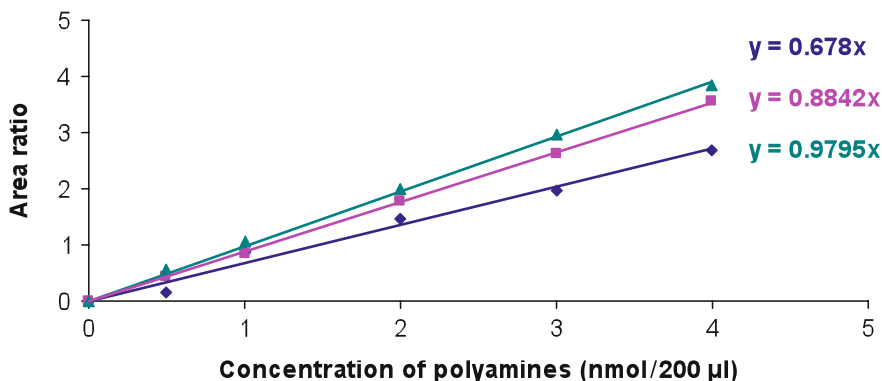


Fig. 3. Standard curves for putrescine, spermidine, and spermine. The linear regression curves and equations from which the quantities of polyamine in unknown dietary samples can be deduced are indicated for putrescine (*filled diamond*), spermidine (*filled square*), and spermine (*filled triangle*).

From the plot illustrated in Fig. 3 above, the regression equations for putrescine, spermidine, and spermine are generally given by:

Area ratio = (Gradient of standard curve) × (Polyamine concentration, nmol/200 µl of acid soluble extract).

Therefore, (Polyamine concentration in nmol/200 µl of acid soluble extract) = (area ratio) / (gradient of standard curve).

3.7. Mathematical Correction for PCA Extraction, Dilution, and Preparation of the Liquefied Extract

Always remember to: (a) correct for the PCA extraction; (b) correct for the dilution used to obtain the best PCA precipitation; (c) correct for the volume of distilled water used to prepare the liquefied dietary extract for solid foods that required liquefaction. This yields the amount of the polyamines in the original weight or volume of the sample. To determine the final concentration of polyamine in the original diet, there is the need to correct the dilutions of the dietary extract used.

1. Correction for PCA extraction. Since 200 µl of the acid soluble extract out of a total volume of 1.2 ml at the end of the PCA extraction is used for the dansylation process, it is important to correct this to reflect the total polyamine load in the 1 ml sample of liquid diet used.

The correction factor for this is given by: $200 \mu\text{l} / 1.2 \text{ ml} = 6$

2. Correction for dilution used to obtain the best PCA precipitation. If there was the need to dilute the liquefied solid diet (or non solid diet), there is the need to correct this to reflect the total polyamine load in the original nonsolid diet or

liquefied solid diet. To do this, it is important to note the exact dilutions used in the form “A in B” where:

- ‘A’ is the volume of the liquefied solid diet (or non solid diet) used in the dilution
- ‘B’ is the total volume after dilution i.e., (volume of liquefied solid diet (nonsolid diet)) + (volume of diluent used)

This correction is achieved by factoring ‘B/A’ in the final calculation to determine the concentration of polyamines in the original nonsolid diet or liquefied solid diet.

3. Correction for the volume of distilled water used to prepare the liquefied dietary extract for solid diet requiring liquefaction. This correction enables us to express the final polyamine content of the diet per weight measure. This is relevant for solid for that needed liquefaction to facilitate PCA extraction of polyamines. It is not applicable to food substances like fruit juices or drinks, the acid soluble portions of which can be directly extracted with PCA without the need for liquefaction. The correction is expressed as:

Total amount of polyamine per weight of solid diet used for liquefaction = (Total volume of distilled water used for liquefaction) × (concentration of polyamine per ml of liquefied diet).

4. Overall calculation incorporating all correction factors (for solid diets requiring liquefaction). Total amount of each polyamine per total weight of solid diet used for liquefaction = ((Area ratio)/(Gradient of standard curve)) × (6 × (b/a) × (volume of distilled water used for liquefaction)).
5. Overall calculation incorporating all correction factors (for liquid diets not requiring liquefaction). Total amount of each polyamine per volume 1 ml of liquid diet = ((Area ratio)/(Gradient of standard curve)) × (6 × (b/a)).

3.8. Examples

3.8.1. Example (for Solid Diet Requiring Liquefaction)

A dietary extract of a solid diet is prepared by liquefying 5 g in 20 ml of distilled water and a 1 in 3.5 dilution is used for PCA extraction per the protocol in Subheading 3. Area ratios obtained from HPLC chromatograms are 0.45, 0.6, and 0.78 for putrescine, spermidine, and spermine, respectively. Calculate the putrescine, spermidine, and spermine content of the 5 g diet using the standard curves shown in Fig 3.

Reminder: Linear regression equations for the polyamines are:

Putrescine: (Area ratio) = 0.678 (Putrescine concentration, nmol/200 µl of acid soluble extract).

Spermidine: (Area ratio) = 0.8842 (Spermidine concentration, nmol/200 µl of acid soluble extract).

Spermine: (Area ratio)=0.9795 (Spermine concentration, nmol/200 μ l of acid soluble extract).

Step 1

From the above formula, the concentration of the polyamines in nmol/200 μ l of acid soluble extract will be given by:

Putrescine: $0.45/0.678=0.664$ nmol of Putrescine/200 μ l of acid soluble extract.

Spermidine: $0.6/0.8842=0.679$ nmol of Spermidine/200 μ l of acid soluble extract.

Spermine: $0.78/0.9795=0.796$ nmol of Spermine/200 μ l of acid soluble extract.

Step 2

Correction for PCA extraction to reflect amount of polyamine per 1 ml of liquefied diet from a 1 in 3.5 dilution of 5 g in 20 ml of distilled water are as follows:

Putrescine: $0.664 \times 6 = 3.98$ nmol of Putrescine/ml liquefied diet from a 1 in 3.5 dilution of 5 g in 20 ml.

Spermidine: $0.679 \times 6 = 4.07$ nmol of Spermidine/ml liquefied diet from a 1 in 3.5 dilution of 5 g in 20 ml.

Spermine: $0.796 \times 6 = 4.78$ nmol of Spermine/ml liquefied diet from a 1 in 3.5 dilution of 5 g in 20 ml.

Step 3

Correction for dilution of 1 in 3.5 to reflect amount of polyamine per 1 ml of liquefied diet of 5 g in 20 ml of distilled water are as follows:

Putrescine: $3.98 \times 3.5 = 13.93$ nmol of Putrescine/ml liquefied diet of 5 g in 20 ml.

Spermidine: $4.07 \times 3.5 = 14.25$ nmol of Spermidine/ml liquefied diet of 5 g in 20 ml.

Spermine: $4.78 \times 3.5 = 16.73$ nmol of Spermine/ml liquefied diet of 5 g in 20 ml.

Step 4

Correction for liquefaction in 20 ml of distilled water to reflect amount of polyamine per 5 g of diet are as follows:

Putrescine: $13.93 \times 20 = 278.6$ nmol of Putrescine/5 g of diet.

Spermidine: $14.25 \times 20 = 285.0$ nmol of Spermidine/5 g of diet.

Spermine: $16.73 \times 20 = 334.6$ nmol of Spermine/5 g of diet.

Overall calculation incorporating all correction factors

Total amount of each polyamine per total weight of solid diet used for liquefaction are as follows:

Putrescine: $(0.45/0.678) \times (6 \times (3.5/1) \times 20) = 278.76$ nmol of Putrescine/5 g of diet.

Spermidine: $[0.6/0.8842] \times [6 \times (3.5/1) \times 20] = 285.00$ nmol of Spermidine/5 g of diet.

Spermine: $[0.78/0.9795] \times [6 \times (3.5/1) \times 20] = 334.46$ nmol of Spermine/5 g of diet.

The results from both methods of calculation are similar.

3.8.2. Example
(for Liquid Diet not
Requiring Liquefaction)

A 1 in 2 dilution of a food drink is used for PCA extraction as per the protocol in Subheading 3. Area ratios obtained from HPLC chromatograms are 0.45, 0.6, and 0.78 for putrescine, spermidine, and spermine, respectively. Calculate the amount of putrescine, spermidine, and spermine contained in 1 ml of the food drink using the standard curves as shown in Fig. 3.

Reminder: Linear regression equations for the polyamines are:

Putrescine: (Area ratio) = 0.678 (Putrescine concentration, nmol/200 μ l of acid soluble extract).

Spermidine: (Area ratio) = 0.8842 (Spermidine concentration, nmol/200 μ l of acid soluble extract).

Spermine: (Area ratio) = 0.9795 (Spermine concentration, nmol/200 μ l of acid soluble extract).

Step 1

From the above formula, the concentration of the polyamines in nmol/200 μ l of acid soluble extract will be given by:

Putrescine: $0.45/0.678 = 0.664$ nmol of Putrescine/200 μ l of acid soluble extract.

Spermidine: $0.6/0.8842 = 0.679$ nmol of Spermidine/200 μ l of acid soluble extract.

Spermine: $0.78/0.9795 = 0.796$ nmol of Spermine/200 μ l of acid soluble extract.

Step 2

Correction for PCA extraction to reflect amount of polyamine per 1 ml of food drink from a 1 in 2 dilution are as follows:

Putrescine: $0.664 \times 6 = 3.98$ nmol of Putrescine/ml food drink from a 1 in 2 dilution
Spermidine: $0.679 \times 6 = 4.07$ nmol of Spermidine/ml food drink from a 1 in 2 dilution
Spermine: $0.796 \times 6 = 4.78$ nmol of Spermine/ml food drink from a 1 in 2 dilution.

Step 3

Correction for dilution of 1 in 2 to reflect amount of polyamine per 1 ml of food drink are as follows:

Putrescine: $3.98 \times 2/1 = 7.96$ nmol of Putrescine/ml of food drink.

Spermidine: $4.07 \times 2/1 = 8.14$ nmol of Spermidine/ml of food drink.

Spermine: $4.78 \times 2/1 = 9.56$ nmol of Spermine/ml of food drink.

Overall calculation incorporating all correction factors

Total content of each polyamine per 1 ml of food drink are as follows:

Putrescine: $[0.45/0.678] \times [6 \times (2/1)] = 7.96$ nmol of Putrescine/ml of food drink.

Spermidine: $[0.6/0.8842] \times [6 \times (2/1)] = 8.14$ nmol of Spermidine/ml of food drink.

Spermine: $[0.78/0.9795] \times [6 \times (2/1)] = 9.56$ nmol of Spermine/ml of food drink.

The results from both methods of calculation are similar.

4. Notes

1. If the supernatant obtained is too small, you may need to use more diluent.
2. Ensure the cap of the Eppendorf tubes are well secured before each vortex mixing to avoid spilling of the contents.
3. Ensure the tip of the Pasteur tubes remains 2–4 cm above the surface of the contents of the plastic tubes.
4. The flow rate of the nitrogen gas should be just enough to cause waves on the surface of the content of the plastic tubes but not to cause bubbling. This ensures gentle drying of the toluene extract to leave the polyamine content at the bottom of the plastic tubes.
5. Ensure all the toluene has evaporated.
6. It is recommended that up to 24 samples including standards are handled at a time.
7. The centrifugation is needed to precipitate any particulate matter, which could otherwise be transferred into the HPLC with the potential to damage the apparatus.
8. A direct substitution of acetonitrile with methanol in the processes described in Subheadings 3.4.1 and 3.4.3 is possible. This will warrant changes to the mobile phase in the HPLC set-up. These changes involve using distilled water as Mobile phase A and methanol as mobile phase B and an elution gradient developed as follows: 0–2 min 72% B, 2–16 min 72–90% of B, 16–20 min 90% B, and 20.01–25 min 72% B. Fluorescence detection is achieved by excitation at 320 nm and emission at 523 nm as before. The retention times for putrescine, 1, 7-diaminoheptane (internal standard), spermidine, and spermine are altered to 7.3, 10.7, 13.9, and 18.6 min, respectively.

Acknowledgment

We thank Gary Cameron (IMS core facilities) for invaluable support with HPLC analysis.

References

1. Eliassen KA, Reistad R, Risøen U, Rønning HF (2002) Dietary polyamines. *Food Chem* 78:273–280
2. Kalac P, Krausová P (2005) A review of dietary polyamines: formation, implications for growth and health and occurrence in foods. *Food Chem* 90:219–230
3. Bardócz S, Grant G, Brown DS, Ralph A, Pusztai A (1993) Polyamines in food – implications for growth and health. *J Nutr Biochem* 4:66–71
4. Milovic V (2001) Polyamines in the gut lumen: bioavailability and biodistribution. *Eur J Gastroenterol Hepatol* 13:1021–1025
5. Okamoto A, Sugi E, Koizumi Y, Yanagida F, Udaka S (1997) Polyamine content of ordinary foodstuffs and various fermented foods. *Biosci Biotechnol Biochem* 61:1582–1584
6. Bardocz S, Duguid TJ, Brown DS et al (1995) The importance of dietary polyamines in cell regeneration and growth. *Br J Nutr* 73:819–828
7. Sawada Y, Pereira SP, Murphy GM, Dowling RH (1994) Origins of intestinal luminal polyamines in man. *Gut* 35:S20
8. Bardocz S, Grant G, Brown DS, Ewen SW, Nevison I, Pusztai A (1990) Polyamine metabolism and uptake during *Phaseolus vulgaris* lectin, PHA-induced growth of rat small intestine. *Digestion* 46:360–366
9. Bardocz S, Brown DS, Grant G, Pusztai A (1990) Luminal and basolateral polyamine uptake by rat small intestine stimulated to grow by *Phaseolus vulgaris* lectin phytohaemagglutinin in vivo. *Biochim Biophys Acta* 1034:46–52
10. Holtta E (1977) Oxidation of spermidine and spermine in rat liver: purification and properties of polyamine oxidase. *Biochemistry* 16:91–100
11. Seiler N, Bolkenius FN, Knodgen B, Mamont P (1980) Polyamine oxidase in rat tissues. *Biochim Biophys Acta* 615:480–488
12. Milovic V, Odera G, Murphy GM, Dowling RH (1997) Jejunal putrescine absorption and the ‘pharmacokinetics’/biotransformation of ingested putrescine in humans. *Gut* 41:A62
13. Teti D, Visalli M, McNair H (2002) Analysis of polyamines as markers of (patho) physiological conditions. *J Chromatogr* 781:107–149
14. Seiler N (1977) Assay procedures for polyamines in urine, serum, and cerebrospinal fluid. *Clin Chem* 23:1519–1526
15. Marton LJ, Russell DH, Levy CC (1973) Measurement of putrescine, spermidine, and spermine in physiological fluids by use of an amino acid analyzer. *Clin Chem* 19:923–926
16. Russell DH, Russell SD (1975) Relative usefulness of measuring polyamines in serum, plasma, and urine as biochemical markers of cancer. *Clin Chem* 21:860–863
17. Kanda S, Takahashi M, Nagase S (1989) Fluorometric assay for polyamines in urine and tissues using electrophoresis on titan iii cellulose acetate. *Anal Biochem* 180:307–310
18. Samejima K, Kawase M, Sakamoto S, Okada M, Endo Y (1976) A sensitive fluorometric method for the determination of aliphatic diamines and polyamines in biological materials by high-speed liquid chromatography. *Anal Biochem* 76:392–406
19. Seiler N, Knödgen B (1980) High-performance liquid chromatographic procedure for the simultaneous determination of the natural polyamines and their monoacetyl derivatives. *J Chromatogr* 221:227–235
20. Wang W, Kucuk O, Franke AA, Liu LQ, Custer LJ, Higuchi CM (1996) Reproducibility of erythrocyte polyamine measurements and correlation with plasma micronutrients in an antioxidant vitamin intervention study. *J Cell Biochem* 62:19–26
21. Kotzabasis K, Christakishampsas MD, Roubelakisangelakis KA (1993) A narrow-bore HPLC method for the identification and quantitation of free, conjugated, and bound polyamines. *Anal Biochem* 214:484–489
22. Seiler N (1983) Liquid chromatographic methods for assaying polyamines using pre-chromatographic derivatization. *Methods Enzymol* 94:10–25
23. Kalac P, Krížek M, Pelikánová T, Langová M, Veskrna O (2005) Contents of polyamines in selected foods. *Food Chem* 90:561–564

Part VII

Polyamines and Disease

Determination of N^1,N^{12} -Diacetylspermine in Urine: A Novel Tumor Marker

Masao Kawakita, Kyoko Hiramatsu, Mari Yanagiya,
Yosuke Doi, and Mieko Kosaka

Abstract

N^1,N^{12} -diacetylspermine (DiAcSpm) is a minor component of human urine that constitutes less than 0.5% of total polyamine species in human urine. Structurally related polyamines and acetylpolyamines were separated and analyzed by HPLC and gas chromatography, and refinement of these procedures led to the identification of this minor component. Subsequent analyses of urines from cancer patients as well as healthy persons revealed that DiAcSpm is a promising candidate for a novel tumor marker. It is much more sensitive than established tumor markers in detecting colorectal and other cancers, and most importantly, is able to detect 60% of early colorectal cancers confined to mucous membranes. Serum CEA is able to detect only about 10% of colorectal cancers at this stage. Collection of urine is easy and does not give any pain to patients, which adds another merit to urinary DiAcSpm as a tumor marker. DiAcSpm-specific antibodies were then developed for simpler determination of DiAcSpm in urine, and the antibodies were used to construct an ELISA system. More recently, a reagent kit for DiAcSpm determination based on colloidal gold aggregation that can be used with automatic biochemical analyzers was also developed.

Key words: Diacetylspermine, Tumor marker, Urine, Cancer diagnosis, Immunoassay, Early cancer detection, ELISA, Automated determination

1. Introduction

There is sound reason for expecting polyamine excretion in urine to increase as a consequence of uncontrolled proliferation of cancer cells, since cell growth and polyamine metabolism are closely related. However, polyamines were not regarded as practical tumor markers (1) until DiAcSpm was identified in human urine (2) and its amount in urines from cancer patients as well as healthy persons was precisely determined (3,4). Assessment via DiAcSpm measurement was characterized by low incidence of

false negative cases and frequent and marked elevation in the urine of cancer patients. It was clearly distinct from total urinary polyamines and individual monoacetylpolyamines whose performance was too poor for a practical tumor marker due to the occurrence of too many false negative as well as false positive cases. This prompted us to develop simpler and more convenient procedures for DiAcSpm determination to replace HPLC analysis whose throughput is too low for routine clinical applications. We developed a procedure to raise and then purify highly specific anti-DiAcSpm polyclonal antibody (5), and the procedure was later used by a commercial company to produce a monoclonal antibody appropriate for the determination of DiAcSpm in urine. Using the purified polyclonal antibody, and later the monoclonal antibody, an ELISA procedure for determination of DiAcSpm was developed. This is sufficient for usual research purposes, but a simpler and automated procedure for determination was needed for wider use in clinical examination. For this purpose, a reagent kit for DiAcSpm analysis compatible with automatic clinical analyzers was recently developed.

Development of ELISA procedure enabled us to carry out extensive clinical studies, and subsequent examination revealed that DiAcSpm was elevated above the cut-off value, which represents mean + 2 SD for healthy persons, in approximately 60% of colorectal cancer patients at earlier clinical stages (stage 0 and stage I) at which cancer lesions were confined within the mucosal layer (Fig. 1) (6). Urinary DiAcSpm was also more effective than CEA and CA15-3 in detecting breast cancers at earlier clinical stages (6). Increased excretion of DiAcSpm in urine from cancer

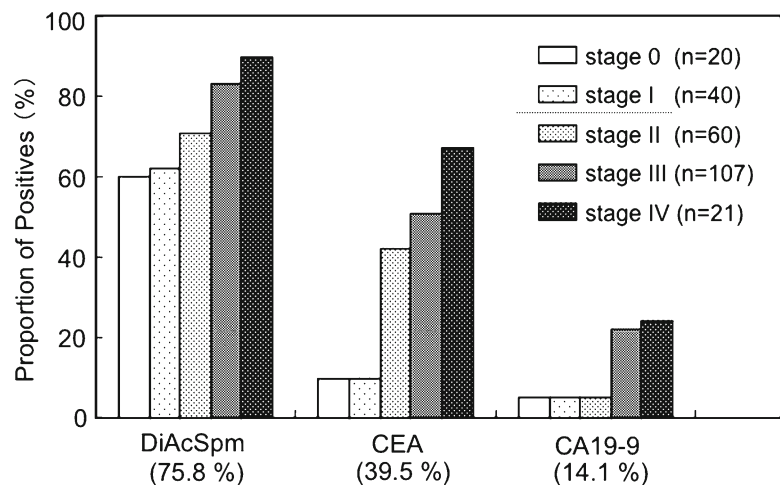


Fig. 1. Sensitivity of urinary DiAcSpm, serum CEA, and serum CA19-9 for colon cancers at various tumor stages. Colon cancer patients were grouped according to tumor stages. The proportion of patients showing marker values above cut-off values with respect to respective markers is represented by bars. Numbers in parentheses represent the overall sensitivity of respective markers.

patients is likely related to rapid growth of cancer tissues in patients. Whether DiAcSpm serves as a tumor marker applicable to a wide variety of cancers is worth examining in future studies.

2. Materials

2.1. Urine Sample Collection

1. Sodium azide solution (10%, w/v) to be added as a preservative is dissolved in water at 100 mg/ml.

2.2. Peptide-Acetylspermine Conjugate as a DiAcSpm-Mimic Used in ELISA Assay

1. A cysteine-containing synthetic peptide with amino acid sequence $\text{NH}_2\text{-CEFLASVIKDTTSDSPAGIDN-COOH}$ (see Note 1) may be obtained from an appropriate company through custom peptide synthesis.
2. *N*-(8-maleimidocapryloxy)succinimide (Dojindo Lab., Kumamoto) to work as a cross-linking bridge between peptide and AcSpm in an amount necessary for the particular experiment (a typical example of preparation of this conjugate is described in Subheading 3.2) is dissolved in tetrahydrofuran at a concentration of 10 mg/ml immediately before use.
3. Tris-HCl buffer (pH 8.0) stock solution: tris(hydroxymethyl)aminomethane (60.0 g) is dissolved in Milli-Q water, pH adjusted to 8.0 by addition of conc. HCl, and the total volume is made to 500 ml with Milli-Q water to give 1 M solution. The solution is autoclaved and stored at room temperature.
4. Tris-buffered urea solution: urea (30 g) is dissolved in Milli-Q water, mixed with 10 ml of 1 M Tris-HCl buffer (pH 8.0), and the total volume is brought to 500 ml with Milli-Q water to give 20 mM Tris-HCl buffer (pH 8.0)-3 M urea solution. The solution is stored refrigerated.
5. Bio-Gel P10 (Bio-Rad, Hercules, CA) is swollen in the Tris-buffered urea solution and packed in a column of 12×700 mm.

2.3. Determination of DiAcSpm by ELISA

1. 20 \times TBS solution: Tris(hydroxymethyl)aminomethane (96.8 g) and NaCl (320 g) are dissolved in Milli-Q water, pH adjusted to 7.6 by addition of about 60 ml of conc. HCl, and the total volume is made to 2,000 ml with Milli-Q water. The solution is autoclaved and stored at room temperature.
2. Washing solution: 20 \times TBS solution (100 ml) and 1/10 dilution of Tween 20 (10 ml) are mixed, and total volume is brought to 2,000 ml with Milli-Q water.
3. Blocking solution: skimmed milk (50 g), 20 \times TBS solution (50 ml), and 1/10 dilution of Tween 20 (5 ml) are mixed, and total volume is brought to 1,000 ml with Milli-Q water.

The solution is dispensed in 50-ml aliquots and stored frozen at -20°C .

4. DiAcSpm stock solution: 1 mM aqueous solution may be stably stored frozen at -20°C . This is diluted appropriately before use (see Note 2).
5. A monoclonal anti-DiAcSpm antibody to be used as primary antibody is a product of TransGenic, Inc. (Kumamoto), but the company is not distributing the antibody as such commercially. Therefore, unfortunately, one has to negotiate with the company to have the antibody available even for research purposes (see Note 3).
6. Horseradish peroxidase-labeled antimouse IgG (Invitrogen) is used at $5,000\times g$ dilution.
7. Antibody diluting solution: One package of phosphate buffer powder (1/15 mol, pH 7.4; Wako Pure Chemical, Osaka) is dissolved in about 500 ml of Milli-Q water, 5 M NaCl (20 ml) is added and total volume is brought to 667 ml with Milli-Q water. The solution is autoclaved and stored at room temperature.
8. Tetramethylbenzidine solution: 3,3',5,5'-tetramethylbenzidine (40 mg) is dissolved in 50 ml of dimethylformamide.
9. 0.2 M Citrate buffer (pH 5.0): citric acid (7.36 g) and sodium citrate (19.12 g) are dissolved in Milli-Q water and brought to 500 ml. The solution is stored refrigerated.
10. Peroxidase reaction medium: tetramethylbenzidine solution (50 ml) and 0.2 M citrate buffer (pH 5.0; 250 ml) are mixed and total volume is brought to 500 ml with Milli-Q water. The solution is stored refrigerated.
11. H_2O_2 solution (1%): prepare fresh before use by mixing 40 μl of 35% H_2O_2 with 1.36 ml of Milli-Q water.
12. 1 N H_2SO_4 for stopping peroxidase reaction and developing yellow color: add 26 ml of conc. H_2SO_4 (36 N) slowly to 910 ml of Milli-Q water.

2.4. Determination of DiAcSpm by Colloidal Gold Aggregation

1. A reagent kit Auto DiAcSpm (Alfresa Pharma Co., Osaka) for DiAcSpm determination is commercially available and may be used in conventional automatic biochemical analyzers. The kit consists of two reagent mixtures, R1 and R2 below. The details of the ingredients of the reagents below are not disclosed.
2. Reagent 1 (R1): buffer solution (pH 6.3) containing BSA-AcSpm conjugate (see below, Subheading 3.4).
3. Reagent 2 (R2): suspension of colloidal gold particles coated with anti-DiAcSpm antibody. R1 and R2 are supplemented with sodium azide at a final concentration of 0.1% as a

preservative. Reagents R1 and R2 are stored at 2–8°C. Do not freeze the reagents.

4. Auto DiAcSpm Standard: this is separately provided by the company as a set of DiAcSpm solutions (pH 4.5) consisting of ten small tubes at different concentrations covering a range of 0–1,000 nM and is used to construct calibration curves. The standard is stored at 2–8°C.

3. Methods

Several methods are found in the literature for the determination of DiAcSpm in urine. In early works, DiAcSpm in urine was identified and determined by gas chromatography and HPLC (2, 7). HPLC analysis involving prior dansylation of polyamines including DiAcSpm has also been described (8). Since these methods are of limited value for routine clinical use for their inconvenience in quickly handling large number of samples, alternative methods using DiAcSpm-specific antibodies were developed. Initially, rabbits were immunized with an antigen with a DiAcSpm-mimicking hapten structure in which *N*-acetylspermine was conjugated to a carrier through an acylamide linkage. An antiserum containing highly specific antibodies against DiAcSpm was thus produced, and anti-DiAcSpm antibody whose cross-reactivity with N^1 -acetylspermine being as low as 0.03% was obtained through several steps of affinity purification (5). A monoclonal anti-DiAcSpm antibody with similar selectivity over N^1 -acetylspermine was later developed using the same strategy. ELISA systems using these and similarly produced antibodies have been developed (5, 9). The ELISA procedure described in (5) was adapted to the monoclonal antibody mentioned above and explained in detail in subsequent sections. More recently, a reagent kit for determination of urinary DiAcSpm was developed, and has now become commercially available. The reagent kit is appropriate for determination of DiAcSpm using an automatic clinical analyzer, and a typical procedure using this reagent kit is also described below. A procedure for determination of DiAcSpm by mass-spectrometry was also described (10).

3.1. Collection and Storage of Urine Samples and Preparation for DiAcSpm Determination

1. Arbitrarily excreted urine (5–10 ml or more) is collected, 2 μ l/ml of 10% sodium azide solution is added, and the sample is stored frozen at –20°C until use (see Note 4).
2. Frozen urine samples are thawed, mixed by inverting sample tubes, and then centrifuged at 3,000 rpm for 5 min at room temperature. The supernatant is saved for DiAcSpm determination.

3.2. Preparation of Peptide-Acetylspermine Conjugate

1. Acetylspermine·3HCl 24.8 mg (70 μ mol) is dissolved in H₂O to give a final volume of 1 ml.
2. Acetylspermine solution is mixed with 5 mg of *N*-(8-maleimidocapryloxy)-succinimide (HMCS) dissolved in 0.5 ml of tetrahydrofuran (see Note 5).
3. The reaction between AcSpm and HMCS starts immediately and proceeds rapidly. The reaction mixture is maintained at neutral pH by adding 1 N NaOH in small aliquots (see Note 6) and is kept at room temperature for 100 min.
4. The reaction mixture is condensed to approximately 0.5 ml under reduced pressure using a centrifugal evaporation system.
5. The reaction mixture containing AcSpm-HMCS conjugate is washed 3 times by extraction with 3 ml of diethyl ether-dichloromethane (2:1) mixture.
6. A synthetic peptide NH₂-CEFLASVIKDTTSDSPAGIDN-COOH 20 mg is dissolved in 0.6 ml of 20 mM Tris-HCl buffer (pH 8.0) and immediately mixed with the AcSpm-HMCS conjugate prepared above.
7. The mixture is kept at room temperature with vigorous shaking for 30 min.
8. The above mixture containing peptide-AcSpm conjugate is applied on a Bio-Gel P-10 column equilibrated with 20 mM Tris-HCl (pH 7.9)-3 M urea, eluted with the same solution at a flow rate of 0.3 ml/min and 2.5-ml fractions are collected.
9. UV absorption of the eluate is monitored at 258 nm (see Note 7), and a small peak eluting at around 25 ml is pooled and stored frozen in small aliquots. The peptide-AcSpm conjugate (DiAcSpm-mimic) is used in the ELISA system described below as a solid-phase antigen to compete with DiAcSpm in urine.

3.3. Determination of DiAcSpm by ELISA

1. Add 50 μ l-aliquot of 0.5 μ g/ml peptide-AcSpm conjugate (DiAcSpm-mimic) to each well of 96-well microtiter plate, and leave the plate for 1 h at room temperature.
2. Discard the DiAcSpm-mimic and wash each well once with washing solution.
3. Add 300 μ l-aliquot of blocking solution to each well for first blocking, and leave the plate overnight at 4°C.
4. Discard the blocking solution and wash each well once with washing solution (see Note 8).
5. An example of a blueprint for making a plate designed for a typical experiment is shown in Fig. 2. The procedure for performing an experiment according to this plan is described below.
6. Add 50 μ l of Milli-Q water to each well.
7. To make twofold serial dilutions of standard samples for calibration curves in quadruplicate, add 50 μ l of 4.0 nM

	1	2	3	4	5	6	7	8	9	10	11	12
A	BL		Sample #1	Sample #1	Sample #2	Sample #2	Sample #3	Sample #3	Sample #4	Sample #4	No DiAcSpm	
B	No DiAcSpm		2x	2x	2x	2x	2x	2x	2x	2x		
C	DiAcSpm 2	2	4x	4x	4x	4x	4x	4x	4x	4x	DiAcSpm 2	2
D	1	1	8x	8x	8x	8x	8x	8x	8x	8x	1	1
E	0.5	0.5	Sample #5	Sample #5	Sample #6	Sample #6	Sample #7	Sample #7	Sample #8	Sample #8	0.5	0.5
F	0.25	0.25	2x	2x	2x	2x	2x	2x	2x	2x	0.25	0.25
G	0.125	0.125	4x	4x	4x	4x	4x	4x	4x	4x	0.125	0.125
H	0.063	0.063	8x	8x	8x	8x	8x	8x	8x	8x	0.063	0.063

Fig. 2. A Sample of microtiter plate for determination of DiAcSpm in urine. A procedure for preparing the plate according this plan is described in detail in the text. The well indicated by BL represent a well for reagent blank without anti-DiAcSpm antibody. Wells indicated by [] are those without competing DiAcSpm, representing 100% color development. Wells indicated by [] with numbers inside represent those for DiAcSpm standard, concentration in nM being indicated by the numbers. Wells indicated by [] are those for serially diluted urine samples.

- authentic DiAcSpm solution to wells C1, C2, C11, and C12, the top wells of each serial dilution, and mix well by pipetting.
- Take 50 μ l of the solution in the top well of each serial dilution and mix well with the content of the second well by pipetting. Repeat this until the last well of the serial dilution is reached, and finally, discard 50 μ l of the content of the bottom well.
 - To make twofold serial dilutions of urine samples in duplicate, add 50 μ l of urine samples 80 \times diluted with water (see Note 9) to the top well of each serial dilution (e.g., well A3) according to the plan in Fig. 1, and mix well by pipetting.
 - Take 50 μ l of the sample in the top well of each serial dilution and mix well with the content of the second well by pipetting. Repeat this until the last well of the serial dilution is reached, and finally, discard 50 μ l of the content of the bottom well.
 - This is repeated until all the serial dilutions as planned are finished.
 - Add 50- μ l aliquot of diluted anti-DiAcSpm antibody solution to each well except well "1A," which is reserved for blank absorption measurement. Add 50 μ l of antibody diluting solution to well "1A."
 - Keep the plate for 1 h at room temperature with constant mixing using a microtiter plate shaker (see Note 10).
 - Thoroughly discard the content of wells by shaking out and then patting the plate against absorptive papers, and then wash each well twice with 280 μ l of washing solution.

15. Add 280 μ l-aliquot of blocking solution to each well for the second blocking, and leave the plate for 45 min (see Note 11) at room temperature.
16. Discard blocking solution by shaking out and wash each well once with washing solution.
17. Add 100- μ l aliquot of diluted HRP-labeled antimouse IgG antibody solution to each well, and keep the plate for 2 h at room temperature with constant mixing using a microtiter plate shaker (see Note 12).
18. Thoroughly discard the content of wells by shaking out and then patting the plate against absorptive papers, and then wash each well 3 times with 280 μ l of washing solution.
19. Add H₂O₂ solution (1%) to appropriate volume of peroxidase reaction medium (prewarmed to room temperature (see Note 12)) in a ratio of 60 μ l/12 ml, mix, and then dispense 100 μ l of the mixture to each well under dim light (see Note 13).
20. Incubate the plate at 30°C for 30 min in the dark (see Note 13).
21. Stop peroxidase reaction by adding 100 μ l of 1 N H₂SO₄ to each well under dim light. Yellow color develops on addition of H₂SO₄, which is stable during subsequent measurement (see Note 14).
22. A₄₅₀ is measured with a microplate reader.
23. A₄₅₀ values of standard sample wells are plotted against the concentration of DiAcSpm to serve as a calibration curve.
24. Of A₄₅₀ values of serially diluted urine sample wells, those that fall within the range of 45–70% of the A₄₅₀ value for the control sample without competing DiAcSpm are used to estimate the DiAcSpm concentration in reference to the calibration curve obtained above. Analytical values for urinary DiAcSpm determined by this procedure are closely correlated with those obtained with HPLC analysis as shown in Fig. 3.

3.4. Determination of DiAcSpm by Colloidal Gold Aggregation

1. The assay is based on specific binding between bovine serum albumin (BSA)-AcSpm conjugate (see Note 15) as a DiAcSpm mimic and a stable red-purple solution of Colloidal Gold-Antibody complexes. BSA-AcSpm conjugate induces a color change from red-purple to gray by causing aggregation of colloidal gold particles. When a urinary sample containing DiAcSpm is added to the system, DiAcSpm competitively binds to the Colloidal Gold-Antibody complexes, and suppresses the color change due to its monovalent nature. A protocol suitable for automatic clinical analyzer is described below.
2. A 7 μ l aliquot of DiAcSpm standard or urine sample (see Note 16) is taken into a reaction cuvette, 180 μ l of R1 (see Note 17) is added, and the content is mixed well.

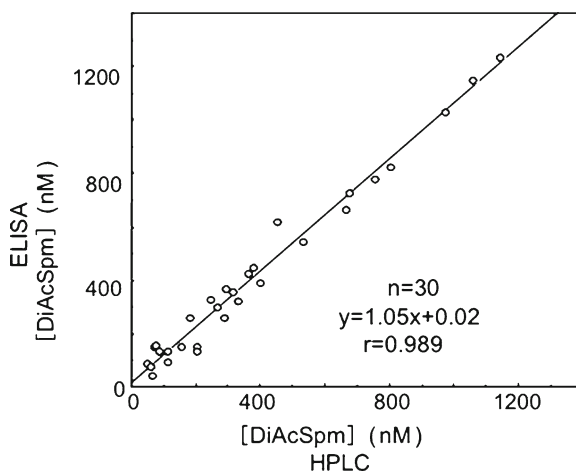


Fig. 3. Comparison between the concentrations of urinary DiAcSpm determined by the ELISA and HPLC procedures. The abscissa indicates DiAcSpm concentration determined by the standard HPLC procedure (2), while the ordinate indicates the corresponding value determined by the ELISA procedure.

3. The cuvette is kept for 5 min at 37°C, then 60 μ l of R2 (see Note 18) is added, and the content is mixed well.
4. Absorbance at 540 nm with 660 nm as a reference wavelength is measured immediately after mixing (Abs 1) and at 5 min after that (Abs 2).
5. The values of (Abs 1–Abs 2) for DiAcSpm standard samples are calculated and used to draw a calibration curve, which is in turn used to estimate DiAcSpm concentrations of urine samples.
6. Using a Hitachi H7070 automatic biochemical analyzer, the coefficients of variation (CV) for within-run and between-run determinations were 1.1–2.5% and 1.1–5.3%, respectively. The assay showed good linearity. Analytical recovery of DiAcSpm was between 94 and 115%. The lower limit of detection was 7.4 nM. The determination of DiAcSpm was not affected by hemoglobin, conjugated bilirubin, free bilirubin, glucose, or ascorbic acid. The slope of the linear regression between the values obtained with this procedure and with ELISA with 505 colorectal cancer patients was 0.92 with correlation coefficient of 0.93.

4. Notes

1. The DiAcSpm mimic is stably adsorbed to microtiter plates and serves as a good solid-phase competing antigen in this assay, but the peptide has not been optimized for this purpose.

Actually, it is a peptide that we had synthesized for other research purpose and happened to be available for us at the time when we were developing this determination procedure.

2. We are using DiAcSpm synthesized and kindly donated by Drs. K. Samejima and A. Shirahata (Josai University), but it is now available from Wako Pure Chemical Industries, Osaka. DiAcSpm at concentrations higher than 100 nM can be stored frozen without appreciable loss, but extensively diluted solutions may not be stable for several days.
3. An ELISA kit for DiAcSpm determination using the monoclonal anti-DiAcSpm antibody is commercially available from TransGenic Inc. (University-based Technology Incubation, Kumamoto). The assay using this kit may be carried out in a way very similar to the one described in Subheading 3.3. Another ELISA kit is available from Yamasa Co. (Chiba). The latter kit is constructed based on the procedure described in ref. (9).
4. DiAcSpm in urine is stable for years under this condition.
5. Tetrahydrofuran is dried over molecular sieve 3A 1/16 prior to use. Drying the solvent for HMCS is very important to have a good yield of peptide-AcSpm conjugate.
6. Acidification proceeds rapidly within 10 min after starting the reaction. Usually about 10 μ l of NaOH is added in a first few minutes and another 10 μ l is added in smaller aliquots during the period that follows.
7. The elution of the peptide can be detected by UV absorption due to phenylalanine.
8. Microtiter plates with bound DiAcSpm-mimic may be stored for a few weeks at 4°C with each well filled with washing solution containing 0.02% sodium azide.
9. This starting dilution is usually appropriate for ordinary urine with creatinine concentration of around 1 g/L and DiAcSpm content of 100–200 nmol/g creatinine. One may start from lower dilutions with dilute urine samples, while extensive dilution (sometimes more than 1,000-fold) may be necessary for accurate determination of urinary DiAcSpm in cancer patients at a terminal stage.
10. Reaction time for competition between DiAcSpm in urine and DiAcSpm-mimic on the plate for binding to anti-DiAcSpm antibody should be controlled precisely for reproducible results.
11. Waiting time for blocking to complete may be flexible but should be longer than 40 min.
12. It is recommended to take appropriate amount of peroxidase reaction medium (12 ml/plate) and bring it to room

temperature during this interval for later use as peroxidase substrate.

13. Blue-colored reaction product resulting from peroxidase reaction with TMB as a substrate is light-sensitive. Erroneous results may be obtained with wells located on the outer rim of the plate if one is not cautious enough of protecting the plate from light.
14. An A_{450} value between 1.3 and 1.5 for a control sample without competing DiAcSpm is appropriate to obtain reliable results. If overreaction is experienced, then shortening the time of peroxidase reaction may be effective in avoiding it.
15. This is prepared according to the procedure described in refs. (5, 11).
16. In case where DiAcSpm concentration is too high and prior dilution is necessary, it should be done by using "Dilution Buffer for Auto DiAcSpm" separately available from Alfresa Pharma.
17. Mix contents of the reagent bottle gently before use.
18. Before daily use, mix the reagent well to achieve a homogeneous suspension of colloidal particles by inverting the bottle more than 20 times.

References

1. Bachrach U (1992) Polyamines as markers of malignancy. *Prog Drug Res* 39:9–33
2. Hiramatsu K, Sugimoto M, Kamei S, Hoshino M, Kinoshita K, Iwasaki K, Kawakita M (1995) Determination of the amounts of polyamines excreted in urine: demonstration of N^1 , N^8 -diacetylspermidine and N^1 , N^{12} -diacetylspermine as components commonly occurring in normal human urine. *J Biochem* 117:107–112
3. Sugimoto M, Hiramatsu K, Kamei S, Kinoshita K, Hoshino M, Iwasaki K, Kawakita M (1995) Significance of urinary N^1 , N^8 -diacetylspermidine and N^1 , N^{12} -diacetylspermine as indicators of neoplastic diseases. *J Cancer Res Clin Oncol* 121:317–319
4. Hiramatsu K, Sugimoto M, Kamei S, Hoshino M, Kinoshita K, Iwasaki K, Kawakita M (1997) Diagnostic and prognostic usefulness of N^1 , N^8 -diacetylspermidine and N^1 , N^{12} -diacetylspermine in urine as novel markers of malignancy. *J Cancer Res Clin Oncol* 123:539–545
5. Hiramatsu K, Miura H, Kamei S, Iwasaki K, Kawakita M (1998) Development of a sensitive and accurate enzyme-linked immunosorbent assay (ELISA) system that can substitute the HPLC analysis for the determination of N^1 , N^{12} -diacetylspermine in human urine. *J Biochem* 124:231–236
6. Hiramatsu K, Takahashi K, Yamaguchi T, Matsumoto H, Miyamoto H, Tanaka S, Tanaka C, Tamamori Y, Imajo M, Kawaguchi M, Toi M, Mori T, Kawakita M (2005) N^1 , N^{12} -Diacetylspermine as a sensitive and specific novel marker for early- and late-stage colorectal and breast cancers. *Clin Cancer Res* 11:2986–2990
7. van den Berg GA, Muskiet F, Kingma AW, van den Silk W, Halie MR (1986) Simultaneous gas-chromatographic determination of free and acetyl-conjugated polyamines in urine. *Clin Chem* 32:1930–1937
8. Vujcic S, Halmekyto M, Diegelman P, Gan G, Kramer DL, Jänne J, Porter CW (2000) Effects of conditional overexpression of spermidine/spermine N^1 -Acetyltransferase on polyamine pool dynamics, cell growth, and sensitivity to polyamine analogs. *J Biol Chem* 275:38319–38328
9. Hamaoki M, Hiramatsu K, Suzuki S, Nagata A, Kawakita M (2002) Two enzyme-linked immunosorbent assay (ELISA) systems for N^1 , N^8 -diacetylspermidine and N^1

- N^{12} -diacetylspermine using monoclonal antibodies. *J Biochem* 132:783–788
10. Kobayashi M, Samejima K, Hiramatsu K, Kawakita M (2002) Mass spectrometric separation and determination of N^1 , N^{12} -diacetylspermine in the urine of cancer patients. *Biol Pharm Bull* 25:372–374
 11. Hiramatsu K, Miura H, Sugimoto K, Kamei S, Iwasaki K, Kawakita M (1997) Preparation of antibodies highly specific to N^1 , N^8 -diacetylspermidine, and development of an enzyme-linked immunosorbent assay (ELISA) system for its sensitive and specific detection. *J Biochem* 121:1134–1138

Spermidine/Spermine-N¹-Acetyltransferase in Kidney Ischemia Reperfusion Injury

Kamyar Zahedi and Manoocher Soleimani

Abstract

Ischemic reperfusion injuries such as acute renal failure, acute liver failure, stroke, and myocardial infarction are prevalent causes of morbidity and mortality. Kidney ischemic reperfusion injury is the leading cause of acute renal failure and dysfunction of transplanted kidneys. Although significant progress has been made in deciphering the factors that contribute to ischemic reperfusion injury, treatment options for these injuries remain scant. Identifying the molecules that contribute to ischemic reperfusion injury and can be therapeutically targeted will lead to development of new approaches for the treatment of such injuries. The expression of spermidine/spermine-N¹-acetyltransferase increases in the kidneys subjected to ischemic reperfusion injury. Furthermore, inactivation of the spermidine/spermine-N¹-acetyltransferase gene reduces the severity of kidney damage after ischemic reperfusion injury. Enhanced expression of spermidine/spermine-N¹-acetyltransferase in cultured cells leads to DNA damage, cell cycle arrest, and disruption of cell matrix interactions. The aforementioned observations strongly suggest that enhanced polyamine back conversion plays an important role in the mediation of tissue damage in renal Ischemic reperfusion injury.

Key words: Ischemic reperfusion injury, Acute renal failure, Spermidine/spermine-N¹-acetyltransferase, Polyamine back conversion

1. Introduction

Tissue damage in ischemic reperfusion injuries (IRI; e.g., acute renal failure (ARF), hepatic shock, stroke, and myocardial infarction) is caused by a temporary cessation of blood flow (ischemia) followed by restoration of blood flow (reperfusion) (1). The ischemia caused by the disruption of blood supply to the affected organ leads to ATP depletion, accumulation of noxious metabolites, and cellular acidosis as a result of switching from aerobic to anaerobic metabolism. Reestablishment of the blood flow and reperfusion causes the production of reactive oxygen intermediates

that contribute to oxidative tissue damage (1, 2). IRI is the major cause of ARF in native kidneys and the foremost cause of delayed graft function and acute rejection in transplanted kidneys (3). ARF is characterized by reduced glomerular filtration rate and retention of nitrogenous waste products, and is among the most prevalent causes of morbidity in hospitalized patients (1). Although a great deal has been learned about the etiology of kidney IRI, its treatment options are primarily limited to supportive interventions.

The expression and activity of spermidine/spermine-N¹-acetyltransferase (SSAT), the rate-limiting enzyme of polyamine back conversion cascade, increases while its ablation reduces the tissue damage in kidneys subjected to IRI (4, 5). Over-expression of SSAT leads to alteration in cell/matrix interactions, induction of DNA damage, and cell cycle arrest (6, 7). These observations suggest that elevated SSAT levels and resultant increase in polyamine back conversion contribute to tissue damage in kidney IRI. The availability of SSAT deficient and site-specific SSAT-ko mice, as well as SSAT over-expressing cells, provides us with powerful model systems to examine the role of polyamine back conversion and the efficacy of its down-regulation in treatment of kidney IRI.

2. Materials

2.1. Surgery

1. Animals. Male C57BL/6 mice (Jackson Laboratories) or appropriate genetically modified male mice on C57BL/6 background are used (see Notes 1 and 2).
2. Balance (Scientech, model SL1000 or equivalent).
3. Ketamine-Xylazine: Mix 1 ml of 100 mg/ml Ketamine 1 ml of 10 mg/ml Xylazine and 8 ml of sterile saline (see Note 3).
4. Betadine.
5. Ethanol.
6. Electric animal clipper.
7. Heating pad (adjustable temperature), temperature adjusted to 36°C.
8. Sterile saline.
9. Sterile surgical equipment and supplies. Individually wrapped sterile latex gloves, fine-tipped surgical scissors, fine-tipped surgical forceps, 60g pressure straight micro clip, micro clip applying forceps, and 7-0 Prolene suture.

2.2. Harvesting of Samples and Assessment of Renal Function

1. Sodium pentobarbital. Dissolve 1 g of sodium pentobarbital in 40 ml of sterile deionized H₂O.
2. Dissection instruments. Dissection tray, scissors, forceps.

3. Liquid nitrogen.
4. Phosphate buffer: Dissolve 21.6 g Na₂HPO₄, 2.7 g NaH₂PO₄ in 500 ml of H₂O adjust pH to 7.4 with HCl then add H₂O to 1,000 ml.
5. Paraformaldehyde: Add 40 g of paraformaldehyde to 500 ml of 0.1 M phosphate buffer pH 7.4 on a heated stir plate. Heat the solution to 65°C to dissolve the paraformaldehyde, add 10 drops of 10 N NaOH and let the solution cool to 40°C. Adjust the volume to 1,000 ml with phosphate buffer pH 7.4.
6. 70% Ethanol.
7. Microcentrifuge.
8. Serum creatinine assay. Commercial kit for serum creatinine assay was purchased from Cayman Chemical Company (Ann Arbor, MI).

2.3. Hematoxylin and Eosin Staining

1. Microscope slides.
2. Glass staining jars or canisters.
3. Xylene.
4. Ethanol (100%; 95 and 70% dilutions of ethanol are in deionized H₂O).
5. 1% aqueous Eosin-Y stock solution: 1 g Eosin-Y in 100 ml of deionized H₂O.
6. 1% aqueous Phloxine B stock solution: 1 g in 100 ml of deionized H₂O.
7. Eosin working solution: 100 ml stock Eosin, 10 ml stock Phloxine B, 780 ml 95% Ethanol, and 4 ml glacial Acetic Acid. Filter this solution before each use to remove oxidized particles.
8. Harris Hematoxylin (Fisher Scientific, Pittsburgh, PA, Cat# BP2699).
9. 1.36% lithium carbonate: 4.7 g lithium carbonate in 350 ml of deionized H₂O.
10. 0.25% Acid alcohol (2.5 ml 95% Ethanol, 988.5 ml of deionized H₂O and 9 ml of HCl).

2.4. RNA Isolation, Size Fractionation, and Northern Blot Analysis

1. TRI Reagent RNA/DNA/Protein Isolation Reagent (Molecular research Center, Inc. Cincinnati, OH).
2. 1-Bromo-3-chloropropane (BCP).
3. Formazol.
4. 2× RNA Master Mix: 60 μl 10× RNA gel buffer (see below), 100 μl formaldehyde, 120 μl H₂O, and 20 μl of 1 mg/ml solution ethidium bromide.

5. 6× Loading buffer: 0.25% bromophenol blue, 0.25% Xylene cyanol, and 30% glycerol in H₂O.
6. Formaldehyde (37%).
7. 10× RNA gel buffer: 200 mM MOPS, 50 mM sodium acetate (CH₃CO₂Na₃·3H₂O), and 10 mM EDTA (20 ml of 0.5 M EDTA solution) dissolve in 500 ml of H₂O, adjust the pH to 7.0 with 10 N NaOH, add H₂O to 1,000 ml, and filter.
8. Seakem LE agarose (Lonza, Rockland, ME).
9. 20× SSPE: Dissolve 175.3 g of NaCl, 27.6 g of NaH₂PO₄, and 9.4 g of EDTA in 800 ml of H₂O. Adjust the pH of the solution to 7.4 with 10 N NaOH and add H₂O to 1,000 ml (final concentrations of components are 150 mM NaCl, 10 mM NaH₂PO₄, and 1 mM EDTA).
10. Sodium phosphate buffer (0.5 M PiB): Dissolve 134 g of Na₂HPO₄ in 800 ml of H₂O, adjust the pH to 7.2 with H₃PO₄, and add H₂O to 1,000 ml.
11. Nytran-N membrane (Whatman, Sanford, ME).
12. 3MM paper (Whatman, Sanford, ME).
13. UV crosslinker (Stratalinker, Stratagene).
14. Prehybridization buffer: 0.1× SSPE and 1% SDS.
15. Hybridization Buffer: 1% crystalline bovine serum albumin (BSA), 7% sodium dodecyl sulfate (SDS), 0.25 M PiB, and 1 mM EDTA.
16. cDNA for Spermidine/spermine-N¹-acetyltransferase, spermine oxidase, and ornithine decarboxylase: All cDNAs were generated by RT-PCR using RNA isolated from kidneys of mice subjected to renal IRI and Super Script First Strand Synthesis Kit for RT-PCR (Invitrogen, Carlsbad, CA). The amplified cDNAs were gel purified on 1.5% Ultra Pure LMP low melting point agarose (Invitrogen, Carlsbad, CA) TAE (0.04 M Tris-acetate, 0.001 M EDTA) gel.
17. Generation of (³²P)-dCTP labeled probes. High Prime (Roch, Indianapolis, IN) or any Klenow polymerase-based kit can be used for generation of radiolabeled DNA probes.
18. Quick Nucleotide Removal Kit (Qiagen, Valencia, CA).
19. Hybridization oven.
20. Wash Buffer A. 0.5% BSA, 0.5% SDS, 20 mM PiB, and 1 mM EDTA.
21. Wash Buffer B: 0.1% SDS, 20 mM PiB, 1 mM EDTA.
22. Storage Phosphor Screen cassette and Phosphor Imager (GE Life Sciences, Piscataway, NJ).
23. Stripping buffer: 1% SDS and 0.1× SSPE.

2.5. Preparation, Size Fractionation by Polyacrylamide Gel Electrophoresis (PAGE), and Western Blot Analysis of Kidney Extracts

1. Isolation solution: 250 mM sucrose and 10 mM triethanolamine, pH 7.6 containing protease inhibitors phenazine methyl sulfonyl fluoride, 0.1 mg/ml; leupeptine 1 µg/ml.
2. Tissue homogenizer.
3. Refrigerated centrifuge.
4. BCA protein assay (Thermo Scientific, Rockford, IL).
5. X Cell II PAGE/Transfer apparatus (Invitrogen, Carlsbad, CA).
6. 2×: Laemmli Sample Buffer: 62.5 mM Tris-HCl, pH 6.8, 25% glycerol, 2% SDS, and 0.01% Bromophenol Blue. Add 50 µl of 2-mercaptoethanol per 950 µl of Laemmli buffer before use.
7. BenchMark prestained protein ladder (Invitrogen, Carlsbad, CA).
8. Running buffer: 25 mM Tris pH 8.6, 192 mM glycine, and 0.1% SDS (dilute 1:10 in H₂O).
9. Precast SDS-12% Tris-Glycine polyacrylamide gels (Invitrogen, Carlsbad, CA).
10. Polyvinylidene difluoride membrane (Invitrogen, Carlsbad, CA).
11. Transfer buffer: 25 mM Tris, 192 mM glycine, 20% methanol, and 0.1% SDS (pH 8.3).
12. Tris buffered saline with Tween-20 (T-TBS): 137 mM NaCl, 20 mM Tris-HCl pH 8.0, and 0.1% Tween-20.
13. Blocking Buffer: 5% nonfat dry milk in T-TBS.
14. Rabbit anti-SSAT antibody (Abcam, Cambridge, MA).
15. Wash Buffer: 2.5% dry milk in T-TBS.
16. Horseradish peroxidase-conjugate donkey antirabbit IgG (Pierce, Rockford, IL).
17. Super Signal West Pico Chemiluminescent Substrate (Thermo Scientific, Rockford, IL).
18. Kodak BioMax XAR film (Fisher Scientific, Pittsburgh, PA).

2.6. Measurement of Polyamine Levels

1. Sterile saline, 0.9%.
2. Perchloric acid (1.2 N).
3. Tissue homogenizer.
4. Microcentrifuge.
5. 2.5 µM 1,7-diaminoheptane in 2 M Na₂CO₃.
6. Dansyl Chloride (Thin Layer chromatography Grade).
7. HPLC grade acetone.

8. Vortex mixer.
9. Heating Block set to 70°C.
10. 100 mg Bakerbond™ spe light load Octadecyl (C₁₈) disposable extraction column (Krackeler Scientific Inc., Albany, NY).
11. Vacuum filtration apparatus (Krackeler Scientific Inc., Albany, NY).
12. Methanol (HPLC grade).
13. ddH₂O (HPLC grade).
14. HPLCsystem(column: Econosphere(C₁₈)5μ4.6 mm × 250 mm HPLC Column (Grace, Deerfield, IL); Waters 616 LC solvent gradient system (Waters Assoc., Milford, MA); Waters Model 2475 fluorescence detector (Waters, Milford, MA); Waters WISP 710B autosampler; and Millennium 32 version 3.2 data collection system and software (Waters, Milford, MA)).
15. Solvent A: 70% 10 mM ammonium acetate – pH 4.4, 30% acetonitrile.
16. Solvent B: 100% acetonitrile.

3. Methods

3.1. Animal Surgery and Harvesting of Specimens

3.1.1. Animal Surgery

1. Anesthetize the animals (25–30 g male C57BL/6 mice) by intraperitoneal injection of 100/10 μg/g body weight ketamine/xylazine (10 μl/g body weight of Ketamine/Xylazine solution) (see Note 3).
2. Once animals are unconscious, shave the abdomen, and swab the abdominal region with Betadine and then ethanol.
3. Place the animals on the surgical drape-covered heating pad (36°C), position the animal abdomen side up, and tape the front and hind paws to the surgical surface (see Note 4).
4. Using fine-tipped surgical scissors make a medial incision from approximately 7-mm above the genital area to 5 mm below the sternum.
5. Move the digestive organs out of the abdominal cavity and wrap in sterile saline-saturated gauze. (Keep the gauze saturated with sterile saline throughout the surgery.)
6. Locate and clamp both renal pedicles with nontraumatic microvascular clamps for 30 min or preferred time based on the desired level of renal injury. Completeness of ischemia can be verified by darkening of the kidneys. Reestablish the blood flow to the kidneys by removal of the clamps (reperfusion) with visual verification of blood return. Animals subjected to sham operation (identical surgical protocol except the renal

pedicles are not clamped) are used as controls. During the procedure, animals should be kept well hydrated and their body temperature needs to be maintained at around 36°C.

7. After removal of the clamps (time point 0), place the digestive organs in the abdominal cavity and close the incision in two layers using 7-0 Prolene Suture (Ethicon, Endo-Surgery Inc. Cincinnati, OH). After closure of the abdominal cavity, each animal should be given 400 µl of saline intraperitoneally. Animals should be kept on a 36°C heat pad during recovery from anesthesia.

3.1.2. Harvesting of Specimens

1. Sacrifice the animal by administering an intraperitoneal injection of sodium pentobarbital (75 µg/g body weight).
2. Bleed the animal by direct cardiac puncture.
3. Harvest the kidneys by affixing the animal to the dissection tray, reopening the incision site, and dissecting the kidney from its surrounding tissue and the renal pedicle. Kidneys are cut in half across the middle (sagittal). Snap freeze one half of the kidney in liquid nitrogen and store at -80°C. Fix the second half of the kidney in 4% paraformaldehyde for 24 h and then transfer to 70% ethanol for paraffin embedding.

3.2. Serum Creatinine Assay

To confirm the efficacy of the surgical protocol in inducing acute renal injury, kidney function needs to be assessed by measuring the serum creatinine levels. Serum creatinine can be determined using the Cayman Chemical Company Creatinine Assay Kit or other assay systems that rely on Jaffe Reaction. To measure the serum creatinine levels:

1. Prepare 1:10 and 1:20 dilution of each serum sample in HPLC-grade water.
2. Prepare the Alkaline Picrate solution by mixing 2 ml of sodium borate, 6 ml of surfactant, 10 ml of color reagent, and 3.6 ml of NaOH solutions provided in the kit.
3. Add 15 µl of creatinine standards or serum sample per well in a 96-well plate.
4. Initiate the reaction by adding 150 µl of Alkaline Picrate solution per well. Cover the plate and incubate on a shaker for 10 min at 25°C.
5. Determine the initial absorbance (Iabs) at 490–500 nm.
6. Add 5 µl of acid solution to each well, cover and incubate on a shaker for 20 min at 25°C.
7. Determine the final absorbance (Fabs) at 490–500 nm.
8. Calculate the adjusted absorbance by subtracting the Fabs from Iabs and further subtracting the adjusted absorbance of

the blank samples from the adjusted absorbance of all other samples (final adjusted absorbance). Obtain a standard curve by plotting the final adjusted absorbance of the standards as a function of their final creatinine concentration. Calculate the creatinine content of the samples by substituting the final adjusted absorbance value of each sample for that of the standard in the equation obtained from linear regression of the standard curve.

3.3. Microscopic Evaluation of Tissue Damage in Kidney IRI

To visually confirm the onset of kidney injury, histology of hematoxylin and eosin (H&E) stained, injured and control kidneys need to be examined (see Note 5).

3.3.1. H&E Staining of Kidney Sections

1. Cut 5 μm sections paraffin embedded kidney and mount onto Superfrost/Plus microscope slides.
2. Deparaffinize the sections in three changes of Xylene (5-min each).
3. Rehydrate in 100% ethanol (2×3 min), 95% ethanol (2×3 min), and 70% ethanol (3 min).
4. Rinse the slides in distilled water (5 min).
5. Stain in hematoxylin (6 min).
6. Rinse in running tap water (20 min).
7. Decolorize in acid alcohol (1–3 s).
8. Rinse in tap water (5 min).
9. Immerse in lithium carbonate (3 s).
10. Rinse in tap water (5 min).
11. Counterstain in Eosin working solution (15 s).
12. Dehydrate in 95% ethanol (2×3 min) and 100% ethanol (2×3 min).
13. Clear slides in two changes of Xylene (5 min/change).
14. Place 100 μl of Cytoseal over the stained tissue and place a cover slip over the tissue, be careful not to trap any air bubbles under the cover slip (perform this step in the fume hood).
15. Assess the onset of kidney injury by examining the H&E-stained kidney sections for tubular dilatation, cast formation, edema, presence of necrotic and apoptotic cells, and tubular inflammation.

3.4. RNA Isolation, Size Fractionation, and Northern Blot Analysis

3.4.1. RNA Isolation

1. Homogenize kidneys in 1 ml/g of tissue of TRI Reagent for 1 min at maximum setting.
2. Store the homogenates for 5 min at room temperature (25°C).
3. Add 100 ml of BCP/1 ml of TRI Reagent, mix using a vortex mixer, store the resulting mixture at room temperature for 15 min, and centrifuge at $12,000 \times g$ for 15 min at 4°C .

4. Collect the aqueous (top) phase, transfer to a new tube and add 0.5 ml of isopropanol/1 ml of TRI Reagent, store at room temperature for 10 min, and centrifuge at 12,000×*g* for 8 min at room temperature (save the organic phase for DNA or protein extraction).
5. Wash the RNA pellet with 75% ethanol, centrifuge at 12,000×*g* for 5 min at room temperature, discard the supernatant, let the pellet dry for 5 min, and resuspend the RNA pellet in 100 ml of Formazol.
6. Determine the RNA concentration by measuring the A₂₈₀ of 1:10 dilution of each sample.

*3.4.2. RNA Size
Fractionation by Agarose
Gel Electrophoresis*

These instructions are for IBI, 1050 Multi Purpose horizontal gel Apparatus (IBI Scientific, Peosta, IA).

1. Prepare 1.2% agarose/formaldehyde denaturing gel by micro-waving 1.2 g of Sea Kem LE agarose in 74 ml of H₂O for 2 min. Let the agarose solution cool to 60°C then add 10 ml of 10× RNA gel buffer and 16.4 ml of formaldehyde (this recipe is for a 100-ml gel). Place the gel tray in a chemical hood, place the appropriate comb in place, pour the gel, and allow the gel to solidify.
2. Prepare 500 ml of 1× RNA gel buffer by mixing 50 ml of 10× RNA gel buffer with 450 ml of H₂O.
3. Prepare the RNA mixture (10–30 μg of RNA in 15 μl of Formazol and 15 μl of RNA Master Mix), denature at 65°C for 10 min, add 2 μl of loading buffer, and place on ice.
4. Place the solidified agarose gel and the tray in the electrophoresis apparatus, pour in the running buffer to fill the chamber, and cover the gel. Remove the comb and load 32 μl of each RNA sample. Run the gel at 100 V. Stop the electrophoretic separation of RNA when the bromophenol blue dye front is approximately 12 cm into the gel.
5. Examine the integrity of isolated RNA and loading accuracy through visualizing the RNA by UV light trans-illumination and take a picture of the gel.

*3.4.3. Transfer of RNA
to Nytran-N Membrane.
Transfer the Size-
Fractionated RNA to
Nytran-N Membrane
by Capillary Transfer*

1. Set up the transfer apparatus by placing a raised, flat plexiglas support surface in a buffer reservoir (Pyrex baking dish). Add the appropriate amount of 10× SSPE to the buffer reservoir (approximately 0.5 cm lower than the support surface). Place a piece of 3MM paper prewetted with 10× SSPE on the support surface with two ends of the paper immersed in the buffer. Place two additional layers of 3MM paper soaked in 10× SSPE over the first layer (the latter set up should be at least 1 cm larger than the gel in all direction). Smooth out the air

bubbles between the filters using a glass rod. Wash the gel in H₂O for 30 min (3 changes, 10 min each) to remove the formaldehyde. Cut the gel to appropriate dimensions, flip the gel over, and place it on the transfer setup. Be certain to squeeze out the air bubbles between the gel and filter papers. Cut a piece of Nytran-N membrane (the dimensions of this membrane should be equal or about 1 mm larger than the gel on all sides) and prewet in deionized H₂O and then 10× SSPE. Place the membrane on the gel and smooth out the air bubbles between the gel and Nytran-N membrane with a glass rod. Place three layers of 10× SSPE soaked layers of 3MM paper on the Nytran-N membrane and add additional 5–8 cm stack of paper towels on top of the 3MM paper (the aforementioned layers need to be approximately 1 mm smaller than the gel on all sides). Place a glass plate on top of the stack of paper towels and place a 500-g weight atop the glass plate.

2. Allow the transfer of size-fractionated RNA to take place.
3. When the transfer is complete (approximately 12–18 h), remove the paper towels and 3MM paper on top of the Nytran-N membrane, label, and peel off the membrane.
4. Confirm the complete transfer of RNA by examining the gel under UV light.
5. Wash the membrane in 5× SSPE for 5 min, take a picture of the membrane, and crosslink the RNA to the Nytran-N membrane using the Auto Crosslink Function of the Stratagene UV Stratalinker.

3.4.4. Generation of Radiolabeled DNA Probes

Gel-purified cDNAs of interest (isolated from cDNA library or generated by RT-PCR using RNA extracted from kidneys of mice subjected to renal IRI) can be used as templates to generate radiolabeled probes. Generate radiolabeled by random priming of cDNA using High Prime random priming kit (other Klenow polymerase-based protocols may also be used). To generate SSAT and SMO probes:

1. Denature 25 ng of appropriate DNA template in 11 µl of H₂O was by heating in a boiling water bath for 5 min.
2. Transfer the DNA to an ice ethanol bath for 1 min. Add 4 µl of High Prime and 5 µl (50 µCi) of (³²P)-dCTP to the cooled DNA mixture and allow the labeling reaction to proceed for 10 min at 37°C.
3. Stop the reaction by adding 2 µl of 0.2 M EDTA pH 8.0.
4. Remove the unincorporated dNTPs using Quick Nucleotide Removal Kit using the protocol provided by the manufacturer.

3.4.5. Hybridization and Visualization of mRNA Bands

Carry out the hybridization reactions at 65°C in a hybridization oven.

1. Wet the hybridization vessel with 10 ml of prehybridization buffer preheated to 65°C.
2. Preheat the hybridization vessel by adding 10 ml of 65°C prehybridization buffer and placing it in the hybridization oven for 5 min.
3. Place the membrane (RNA side facing away from the vessel wall) in the hybridization vessel containing prehybridization buffer and incubate at 65°C for 1 h.
4. Discard the prehybridization buffer and add 10 ml of preheated (65°C) hybridization buffer and incubate at 65°C for 30 min.
5. Denature the radiolabeled probe by boiling in a water bath for 5 min and then transfer the tube to an ethanol/ice bath for 1 min.
6. Replace the hybridization buffer in the vessel with fresh buffer, add the denatured probe to the side of the hybridization vessel, return the vessel to the hybridization oven, and allow hybridization to proceed for 12–16 h at 65°C.
7. Prewarm wash buffer A and B to 65°C.
8. Discard the hybridization buffer containing the labeled probe.
9. Wash the membrane in 15 ml of wash buffer A for 10 min at 65°C (repeat 3 times).
10. Wash the membrane in 15 ml of wash buffer B for 10 min at 65°C (repeat 4 times).
11. Rinse the membrane in 25°C 10 mM phosphate buffer (do not allow the membrane to dry if it is going to be reprobated).
12. Place the membrane in a sealable bag, smooth out the air bubbles, and seal the bag.
13. Place the membrane in a Phosphor Screen cassette and visualize the signal using a Phosphor Imager.

3.4.6. Stripping and Reprobing the Membrane

If the blot is going to be reprobated for detection of other transcripts, it has to be stripped and the dissociation of labeled probe from the membrane has to be confirmed.

1. Preheat 500 ml of the stripping buffer to 95°C. At the same time, preheat a pyrex dish containing 200 ml of deionized H₂O to 95°C.
2. Discard the deionized H₂O and pour 200 ml of stripping buffer into the preheated pyrex dish and then place the blot in preheated stripping buffer in the pyrex dish for 5 min.
3. Discard the stripping buffer and replace with 200 ml of fresh buffer and carry out the stripping protocol for an additional 10 min.

4. Place the blot in 10 mM phosphate buffer for 5 min at 25°C.
5. Place the membrane in a sealable bag as described in the previous section and repeat the phosphor imaging protocol to confirm the efficiency of the stripping procedure.

3.5. Preparation, Size Fractionation, and Western Blot Analysis of Kidney Extracts

3.5.1. Preparation of Kidney Extracts

1. Homogenize the tissue samples in 4 ml of ice-cold isolation solution with three bursts of 30 s using a Polytron homogenizer.
2. Centrifuge the homogenate at $1,000\times g$ (4,000 rpm using SS-34 Rotor) for 10 min at 4°C. The nuclei and cell debris will be in the pellet.
3. Collect the supernatant and determine the protein content by BCA protein assay (Pierce, Rockford, IL) following the manufacturer's protocol.

3.5.2. Size Fractionation of Kidney Extracts by SDS-PAGE

This protocol is designed for X Cell II PAGE/Transfer apparatus (Invitrogen, Carlsbad, CA).

1. Dilute 50 µg of protein from each extract with Laemmli sample buffer (1:1).
2. Heat the samples and the molecular weight standard (BenchMark Prestained Protein Ladder) for 10 min at 95–100°C.
3. Load the sample onto an SDS-12% polyacrylamide gel and perform the electrophoretic separation of proteins at 110 V until the bromophenol dye front is within 5 mm of the bottom of the gel.

3.5.3. Transfer of Size-Fractionated Kidney Extracts to Polyvinylidene Difluoride Membrane

The directions in this section are for X Cell II PAGE/Transfer apparatus (Invitrogen, Carlsbad, CA).

1. Prewet a sheet of polyvinylidene difluoride membrane that was cut to the size of the gel.
2. Prewet four sheets of 3MM paper and four foam pads in distilled water and then transfer buffer.
3. In a shallow container filled with transfer buffer, assemble the transfer cassette. Place two prewetted foam pads on the transfer tray. Roll out the air bubbles using a glass rod. Place two sheets of prewetted 3MM paper on the foam pads and roll out the air bubbles. Disassemble the gel unit and extract the gel. Place the gel on 3MM paper and roll out the bubbles. Place the prewetted polyvinylidene difluoride membrane on the gel and roll out the bubbles. Place two sheets of prewetted 3MM paper on the polyvinylidene difluoride membrane and roll out the bubbles. Place two prewetted foam pads on the filter papers and roll out the bubbles. Close the transfer tray.

The cassette is now ready to be placed in the transfer apparatus filled with transfer buffer.

4. Place the cassette in the transfer tank such that the nitrocellulose membrane is between the gel and the anode. Transfer takes place by electrophoresis at a constant power of 110 V for 90 min.

3.5.4. Immunodetection of SSAT in Kidney Extracts

Upon completion of the transfer, disassemble the cassette as follows:

1. Remove the top sponge and 3MM paper layers.
2. Remove the gel and mark the top left corner of the membrane (the prestained protein standards should be visible on the membrane).
3. Block the membrane in 50 ml of blocking buffer for 30 min at 25°C on a rocking platform.
4. Discard the buffer and add fresh blocking buffer containing 2 µg/ml of rabbit anti-SSAT antibody. Allow the binding to proceed at 4°C on a rocking platform for 12–18 h.
5. Remove the primary antibody and wash the membrane 5 times for 5-min each with 50 ml of blocking buffer.
6. Prepare a fresh 1:1,000 dilution of horseradish peroxidase conjugated donkey antirabbit antibody in blocking buffer. Incubate the membrane in secondary antibody for 1 h at 25°C on a rocking platform.
7. Discard the secondary antibody and wash the membrane 5 times for 5-min each with wash buffer.
(The remaining steps need to be performed in a dark room.)
8. Mix 5 ml each of solution A and B of the Super Signal West Pico Chemiluminescent Substrate.
9. Incubate the blot in the substrate for 2 min.
10. Place the blot in a plastic sleeve and then place the sleeve in a X-ray cassette.
11. Expose the membrane to X-ray film for 30 s (based on the strength of the signal adjust the exposure time as needed).

3.6. Measurement of Polyamine Levels (see Note 6)

3.6.1. Perchloric Acid Extraction of Tissue Samples

1. Homogenize 100–150 mg of each sample in 1 ml of saline (samples need to be flash frozen and stored at –70°C upon harvest and weighed before homogenization).
2. Mix 400 µl of each homogenate with 400 µl of 1.2 N perchloric acid (PCA) in a 1.5-ml microcentrifuge tube.
3. Centrifuge the samples for 20 min at 12,000 × *g* and transfer the supernatants to new microcentrifuge tubes (save the pellets).

for determination of protein content needed for final normalization of polyamine content to the protein levels).

4. Store the extracts in -70°C until ready for HPLC analysis.

3.6.2. Dansylation of Extracted Supernatants

1. Preheat a heating block to 70°C . Dispense $50\ \mu\text{l}$ of PCA extracted samples or $25\ \mu\text{l}$ of $20\ \mu\text{M}$ polyamine standard into $1.5\ \text{ml}$ microcentrifuge tubes.
2. Add $200\ \mu\text{l}$ of $2\ \text{M}\ \text{Na}_2\text{CO}_3$ containing $2.5\ \mu\text{M}$ 1,7-diaminoheptane to each sample as internal standard.
3. Prepare the dansyl chloride solution by adding $0.8\ \text{ml}$ of $0.1\ \text{g/ml}$ stock solution to $4.5\ \text{ml}$ HPLC grade acetone.
4. Add $200\ \mu\text{l}$ of the dansyl chloride/acetone to each tube and mix for $15\ \text{s}$ using a vortex mixer. Place the tubes in a heating block set at 70°C for $3\ \text{min}$, release pressure by uncapping the tube briefly, and then mix the samples for $15\ \text{s}$ using a vortex mixer (repeat 3 times). Store the dansylation reactions in the dark and let them cool to room temperature.
5. Set up the appropriate number of $100\ \text{mg}$ Bakerbond™ spe light load C_{18} disposable extraction column in a vacuum apparatus. Condition columns with two column volumes of HPLC grade methanol followed by two column volumes of HPLC grade water. Transfer the contents of each tube to a column. Rinse each tube with $300\ \mu\text{l}$ HPLC grade water and add to rinse solution to the appropriate column. Using vacuum, draw sample through the column and discard the eluate. Wash with two column volumes of HPLC grade water and discard the eluate. Insert collection tubes into the vacuum apparatus. Add $1.0\ \text{ml}$ of methanol draw through and collect the eluate for HPLC analysis.

3.6.3. HPLC Analysis of Polyamines

1. Inject a $50\text{-}\mu\text{l}$ aliquot of each dansylated sample onto a $250\times 4.6\ \text{mm}$, $5\ \mu$ particle size Econosphere C18 column with a column temperature of 50°C .
2. Elute by a two solvent gradient with the flow rate of $0.79\ \text{ml}$ per min. Begin the gradient at 100% solvent A and progress linearly to 82% solvent B over $30\ \text{min}$ with an additional 15-min hold at 82% solvent B.
3. Detect the presence of polyamines by assessing the fluorescence of eluted peaks with excitation wavelength of $340\ \text{nm}$ and emission wavelength of $520\ \text{nm}$ (elution times: Putrescine, $20\text{--}22\ \text{min}$; Spermidine, $25\text{--}27\ \text{min}$; Spermine, $28\text{--}30\ \text{min}$).
4. Collect and analyze the results using Waters Millennium 32 chromatography software version 3.2 (Milford, MA).

5. Equilibrate the column with 100% solvent A for 8 min between sample injections. Express the polyamine levels as pmol of polyamine/mg of protein.

4. Notes

1. Male C57BL/6 mice or animals completely bred on C57BL/6 background are used in our studies. The C57BL/6 strain has been chosen because (a) of its susceptibility to renal ischemic reperfusion injury (8); and (b) most knock out strains are bred on to this background.
2. We only use male animals in our studies since they are more susceptible to renal ischemic reperfusion injury than female mice (9).
3. Animals in our studies are anesthetized using ketamine-xylazine rather than volatile anesthetics (e.g., isoflurane) because the latter reduce the severity of kidney damage caused by renal ischemic reperfusion injury (10, 11).
4. The severity of injury is affected by the body temperature. Therefore, during the procedure animals are kept on a 36°C heating pad in order to keep their body temperature stable (12).
5. In addition to H&E stain, tissue sections can be stained for activated caspase 3 and inflammatory infiltrates to assess the onset of apoptotic and inflammatory response respectively.
6. The use of difluoromethylornithine and MDL72527, which inhibit ornithine decarboxylase and polyamine oxidases respectively, as well as available knock out animals can specifically address the role of different polyamine pathway enzymes in the mediation of ischemic reperfusion injuries.

Acknowledgements

The authors would like to thank Dr. Debora L. Kramer, Ms. Paula Diegelman, and Ms. Sharon L. Barone for their help with this manuscript. This work was supported by National Institutes of Health Grant RO1DK62809, Veterans Administration Merrit Review Award, and funds from the Center on Genetics of Transport at the University of Cincinnati.

References

1. Bonventre JV (1993) Mechanisms of ischemic acute renal failure. *Kidney Int* 43:1160–1178
2. Ambrosio G, Zweier JL, Duilio C, Kuppasamy P, Santoro G, Elia PP, Tritto I, Cirillo P, Condorelli M, Chiariello M et al (1993) Evidence that mitochondrial respiration is a source of potentially toxic oxygen free radicals in intact rabbit hearts subjected to ischemia and reflow. *J Biol Chem* 268:18532–18541
3. Thadhani R, Pascual M, Bonventre JV (1996) Acute renal failure. *N Engl J Med* 334:1448–1460
4. Zahedi K, Wang Z, Barone S, Prada AE, Kelly CN, Casero RA, Yokota N, Porter CW, Rabb H, Soleimani M (2003) Expression of SSAT, a novel biomarker of tubular cell damage, increases in kidney ischemia-reperfusion injury. *Am J Physiol Renal Physiol* 284:F1046–F1055
5. Zahedi K, Lentsch AB, Okaya T, Barone S, Sakai N, Witte DP, Arend LJ, Alhonen L, Jell J, Janne J, Porter CW, Soleimani M (2009) Spermidine/spermine-*N*¹-acetyltransferase ablation protects against liver and kidney ischemia reperfusion injury in mice. *Am J Physiol Gastrointest Liver Physiol* 296:G899–G909
6. Zahedi K, Bissler JJ, Wang Z, Josyula A, Lu L, Diegelman P, Kisiel N, Porter CW, Soleimani M (2007) Spermidine/spermine *N*¹-acetyltransferase overexpression in kidney epithelial cells disrupts polyamine homeostasis, leads to DNA damage, and causes G2 arrest. *Am J Physiol Cell Physiol* 292:C1204–C1215
7. Wang Z, Zahedi K, Barone S, Tehrani K, Rabb H, Matlin K, Casero RA, Soleimani M (2004) Overexpression of SSAT in kidney cells recapitulates various phenotypic aspects of kidney ischemia-reperfusion injury. *J Am Soc Nephrol* 15:1844–1852
8. Burne MJ, Haq M, Matsuse H, Mohapatra S, Rabb H (2000) Genetic susceptibility to renal ischemia reperfusion injury revealed in a murine model. *Transplantation* 69:1023–1025
9. Wei Q, Wang MH, Dong Z (2005) Differential gender differences in ischemic and nephrotoxic acute renal failure. *Am J Nephrol* 25:491–499
10. Kim M, Kim N, D'Agati VD, Emala CW Sr, Lee HT (2007) Isoflurane mediates protection from renal ischemia-reperfusion injury via sphingosine kinase and sphingosine-1-phosphate-dependent pathways. *Am J Physiol Renal Physiol* 293:F1827–F1835
11. Lee HT, Kim M, Kim N, Billings FT 4th, D'Agati VD, Emala CW Sr (2007) Isoflurane protects against renal ischemia and reperfusion injury and modulates leukocyte infiltration in mice. *Am J Physiol Renal Physiol* 293:F713–F722
12. Delbridge MS, Shrestha BM, Raftery AT, El Nahas AM, Haylor JL (2007) The effect of body temperature in a rat model of renal ischemia-reperfusion injury. *Transplant Proc* 39:2983–2985

Use of Polyamine Metabolites as Markers for Stroke and Renal Failure

Kazuei Igarashi and Keiko Kashiwagi

Abstract

Acrolein and H_2O_2 are among the metabolic products of spermine and spermidine, and it was found that acrolein was more toxic than H_2O_2 . It was determined whether acrolein can serve as a biochemical marker for stroke (brain infarction) and chronic renal failure. Since acrolein rapidly reacts with lysine residues in protein, protein-conjugated acrolein (PC-Acro) was measured. PC-Acro was increased at the locus of brain infarction and in plasma in a mouse model of stroke involving photochemically induced thrombosis. An increase in PC-Acro in plasma was found to be a good biochemical marker in patients with stroke or with chronic renal failure. Using a receiver operating characteristic curve, the combined measurement of PC-Acro, IL-6 and CRP together with age indicated silent brain infarction (SBI) with 89% sensitivity and 91% specificity. The procedures to measure PC-Acro and polyamine oxidases [spermine oxidase (SMO) and acetylpolyamine oxidase (ACPAD)], and its application as markers in stroke and chronic renal failure are described in this chapter.

Key words: Acrolein, Biochemical marker, Brain infarction, Chronic renal failure, Polyamine metabolite, Polyamine oxidase

1. Introduction

Polyamines exist mostly as polyamine-RNA complexes and affect translation at various steps (1, 2). However, addition of spermidine or spermine to culture medium containing ruminant serum inhibits cellular proliferation (3). This effect is caused by polyamine oxidation products that are generated by serum amine oxidase (4). Ruminant serum amine oxidase produces H_2O_2 and acrolein ($CH_2=CH-CHO$) (Fig. 1a) (5). Similarly, spermine oxidase (SMO) in cells produces H_2O_2 and 3-aminopropanal, which may be converted to acrolein as shown in Fig. 1a. Thus, we compared the toxicity of H_2O_2 and acrolein in a cell-culture system (see

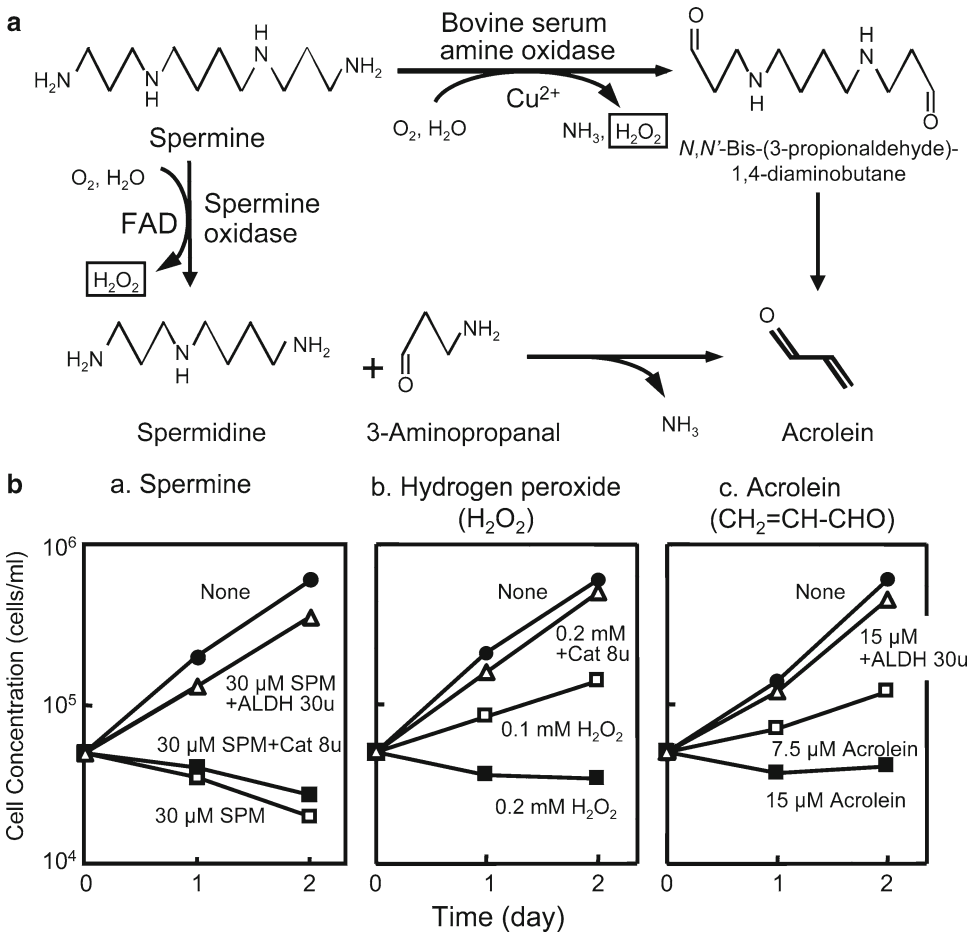


Fig. 1. Acrolein production from spermine by amine oxidase in ruminant serum and by spermine oxidase (SMO) (a), and effect of spermine, hydrogen peroxide, and acrolein on cell growth of FM3A cells (b). Culture of FM3A cells was described in 3.1. (ba) Toxic effect of 30 μM spermine was restored by 30 units of aldehyde dehydrogenase but not by 8 units of catalase. (bb, bc) 0.1–0.2 mM H_2O_2 inhibits cell growth, whereas 7.5–15 μM acrolein inhibits cell growth at the same extent. Figures are taken from Sharmin et al. (6).

Note 1 and Fig. 1b), and found that acrolein is a major toxic compound produced from spermine (6).

Polyamines have been suggested to be one of the uremic “toxins,” which accelerate the progression of uremia (7). However, this idea has not been carefully explored. We determined the level of polyamines, together with polyamine oxidase (PAO) activity and the level of protein-conjugated acrolein (PC-Acro) in plasma of patients with renal failure (Table 1). We found that PC-Acro and PAO in plasma were well correlated with the severity of chronic renal failure (8, 9) (see Note 4). The results suggest that PC-Acro may be increased in plasma of patients having other pathologies that involve cell damage. Stroke is a sudden focal neurological deficit caused by vascular insult, accompanied by cell damage in the central nervous system. At present, there is no

Table 1
Polyamine and PC-Acro contents and SMO in plasma of normal subjects and patients with chronic renal failure^a

Category of subjects ^b	Level (pmol/mL plasma) of polyamine			SMO (nmol/mL of plasma)	Acrolein content (nmol/mL of plasma)	FDP-Lys (nmol/mL of plasma)
	Putrescine	Spermidine	Spermine			
Normal (<i>n</i> = 19)	49.5 ± 31.2	72.9 ± 34.9	30.7 ± 39.5	1.66 ± 0.97	0.53 ± 0.18	31.2 ± 8.80
Moderate (<i>n</i> = 13)	107 ± 86.2*	68.9 ± 53.4	9.22 ± 7.58	3.56 ± 2.10**	1.02 ± 0.98	138 ± 51.1***
Severe (<i>n</i> = 9)	91.0 ± 29.8***	46.1 ± 15.4**	7.55 ± 6.56*	3.96 ± 3.19**	1.42 ± 0.84**	170 ± 85.8***

Moderate, <8 mg of serum creatinine per dL; severe, >8 mg of serum creatinine per dL. Creatinine in plasma was determined by a standard method for blood chemistry, the creatinase-peroxidase (CRTNas-POD) method. Amino acids in plasma were removed by cellulose phosphate column chromatography before polyamine analysis. To 1.8 mL of plasma, 0.2 mL of 50% trichloroacetic acid (TCA) was added and centrifuged for 10 min at 12,000 × *g*. The supernatant thus obtained was neutralized with 6 N KOH, and applied to a cellulose phosphate column (1 mL) previously equilibrated with a buffer containing 0.1 M boric acid-Na₂CO₃ and 0.025 M NaCl (pH 8.0). Amino acids were eluted with 10 mL of the same buffer, and polyamines were then eluted with 3 mL of a buffer containing 0.2 M boric acid-Na₂CO₃ and 0.8 M NaCl (pH 8.0). Polyamine contents were measured by HPLC as described previously (18). Acrolein was determined by HPLC, as described previously (8). Results are means ± SD; **p* < 0.05, ***p* < 0.01 and ****p* < 0.001 vs. normal subjects. Table is taken from Igarashi et al. (9). Data shown in the Table indicate that acrolein is produced from spermine and spermidine and it is higher in the plasma of patients with chronic renal failure (see Note 4).

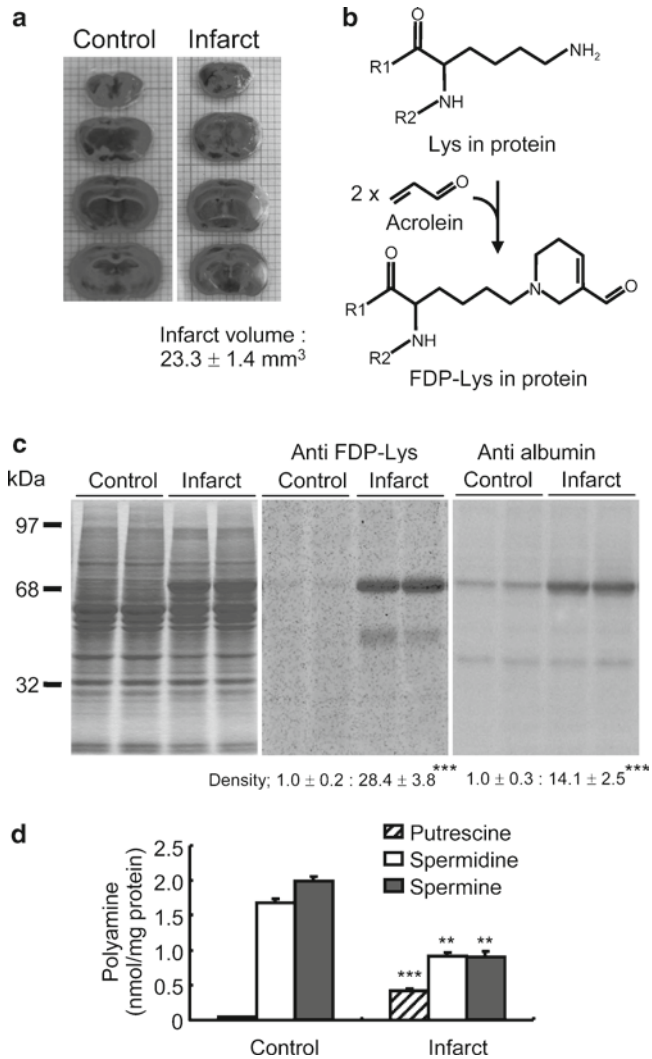


Fig. 2. Correlation between brain infarction and PC-Acro. (a) Infarct volume at 24 h after the induction of infarction. The infarct volume in each mouse was determined from the sum of infarct area in all brain slices. Average infarct volume of 10 mice is shown. (b) Formation of FDP-Lys from acrolein in protein. (c) Total proteins (20 μg) were stained with Coomassie Brilliant Blue R250 after SDS-polyacrylamide gel electrophoresis, and the levels of PC-Acro and albumin were estimated by Western blotting using antibodies against bovine serum albumin conjugated acrolein and mouse albumin. Relative levels of PC-Acro and albumin were estimated by measuring the density of band of 10 mice with a LAS1000 imaging analyzer (Fuji Film). (d) Polyamine content in brain tissues in control and PIT mice. Polyamine content was measured using 10 mice in each group. Data are shown as mean \pm S. E. ** $p < 0.01$; *** $p < 0.001$ compared with control mice. Figures are taken from Saiki et al. (14).

simple biochemical marker for diagnosis of stroke. We found that PC-Acro and PAO are good biomarkers of stroke (10) (see Notes 2 and 3) in both mouse models (Fig. 2) and human patients (Fig. 3). Furthermore, silent brain infarction (SBI) was indicated

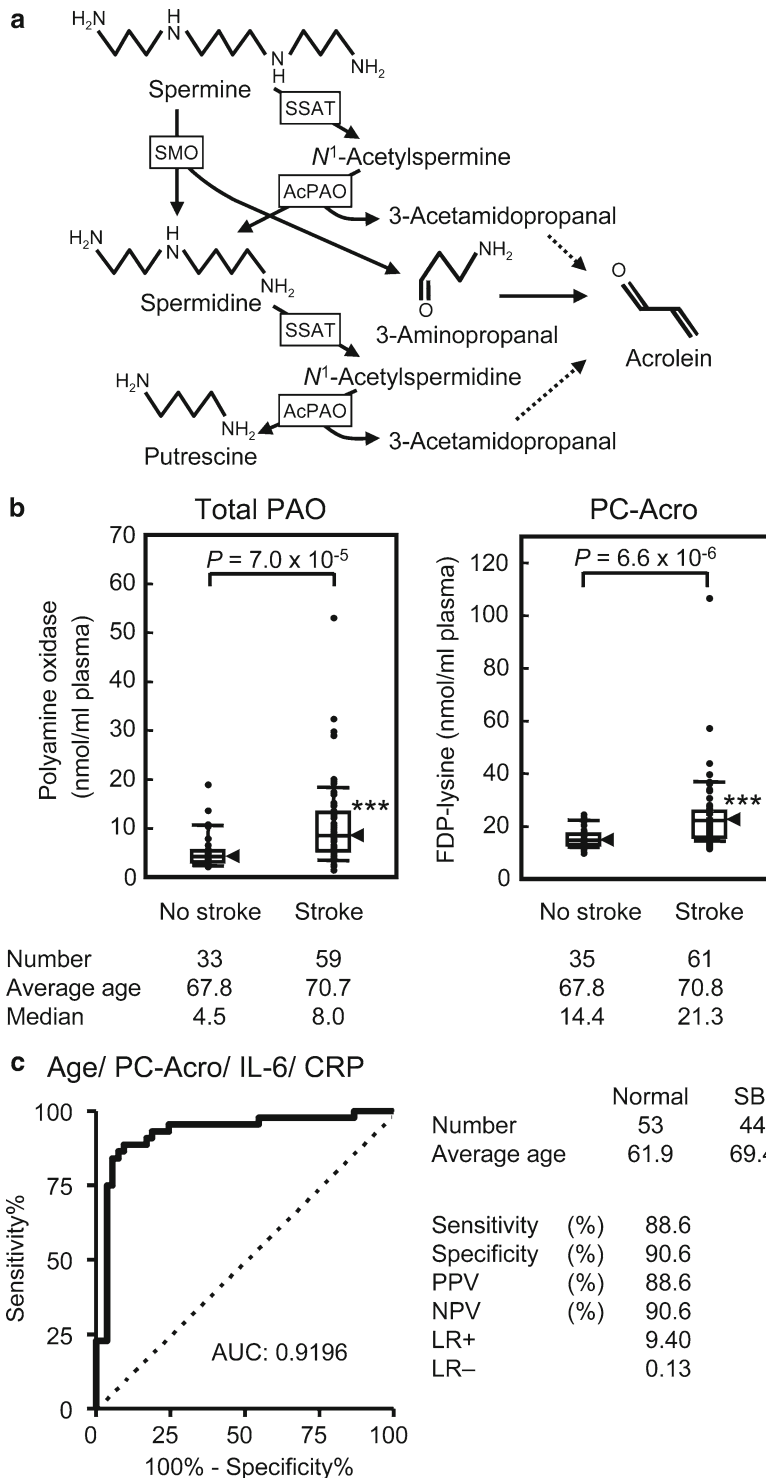


Fig. 3. Acrolein production in mammalian cells (a), correlation between stroke and levels of total PAO and PC-Acro (b) and ROC curve of age/PC-Acro/IL-6/CRP for detection of silent brain infarction (c). (a) Acrolein can be produced either by SMO or by spermidine/spermine *N*-acetyltransferase (SSAT) and acetylpolyamine oxidase (AcPAO). (b) The levels of Total PAO (SMO plus AcPAO) and PC-Acro in plasma were significantly higher in stroke patients than subjects without stroke. *** $p < 0.001$ compared with subjects without stroke. (c) Silent brain infarction can be detected with 89% sensitivity and 91% specificity with ROC curve of age/PC-Acro/IL-6/CRP. Figures are taken from Tomitori et al. (10) and Yoshida et al. (11).

with 89% sensitivity and 91% specificity by measuring PC-Acro, interleukin-6 (IL-6), and C-reactive protein (CRP) together with age (11). In this chapter, the procedures to measure PC-Acro and PAO, and its application as biochemical markers in stroke and chronic renal failure are discussed.

2. Materials

2.1. Cell Culture of Mouse Mammary Carcinoma FM3A Cells

1. Mouse mammary carcinoma FM3A cells (Japan Health Science Foundation).
2. ES medium (Nissui Pharmaceutical Co., Tokyo).
3. Heat-inactivated fetal calf serum.

2.2. Preparation of Photochemically Induced Thrombosis Model Mice (see Note 2)

1. Male C57BL/6 mice (7-week-old) were purchased from Japan SLC Inc. (Hamamatsu, Japan).
2. 3% Isoflurane (Abbott Japan).
3. Rose Bengal.
4. Xenon lamp (Hamamatsu Photonics Japan).
5. 5% Triphenyltetrazolium chloride solution.
6. NIH image program.

2.3. Subjects

1. 35 Control subjects without stroke (20 males, 15 females; 67.8 ± 2.3 years of age), 62 patients with stroke (33 males, 29 females; 70.7 ± 1.7 years of age).
2. For detection of SBI, 114 elderly volunteers (53 males, 61 females; 65.5 ± 8.4 years of age, range 45–88 years of age).
3. For estimation of chronic renal failure, normal subjects (14 males, 6 females; average age 30) and patients with chronic renal failure who have never had hemodialysis (12 males, 8 females; average age 65) (see Note 4).

2.4. Measurement of PC-Acro, Albumin, and Polyamines

1. Ultra-Turrax homogenizer.
2. Buffer A: 10 mM Tris/HCl, pH 7.5, 1 mM dithiothreitol, 10% glycerol, 0.2 mM EDTA, and 0.02 mM FUT-175 (6-amino-2-naphthyl-4-guanidinobenzoate), a protease inhibitor.
3. Antibodies [polyclonal antibody against bovine serum albumin conjugated acrolein (MoBiTec Germany), and antibody against mouse albumin (Bethyl USA)].
4. ACR-LYSINE ADDUCT ELISA system (NOF Corporation).
5. Microplate reader Bio-Rad Model 550.
6. 5% Trichloroacetic acid (5% TCA).

**2.5. Assays
for Spermine Oxidase
and Acetylpolyamine
Oxidase in Plasma**

1. Reaction mixture (0.075 mL) containing 10 mM Tris-HCl, pH 7.5, 0.2 mM spermine for SMO or *N*¹-acetylspermine for acetylpolyamine oxidase (AcPAO), and 0.065 mL plasma.

**2.6. Measurement
of Interleukin-6 and
C-Reactive Protein**

1. Endogen human IL-6 ELISA kit (Pierce Biotechnology, Inc.).
2. Human CRP ELISA kit (Alpha Diagnostic).
3. Microplate reader Hitachi MTP-800AFC.

2.7. Imaging

1. 1.5-T magnetic resonance imaging (MRI) unit (Signa; GE Medical Systems).

2.8. Statistics

1. GraphPad Prism® Software (GraphPad Software).
2. Artificial neural networks using NEUROSIM/L software (Fujitsu).

3. Methods

The toxicity of acrolein and hydrogen peroxide (H₂O₂) on cell growth was compared in mouse mammary carcinoma FM3A cells, and it was found that acrolein is about tenfold more toxic than H₂O₂. Increase in PC-Acro together with decrease in spermidine and spermine in brain tissue of brain infarction was determined in photochemically induced thrombosis (PIT) model mice. The level of PC-Acro in plasma has been developed as a biochemical marker, with measuring PAOs, IL-6, and/or CRP to detect brain infarction, SBI, and renal failure.

**3.1. Effect of Spermine,
Acrolein, and Hydrogen
Peroxide on the
Growth of FM3A Cells**

FM3A cells (5×10^4 cells/mL) were cultured in ES medium, supplemented with 50 units/mL streptomycin, 100 units/mL penicillin G, and 2% heat-inactivated fetal calf serum at 37°C in an atmosphere of 5% CO₂ in air (12) in the presence and absence of spermine, acrolein, H₂O₂, catalase, and/or aldehyde dehydrogenase (see Note 1).

**3.2. Preparation
of Photochemically
Induced Thrombosis
Model Mice**

All animal experiments were approved by the Institutional Animal Care and Use Committee of Chiba University and carried out according to the Guidelines for Animal Research of Chiba University. Eight-week-old male mice weighing 22–26 g were anesthetized with inhalation of 3% isoflurane. Anesthesia was continued with 1.5% isoflurane during operation, and body temperature was kept at $37 \pm 1^\circ\text{C}$ with a heating pad. The thrombotic occlusion of the middle cerebral artery (MCA) was induced by photochemical reaction (13): an incision was made between

the left orbit and the external auditory canal, and the temporalis muscle was detached from dura mater to expose the proximal section of the MCA (see Note 2). Immediately after intravenous injection of photosensitizer, Rose Bengal (20 mg/kg), through a jugular vein, green light (wavelength: 540 nm) emitted from a xenon lamp illuminated the MCA for 10 min. After MCA occlusion, incised skin was restored. At 24 h after the induction of PIT stroke, the brain was removed and sectioned into 2 mm thick coronal slices. Each slice was incubated with 5% triphenyltetrazolium chloride solution at 37°C for 30 min. The volume of infarction was analyzed on a Macintosh computer using the NIH image program (14).

3.3. Subjects and Collection of Blood

Plasma samples were collected from 35 control subjects without stroke (20 males, 15 females; 67.8 ± 2.3 years of age) and 62 patients with stroke (33 males, 29 females; 70.7 ± 1.7 years of age). Stroke patients were defined as having focal infarcts detected by MRI or computed tomography (CT) (41 patients were lacunar and 21 patients were large artery), and managed according to Japanese Guideline for the Management of Stroke (2004). In brief, edaravone, ozagrel, and argatroban were medicated to the patients within the first 10–14 days, and ticlopidine hydrochloride or aspirin was medicated after a few days to weeks of onset of stroke. For detection of SBI, we examined 114 elderly volunteers (53 males, 61 females; 65.5 ± 8.4 years of age, range 45–88 years of age). All participants were healthy volunteers and were living independently at home without apparent history of stroke and dementia. For estimation of chronic renal failure, blood was obtained from normal subjects (14 males, 6 females; average age 30) and from patients with chronic renal failure who have never had hemodialysis (12 males, 8 females; average age 65). Informed consent was given by each participant, and our study protocol was approved by the ethics committees of Graduate School of Medicine, and of Pharmaceutical Sciences, Chiba University. Experiments were conducted in accordance with the Declaration of Helsinki principles. Blood containing 3 unit/mL heparin was centrifuged at $1,500 \times g$ for 10 min at 4°C, and plasma was carefully collected to avoid contamination by erythrocytes.

3.4. Measurement of PC-Acro, Albumin, and Polyamines (see Notes 2–4)

Brain tissues at the locus of infarction of PIT model mice and at the same locus of control mice were homogenized using an Ultra-Turrax homogenizer in 0.5 mL of Buffer A in 2.4. Total proteins (20 μ g) were stained with Coomassie Brilliant Blue R-250 after SDS-polyacrylamide gel electrophoresis (15), and the level of PC-Acro was measured by Western blotting (16) using 20 μ g protein of tissue homogenate and polyclonal antibody against bovine serum albumin conjugated acrolein (see Note 2). The level

of albumin was similarly measured using antibody against mouse albumin. PC-Acro, in which acrolein is converted to *N*^ε-(3-formyl-3,4-dehydropiperidino-lysine) (FDP-Lys), in plasma was measured by the method of Uchida et al. (17) using ACR-LYSINE ADDUCT ELISA system and 0.05 mL plasma. After the reaction was terminated, absorbance at 450 nm was measured by a microplate reader Bio-Rad Model 550. Polyamines in brain tissues and plasma were extracted with 5% TCA and measured by HPLC as previously described (18) (see Notes 2 and 3). Protein was determined by the method of Lowry et al. (19). Values for PC-Acro content in patients with stroke are shown in Fig. 3 and for patients with chronic renal failure in Table 1. Polyamine levels in these patients are shown in Table 1.

3.5. Assays for Spermine Oxidase and Acetylpolyamine Oxidase in Plasma

The reaction mixture in 2.5 was incubated at 37°C for 48 h. To 0.02 mL of the reaction mixture, 0.55 mL of 5% TCA was added and centrifuged at 12,000 × *g* for 10 min. A 10 μL aliquot of the supernatant was used for the polyamine measurement by HPLC (18). The activity of SMO and AcPAO was expressed as nmol spermidine increase per ml plasma. Table 1 shows values.

3.6. Measurement of Interleukin-6 and C-Reactive Protein

IL-6 and high sensitive CRP were measured using Endogen Human IL-6 ELISA kit and human CRP ELISA kit, respectively, according to the manufacturer's protocol. After the reaction was terminated, absorbance at 450 nm was measured by a microplate reader Hitachi MTP-800AFC.

3.7. Imaging

For imaging of SBI, all subjects underwent T1- and T2-weighted MRI, and fluid-attenuated inversion recovery (FLAIR) in parallel with collection of blood samples. FLAIR images were used to distinguish infarcts from dilated perivascular spaces. All MRI was performed in 5–10 mm thickness with 1–2 mm slice gap with a 1.5-T MRI unit. A standard head coil with a receive–transmit birdcage design was used. The maximum size of focal infarcts was measured using 5 or 10 mm length calibration accompanied in each image. The diagnosis of SBI was made as follows: (1) spotty areas ≥ 3 mm in diameter showing with high intensity in the T2 and FLAIR images and low intensity in the T1 image, (2) lack of neurological signs and/or symptoms that can be explained by the MRI lesions, and (3) no medical history of clinical stroke (20). “Normal” subjects are defined as subjects with: (1) no spotty areas; (2) lack of neurological signs and/or symptoms; and (3) no medical history of clinical stroke. An interpreter study for evaluating the MRI lesions was performed by two independent medical doctors experienced in studies of brain disease in a blind fashion. The agreement rate was more than 99%. Through this diagnosis, 97 subjects were classified into 53 normal and 44 SBI subjects. Seventeen subjects were judged to have less than 3 mm infarction, and excluded from SBI.

3.8. Statistics

Statistical calculations were performed with GraphPad Prism® Software. Values are indicated as means \pm S. D. or median \pm interquartile deviation. Groups were compared using Wilcoxon rank sum test. Difference in each marker or combination of various markers in SBI vs. no stroke was evaluated using a receiver operating characteristic (ROC) curve (21). ROC curve analysis was performed with artificial neural networks (22). Candidates of cutoff values and their sensitivity and specificity were calculated with the neural networks and the cutoff value was set up as the closest point on ROC curve from the P point, that is sensitivity = 1 and 1-specificity = 0. Sensitivity, specificity, positive- and negative-predictive values (PPV and NPV), and positive- and negative-likelihood (LR+ and LR-) were calculated with the standard method (23).

4. Notes

1. It is known that polyamines (spermine and spermidine) inhibit cell growth in the presence of fetal calf serum. The viable cell number was counted in the presence of 0.25% trypan blue. The inhibitory effect of spermine was seen with mouse mammary carcinoma FM3A cells exposed to spermine in the presence of FCS (Fig. 1b). The toxicity is caused by factors produced from polyamines by amine oxidase. The evidence for this is that aminoguanidine, an inhibitor of amine oxidase, reduced or prevented the toxic effects of polyamines. Polyamines are converted to aminoaldehydes and H_2O_2 by amine oxidase (Fig. 1a). Then, acrolein is spontaneously formed from aminoaldehydes. The addition of aldehyde dehydrogenase, but not catalase, to the culture medium could prevent the effects of spermine on cell growth (Fig. 1b). Furthermore, the concentration of acrolein (7.5–15 μM) necessary for inhibition of cell growth was much lower than that of H_2O_2 (100–200 μM). The results suggest that acrolein is more strongly involved than H_2O_2 in the inhibition of cell growth by spermine (6).
2. To show that the increase in PC-Acro at the locus of infarction and in plasma is well correlated with the induction of acrolein, experiments were performed using PIT model mice. The volume of the infarction was determined by staining 2 mm thick coronal slices with triphenyltetrazolium. This stains the viable brain tissue red, whereas infarct tissue remains unstained. Under our experimental conditions, the average volume of infarction at 24 h after photoinduction was 23 mm³ (Fig. 2a). Acrolein may be formed from spermine and spermidine by SMO, spermidine/spermine *N*¹-acetyltransferase (SSAT), and AcPAO

(see Fig. 3a). Because free acrolein is rapidly converted to PC-Acro through its interaction with lysine side chains in proteins (Fig. 2b), PC-Acro at the locus of brain infarction was 28-fold higher than that at the same locus of control mice (Fig. 2c). The protein was also stained with antibody against albumin, suggesting that most of PC-Acro is acrolein conjugated with albumin.

We measured the levels of polyamines at the locus of brain infarction in comparison with the level at the same locus of control mice to confirm that acrolein is mainly produced from spermine and spermidine. As shown in Fig. 2d, the levels of both spermine and spermidine decreased significantly after the infarction, whereas the level of putrescine increased. The results strongly suggest that acrolein is produced during the conversion of spermine to spermidine and spermidine to putrescine. The size of infarction decreased significantly when 100 mg/kg of MDL72527, an inhibitor of PAOs, was added (24). The data support the idea that a toxic compound acrolein is produced from spermine and spermidine by PAOs during brain infarction. It was also found that PC-Acro in plasma was significantly higher in PIT model mice than in control mice.

3. PC-Acro is formed from 3-aminopropanal produced by SMO and less effectively from 3-acetamidopropanal produced by SSAT and AcPAO (Fig. 3a). Accordingly, the activities of SMO and AcPAO were measured together with the level of PC-Acro (FDP-lysine) in plasma of the patients with stroke. As shown in Fig. 3b, the levels of total PAO (SMO plus AcPAO) and PC-Acro were significantly higher in the plasma of patients with stroke. When we analyzed the level of polyamines in plasma, there was a tendency for putrescine levels to be increased, whereas levels of spermine and spermidine were significantly decreased after stroke. The results support the idea that AcPAO and SMO are released from nerve, glia, or other cells during the early period of stroke, leading to reduced levels of spermidine and spermine and increased levels of PC-Acro. The size of stroke was nearly parallel with the multiplied value of PC-Acro and total PAO. After the onset of stroke, an increase in AcPAO first occurred, followed by increased levels of SMO and finally PC-Acro.

It has been reported that SBI increases the risk of subsequent stroke (25, 26) and dementia (26). It is, therefore, valuable to detect SBI at an early period by biochemical markers, because measurement of biochemical markers in blood is common and economical compared to diagnostic imaging such as MRI and CT. Thus, we investigated whether SBI can be detected by measuring acrolein, PAO, or other biomarkers.

Several biomarkers were measured in the plasma of 53 normal subjects and 44 subjects with SBI. It was found that the levels of PC-Acro, IL-6, and CRP were significantly higher in SBI than in normal subjects. Total PAO was slightly higher in SBI than in normal subjects. Since the probability of SBI was increased with age, values were analyzed including age as a factor. When the combined measurements of PC-Acro, IL-6, and CRP were evaluated together with age using a ROC curve, SBI was indicated with 89% sensitivity and 91% specificity. The results indicate that measurement of PC-Acro together with IL-6 and CRP makes it possible to identify SBI with high sensitivity and specificity.

4. The polyamine content and SMO activity in plasma of patients with renal failure were measured. Plasma was divided into moderate (<8 mg/dL) and severe (>8 mg/dL) classes according to the value of serum creatinine. The level of putrescine in plasma of patients with renal failure was higher than that in normal subjects, whereas spermidine and spermine levels were lower. We subsequently determined the activity of SMO in plasma. SMO in plasma of patients with renal failure was higher than that in normal subjects. In general, the change of polyamine levels and the increase in SMO were greater in patients with severe renal failure than in those with moderate failure (Table 1). The results suggest that acrolein, a toxic compound, is produced from spermidine and spermine by PAO in the plasma of patients with renal failure.

PC-Acro in plasma was then measured. As shown in Table 1, PC-Acro was increased in plasma of patients with renal failure. PC-Acro in plasma of uremic patients was equivalent to 140–170 μ M, which is about fivefold higher than in plasma of normal subjects.

Patients with severe renal failure undergo hemodialysis (HD). Thus, we tested whether the levels of polyamines, SMO, and PC-Acro in plasma of HD patients decreased by HD. Blood was taken just before HD. Although the level of polyamines did not change significantly compared with that of the patients without HD, the level of SMO and PC-Acro decreased greatly in HD patients (9). The results indicate that HD is effective for decreasing a toxic compound, acrolein.

Acknowledgments

We are grateful to Drs. K. Williams and A. J. Michael for critical reading of the manuscript prior to submission. This study was supported in part by Grants-in-Aid for Scientific Research from the Ministry of Education, Culture, Sports, Science, and Technology, Japan.

References

1. Igarashi K, Kashiwagi K (2000) Polyamines: mysterious modulators of cellular functions. *Biochem Biophys Res Commun* 271:559–564
2. Igarashi K, Kashiwagi K (2010) Modulation of cellular function by polyamines. *Int J Biochem Cell Biol* 42:39–51
3. Gaugas JM, Dewey DL (1979) Evidence for serum binding of oxidized spermine and its potent G1-phase inhibition of cell proliferation. *Br J Cancer* 39:548–557
4. Bachrach U (1970) Oxidized polyamines. *Ann N Y Acad Sci* 171:939–956
5. Tabor CW, Tabor H, Bachrach U (1964) Identification of the aminoaldehydes produced by the oxidation of spermine and spermidine with purified plasma amine oxidase. *J Biol Chem* 239:2194–2203
6. Sharmin S, Sakata K, Kashiwagi K, Ueda S, Iwasaki S, Shirahata A, Igarashi K (2001) Polyamine cytotoxicity in the presence of bovine serum amine oxidase. *Biochem Biophys Res Commun* 282:228–235
7. Campbell RA, Talwalkar Y, Bartos D, Bartos F, Musgrave J, Harner M, Puri H, Grettie D, Dolney AM, Loggan B (1978) Polyamines, uremia and hemodialysis. In: Campbell RA, Morris DR, Bartos D, Daves GD Jr (eds) *Advances in polyamine research*. Raven, New York, pp 319–343
8. Sakata K, Kashiwagi K, Sharmin S, Ueda S, Irie Y, Murotani N, Igarashi K (2003) Increase in putrescine, amine oxidase, and acrolein in plasma of renal failure patients. *Biochem Biophys Res Commun* 305:143–149
9. Igarashi K, Ueda S, Yoshida K, Kashiwagi K (2006) Polyamines in renal failure. *Amino Acids* 31:477–483
10. Tomitori H, Usui T, Saeki N, Ueda S, Kase H, Nishimura K, Kashiwagi K, Igarashi K (2005) Polyamine oxidase and acrolein as novel biochemical markers for diagnosis of cerebral stroke. *Stroke* 36:2609–2613
11. Yoshida M, Tomitori H, Machi Y, Katagiri D, Ueda S, Horiguchi K, Kobayashi E, Saeki N, Nishimura K, Ishii I, Kashiwagi K, Igarashi K (2009) Acrolein, IL-6 and CRP as markers of silent brain infarction. *Atherosclerosis* 203:557–562
12. Ayusawa D, Iwata K, Seno T (1981) Alteration of ribonucleotide reductase in aphidicolin-resistant mutants of mouse FM3A cells with associated resistance to arabinosyladenine and arabinosylcytosine. *Somatic Cell Genet* 7:27–42
13. Tanaka Y, Marumo T, Omura T, Yoshida S (2007) Quantitative assessments of cerebral vascular damage with a silicon rubber casting method in photochemically-induced thrombotic stroke rat models. *Life Sci* 81:1381–1388
14. Saiki R, Nishimura K, Ishii I, Omura T, Okuyama S, Kashiwagi K, Igarashi K (2009) Intense correlation between brain infarction and protein-conjugated acrolein. *Stroke* 40:3356–3361
15. Laemmli UK (1970) Cleavage of structural proteins during the assembly of the head of bacteriophage T4. *Nature (London)* 227:680–685
16. Nielsen PJ, Manchester KL, Towbin H, Gordon J, Thomas G (1982) The phosphorylation of ribosomal protein S6 in rat tissues following cycloheximide injection, in diabetes, and after denervation of diaphragm. A simple immunological determination of the extent of S6 phosphorylation on protein blots. *J Biol Chem* 257:12316–12321
17. Uchida K, Kanematsu M, Morimitsu Y, Osawa T, Noguchi N, Niki E (1998) Acrolein is a product of lipid peroxidation reaction. Formation of free acrolein and its conjugate with lysine residues in oxidized low density lipoproteins. *J Biol Chem* 273:16058–16066
18. Igarashi K, Kashiwagi K, Hamasaki H, Miura A, Kakegawa T, Hirose S, Matsuzaki S (1986) Formation of a compensatory polyamine by *Escherichia coli* polyamine-requiring mutants during growth in the absence of polyamines. *J Bacteriol* 166:128–134
19. Lowry OH, Rosebrough NJ, Farr AL, Randall RJ (1951) Protein measurement with the Folin phenol reagent. *J Biol Chem* 193:265–275
20. Hoshi T, Kitagawa K, Yamagami H, Furukado S, Hougaku H, Hori M (2005) Relations of serum high-sensitivity C-reactive protein and interleukin-6 levels with silent brain infarction. *Stroke* 36:768–772
21. Henry JA, McNeil BJ (1982) The meaning and use of the area under a receiver operating characteristic (ROC) curve. *Radiology* 143:29–36
22. Ellenius J, Groth T, Lindahl B, Wallentin L (1997) Early assessment of patients with suspected acute myocardial infarction by biochemical monitoring and neural network analysis. *Clin Chem* 43:1919–1925
23. Brenner H, Gefeller O (1997) Variation of sensitivity, specificity, likelihood ratios and predictive values with disease prevalence. *Stat Med* 16:981–991
24. Dogan A, Rao AM, Hatcher J, Rao VL, Baskaya MK, Dempsey RJ (1999) Effects of

- MDL 72527, a specific inhibitor of polyamine oxidase, on brain edema, ischemic injury volume, and tissue polyamine levels in rats after temporary middle cerebral artery occlusion. *J Neurochem* 72:765–770
25. Kobayashi S, Okada K, Koide H, Bokura H, Yamaguchi S (1997) Subcortical silent brain infarction as a risk factor for clinical stroke. *Stroke* 28:1932–1939
 26. Vermeer SE, Hollander M, van Dijk EJ, Hofman A, Koudstaal PJ, Breteler MM (2003) Silent brain infarcts and white matter lesions increase stroke risk in the general population: the Rotterdam Scan Study. *Stroke* 34:1126–1129

Methods to Evaluate Alterations in Polyamine Metabolism Caused by *Helicobacter pylori* Infection

Alain P. Gobert, Rupesh Chaturvedi, and Keith T. Wilson

Abstract

Helicobacter pylori is a Gram-negative bacteria that infects the human stomach of half of the world's population. Colonization is followed by infiltration of the gastric mucosa by lymphocytes and myeloid cells. These cells are activated by various bacterial factors, causing them to produce immune/inflammatory mediators, including reactive nitrogen species and polyamines that contribute to cellular damage and the pathogenesis of *H. pylori*-associated gastric cancer. In vitro experiments have revealed that *H. pylori* induces macrophage polyamine production by upregulation of the arginase 2/ornithine decarboxylase (ODC) metabolic pathway and enhances hydrogen peroxide synthesis through the activity of spermidine oxidase (SMO). In this chapter, we present a survey of the methods used to analyze the induction and the role of the enzymes related to polyamine metabolism, i.e., arginase, ODC, and SMO in *H. pylori*-infected macrophages.

Key words: Macrophage, Arginase, Ornithine decarboxylase, Spermine oxidase, *Helicobacter pylori*

1. Introduction

Worldwide, human infection with *Helicobacter pylori* is the main cause of chronic gastritis, peptic ulcer, and gastric cancer (1). Importantly, gastric cancer is the second-leading cause of cancer death worldwide. The persistence of this pathogen in the stomach despite a strong induction of a mucosal immune response is a critical hallmark of the infection (2). It is therefore of importance to determine how *H. pylori* modulates the innate immune response of the cells with which it interacts, such as gastric epithelial cells and macrophages.

Enzymes that metabolize L-arginine are essential for macrophage function. First, inducible nitric oxide (NO) synthase (iNOS) converts L-arginine into citrulline and NO. The free radical NO possesses numerous antimicrobial (3) and proinflammatory

properties (4). In addition, L-arginine is also a substrate for both arginase 1 and arginase 2. Therefore, through consumption of L-arginine, arginase is a natural competitor of iNOS by decreasing substrate availability. Arginase synthesizes L-ornithine, which is metabolized by ornithine decarboxylase (ODC) into the diamine putrescine that serves as the precursor to the polyamines, spermidine and spermine. Intracellular polyamine catabolism occurs through two distinct enzymatic pathways: (a) spermidine/spermine N^1 -acetyltransferase (SSAT) acetylates both spermine and spermidine, providing acetylated polyamines as substrates for further backconversion to putrescine by N^1 -acetylpolyamine oxidase (APAO); and (b) spermine oxidase (SMO), also termed polyamine oxidase (PAOI), directly converts spermine to spermidine. Of importance, both metabolic pathways generate hydrogen peroxide.

We have shown that *H. pylori*: (a) induces macrophage apoptosis through the arginase 2/ODC/SMO pathway (5–7) and (b) regulates iNOS translation in macrophages by increasing ODC expression and endogenous polyamine synthesis (8). Furthermore, the induction of ODC and its biological consequences is dependent on c-Myc binding to the ODC promoter (7). Together these data suggest that there is a strong interaction between *H. pylori* and the inducible metabolism of L-arginine in macrophages (Fig. 1).

The modulation of the induction of arginase 2, ODC, and SMO in macrophages by *H. pylori* may occur at both the transcriptional and translational levels. Below we will describe

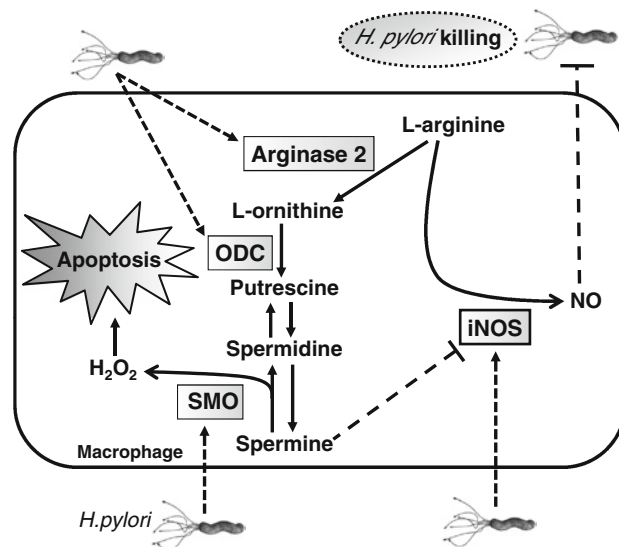


Fig. 1. *Helicobacter pylori* stimulated synthesis and metabolism of polyamines in macrophages. *H. pylori* stimulates expression of iNOS, arginase 2, ODC, and SMO. High output iNOS-derived NO kills *H. pylori*. Polyamines are synthesized through the arginase 2/ODC metabolic pathway. Spermine inhibits iNOS translation. The backconversion of spermine to spermidine by SMO releases H₂O₂ that induces macrophage apoptosis.

straightforward assay protocols for understanding the regulation of polyamine metabolism and its role in *H. pylori*-infected macrophages. These include: transient transfection of macrophages with small interfering RNA (siRNA) or reporter plasmids, analysis of mRNA expression by reverse transcription (RT)-polymerase chain reaction (PCR) and real-time PCR, detection of proteins by Western blotting, and determination of relevant enzymes activities involved in polyamine metabolism.

It should be noted that our laboratory also works extensively on the response to *H. pylori* in other experimental systems. Space does not permit description of these experimental protocols in the current chapter, but we would like to refer the reader to our published protocols for isolation of mouse peritoneal macrophages (5, 8) and mouse gastric macrophages (9) and infection of mice with *H. pylori* (5). Additionally, information about the adaptation of the macrophage protocols described below to the gastric epithelial cell model has been described by our laboratory (10).

2. Materials

2.1. Cell Culture

1. The RAW 264.7 murine macrophage cell line was obtained from the ATCC.
2. Complete RAW 264.7 cell culture medium: Dulbecco's Modified Eagle's Medium with glutamine (DMEM; Invitrogen, Carlsbad, CA) supplemented with 10% decompartmented (heat-inactivated) fetal bovine serum (FBS; Invitrogen), 1% sodium pyruvate, 10 mM HEPES, 100 U/ml penicillin, and 100 µg/ml streptomycin.

2.2. Transfections

1. SMO siRNA sequences: 5'-GGACGUGGUUGAGGAAUUC-3' and 5'-CCUGCACCAACUCCUUAAG-3'; ODC siRNA sequences: 5'-CUCAUGAAACAGAUCCAGA-3' and 5'-UCUGGAUCUGUUUCAUGAG-3'. siRNAs were purchased from Qiagen (Valencia, CA).
2. Prepare 20 µM stock solutions of the above siRNA duplexes dissolved in 10 mM Tris-HCl, pH 7.5, 1 mM ethylenediaminetetraacetic acid (EDTA) buffer.
3. The pcDNA3.1-SMO plasmid contains the gene encoding SMO under the control of the constitutive SV40 promoter; this plasmid is provided by RA Casero, Jr. (Department of Oncology, Johns Hopkins University School of Medicine, Baltimore, MD).
4. The pSV-β-galactosidase plasmid is obtained from Promega (Madison, WI).

5. Lipofectamine 2000 transfection reagent (Invitrogen).
6. OptiMEM medium (Invitrogen).
7. β -galactosidase Enzyme Assay System with Reporter Lysis Buffer kit (Promega).

2.3. RNA Extraction and PCR

1. Add 1 ml of diethylpyrocarbonate (DEPC) to 1 l of distilled water, treat from 6 h to overnight, and autoclave for 20 min at 120°C.
2. Prepare a solution of 75% ethanol in DEPC water.
3. A 5 \times RT buffer is composed of 50 mM Tris-HCl (pH 9), 250 mM KCl, and 0.5% Triton X-100, all obtained from Sigma (St. Louis, MO).
4. RT mastermix, for each sample: 4 μ l of 5 \times RT buffer, 1 μ l of 10 mM deoxyribonucleotide triphosphate (dNTP), 2 μ l of 0.1 M dithiothreitol (DTT), 1 μ l of 40 U/ μ l RnaseOUT, and 0.5 μ l of 100 U/ml SuperScript II Reverse Transcriptase[®], all obtained from Invitrogen.
5. 10 \times PCR buffer: 500 mM KCl, 100 mM Tris-HCl (pH 8.3), and 15 mM MgCl₂.
6. Sense and antisense primer sequences and PCR product sizes are as follows: murine iNOS, 5'-GCCTCGCTCTGGA AAGA-3' and 5'-TCCATGCAGACAACCTT-3', 499 bp or 5'-CACCTTGGAGTTCACCCAGT-3' and 5'-ACCACTCG TACTTGGGATGC-3', 170 bp; murine arginase 1, 5'-AA GAAAAGGCCGATTCACCT-3' and 5'-CACCTCCTCTG CTGTCTTCC-3', 201 bp; murine arginase 2, 5'-ACAGGGT TGCTGTCAGCTCT-3' and 5'-TGATCCAGACAGCCA TTTCA-3', 298 bp; murine ODC, 5'-CAGCAGGCTT CTCTTGGAAC-3' and 5'-CATGCATTTTCAGGCAGG TTA-3', 602 bp; murine SMO, 5'-CACGTGATTGTGACC GTTTC-3' and 5'-TGGGTAGGTGAGGGTACAGTC-3', 222 bp; murine APAO, 5'-CTTTTCCAGGGGAGAC CTTC-3' and 5'-CACACCACCTGGATGAACTG-3', 250 bp; murine SSAT, 5'-GACCCCTGAAGGACATAGCA-3' and 5'-CCGAAGCACCTCTTCTTTTG-3', 248 bp; and murine/human β -actin, 5'-CCAGAGCAAGAGAGG TATCC-3' and 5'-CTGTGGTGGTGAAGCTGTAG-3', 436 bp. The stock concentration of each primer is 15 pmol/ μ l, and they are stored at -20°C.
7. PCR mastermix, for each sample: 2.5 μ l of 10 \times PCR buffer, 1 μ l of 50 mM MgCl₂, 0.5 μ l of 10 mM dNTP, 0.5 μ l of 25 U/ μ l Platinum *Taq* DNA polymerase (Invitrogen). Add (a) 0.5 μ l each of the of 5' and 3' murine iNOS, arginase 1 or 2, ODC, SMO, APAO, or SSAT primers, and (b) 0.1 μ l each of the of 5' and 3' murine β -actin primers. Complete with 18.9 μ l of DEPC H₂O.

8. 10× Tris-acetate-EDTA (TAE): 48.4 g/l Tris base, 10.9 g/l glacial acetic acid, and 2.92 g/l EDTA, pH 8.0.

2.4. Reporter Gene for ODC Promoter

1. Primer sequence for ODC promoter region: sense, 5'-GGGGTACCTGTCCGACACGAG-3'; antisense, 5'-GGAAGATCTTTAGCCAAGAAGACTC-3', 2.8 kbp.
2. The ODC-CAT plasmid is provided by JL Cleveland (St. Jude Children's Research Hospital, Memphis, TN).
3. The Luciferase Reporter pGL3-Enhancer vector (Promega) contains an SV40 enhancer located downstream of the luciferase gene (*luc+*) and the poly(A) signal, and an ampicillin resistance gene.

2.5. Western Blot

1. Stock solution of 100 mM phenylmethanesulphonylfluoride (PMSF): 0.174 g PMSF in 10 ml ethanol; keep at -20°C .
2. Radioimmunoprecipitation (RIPA) buffer: Tris-HCl 50 mM, pH 7.4, sodium deoxycholate 0.25%, NaCl 150 mM, EDTA 1 mM, Na_3VO_4 1 mM, NaF 1 mM. Before use, add 1 mM PMSF, 1% NP-40, and an antiprotease cocktail (Sigma).
3. The following 6× protein loading buffer can be prepared in advance and stored at -20°C : Tris-HCl 375 mM, pH 6.8, 3 ml glycerol, 1 g SDS, 0.93 g DTT, and 1.2 mg bromophenol blue, in a final volume of 10 ml.
4. A 5× solution of electrophoresis running buffer consists of Tris 125 mM, glycine 960 mM and SDS 0.5%, and stocked at 4°C .
5. A 5× solution of transfer buffer is composed of 125 mM Tris and 950 mM glycine. The working TB buffer is: 20% 5× TB buffer, 20% methanol and 60% H_2O .
6. Tris-buffered saline with Tween (TBS-T): Prepare 10× stock with 1.37 M NaCl, 27 mM KCl, 250 mM Tris-HCl, pH 7.4, and 1% Tween-20.
7. Blocking buffer: 5% nonfat dry milk in TBS-T.
8. Antibody dilution buffer: TBS-T supplemented with 2% bovine serum albumin.
9. Stripping buffer: Tris-HCl 62.5 mM, pH 6.8, SDS 2%, and 0.8% β -mercaptoethanol. Warm this buffer to 50°C before use.

2.6. Arginase and ODC Activity Assays

1. Arginase activity lysis buffer: 0.1% Triton X100, 0.01% pepstatin, 0.01% aprotinin, and 0.01% antipain in distilled H_2O . Make fresh as required.
2. 9% α -isonitrosopropiophenone (Sigma) dissolved in ethanol.
3. ODC lysis buffer: 1 mM Tris-HCl (pH 7.4), 1 mM EDTA, 0.05 mM pyridoxal-5'-phosphate, and 5 mM DTT.

2.7. SMO, APAO, and SSAT Activity assays

1. Borate buffer: 4.76 g boric acid and 2.54 g sodium tetraborate in 1 l of distilled H₂O. Equilibrate to pH 8.4 with NaOH.
2. Assay reaction mixture for SMO activity: 5.7 U/ml of horseradish peroxidase (HRP) and 50 μM spermine (6, 10) in 80 mM borate buffer, pH 9.0.
3. Assay reaction mixture for APAO activity: 5.7 U/ml of HRP and 50 μM N¹-acetylspermine (Fluka Chemie, Buchs, Switzerland) in 80 mM borate buffer, pH 9.0.
4. Luminol: Prepare fresh just before addition to assay reaction mixture as 100 nM solution in H₂O.
5. The SSAT assay reaction mixture is composed of 3 mM spermidine and 12.7 μM l-(¹⁴C)acetyl-CoA (specific activity, 63 mCi/mmol).

2.8. Griess Reagents

1. Griess A: sulfanilamide 1% in HCl 1.2 N.
2. Griess B: naphthylethylenediamine 0.3% in distilled H₂O.
3. Keep solutions at 4°C and protect from light.

3. Methods**3.1. Cell Culture and Infection**

1. *H. pylori* is cultured on trypticase soy agar blood agar plates (BD Biosciences, Sparks, MD) at 37°C under 5% CO₂. The day before the infection, bacteria are grown overnight on plates and are then harvested using a cotton tip in sterile phosphate buffered saline (PBS) solution. Bacteria are washed once and resuspended in complete DMEM without antibiotics. The absorbance (*A*) is measured at of 600 nm; we have reported that a solution of 10⁹ bacteria/ml corresponds to an *A*_{600 nm} of 1 (11).
2. The murine macrophage cell line RAW 264.7 (ATCC # TIB-71) is maintained in complete DMEM in T75 flasks. The day of the experiment, adherent cells are washed twice with 10 ml PBS, detached from the culture flask using a scraper, and centrifuged at 300×*g* for 10 min. Pellets are resuspended with 1 ml of complete medium without antibiotics (see Note 1); then 5 ml of this same medium is added. Cells are counted using a hemocytometer and are plated on 6-well plates (2–4 × 10⁶ cells/well in 2 ml) or on 24-well plates (0.5–1 × 10⁶ cells/well in 1 ml) for 2 h. Medium is removed and fresh complete medium without antibiotics is added to the wells. Bacteria are added to the cells at a multiplicity of infection (MOI; number of bacteria per cells) of 1–100 together with pharmacological inhibitors of iNOS, arginase, ODC, or SMO

if required; inhibitors of signal transduction or of transcriptional factors are added 30 min prior to the infection. At the end of the infection (see Note 2), cocultures are washed with PBS and RNA or proteins are extracted from cells. In addition to live bacteria directly cocultured with the macrophages, the reader is referred to other studies documenting methods for coculture of *H. pylori* separated from macrophages by Transwell filter supports (5), and other preparations of *H. pylori* that can be used, including lysates prepared in a French Pressure Cell (11) and water extracts (12).

3.2. Transient Transfection of Macrophages

1. Transfection of siRNA for ODC or SMO in macrophages: To knock-down *H. pylori*-induced expression of SMO or ODC, we developed an siRNA-based approach. These strategies are particularly useful because the SMO inhibitor, MDL 72527 also blocks APAO, and the ODC inhibitor, α -difluoromethylornithine does not prevent spermine accumulation in short-term culture. For these studies, plate 2×10^6 cells in 6-well plates and grow them in complete culture medium overnight. The next day, discard the medium and add 1 ml of OptiMEM medium (Invitrogen). For each well, mix 20 μ l of the 20 μ M stock solution of either SMO, ODC, or control scrambled siRNA with 100 μ l of OptiMEM medium, and incubate for 15 min at room temperature. Add this mixture to a solution containing 5 μ l of Lipofectamine 2000 in 100 μ l of OptiMEM and incubate for 15 min at room temperature. Gently overlay this combination of siRNA, lipid transfection reagent, and medium on RAW 264.7 cells, and incubate for 18 h. Wash the cells, add complete medium without antibiotics, and proceed with *H. pylori* infection. To confirm knockdown of SMO in macrophages, analyze SMO mRNA expression by RT-PCR/real-time PCR after an infection of 6 h by *H. pylori*, as described in Subheading 3.3. ODC knockdown can be confirmed by RT-PCR/real-time PCR or immunoblotting (see Subheading 3.5).
2. Transfection of plasmid expressing SMO in macrophages: To overexpress SMO activity in macrophages, RAW 264.7 cells are transfected with the pcDNA3.1-SMO plasmid; the pSV- β -galactosidase plasmid is transfected concomitantly to determine the efficacy of transfection. Plate 5×10^6 cells in 6-well plates and grow them in complete culture medium overnight. The next day, discard the medium and add 800 μ l of OptiMEM medium. For each well, mix 400 ng of pSV- β -galactosidase and 200 ng of pcDNA3.1-SMO plasmids in a final volume of 100 μ l of OptiMEM. Separately mix 20 μ l LipofectAMINE Plus with 100 μ l of OptiMEM medium. Incubate both tubes for 15 min at room temperature. Mix both solutions and incubate

the mixture for 15 min at room temperature before adding it to cells. Incubate the RAW 264.7 cells for 18 h, change the medium to complete DMEM, and activate cells with *H. pylori*. Measure transfection efficiency by measuring β -galactosidase activity in transfected cells using the β -galactosidase Enzyme Assay System with Reporter Lysis Buffer kit. SMO enzyme activity is measured as described in Subheading 3.8.

3.3. mRNA Analysis

1. RNA extraction: Wells containing RAW 264.7 cells are washed twice with PBS and the liquid is completely removed. TRIzol (1 ml; Invitrogen) is directly added to the cells for 10 min. The plates are then gently vortexed and the lysates are harvested in RNase-free 1.5 ml Eppendorf tubes (see Notes 3 and 4). Add 0.2 ml chloroform and mix vigorously by manual shaking for 30 s; do not use a vortex. Leave the tubes at room temperature for 10 min. Centrifuge at $12,000 \times g$ at 4°C for 15 min. Carefully collect the upper aqueous phase and transfer to new 1.5 ml Eppendorf tubes and add 0.5 ml isopropanol. Gently mix the contents by repeatedly inverting and let tubes stand at room temperature for 10 min. Centrifuge at $12,000 \times g$ at 4°C for 15 min. Aspirate the supernatant and resuspend the pellet in 1 ml of 75% ethanol in DEPC water. Centrifuge at $8,000 \times g$ at 4°C for 10 min, and again remove the supernatant. Dry the pellet (see Note 5) and add 20 μl DEPC H_2O . RNA is then solubilized by incubation of the tubes at 56°C for 20 min.
2. Removing of residual DNA. Each RNA sample is treated with DNase I obtained from Promega according to the manufacturer's protocol (see Note 6).
3. Quantify the RNA suspension after diluting 50–100 times in DEPC water and reading absorbance at A_{260} and A_{280} to measure nucleic acid and protein concentration, respectively (see Note 7). Ideally, the A_{260}/A_{280} ratio should be close to 2 for high purity nucleic acid. RNA concentration is determined by the following formula: $(\text{RNA}) (\mu\text{g}/\mu\text{l}) = (A_{260} \times 40 \times \text{dilution factor}) / 1,000$. RNA is stored at -80°C .
4. RT: This step corresponds to the synthesis of cDNA from messenger RNA (mRNA). All the steps described below are performed on ice. Add 1 μl of Oligo dT (500 $\mu\text{g}/\text{ml}$) to 10.5 μl of a solution of DEPC water containing 2 μg total RNA. Incubate at 65°C for 5 min and chill quickly on ice. Centrifuge the tubes briefly and add 8.5 μl of RT mastermix to each sample. Incubate 50 min at 42°C , and 15 min at 70°C to stop the reaction. cDNA samples are stored at -20°C . Amplification of cDNA is then performed by PCR and/or real-time PCR.
5. PCR: Prepare one PCR mastermix for all the samples; dispense 24 μl in 0.2 ml Eppendorf tubes and add 1 μl of each

cDNA in each tube. PCR is conducted in an iCycler apparatus (Bio-Rad, Hercules, CA). One PCR cycle consists of the following: 94°C for 2 min (94°C for 30 s, 59°C for 30 s, and 72°C for 60 s) for a total cycle number of 30–35; 72°C for 5 min. Harvest 10 µl of PCR product and add 2 µl of Loading Buffer; perform the electrophoresis on 1.5% agarose gel in 1× TAE buffer containing 0.4 µg/ml ethidium bromide (see Note 8). Stained bands are visualized under UV light and photographed. An example of *H. pylori*-stimulated ODC mRNA expression is shown in Fig. 2d.

6. Real-time PCR: cDNA (1 µl) is amplified by the SYBR® Green SuperMix for iQ kit (Bio-Rad) containing 0.12 pmol/µl each of sense and antisense primers, in a Bio-Rad iQ5 real-time PCR machine. One PCR cycle consists of the following: 94°C for 2 min (94°C for 30 s, 59°C for 30 s, and 72°C for 30 s) for a total cycle number of 45; 72°C for 2 min. For each

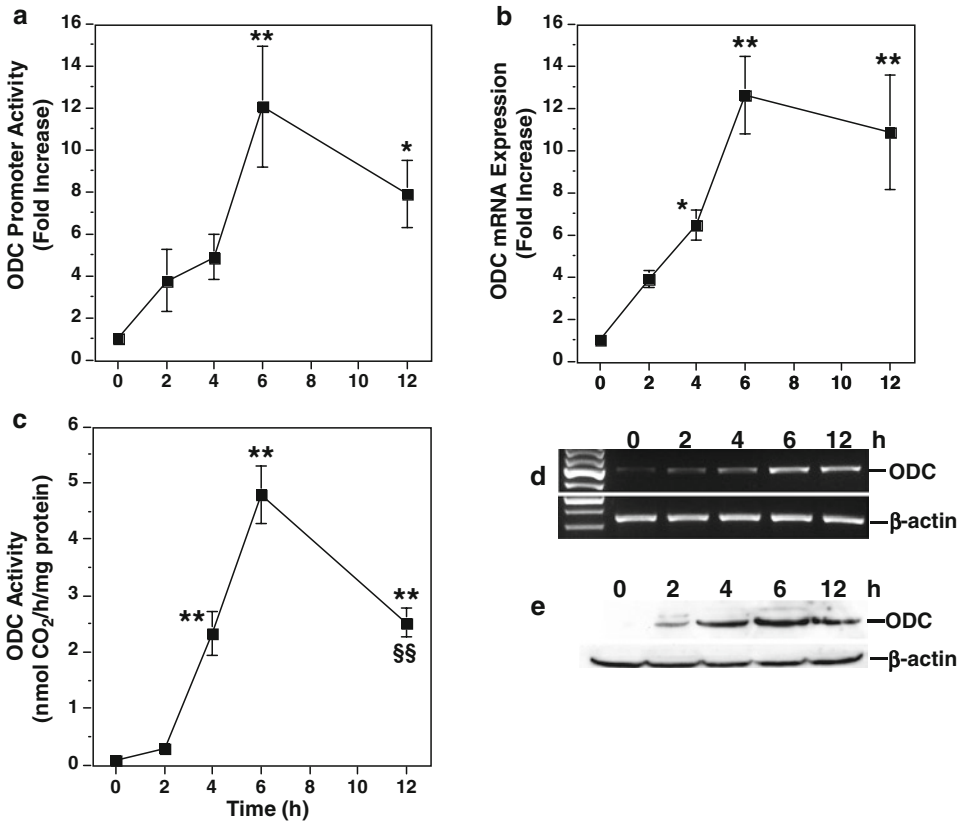


Fig. 2. Time course of induction of ODC in *H. pylori*-stimulated macrophages. RAW 264.7 cells were exposed to *H. pylori* for the times indicated. (a) promoter activity determined by luciferase reporter assay using a -264-bp functional ODC promoter. (b) mRNA levels determined by real-time PCR. (c) ODC activity determined by radiochemical assay. (d) RT-PCR for ODC. (e) Western blot for ODC (53 kDa) and β-actin (42 kDa). *, $p < 0.05$; **, $p < 0.01$ vs. time 0; in (a–c), each experiment was performed a minimum of three times, each in duplicate. In (d) and (e), the data are representative of three experiments (Reproduced from ref. (7) with permission from The American Society for Biochemistry and Molecular Biology).

sample, the cycle threshold (Ct; number of PCR cycles needed to get a fluorescent signal) is provided by the software of the individual real-time PCR machine. Variations in crossing point reflect different DNA quantities between samples. Results are calculated using the comparative Ct method in which the amount of target gene mRNA is normalized to the internal control β -actin and in which mRNA expression in *H. pylori* infected cells (Hp) is compared to uninfected cells (Ctrl). The following formula is used:

$$\begin{aligned} &\text{Gene expression (fold increase/Ctrl)} \\ &= 2^{[\text{Ct } \beta\text{-actin(Ctrl)} - \text{Ct gene(Ctrl)}] - [\text{Ct } \beta\text{-actin(Hp)} - \text{Ct gene(Hp)}]} \end{aligned}$$

Representative published data for *H. pylori*-stimulated ODC mRNA expression is shown in Fig. 2b.

3.4. Luciferase Assay for ODC Promoter

1. Construction of the gene reporter: To generate desired promoter constructs, perform PCR using 2 μg ODC-CAT plasmid as a template with 0.5 pmol/l each of ODC promoter region primers and the Phusion™ High-Fidelity PCR Master Mix (New England Biolabs, Inc, Ipswich, MA), in a final volume of 50 μl . Use the following conditions for PCR: 95°C for 3 min; 30 cycles as follows: 98°C for 1 min, 50°C for 1 min, and 72°C for 2.5 min; 10 min at 72°C. Run PCR products on a 0.7% agarose gel in 1 \times TAE buffer containing 0.4 $\mu\text{g/ml}$ ethidium bromide (see Note 8). Excise the 2.8 kbp band from the gel with a razor blade, and purify the PCR product using QIA Quick Gel Extraction kit from Qiagen. Measure the concentration of the DNA, using spectrophotometry, and adjust the concentration of the PCR product to 0.2 $\mu\text{g}/\mu\text{l}$. To 20 μl of purified PCR product, add 1 μl of 0.5 mM dNTP and 5 units of the DNA polymerase I Klenow fragment (New England Biolabs, Inc.) and incubate at 30°C for 15 min. Stop the reaction by heating to 75°C for 10 min. In parallel, the pGL3-Enhancer vector plasmid is linearized with 20 units of the restriction enzyme KpnI (New England Biolabs, Inc.) overnight at 24°C. This plasmid is then isolated by electrophoreses on an 0.7% agarose gel, treated with the Klenow fragment, and purified using the QIA Quick Gel Extraction kit (Qiagen), as described above. Combine 50 ng of pGL3-Enhancer vector with 1 μg of the insert corresponding to the ODC promoter region. Adjust volume to 10 μl with distilled H₂O, add 10 μl of 2 \times Quick Ligation Buffer (New England Biolabs, Inc.) and 1 μl of Quick T4 DNA Ligase (New England Biolabs, Inc.); mix thoroughly, centrifuge briefly, and incubate at 25°C for 5 min. Chill on ice and store this pGL3-ODC minimal functional promoter plasmid at -20°C. Editor's note: mouse genomic DNA could be used in place of the ODC-CAT construct to obtain the promoter region by the PCR method detailed here.

2. The reporter gene is introduced into the competent *Escherichia coli* strain DH5 α and selected on Luria Bertani (LB) agar plates containing 25 $\mu\text{g}/\text{ml}$ ampicillin.
3. Selection of the clones containing pGL3-ODC plasmid: Transformed *E. coli* are then spread on LB plates. Isolated colonies are harvested and grown on 10 ml LB broth overnight. Half of the culture is frozen in 10% glycerol, and half is used to isolate the plasmid using the QIAprep Spin Miniprep Kit (Qiagen). Digest the plasmid with 20 units of the restriction enzyme XbaI (New England Biolabs, Inc.) overnight at 24°C and run on a 0.7% agarose gel. Check for 5.0 kpb band and keep the colonies that have been transformed.
4. Transient transfection and luciferase assay: RAW 264.7 cells are transfected with the purified pGL3-ODC and the pSV- β -galactosidase plasmids as described in Subheading 3.2. Transfection efficiency is evaluated by measuring β -galactosidase activity in transfected cells using the β -galactosidase Enzyme Assay System with Reporter Lysis Buffer kit (Promega). After infection with *H. pylori*, luciferase activity is measured using the Luciferase Assay System (Promega) following the manufacturer's instructions. Representative data are shown in Fig. 2a.

3.5. Immunoblotting for ODC

1. Scrape the RAW 264.7 cells in 1 ml PBS and harvest them in 1.5 ml Eppendorf tubes. Spin at 300 $\times g$ for 10 min and discard the supernatant.
2. On ice, suspend each pellet with 100 μl of RIPA buffer; incubate for 20 min.
3. Centrifuge the lysate at 12,000 $\times g$ for 20 min at 4°C. Transfer the supernatants to ice-chilled Eppendorf tubes and measure protein concentration.
4. Dilute 30 μg of each protein sample in a final volume of 20 μl of RIPA buffer, add 4 μl of loading buffer, and boil the samples for 5 min. Chill on ice.
5. Load samples and the colored molecular weight markers in 12.5% Tris-HCl polyacrylamide Criterion Precast Gels (Bio-Rad).
6. Electrophoresis is performed in 1 \times running buffer at 100 V in a Criterion™ Cell (Bio-Rad), until the dye front reaches the bottom of the gel. The samples that have been separated by SDS-page are then transferred to nitrocellulose membrane.
7. Cut a nitrocellulose membrane and two pieces of GB005 Whatman filter paper to the same size as the gel, and incubate them in the transfer buffer at 4°C for 15 min. The gel unit is disconnected from the power supply and disassembled. On the base of the Transblot SD Semidry Transfer Cell apparatus

- (Bio-Rad), place one wet filter paper, the gel, the nitrocellulose membrane (see Note 9), and then the second filter paper. Gently roll a pipette on this block to remove bubbles present between the gel and the membrane. Transfer is performed at 400 mA for 1 h. The colored molecular weight markers should be clearly visible on the membrane.
8. The nitrocellulose is then incubated in 20 ml blocking buffer for 2 h at room temperature on a rocking platform.
 9. Wash the membrane 2 times 5 min with 20 ml TBS-T.
 10. Incubate the membrane with the rabbit polyclonal anti-ODC antibody (Santa Cruz Biotechnology, Santa Cruz, CA; 1:1,000 dilution) overnight at 4°C and wash membrane three times with TBS-T for 15 min.
 11. Incubate the membrane with a goat anti-rabbit IgG secondary antibody conjugated with HRP (Sigma; 1:5,000 dilution) for 1 h at room temperature, and wash 3 times with TBS-T for 15 min.
 12. After the final wash, mix 2 ml each of both the ECL reagents (Invitrogen) according to the manufacturer's instructions, and incubate membrane in this solution for 5 min. Remove membrane, gently blot on Kim wipes, and place it in between plastic sheets. In a dark room, expose the blot to Bio-Max ML film (Kodak, Rochester, NY) for 30 s to 5 min in an X-ray film cassette. Develop exposed film in developer. Films can be digitized using a flatbed scanner. A representative example of *H. pylori*-stimulated ODC protein expression as detected by Western blotting is shown in Fig. 2e.
 13. Once a satisfactory exposure is obtained, incubate the blot in stripping buffer for 30 min at 50°C. Wash membrane 3 times for 10 min each with 100 ml of TBS-T and incubate again in blocking buffer.
 14. The membrane can then be reprobed using mouse anti- β -actin (Sigma; 1:10,000 dilution) as a loading control; washes, secondary antibody addition, and ECL detection are performed as described above. A blot of β -actin after a strip of the membrane is depicted in Fig. 2e.

3.6. Determination of Arginase Activity

Arginase activity is measured in RAW 264.7 macrophages using the micromethod described by Corraliza et al. (13).

1. Macrophages are harvested at the end of the experiment, counted, and 2×10^5 cells are isolated in a 1.5 ml Eppendorf tube.
2. After washing with PBS, the pellet is resuspended in 50 μ l of arginase activity lysis buffer. Tubes are vortexed and incubated 15 min on ice.

3. In parallel, serial dilutions of recombinant bovine arginase (Sigma) are prepared as a standard curve.
4. 5 μl of a solution of 100 mM MnCl_2 in PBS is added to each sample and to the standards for 10 min at 55°C. Then, 50 μl of a solution of 0.5 M L-arginine in PBS is added to each sample for 1 h at 37°C. The reaction is stopped by the addition of 400 μl of an acid mixture of $\text{H}_2\text{SO}_4/\text{H}_3\text{PO}_4/\text{H}_2\text{O}$ (1:3:7).
5. The concentration of urea synthesized by arginase metabolism is determined by addition of 25 μl of 9% α -isonitrosopropiophenone for 45 min at 100°C. The colored product is quantified by $A_{540\text{ nm}}$ in a spectrophotometer.

3.7. Assay for ODC Activity

ODC activity is determined by a radiometric analysis in which the amount of $^{14}\text{C}]O_2$ liberated from L- ^{14}C ornithine is measured.

1. Macrophages (2×10^5) are lysed in 500 μl of ODC lysis buffer. Cells are freeze/thawed once, followed by sonication on ice with 3×30 s pulses using an Ultrasonic Processor set at an amplitude of 50.
2. Prepare 2.5 cm diameter disks of Whatman filter paper impregnated with 20 μl of 2 N NaOH. These are left to dry at room temperature.
3. After centrifugation at $12,000 \times g$ for 15 min, 300 μl of the macrophage lysate supernatants are incubated at 37°C with 10 nmol L- ^{14}C ornithine (specific activity, 47.7 mCi/mmol; NEN, Boston, MA) for 15 min in a 15 ml glass tube fitted with a rubber stopper and a center well assembly containing the Whatman filter paper; the $^{14}\text{C}]O_2$ liberated by the activity of the ODC is trapped on the filter paper. The reaction is stopped with 300 μl of 10% trichloroacetic acid. The rest of each lysate is used for measurement of protein concentration.
4. $^{14}\text{C}]O_2$ present on the filter paper is analyzed by liquid scintillation counting.
5. From the cpm value measured, the amount of $^{14}\text{C}]O_2$ present in each sample is calculated using the following formula:

$$^{14}\text{C}]O_2(\text{fmol}) = \text{cpm} / [2.10^9 \times \text{specific activity (Ci/mmol)}].$$
6. ODC activity is expressed as nmol $\text{CO}_2/\text{h}/\text{mg}$ protein. Representative data are shown in Fig. 2c.

3.8. Measurement of SMO and APAO Activity

The same assay is used to determine PAOI and APAO activity. Only the reaction mixture is different between the assays.

1. Harvest 5×10^6 macrophages in 500 μl borate buffer (for 6-well plates) on ice, and homogenize with an Ultra-Turrax

- (IKA Works, Wilmington, NC). Centrifuge at $12,000 \times g$ for 10 min and collect the supernatant.
2. Measure protein concentration using BCA protein estimation kit (Pierce/Thermo Scientific, Rockford, IL) as described in the manufacturer's instructions.
 3. On ice, add 100 μ l of cell lysate to 100 μ l of assay reaction mixture and incubate for 2 min at 37°C (see Note 10).
 4. For the standard curve, prepare solutions of H_2O_2 (0–160 nmol) in 100 μ l of cell lysis buffer and 100 μ l of assay buffer in 12 \times 75 mm glass tubes.
 5. Transfer the unknown and standard tubes to a luminometer. Add 10 μ l of 100 nM luminol using an injector, and integrate the resulting chemiluminescence for 20 s.
 6. Express activities as nmol of H_2O_2 /min/mg of protein.

3.9. Determination of SSAT Activity

1. Scrape 5×10^6 RAW 264.7 cells in 250 μ l borate buffer and homogenize with an Ultra-Turrax (IKA Works, Wilmington, NC) and measure protein concentration with BCA protein kit.
2. Add 100 μ l of RAW 264.7 lysates to 100 μ l SSAT assay reaction mixture and incubate for 10 min at room temperature.
3. Stop reaction by adding 10 μ l of 1 M hydroxylamine, and boil for 3 min.
4. Spot the resulting samples onto P-81 phosphocellulose disks and wash the disks twice with 10 ml of 100% methanol.
5. Transfer disks in 5 ml of biodegradable scintillation fluid in counting vials and measure radioactivity in a scintillation counter.
6. From the cpm value measured, the amount of [^{14}C]acetyl-CoA incorporated into spermidine in each sample is calculated, using the following formula:

$$\begin{aligned} &L-[^{14}C]\text{acetylspermidine (fmol)} \\ &= \text{cpm} / [2.10^9 \times \text{specific activity (Ci/mmol)}]. \end{aligned}$$

7. Express enzyme activity as nmol of L-[^{14}C]acetylspermidine formed/min/mg of protein.

3.10. Measurement of NO_2^- Concentration

NO_2^- and NO_3^- concentration in a cell supernatant is a reliable indicator of NO production by activated macrophages. Here, we present the Griess reaction that allows spectrophotometric detection of NO_2^- (see Note 11).

1. Place 50 μ l of each cell supernatant in wells of 96-well plates in duplicate; add 60 μ l of Griess A and then 60 μ l of Griess B.
2. To ensure accurate NO_2^- quantitation, prepare a reference curve with $NaNO_2$ for each assay (from 0 to 100 μ M), using the same cell culture medium used for experimental samples.

3. Incubate at room temperature for 5–10 min, protected from light. A purple/magenta color will begin to form immediately. Measure $A_{540\text{ nm}}$ in a plate reader.

3.11. Measurement of Apoptosis

1. Plate 5×10^5 RAW 264.7 cells and stimulate with *H. pylori*.
2. Scrape the cells and collect them in the cell culture supernatant. Centrifuge at $1,000 \times g$ at 4°C for 10 min.
3. Discard the supernatant and use the Annexin V-FITC Apoptosis Detection kit I from BD Biosciences to analyze the apoptosis by flow cytometry.

4. Notes

1. The cells have to be first dissolved in 1 ml medium with a Pipetman to ensure a proper dissolution of the pellet before adding more medium.
2. The time of infection varies according to the type of experiment. Usually, mRNA expression and protein analysis are performed 3–9 and 6–24 h after the beginning of the infection, respectively. NO_2^- concentration and apoptosis are analyzed 24–48 h postinfection. We recommend performing a kinetic analysis of earlier time points as appropriate.
3. Samples can be stored frozen at -20 or -80°C in TRIzol for 3 and 12 months, respectively.
4. The material will be very viscous at this stage owing to release of DNA, and thus hard to pipette. The viscosity will decrease if samples are frozen at -20 or -80°C .
5. The use of a vacuum chamber is advised.
6. DNase treatment is a recommended step. Contaminating DNA fragments will remain in the cDNA samples if not removed. As such, this DNA will be amplified by PCR along with the cDNA, and results could be compromised. To check for proper removal of contaminating DNA, it is suggested to perform PCR using $0.2\ \mu\text{g}$ RNA as a template instead of $1\ \mu\text{l}$ cDNA; no amplification should be observed if there is no DNA contamination.
7. We use a 96-well quartz microplate for absorbency determinations in the ultraviolet region of the light spectrum. Additionally, different disposable microplates with no background absorbance characteristics in the UV range are commercially available.
8. Add agarose to TAE buffer in an Erlenmeyer flask and cover it with plastic wrap and pierce a hole in the wrap for ventilation. Weigh the beaker and solution. Microwave the agarose

solution for periods of 1 min. Between each series, take out the flask from the microwave using high heat gloves and swirl gently the solution to resuspend any remaining agarose particles; any microwaved solution may be superheated and could foam over the container's rim if agitated. It is important to check the boiling of this solution in the microwave to avoid an overflow. Agarose is dissolved when a clear solution is obtained. Add enough hot distilled water to return the contents to the original weight; mix continuously. Then, let the temperature cool down to 55°C. Add ethidium bromide under a fume hood, mix thoroughly, and pour into gel casting apparatus.

9. One corner of the gel and the membrane are cut to allow orientation to be tracked. Also, wet transfer of SDS-PAGE gels to membranes can be used.
10. We have found that the standard curve is linear for values between 5 and 80 nmol of H₂O₂. Therefore, samples should be diluted to fit in this linear range.
11. When produced by activated cells, NO reacts with itself and water in the presence of oxygen to form NO₂⁻. Nonetheless, other reactive nitrogen species, including NO₃⁻, can be synthesized. To measure NO₃⁻ concentration, NO₃⁻ should be converted into NO₂⁻ by a NO₃⁻ reductase prior to performing the Griess assay. Numerous kits are commercially available to perform this experiment.

Acknowledgements

This work was supported by R01 DK053620, R01 AT004821, P01 CA116087, P01 CA028842, P30 DK058404 (Vanderbilt Digestive Disease Center), and a Merit Review Grant from the Office of Medical Research, Department of Veterans Affairs. APG is also supported by a grant from Philippe Foundation.

References

1. Cover TL, Blaser MJ (2009) *Helicobacter pylori* in health and disease. *Gastroenterology* 136:1863–1873
2. Wilson KT, Crabtree JE (2007) Immunology of *Helicobacter pylori*: insights into the failure of the immune response and perspectives on vaccine studies. *Gastroenterology* 133: 288–308
3. Gobert AP, McGee DJ, Akhtar M, Mendz GL, Newton JC, Cheng Y, Mobley HL, Wilson KT (2001) *Helicobacter pylori* arginase inhibits nitric oxide production by eukaryotic cells: a strategy for bacterial survival. *Proc Natl Acad Sci U S A* 98:13844–13849
4. Gobert AP, Cheng Y, Akhtar M, Mersey BD, Blumberg DR, Cross RK, Chaturvedi R, Drachenberg CB, Boucher JL, Hacker A, Casero RA Jr, Wilson KT (2004) Protective role of arginase in a mouse model of colitis. *J Immunol* 173:2109–2117
5. Gobert AP, Cheng Y, Wang JY, Boucher JL, Iyer RK, Cederbaum SD, Casero RA Jr, Newton

- JC, Wilson KT (2002) *Helicobacter pylori* induces macrophage apoptosis by activation of arginase II. *J Immunol* 168:4692–4700
6. Chaturvedi R, Cheng Y, Asim M, Bussiere FI, Xu H, Gobert AP, Hacker A, Casero RA Jr, Wilson KT (2004) Induction of polyamine oxidase 1 by *Helicobacter pylori* causes macrophage apoptosis by hydrogen peroxide release and mitochondrial membrane depolarization. *J Biol Chem* 279:40161–40173
 7. Cheng Y, Chaturvedi R, Asim M, Bussiere FI, Scholz A, Xu H, Casero RA Jr, Wilson KT (2005) *Helicobacter pylori*-induced macrophage apoptosis requires activation of ornithine decarboxylase by c-Myc. *J Biol Chem* 280:22492–22496
 8. Bussiere FI, Chaturvedi R, Cheng Y, Gobert AP, Asim M, Blumberg DR, Xu H, Kim PY, Hacker A, Casero RA Jr, Wilson KT (2005) Spermine causes loss of innate immune response to *Helicobacter pylori* by inhibition of inducible nitric-oxide synthase translation. *J Biol Chem* 280:2409–2412
 9. Chaturvedi R, Asim M, Lewis ND, Algood HM, Cover TL, Kim PY, Wilson KT (2007) L-arginine availability regulates inducible nitric oxide synthase-dependent host defense against *Helicobacter pylori*. *Infect Immun* 75:4305–4315
 10. Xu H, Chaturvedi R, Cheng Y, Bussiere FI, Asim M, Yao MD, Potosky D, Meltzer SJ, Rhee JG, Kim SS, Moss SF, Hacker A, Wang Y, Casero RA Jr, Wilson KT (2004) Spermine oxidation induced by *Helicobacter pylori* results in apoptosis and DNA damage: implications for gastric carcinogenesis. *Cancer Res* 64:8521–8525
 11. Wilson KT, Ramanujam KS, Mobley HL, Musselman RF, James SP, Meltzer SJ (1996) *Helicobacter pylori* stimulates inducible nitric oxide synthase expression and activity in a murine macrophage cell line. *Gastroenterology* 111:1524–1533
 12. Gobert AP, Mersey BD, Cheng Y, Blumberg DR, Newton JC, Wilson KT (2002) Cutting edge: urease release by *Helicobacter pylori* stimulates macrophage inducible nitric oxide synthase. *J Immunol* 168:6002–6006
 13. Corraliza IM, Campo ML, Soler G, Modolell M (1994) Determination of arginase activity in macrophages: a micromethod. *J Immunol Methods* 174:231–235

High-Resolution Capillary Gas Chromatography in Combination with Mass Spectrometry for Quantification of Three Major Polyamines in Postmortem Brain Cortex

Gary Gang Chen, Laura M. Fiori, Orval A. Mamer, and Gustavo Turecki

Abstract

There is considerable evidence supporting a role of the polyamine system in the etiology and pathology of mental disorders. Changes in the expression and activity of polyamine anabolic/catabolic enzymes, as well as in the levels of individual polyamines, have been found in many psychiatric conditions, including schizophrenia, mood disorders, anxiety, and suicidal behavior. Recent microarray studies have found that spermidine/spermine-*N*¹-acetyltransferase (SAT1, SSAT), the key enzyme in charge of the polyamine catabolic pathway, is downregulated in brain tissue of individuals who were depressed and died by suicide. To provide further insight into the downstream effects of altered SAT1 expression, we developed a quantitative gas chromatography-mass spectrometry method for measurement of polyamine concentrations in postmortem human brain tissues. This protocol employs a conventional electron ionization method with total ion and selected ion monitoring. This method can accurately measure the levels of the polyamines putrescine, spermidine, and spermine from very small quantities (1–50 mg) of postmortem brain tissues, with quantitation limits down to 10 ng/g of wet tissue for putrescine and 100 ng/g for spermidine and spermine.

Key words: Polyamines, Putrescine, Putrescine-D4, Spermidine, Spermine, 1,7-Diaminoheptane, Spermidine/spermine-*N*¹-acetyltransferase (SAT1, SSAT), Gas chromatography-mass spectrometry

1. Introduction

The polyamines, including putrescine (PUT), spermidine (SPD), and spermine (SPM), belong to a family of biogenic amines which play critical roles in many biological processes including cell proliferation and differentiation, apoptosis, angiogenesis, aging, and inflammation (1–5). Recent studies by our group have also implicated the polyamine system in suicide and depression (6, 7). At physiological pH, the polyamines are positively charged,

allowing them to interact with anionic biomolecules such as DNA, RNA, phospholipids, and proteins. The intracellular levels of the polyamines are tightly controlled by the balance between the complex anabolic and catabolic pathways that allows rapid and efficient changes to polyamine levels in reaction to specific cellular and behavioral needs (8). As our recent studies demonstrated alterations in the expression of several polyamine anabolic and catabolic genes in multiple brain regions of suicide completers, we were interested in determining if these changes in gene expression resulted in alterations in the levels of the polyamines themselves (6, 9, 10). Polyamine analysis from postmortem brain tissue has been previously performed through high performance liquid chromatography (HPLC) by Gilad and colleagues in the 1990s (11). More recently, a gas chromatography-mass spectrometry (GC-MS) method employing a single derivatization process for the analysis of neurochemicals and putrescine from rat hippocampal slices has been reported (12). As there were no suitable quantitative GC-MS methods for the analysis of the three major polyamines, PUT, SPD, and SPM from complex biological sources such as postmortem brain samples, we developed a dedicated GC-MS method for the extraction and measurement of these polyamines from postmortem brain tissues (13). The efficiency of this GC-MS method is based on an effective two-phase extractive derivatization strategy. This analytical method is robust and efficient, and can be readily adapted to use in other biological samples such as blood and urine.

2. Materials

2.1. Instruments, Equipment, and Related Materials

1. An Agilent bench-top 6890GC/MSD5973N Chemstation system (Agilent Technologies, Inc. Santa Clara, CA, USA) equipped with an autosampler was employed for this work.
2. Helium gas (99.999%).
3. Nitrogen gas (pre-purified grade).
4. Deionized water.
5. Dry ice.
6. Derivatization station with heating block (Tecam, Dri-Block DB-3, or equivalent product).
7. Microtissue homogenizer.
8. Centrifuge and microcentrifuge.
9. Analytical balance (measuring at the nanogram scale).
10. -80°C Freezer.
11. Crimper for seal derivatization vials.

12. Vortex.
13. Heating block.
14. pH paper and pH meter.
15. Derivatization vials (2 ml, 12×32 mm, 9–425, clear glass, screw thread, Chromatographic Specialties Inc. C779199; or equivalent product); Derivatization vial screw cap (9 mm, BLUE, W/RED PTFE/WHITE SIL SEPT, Chromatographic Specialties Inc. C779200B; or equivalent product).
16. GC-MS autosampler vials (microval, C/T, 250 µl, 12×32 mm, Chromatographic Specialties Inc. SB200046; or equivalent product); and autosampler vial seals (CRIMP TOP, 11 mm, SILVER ALU, W/TEF/OR RUB SEPT Chromatographic Specialties Inc. C221150C; or equivalent product).
17. Glass syringes (10–100 µl scale, Agilent Gold Standard; or equivalent product).
18. Glass pipettes (7").

2.2. Chemicals

1. Polyamine standards: PUT, SPD, SPM, and 1,7-diaminoheptane (DAH) as free bases were obtained from Sigma.
2. Ethyl acetate (derivatization grade, Sigma).
3. Ethyl chloroformate (ECF).
4. Trifluoroacetic acid anhydride (TFAA).
5. Putrescine-D4 (PUT-D4) was purchased from CDN isotopes (Pointe-Claire, QC, Canada) with 98% atom deuterium.
6. Diethyl ether.
7. Hexane.
8. Methanol.
9. HCl.
10. NaOH.
11. NaCl.
12. Anhydrous sodium sulfate.

2.3. Tissue Samples

1. Postmortem brain tissue samples were acquired from the Quebec Suicide Brain Bank (www.douglasrecherche.qc.ca/suicide) following IRB approval.

2.4. Preparation of Polyamine Standards

1. Stock standard solutions are prepared by dissolving each polyamine in 0.1 M HCl at a final concentration of 10 mg/ml, then stored at –80°C (see Note 1).
2. Working standard solutions of each polyamine at concentrations of 10, 100 ng, 1, 10, 100 µg, and 1 mg/ml are prepared by sequential dilutions of the stocks in 0.1 M HCl.

3. Methods

GC-MS can provide the absolute quantification of a given metabolite in a concentration range of up to four orders of magnitude provided that proper external and internal standards have been used. However, it must be kept in mind that each step during the sample extraction, preparation, and analysis can introduce general and specific losses, which depend on the source of the biological sample, extraction method, and analytical technique used.

Traditional liquid–liquid extraction has many disadvantages such as matrix effects, formation of emulsions, and the use of hazardous solvents, and typically requires more complicated isolation protocols. However, given the complexity of polyamine extraction and derivatization, the liquid–liquid extraction strategy described here actually reduced total solvent exchanges, sample transfer manipulations, and drying steps compared to solid phase extraction and conventional organic solvent extraction methods, thus reducing the overall time required. For a batch of 10–20 samples, the extraction and derivatization procedures take approximately 2 days. The GC-MS analysis of one sample takes approximately 85–90 min. The time required to analyze GC-MS data depends on the quality of the running results: for high quality running data, it typically requires approximately 30 min to process each sample.

3.1. Internal Standardization and Calibration

A pilot experiment needs to be performed to determine the levels of PUT-D4 and DAH needed as internal standards to represent endogenous PUT, SPD, and SPM, respectively. Following this, one can build a calibration curve using known concentrations of the polyamine standards as follows:

1. Add 500 ng each of PUT-D4 and DAH into six 0.5 ml aliquots of 0.1 M HCl.
2. Add PUT, SPD, and SPM using polyamine working stocks to yield final concentrations of 1, 10, 100 ng, 1, 10, and 100 µg/ml in a final volume of 1 ml.
3. These samples will be used to obtain the limit of detection (LOD) and linearity of response (the calibration range). A good calibration curve can give a linear response in up to four magnitudes of concentrations. An example calibration curve is shown in Fig. 1 and the selected ion chromatograms for the derivatives of three polyamines plus two internal standards (I.S) is given in Fig. 2. The LOD is 0.1 ng/g for PUT and 10 ng/g for both SPD and SPM. All three polyamines showed good linearity in physiological polyamine ranges (1–10 µg/g wet tissue).

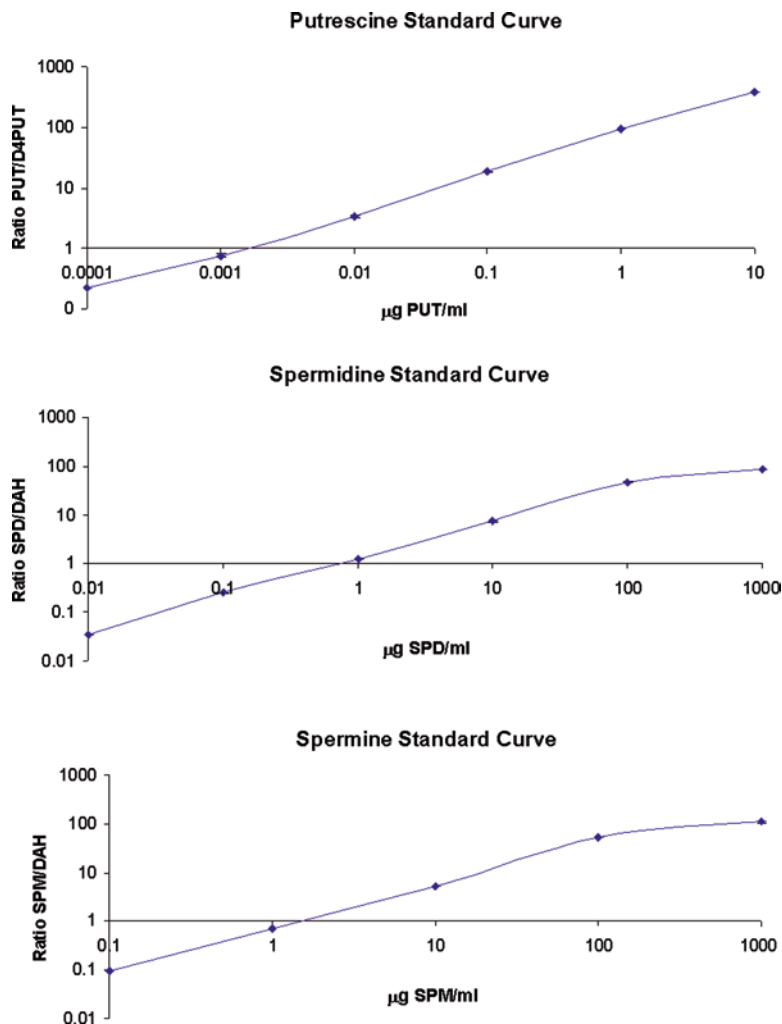


Fig. 1. Calibration curves for PUT, SPD, and SPM. Calibration curves were performed using 0.1 M HCl. The weights of target analytes per milliliter of calibrating sample is plotted against the intensity ratios of the measured analytes and standards.

3.2. Polyamine Extraction from Brain Tissues

1. To approximately 50 mg of thawed brain tissue, add internal standards, PUT-D4 and DAH, at 10 ng each per mg of tissue (see Note 2). The pilot experiment and calibration curves indicate the amount of putrescine-D4 and DAH needed to be added as internal standards per milligram of tissue.
2. Homogenize tissue samples with added internal standards on ice with 10 volumes (0.5 ml) of 0.1 M HCl (see Note 3).
3. Centrifuge at $12,000\times g$ for 15 min at 4°C.
4. Collect the supernatant containing the soluble polyamines.
5. Resuspend the pellet in 10 volumes of 0.1 M HCl, and repeat steps 2 and 3.

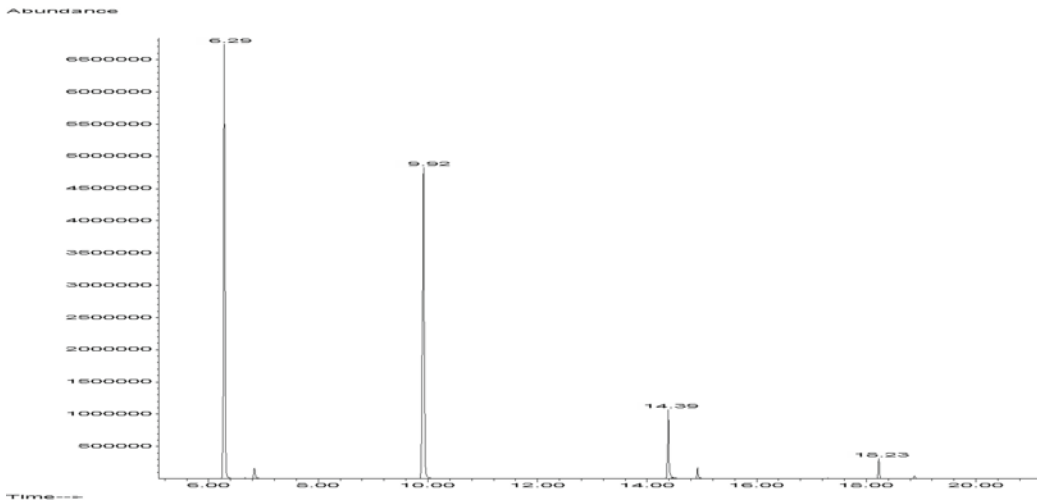


Fig. 2. Composite selected ion chromatograms for the derivatives of five polyamines from HP-5MS capillary column separation by GC-MS. Detailed conditions are described in the Subheading 3. Peaks: 6.28 min = PUT and PUT-D4; 9.92 min = DAH; 14.39 min = SPD; 18.23 min = SPM.

6. Combine the supernatants and bring the final volume to 2 ml with 0.1 M HCl.
7. Add 3 ml of diethyl ether to the supernatant and vortex for 5 min at room temperature.
8. Centrifuge the sample at $12,000 \times g$ for 20 min at room temperature. At this point, the emulsion is broken and two layers can be clearly seen.
9. Discard the upper ether layer without disrupting the lower aqueous phase.
10. Repeat steps 7 and 8 on the aqueous phase.
11. The aqueous layer contains polyamines and other biogenic amines, and can be stored at -80°C until use.

3.3. Polyamine Derivatization with Ethyl Chloroformate and Trifluoroacetic Acid Anhydride

1. To 0.5 ml aliquots of polyamine standards, as well as the aqueous layer from the polyamine extraction step, add 5 M NaOH to obtain a final pH = 10. This can be performed using pH paper and a pH meter (see Note 4).
2. To carry out the N-ethoxycarbonylation of the polyamines, add 1 ml of diethyl ether containing 50 μl of ECF to the above sample. Shake the reaction mixture at room temperature for 30 min, until no more CO_2 gas is released.
3. Centrifuge at $1,200 \times g$ for 5 min at room temperature. Transfer the ether layer containing the polyamine derivatives to a separate derivatization glass vial.
4. Repeat the above polyamine N-ethoxycarbonyl (N-EOC) derivatization by reextracting the aqueous phase with 1 ml of diethyl ether containing 50 μl ECF. Additional repeats of this step do not increase recoveries.

5. Combine the two ether extracts and add approximately 50 mg of dry anhydrous sodium sulfate and vortex for 5 s several times over a 5 min period. This step ensures that any trace amount of water will be absorbed by the anhydrous sodium sulfate.
6. Transfer the ether extract into a derivatization vial that can be sealed with a Teflon coated cap, and evaporate to near dryness under a slow stream of nitrogen gas (see Note 5).
7. Dissolve the dried residues in 100 μ l of ethyl acetate.
8. Add 200 μ l of fresh trifluoroacetic anhydride into the above derivatization vial containing the N-EOC polyamines in ethyl acetate and seal the vial immediately. This step allows the trifluoroacetylation of the remaining N-H bonds of the N-EOC polyamine derivatives.
9. Place the vial in a 75°C heating block for 1 h to complete the N-trifluoroacetyl (N-TFA) derivatization reaction.
10. Cool the vial and evaporate to dryness under nitrogen gas.
11. Dissolve the residue in 200 μ l of ethyl acetate. Transfer 100 μ l to an autosampler vial. This sample is now ready to be analyzed by GC-MS (see Note 6). The remaining 100 μ l can be stored at -20°C.

3.4. GC-MS Conditions for Measurement of Polyamines from Postmortem Brains

All mass spectra are acquired in electron ionization (EI) mode for full scan and SIM with an Agilent bench-top HP6890/MSD5973N Chemstation system. Detailed conditions are listed below:

1. A HP-5MS capillary GC column (25 m, 0.25 mm i.d. and 0.25 μ m thickness) was used.
2. Helium carrier gas was set to a column head pressure of 8.5 psi at a flow rate of 1.0 ml/min.
3. Aliquots of 2 μ l of sample were injected in splitless mode with a 5 min solvent delay.
4. The GC oven was programmed from 140 to 210°C at 8°C/min followed by a 2 min hold, then to 300°C at 20°C/min, followed by a 4 min hold. A final temperature increase to 320°C at 20°C/min was held as bake out for 4 min.
5. Other instrument temperatures were: source 200°C, quadrupole sector 150°C, interface 250°C, and injector 260°C.
6. The source pressure was 1.8×10^{-5} torr.
7. Full scans at 2 s/scan were over the mass range m/z 10–700.
8. A total of 14 ions for four ion groups were selected for monitoring: PUT, PUT-D4, DAH, SPD, and SPM (Table 1).
9. All ions listed in Table 1 were monitored during GC-MS data acquisitions, with the characters ions in bold used for quantification purpose (see Note 7).

Table 1
Ions monitored in electron ionization-selected ion monitoring (EI-SIM) mode

Polyamines	[M]	[M-69]	[M-73]	[M-258]
PUT	424	355		166
PUT-D ₄	428	359		170
DAH	466	397		
SPD	553		480	295
SPM	682		609	424

Ions with masses in bold were used to quantify sample polyamines. Other ions were monitored to verify the identities of individual amines

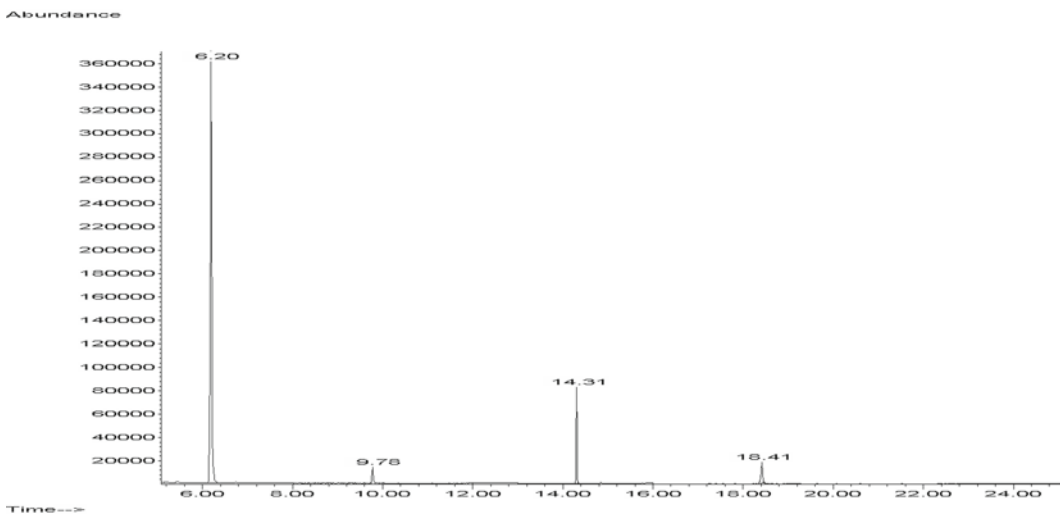


Fig. 3. Total ion chromatograms of the GC-MS analysis, in the selected ion monitoring (SIM) mode, of three major polyamines and internal standard derivatives from the postmortem brain cortex of a patient. GC conditions are described in the method section. Peaks: 6.20 min=PUT-D₄ (I.S) and PUT 9.78 min=DAH (I.S); 14.31 min=SPD; 18.41 min=SPM.

10. Due to the limitation of postmortem brain tissue samples, we could not prepare sample in triplicates. However, samples were analyzed by triplicate injections for statistical analysis (see Note 8).
11. An example selected ion monitoring chromatogram for the internal standards and the three major polyamines extracted from the cortex of a patient brain is given in Fig. 3.

3.5. Data Analysis

1. GC-MS data analysis was carried out with Chemstation software (Agilent Technologies) (see Note 9).
2. Statistical analyses were performed using SPSS 15.0.

3. Student *t*-tests were used to assess differences in PUT, SPD, and SPM levels between controls and suicides.
4. Pearson correlations were used to assess relationships between sample characteristics and polyamine levels.

4. Notes

1. The stable isotope putrescine-D4 is used as internal standard for putrescine. DAH is used as the internal standard for SPD and SPM, as we were unable to obtain isotope labeled analogs for these polyamines commercially.
2. Generally speaking, 10 mg of postmortem frozen brain tissue is sufficient for one experiment. However, 50 mg of tissue is used when including technical replicates.
3. This should produce an emulsion that can be broken by centrifugation.
4. The key step of this dual derivatization is the N-ethyl-oxycarbonylation of polyamines with ECF to form urethanes in the aqueous layer under mild alkaline conditions, ideally at pH 10. At pH > 11, hydrolysis of urethanes has been observed, whereas under pH < 9, the protonated polyamines will prevent complete derivatization of amino groups.
5. Ensure that the nitrogen tube is well positioned inside the vial to exclude condensing of atmospheric water mist in the vial. The purpose here is to remove as much of the ether as possible but leave behind the N-EOC polyamine derivatives.
6. For best analytical results, keep the derivatized samples at -20°C before analysis and use within 1 week of derivatizing.
7. A fragment at *m/z* 327 produces a strong ion signal. However, SPD, spermine, as well as many other biogenic amines can produce this *m/z* 327 ion fragment under the same derivatization and GC-MS analytical conditions. Consequently, it cannot be used for quantification of SPD and spermine.
8. After approximately 200 sample injections, the ion source of the mass spectrometry detector will need to be cleaned. At this stage, the injector, inlet septum, and inlet liner will also need to be replaced. For best running results, a long-life inlet septum should be used (Agilent Longlife Non-stick 11 mm Inlet sept, Part No.5183-4761-100).
9. The evaluation and manual check for misidentified metabolites can become the bottleneck of the whole GC-MS analysis if complicated running results were obtained. This is usually caused by the accumulation of impurities in the GC column from badly extracted samples and an incomplete derivatization process.

Acknowledgments

This work was supported by a Canadian Institutes for Health Research grant to GT (MOP-79253).

References

1. Casero RA, Pegg AE (2009) Polyamine catabolism and disease. *Biochem J* 421:323–338
2. Igarashi K, Kashiwagi K (2010) Modulation of cellular function by polyamines. *Int J Biochem Cell Biol* 42:39–51 (originally published online 9 July 2009, at <http://dx.doi.org/10.1016/j.biocel.2009.07.009>)
3. Pegg AE (2009) Mammalian polyamine metabolism and function. *IUBMB Life* 61:880–894
4. Casero RA Jr, Marton LJ (2007) Targeting polyamine metabolism and function in cancer and other hyperproliferative diseases. *Nat Rev Drug Discov* 6:373–390
5. Pegg AE (2008) Spermidine/spermine-N(1)-acetyltransferase: a key metabolic regulator. *Am J Physiol Endocrinol Metab* 294:E995–E1010
6. Sequeira A, Gwady FG, Ffrench-Mullen JM, Canetti L, Gingras Y, Casero RA Jr et al (2006) Implication of SSAT by gene expression and genetic variation in suicide and major depression. *Arch Gen Psychiatry* 63:35–48
7. Fiori LM, Turecki G (2008) Implication of the polyamine system in mental disorders. *J Psychiatry Neurosci* 33:102–110
8. Wallace HM, Fraser AV, Hughes A (2003) A perspective of polyamine metabolism. *Biochem J* 376:1–14
9. Sequeira A, Klempan T, Canetti L, Ffrench-Mullen J, Benkelfat C, Rouleau GA et al (2007) Patterns of gene expression in the limbic system of suicides with and without major depression. *Mol Psychiatry* 12:640–655
10. Klempan TA, Rujescu D, Merette C, Himmelman C, Sequeira A, Canetti L et al (2009) Profiling brain expression of the spermidine/spermine N(1)-acetyltransferase 1 (SAT1) gene in suicide. *Am J Med Genet B Neuropsychiatr Genet* 150B:934–943
11. Gilad GM, Gilad VH, Casanova MF, Casero RA Jr (1995) Polyamines and their metabolizing enzymes in human frontal cortex and hippocampus: preliminary measurements in affective disorders. *Biol Psychiatry* 38:227–234
12. Wood PL, Khan MA, Moskal JR (2006) Neurochemical analysis of amino acids, polyamines and carboxylic acids: GC-MS quantitation of tBDMS derivatives using ammonia positive chemical ionization. *J Chromatogr B Analyt Technol Biomed Life Sci* 831:313–319
13. Chen GG, Turecki G, Mamer OA (2009) A quantitative GC-MS method for three major polyamines in post-mortem brain cortex. *J Mass Spectrom* 44:1203–1210

Spermine Synthase Deficiency Resulting in X-Linked Intellectual Disability (Snyder–Robinson Syndrome)

Charles E. Schwartz, Xiaojing Wang, Roger E. Stevenson,
and Anthony E. Pegg

Abstract

Polyamines, small positively charged molecules, are vital for cell proliferation and differentiation. They are found ubiquitously in eukaryotic cells. Additionally, they interact with a wide range of other molecules and some membrane associated receptors. Polyamines, spermidine and spermine, are synthesized by two aminopropyltransferases, spermidine synthase and spermine synthase. Recently, mutations in the latter enzyme have been shown to be responsible for an X-linked intellectual disability condition known as Snyder–Robinson syndrome. Spermine synthase deficiency is thus far the only known polyamine deficiency syndrome in humans.

Key words: Spermine, Spermine synthase, X-linked intellectual disability, Snyder–Robinson syndrome, Polyamine deficiency

1. Introduction

Polyamines are ubiquitous in eukaryotic cells and their presence is critical for cell growth and differentiation (1, 2). Polyamines are rather simple small molecules that interact with a variety of molecules ranging from nucleic acids to proteins. As a result, they are involved in numerous cellular processes: transcription, translation, and modulation of ion channel activities (3–5).

The polyamines, spermidine and spermine, are synthesized by two aminopropyltransferases (6). Spermidine synthase converts putrescine to spermidine and spermine synthase (SMS) converts spermidine to spermine. The aminopropyl group, in both reactions, comes from decarboxylated *S*-adenosylmethionine (dcAdoMet) and its transfer forms 5'-methylthioadenosine (MTA) as a by-product.

Recently, mutations in *hSMS* have been found to be associated with an X-linked mental retardation (MR) condition, Snyder–Robinson syndrome (SRS) (7–9). SMS deficiency is the first known polyamine deficiency in humans. Affected males have MR, hypotonia, cerebellar circuitry dysfunction, thin habitus, and kyphoscoliosis. Biochemically, the patients have almost no SMS activity, low levels of intracellular spermine, and elevated spermidine/spermine levels. This phenotype clearly establishes a critical role of spermine in cognitive and cerebellar function.

SRS was one of the earliest reported X-linked mental retardation (XLMR) conditions (10). It was initially described as a nonsyndromic XLMR entity meaning the affected males were not thought to have any physical features distinguishing them from their normal brothers (OMIM 309583). However, they were hypotonic and had an unsteady gait in addition to MR. A follow-up analysis of the family in 1996 (11) identified additional clinical findings which included facial asymmetry, narrow or cleft palate, nasal dysarthric speech, diminished muscle mass, kyphoscoliosis, and long great toes. Some of the males were also noted to have experienced seizures.

Along with the clinical delineation of SRS in 1996, Arena et al. (11) were able to map the syndrome to Xp21.3-p22.12. This allowed positional mapping and candidate gene screening to occur. As a result, Cason et al. (7) were able to show that a nucleotide alteration, c.329+5 G>A, in the spermine synthase (*hSMS*) gene segregated in the SRS family. This G→A substitution caused aberrant splicing of *hSMS* which resulted in the absence of exon 4 and truncation of the protein (7).

Subsequent to the identification of the link between SRS and *hSMS*, three additional families were identified (8, 9) (Boyd and Schwartz, unpublished data). This has allowed for a further refinement of the clinical phenotype characteristics of SRS, summarized in Table 1. Thus, SRS should be suspected in any male with mild–moderate MR, thin habitus, muscle hypoplasia, kyphoscoliosis, some facial asymmetry, a prominent lower lip, and long great toes.

Males with SRS have almost no measurable SMS activity as measured in their lymphocytes or fibroblasts in culture as summarized in Table 2. The males from the original SRS do have measurable SMS activity (2–10% control) most likely due to the fact that their mutation affects splicing of the *hSMS* gene resulting in the presence of a low level of normal transcript and thus normal protein (7). The other known SRS families have deleterious mutations present in all the transcripts, thus adversely affecting the function of all SMS protein synthesized (8, 9) (Boyd and Schwartz, unpublished data). Coincidental with the lack of or low levels of SMS activity, males with SRS have decreased levels of cellular spermine and significantly elevated levels of cellular spermidine (Table 2). As a result, the spermidine/spermine (Spd/Spm) ratio is two- to fivefold higher as compared to controls. Genetic and

Table 1
Clinical features in the reported affected families with SRS

Physical features	Family 1 (10, 11)	Family 2 (8)	Family 3 (9)	Family 4 (Boyd and Schwartz, unpublished)	Total
Number of males	5	3	2	2	12
Mental retardation	5/5	3/3	2/2	2/2	12/12
Asthenic body build	5/5	3/3	2/2	2/2	12/12
Diminished muscle bulk	5/5	3/3	2/2	2/2	12/12
Prominent lower lip	5/5	3/3	2/2	0/2	10/12
Speech abnormalities	5/5	3/3	2/2	2/2	12/12
Osteoporosis	4/4	1/1	2/2	2/2	9/9
Long hands	5/5	1/3	2/2	1/2	9/12
Kyphoscoliosis	4/5	3/3	1/2	2/2	10/12
High, narrow, or cleft palate	3/5	1/1	2/2	2/2	8/10
Facial asymmetry	4/5	0/3	2/2	1/2	7/12
Unsteady gait	1/5	3/3	2/2	2/2	8/12

Table 2
Spermidine/spermine ratios and SMS activity

	Spermidine	Spermine (pmol/mg protein)	Spd/Spm	SMS activity (pmol/h/mg protein)
<i>Family 1</i>				
Patient 1	11.86	9.90	1.20	63
Patient 2	9.31	6.27	1.48	49
<i>Family 2</i>				
Patient 1	23.16	8.18	2.83	<1
Patient 2	23.84	9.39	2.54	<1
<i>Family 3</i>				
Patient 1	23.55	8.51	2.77	4
Patient 2	23.58	7.61	3.76	<1
<i>Family 4</i>				
Patient 1	12.82	4.38	2.92	<1
Patient 2	13.25	5.86	2.26	<1
<i>Controls</i>				
1	6.93	11.93	0.58	437
2	8.28	13.08	0.63	457

biochemical confirmation of SRS requires analysis of the *hSMS* gene and measurement of SMS activity and polyamine content in cells derived from patients. The assay described below is a very sensitive method to assay SMS. It is modified from that described in previous publications (12, 13) and measures the formation of [³⁵S]MTA from [³⁵S]dcAdoMet. Measurement of cellular polyamines can be made using a variety of methods including pre- and postcolumn derivatization with separation by HPLC (14, 15) and by analysis by gas chromatography/mass spectrometry (16, 17).

2. Materials

2.1. Spermine Synthase Assay

1. Sodium phosphate buffer: 0.5 mM pH 7.5.
2. Spermidine trihydrochloride (Sigma): 100 mM.
3. *S*-adenosyl-3-thio-1,8-diaminooctane (AdoDATO) (18) (20 μM) or other spermidine synthase inhibitors (see Notes 1 and 2).
4. [³⁵S]-decarboxylated *S*-adenosylmethionine ([³⁵S]-dcAdoMet) (see Notes 3 and 4).
5. Minicolumns filled with cellulose phosphate resin (see Note 5).
6. HCl.
7. EDTA.
8. β-Mercaptoethanol.
9. Sodium phosphate buffer: 0.1 M pH 7.2 (3.42 ml 1 M Na₂HPO₄, 1.58 ml 1 M NaH₂PO₄ in 40 ml water). Adjust pH to 7.2 with 1 M NaOH. Adjust volume to 50 ml with water.
10. Buffer A: 50 mM NaPO₄ pH 7.2, 0.3 mM EDTA, 10 mM β-mercaptoethanol (25 ml water, 25 ml 0.1 M sodium phosphate buffer pH 7.2, 30 μl 0.5 M EDTA pH 8.0, 35 μl 14.3 M β-mercaptoethanol).
11. BCS Biodegradable Counting Scintillant (Amersham Biosciences).
12. PYREX® disposable culture tube (Corning).
13. Disposable Pasteur pipettes (Corning).
14. Borosilicate glass scintillation vials, 20 mL (Fisher, 03-337-7).
15. Multi-Purpose Scintillation Counter (BECKMAN COULTER™ LS6500).

3. Methods

3.1. Molecular Genetic Analysis

SRS results from mutations in the *hSMS* gene. To date, four mutations are known, three of which eliminate all enzymatic activity

Table 3
SMS mutations information in known SRS families

Family	DNA mutation	Protein alteration	SMS activity
1	c.329+5 G>A	truncating p.I88fx111	10% Normal
2	c.267 G>A	p.G56S	0
3	c.496 T>G	p.V132G	0
4	c.4449 T>C	p.I150T	0

(Table 3). The c.329+5 G>A mutation, by virtue of it causing alternative splicing (removing exon 4) and subsequent truncation of the SMS protein, removes the active site. The p.G56S mutation occurs in the amino terminal end of SMS, which is critical for dimer formation (19). As SMS functions as a dimer, the result is loss of activity and protein instability. The two other mutations, p.V132G and p.I150T alter the three dimensional structure of the protein reducing dimer formation, decreasing stability and virtually eliminating enzymatic activity.

1. Mutation screening of the *SMS* gene can be conducted on genomic DNA. Presently primers are designed flanking each of the 11 exons that contain the coding sequence for *SMS*. The amplicons extend at least 50 bp into intronic sequence on either side of each exon. Utilization of M13 tails allows for efficient amplifications of all 11 exons for sequencing under the same PCR conditions (8, 9).

3.2. Spermine Synthase Assay

1. Pellets of fibroblast or lymphoblast cells are homogenized in buffer A.
2. The homogenate is centrifuged at 10,000 rpm (30,000×g) for 20 min at 4°C.
3. The supernatant extract is removed and stored frozen at -70°C until needed.
4. The protein concentration in the supernatant extract is determined.
5. Assay tubes are set up containing 0.1 ml assay solution consisting of 40 µl 0.5 M Na phosphate buffer pH 7.5, 4 µl 1 mM AdoDATO, 10 µl 10 mM spermidine and 6 µl [³⁵S]dcAdoMet and 40 µl water giving final concentrations of 0.1 M Na phosphate buffer, 20 µM AdoDATO, 1.0 mM spermine, and 80,000–100,000 dpm of [³⁵S]dcAdoMet (see Note 6).
6. Add to each assay tube 0.1 ml of supernatant extract from cell culture (see Note 7). Blank assays are also set up using Buffer A.
7. Cover tubes and incubate at 37°C for 1 h.

8. Place the tubes and add 1 ml of 25 mM HCl to stop the reaction.
9. Minicolumns of Cellex P or equivalent resin (see Notes 5 and 8) are washed with two aliquots of 2 ml 0.5 N HCl, then once with 2 mL of distil water and equilibrated by passage of three aliquots of 2 ml of 25 mM HCl. The columns are then placed over scintillation vials.
10. Each assay sample is transferred to its corresponding column. After the sample flows though the column into the scintillation vial, 2 ml of 25 mM HCl is added to each column and allowed to drain into same vial (see Note 9).
11. The vials are taken and add 15 ml BCS Counting Scintillant. After capping and vigorous mixing, the radioactivity is determined in a scintillation counter.
12. The radioactivity present in the sample minus that present in the blank represents the SMS activity. Results are expressed as dpm [³⁵S]MTA formed per microgram of protein added (see Note 7). Samples from SRS patients have <10% of the activity present in control samples.
13. The columns can be reused. Clean using two aliquots of 2 ml 0.5 N HCl, then two aliquots of 2 mL of distil water and three aliquots of 2 mL of 25 mM HCl. Discard effluent in radioactive waste. Store them in the refrigerator in a covered container so they do not dry out.

3.3. Polyamine Assay

1. The cellular spermine concentration and spermidine:spermine ratio can readily be assayed by a variety of methods. Older methods based on HPLC separation of either dansyl derivatives (14) or the polyamines themselves with detection postcolumn by reaction with *o*-phthalaldehyde (15) and more recent methods using gas chromatography/mass spectrometry, which are described in this volume (16, 17) are suitable for this purpose.

4. Notes

1. If crude cell extracts, which contain significant amounts of putrescine are used, the assay does not distinguish between spermidine synthase and SMS activity. Rather than dialyze the extracts to remove putrescine, we add AdoDATO which is a potent and specific mechanism-based spermidine synthase inhibitor (18). This is not commercially available but its synthesis is published (18, 20).
2. Other spermidine synthase inhibitors such as trans-4-methylcyclohexylamine should also work for this purpose (21, 22).

3. This is not now commercially available but procedures for its synthesis are described in references (13, 23).
4. The advantage of using [³⁵S]-dcAdoMet is that [³⁵S]methionine needed for its synthesis is relatively inexpensive and is available at a very high specific activity. The disadvantage is that synthesis requires the use of two enzymes, *S*-adenosylmethionine (AdoMet) synthetase and AdoMet decarboxylase. The requirement for the former can be eliminated by using [³H-*methyl*] AdoMet or [¹⁴C-*methyl*] AdoMet which are commercially available but these are much more expensive and, particularly in the case of the latter, have a much lower specific activity lowering the sensitivity of the assay.
5. We use Cellex P from BioRad. The material is stable for several years at room temperature, as is the suspended slurry when stored in 25 mM HCl at 4°C. The minicolumns are made by plugging a Pasteur pipette with glass wool and then by adding about 1 ml of a cation exchange resin. Any weak cation exchange resin can be used although it may be necessary to modify the acid concentrations to ensure that dcAdoMet is fully retained and that all MTA formed is present in the first flow-through and wash used for scintillation counting.
6. In order to maximize sensitivity we do not add unlabeled dcAdoMet for assays in which samples from different sources are being compared within the same assay. If an accurate quantification of SMS activity as pmol product per mg protein formed per hour is required then unlabeled dcAdoMet is added at a final concentration of 2 μM. This is sufficient to give a near maximal rate of reaction. The amount of [³⁵S] dcAdoMet may need to be increased to obtain enough radioactive product for accurate measurement but the amount of the labeled material is negligible compared to the unlabeled and no adjustment to the overall concentration is needed.
7. The amount of cell extract needs to be determined by preliminary testing to obtain a production of [³⁵S]MTA that is less than 15% of the input of [³⁵S]dcAdoMet substrate and sufficient to give at least twice the background obtained when no extract is added to ensure accurate measurement. It is important to also ensure that the reaction is proportional to the amount of protein added by using at least two concentrations of extract giving results within this range.
8. Since these columns will drain at different rates, it is a good idea to treat many more columns that are necessary and then pick out the ones they are draining the fastest for use. We use a piece of Plexiglas with holes drilled in it to hold the columns. While we preparing the columns, the Plexiglas can be placed over a waster container, and then before the samples added, the Plexiglas and columns can be situated over empty scintillation

vials. For this step, we place the vials in one of the cardboard containers they were shipped in and then place the Plexiglas with the columns on top.

9. The principle of the separation is that the weakly charged [³⁵S]MTA product passes through the column, whereas the remaining [³⁵S]dcAdoMet substrate, which is strongly positively charged, is retained. Assay of the flow-through by scintillation counting indicates the amount of [³⁵S]MTA product formed. MTA is rapidly degraded in mammalian cells by MTA phosphorylase, which converts it to adenine and methylthioribose-1-phosphate (24, 25). This does not affect this assay since the [³⁵S]methylthioribose-1-phosphate has no charge and is not retained on the columns.

References

1. Cohen SS (1998) A guide to the polyamines. Oxford University Press, New York
2. Pegg AE (2009) Mammalian polyamine metabolism and function. *IUBMB Life* 61:880–894
3. Williams K (1997) Interactions of polyamines with ion channels. *Biochem J* 325:289–297
4. Nichols CG, Lopatin AN (1998) Inward rectifier potassium channels. *Annu Rev Physiol* 59:171–191
5. Gerner EW, Meyskens FL Jr (2004) Polyamines and cancer: old molecules, new understanding. *Nat Rev Cancer* 4:781–792
6. Ikeguchi Y, Bewley M, Pegg AE (2006) Aminopropyltransferases: function, structure and genetics. *J Biochem* 139:1–9
7. Cason AL, Ikeguchi Y, Skinner C, Wood TC, Lubs HA, Martinez F, Simensen RJ, Stevenson RE, Pegg AE, Schwartz CE (2003) X-Linked spermine synthase gene (SMS) defect: the first polyamine deficiency syndrome. *Eur J Human Genet* 11:937–944
8. de Alencastro G, McCloskey DE, Kliemann SE, Maranduba CM, Pegg AE, Wang X, Bertola DR, Schwartz CE, Passos-Bueno MR, Sertie AL (2008) New SMS mutation leads to a striking reduction in spermine synthase protein function and a severe form of Snyder-Robinson X-linked recessive mental retardation syndrome. *J Med Genet* 45:539–543
9. Becerra-Solano LE, Butler J, Castañeda-Cisneros G, McCloskey DE, Wang X, Pegg AE, Schwartz CE, Sánchez-Corona J, Garcia-Ortiz JE (2009) A missense mutation, p.V132G, in the X-linked spermine synthase gene (SMS) causes Snyder-Robinson syndrome. *Am J Med Genet A* 149A:328–335
10. Snyder RD, Robinson A (1969) Recessive sex-linked mental retardation in the absence of other recognizable abnormalities. Report of a family. *Clin Pediatr (Phila)* 8:669–674
11. Arena JF, Schwartz C, Ouzts L, Stevenson R, Miller M, Garza J, Nance M, Lubs H (1996) X-linked mental retardation with thin habitus, osteoporosis, and kyphoscoliosis: linkage to Xp21.3-p22.12. *Am J Med Genet* 64:50–58
12. Mackintosh CA, Pegg AE (2000) Effect of spermine synthase deficiency on polyamine biosynthesis and content in mice and embryonic fibroblasts and the sensitivity of fibroblasts to 1,3-bis(2-chloroethyl)-N-nitrosourea. *Biochem J* 351:439–447
13. Wiest L, Pegg AE (1998) Assay of spermidine and spermine synthase. In: Morgan DML (ed) *Methods in molecular biology*. 79. Polyamine protocols. Humana, Totowa, pp 51–58
14. Kabra PM, Lee HK, Lubich WP, Marton LW (1986) Solid-phase extraction and determination of dansyl derivatives of unconjugated and acetylated polyamines by reversed-phase liquid chromatography; improved separation systems for polyamines in cerebrospinal fluid, urine and tissue. *J Chromatogr Biomed Appl* 380:19–32
15. Seiler N, Knödgen B (1985) Determination of polyamines and related compounds by reversed-phase high-performance liquid chromatography: improved separation systems. *J Chromatogr* 339:45–57
16. Häkkinen MR (2010) Polyamine analysis by LC-MS. In: Pegg AE, Casero RA Jr (eds) *Methods in molecular biology* 720. Polyamine protocols Chapter 33. Humana, Totowa

17. Chen GG, Fiori LM, Mamet OA, Turecki G (2010) High-resolution capillary gas chromatography (GC) in combination with mass spectrometry (MS) for quantification of three major polyamines in post-mortem brain cortex. In: Pegg AE Casero RA Jr (eds) *Methods in molecular biology* 720. Polyamine protocols Chapter 27. Humana, Totowa
18. Tang KC, Pegg AE, Coward JK (1980) Specific and potent inhibition of spermidine synthase by the transition-state analog, S-adenosyl-3-thio-1, 8-diaminooctane. *Biochem Biophys Res Commun* 96:1371–1377
19. Wu H, Min J, Zeng H, McCloskey DE, Ikeguchi Y, Loppnau P, Michael AJ, Pegg AE, Plotnikov AN (2008) Crystal structure of human spermine synthase: implications of substrate binding and catalytic mechanism. *J Biol Chem* 283:16135–16146
20. Tang KC, Mariuzza R, Coward JK (1981) Synthesis and evaluation of some stable multisubstrate adducts as specific inhibitors of spermidine synthase. *J Med Chem* 24:1277–1284
21. Shirahata A, Morohoshi T, Samejima K (1988) Trans-4-methylcyclohexylamine, a potent new inhibitor of spermidine synthase. *Chem Pharm Bull* 36:3220–3222
22. Shirahata A, Morohoshi T, Fukai M, Akatsu F, Samejima K (1991) Putrescine or spermidine binding site of aminopropyltransferases and competitive inhibitors. *Biochem Pharmacol* 41:205–212
23. Pegg AE (1983) Assay of aminopropyltransferases. *Methods Enzymol* 94:260–265
24. Pegg AE, Williams-Ashman HG (1969) Phosphate-stimulated breakdown of 5'-methylthioadenosine by rat ventral prostate. *Biochem J* 115:241–247
25. Albers E (2009) Metabolic characteristics and importance of the universal methionine salvage pathway recycling methionine from 5'-methylthioadenosine. *IUBMB Life* 61:1132–1142

Part VIII

Chemistry and Analysis

Chapter 29

Methylated Polyamines as Research Tools

Alex R. Khomutov, Janne Weisell, Maxim A. Khomutov,
Nikolay A. Grigorenko, Alina R. Simonian, Merja R. Häkkinen,
Tuomo A. Keinänen, Mervi T. Hyvönen, Leena Alhonen,
Sergey N. Kochetkov, and Jouko Vepsäläinen

Abstract

Earlier unknown racemic β -methylspermidine (β -MeSpd) and γ -methylspermidine (γ -MeSpd) were synthesized starting from crotononitrile or methacrylonitrile and putrescine. Lithium aluminum hydride reduction of the intermediate di-Boc-nitriles resulted in corresponding di-Boc-amines, which after deprotection gave target β - and γ -MeSpd's. To prepare α -MeSpd, the starting compound, 3-amino-1-butanol, was converted into *N*-Cbz-3-amino-1-butyl methanesulfonate, which alkylated putrescine to give (after deprotection of amino group) the required α -MeSpd. Novel β - and γ -MeSpd's in combination with earlier α -MeSpd are useful tools for studying enzymology and cell biology of polyamines.

Key words: Polyamines, C-methylated spermidine analogs

1. Introduction

Alkylated polyamine derivatives are widely used as a research tool in polyamine biochemistry and cell biology. Most important are different *N,N'*-terminally bis-alkylated derivatives of Spm and its homologs, including conformationally restricted analogs with up to 12 amino groups in the polyamine backbone (1, 2). C-Alkylated (methylated) derivatives of Spm and Spd are much less investigated; in 1992, α -MeSpd was proved to be capable of substitution for Spd in supporting the growth of cells with a depleted polyamine pool (3). Moreover, α -MeSpd was not a substrate of spermidine/spermine *N*¹-acetyltransferase (SSAT) imparting catabolic stability (3). Even more sterically hindered *gem*-dimethyl Spds were also

capable to overcome acute polyamine deficiency (4). Recently, (*R*)- and (*S*)-isomers of α -MeSpd and α -MeSpm, as well as (*R,R*)-, (*R,S*)-, and (*S,S*)-diastereomers of α,α' -Me₂Spm were synthesized (5). Using these compounds it was possible to prevent the development of acute pancreatitis in SSAT-transgenic rats (6); to reveal dormant stereospecificity of acetyl-polyamine oxidase (7) and to discover an original approach to regulate its stereospecificity (8); to find dormant stereospecificity of deoxyhypusine synthase (9). Furthermore, it proved possible to regulate individually the activity of the key enzymes of polyamine metabolism by using different enantiomers of α -methylated polyamines (10).

However, the diversity and complexity of polyamine cellular functions in conjunction with several enzymes and regulatory proteins being involved in their metabolism makes it impossible to use single type of analog for all purposes. Hence, we designed and prepared two novel *C*-methylated Spd derivatives, considering that each of these compound might have its own target that will distinguish their effect(s) on polyamine metabolism and will be helpful for the investigation of the exact cellular functions of Spm and Spd. This paper presents synthesis of two first representatives of this family β -MeSpd and γ -MeSpd, as well as an earlier known α -MeSpd.

Methods being suitable for the preparation of racemic α -, β -, and γ -MeSpds in a gram scale are presented.

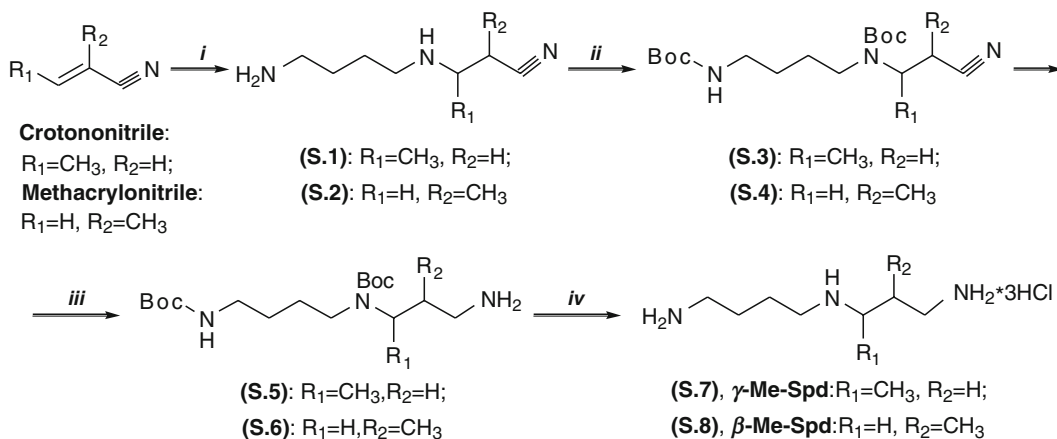
2. Materials

1. Crotononitrile (*cis+trans*), >98%.
2. Methacrylonitrile, >99%.
3. 1,4-Diaminobutane, 99%.
4. Ethyl 3-aminobutyrate, tech., 90%.
5. Benzyl chloroformate (Cbz-Cl), tech., 95%.
6. Palladium, 10% on activated carbon (Pd/C).
7. Methanesulfonyl chloride (Ms-Cl), $\geq 99\%$.
8. Di-*tert*-butyl dicarbonate (Boc₂O), >98%.
9. Lithium aluminum hydride (LiAlH₄), 95%.
10. Filter agent Celite® 545.
11. HCl, 37%.
12. Acetic acid, glacial (AcOH), 99.8%.
13. Ethyl alcohol, $\geq 99.8\%$ (abs. EtOH).
14. Methyl alcohol (MeOH), analytical grade.
15. Diethyl ether (Et₂O), anhydrous, reagent grade.

16. Chloroform (CHCl_3), reagent grade.
17. Dichloromethane (DCM), reagent grade.
18. 1,4-Dioxane (dioxane), reagent grade.
19. Tetrahydrofuran (THF), reagent grade.
20. Pyridine (Py), 99+%.
21. 1-Butanol (*n*-BuOH), 99.5%.
22. Ammonium hydroxide, 25% (NH_4OH), reagent grade.
23. Ninhydrin spray reagent.
24. Tetrabromophenol blue, sodium salt.
25. Sodium (Na).
26. Calcium chloride (CaCl_2), anhydrous.
27. Phosphorus pentoxide (P_2O_5).
28. Magnesium sulfate, anhydrous (MgSO_4).
29. Saturated sodium bicarbonate solution (sat. NaHCO_3).
30. 10% Water solution of citric acid.
31. Saturated sodium chloride (NaCl) solution (brine).
32. Glass chromatography column (6×12-cm) with a glass filter (porosity 3, G3) and a joint at the top.
33. Silica gel (e.g., Kieselgel 60, 0.040–0.063 mm; Merck).
34. TLC plates: Silica-coated aluminum sheets, Silica gel 60 F₂₅₄, Merck.
35. Vacuum desiccator.
36. Rotary evaporator equipped with water aspirator.
37. Vacuum oil pump.
38. Balloon of hydrogen.

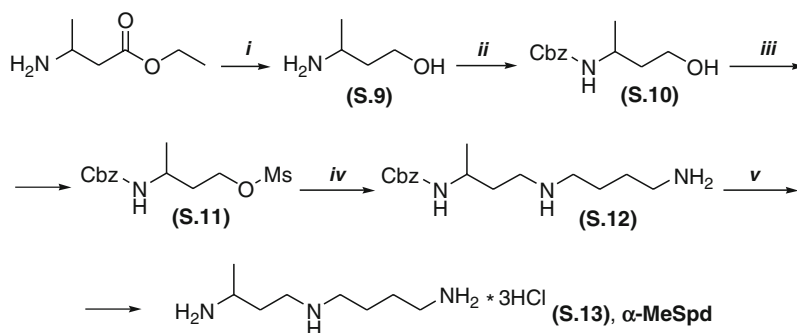
3. Methods

The suggested syntheses of earlier unknown γ -MeSpd (S.7) and β -MeSpd (S.8) are four step protocols (Fig. 1). The first step was the addition of putrescine to crotononitrile or methacrylonitrile and the nitriles (S.1 and S.2) were isolated by distillation with excellent or good yields. At the second step, primary and secondary amino groups of these nitriles were protected with Boc-group under standard conditions using Boc_2O . Thus, obtained di-Boc-nitriles (S.3 and S.4) were reduced by LiAlH_4 at the temperature below -5°C under the conditions similar to that, being described in (11), to give di-Boc-amines (S.5 and S.6) as key intermediates, which were purified by flash-chromatography on silica gel. At the



i- $\text{NH}_2(\text{CH}_2)_4\text{NH}_2/20^\circ\text{C} \rightarrow 90^\circ\text{C}$; *ii*- $\text{Boc}_2\text{O}/\text{THF}$; *iii*- $\text{LiAlH}_4/\text{Et}_2\text{O}/-5^\circ\text{C}$; *iv*- $\text{HCl}/\text{EtOH}/\text{H}_2\text{O}$.

Fig. 1. Syntheses of $\beta\text{-MeSpd}$ and $\gamma\text{-MeSpd}$.



i- $\text{LiAlH}_4/\text{THF}/\Delta$; *ii*- $\text{Cbz-Cl}/\text{H}_2\text{O}/\text{NaHCO}_3$; *iii*- $\text{Ms-Cl}/\text{Et}_3\text{N}/\text{DCM}$; *iv*- $\text{NH}_2(\text{CH}_2)_4\text{NH}_2/\text{THF}$;
v- $\text{H}_2/\text{MeOH}/\text{AcOH}/\text{Pd}/\text{C}$

Fig. 2. Synthesis of $\alpha\text{-MeSpd}$.

last step, Boc-groups were removed by acidic hydrolysis that after crystallization afforded target $\gamma\text{-MeSpd}$ (S.7) and $\beta\text{-MeSpd}$ (S.8) with overall yields 45 and 27%, as calculated for crotononitrile or methacrylonitrile, respectively.

The preparation of $\alpha\text{-MeSpd}$ (S.13) was performed according to (7, 12) starting from commercially available ethyl 3-aminobutyrate (Fig. 2), which was reduced by LiAlH_4 into 3-amino-1-butanol (S.9) with subsequent conversion into *N*-Cbz-3-amino-1-butyl methanesulfonate (S.11). Alkylation of the excess of putrescine with the mesylate (S.11) resulted in corresponding *N*-Cbz-derivative (S.12), which after deprotection gave target $\alpha\text{-MeSpd}$ (S.13) with overall yield 48% as calculated for ethyl 3-aminobutyrate.

It is essential to carry out all operations involving organic solvents and reagents in a well-ventilated fume hood, and wear gloves and protective glasses.

3.1. Synthesis of 3-Methyl-8-Amino-4-Azaoctanenitrile (S.1)

1. Weight 1,4-diaminobutane (58.9 g, 0.67 mol) into 100-mL round bottom flask containing a stir bar, add abs. EtOH (8 mL) and cool the obtained solution to +4°C with stirring.
2. To the resulting solution add dropwise crotononitrile (8.97 g, 0.134 mol) (see Note 1) using a pressure-equalizing dropping funnel and continue stirring at 20°C for 2 h.
3. Replace pressure-equalizing dropping funnel with vertical condenser and continue stirring for 2 h at 60°C and then for 2.5 h at 90°C.
4. Cool the reaction mixture and distil the excess of 1,4-diaminobutane at 10–15 mmHg, cool the distillation flask, transfer the liquid into a smaller flask equipped with Vigreux distilling head with a condenser and continue distillation at 0.75–0.5 mmHg using an oil pump. Collect the fraction with bp 102–103°C/0.75 mmHg to get pure (see Note 2) S.1 (17.6 g, 84.7%), n_D^{20} 1.4688. *Rf* 0.38 (dioxane–25% ammonia, 8:2 (v/v)). ¹H-NMR (CDCl₃) δ: 3.02–2.95 (1H, m, CH₂CH), 2.67 (2H, t, *J* 6.8, CH₂NH₂), 2.59 (2H, t, *J* 6.6, NHCH₂), 2.45–2.36 (2H, m, NCCH₂), 1.51–1.41 (4H, m, CH₂CH₂CH₂CN), 1.85 (3H, d, *J* 6.6, CH₃), 1.05–0.95 (3H, m, NH+NH₂). ¹³C-NMR (CDCl₃) δ: 118.32, 50.36, 47.12, 42.09, 31.50, 28.24, 25.29, 20.94. Found, %: C 61.87; H 11.11; N 27.00. C₈H₁₇N₃. Calculated, %: C 61.89; H 11.04; N 27.07.

3.2. Synthesis of 2-Methyl-8-Amino-4-Azaoctanenitrile (S.2)

1. Repeat steps 1–4 for the synthesis of S.1, starting from 1,4-diaminobutane (55.4 g, 0.63 mol) and methacrylonitrile (17.16 g, 0.256 mol) in EtOH (8 mL) to obtain S.2 (18.8 g, 47%), bp 101°C/0.5 mmHg, n_D^{20} 1.4646, *Rf* 0.41 (dioxane–25% ammonia, 8:2 (v/v)). ¹H-NMR (CDCl₃) δ: 2.87–2.61 (7H, m, CH₂NH₂ + CH₂NHCH₂ + CHCN); 1.56–1.45 (4H, m, CH₂CH₂CH₂NH₂); 1.37 (3H, s, NH+NH₂); 1.31 (3H, d, *J* 6.6, CH(CH₃)). Found, %: C 61.63; H 11.20; N 27.03. C₈H₁₇N₃. Calculated, %: C 61.89; H 11.04; N 27.07.

3.3. Synthesis of 3-Methyl-8-(*N*-tert-Butyloxycarbonyl) Amino-4-(*N*-tert-Butyloxycarbonyl) Azaoctanenitrile (S.3)

1. Dissolve S.1 (1.55 g, 10 mmol) in THF (20 mL) into 50-mL round bottom two-necked flask containing a stirring bar and place the flask in the bath with room temperature water. Add dropwise (see Note 3) with stirring a solution of Boc₂O (4.41 g, 20 mmol) in THF (10 mL) and leave the reaction mixture overnight at 20°C.

2. Evaporate the reaction mixture to dryness in vacuo, using rotary evaporator. Take the residual oil into DCM (40 mL) and transfer it into a 100-mL separatory funnel. Wash subsequently with 10% citric acid (3 × 15 mL), H₂O (5 mL), sat. NaHCO₃ (10 mL), H₂O (5 mL), and brine (15 mL).
3. Dry the DCM solution over MgSO₄ overnight and evaporate it to dryness in vacuo using rotary evaporator.
4. Dry the residual oil in vacuum desiccator over P₂O₅ (change P₂O₅ after 4 h and then leave overnight over a fresh portion of P₂O₅) to obtain S.3 (3.5 g, 99%) as a colorless viscous oil, *R*_f 0.33 (EtOAc–hexane, 1:2 (v/v)). ¹H-NMR (CDCl₃) δ: 4.57 (1H, bs, NHBoc); 4.06–3.98 (1H, m, CH(CH₃)); 3.22–3.10 (4H, m, CH₂NHBoc + CH₂N(Boc)–); 2.75–2.50 (2H, m, CH₂CN); 1.60–1.49 (4H, m, CH₂CH₂CH₂NHBoc); 1.46 (9H, s, >N–C(O)–OC(CH₃)₃); 1.43 (9H, s, –NH–C(O)–OC(CH₃)₃); 1.33 (3H, d, *J* 6.8, CH(CH₃)). Found, %: C 60.54; H 9.16; N 11.74. C₁₈H₃₃N₃O₄. Calculated, %: C 60.82; H 9.36; N 11.82.

3.4. Synthesis of 2-Methyl-8-(*N*-tert-Butyloxycarbonyl) Amino-4-(*N*-tert-Butyloxycarbonyl) Azaoctanenitrile (S.4)

1. Repeat steps 1–4 for the synthesis of S.3, starting from S.2 (1.55 g, 10 mmol) and Boc₂O (4.41 g, 20 mmol) in THF (30 mL) to obtain S.4 (3.55 g, 94%) as colorless viscous oil, *R*_f 0.35 (EtOAc–hexane, 1:2 (v/v)). ¹H-NMR (CDCl₃) δ: 4.65 (1H, bs, NHBoc); 3.52–3.01 (7H, m, CH₂CH₂NHBoc + CH₂N(Boc)– + CH₂NHBoc + CHCH₃); 1.60–1.37 (22H, m, CH₂CH₂CH₂NHBoc + 2 * C(CH₃)₃); 1.26 (3H, d, *J* 6.9, CHCH₃). [M + Na]⁺ calc. for C₁₈H₃₃N₃O₄ 378.2369 obs. 378.2358.

3.5. Synthesis of 1-Amino-3-Methyl-8-(*N*-tert-Butyloxycarbonyl) Amino-4-(*N*-tert-Butyloxycarbonyl) Azaoctane (S.5)

1. Weigh LiAlH₄ (0.95 g, 25 mmol) into 100-mL three-necked (vertical) round bottom flask equipped with effective mechanical stirrer, thermometer, and a pressure-equalizing dropping funnel equipped with a tube with KOH or CaCl₂ (see Note 4) and add slowly in abs. Et₂O (25 mL) (see Note 5) with cooling (see Note 6) and slow stirring.
2. Cool the obtained suspension to –20°C and with stirring add slowly (see Note 7) a solution of S.3 (3.55 g, 10 mmol) in abs. Et₂O (15 mL) maintaining the temperature below –10°C (see Note 8).
3. Continue stirring of the reaction mixture for additional 1 h, maintaining the temperature between –10 and –5°C (see Note 8).
4. Cool to –25°C and quench the reaction mixture with subsequent dropwise additions of H₂O (1.4 mL), 20% (w/w) NaOH (1.3 mL), H₂O (3.5 mL), and finally with 40% (w/w) NaOH (4.1 mL) – all additions with very effective stirring maintaining all the time the temperature below –10°C.

5. Allow the reaction mixture to warm to room temperature, separate the organic phase, extract the residue with Et₂O (3 × 15 mL), and wash the combined Et₂O extracts with sat. NaHCO₃ (2 × 15 mL), H₂O (5 mL), brine (15 mL), and dry over K₂CO₃ for 12 h.
6. Evaporate ether in vacuo using rotary evaporator and dissolve the residue in CHCl₃-MeOH, 98:2 (v/v) mixture (7 mL).
7. Prepare a slurry of 120 g of silica gel in CHCl₃-MeOH, 98:2 (v/v) mixture (500 mL), containing 0.7 mL of Et₃N/1 L of the eluent, and pour it in one portion into a 6 × 12 cm chromatography column equipped with a forecolumn of a proper size. Wash this column with CHCl₃-MeOH, 98:2 (v/v) mixture (150 mL), containing 0.5 mL of Et₃N/1 L of the eluent.
8. Apply carefully the solution from step 6 on the top of silica gel and wash the column with CHCl₃-MeOH, 98:2 (v/v) mixture (150 mL), containing 0.5 mL of Et₃N/1 L of the eluent, collecting 10 mL fractions.

Analyze fractions by TLC (see Note 9) using dioxane-25% ammonia, 98:2 (v/v) mixture and combine the fractions containing only S.5. Evaporate the volatile material from the combined fractions in vacuo using rotary evaporator, coevaporate the residue with dioxane (15 mL), and dry the residual oil in vacuum desiccator over P₂O₅ (change P₂O₅ after 4 h and then leave overnight over a fresh portion of P₂O₅) to obtain S.5 (2.73 g, 76%) as a colorless viscous oil, *R_f* 0.28 (dioxane-25% ammonia, 98:2 (v/v)). ¹H-NMR for the major isomer (CDCl₃) δ: 4.56 (1H, bs, NHBoc); 4.30 (1H, bm, CH(CH₃)); 3.19-2.98 (4H, m, CH₂NHBoc + CH₂N(Boc)-); 2.74-2.57 (2H, m, CH₂NH₂); 2.24 (2H, bs, CH₂NH₂); 1.66-1.39 (24H, m, CH₂CH₂CH₂NHBoc + CH₂CH₂NH₂ + -C(CH₃)₃ + -C(CH₃)₃); 1.15 (3H, d, *J* 6.8, CH(CH₃)). Found, %: C 59.89; H 10.19; N 11.80. C₁₈H₃₇N₃O₄. Calculated, %: C 60.14; H 10.37; N 11.68. [M+H]⁺ calc. for C₁₈H₃₈N₃O₄ 360.2862 obs. 360.2862.

**3.6. Synthesis of
1-Amino-2-Methyl-8-
(N-tert-
Butyloxycarbonyl)
Amino-4-(N-tert-
Butyloxycarbonyl)
Azaoctane (S.6)**

1. Repeat steps 1-8 for the synthesis of S.5, starting from S.4 (3.55 g, 10 mmol) and LiAlH₄ (0.95 g, 25 mmol) to obtain S.6 (2.92 g, 81%) as a viscous oil, *R_f* 0.42 (dioxane-25% ammonia, 98:2 (v/v)). ¹H-NMR for the major isomer (CDCl₃) δ: 4.58 (1H, s, -NHBoc); 3.23-3.08 (5H, m, CH₂NHBoc + CH₂CH₂N(Boc)- + CH₂N(Boc)); 2.96 (1H, dd, ²*J*_{HH} 14.2, *J* 6.8, CH₂NBoc); 2.67-2.50 (2H, m, CH₂NH₂); 1.89-1.79 (3H, m, CHCH₃ + NH₂); 1.59-1.51 (2H, m, CH₂CH₂CH₂); 1.49-1.40 (20H, m, + CH₂CH₂CH₂ + 2*C(CH₃)₃); 0.90 (3H, d, *J* 6.8, CHCH₃). Found, %: C 60.18; H 10.33; N 11.70. C₁₈H₃₇N₃O₄. Calculated, %: C 60.14; H 10.37; N 11.68. [M+H]⁺ calc. for C₁₈H₃₇N₃O₄ 360.2862 obs. 360.2867.

3.7. Synthesis of 1,8-Diamino-3-Methyl-4-Azaoctane Trihydrochloride, γ -MeSpd (S.7)

1. Dissolve S.5 (0.72 g, 2 mmol) in EtOH (30 mL), add to this solution in one portion 37% HCl (3.0 mL) and leave at 20°C, controlling the deprotection process by TLC in dioxane–25% ammonia, 98:2 (v/v).
2. Evaporate the reaction mixture to dryness in vacuo using rotary evaporator, coevaporate the semisolid residue with abs. EtOH (3 × 15 mL) and recrystallize from abs. EtOH to obtain S.7 (0.38 g, 70.7%), mp 231–232°C, *R_f* 0.24 (*n*-butanol–AcOH–pyridine–H₂O, 4:2:1:2 (v/v)). ¹H-NMR (CDCl₃) δ : 3.48–3.41 (1H, m, CH(CH₃)); 3.20–3.03 (6H, m, H₂NCH₂(CH₂)₂CH₂NH + NH₂CH₂); 2.24–2.17 (1H, m, CHCH₂); 2.00–1.91 (1H, m, CHCH₂); 1.83–1.74 (4H, m, C–CH₂CH₂–C); 1.37 (3H, d, *J* 6.7, CH(CH₃)). Found, %: C 35.52; H 9.17; N 15.47. C₈H₂₄Cl₃N₃. Calculated, %: C 35.77; H 9.00; N 15.64.

3.8. Synthesis of 1,8-Diamino-2-Methyl-4-Azaoctane Trihydrochloride, β -MeSpd (S.8)

1. Repeat steps 1 and 2 for the synthesis of S.7, starting from S.6 (1.44 g, 4 mmol) to obtain S.8 (0.81 g, 75%), mp 189–192°C, *R_f* 0.22 (*n*-butanol–AcOH–pyridine–H₂O, 4:2:1:2 (v/v)). ¹H-NMR (D₂O) δ : 3.19–2.90 (8H, m, CHCH₂NH₂ + CH₂NHCH₂– + CH₂NH₂); 2.39–2.28 (1H, m, CH(CH₃)); 1.85–1.72 (4H, m, CH₂CH₂CH₂NH); 1.16 (3H, d, *J* 6.8, CH(CH₃)). Found, %: C 35.84; H 9.09; N 15.74. C₈H₂₄Cl₃N₃. Calculated, %: C 35.77; H 9.00; N 15.64.

3.9. Synthesis of 3-Amino-1-Butanol (S.9)

1. Weigh LiAlH₄ (8 g, 0.21 mol) into 1.0-L three-necked (vertical) round bottom flask equipped with effective mechanical stirrer, vertical condenser (see Note 4), and a pressure-equalizing dropping funnel and add slowly anhydrous THF (150 mL) (see Note 5) with gentle stirring.
2. To the obtained suspension add dropwise, with stirring, a solution of freshly distilled ethyl 3-aminobutyrate (13.5 g, 0.103 mol) in abs. THF (50 mL) at such a speed to maintain gentle boiling of THF (see Note 10).
3. Reflux the reaction mixture with stirring for 3 h and then leave it at 20°C for 16 h without stirring.
4. Quench the reaction mixture (see Note 11) by subsequent slow dropwise additions of water (11.4 mL), 20% (w/w) NaOH (10.6 mL), water (29.0 mL), and finally with 40% (w/w) NaOH (34.2 mL) – all with vigorous stirring.
5. Cool the reaction mixture to 20°C, separate the organic layer by decantation and extract solids with hot CHCl₃ (4 × 80 mL). Dry the combined organic extracts over MgSO₄ for 16 h. Distil out the solvents at atmospheric pressure using effective Vigreux column.
6. Distil the residue and obtain S.9 (7.3 g, 80%) as a colorless liquid, bp 108–109°C/42 mmHg, n_D^{20} 1.4537. ¹H NMR

(CDCl₃) δ: 3.79–3.68 (2H, m, CH₂O), 3.12–3.03 (1H, m, MeCH), 2.58 (3H, bs, OH, NH₂), 1.62–1.54 (1H, m, CHCH₂), 1.50–1.40 [1H, m, CHCH₂ (due to chiral center on the next carbon, these CH₂-protons have different chemical shifts)], 1.09 (3H, d, *J* 6.5, CH₃).

3.10. Synthesis of *N*-(Benzyloxycarbonyl)-3-Amino-1-Butanol (S.10)

1. Charge 250 mL round bottom three-necked flask equipped with an effective mechanical stirrer with NaHCO₃ (4.2 g, 50 mmol), 2 M aq. Na₂CO₃ (50 mL), S.9 (4.45 g, 50 mmol), and THF (60 mL). Cool (+4°C) the obtained suspension and add Cbz-Cl (7.5 mL, 50.5 mmol) in five portions with 20 min interval with very effective mechanic stirring. Continue stirring for 1 h at 0°C to +4°C and then for 4 h at 20°C.
2. Separate the organic layer, extract water suspension with EtOAc (2 × 15 mL) and evaporate combined organic extracts to dryness in vacuo using a rotary evaporator.
3. Dissolve the residue in CHCl₃ (120 mL), transfer the obtained solution into a separating funnel, wash subsequently with H₂O (20 mL), 0.5 M H₂SO₄ (3 × 15 mL), H₂O (2 × 10 mL), sat. NaHCO₃ (2 × 15 mL), H₂O (15 mL), brine (25 mL); and dry over MgSO₄ for 12 h.
4. Remove CHCl₃ in vacuo using rotary evaporator, dry resulting semisolid residue at 0.5 mmHg at 30°C for 60 min and then treat the residue with a mixture of Et₂O (25 mL) and hexane (50 mL), leave the obtained suspension at +4°C for couple of hours, separate the product by filtration using glass filter (G3), wash with hexane and dry it overnight in air to obtain S.10 (10.1 g, 90%) as a colorless solid. Analytical sample was recrystallized from EtOAc–hexane to provide S.10, having mp 58–58.5°C; *R_f* 0.38 (CHCl₃–MeOH, 97:3); ¹H NMR (CDCl₃) δ: 7.37–7.28 (5H, m, Ph), 5.09 (2H, s, CH₂Ph), 4.75 (1H, bs, NHCbz), 4.01–3.93 (1H, m, MeCH), 3.67–3.59 (2H, m, CH₂O), 2.98 (1H, bs, OH), 1.83–1.72 (1H, m), 1.45–1.35 [1H, m, CHCH₂ (due to chiral center on the next carbon, these CH₂-protons have different chemical shifts)], 1.20 (3H, d, *J* 6.5, CH₃).

3.11. Synthesis of *N*-(Benzyloxycarbonyl)-3-Amino-1-Butyl Methanesulfonate (S.11)

1. Charge 250 mL round bottom two-necked flask with S.10 (8.92 g, 40 mmol), Et₃N (8.45 mL, 60.7 mmol), dry DCM (95 mL), and a stirring bar.
2. Cool the reaction mixture to +4°C and add Ms-Cl (3.3 mL, 42.6 mmol) in DCM (15 mL) dropwise with stirring within 30 min. Continue stirring for additional 30 min at +4°C and then for 1.5 h at 20°C. Remove Et₃N hydrochloride by filtration and wash the filtrate subsequently with sat. NaHCO₃ (4 × 20 mL), H₂O (15 mL), 0.5 M H₂SO₄ (4 × 20 mL), H₂O

(20 mL), sat. NaHCO_3 (15 mL), H_2O (10 mL), brine (25 mL), and dry over MgSO_4 for 12 h.

- Remove CHCl_3 in vacuo using rotary evaporator and dry resulting solid at 0.5 mmHg at 30°C for 60 min. The obtained S.11 (98%) is pure enough to alkylate 1,4-diaminobutane. Analytical sample was recrystallized from *i*-PrOH to provide S.11, having mp $74.5\text{--}75^\circ\text{C}$; R_f 0.62 ($\text{CHCl}_3\text{--MeOH}$, 97:3). $^1\text{H NMR}$ (CDCl_3) δ : 7.35–7.25 (5H, m, C_6H_5); 5.08 (2H, s, PhCH_2); 4.27 (2H, t, J 6.0, MsOCH_2); 2.96 (3H, s, CH_3SO_2); 2.00–1.79 (2H, m, OCH_2CH_2); 1.22 (3H, d, J 6.5, CHCH_3). Calculated, %: C 51.81; H 6.36; N 4.65. $\text{C}_{13}\text{H}_{19}\text{NO}_5$. Found, %: C 51.95; H 6.64; N 4.74.

**3.12. Synthesis
of *N*-(
(Benzyloxycarbonyl)-
1,8-Diamino-5-
Azanonane (S.12)**

- Place in 250 mL round bottom flask a solution of S.11 (7.5 g, 25 mmol) in dry THF (50 mL) and cool it to 0°C . To the resulting solution add in one portion cooled (0°C) solution of 1,4-diaminobutane (35.1 g, 400 mmol) in dry THF (50 mL) and keep the reaction mixture for 12 h at 0°C and 16 h at 20°C .
- Evaporate THF and excess of 1,4-diaminobutane in vacuo using first water aspirator and then vacuum oil pump (see Note 12). Add to the residue 2 M NaOH (25 mL) and H_2O (5 mL). Transfer the obtained mixture into a separating funnel and extract with DCM (30 mL and 2×5 mL) (see Note 13) and dry the combined extracts over K_2CO_3 . Remove DCM in vacuo using rotary evaporator and dissolve the residue in dioxane–25% ammonia, 93:7 (v/v) mixture (20 mL).
- Prepare a slurry of 130 g of silica gel in dioxane–25% ammonia, 93:7 (v/v) mixture (600 mL), and pour it in one portion into a 6×12 cm chromatography column being equipped with a forcolumn of a proper size. Wash this column with dioxane–25% ammonia, 93:7 (v/v) mixture (200 mL).
- Apply carefully 1/3 of the solution from step 2 on the top of silica gel and elute the column with dioxane–25% ammonia, 93:7 (v/v) mixture, collecting 15 mL fractions.
- Analyze fractions by TLC using dioxane–25% ammonia, 9:1 (v/v) mixture and combine the fractions containing only S.12. Evaporate the volatile material from the combined fractions in vacuo using rotary evaporator, coevaporate the residue with dioxane (2×25 mL) and dry the residual oil in vacuum desiccator over P_2O_5 (change P_2O_5 after 4 h and then leave overnight over a fresh portion of P_2O_5) to obtain S.12 (5.63 g, 77%) as a viscous oil: R_f 0.15 (dioxane–25% ammonia, 9:1). $^1\text{H NMR}$ (CDCl_3) δ : 7.37–7.27 (5H, m, Ph), 5.57 (1H, bs, NHcbz), 5.08 (2H, s, CH_2Ph), 3.85–3.76 (1H, m, MeCH), 2.74–2.52 (6H, m, CH_2NH), 1.71–1.41 (6H, m, CCH_2C), 1.40 (3H, bs, NH, NH_2), 1.17 (3H, d, J 6.5, CH_3).

**3.13. Synthesis
of 1,8-Diamino-5-
Azanonane
Trihydrochloride,
 α -MeSpd (S.13)**

1. Place in 100 mL round bottom flask a solution of S.12 (5.2 g, 17.7 mmol) in a mixture of AcOH–MeOH (1:1, 40 mL), a stir bar, and add a suspension of Pd/C in MeOH (~1 mL).
2. Wash the system with a slow (see Note 14) hydrogen flow (see Note 15).
3. Switch on the magnetic stirrer to get as effective stirring as possible. Continue hydrogenation until the disappearance of the starting material (control with TLC using dioxane–25% ammonia, 8:2).
4. Load a suspension of Celite® 545 in MeOH on 10-mL glass funnel, wash the Celite layer with MeOH and filtrate the reaction mixture through Celite (see Note 16). Wash the catalyst with MeOH and evaporate the combined filtrates to dryness in vacuo using rotary evaporator. Coevaporate the semisolid residue with abs. EtOH (20 mL), dissolve the residue in the minimal volume of boiling MeOH, add boiling abs. EtOH until the beginning of crystallization. Allow the mixture to cool to 20°C, then put it in refrigerator for couple of hours and finally leave it overnight at –20°C.
5. Filter α -MeSpd off, wash it with abs. EtOH and dry in vacuum desiccator over P₂O₅/KOH to obtain S.13 (4.23 g, 89%) as colorless crystals, mp 191–192°C; *Rf* 0.28 (*n*-butanol–AcOH–pyridine–H₂O, 4:2:1:2). ¹H NMR (D₂O) δ : 3.53 (1H, m, MeCH), 3.21 (2H, m, NCH₂), 3.15 (2 H, m, NCH₂), 3.07 (2H, m, NCH₂), 2.16 (1H, m, CCH₂C), 2.02 [1H, m, CCH₂C (due to chiral center on the next carbon, these CH₂-protons have different chemical shifts)], 1.86–1.74 (4H, m, CCH₂C), 1.36 (3H, d, *J* 6.5, CH₃). Calculated, %: C 35.76; H 9.00; N 15.64. C₈H₂₄N₃Cl₃. Found, %: C 35.88; H 9.10; N 15.63.

4. Notes

1. Crotononitrile and methacrylonitrile may be dried over a small portion of CaCl₂ and then distilled at atmospheric pressure. In the distillation flask and in the receiving flask(s) a few crystals of hydroquinone must be added.
2. Usually a second distillation is necessary to obtain a pure product. Use TLC control of the distillate in dioxane–25% ammonia, 8:2 (v/v). In this system 1,4-diaminobutane has *Rf* only about 0.03–0.05.
3. In larger scale synthesis more effective cooling is required, because the reaction is slightly exothermic.

4. A funnel (a condenser for the synthesis of S.9) must be equipped with *a tube with KOH or CaCl₂* being connected to a funnel (condenser) with enough long rubber tube and *placed directly in the ventilation hole of the hood* – evolution of hydrogen!
5. Use freshly distilled (over Na, or LiAlH₄) Et₂O, or THF (for the synthesis of S.9).
6. For cooling it is better to use heptane–dry CO₂ or heptane–liquid N₂ baths. In the case of larger scale synthesis, for safety reasons, it is necessary to use four-necked flask additionally equipped with a condenser being protected from air moisture (see Note 5).
7. The temperature rises up from –20 to –10°C after the addition of the first drop of the nitrile solution.
8. Warming of the reaction mixture to the temperature higher than –5°C gives rise to some by-products, which are difficult to separate from the target S.5.
9. To develop di-Boc-nitrile on TLC use 0.02% (w/v) solution of sodium salt of tetrabromophenol blue in water. Boc-derivatives appear as pale spots on the blue-lilac background.
10. After the addition of each quarter of THF solution of ethyl 3-aminobutyrate reflux the reaction mixture for 5 min.
11. This is very exothermic reaction. During dropwise addition THF starts boiling and cooling (see Note 6) is necessary to keep THF boiling gently.
12. Do not heat the distillation flask over 40°C to avoid yellow-brown color.
13. Extension of the extraction is not necessary, since third 5 mL DCM extract contains practically no S.12, but mainly 1,4-diaminobutane.
14. Bubbles of hydrogen can easily be counted using a bubble-counter, being placed after the hydrogenation apparatus.
15. Equip the outlet of the bubble-counter with a rubber tube, the end of which is *placed directly in the ventilation hole of the hood*.
16. Cellite layer prevents clogging of the glass filter pores.

Acknowledgments

This work was supported by the Academy of Finland (project nos. 124185 and 128702), the Russian Foundation for Basic Research (project nos. 09-04-01272, and 08-04-91777), and the program Molecular and Cell Biology of the Presidium of the Russian Academy of Sciences.

References

1. Casero RA Jr, Woster PM (2009) Recent advances in the development of polyamine analogues as antitumor agents. *J Med Chem* 52:4551–4573
2. Casero RA Jr, Marton LJT (2007) Targeting polyamine metabolism and function in cancer and other hyperproliferative diseases. *Nat Rev Drug Discov* 6:373–390
3. Lakanen JR, Coward JK, Pegg AE (1992) α -Methyl polyamines: metabolically stable spermidine and spermine mimics capable of supporting growth in cells depleted of polyamines. *J Med Chem* 35:724–734
4. Nagarajan S, Ganem B, Pegg AE (1988) Studies of non-metabolizable polyamines that support growth of SV-3T3 cells depleted of natural polyamines by exposure to α -difluoromethylornithine. *Biochem J* 254:373–378
5. Grigorenko NA, Khomutov AR, Keinänen TA, Järvinen A, Alhonen L, Jänne J, Vepsäläinen J (2007) Synthesis of novel optical isomers of α -methylpolyamines. *Tetrahedron* 63:2257–2262
6. Räsänen TL, Alhonen L, Sinervirta R, Keinänen T, Herzig K-H, Suppola S, Khomutov AR, Vepsäläinen J, Jänne J (2002) A polyamine analogue prevents acute pancreatitis and restores early liver regeneration in transgenic rats with activated polyamine catabolism. *J Biol Chem* 277:39867–39872
7. Järvinen AJ, Cerrada-Gimenez M, Grigorenko NA, Khomutov AR, Vepsäläinen JJ, Sinervirta RM, Keinänen TA, Alhonen LI, Jänne JE (2006) α -Methyl polyamines: efficient synthesis and tolerance studies *in vivo* and *in vitro*. First evidence for dormant stereospecificity of polyamine oxidase. *J Med Chem* 49:399–406
8. Järvinen AJ, Keinänen TA, Grigorenko N, Khomutov AR, Uimari A, Vepsäläinen J, Närvänen A, Alhonen L, Jänne J (2006) Guide molecule-driven stereospecific degradation of α -methylpolyamines by polyamine oxidase. *J Biol Chem* 281:4589–4595
9. Hyvönen MT, Keinänen TA, Cerrada-Gimenez M, Sinervirta R, Grigorenko N, Khomutov AR, Vepsäläinen J, Alhonen L, Jänne J (2007) Role of hypusinated eukaryotic translation initiation factor 5A in polyamine depletion-induced cytostasis. *J Biol Chem* 282:34700–34706
10. Hyvönen MT, Howard MT, Anderson CB, Grigorenko N, Khomutov AR, Vepsäläinen J, Alhonen L, Jänne J, Keinänen TA (2009) Divergent regulation of the key enzymes of polyamine metabolism by chiral α -methylated polyamine analogs. *Biochem J* 422:321–328
11. Lebreton L, Jost E, Carboni B, Annat J, Vaultier M, Dutartre P, Renault P (1999) Structure-immunosuppressive activity relationships of new analogues of 15-deoxyspergualin. 2. Structural modification of the spermidine moiety. *J Med Chem* 42:4749–4763
12. Grigorenko NA, Vepsäläinen J, Järvinen A, Keinänen TA, Alhonen L, Jänne J, Kritsyn AM, Khomutov AR (2004) A new synthesis of α -methylspermidine. *Bioorg Khim* 30:441–445

Fluorescent Substrates for Polyamine Catabolic Enzymes and Transport

Koichi Takao and Akira Shirahata

Abstract

The most widely used methods for measuring polyamine enzyme activities are radioisotope methods that measure the radioactivity of compounds produced from radiolabeled substrate by the enzyme reaction. Several fluorescent polyamines have been developed for the measurement of the polyamine transport system (PTS) or transglutaminase. Although fluorophores in the fluorescent polyamines may affect the affinity of the polyamine moiety to the enzyme protein, the assays that use fluorescent substrate are sensitive and simple for common laboratory usage.

In this chapter, the uses of dansyl polyamines with a simple high-performance liquid chromatography system for the measurement of the PTS and polyamine catabolic enzymes including spermidine/spermine N¹-acetyltransferase and N¹-acetylpolyamine oxidase are described.

Key words: Dansyl polyamine, Spermidine/spermine-N¹-acetyltransferase (SSAT), N¹-Acetylpolyamine oxidase (APAO), Polyamine transport system (PTS), Polyamine, High-performance liquid chromatography (HPLC)

1. Introduction

The most widely used methods for measuring polyamine enzyme activities are radioisotope methods that measure the radioactivity of compounds produced from radiolabeled substrate by the enzyme reaction (1). The nonradioisotope methods include high-performance liquid chromatography (HPLC) methods that measure the products from natural polyamine substrates or fluorinated polyamines by postcolumn labeling with *o*-phthalaldehyde (2, 3) or precolumn dansyl-derivatization (4). Mass spectrometry with stable-isotope-labeled polyamines (5) or methods that detect the formation of nonpolyamine products, such as hydrogen peroxide (6) or methylthioadenosine (7), is also useful for the assay of polyamine enzymes.

There are several fluorescent substrates for polyamine enzymes. These substrates are mainly used for the measurement of the polyamine transport system (PTS) activity with flow cytometry or the measurement of transglutaminase activity with HPLC (8–13). Although the hydrophobicity or the relatively large molecular size of the fluorophore in the fluorescent polyamine may affect the affinity of the polyamine moiety to the enzyme, the assay methods using fluorescent substrate are sensitive and simple for common laboratory usage.

In this chapter, the uses of dansyl polyamines with a simple HPLC system for the measurement of polyamine enzymes including spermidine/spermine- N^1 -acetyltransferase (SSAT) (14), N^1 -acetylpolyamine oxidase (APAO) (15), and PTS (16) are described.

SSAT is a primarily cytosolic enzyme found in various tissues in higher organisms, although there is also a mitochondrial form (17) of SSAT whose function is unknown. SSAT catalyzes the acetylation of a primary amine separated from another nitrogen atom by a three-carbon aliphatic chain of the polyamines (18). Based on the loose substrate specificity of SSAT, N^1 -dansyl norspermine (DNS333) can be used for the fluorescent substrate of SSAT. SSAT acetylates DNS333 to N^1 -acetyl- N^{11} -dansyl norspermine (AcDNS333), which is detected by HPLC (Fig. 1) (14).

APAO is a constitutive enzyme that catalyzes the oxidative cleavage of natural substrates, N^1 -acetylspermidine and N^1 -acetylspermine, to liberate 3-acetamidopropanal and form putrescine and spermidine, respectively. APAO is a flavoprotein located in the peroxisomes of animal cells, and its enzyme activity

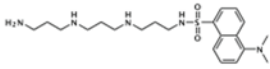
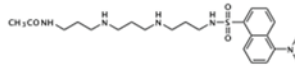
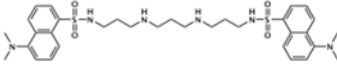
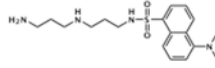
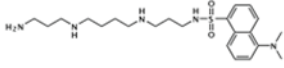
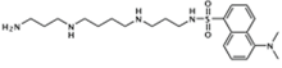
Polyamine enzyme	Substrate	Product or substrate to be determined by HPLC
SSAT	DNS333 	AcDNS333 
APAO	DiDNS333 	DNS333 
PTS	DNS343 	DNS343 

Fig. 1. Structures of dansyl polyamine substrates and products to be determined by HPLC.

is abundantly expressed in nearly all vertebrate tissues (19). Based on the substrate specificities of APAO, it is predicted that the two anionic centers and a hydrophobic region are present in the active site of APAO in addition to the cleavage site of the acetamidopropyl group, and the catalytic reaction requires a positive charge at a 3 or 4 methylene chain interval from the cleavage site (20); therefore, N¹, N¹¹-didansyl norspermine (DiDNS333) is used as the fluorescent substrate of APAO. DiDNS333 is cleaved by APAO to N-dansylamidopropanal (DNS3al) and N¹-dansyl norspermidine (DNS33), which is detected by HPLC (Fig. 1) (15).

Most mammalian cells take up polyamines by carrier-mediated, sodium- and energy-dependent mechanisms. The cells appear to have a single transport system for the three polyamines. The PTS is fully integrated into the cellular regulatory system for the control of intracellular polyamine levels. Although the PTS gene has not been identified in mammalian cells, some of the properties of PTS are known. PTS is inducible and saturable. Depletion of the intracellular polyamine content leads to a marked increase in the rate of polyamine uptake that scarcely affects the affinities to polyamines, while an increase in the intracellular polyamine level downregulates PTS activity (21, 22). The uptake of several fluorescent polyamines via the PTS has been assessed by flow cytometry to determine the PTS activity. In the present protocol, N¹-dansylspermine (DNS343), a fluorescent substrate of PTS, is incorporated into cells via the PTS and measured by HPLC (Fig. 1) (16).

2. Materials

The majority of the reagents are common laboratory reagents and may be purchased from a preferred supplier. Preparation and use of stocks is dictated by standard laboratory practice.

2.1. Synthesis of Fluorescent Substrates

1. Free polyamines: spermine, norspermine, norspermidine.
2. Ethyl trifluoroacetate, di-tert-butyl dicarbonate (BOC₂O), triethylamine, ammonia aq. solution, dansyl chloride, acetic anhydride (Ac₂O), trifluoroacetic acid, hydrochloric acid, chloroform, methanol, ethanol, ethyl acetate, hexane, silica gel (C-300).

2.2. HPLC Analysis of Fluorescent Substrates

1. HPLC system apparatus: Chromatopac C-R8A, System controller SCL-10A_{VP}, auto injector SIL-10AD_{VP}, liquid chromatograph pump LC-10D_{VP}, degasser DGU-14A, column oven CTO-10A_{VP}, fluorescence detector RF-10A_{XL} (Shimadzu) (see Note 1).
2. 4.6 mm ϕ \times 150 mm TSKgel-ODS80_{TM} column (Tosoh).
3. Methanol (liquid chromatography grade), sodium octanesulfonate (ion-pair reagent grade), trifluoroacetic acid (amino acid analysis grade).

2.3. Cell Culture

1. HTC cell line (Morris hepatoma 7288c, Dainippon Pharmaceuticals).

Culture medium: Minimum essential medium – Eagle's medium – containing 10% fetal bovine serum (FBS), 1% penicillin-streptomycin solution (containing 5,000 units/mL penicillin and 5 mg/mL streptomycin).

2. 0.25% trypsin solution: 2.5% trypsin is diluted in PBS.

2.4. SSAT Assay

All aqueous solutions should be prepared with distilled, deionized water.

1. 1.0 M Tris–HCl buffer, pH 7.8, at 37°C: Use ultrapure grade Tris base. Adjust to the appropriate pH at 37°C by using concentrated HCl. Store at –20°C (see Note 2).
2. 0.5 mM Acetyl-CoA solution: Store at –20°C.
3. 0.4 mM N¹-Dansylnorspermine solution: N¹-dansylnorspermine tetrahydrochloride is dissolved in 0.01 M HCl. Store at –20°C (see Note 3).
4. 50% Trichloroacetic acid solution: Store at room temperature.

2.5. Stock Solutions for APAO Assay

1. 1.0 M Tris–HCl buffer containing 10 mM EDTA, pH 9.0: Use ultrapure grade Tris base. Adjust to the appropriate pH at 37°C by using concentrated HCl. Store at –20°C (see Note 2).
2. 0.2 mM Dithiothreitol solution: Store in aliquots at –20°C.
3. 0.35 mM Pargyline solution: Store at –20°C.
4. 5.6 mM Aminoguanidine solution: Store at –20°C.
5. 0.5 mM N¹,N¹¹-Didansylnorspermine solution: N¹,N¹¹-didansylnorspermine tetrahydrochloride is dissolved in 0.01 M HCl. Store at –20°C (see Note 3).
6. 20% Trichloroacetic acid solution: Store at room temperature.

2.6. Stock Solutions for PTS Assay

1. 1 mM N¹-dansylspermine solution: N¹-dansylspermine tetrahydrochloride is dissolved in 0.01 M HCl. Store at –20°C after filter sterilization (see Note 3).
2. 10% Trichloroacetic acid solution: Store at room temperature.

3. Methods**3.1. Synthesis of N¹-Dansylnorspermine (DNS333) and N¹-Dansylspermine (DN343)**

1. Norspermine (333) (1 eq) and triethylamine (4 eq) are dissolved in methanol (10 mL/meq) at –78°C (acetone-dry ice). One primary amino group of 333 is selectively protected by the reaction with ethylfluoroacetate (1 eq) that is added dropwise over 30 min. After an additional 30 min of stirring, the temperature is increased to 0°C to afford predominantly the

mono-trifluoroacetamide form. Immediately, the remaining three amino functional groups are protected with BOC_2O (3 eq) at 25°C and stirred for an additional 15 h to obtain fully protected 333. The trifluoroacetyl-protecting group is then cleaved by increasing the pH of the solution to above 11 with concentrated aqueous ammonia and then stirring at 25°C for 15 h, to afford tri-Boc-333. The tri-Boc-333 is purified by silica gel column chromatography with a solvent system of chloroform:methanol:ammonia (see Note 4).

2. The tri-Boc-333 is dissolved in methanol (10 mL/meq). The free primary amine of tri-Boc-333 (1 eq) is reacted with dansyl chloride (DNS-Cl) (1 eq) in the presence of triethylamine (1 eq). After purification over silica gel column chromatography with a solvent system of chloroform:methanol:ammonia, a single band of tri-Boc-DNS333 is obtained.
3. The tri-Boc-DNS333 is dissolved in trifluoroacetic acid to cleave the Boc groups and evaporated to yield DNS333 tetratrifluoroacetate. The DNS333 tetratrifluoroacetate is dissolved in hydrochloric acid for exchange of hydrochloride salt. The DNS333 tetrahydrochloride is recrystallized from ethanol-water.
4. DNS343 is synthesized according to the method above for the synthesis of DNS333 with norspermine substituted by spermine.

3.2. Synthesis of *N*¹-Acetyl-*N*¹¹-Dansylnorspermine (AcDNS333)

1. 333 (1 eq) and triethylamine (4 eq) are dissolved in methanol (10 mL/meq). Two primary amino functional groups of 333 are selectively protected by the reaction with ethyl trifluoroacetate (2 eq). The remaining two amino functional groups are protected with BOC_2O (2 eq) to afford fully protected norspermine. The trifluoroacetyl-protecting groups are then cleaved by increasing the pH of the solution to above 11 with concentrated aqueous ammonia and then stirring at 25°C for 15 h to afford di-Boc-333. The di-Boc-333 is purified by silica gel column chromatography with a solvent system of chloroform:methanol:ammonia.
2. The di-Boc-333 is dissolved in methanol (10 mL/meq). One of the free primary amines of di-Boc-333 (1 eq) is reacted with DNS-Cl (1 eq) in the presence of triethylamine (1 eq). After purification by silica gel column chromatography with a solvent system of chloroform:methanol:ammonia, a single band of di-Boc-*N*¹-dansyl333 (di-Boc-DNS333) is obtained.
3. The di-Boc-DNS333 is dissolved in methanol (10 mL/meq) with triethylamine (1 eq). The free primary amine of di-Boc-DNS333 (1 eq) is reacted with Ac_2O (1 eq). After purification by silica gel column chromatography with a solvent system of chloroform:methanol:ammonia, a single band of di-Boc-*N*¹-acetyl-*N*¹¹-DNS333 (di-Boc-AcDNS333) is obtained.

4. The di-Boc-AcDNS333 is dissolved in trifluoroacetic acid to cleave the Boc groups and evaporated to yield AcDNS333 tetratrifluoroacetate. The AcDNS333 tetratrifluoroacetate is dissolved in hydrochloric acid for exchange of hydrochloride salt. The AcDNS333 tetrahydrochloride is recrystallized from ethanol-water.

3.3. Synthesis of *N*'-Dansylnorspermidine (DNS33)

DNS33 is synthesized by the method used for the synthesis of DNS333 (see Subheading 3.1, step 1) with norspermine replaced by norspermidine (33).

1. Norspermidine (33) (1 eq) and triethylamine (3 eq) are dissolved in methanol (10 mL/meq). One primary amino group of 33 is protected by the reaction with ethyltrifluoroacetate (1 eq) that is added drop-wise over 30 min. The remaining two amino functional groups are protected with BOC_2O (2 eq) to afford fully protected 33. The trifluoroacetyl-protecting group is then cleaved with *conc. aq.* ammonia, to afford di-Boc-33. The di-Boc-33 is purified by silica gel chromatography with a solvent system of chloroform:methanol:ammonia.
2. The di-Boc-33 is dissolved in methanol (10 mL/meq) with triethylamine (1 eq). A free primary amino group of di-Boc-33 (1 eq) is reacted with DNS-Cl (1 eq). After purification by silica gel column chromatography with a solvent system of chloroform:methanol:ammonia, a single band of di-Boc-DNS33 is obtained.
3. The di-Boc-dansylnorspermidine is dissolved in trifluoroacetic acid to cleave the Boc groups and evaporated to yield DNS33 tritrifluoroacetate. The DNS33 tritrifluoroacetate is dissolved in hydrochloric acid for exchange of hydrochloride salt. The DNS33 trihydrochloride is recrystallized from ethanol-water.

3.4. Synthesis of *N*¹,*N*¹¹-Didansylnorspermine (DiDNS333)

1. The di-Boc-333 (1 eq), described above (see Subheading 3.2, step 1), is dissolved in methanol with triethylamine (2 eq). The two free primary amines of di-Boc-333 are reacted with DNS-Cl (2 eq). After purification by silica gel column chromatography with a solvent system of chloroform:methanol:ammonia, a single band of di-Boc-*N*¹, *N*¹¹-didansylnorspermine (di-Boc-DiDNS333) is obtained.
2. The di-Boc-DiDNS333 is dissolved in trifluoroacetic acid to cleave the Boc groups and evaporated to yield DiDNS333 tetratrifluoroacetate. The DiDNS333 tetratrifluoroacetate is dissolved in hydrochloric acid for exchange of hydrochloride salt. The DiDNS333 tetrahydrochloride is recrystallized from ethanol-water.

3.5. HPLC Analysis of Fluorescent Substrates

1. The HPLC system, as described in Subheading 2.2, contains a TSKgel-ODS80_{TM} column (4.6 mm^o × 150 mm) that is equilibrated with elution buffer (methanol:water (75:25) containing 8 mM sodium octanesulfonate and 0.1% trifluoroacetic acid). The flow rate is 1 mL/min, and the column oven temperature is 40°C. The fluorescence is detected at an excitation wavelength of 333 nm and an emission wavelength of 544 nm.
2. Start each analysis by injecting a working standard. The chromatograms of the dansyl polyamine standards (DNS333 and AcDNS333 for SSAT assay, DNS33 and DiDNS333 for APAO assay, DNS343 for PTS assay) are shown in Fig. 2 (see Note 5). The detection limits of the dansyl polyamines in this system are approximately 30 fmol, and a linearity of the peak area of dansyl polyamines is present at least until 20 pmol.
3. Start the sample analysis when the chromatogram of the standards is satisfactory.

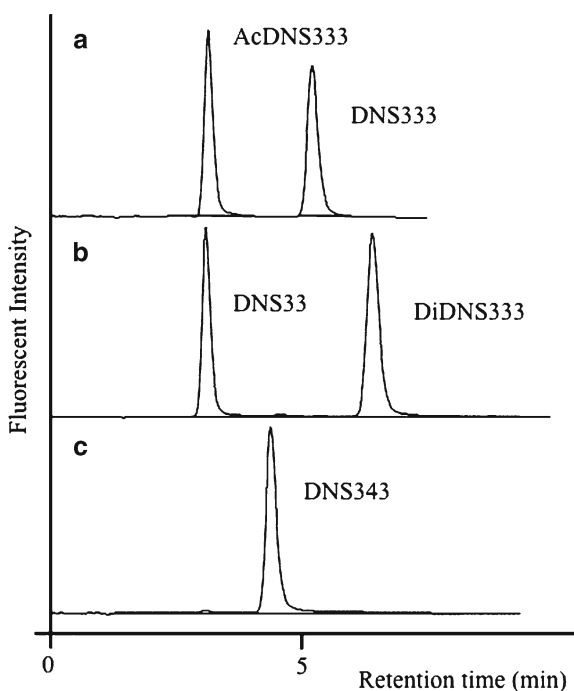


Fig. 2. HPLC chromatograms of dansyl polyamine substrates and products. Ten μL of standard solutions containing 1 pmol of each dansyl polyamine were subjected to HPLC, as described in the text. (a) Substrate (DNS333) and product (AcDNS333) for SSAT reaction. (b) Substrate (DiDNS333) and product (DNS33) for APAO reaction. (c) Substrate (DNS343) for PTS.

3.6. Maintenance of HTC Cells in Culture

Subculture HTC cells every 3 or 4 days in 10-cm culture dishes in MEM-Eagle medium supplemented with 10% FBS, 50 units/mL penicillin, and 50 $\mu\text{g}/\text{mL}$ streptomycin.

All solutions are filter sterilized.

1. Remove the medium from a confluent monolayer of cells and rinse the cells with PBS.
2. Add 1 mL of trypsin (0.25%) solution in PBS to the 10-cm dish and tilt the dish to thoroughly wet the cell monolayer. Return the dish to the incubator.
3. After 3 min, remove the dish from the incubator and examine under the microscope. The cells should round up and begin to detach from the surface. Smartly tap the side of the dish 2 or 3 times to aid cell detachment. Prolonged exposure to trypsin can damage the cells and reduce viability.
4. Add an equal volume of MEM medium with FBS and draw the cell suspension up and down several times through a narrow bore pipette to break up any cell clumps. Dilute the cells in fresh medium, and plate 5×10^5 cells per 10-cm culture dish.
5. Return the cells to the incubator.

3.7. Preparation of SSAT Enzyme from HTC Cells

1. Seed the HTC cells at a density of 5×10^5 cells per 10-cm culture dish. After the cells become attached to the dish, treat the cells with 25 μM $\text{N}^1, \text{N}^{11}$ -diethylnorspermine and 1 mM aminoguanidine for SSAT induction.
2. After 24 h, wash the cultured cells 3 times with 3 mL of PBS. Then, scrape off the cells by using a rubber policeman and collect them by centrifugation. Store the collected cells at -80°C until use.
3. Sonicate the collected cells in PBS on ice and then centrifuge the cells at $105,000 \times g$ at 4°C .
4. Dialyze the supernatant against 0.1 M Tris-HCl, pH 7.8, at 4°C , and use the resultant crude extract as the enzyme solution for the SSAT assay. Store the extract at -80°C until use.

3.8. Assay Method for SSAT with DNS333 (see Note 6)

All solutions should be kept at 4°C until the start of the assay. Reaction tubes and all assay solutions should be chilled and kept on ice prior to the incubation.

1. Prepare a stock assay mixture in which each 80- μL aliquot is to be added to one reaction tube consisting of: 10 μL of 1 M Tris-HCl buffer (pH 7.8), 10 μL of 0.5 mM Acetyl-CoA solution, 10 μL of 0.4 mM DNS333 solution, and 50 μL of distilled water.
2. To start the reaction, add 20 μL of enzyme solution to each tube. The final reaction volume of all tubes should be 100 μL .

Also include blank reactions that substitute 20 μL of water or buffer for enzyme solution.

3. Incubate tubes at 37°C (see Notes 7–11).
4. Stop the reaction by adding 50 μL of 30% trichloroacetic acid solution.
5. After centrifugation, inject the aliquots of diluted supernatant into the column and perform HPLC analysis as described in Subheading 3.5.

3.9. Preparation of APAO Enzyme from Rat Liver

1. Homogenize rat livers at 4°C with 4 volumes of 0.25 M sucrose-10 mM Tris-HCl buffer, pH 7.4, by using a Potter-Elvehjem homogenizer.
2. Centrifuge the homogenate at 600 $\times g$ for 10 min at 4°C.
3. Centrifuge the supernatant at 15,000 $\times g$ for 10 min at 4°C.
4. Suspend the pellet in 0.1% Triton X-100 dissolved in buffer A (10 mM Tris-HCl buffer, pH 7.8, containing 0.1 mM EDTA and 0.1 mM DTT) at 4°C.
5. Centrifuge the suspension at 25,000 $\times g$ for 30 min at 4°C.
6. Dialyze the supernatant against buffer A at 4°C.
7. Use the crude extract as the enzyme solution for the APAO assay. Store extract at -80°C until use.

3.10. Assay Method for APAO with DiDNS333 (see Note 12)

All solutions should be kept at 4°C until the start of the assay. Reaction tubes and all assay solutions should be chilled and kept on ice prior to the incubation.

1. Prepare a stock assay mixture in which each 80- μL aliquot is to be added to one reaction tube consisting of: 10 μL of 1 M Tris-HCl buffer, pH 9.0, containing 10 mM EDTA, 10 μL of 0.2 mM DTT solution, 10 μL of 0.36 mM pargyline solution, 10 μL of 5.6 mM aminoguanidine solution, 10 μL of 0.5 mM DiDNS333 solution, and 30 μL of distilled water (see Note 13).
2. Add 20 μL of enzyme solution to each tube to initiate the reaction. The final reaction volume of all tubes should be 100 μL . Also include blank reactions that substitute 20 μL of water or buffer for the enzyme solution.
3. Incubate tubes at 37°C (see Note 7).
4. Stop the reaction by adding 100 μL of 20% trichloroacetic acid solution.
5. Centrifuge the reaction mixtures to perform HPLC analysis as described in Subheading 3.5.
6. Use the peak area to determine enzyme activity.

**3.11. Analysis
of Polyamine
Transport with DNS343
(see Note 14)**

All solutions are sterilized by filtration through a 0.2- μ m filter.

1. Seed HTC cells by plating 5×10^5 cells per 10-cm culture dish.
2. After cells attach to the dish, add medium containing 50 mM aminoguanidine solution (0.2 mL in 10 mL culture medium) and 1 mM DNS343 (0.1 mL in 10 mL culture medium) to the monolayer (see Note 15).
3. Incubate cells for 2 h at 37°C (see Notes 16 and 17).
4. Wash the attached cells three times with 3 mL of PBS on ice.
5. Use a rubber policeman to scrape off and harvest cells on ice.
6. Use a hemocytometer slide to count cells.
7. Centrifuge the suspended cells at 4°C to collect the cells.
8. Add 200 μ L of 10% TCA to the resulting cell pellets.
9. Vibrate the solutions, and if necessary, sonicate the solutions.
10. Centrifuge the solutions and collect the supernatants.
11. Perform an HPLC analysis of the supernatants, as described in Subheading 3.5.
12. Use the peak area to determine enzyme activity.

4. Notes

1. The simplest HPLC apparatus requires an HPLC pump, sample injector (manual or auto), C18 column, fluorescence detector, and recorder.
2. Because the pH of Tris has a significant temperature coefficient, it is important to adjust the pH of buffers to the intended pH at the temperature at which they are to be used.
3. Stock solutions of amines, such as DNS333, DNS343, DiDNS333, and polyamine, are dissolved in 0.01 M HCl, because such amines dissolved in water may degrade during storage.
4. The purification by silica gel column chromatography is important, because the contaminants di-Boc-333 and tetra-Boc-333 are difficult to remove from tri-Boc-333 after the dansylation.
5. The advantages of this HPLC method are that it is quick and convenient, it has good resolution between dansyl polyamines of very similar structure, and it easily accommodates the inclusion of an internal standard, which improves quantification.

The disadvantage of this HPLC method is that heparin strongly affects the HPLC separation of dansyl polyamines. Therefore, EDTA is the recommended anticoagulant.

6. The K_m values of DNS333 and acetyl-CoA for the SSAT from HTC cells are approximately 11 and 13 μM , respectively.
7. The time chosen must be such that the rate of conversion of product to substrate is linear with time and that <2% of the substrate has been consumed.
8. As nonenzymatic acetylation of DNS333 increases with time, SSAT activity is produced by subtracting the amount of AcDNS333 detected for the assay without the enzyme from that for the assay with the enzyme.
9. As copper-dependent amine oxidases (e.g., porcine diamine oxidase from the kidney and bovine serum amine oxidase) degrade DNS333 to DNS33, aminoguanidine should be added to the assay mixture. The existence of the amine oxidase can be detected by the reaction without acetyl-CoA in the assay mixture.
10. As APAO degrades DNS333 to DNS3al and 33, MDL72527 must be added to the assay when the sample contains APAO. The existence of the amine oxidase is measured without acetyl-CoA in the assay mixture. The level of DNS333 decreases with time.
11. MDL72527 is synthesized according to the method described by Bey et al. (23).
12. The K_m value of DiDNS333 for the APAO from rat liver is approximately 3.5 μM .
13. APAO degrades DiDNS333 to DNS33 and DNS3al. DNS3al reacts with aminoguanidine in the assay mixture and is detected as two peaks in the chromatogram. Thus, DNS33 is used to measure the APAO activity.
14. The K_m value of DNS343 for the PTS in HTC cells is approximately 1.5 μM .
15. FBS contains an amine oxidase that will oxidize polyamines to cytotoxic aldehyde. Therefore, aminoguanidine must be added to the culture medium. Care should be taken when using aminoguanidine, because it can affect cell growth and the intracellular polyamine contents (24).
16. The PTS activity must be measured at a point when the time course for uptake is linear. A suitable time point must be found by preliminary experiments.
17. As the DNS343 is degraded by APAO, MDL72527 should be added when cells have high APAO activity (e.g., Chinese hamster ovary cells).

References

- Morgan DML (1998) Polyamine Protocols. Methods in molecular biology, vol 79. Humana Press, Totowa
- Halline AG, Brasitus TA (1990) Reversed phase high performance liquid chromatographic method for the measurement of polyamine oxidase activity. *J Chromatogr* 533:187–194
- Baillon JG, Mamont PS, Wagner J, Gerhart R, Lux P (1988) Fluorinated analogues of spermidine as substrates of spermine synthase. *Eur J Biochem* 176:237–242
- Vujcic S, Diegelman P, Bacchi C, Kramer D, Porter CW (2002) Identification and characterization of a novel flavin-containing spermine oxidase of mammalian cell origin. *Biochem J* 367:665–675
- Xu YJ, Hara T, Samejima K, Sasaki H, Kobayashi M, Takahashi A, Niitsu M (2002) Simultaneous determination of endogenous and orally administered ¹⁵N-labeled polyamines in rat organs. *Anal Biochem* 301:255–260
- Suzuki O, Matsumoto T, Katsumata Y (1984) Determination of polyamine oxidase activities in human tissues. *Experientia* 40:838–839
- Enomoto K, Nagasaki T, Yamauchi A, Onoda J, Sakai K, Yoshida T, Maekawa K, Kinoshita Y, Nishino I, Kikuoka S, Fukunaga T, Kawamoto K, Numata Y, Takemoto H, Nagata K (2006) Development of high-throughput spermidine synthase activity assay using homogeneous time-resolved fluorescence. *Anal Biochem* 351:229–240
- Aziz SM, Yatin M, Worthen DR, Lipke DW, Crooks PA (1998) A novel technique for visualizing the intracellular localization and distribution of transported polyamines in cultured pulmonary artery smooth muscle cells. *J Pharm Biomed Anal* 17:307–320
- Cullis PM, Green RE, Merson-Davies L, Travis N (1999) Probing the mechanism of transport and compartmentalization of polyamines in mammalian cells. *Chem Biol* 6:717–729
- Soulet D, Covassin L, Kaouass M, Charest-Gaudreault R, Audette M, Poulin R (2002) Role of endocytosis in the internalization of spermidine-C₇-BODIPY, a highly fluorescent probe of polyamine transport. *Biochem J* 367:347–357
- Phanstiel O IV, Kaur N, Delcros J-D (2007) Structure-activity investigations of polyamine-anthracene conjugates and their uptake via the polyamine transporter. *Amino Acids* 33:305–313
- Guminski Y, Grousseau M, Cugnasse S, Brel V, Annereau J-P, Vispe S, Guilbaud N, Barret J-M, Bailly C, Imbert T (2009) Synthesis of conjugated spermine derivatives with 7-nitrobenzoxazole (NBD), rhodamine and bodipy as new fluorescent probes for the polyamine transport system. *Bioorg Med Chem Lett* 19:2474–2477
- Wu Y-W, Tsai Y-H (2006) A rapid transglutaminase assay for high throughput screening applications. *J Biomol Screen* 11:836–843
- Takao K, Miyatake S, Fukazawa K, Wada M, Sugita Y, Shirahata A (2008) Measurement of spermidine/spermine-N¹-acetyltransferase activity by high-performance liquid chromatography with N¹-dansylspermine as the substrate. *Anal Biochem* 376:277–279
- Takao K, Sugita Y, Shirahata A (2010) Assay of N¹-acetyl polyamine oxidase with N¹, N¹¹-didansylspermine as the substrate by ion-pair reversed phase high performance liquid chromatography. *Biol Pharm Bull* 33:1089–1094
- Takao K, Sugita Y, Shirahata A (2010) Evaluation method for polyamine uptake by N¹-dansylspermine. *Amino Acids* 38:533–539
- Holst CM, Nevsten P, Johansson F, Carlemalm E, Oredsson SM (2008) Subcellular distribution of spermidine/spermine N¹-acetyltransferase. *Cell Biol Int* 32:39–47
- Pegg AE (2008) Spermidine/spermine N¹-acetyltransferase: a key metabolic regulator. *Am J Physiol Endocrinol Metab* 294:E995–E1010
- Seiler N (1995) Polyamine oxidase, properties and functions. *Prog Brain Res* 106:333–344
- Takao K, Shibata S, Ozawa T, Wada M, Sugita Y, Samejima K, Shirahata S (2009) A conceptual model of the polyamine binding site of N¹-acetyl polyamine oxidase developed from a study of polyamine derivatives. *Amino Acids* 37:401–405
- Seiler N, Dezeure F (1990) Polyamine transport in mammalian cells. *Int J Biochem* 22:211–218
- Seiler N, Delcros JD, Molinoux JP (1996) Polyamine transport in mammalian cells. An update. *Int J Biochem* 28:843–861
- Bey P, Bolkenius FN, Seiler N, Casara P (1985) N-2, 3-butadienyl-1, 4-butanediamine derivatives: potent irreversible inactivators of mammalian polyamine oxidase. *J Med Chem* 28:1–2
- Brunton VG, Grant HM, Wallace HM (1994) Spermine toxicity in BHL-21/C13 cells in the presence of bovine serum: the effect of aminoguanidine. *Toxicol In Vitro* 8:337–341

Use of Polyamine Derivatives as Selective Histone Deacetylase Inhibitors

Patrick M. Woster

Abstract

Histone acetylation and deacetylation, mediated by histone acetyltransferase and the 11 isoforms of histone deacetylase, play an important role in gene expression. Histone deacetylase inhibitors have found utility in the treatment of cancer by promoting the reexpression of aberrantly silenced genes that code for tumor suppressor factors. It is unclear which of the 11 histone deacetylase isoforms are important in human cancer. We have designed a series of polyaminohydroxamic acid (PAHA) and polyaminobenzamide (PABA) histone deacetylase inhibitors that exhibit selectivity among four histone deacetylase isoforms. Although all of the active inhibitors promote reexpression of tumor suppressor factors, they produce variable cellular effects ranging from stimulation of growth to cytostasis and cytotoxicity. This chapter describes the procedures used to quantify the global and isoform-specific inhibition caused by these inhibitors, and techniques used to measure cellular effects such as reexpression of tumor suppressor proteins and hyperacetylation of histones H3 and H4. Procedures are also described to examine the ability of PAHAs and PABAs to utilize the polyamine transport system and to induce overexpression of the early apoptotic factor annexin A1.

Key words: Histone deacetylase, Polyaminohydroxamic acid, Polyaminobenzamide, Annexin A1, Polyamine transport, Breast cancer

1. Introduction

Chromatin architecture, which is strongly influenced by post-translational modifications of histones, is a key factor in the regulation of gene expression (1–3). Several posttranslational modifications of histones (4, 5) mediate epigenetic chromatin remodeling, and histone acetylation/deacetylation are the best-characterized processes (1, 6). The acetylation status of histones is controlled by a balance between two enzymes, histone acetyltransferase (HAT), which promotes histone hyperacetylation, and the histone deacetylases (HDACs), which catalyze acetyl group

cleavage (6, 7). Normal mammalian cells exhibit an exquisite level of control of chromatin architecture by maintaining a balance between these two enzymes (8). There are 11 known zinc-dependent HDAC isoforms (9–11) that belong to four structural classes: class I (isoforms 1–3 and 8) (12), class IIa (isoforms 4, 5, 7, and 9) (9), class IIb (isoforms 6 and 10) (9), and class IV (HDAC 11) (9).

In some tumor cells, hypoacetylation of histones results in aberrant gene silencing leading to the underexpression of growth-regulatory proteins such as the cyclin-dependent kinase inhibitor p21^{Waf1}, thus contributing to tumorigenesis (1, 6). Despite extensive study, it is still uncertain which HDAC isoforms play the most important roles in human cancer. Histone hyperacetylation caused by HDAC inhibitors such as trichostatin A (TSA, **1**, Fig. 1), *N*-(2-aminophenyl)-4-[*N*-(pyridin-3-ylmethoxycarbonyl)-aminomethyl]benzamide (MS-275, **2**, Fig. 1), and suberoylanilide hydroxamic acid (SAHA, **3**, Fig. 1) can cause growth arrest in a wide range of transformed cells, and can inhibit the growth of human tumor xenografts (6, 7, 12–14), especially when used in combination with DNA methyltransferase (DNMT) inhibitors (15–18). Although several HDAC inhibitors are in clinical trials and one agent has been marketed, dose-limiting toxicity remains a problem (19). Most existing HDAC inhibitors do not discriminate between the 11 isoforms of HDAC. Isoform-specific HDAC inhibitors would be of great value in elucidating the roles of HDAC isoforms in both normal and cancer cells, but very few isoform selective inhibitors have been synthesized.

HDAC inhibitors such as **1–3** possess three structural features that are required for optimal activity: an aromatic cap group, an aliphatic chain, and a metal binding functional group (Fig. 2).

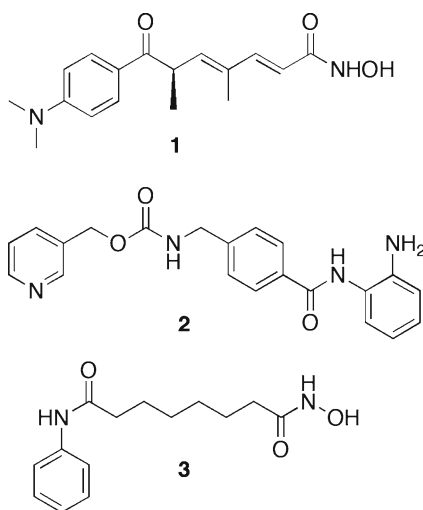


Fig. 1. Histone deacetylase inhibitors trichostatin A (**1**), MS-275 (**2**) and SAHA (**3**).

4 and **5** (Fig. 2), inhibited HDAC in this assay by 75% at a 1.0 μM concentration. Compound **5** at 1.0 μM produced significantly greater induction of acetylated histone H3 (AcH3) and acetylated histone H4 (AcH4) than a like concentration of **2**, and was markedly more effective at reexpressing the cyclin-dependent kinase inhibitor p21^{Waf1} in the ML-1 mouse leukemia cell line. Compound **6** at 1.0 μM (Fig. 2) inhibited the HDAC mixture by 51.5%, but caused a 253-fold induction of acetylated α -tubulin while only causing a minimal increase in AcH3, AcH4, and p21^{Waf1} (**21**), suggesting that **6** shows a marked selectivity toward HDAC 6, which is known to deacetylate α -tubulin (**22**). Compound **6** was later found to inhibit HDAC 6 by 99.7% at 1.0 μM .

Using the same design strategy, a series of polyaminobenzamides (PABAs) and their homologues were synthesized and evaluated as inhibitors of HDAC (**21**). Compound **7** (Fig. 3), one of the first entries in the series, exhibits an IC_{50} value against global HDAC from the HeLa cell lysate of 4.9 μM , which is comparable to the reported IC_{50} value for **2** (4.8 μM) (**23**). Analogues in the PABA series were evaluated against global HDAC and against 4 HDAC isoforms representing Class I (HDAC 1, 3, and 8) and Class II (HDAC 6). Isoform selectivity among the four HDACs evaluated varied significantly, demonstrating that global percent HDAC inhibition is a composite of strong and weak inhibition at different isoforms. The observed HDAC selectivity with PAHAs and PABAs is in part due to structural variations in their polyamine side chains (**24**). PAHA and PABA HDAC inhibitors were also evaluated for their ability to utilize the polyamine transport system (**25**). The hydroxamic acid-containing PAHAs, with pK_a values of approximately 9, are not substrates for the mammalian transporter, while PABAs such as **7** are effectively imported using the polyamine transport system (**21**).

The most active global HDAC inhibitors in the PABA series were evaluated against MCF7 wild-type tumor cells in vitro, and structure-dependent variations in growth inhibitory activity were observed, as exemplified by PABA compounds **8–10** (Fig. 3). All these three analogues inhibited global HDAC between 30 and 40%. However, compounds **8** and **10** showed a marked selectivity for HDAC 1, while compound **9** has negligible activity against this isoform. Over a range of concentrations between 0.3 and 30 μM , benzamide **8** appeared to stimulate tumor cell growth, while **9**, which features a shorter linker chain region and an α -ketoamide metal-binding moiety, was cytostatic. However, benzamide **10**, featuring a shorter polyamine substituent, initiated apoptotic cell death in the MCF7 cell line, with an IC_{50} of 0.9 μM . In the MCF10A normal breast epithelial cell line, **10** exhibited an IC_{50} of 24 μM , and thus demonstrated significant selectivity for tumor cells. Subsequent experiments showed that **10**, but not **8**, promoted the induction of annexin A1, an early intermediate in the

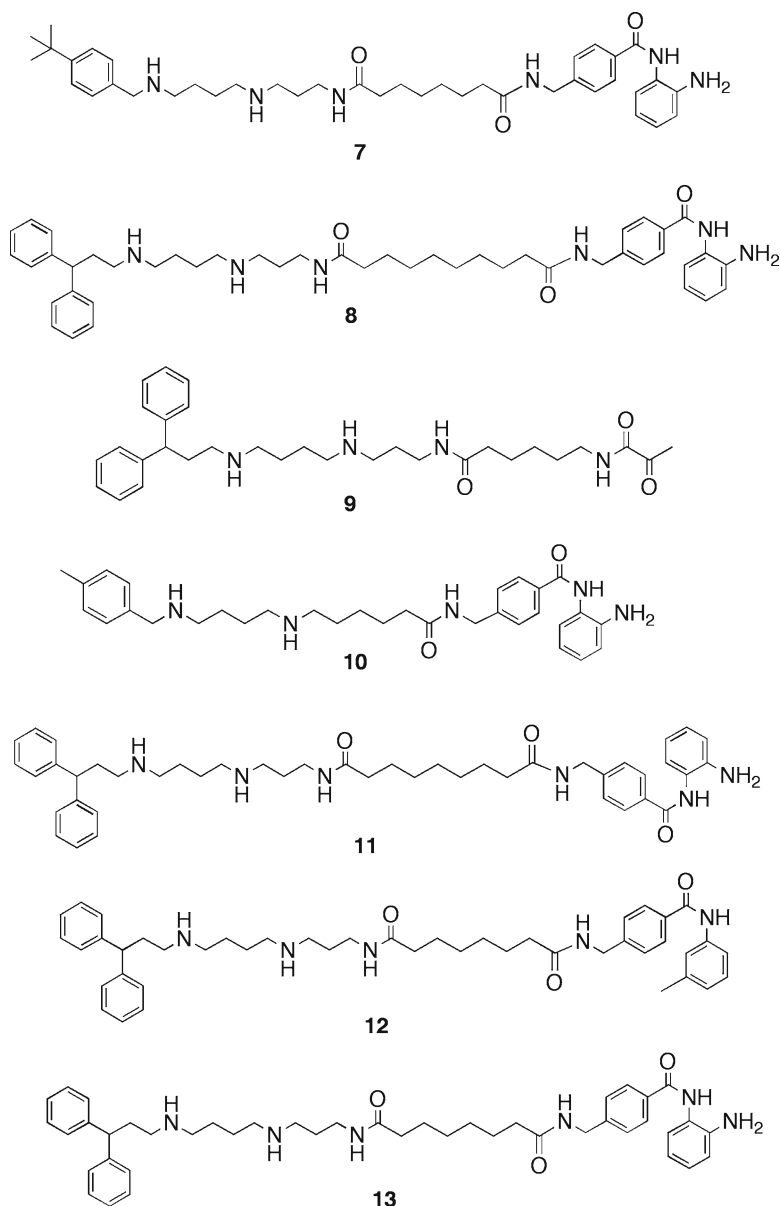


Fig. 3. Polyaminobenzamide (PABA) HDAC inhibitors 7–13.

apoptosis pathway (26). HDAC inhibitors have been shown to promote apoptosis through induction of annexin A1, and recent studies suggest that breast tumors expressing high levels of annexin I are more likely to respond to neoadjuvant chemotherapy than cells with low levels of the protein (27).

Aberrant HDAC activity plays a role in other diseases where an HDAC inhibitor with no inherent cytotoxicity would be of great value. Recent studies have suggested that histone acetylation status plays a role in the development of diabetes mellitus (28, 29)

and that HDAC inhibitors may serve as a novel class of agents for the treatment of diabetes and its complications (30, 31). We thus evaluated PABA HDAC inhibitors for their cytoprotective effects against IL-1 β -induced damage to isolated β -cells. Three PABAs, compounds **11**–**13** (Fig. 3), significantly inhibited HDAC activity and increased the acetylation of histone H4 in isolated β -cells. These compounds further exerted no toxic effects on metabolic cell viability in these cells. PABA **11** protected against IL-1 β -mediated loss in β -cell viability (32). Remarkably, compound **11** differs from **13**, which does not protect against this loss in β -cell viability, by only a single carbon in the linker chain region. Compound **11** was also able to attenuate IL-1 β -induced iNOS expression and subsequent NO release. These data suggest that the cytoprotective properties of **11** against IL-1 β -mediated effects may, in part, be due to inhibition of IL-1 β -induced transactivation of NF κ B in these cells. A novel HDAC inhibitor such as **11** that can prevent IL-1 β -mediated effects on isolated β -cells supports the development of nontoxic PABAs to prevent deleterious effects of cytokines and the onset of autoimmune diabetes.

This chapter describes the procedures used to quantify inhibition caused by these inhibitors and to measure cellular effects such as reexpression of tumor suppressor proteins and hyperacetylation of histones H3 and H4. Procedures are also described to examine their ability to utilize the polyamine transport system and to induce overexpression of the early apoptotic factor annexin A1. A full description of the synthesis of PAHA and PABA HDAC inhibitors is beyond the scope of this manuscript. A full description of these syntheses, including step-by-step procedures and reaction conditions, can be found in refs. (20) and (21).

2. Materials

2.1. HDAC Inhibition Assay

1. Fluor de Lys[®] HDAC Assay Kit AK500 (BIOMOL International, LP, Plymouth Meeting, CA).
2. 96-Well microplates (BD Falcon Microtest 96-well Assay Optilux, Black/Clear Bottom, TC) Surface (BD Biosciences, Franklin Lakes, NJ).
3. Assay buffer: 50 mM Tris-HCl, pH 8.0, 137 mM NaCl, 2.7 mM KCl, 1 mM MgCl₂.
4. SpectraMax M5 plate reader (Molecular Devices, Sunnyvale, CA).

2.2. Isoform Selectivity Studies

1. Fluorogenic HDAC Assay Kit (BPS Bioscience, San Diego, CA).
2. HDAC 1 (C-Flag) (BPS Bioscience, San Diego, CA).

3. HDAC 3 (NcoR2) (BPS Bioscience, San Diego, CA).
4. HDAC 6 (BPS Bioscience, San Diego, CA).
5. HDAC 8 (BPS Bioscience, San Diego, CA).
6. Fluorogenic HDAC Substrate 1 (BPS Bioscience, San Diego, CA).
7. 96-Well microplates (BD Falcon Microtest 96-well Assay Optilux, Black/Clear Bottom, TC) Surface (BD Biosciences).
8. Assay buffer: 50 mM Tris-HCl, pH 8.0, 137 mM NaCl, 2.7 mM KCl, 1 mM MgCl₂.
9. SpectraMax M5 plate reader (Molecular Devices, Sunnyvale, CA).

2.3. HDAC Cellular Assay

1. MCF7 Human breast carcinoma cells (ATCC, Manassas, VA).
2. MCF10A Human breast carcinoma cells (ATCC, Manassas, VA).
3. MCF7 culture medium: RPMI 1640 (ATCC, Manassas, VA) supplemented with 10% fetal bovine serum (FBS, Atlanta Biologicals, Lawrenceville, GA), 10 µg/mL insulin (Sigma/Aldrich, St. Louis, MO), 100 IU/100 µg/mL penicillin/streptomycin solution (Mediatech, Manassas, VA).
4. MCF10A culture medium: DMEM/Ham's F12:50/50 (Mediatech, Manassas, VA) supplemented with 5% horse serum (Atlanta Biologicals, Lawrenceville, GA), 20 ng/mL epidermal growth factor, 100 ng/mL cholera toxin, 10 µg/mL insulin, 500 ng/mL hydrocortisone (Sigma/Aldrich, St. Louis, MO), 100 IU/100 µg/mL penicillin/streptomycin solution (Mediatech).
5. Cell detaching solution: TrypLE Express (Gibco, Bethesda, MD).
6. HDAC Fluorometric Cellular Assay Kit AK503 (BIOMOL International, LP, Plymouth Meeting, CA).
7. 96-Well microplates (BD Falcon Microtest 96-well Assay Optilux, Black/Clear Bottom, TC Surface (BD Biosciences, Franklin Lakes, NJ).
8. SpectraMax M5 plate reader (Molecular Devices, Sunnyvale, CA).

2.4. Cell Culture

1. MCF7 Human breast carcinoma cells (ATCC).
2. MCF10A Human breast carcinoma cells (ATCC).
3. MCF7 culture medium: RPMI 1640 (ATCC) supplemented with 10% fetal bovine serum (FBS, Atlanta Biologicals), 10 µg/mL insulin (Sigma/Aldrich), 100 IU/100 µg/mL penicillin/streptomycin solution (Mediatech).
4. MCF10A culture medium: DMEM/Ham's F12:50/50 (Mediatech) supplemented with 5% horse serum (Atlanta Biologicals), 20 ng/mL epidermal growth factor, 100 ng/mL

cholera toxin, 10 µg/mL insulin, 500 ng/mL hydrocortisone (Sigma/Aldrich), 100 IU/100 µg/mL penicillin/streptomycin solution (Mediatech).

- INS 832/13 culture medium: RPMI 1640 medium containing 10% heat-inactivated fetal bovine serum supplemented with 100 IU/mL penicillin and 100 IU/mL streptomycin, 1.0 mM sodium pyruvate, 50 µM 2-mercaptoethanol, and 10 mM HEPES (pH 7.4).

2.5. Determination of Cell Viability for MCF-7 and MCF 10A Cells In Vitro

- MCF7 Human breast carcinoma cells (ATCC).
- MCF10A Human breast carcinoma cells (ATCC).
- MCF7 culture medium: RPMI 1640 (ATCC) supplemented with 10% fetal bovine serum (FBS, Atlanta Biologicals), 10 µg/mL insulin (Sigma/Aldrich), 100 IU/100 µg/mL penicillin/streptomycin solution (Mediatech).
- MCF10A culture medium: DMEM/Ham's F12:50/50 (Mediatech) supplemented with 5% horse serum (Atlanta Biologicals), 20 ng/mL epidermal growth factor, 100 ng/mL cholera toxin, 10 µg/mL insulin, 500 ng/mL hydrocortisone (Sigma/Aldrich), 100 IU/100 µg/mL penicillin/streptomycin solution (Mediatech).
- Cell detaching solution: TrypLE Express (Gibco).
- CellTiter 96^R AQ_{ucous} One Solution Cell Proliferation Assay Kit (Promega, Madison, WI).
- CellTiter 96^R AQ_{ucous} One Solution Reagent; MTS (3-[4,5-dimethylthiazo-2-yl]-2,5-diphenyltetrazolium bromide) (Promega, Madison, WI).
- 96-Well flat bottom plates (Corning, Corning, NY).
- Microplate reader (E max precision microplate reader) (Molecular Devices, Sunnyvale, CA).

2.6. Western Blotting

- 125 mM Tris-HCl, pH 6.8.
- BCATM Protein Assay Reagent Kit (PIERCE, Rockford, IL).
- Millipore Immobilon Western Chemiluminescent HRP Substrate.
- Science Lab Image Gauge software (FujiFilm, USA).

2.7. Determination of Histone Acetylation by Western Blotting

2.7.1. Determination of Acetylated Histones H3 and H4 in ML-1 Human Acute Myeloid Leukemia Cells

- Buffer A: 25 mM HEPES, pH 7.9, 150 mM NaCl, 0.5 mM EDTA, 0.1% Triton X, 10% Glycerol, 0.1% mg/mL BSA.
- Lysis Buffer B: 10 mM Tris-HCl pH 7.6, 0.25 M sucrose, 3 mM calcium chloride, and 5 mM butyric acid.
- Primary antibodies against acetyl-histone H3 (diluted 1:1,000), acetyl-histone H4 (diluted 1:500), and histone – H2A (diluted 1:1,000) (Upstate Biotechnologies, Lake Placid, NY).

4. Odyssey blocking buffer #927-40000 (Li-Cor Bioscience, Lincoln, NE).
5. Infrared labeled antibodies: anti-mouse IRdye 800, anti-rabbit AlexaFluor 680 (Li-Cor Bioscience, Lincoln, NE).
6. PBS-T (phosphate-buffered saline (PBS) containing 0.1% Tween 20).

2.7.2. Determination of Acetylated Histones H3 and H4 in Insulin-Secreting Rat INS-832/31 Cells

1. 1× Cell lysis buffer : 20 mM Tris-HCl pH 7.5, 150 mM NaCl, 1.0 mM EDTA, 1.0 mM EGTA, 1% Triton X-100, 2.5 mM sodium pyrophosphate, 1.0 mM β -glycerophosphate, 1.0 mM Na_3VO_4 , 1.0 $\mu\text{g}/\text{mL}$ Leupeptin, 1.0 mM PMSF (see Note 1).
2. 3× Sample loading buffer: 2.4 mL of 1.0 M Tris-HCl pH 6.8 stock, 3 mL of 20% SDS stock, 3 mL of 100% Glycerol, 1.6 mL β -mercaptoethanol, 6.0 mg bromophenol blue, diluted to 10 mL with dH_2O .
3. Antibodies (Cell Signaling Technologies, Danvers, MA): Histone H4- 2592- Rabbit, AcH4- 2594 S- Rabbit, Histone H3- 9715- Rabbit, AcH3- 9649 S- Rabbit.
4. Insulin-secreting rat INS-832/31 cells (33).

2.8. Determination of Annex 1A expression

1. MCF7 Human breast carcinoma cells (ATCC).
2. MCF7-AnxA1 stable cells, transfected with annexin A1 with GFP (provided by Dr. F. Hirata at Wayne State University).
3. MCF10A Human breast carcinoma cells (ATCC).
4. MCF7 culture medium: RPMI 1640 (ATCC) supplemented with 10% fetal bovine serum (FBS, Atlanta Biologicals), 10 $\mu\text{g}/\text{mL}$ insulin (Sigma/Aldrich), 100 IU/100 $\mu\text{g}/\text{mL}$ penicillin/streptomycin solution (Mediatech).
5. MCF7-AnxA1 culture medium: Minimum essential medium, Eagle with Earle's balanced salt solution (ATCC, Manassas, VA) supplemented with 10% fetal bovine serum (FBS, Atlanta Biologicals), 10 $\mu\text{g}/\text{mL}$ insulin (Sigma/Aldrich), 100 IU/100 $\mu\text{g}/\text{mL}$ penicillin/streptomycin solution (Mediatech).
6. MCF10A culture medium: DMEM/Ham's F12:50/50 (Mediatech) supplemented with 5% horse serum (Atlanta Biologicals), 20 ng/mL epidermal growth factor, 100 ng/mL cholera toxin, 10 $\mu\text{g}/\text{mL}$ insulin, 500 ng/mL hydrocortisone (Sigma/Aldrich), 100 IU/100 $\mu\text{g}/\text{mL}$ penicillin/streptomycin solution (Mediatech).
7. Cell detaching solution: TrypLE Express (Gibco).
8. Cell lysis buffer: 10 mM Tris-HCl, pH 7.4, 1% SDS, 1 mM EDTA, 1 mM EGTA, 2 mM PMSF, 3 mM-activated Na_3VO_4 , protease inhibitor cocktail.

9. BCA™ Protein Assay Reagent Kit (PIERCE).
10. Polyacrylamide gel: 10% Bis-Tris precast (Bio-Rad Labs, Hercules, CA).
11. Gel running buffer: XT MOPS running buffer (Bio-Rad Labs, Hercules, CA).
12. Precision Plus protein standards (Bio-Rad Labs, Hercules, CA).
13. Sample buffer: XT Sample Buffer (Bio-Rad Labs, Hercules, CA).
14. Blotting buffer: PVDF Westran clear signal membrane (Whatman, Sanford, ME).
15. Transfer buffer: Towbin's Bis-Tris/Glycin/20% methanol without SDS.
16. Antibodies: Anti-Annexin A1 antibody (Santa Cruz Biotechnology, Santa Cruz, CA), anti- β -actin antibody (Sigma-Aldrich, St. Louis, MO), anti-mouse IgG horseradish peroxidase-conjugated antibody (Bio-Rad Labs, Hercules, CA).
17. Immunodetection reagents: ECL advance western blotting detection reagent (Amersham, Piscataway, PA).
18. 6-Well flat bottom plates (Corning).
19. PBS: Mediatech, Manassas, VA).
20. Tris-buffered saline (TBS): 20 mM Tris-HCl, pH 7.5, 137 mM NaCl.
21. Chemiluminescence detection and analyzer, Fuji LAS-1000 Plus and Science Lab Image Gauge (Fuji Film, USA).

2.9. Polyamine Uptake Assay

1. MCF7 Human breast carcinoma cells (ATCC).
2. MCF10A Human breast carcinoma cells (ATCC).
3. MCF7 culture medium: RPMI 1640 (ATCC) supplemented with 10% fetal bovine serum (FBS, Atlanta Biologicals), 10 μ g/mL insulin (Sigma/Aldrich), 100 IU/100 μ g/mL penicillin/streptomycin solution (Mediatech).
4. MCF10A culture medium: DMEM/Ham's F12:50/50 (Mediatech) supplemented with 5% horse serum (Atlanta Biologicals), 20 ng/mL epidermal growth factor, 100 ng/mL cholera toxin, 10 μ g/mL insulin, 500 ng/mL hydrocortisone (Sigma/Aldrich), 100 IU/100 μ g/mL penicillin/streptomycin solution (Mediatech).
5. Cell detaching solution: TrypLE Express (Gibco).
6. [3 H]-spermidine trihydrochloride (Perkin-Elmer, Boston, MA) (see Note 2).
7. Spermidine trihydrochloride (Acros Organics, Morris Plains, NJ).
8. PBS-T (PBS containing 0.1% Tween 20).
9. BCA™ Protein Assay Reagent Kit (PIERCE).
10. 24-Well plates, flat bottom (Corning).

3. Methods

3.1. HDAC Inhibition Assay

1. HDAC inhibition activity was evaluated *in vitro* by using HDAC fluorimetric assay/drug discovery kit AK500. The assay was performed in a 96-well plate. 30-fold diluted HeLa extract was used as source of HDAC activity.
2. The Fluor de Lys™ substrate containing acetylated lysine side chains was normalized by plotting a standard curve at various substrate concentrations.
3. A 10 μL portion of the desired inhibitor molecule (5 μM final concentration) in assay buffer, 25 μL of Fluor de Lys™ substrate (250 μM), 0.5 μL of HeLa cell extract (6–9 mg/mL), and 14.5 μL assay buffer were incubated at 37°C in an appropriate well of the microtiter plate for 30 min (see Note 3).
4. The reaction was stopped by adding 50 μL Fluor de Lys™ developer cocktail, and the plate was incubated at room temperature for 15 min.
5. Fluorescence was measured using a SpectraMax M5 plate reader (excitation wave length 360 nm, emission wave length 450 nm).

3.2. Isoform Selectivity Studies

1. Inhibition of individual HDAC isoform activity was evaluated using a Fluorogenic HDAC Assay Kit (BPS Bioscience) performed in a 96-well plate. Human recombinant HDAC immunoprecipitates were used as the source of HDAC activity.
2. A 10 μL portion of the desired inhibitor molecule (5 μM final concentration) in assay buffer, 5 μL of substrate (200 μM), 5.0 μL HDAC 6 (0.2 $\mu\text{g}/\mu\text{L}$), HDAC 3 (0.2 $\mu\text{g}/\mu\text{L}$), HDAC 1 (0.04 $\mu\text{g}/\mu\text{L}$) or HDAC 8 (0.6 $\mu\text{g}/\mu\text{L}$), and 35.0 μL assay buffer were incubated at 37°C in an appropriate well of the microtiter plate for 30 min.
3. The reaction was stopped by adding 50 μL of the developer cocktail.
4. The plate was incubated at room temperature for 15 min.
5. Fluorescence was measured using a SpectraMax M5 plate reader (excitation wave length 360 nm, emission wave length 450 nm).

3.3. HDAC Cellular Assay

1. Cells were seeded in 200 μL of the appropriate medium at 7,000 cells per well without phenol red, and were cultured at 37°C in 5% CO_2 for 2.5 days (80% confluences in a 96-well microplate).
2. Cells were exposed to test compounds in 100 μL of medium for 6 days. The medium containing the compound was changed every 3 days.

3. Medium was replaced with 50 μL /well of media containing 200 μM of the Fluor de LysTM substrate. The plates were incubated at 37°C for 3 h and 40 min.
4. The reaction was stopped by adding 50 μL Fluor de LysTM developer cocktail containing 1 \times developer in cold lysis buffer and 2 mM trichostatin A.
5. The plate was incubated at 37°C for 15 min.
6. Fluorescence was measured using a SpectraMax M5 plate reader (excitation wave length 360 nm, emission wave length 450 nm).

3.4. Cell Culture

1. Human breast carcinoma MCF-7 (HTB-22) was maintained in the logarithmic phase at 37°C in a 5% CO₂ humidified atmosphere in the medium described above.
2. Human mammary epithelial cells (MCF 10A) were obtained from Karmanos Cancer Institute, Detroit, MI, and grown in the logarithmic phase at 37°C in a 5% CO₂ humidified atmosphere in the DMEM described above.
3. INS 832/13 cells were cultured in the medium described above at 37°C in a 5% CO₂ humidified atmosphere. The medium was changed twice weekly and cells were trypsinized and subcloned weekly.

3.5. Determination of Cell Viability for MCF-7 and MCF 10A Cells In Vitro

1. 7,500 Cells/well in 200 μL medium were seeded in a 96-well plate, and the cells were allowed to attach at 37°C in 5% CO₂ for 2.5 days.
2. The medium was aspirated, and cells were treated with 200 μL fresh medium containing gradually increasing concentrations of the test compound. The cells were incubated for 6 days at 37°C in 5% CO₂. Medium containing compounds was replaced every 3 days.
3. After 6 days, the medium was removed and replaced with a mixture of 100 μL phenol red free medium and 20 μL of the MTS reagent solution. The cells were incubated for another 4 h at 37°C under 5% CO₂ environment.
4. Absorbance was measured at 490 nm on a microplate reader equipped with SOFTmax PRO 4.0 software to determine the cell viability.

3.6. Western Blotting

1. Protein extracts were prepared in 125 mM Tris-HCl (pH 6.8), denatured using 4% SDS.
2. Protein content was quantitated using the BCATM Protein Assay Reagent Kit.
3. Extracts were subjected to polyacrylamide gel electrophoresis (PAGE) and electroblotted to nitrocellulose.

4. Blots were probed with antibodies and developed with Millipore Immobilon Western Chemiluminescent HRP Substrate.
5. Chemiluminescence was detected by Luminescence Image Analyzer, Fuji LAS-1000 Plus or Odyssey Infrared Imaging system.
6. Bands were analyzed by the Science Lab Image Gauge software (Fuji Photo Film).

3.7. Determination of Histone Acetylation

3.7.1. Determination of Acetylated Histones H3 and H4 in ML-1 Human Acute Myeloid Leukemia Cells

1. ML-1 human acute myeloid leukemia cells were seeded at the rate of 2×10^6 cells/T-25 flask in 5.0 mL McCoy's 5A medium containing 9% fetal bovine serum and allowed to attach overnight.
2. Cells were treated with appropriate concentration of PABAs and PAHAs in the presence of 1.0 mM aminoguanidine and incubated for 24 h at 37°C with 5% CO₂.
3. At the end of 24 h, cells were harvested with trypsin and were converted to pellets, which were washed with 1× PBS and repelleted.
4. The pellet was resuspended in buffer A and protease inhibitors (~200 µL per T-25 flask).
5. The samples were transferred to chilled 1.5 mL tubes and were incubated on ice for 20 min. Nuclei were collected by centrifugation at 14,000 rpm for 15 min.
6. The pellets were resuspended in 250 µL ice cold lysis buffer B. 0.4 N Sulfuric acid was added to the samples, and they were incubated at 4°C overnight.
7. Debris was pelleted by centrifugation and the supernatant was collected. Histones were precipitated by addition of 10 volumes of acetone and incubated at -20°C overnight.
8. Pellets were collected by centrifugation, briefly dried under vacuum and resuspended in ddH₂O.
9. Proteins (10–20 µg per lane) are separated on 15% SDS-PAGE and visualized by Western blot analysis (see Subheading 3.6) using primary antibodies against AcH3, H4, and H2A.
10. The immunoreactive proteins were quantified using Odyssey Infrared Imaging System.

Protein was transferred to PVDF, and the membrane was blocked for 1 h with Odyssey blocking buffer. Primary antibodies in the same dilution as mentioned above were added to the blocking buffer along with 0.1% Tween 20. The membrane was washed 5 times with PBS-T for 5 min. Infrared labeled antibodies anti-mouse IRdye 800 and anti-rabbit AlexaFluor 680 were diluted in

blocking buffer with 0.1% Tween 20 to 1:4,000. The antibody solution was added to the membrane and it was rocked for 1 h at room temperature. It was washed again for 5 min, and the membrane is scanned on Odyssey Infrared Imaging system.

3.7.2. Determination of Acetylated Histones H3 and H4 in Insulin-Secreting Rat INS-832/31 Cells

1. INS-832/13 (33) cells were cultured for 2 days in a 24-well plate in RPMI media.
2. The media was aspirated and the cells were rinsed twice with ice cold PBS.
3. 50 μ L of ice cold 1 \times cell lysis buffer was pipetted into each well and immediately scraped and collected into microcentrifuge tubes such that 3 wells were combined per tube.
4. The cells were then lysed by sonication.
5. Cell lysate protein concentration was then quantitated using Bio-Rad's Bradford reagent standardized with BSA.
6. 10 μ g of protein was then taken from each sample and combined with a 1:3 ratio of 3 \times sample loading buffer.
7. The proteins were then separated on a 12% SDS-PAGE gel.
8. The proteins were then transferred, overnight, to a nitrocellulose membrane by wet transfer.
9. The membrane was then blocked with 5% BSA in TBST for 1 h with gentle agitation.
10. The 1 $^{\circ}$ antibody was diluted 1:1,000 in 5% BSA in TBST and applied over night to the membrane at 4 $^{\circ}$ C with gentle agitation.
11. The membrane was then washed 3 \times 10 min in TBST with gentle agitation.
12. The 2 $^{\circ}$ antibody was then applied to the membrane with a dilution of 1:1,000 in 5% BSA in TBST for 1 h. The 2 $^{\circ}$ anti-rabbit antibody was purchased from GE Health Sciences #NA931V.
13. The membrane was then washed 3 \times 10 min in TBST.
14. The membrane was then developed with ECL Plus (GE Health Science).
15. The blot was then imaged using a Kodak Image Station 4000R Pro.

3.8. Determination of Annex 1A Expression

1. Cells were seeded at the rate of 1.0×10^6 cells/well in 6-well plate in 2 mL of the indicated medium and allowed to grow to 90% confluency.
2. Cells were treated with an appropriate concentration of inhibitor and incubated for 2.5 days at 37 $^{\circ}$ C with 5% CO $_2$.
3. Cells were detached using the cell detaching solution, and washed twice with PBS.

4. A 120 mM portion of lysis buffer was added, and the cells were incubated for 5 min on ice.
5. The lysed cells were collected with a scraper, samples were transferred to chilled 1.5 mL tubes, and nuclei were collected by centrifugation at 15,000 rpm for 5 min at 4°C.
6. The pellets were resuspended in 80 μ L ice cold lysis buffer. Samples were sonicated 3 times for 10 s followed by 10 s break in between them and boiled for 5 min at 95°C.
7. Protein content was quantitated using BCA™ Protein Assay Reagent Kit.
8. Proteins (10 or 3 μ g per lane) were separated by SDS-PAGE.
9. Protein was transferred to PVDF membrane and blocked overnight at 4°C with 1% ECL blocking buffer.
10. Blots were probed with primary antibodies against annexin A1 and β -actin diluted in blocking buffer, then washed 4 times with 1% TBS for 10 min on a shaker.
11. Blots were then treated with anti-m-IgG-HRP diluted in blocking buffer with 0.1% Tween 20.
12. The membrane was washed 4 times with 1% TBS with 0.1% Tween 20 for 10 min on a shaker.
13. The membrane was developed with ECL advance blotting reagent.
14. Chemiluminescence signals were detected with the Fuji LAS-1000 Plus, and bands were analyzed by the Science Lab Image Gauge software.

3.9. Polyamine Uptake Assay

1. MCF7 cells were seeded at the rate of 5×10^5 cells/well or MCF10A cells were seeded at 3×10^5 cells/well in the appropriate medium and cultured for 2.5 days at 37°C in 5% CO₂ in 24-well plates. Cells were allowed to exponential growth at 37°C for 2.5 days.
2. The medium was removed by aspiration and replaced with 0.5 mL serum-free medium to each well and allowed to incubate for 1 h at 37°C in 5% CO₂.
3. A mixture of ³H spermidine trihydrochloride (34) and unlabeled spermidine (5 μ L, 96 μ M) was added to each well with increasing concentrations of PAHA or PABA inhibitor from 0.3–30 μ M and incubated at 37°C for 30 min.
4. Medium containing residual ³H spermidine was aspirated, and cells were placed on ice and rinsed 3 times with 1 mL cold phosphate-buffer saline (PBS).
5. Cells were digested for 1 h at room temperature in 400 μ L 1 N NaOH.

6. Prior to determination of cell associated radioactivity, 400 μL of the cell digest was neutralized with 420 μL of 1 N acetic acid.
7. The 720 μL of neutralized digest was added to 4 mL of scintillation fluid, and the radioactivity was counted using a β -rack liquid scintillation counter (Perkin Elmer, MA).

4. Notes

1. Utilization of this lysis buffer is important to prevent the loss of acetyl groups. If you are not probing for acetylated histones, then other lysis buffers may be substituted.
2. Use of tritiated substances requires institutional training and approval by the office of radiation safety. All procedures should be carried out in areas within laboratories that have been approved for use of radioisotopes. Radioactive waste should be disposed of in approved containers.
3. All aqueous solutions should be prepared in water that has a resistivity of 18.2 $\text{M}\Omega\text{-cm}$ and total organic content of less than five parts per billion.
4. Acetylated histones must be probed first because stripping will remove the acetyl groups.

References

1. Marks PA, Richon VM, Breslow R, Rifkind RA (2001) Histone deacetylase inhibitors as new cancer drugs. *Curr Opin Oncol* 13:477–483
2. Luger K, Mader AW, Richmond RK, Sargent DF, Richmond TJ (1997) Crystal structure of the nucleosome core particle at 2.8 Å resolution. *Nature* 389:251–260
3. Jenuwein T, Allis CD (2001) Translating the histone code. *Science* 293:1074–1080
4. Herman JG, Baylin SB (2003) Gene silencing in cancer in association with promoter hypermethylation. *N Engl J Med* 349:2042–2054
5. Robertson KD (2001) DNA methylation, methyltransferases, and cancer. *Oncogene* 20:3139–3155
6. Johnstone RW (2002) Histone-deacetylase inhibitors: novel drugs for the treatment of cancer. *Nat Rev Drug Discov* 1:287–299
7. Marks P, Rifkind RA, Richon VM, Breslow R, Miller T, Kelly WK (2001) Histone deacetylases and cancer: causes and therapies. *Nat Rev Cancer* 1:194–202
8. Shogren-Knaak M, Ishii H, Sun JM, Pazin MJ, Davie JR, Peterson CL (2006) Histone H4-K16 acetylation controls chromatin structure and protein interactions. *Science* 311(5762):844–847
9. Haberland M, Montgomery RL, Olson EN (2009) The many roles of histone deacetylases in development and physiology: implications for disease and therapy. *Nat Rev Genet* 10:32–42
10. Gray SG, Ekstrom TJ (2001) The human histone deacetylase family. *Exp Cell Res* 262:75–83
11. Taunton J, Hassig CA, Schreiber SL (1996) A mammalian histone deacetylase related to the yeast transcriptional regulator Rpd3p. *Science* 272:408–411
12. Grozinger CM, Schreiber SL (2002) Deacetylase enzymes: biological functions and the use of small-molecule inhibitors. *Chem Biol* 9:3–16
13. Weinmann H, Ottow E (2004) Recent advances in the medicinal chemistry of histone deacetylase inhibitors. *Ann Rep Med Chem* 39:185–196
14. Kouraklis G, Theocharis S (2006) Histone deacetylase inhibitors: a novel target of anticancer therapy (review). *Oncol Rep* 15:489–494

15. Cameron EE, Bachman KE, Myohanen S, Herman JG, Baylin SB (1999) Synergy of demethylation and histone deacetylase inhibition in the re-expression of genes silenced in cancer. *Nat Genet* 21:103–107
16. Herman JG, Civin CI, Issa JP, Collector MI, Sharkis SJ, Baylin SB (1997) Distinct patterns of inactivation of p15INK4B and p16INK4A characterize the major types of hematological malignancies. *Cancer Res* 57:837–841
17. Herman JG, Jen J, Merlo A, Baylin SB (1996) Hypermethylation-associated inactivation indicates a tumor suppressor role for p15INK4B. *Cancer Res* 56:722–727
18. Corn PG, Smith BD, Ruckdeschel ES, Douglas D, Baylin SB, Herman JG (2000) E-cadherin expression is silenced by 5' CpG island methylation in acute leukemia. *Clin Cancer Res* 6:4243–4248
19. Ryan QC, Headlee D, Acharya M, Sparreboom A, Trepel JB, Ye J, Figg WD, Hwang K, Chung EJ, Murgo A, Melillo G, Elsayed Y, Monga M, Kalnitskiy M, Zwiebel J, Sausville EA (2005) Phase I and pharmacokinetic study of MS-275, a histone deacetylase inhibitor, in patients with advanced and refractory solid tumors or lymphoma. *J Clin Oncol* 23:3912–3922
20. Varghese S, Gupta D, Baran T, Jiemjit A, Gore SD, Casero RA Jr, Woster PM (2005) Alkyl-substituted polyaminohydroxamic acids: a novel class of targeted histone deacetylase inhibitors. *J Med Chem* 48:6350–6365
21. Varghese S, Senanayake T, Murray-Stewart T, Doering K, Fraser A, Casero RA, Woster PM (2008) Polyaminohydroxamic acids and polyaminobenzamides as isoform selective histone deacetylase inhibitors. *J Med Chem* 51:2447–2456
22. Hubbert C, Guardiola A, Shao R, Kawaguchi Y, Ito A, Nixon A, Yoshida M, Wang XF, Yao TP (2002) HDAC6 is a microtubule-associated deacetylase. *Nature* 417:455–458
23. Suzuki T, Ando T, Tsuchiya K, Fukazawa N, Saito A, Mariko Y, Yamashita T, Nakanishi O (1999) Synthesis and histone deacetylase inhibitory activity of new benzamide derivatives. *J Med Chem* 42:3001–3003
24. Casero RA Jr, Woster PM (2009) Recent advances in the development of polyamine analogues as antitumor agents. *J Med Chem* 52:4551–4573
25. Seiler N, Delcros JG, Moulinoux JP (1996) Polyamine transport in mammalian cells. An update. *Int J Biochem Cell Biol* 28:843–861
26. Tabe Y, Jin L, Contractor R, Gold D, Ruvolo P, Radke S, Xu Y, Tsutusmi-Ishii Y, Miyake K, Miyake N, Kondo S, Ohsaka A, Nagaoka I, Andreeff M, Konopleva M (2007) Novel role of HDAC inhibitors in AML1/ETO AML cells: activation of apoptosis and phagocytosis through induction of annexin A1. *Cell Death Differ* 14:1443–1456
27. Chuthapitsith S, Bean BE, Cowley G, Eremin JM, Samphao S, Layfield R, Kerr ID, Wiseman J, El-Sheemy M, Sreenivasan T, Eremin O (2009) Annexins in human breast cancer: Possible predictors of pathological response to neoadjuvant chemotherapy. *European Journal of Cancer* 45(7):1274–81
28. Gowri PM, Yu JH, Shaufel A, Sperling MA, Menon RK (2003) Recruitment of a repressor complex at the growth hormone receptor promoter and its potential role in diabetic nephropathy. *Mol Cell Biol* 23:815–825
29. Miao F, Gonzalo IG, Lanting L, Natarajan R (2004) In vivo chromatin remodeling events leading to inflammatory gene transcription under diabetic conditions. *J Biol Chem* 279:18091–18097
30. Gray SG, De Meyts P (2005) Role of histone and transcription factor acetylation in diabetes pathogenesis. *Diab Metab Res Rev* 21:416–433
31. Lee HB, Noh H, Seo JY, Yu MR, Ha H (2007) Histone deacetylase inhibitors: a novel class of therapeutic agents in diabetic nephropathy. *Kidney Int Suppl* (106):S61–S66
32. Susick L, Senanayake T, Veluthakal R, Woster PM, Kowluru A (2009) A novel histone deacetylase inhibitor prevents IL-1beta-induced metabolic dysfunction in pancreatic beta-cells. *J Cell Mol Med* 13(8B):1877–85
33. Hohmeier HE, Mulder H, Chen G, Henkel-Rieger R, Prentki M, Newgard CB (2000) Isolation of INS-1-derived cell lines with robust ATP-sensitive K⁺ channel-dependent and -independent glucose-stimulated insulin secretion. *Diabetes* 49:424–430
34. Aziz SM, Yatin M, Worthen DR, Lipke DW, Crooks PA (1998) A novel technique for visualizing the intracellular localization and distribution of transported polyamines in cultured pulmonary artery smooth muscle cells. *J Pharm Biomed Anal* 17:307–320

Chapter 32

Measurement of Polyamine pK_a Values

Ian S. Blagbrough, Abdelkader A. Metwally, and Andrew J. Geall

Abstract

The extent of ionization of the polyamines is an important factor in their interactions with cellular components. The pK_a is the pH at which a functional group is 50% ionized. For compounds such as polyamines with more than one ionizable center (atom or functional group), there is a pK_a value for each center of ionization. This chapter describes the pK_a values for each amine group in many important polyamines, the factors influencing these values and methods for their determination using potentiometric titration and nuclear magnetic resonance spectroscopy.

Key words: Ionization, Potentiometry, Nuclear magnetic resonance spectroscopy, DNA condensation, Henderson–Hasselbalch equation

1. Introduction

The pK_a is the pH at which a functional group (or a molecule if it only has one ionizable group) is 50% ionized. pK_a is defined as $-\log K_a$, where K_a is the dissociation constant (not association) of the reaction:

$[H^+] + [A^-] = [HA]$. In other words, $K_a = [H^+][A^-]/[HA]$, and its units are therefore molar. The Henderson–Hasselbalch equation (1–4) describes the relationship between pK_a, pH, and the ratio of ionized to nonionized species:

$pH = pK_a + \log_{10}[A^-]/[HA]$ or $pH = pK_a + \log_{10}[\text{conjugate base}]/[\text{acid}] = pK_a + \log_{10}[\text{base}]/[\text{conjugate acid}]$, perhaps better shown as:

$$\begin{aligned} pH &= pK_a + \log \frac{[\text{conjugate base}]}{[\text{acid}]} = pK_a + \log \frac{[A^-]}{[HA]} \\ &= pK_a - \log \frac{[\text{conjugate acid}]}{[\text{base}]} = pK_a - \log \frac{[BH^+]}{[B]} \end{aligned}$$

this apparent inversion follows as: $+\log[\text{conjugate base}]/[\text{acid}] = -\log[\text{acid}]/[\text{conjugate base}]$.

For compounds with more than one ionizable center (atom or functional group), for example polyamines and amino acids, there is a pK_a value for each center of ionization (see examples and Figs. 1–4 and Table 1 at the end of this section). The pK_a of each amine group in a polyamine is affected by the type of amine (primary, secondary, tertiary, or quaternary), electronic factors more than steric factors, the position of the amine group in the compound (e.g., if it is conjugated to an aromatic ring), and especially by the number of (usually, but not exclusively) carbon atoms between neighboring amines (Fig. 1).

There are three methods used to determine pK_a values. The most common is potentiometric titration, and this is automated and the easiest, given sufficient material. The second is spectroscopic using nuclear magnetic resonance (NMR) spectroscopy; while this requires significantly more compound, it is (should be) entirely recoverable after the measurement, albeit as its salt or corresponding free base. This is now generally available given the ready availability of high-field NMR spectrometers in chemistry and biochemistry departments and in many (pharmaceutical) analytical laboratories. However, it is not as routine as potentiometric titration, but it does provide a wealth of other useful (spectroscopic) information along the way. NMR determination involves measuring chemical shifts as a function of pH, and offers the advantage of measuring pK_a in solutions that are not pure, e.g., in the presence of biological fluids or even of impurities, something which cannot be achieved by potentiometry (5). NMR also allows the (overall) sequence of polyamine protonation to be determined or even followed. The NMR experimental time will depend on the concentration and exact nucleus being observed, which can itself be a practical problem for species only in micromolar concentrations. The third method is spectrophotometric. While this adds a historical perspective, its use requires visible or

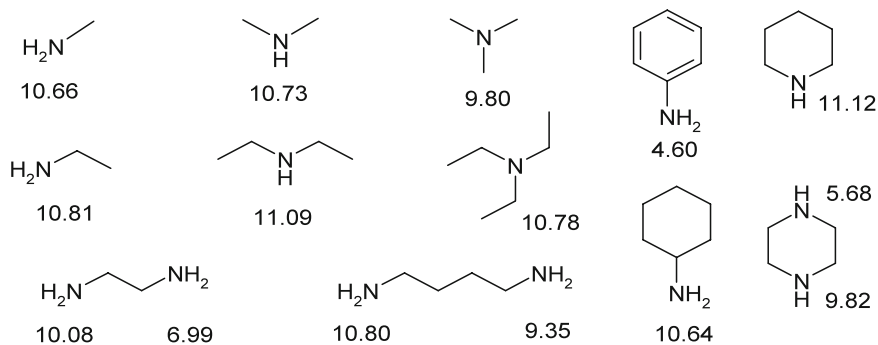


Fig. 1. pK_a values of different simple mono- and diamines.

Table 1
Potentiometrically measured pK_a values of steroidal polyamine conjugates and the net positive charge (at pH 7.4) calculated using the Henderson–Hasselbalch equation (27)

Polyamine	Measured pK _a s	Net charge
Spermine (3.4.3)	10.9 ± 0.01 10.1 ± 0.01 8.9 ± 0.01 8.1 ± 0.01	3.8
3.4.3-cholesteryl-3-carbamate 1	10.1 ± 0.06 8.6 ± 0.06 7.3 ± 0.05	2.4
3.3.3-cholesteryl-3-carbamate 2	10.7 ± 0.04 8.8 ± 0.02 7.2 ± 0.02	2.3
3.2.3-cholesteryl-3-carbamate 3	10.0 ± 0.02 8.0 ± 0.02 5.5 ± 0.02	1.8
2.3.2-cholesteryl-3-carbamate 4	9.3 ± 0.01 7.6 ± 0.01 5.7 ± 0.01	1.6
2.2.2.2-cholesteryl-3-carbamate 5	9.9 ± 0.20 8.4 ± 0.20 6.3 ± 0.21 3.9 ± 0.21	2.0
2.2.2.2.2-cholesteryl-3-carbamate 6	10.2 ± 0.10 8.6 ± 0.08 7.2 ± 0.09 4.4 ± 0.09 2.5 ± 0.28	2.3
Diocetyldecylglycylspermine (DOGS, Transfectam) (32)	10.5 9.5 8.4 5.5	2.9

UV chromophores, and these are lacking in typical polyamines; thus there are no obvious literature examples within polyamine research. There are numerous software packages for the prediction of pK_a values (6).

The measurement of pK_a data is crucial to study and understand many biological processes. For example, the ionization of spermine at physiological pH is essential for its electrostatic binding to the negatively charged phosphate groups of DNA. The distribution of charge on the surface of polyamines has profound

effect on the interaction with and conformational change induction of DNA (7). The amphiphilic nature of many phospholipids, being a major component of mammalian cell membrane, is attributed to the ionization of their phosphate groups in the physiological pH. The distribution (partition) of polyamines, as their free bases, into lipid bilayers is important for their interaction with ligand- or voltage-gated cation channels over extended periods of time (8–13).

The importance of polyamine pK_a in relation to their biological activities has been pointed out in many studies. Bergeron et al. pointed out the importance of ionization pattern of series of analogs and homologs of N^1, N^{12} -diethylspermine for their biological activity (14), where the tetracationic species showed better uptake by cells compared to the dicationic species. Binding of spermine to an autonomous domain of the regulatory subunit of protein kinase CK2 was lowered when the highly acidic binding domain of B subunit of CK2 was modified by introducing alanine to replace three glutamic acids (15). The binding of several polyamines to human serum albumin is also attributed to the protonation of the amine groups at physiological pH (16). The binding of polynucleotides such as DNA and siRNA to fatty acid derivatives of spermine (17) and aminoglycoside-polyamine conjugates (18) is also dependant on the protonation of the polyamines, which in turn depend on the pK_a values of the individual amine groups.

1.1. Worked Examples

Examples of pK_a values of different simple mono- and diamines (19, 20) are shown in Fig. 1. The increase in alkyl chain length or in number of alkyl substituents increases pK_a ; however, steric effects may lower pK_a as seen between trimethyl- and triethylamine and the corresponding dimethyl- and diethylamine. The aromatic amine aniline has a significantly lower pK_a value than hexylamine due to the delocalization of the electron lone-pair into the aromatic ring.

With regard to the simple linear polyamines (Fig. 2), spermidine, pK_a values are from potentiometry (21): 10.81, 9.94, 8.40; and also from potentiometry (22) (at 51 mM): 10.84 ± 0.10 , 10.06 ± 0.10 , 8.57 ± 0.11 ; and from potentiometry (23): 10.89 ± 0.05 , 9.81 ± 0.02 , 8.34 ± 0.03 ; and from NMR (22) (at 51 mM): 10.90 ± 0.21 , 9.71 ± 0.12 , 8.25 ± 0.09 . pK_a values from potentiometry (21) for: 6-fluorospermidine 10.40, 9.55, 7.18; 7-fluorospermidine 10.28, 9.00, 7.80; 6,6-difluorospermidine 10.34, 9.29, 5.70; 7,7-difluorospermidine 10.25, 8.24, 6.64; 2,2-difluorospermidine 10.32, 7.30, 5.50; 6-fluorospermine from NMR (24): 10.7, 9.7, 8.04, 6.62; 6,6-difluorospermine from NMR (24): 10.7, 9.8, 7.74, 5.11. pK_a values for thermospermine (3.3.4) from potentiometry (25) (at 3 mM): 11.14, 10.49, 9.23, 7.58, therefore the total charge on thermospermine at pH=7.4 is calculated to be +3.587. The fluorinated analogs

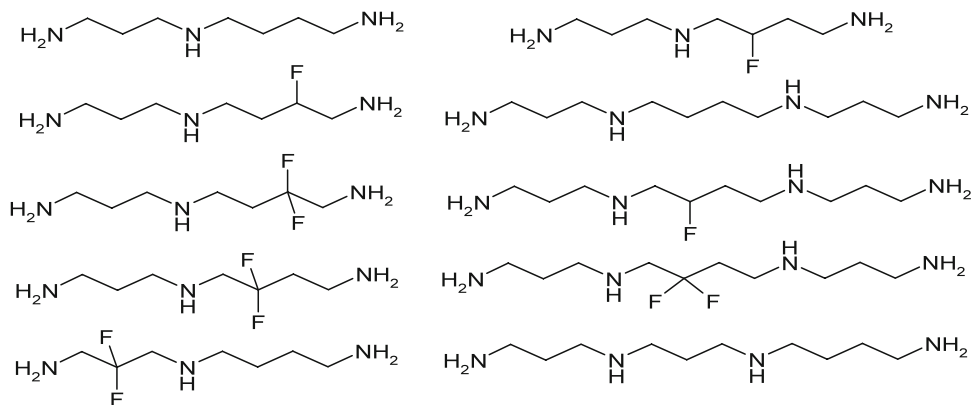


Fig. 2. Simple linear polyamines, spermidine (3.4), spermine (3.4.3), and thermospermine (3.3.4).

have different protonation constants according to the fluorination site. When these fluorinated spermidine analogs were used as substrates for the enzyme spermine synthase, there was a change in the affinity constant according to the substrate used. 6-Fluorospermidine did not affect the affinity constant while the 6,6-difluorospermidine reduced the affinity constant five-fold (21). These data reflect the effect of changing protonation constants on the biochemical activity of substrates. Taking spermine as a detailed worked example, at $pH = 7.4$, pK_a values from potentiometry (26): 10.80, 10.02, 8.85, 7.96 (charge = +3.748), and also from potentiometry (27): 10.9, 10.1, 8.9, 8.1 (charge = +3.801), and from NMR (5): 11.20, 10.30, 9.05, 8.18 (charge = +3.835). At the slightly lower $pH = 6.8$, spermine is “effectively fully protonated,” charge = +3.954 (5).

In order to investigate DNA condensation and gene delivery, we have designed and synthesized a series of polyamine cholesteryl carbamates as potential vectors where both the positive charge and its regiochemical distribution have been varied along the polyamine moiety. Others have investigated polyethylenimines (PEI) in this context (Fig. 3). The charge on the polyamine conjugates has been determined by measuring the pK_a s (Table 1) potentiometrically, using a Sirius PCA101 automated titrator (27). The net positive charge carried by these molecules at physiological pH (7.4) has then been calculated using the Henderson–Hasselbalch equation (Table 1). The pK_a s of polyamines are a function of the interamine distance as well as their substituents. It is important to recognize that any charge is shared across several of the basic centers and that it cannot be attributed to a single point. With the specific examples of fluorinated polyamine analogs, e.g., 7,7-difluorospermidine, the pK_a s of polyamines near to the electron withdrawing fluorines are significantly lowered (21, 24), and therefore the first positive charge is predominantly

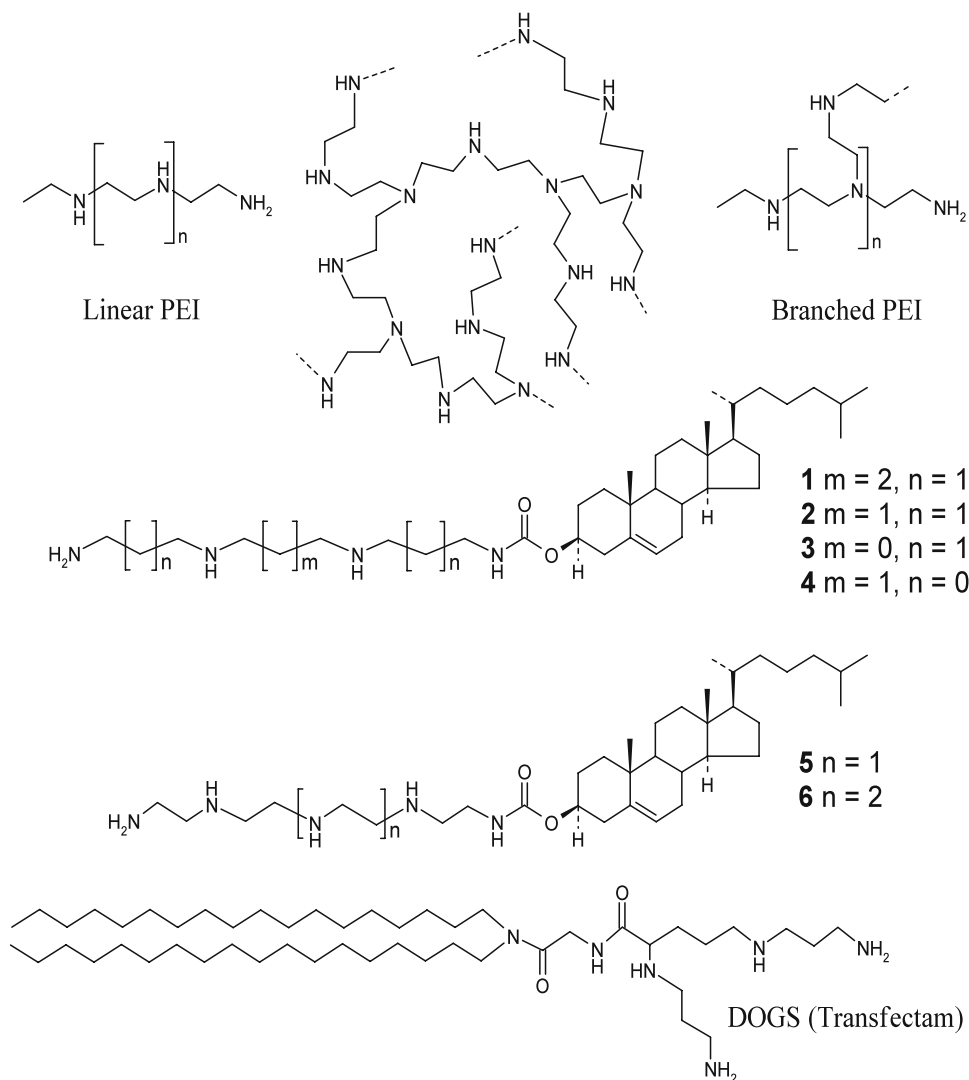


Fig. 3. Polyethylenimines (PEIs), some of our cholesteryl polyamine carbamates **1–6**, and the lipopolyamine dioctadecylglycylspermine (DOGS, Transfectam) used in gene delivery.

on one primary amine (N^1) until $\text{pH}=9$ when the second charge develops on the secondary amine (N^4) until $\text{pH}=7$. Even when the first charge is introduced principally on the primary amine, e.g., of unsubstituted spermidine, it is also distributed on to the secondary amines. This has been demonstrated using unsymmetrical triamine, spermidine (22) and illustrates that not all amines are fully protonated at physiological pH. Furthermore, there exists a series of complex equilibria between the ammonium ions and the corresponding amines. This series of molecules (Table 1) all carry different net charges at $\text{pH} 7.4$, which are distributed on varying lengths of methylene chain and could therefore reasonably

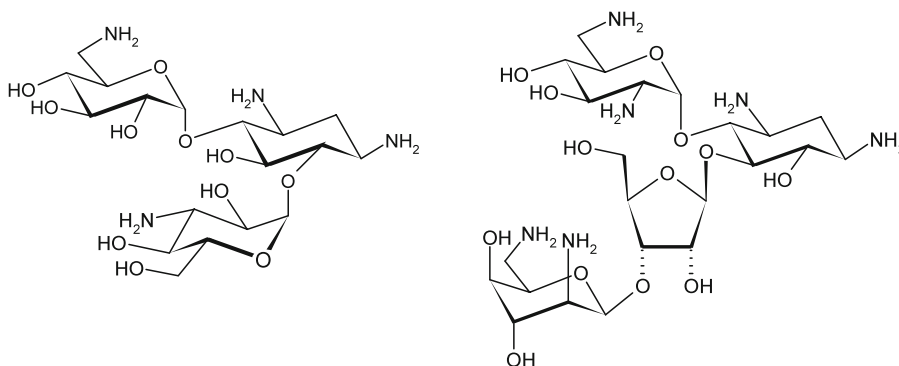


Fig. 4. Aminoglycosides are structurally more complex polyamines e.g. kanamycin A (left) and neomycin B (right).

be expected to impart differences in biological activity, e.g., in binding to polynucleic acids (DNA or siRNA).

Kanamycin A and neomycin B (Fig. 4) are indeed polyamines, just not linear molecules. Furthermore, they deserve special consideration of their pK_a data as they show how steric and electronic effects significantly come into play. Kanamycin A has pK_a values of 9.03, 8.16, 7.42, 6.19 (28). The fact that one of these bases has a pK_a value below 7.4, and another at around 7.4 means that only 2.4 positive charges are carried at $pH=7.4$ from the Henderson–Hasselbalch equation: $pK_a = pH - \log[\text{conjugate base}]/[\text{acid}]$. Similarly, neomycin B, with its pK_a values of 8.8, 8.6, 8.1, 7.6, 7.6 (sic), 5.7 (29), for six seemingly similar primary amine functional groups, carries only 4.0 positive charges at $pH=7.4$.

A few points should be emphasized about working the Henderson–Hasselbalch equation with regard to the significance of significant figures. The key is $\log_{10}[1]=0$, so $\log_{10}[\text{conjugate base}]/[\text{acid}]=0$ when $[\text{conjugate base}]=[\text{acid}]$. At this point $pH=pK_a$, so the species is 50% ionized. If working without the accuracy of dp, then, e.g., the spermine pK_a data can simply be interpreted as the molecule carrying 4 positive charges at $pH=7.4$. If it is important to work to 1 dp (2 SF), as in DNA or siRNA charge neutralization for DNA condensation and gene delivery (30), then the charge on spermine is +3.8, for 2 dp 3.80, and for 3 dp 3.801. Remembering that amines are never really “fully” protonated, as there is always a tiny fraction of the molecules which is uncharged, as the value only “approaches” 1.0 asymptotically, e.g., from “1,000 charged/1,001 total molecules,” etc. The above PEI (Fig. 3) and aminoglycoside (Fig. 4) examples show that one cannot simply count-up the number of basic nitrogens and call that the number of (“fully”) protonated groups at physiological pH. Therefore, care must be exercised with the interpretation of pK_a data.

2. Materials

2.1. Materials for Potentiometry

1. A series of standard buffers (pH=4.01, 7.00, and 10.00) supplied as solutions or as tablets to be dissolved in deionized CO₂-free water.
2. Standard solution that will be used for the titration. This can be NaOH, KOH, and Me₄NOH. The titrant is better being freshly prepared with deionized CO₂-free water.
3. The sample polyamine (polyammonium ion), usually as its hydrochloride (or trifluoroacetate) salt, is dissolved in a solution of the supporting electrolyte (e.g., NaClO₄, KNO₃, or NaCl). A concentration of 1 μM of the polyamine is usually sufficient.

2.2. Materials for NMR Spectroscopy

1. Several potassium salts (see Note 1) are used to prepare standard buffer solutions in D₂O that can be used to calibrate the electrodes of the pH Meter: KD₂PO₄ (0.025 M) + K₂DPO₄ (0.025 M), pD=7.39, and KDCO₃ (0.025 M) + K₂CO₃ (0.025 M), pD=10.60 (5).
2. Dissolve the polyamine sample as, e.g., its hydrochloride (or trifluoroacetate) salt in D₂O at an appropriate concentration typically around 50 mM. The pD of the stock polyamine solution (0.5 ml) can be changed by the addition of a small volume (μl) of concentrated DCl or KOD solutions (see Note 2).

3. Methods

3.1. Methods for Potentiometry

1. Calibrate the electrode(s) using a series of standard buffers (see Notes 3 and 4)
2. The temperature at which all the measurements are done should be kept constant all the time (and recorded and reported!).
3. The titration and data recording are normally controlled by means of computerized systems; however, if manual titration is to be carried out, the burette should be calibrated before use and washed with deionized water and titrant according to standard procedures.
4. Place the electrode (if combined type electrode) or electrodes (if separate reference electrode) in the polyamine solution.
5. Start the titration (whether manually or automatically operated), make sure to allow enough time (several minutes) between each addition of the titrant to get a fixed pH reading before proceeding. In automated systems, follow the manufacturer's instructions.

6. After reaching a specific pH (e.g., 11 or 12), the titration is stopped and the data are processed using the appropriate computer software packages for titration curve fitting, calculating the equivalence point (end point), and calculating the polyamine pK_a values (deconvolution) (see Note 5).

3.2. Methods for NMR Spectroscopy

1. The NMR experimental conditions such as spectrometer frequency, pulse width, and acquisition time should be adjusted according to the field-frequency (100, 270, 300, 400, 500 MHz, or even though less common and certainly not required, 600 and 750 MHz). The acquisition time will depend on whether pulsing on 1H or ^{13}C and whether the sample is 5 or 50 mg (typically) per 0.5 ml, and this can be 5 min (best) for each pH data point, but obviously using more dilute samples or ^{13}C acquisition may require 2–24 h per pH value (not a laboratory friendly approach as 12–24 pH data points will be required to generate a full pH titration curve across a typical range 3–12).
2. The temperature during the pD determination should be kept constant throughout the measurements (and recorded and reported!).
3. The 1H or ^{13}C spectra are recorded as well as 2D NMR data (such as HMQC) according to the standard procedures related to the instruments used. 2D NMR can facilitate assignments of overlapped 1H peaks obtained at the same time as the different pH measurements for the pK_a data.
4. The chemical shifts data are then processed using specific software packages (e.g., HYPNMR2000) to calculate the pK_a values (measured in D_2O).
5. An adjustment must be made for actually measuring pD values when pH is required. Glasoe and Long (31) showed that the relationship is $pD - 0.4 = pH$.

4. Notes

1. Potassium salts are preferred more than sodium salts to avoid the interference of sodium with the sensitivity of the electrode at pD >9.00.
2. The total activity of ions in the solution will not need adjustment with an inert salt.
3. The concentration of ions in the media and temperature must be kept constant at all times.
4. Always refer to the pH-meter manufacturer's instructions about calibrating the instrument.

5. The titration curve is a plot of electromotive force (EMF) versus pH. Software detects the equivalence point by curve fitting according to data points, then finding the second derivative of the curve equation, and solving the equation.

Acknowledgements

We thank the BBSRC (A.J.G.) and the Egyptian Government (A.A.M.) for PhD studentships and Celltech Therapeutics, Slough, UK for a CASE award (to A.J.G.).

References

1. Henderson LJ (1908) Concerning the relationship between the strength of acids and their capacity to preserve neutrality. *Am J Physiol* 21:173–179
2. Henderson LJ (1908) The theory of neutrality regulation in the animal organism. *Am J Physiol* 21:427–448
3. Hasselbalch KA (1916) Die Berechnung der Wasserstoffzahl des Blutes aus der freien und gebundenen Kohlensäure desselben, und die Sauerstoffbindung des Blutes als Funktion der Wasserstoffzahl. *Biochem Z* 78:112–144
4. Po N, Senozan M (2001) Henderson–Hasselbalch equation: its history and limitations. *J Chem Educ* 78:1499–1503
5. Frassinetti C, Ghelli S, Gans P, Sabatini A, Moruzzi MS, Vacca A (1995) Nuclear magnetic resonance as a tool for determining protonation constants of natural polyprotic bases in solution. *Anal Biochem* 231:374–382
6. Meloun M, Bordovská S (2007) Benchmarking and validating algorithms that estimate pKa values of drugs based on their molecular structures. *Anal Bioanal Chem* 389:1267–1281
7. Basu HS, Schwietert HCA, Feuerstein BG, Marton LJ (1990) Effects of variation in the structure of spermine on the association with DNA and the induction of DNA conformational changes. *Biochem J* 269:329–334
8. Usherwood PNR, Blagbrough IS (1989) Amino acid synapses and receptors. In: McFarlane NR (ed) *Progress and prospects in insect control*, Monograph No 43. Farnham, London, pp 45–58
9. Usherwood PNR, Blagbrough IS (1989) Antagonism of insect muscle glutamate receptors - with particular reference to arthropod toxins. In: Narahashi T, Chambers JE (eds) *Insecticide action from molecule to organism*, ACS Symposium Series. Plenum, New York, pp 13–31
10. Usherwood PNR, Sudan H, Standley C, Blagbrough IS, Bycroft BW, Mather AJ (1990) The mechanisms of neurotoxicity of low molecular weight spider toxins. In: Volans GN, Sims J, Sullivan FM, Turner P (eds) *Basic science in toxicology*. Taylor & Francis, London, pp 569–579
11. Usherwood PNR, Blagbrough IS (1991) Spider toxins affecting glutamate receptors: polyamines in therapeutic neurochemistry. *Pharmacol Ther* 52:245–268
12. Usherwood PNR, Blagbrough IS, Brackley PTH, Kerry CJ, Sudan HL, Nakanishi K (1992) Polyamines and polyamine-containing toxins - modulators and antagonists of excitatory amino acid receptors. In: Kawai N, Nakajima T, Barnard E (eds) *Neuroreceptors, ion channels and the brain*. Elsevier, Amsterdam, pp 11–20
13. Usherwood PNR, Blagbrough IS (1994) Electrophysiology of polyamines and polyamine amides. In: Carter C (ed) *The neuropharmacology of polyamines*. Academic, London, pp 185–204
14. Bergeron RJ, McManis JS, Weimar WR, Schreier KM, Gao FL, Wu QH, Ortiz-Ocasio J, Luchetta GR, Porter C, Vinson JRT (1995) The role of charge in polyamine analog recognition. *J Med Chem* 38:2278–2285

15. Leroy D, Heriche JK, Filhol O, Chambaz EM, Cochet C (1997) Binding of polyamines to an autonomous domain of the regulatory subunit of protein kinase CK2 induces a conformational change in the holoenzyme – a proposed role for the kinase stimulation. *J Biol Chem* 272:20820–20827
16. Ouameur A, Mangier E, Diamantoglou S, Rouillon R, Carpentier R, Tajmir-Riahi H (2004) Effects of organic and inorganic polyamine cations on the structure of human serum albumin. *Biopolymers* 73:503–509
17. Ahmed OAA, Pourzand C, Blagbrough IS (2006) Varying the unsaturation in N4, N9-dioctadecanoyl spermines: nonviral lipopolyamine vectors for more efficient plasmid DNA formulation. *Pharm Res* 23:31–40
18. Rege K, Ladiwala A, Hu SH, Breneman CM, Dordick JS, Cramer SM (2005) Investigation of DNA-binding properties of an aminoglycoside-polyamine library using quantitative structure-activity relationship (QSAR) models. *J Chem Inf Model* 45:1854–1863
19. Perrin DD (1965) Dissociation constants of organic bases in aqueous solution Butterworths, London, p 137
20. Albert A, Serjeant EP (1971) The determination of ionization constants. Chapman & Hall, London, pp 91–96
21. Baillon JG, Mamont PS, Wagner J, Gerhart F, Lux P (1988) Fluorinated analogs of spermidine as substrates of spermine synthase. *Eur J Biochem* 176:237–242
22. Kimberly MM, Goldstein JH (1981) Determination of pK_a values and total proton distribution pattern of spermidine by Carbon-13 nuclear magnetic resonance titrations. *Anal Chem* 53:789–793
23. Palmer BN, Powell HKJ (1974) Polyamine complexes with seven-membered chelate rings: Complex formation of 3-azaheptane-1,7-diamine, 4-azaoctane-1,8-diamine (spermidine), and 4,9-diazadodecane-1,12-diamine (spermine) with copper(II) and hydrogen ions in aqueous solution. *J Chem Soc Dalton Trans* 2089–2092
24. Frassinetti C, Alderighi L, Gans P, Sabatini A, Vacca A, Ghelli S (2003) Determination of protonation constants of some fluorinated polyamines by means of ^{13}C NMR data processed by the new computer program HypNMR2000. Protonation sequence in polyamines. *Anal Bioanal Chem* 376:1041–1052
25. Takeda Y, Samejima K, Nagano K, Watanabe M, Sugeta H, Kyogoku Y (1983) Determination of protonation sites in thermospermine and in some other polyamines by ^{15}N and ^{13}C nuclear magnetic resonance spectroscopy. *Eur J Biochem* 130:383–389
26. Palmer BN, Powell HKJ (1974) Complex formation between 4,9-diazadodecane-1,12-diamine (spermine) and copper(II) ions and protons in aqueous solution. *J Chem Soc Dalton Trans* 2086–2089
27. Geall AJ, Taylor RJ, Earll ME, Eaton MAW, Blagbrough IS (2000) Synthesis of cholesteryl polyamine carbamates: pK_a studies and condensation of calf thymus DNA. *Bioconjug Chem* 11:314–326
28. Szczepanik W, Kaczmarek P, Sobczak J, Bal W, Gatner K, Jezowska-Bojczuk M (2002) Copper(II) binding by kanamycin A and hydrogen peroxide activation by resulting complexes. *New J Chem* 26:1507–1514
29. Clouet-d'Orval B, Stage TK, Uhlenbeck OC (1995) Neomycin inhibition of the hammerhead ribozyme involves ionic interactions. *Biochemistry* 34:11186–11190
30. Geall AJ, Blagbrough IS (2000) Rapid and sensitive ethidium bromide fluorescence quenching assay of polyamine conjugate-DNA interactions for the analysis of lipoplex formation in gene therapy. *J Pharm Biomed Anal* 22:849–859
31. Glasoe PK, Long FA (1960) Use of glass electrodes to measure acidities in deuterium oxide. *J Phys Chem* 64:188–190
32. Remy J-S, Sirlin C, Vierling P, Behr J-P (1994) Gene transfer with a series of lipophilic DNA-binding molecules. *Bioconjug Chem* 5:647–654

Polyamine Analysis by LC-MS

Merja R. Häkkinen

Abstract

This chapter describes a protocol to analyze polyamines without any derivatization steps utilizing LC-MS/MS. Polyamines are separated by reversed phase LC prior MS analysis using heptafluorobutyric acid as MS compatible volatile ion-pairing agent, and selective and sensitive MS detection is performed using MS/MS in selected reaction monitoring mode.

Key words: LC-MS/MS, Method development, Validation, Polyamines, Polyamine analogs, Selected reaction monitoring

1. Introduction

Due to the poorly volatile, nonfluorescent, and weakly UV absorbing nature of polyamine backbone, most of the existing methods to quantify polyamines and their analogs and metabolites are based on analysis of different derivatives (1). However, several drawbacks have been associated with the derivatization, including possible derivatization of other compounds present in the matrix or diverse reactivities of the analytes, as well as instability of the derivatization products. Undesired side reactions and unreacted derivatization agent may need extensive clean-up procedures prior analysis to avoid comigration or interference during the separation of analytes. Thus, direct methods, which do not require derivatization, can sometimes be more feasible. In addition, traditional polyamine quantification using LC and UV detection of derivatives suffers from lack of sensitivity and selectivity as the analysis relies on retention time, peak area, and UV spectral character, especially if interferences from coeluting or overlapping peaks are present. Furthermore, with diluted samples, more selective and sensitive

analytical methods are required. Tandem mass spectrometric (MS/MS) detection and quantification utilizing electrospray ionization (ESI), combined to liquid chromatography/mass spectrometry (LC-MS), is among the most powerful methods for the analysis of metabolites (2), which has not yet been utilized widely in polyamine analysis, especially without derivatization. This chapter offers a protocol to analyze polyamines utilizing LC-MS/MS without any derivatization steps.

In ESI source, gas-phase ions are formed from analytes. In very complex matrices, like biological samples, several compounds may have the same mass-to-charge (m/z). Selectivity of the method is enhanced using MS/MS. In this technique the isolated precursor ion (normally protonated molecule) of a compound formed in the ESI source is selectively collided with neutral gas molecules (like nitrogen) to generate a characteristic set of product ions utilizing collision-induced dissociation (CID). Precursor ion fragmentation is induced by increasing the kinetic energy (collision energy) of the precursor ion. As the precursor ion fragmentation in the majority of cases provides a unique fragment, the most specific way to perform MS quantification is by using a mass spectrometer capable of MS/MS fragmentation and selective fragment ion detection, such as with a triple quadrupole (QQQ) mass spectrometer (3–5).

MS/MS quantifications are mostly performed using selected reaction monitoring (SRM). In SRM, both mass analyzers in the MS instrument are set on a specific mass, and the signal (or peak) obtained represents the precursor-to-product ion transition for a specific ion pair (4). Typically by using QQQ instrument, the first quadrupole isolates the selected precursor ion with a narrow isolation width, then the second quadrupole is used only for the fragmentation of this ion by CID, and finally the third quadrupole is programmed to detect product ion with known m/z value (6). The parent ion has to dissociate to all the monitored product ions and the ratio of the product ions should match a known value for the experimental conditions (4). This combination of the specific parent mass and the unique fragment ions is used to selectively monitor for the compounds to be quantified. In addition to selectivity, a relative increase in sensitivity is achieved due to the dramatic reduction of the chemical noise (3).

The optimization of the SRM method consists of three steps. First, the precursor ion should be isolated with the highest efficiency. This includes the selection of the fragmentor voltage. In order to achieve the best signal response and sensitivity, also instrument-specific MS/MS parameters need to be optimized, like capillary voltage, nebulizer gas pressure, and drying gas flow and temperature. The second step is the study of fragmentation of precursor ions and the optimization of the collision cell voltage for each analyte. These can be tested without chromatography by

using flow injection analysis (FIA), where the LC injector is connected directly to the ion source (3). The third step is the selection of the most sensitive and/or selective transition from the precursor ion to the selected product ion for the quantification. A good practice is to avoid, if possible, product ions obtained by loss of a water or ammonium molecule, as these fragmentations are not very selective. Monitoring also other significant transitions (so-called qualifier ions) enables to increase the selectivity of the method (7).

Generally, extensive chromatographic separation for analytes is not necessary for the SRM analysis since there is usually only a single peak for the analyte detected in an entire chromatographic run. However, the probability of observing multiple peaks due to the endogenous compounds from the complex biological samples sharing the same SRM transition for a given analyte is increased with small molecular weight compounds such as polyamines. Therefore, appropriate chromatographic separation for very small molecules prior to mass spectrometric detection becomes essential. Traditional reversed phase separation of underivatized polyamines is challenging due to their low-column retention and susceptibility to undergo severe tailing (8, 9). Ion-pairing chromatography utilizing lipophilic ions, termed ion-pairing reagents, as mobile phase additives has been widely used as an effective way to obtain adequate retention of polar analytes (10). Conventionally, the polyamine separation has been performed with alkyl or aryl sulfonates as anionic ion-pairing reagents (11). However, these nonvolatile ion-pairing reagents are not recommended for LC-MS as they cause ion source contamination, increase background, and cause strong signal suppression in MS. Volatile perfluorinated carboxylic acids as ion-pairing reagents are normally adapted for LC/MS systems as they are more compatible with the MS source. Among the most commonly used ion-pairing agents in LC-ESI-MS analysis of polar basic compounds is heptafluorobutyric acid (HFBA) (12), which is also suitable for underivatized polyamine separations by C18 reversed phase column (9, 13).

HFBA, as an additive in the LC separations, has two important functions in the analysis of polyamines. It enables the chromatographic separation of the highly polar analytes, giving them good symmetrical peak shapes, and prevents the unwanted interaction of these basic analytes with free silanol groups in the column and with capillaries in the instrument. However, HFBA is known to suppress ionization in the MS in some extent, thus lowering the sensitivity of the method. The addition of propionic acid has been demonstrated to decrease this suppression to some extent (14–16). For example, addition of isopropanol/propionic acid (75:25 to the column flow) has been shown to increase polyamine signal in ESI with HFBA as a solvent additive by four to tenfold (9). However, sometimes addition of isopropanol/propionic acid

may result in severe background (13), and it also complicates the chromatography in some extent. Therefore, propionic acid addition has not been utilized in this protocol, but it is worthwhile to remember this option as one solution, if the sensitivity of the analysis method needs to be increased.

The addition of ion-pairing reagents to the mobile phase is expected to retain not only polar analytes, but also some of the polar endogenous components in biological samples as well as exogenous materials from solvents and containers. These coextracted and coeluting substances may alter the amount of the charged analyte ions to reach the gas-phase. This may either suppress or enhance the analyte signal, and these alterations in signal response may be hidden in the chromatography, but still have a negative impact on the method's sensitivity and selectivity. The previous phenomenon is called matrix effect, which is said to be the Achilles' heel of quantitative LC-MS/MS measurements (17). Matrix effect can be assessed either by the postcolumn infusion method (18) or by the postextraction addition method (19). The deleterious matrix effects may be minimized by modification and improvement of the sample extraction methodology and chromatographic separation. One technique that can be used to diminish matrix effects is the application of internal standards (ISs, see below). Especially, the use of stable isotope-labeled analogs as ISs is recommended, as matrix effect should not affect the relative efficiency of ionization of the analyte and its coeluting stable isotope-labeled IS. However, the elimination of the coeluting compounds is still advisable, since their presence could reduce the method's sensitivity and may lead to false negative results for low concentrated samples (19, 20).

When performing MS quantification, IS is added to every sample to be measured to enhance the reliability of the method. An appropriate IS will control for the ionization variability, which may happen in the MS detection, as well as any losses during extraction and sample preparation, if added at the beginning of the sample work-up. The added amount of the IS should be well above the lower limit of quantification (LLOQ), but not so high as to suppress the ionization of the analyte. IS should be added at the same concentration in every sample including the standards, but it is not necessary to know the exact concentration of IS. The analytes and IS are then extracted, separated by LC, and finally analyzed by MS/MS. The quantification is achieved by comparing the peak area ratios of the analyte ions and IS ions, with the peak-area ratios of the calibrators used in preparing a standard curve. The best IS is an isotopically labeled version of the molecule to be quantified, since the physicochemical properties of an isotopically labeled analog are virtually identical with those of the analyte, but it has a different m/z value in MS. Other possibilities for an IS are, for example, structural analogs of the analyte.

However, it should be noted that if the analyte and the structural analog differ in functional groups, the IS is less likely to be suitable than when the difference is in the carbon backbone of the molecule. Also, substitution or rearrangement of heteroatoms is more likely to result in altered charge distribution of the molecule than changes to carbon–hydrogen groups (6, 21). In contrast, isotope-labeled analogs may suffer from ion suppression or enhancement by the analyte at high concentrations and vice versa. This may have a great impact on the accuracy of other measurements in the same chromatographic run, if only one IS is used for several analytes. Also, due to the other possible differences in matrix profile, corresponding IS may be required for each analyte, if more than one compound is determined in the same analysis. However, this may not be always possible; so if limited number of ISs is available, the use of the dual quantification based on different ISs may be feasible (22).

2. Materials

2.1. LC-MS/MS Solutions

Make fresh as required; solvents can be used approximately up to 1 week:

1. Solvent A: 0.1% (v/v) HFBA (>99%) in water.
2. Solvent B: 0.1% (v/v) HFBA in ultragradient HPLC grade acetonitrile.
3. Solvent for needle wash: 50% (v/v) acetonitrile in ultrapure water.

2.2. Sample Preparation

1. Deuterated polyamines as internal standards (see Note 1).
2. Sample buffer: 90 mM glycine-sodium hydroxide pH 9.5 containing 5% formic acid (see Note 2). Store buffers at +4°C.
3. 0.5% HFBA in water (see Note 2). Make fresh as required.

3. Methods

3.1. Instrumental Parameters

1. Instrumental parameters for Agilent 6410 Triple Quad LC/MS, which have given the best ion abundances for polyamine measurements, are explained in the following. Check the parameters with your instrument. Capillary voltage = 4,000 V. Nebulizer gas pressure = 40 psi. Drying gas flow = 8 L/min. Drying gas temperature = 300°C.

3.2. Flow Injection Analysis

To get the best sensitivity for MS/MS analysis, define the optimal values for fragmentor and collision energy.

1. Prepare individual samples from each analyte. For example, 100 μM in water, with 1 μL injections, is suitable for FIA.
2. Define the optimal fragmentor voltage value for each measured analyte. Use, for example, m/z 50–450, and test fragmentor energies 0, 30, 60, 90, and 120 V. Select the value, which gives the highest precursor ion abundance (see Note 3). Use the same parameters for deuterated internal standards.
3. Use the optimal fragmentor voltage value and define the generating product ions for each of the measured analyte. At the same time, you can determine the optimal collision energies for each of these selected ions. Use, for example, m/z 10–400, and check collision energies 0, 5, 10, 15, and 20 V (see Notes 4 and 5). Use the same parameters for deuterated internal standards.

3.3. Chromatographic Conditions

1. Column: Phenomenex Gemini reversed phase C18 column (3 μm , 110 \AA , 50 \times 2 mm) (see Note 6). Column temperature 25°C. Guard column: Phenomenex C18 guard column (4 \times 2 mm).
2. Gradient for sample analysis is shown in Table 1 (see Notes 6–8). Test the best gradient for separation of your analytes.
3. Sample injection with needle wash: Use 10 μL injection with 10 s needle wash (see Note 9).
4. Clean-up run: Use 50 μL blank (water or solvent A) injection with 20 s needle wash as a sample in clean-up run. Gradient for clean-up run is shown in Table 2 (see Notes 9 and 10).

3.4. SRM Method Development and Optimization

1. Select the quantifier and qualifier ions from the measured product ions (see Notes 4 and 11).
2. Make acquisition method by using these ions.

Table 1
Gradient for sample analysis by 50 \times 2 mm column

Time (min)	Solvent B (%)
0–12	2–50
12–12.5	50–50
12.5–13	50–2
13–20	2–2

Table 2
Shorter gradient for clean-up run, if more than one clean-up runs are needed

Time (min)	Solvent B (%)
0–5	2–80
5–6	80–80
6–11	80–2

3. Determine dwell time as ~50 ms (see Note 12).
4. If needed, use more than one time segment (see Notes 12 and 13).
5. Test that there is no interference of selected ion transitions of standards to the internal standards ion transition channels: Use concentrated sample without internal standards, like a sample including: 50 μL std60 (see chapter 3.4.1) + 50 μL water + 25 μL 0.5% HFBA. Run the sample using gradient for sample analysis (see Note 11).
6. Test that there is no interference of selected ion transitions of the internal standards to standards ion transition channels: Use sample without standards, like a sample including: 50 μL 1 μM internal standard mixture (zero sample see chapters 3.4.1 and 3.4.2) + 50 μL water + 25 μL 0.5% HFBA.
7. Test that there is no deleterious matrix effect using postcolumn infusion method:
 - (a) Use T-split to deliver a constant flow (~7 $\mu\text{L}/\text{min}$) of mixture of measured analytes (like a sample including: 100 μL 1 μM std + 100 μL 1 μM IS + 50 μL 0.5% HFBA (see chapters 3.4.1 and 3.4.2)) into the LC eluent after the chromatographic column, but before MS detection using an infusion pump.
 - (b) Inject a sample extract free of added analyte (or other control sample close to the used matrix) and run with the chromatographic conditions described above.
 - (c) Investigate the matrix effect over the entire run (see Note 14).

3.5. Sample Preparation

3.5.1. Working Solution

1. Weigh the standards with analytical balance, and prepare the stock solution containing all calibration standards as 1 mM concentration in the selected buffer.
2. From this 1 mM stock solution, dilute with the buffer to have 60, 30, 10, 3, 1, 0.3, 0.1, and 0.03 μM working solutions for calibration standards.

3. Prepare also 20, 2, 0.2, 0.05 μM working solutions for quality control samples.
4. Filter both the calibration standard and quality control sample working solutions through 0.22 μm filter.
5. Prepare the solution containing all internal standards as 1 μM concentration in the water (see Note 15).

3.5.2. Samples for LC-MS/MS Measurements

1. Standard samples for calibration: Pipet 50 μL of standard working solution, 50 μL of 1 μM internal standard working solution, and 25 μL 0.5% HFBA in a polypropylene tube (see Note 16).
2. Blank standard for calibration: Pipet 50 μL of buffer, 50 μL of 1 μM water, and 25 μL 0.5% HFBA in a polypropylene tube.
3. Zero sample for calibration: Pipet 50 μL of buffer, 50 μL of 1 μM internal standard working solution, and 25 μL 0.5% HFBA in a polypropylene tube.
4. Samples and QC samples: Pipet 50 μL of sample or QC sample, 50 μL of 1 μM internal standard working solution, and 25 μL 0.5% HFBA in a polypropylene tube.
5. After vortexing, transfer all the samples into Agilent 250 μL polypropylene vial inserts (Product number 5182-0549).

3.6. Assay Validation

1. Analyze calibration standards and QC samples before the samples within each analysis batch. Use U.S. Food and Drug Administration guidelines for bioanalytical method validation (23) (see Notes 17 and 18).
2. Construct calibration curves from the peak-area ratios of each analyte to their internal analogs using a $1/\times$ weighted least squares regression model (see Note 19).

4. Notes

1. General synthesis protocols for deuterium-labeled polyamines are available in (24), if the required isotopically labeled polyamine structure is not commercially available. Usually two to three mass units higher molecular mass of IS compared to molecular mass of analyte is sufficient to avoid interference by natural isotopes of the analyte at the m/z value of the labeled compound. You can estimate the needed number of isotope atoms by calculating isotope pattern of the analyte.
2. Plain water should be avoided as the polyamines tend to absorb to different surfaces, especially to the glass or to the

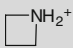
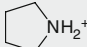
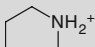
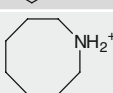
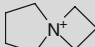
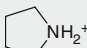
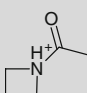
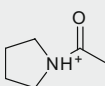
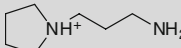
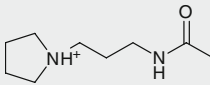
filters. 0.5% HFBA is added during LC-MS/MS sample preparation to enable column retention and symmetrical peak shapes as well as to reduce unwanted polyamine–silanol interactions and retention of polyamines to instrument’s capillaries. Some samples may also contain (or be prepared in) 5% sulfosalicylic acid, which are also applicable for LC-MS/MS analysis, if more HFBA (5% in the sample) is used in the LC-MS/MS sample preparation. This can be achieved easily by changing 0.5% HFBA to 10% HFBA in water in sample preparation.

3. Use the extracted ion chromatogram (EIC) to see the ion abundances. The best fragmentor voltage value is the one that gives the highest peak area. Usually diamines have lower fragmentor voltage, like 60 V, and higher polyamines around 90 V with Agilent 6410 Triple Quad LC/MS. See examples in Table 3.
4. Use EIC to see the ion abundances. The best collision energy voltage value for the product ion is the one which gives the highest peak area for that product ion. Higher collision energy fragments the precursor ion to smaller fragments. In Table 3 are listed some precursor to product ion transitions, fragmentor voltage, and collision energy voltage values for most common di- and polyamines from previous studies (9, 13).

Table 3
Precursor to product ion transitions, and fragmentor voltage and collision energy voltage values for most common di- and polyamines

	Precursor ion (<i>m/z</i>)	Fr (V)	Quantifier ion (<i>m/z</i>)	CID (V)	Qualifier ion (<i>m/z</i>)	CID (V)
DAP	75	60	58	5	–	–
PUT	89	60	72	5	–	–
CAD	103	60	86	5	–	–
DAH	131	60	114	5	55	15
SPD	146	90	112	10	72	15
<i>N</i> ¹ -AcSPD	188	90	100	15	72	15
<i>N</i> ⁸ -AcSPD	188	90	114	15	72	20
SPM	203	90	112	15	129	10
<i>N</i> ¹ -AcSPM	245	90	129	10	112	20

Table 4
Some of the probable product ion structures for the most common polyamines and their acetylated derivatives

	Precursor ion (<i>m/z</i>)	Product ion (<i>m/z</i>)	Possible product ion structure	Examples of other product ions (<i>m/z</i>)
DAP	75	58		–
PUT	89	72		–
CAD	103	86		–
DAH	131	114		55
SPD	146	112		129
		72		
<i>N</i> ¹ -AcSPD	188	100		171, 72
<i>N</i> ⁸ -AcSPD	188	114		171, 112, 84, 72, 58
SPM	203	129		112, 84
<i>N</i> ¹ -AcSPM	245	171		129, 112, 100

- In Table 4 are presented some of the probable product ion structures for the most common polyamines and their acetylated derivatives. These structures can be also used to predict fragmentation and product ions of other polyamine analogs (e.g., *N*-alkylated, as well as isotopically labeled polyamine analogs).
- LC-MS/MS chromatograms from the mixture of nine di- and polyamines which were analyzed using 50 × 2 mm column are shown in Fig. 1. Depending on the analytes, also shorter column (30 × 2 mm) may be appropriate. However, longer (50 × 2 mm) column enables better analysis of small diamines (PUT and DAP) from samples having large amount of junk in the solvent front of the column (e.g., cell extracts containing

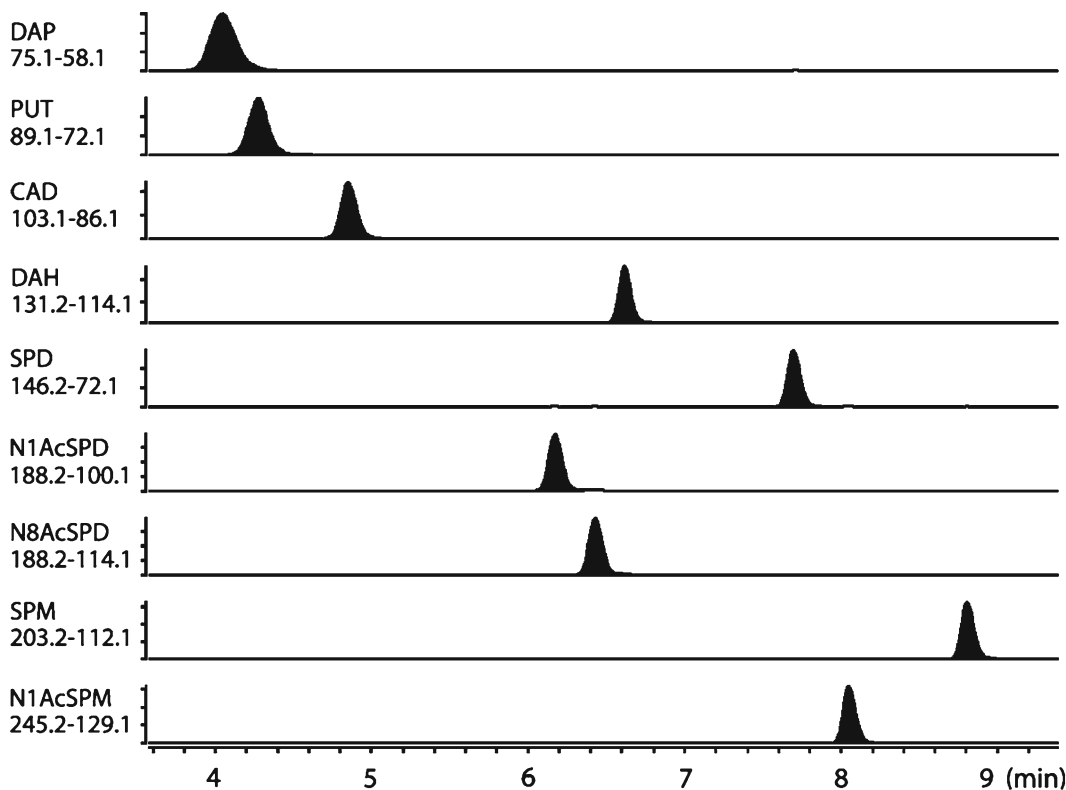


Fig. 1. Representative LC-MS/MS chromatograms from the mixture of nine di- and polyamines, which were analyzed using 50×2 mm column and Table 1 gradient. *DAP* propane-1,3-diamine; *PUT* butane-1,4-diamine; *CAD* pentane-1,5-diamine; *DAH* heptane-1,7-diamine; *SPD* *N*-(3-aminopropyl)butane-1,4-diamine; *N1AcSPD* *N*-[3-(4-aminobutylamino)propyl]acetamide; *N8AcSPD* *N*-[4-(3-aminopropylamino)butyl]acetamide; *SPM* *N,N'*-bis(3-aminopropyl)butane-1,4-diamine; *N1AcSPM* *N*-[3-[4-(3-aminopropylamino)butylamino]propyl]acetamide.

Table 5
Gradient for sample analysis by 30×2 mm column

Time (min)	Solvent B (%)
0–10	2–50
10–10.5	50–50
10.5–11	50–2
11–16	2–2

5% sulfosalicylic acid). Test the best column for your samples. It should also be noted that not all C18 columns available are suitable for polyamines, as some of them may give severe tailing or even double peaks for higher polyamines.

7. Example of gradient for sample analysis by 30×2 mm column is shown in Table 5.

8. Some polyamine analogs, lipids, or other impurities may in time get absorbed to the column material (or react with free silanol groups) and change the lipophilicity of the column. This may cause the retention times of the analytes to become short.
9. Some higher polyamines in the sample, like SPM, may get absorbed in the column and capillary surfaces in some extent, especially after concentrated samples, and contaminate next sample run. This may be reduced with needle wash after sample injection, as well as performing one or more clean-up runs after concentrated samples.
10. Clean-up can be performed using the same gradient as for the analysis. If more than one clean-up runs are needed (e.g., in the case of very high concentrations of spermine before samples without spermine), the shorter gradient shown in Table 2 may be more convenient as the first clean-up run. You may use same clean-up run conditions for 30×2 mm column.
11. The ideal quantifier ion is product ion, which does not have high abundance and least background in the channel and does not cause interference to other measured transitions. A good practice is to avoid, if possible, product ions obtained by loss of a water or ammonium molecule, as these fragmentations are not very selective. Monitoring also other significant transitions for the same analyte (so-called qualifier ions) enables to increase the selectivity of the method.
12. Optimal number of points across the chromatographic peak is at least 15–20. This can be achieved by specifying dwell time for analytes so that MS has time to measure the same analyte 20 times during peak elution. However, too short dwell time may increase S/N ; thus if several analytes are being measured, it might be better to add more than one time segments to the method in order to achieve higher dwell time for each analyte. Usually, dwell times 20–100 ms are practical for Agilent 6410 Triple Quad LC/MS. However, minimum dwell time is instrument-specific, thus check also the instrument manual.
13. Remember to follow any retention time changes, as only those specified ion transitions at the particular time segment are being measured.
14. Usually, the matrix effect is strongest in the solvent front.
15. The same solution batch is used in all LC-MS/MS samples.
16. If you use 5% sulfosalicylic acid as a buffer in sample preparation, use 10% HFBA solution instead of 0.5% HFBA.
17. Measure five replicates of QC samples at three or four concentrations within analyze batch. Use R.S.D. of the concentrations as an index of precision. Precision should be better

than 15% R.S.D, except for LLOQ (see Note 18). Compare the mean experimental concentrations of QC samples with their nominal values and use percentage values as the index of accuracy. Accuracy should be within 85–115%, except for LLOQ (see Note 18).

18. The lower limit of quantification (LLOQ) is the lowest working solution concentration analyzed with accuracy within 80–120% and precision better than 20% R.S.D. Include six 0.03 μM calibration standard samples within analyze batch and verify LLOQ by calculating precision and accuracy.
19. Usually, linear or quadratic fit is suitable.

References

1. Teti D, Visalli M, McNair H (2002) Analysis of polyamines as markers of (patho)physiological conditions. *J Chromatogr B* 781:107–149
2. Kostianen R, Kotiaho T, Kuuranne T, Auriola S (2003) Liquid chromatography/atmospheric pressure ionization-mass spectrometry in drug metabolism studies. *J Mass Spectrom* 38: 357–372
3. Politi L, Groppi A, Poletini A (2006) Ionization, ion separation and ion detection in LC-MS. In: Poletini A (ed) *Applications of LC-MS in toxicology*. Pharmaceutical Press, London, pp 1–22
4. Glish GL, Vachet RW (2003) The basics of mass spectrometry in the twenty-first century. *Nat Rev Drug Discov* 2:140–150
5. Principles of MS Quantitation (2009) Available at: <http://www.ionsource.com/tutorial/msquan/requantoc.htm/>
6. Holčápek M, Kolarová L, Nobilis M (2008) High-performance liquid chromatography-tandem mass spectrometry in the identification and determination of phase I and phase II drug metabolites. *Anal Bioanal Chem* 391:59–78
7. Capote FP, Jiménez RJ, Granados JM, de Castro MDL (2007) Identification and determination of fat-soluble vitamins and metabolites in human serum by liquid chromatography/triple quadrupole mass spectrometry with multiple reaction monitoring. *Rapid Commun Mass Spectrom* 21:1745–1754
8. Feistner GJ (1994) Metabolites of Erwinia 9. Profiling of basic-amino-acids and polyamines in microbial culture supernatants by electrospray mass-spectrometry. *Biol Mass Spectrom* 23:784–792
9. Häkkinen MR, Keinänen TA, Vepsäläinen J, Khomutov AR, Alhonen L, Jänne J, Auriola S (2007) Analysis of underivatized polyamines by reversed phase liquid chromatography with electrospray tandem mass spectrometry. *J Pharm Biomed Anal* 45:625–634
10. Cecchi T (2008) Ion pairing chromatography. *Crit Rev Anal Chem* 38:161–213
11. Khuhawar MY, Qureshi GA (2001) Polyamines as cancer markers: applicable separation methods. *J Chromatogr B* 764:385–407
12. Kostianen R, Kauppila TJ (2009) Effect of eluent on the ionization process in liquid chromatography-mass spectrometry. *J Chromatogr A* 1216:685–699
13. Häkkinen MR, Keinänen TA, Vepsäläinen J, Khomutov AR, Alhonen L, Jänne J, Auriola S (2008) Quantitative determination of underivatized polyamines by using isotope dilution RP-LC-ESI-MS/MS. *J Pharm Biomed Anal* 48:414–421
14. Kuhlmann FE, Apffel A, Fischer SM, Goldberg G, Goodley PC (1995) Signal enhancement for gradient reverse-phase high-performance liquid chromatography electrospray ionization mass spectrometry analysis with trifluoroacetic acid and other strong acid modifiers by postcolumn addition of propionic acid and isopropanol. *J Am Soc Mass Spectrom* 6:1221–1225
15. Apffel A, Fischer S, Goldberg G, Goodley PC, Kuhlmann FE (1995) Enhanced sensitivity for peptide mapping with electrospray liquid chromatography-mass spectrometry in the presence of signal suppression due to trifluoroacetic acid-containing mobile phases. *J Chromatogr A* 712:177–190
16. Shou WZ, Naidong W (2005) Simple means to alleviate sensitivity loss by trifluoroacetic acid (TFA) mobile phases in the hydrophilic interaction chromatography-electrospray tandem mass spectrometric (HILIC-ESI/MS/MS) bioanalysis of basic compounds. *J Chromatogr B* 825:186–192

17. Taylor PJ (2005) Matrix effects: the Achilles heel of quantitative high-performance liquid chromatography-electrospray-tandem mass spectrometry. *Clin Biochem* 38:328–334
18. Bonfiglio R, King RC, Olah TV, Merkle K (1999) The effects of sample preparation methods on the variability of the electrospray ionization response for model drug compounds. *Rapid Commun Mass Spectrom* 13:1175–1185
19. Matuszewski BK, Constanzer ML, Chavez-Eng CM (2003) Strategies for the assessment of matrix effect in quantitative bioanalytical methods based on HPLC-MS/MS. *Anal Chem* 75:3019–3030
20. Eeckhaut AV, Lanckmans K, Sarre S, Smolders I, Michotte Y (2009) Validation of bioanalytical LC-MS/MS assays: evaluation of matrix effects. *J Chromatogr B* 877:2198–2207
21. Taylor PJ (2006) Method development and optimisation of LC-MS. In: Polettini A (ed) *Applications of LC-MS in toxicology*. Pharmaceutical Press, London, pp 23–42
22. Kronstrand R, Josefsson M (2006) Quantification using LC-MS. In: Polettini A (ed) *Applications of LC-MS in toxicology*. Pharmaceutical Press, London, pp 43–70
23. US Department of Health and Human Services Food and Drug Administration, Center for Drug Evaluation and Research (CDER) (2001) Guidance for industry, bioanalytical method validation. Available at: <http://www.fda.gov/cder/guidance/4252fnl.pdf>
24. Häkkinen MR, Keinänen TA, Khomutov AR, Auriola S, Weisell J, Alhonen L, Jänne J, Vepsäläinen J (2009) Synthesis of novel deuterium labeled derivatives of N-alkylated polyamines. *Tetrahedron* 65:547–562

INDEX

A

- 3-Acetamidopropanal..... 405, 464
 Acetylation12, 17, 21, 173, 464, 473, 475,
 479, 480, 482–483, 487–488
 Acetylpolyamine oxidase (APAO). *See* *N*¹-Acetylpolyamine
 oxidase
*N*¹-Acetylpolyamine oxidase (APAO)12, 410, 464
 Acrolein, protein-conjugated (PC-Acro)..... 396
 Action potential..... 113
 S-Adenosylmethionine (AdoMet).....6, 40, 162, 219,
 220, 224, 228, 231, 306, 443
 S-Adenosylmethionine decarboxylase
 (AdoMetDC)5, 6, 11, 12, 14, 40–42, 45,
 88, 101, 160, 162–163, 219–234, 310, 437,
 440, 441, 443, 444
 Adipocyte differentiation..... 21
 African sleeping sickness14, 219, 310
 Agmatine..... 3, 4, 6, 45, 48, 81, 82, 100, 101, 106
 Agmatine deiminase 5
 Agmatine iminohydrolase..... 40
 Alanine racemase..... 42–45
 Allosteric.....219–234
 α -(methyl)spermidine (α -MeSpd)..... 449, 450, 452, 459
 α -(methyl)spermine (α -MeSpm)..... 450
 Amine..... 5, 6, 196, 346, 464, 467, 494, 496, 498, 499
 Amine oxidase 62, 184, 395, 396, 404, 473
 3-Aminopropanal 12, 13, 174, 395, 405
 Aminopropylagmatine..... 6, 82, 86, 94, 99–101, 106
 Aminopropyltransferase 5, 6, 40, 42, 45–46,
 101, 106, 437
 AMPA receptors.....20
 Annexin..... 423, 478–480, 483, 484, 489
 Antiporter.....296, 305, 318
 Antizyme (AZ)..... 10, 14, 22, 40, 131, 237–264
 Antizyme inhibitor (AZI)14, 240–241,
 252–255, 258, 269–278
 Apoptosis..... 12, 18, 19, 22, 137, 269, 410, 423, 427, 479
Arabidopsis thaliana 12, 184
 Arginase..... 19, 410, 412–414, 420–421
 Arginine.....4, 5, 11, 12, 17, 40–43, 52, 144,
 263, 299, 310, 311, 340, 409, 410, 421
 Arginine decarboxylase (ADC)5, 11, 12,
 40–43, 45, 106
 Aspartic- β -semialdehyde..... 6, 7

B

- Biomarker19, 398, 405, 406
 Brain infarction398, 399, 401, 405
 Butylamine 195

C

- Cadaverine..... 3, 4, 42, 81, 82, 230, 232, 296, 305, 312
 Caldine 3, 82, 90
 Caldohexamine..... 82, 85, 91, 93,
 96–97, 104
 Caldopentamine 82–84, 90–96, 100, 101
 Cancer
 breast 279, 368
 chemoprevention 10, 17
 colorectal.....131, 368, 375
 diagnosis 18
 early detection 368
 gastric 409
 therapy..... 18, 22
 Capillary electrophoresis..... 351
 Carboxynorspermidine decarboxylase
 (CANSDC)7, 42, 43, 45–47
 Carboxynorspermidine synthase. *See* Carboxyspermidine
 synthase
 Carboxyspermidine dehydrogenase. *See* Carboxyspermidine
 synthase
 Carboxyspermidine synthase (CANSDH)7, 46, 47
 Carcinogenesis..... 10, 19, 129–140, 174
 Caveolin.....17, 340, 344
 Chagas disease14, 16, 310
 Chemiluminescence..... 55, 174, 175, 180, 422,
 484, 487, 489
 CHO cell lines
 HSPG deficient (pgsD-677) 328, 333
 wild type 329
 Cholesterol 144, 145, 148
 Chromatin, remodelling 475

c-Myc. See Oncogene

Cofactor14, 43, 187, 192, 195, 220, 221
Colloidal gold aggregation..... 370–371

D

Dansyl23, 191, 357, 463, 464, 469, 472, 473
Dansylation 23, 186, 191, 353, 355–356,
359, 371, 392, 472
Dansyl chloride.....186, 191, 352, 356, 383, 392, 465, 467
Deafness160
Decarboxylated S-adenosylmethionine
(dcAdoMet)..... 5, 40, 45, 88, 101, 160,
162, 219–234, 310, 437, 440, 443
Deoxyhypusine 8, 13, 195–197, 200–203,
207–209, 213–215
Deoxyhypusine hydroxylases (DOHH)..... 14, 207–215
Deoxyhypusine synthase (DHS).....7, 13, 195–204,
208, 211, 214, 450
Diabetes 19, 479, 480
N¹,N¹²-Diacetylspermine (DiAcSpm)..... 18, 367–377
Diamine3, 4, 279, 312, 410, 494, 496, 513, 515
Diamine oxidase12, 175, 180, 184, 192, 350, 473
1,4-Diaminobutane. See Putrescine
Diaminobutyrate 46
1,4-Diaminobutyric acid 4, 5
1,5-Diaminopentane. See Cadaverine
Diaminopimelate decarboxylase (DAPDC)42, 43, 45
1,3-Diaminopropane 3, 4, 6–8, 82, 85, 96,
183, 196, 202
Diatom 6, 46
Diet17, 18, 133, 144, 145, 161, 339,
340, 345, 349–363
 α -Difluoromethylornithine (DFMO).....10, 14, 53,
54, 56, 60, 62, 71, 73–76, 309, 333, 339, 415
Dioxygenases 208
DNA condensation.....104, 497, 499
DNA methyltransferase (DNMT) 476

E

Edema 144, 145, 147, 149–152, 386
eIF5A 8, 9, 13, 14, 57, 58, 60, 62, 63,
195–199, 201–204, 207–212, 214, 215
Electrospray ionization (ESI)..... 506, 507
ELISA146, 148, 151, 185, 188, 246,
247, 351, 368–376, 400, 401, 403
Endocytic uptake..... 17
Endocytosis, caveolar..... 340
Escherichia coli..... 5, 16, 41–46, 48, 51, 52,
54–56, 58–61, 81, 88, 103, 105, 106, 114, 116,
184, 187, 193, 223, 225, 226, 233, 240, 242,
252, 256, 264, 295–306, 340, 419
Eukaryote9, 13, 41, 45, 46, 51, 195, 237
Eukaryotic. See Eukaryote
Evolution39–45, 130, 139, 222, 228, 460

F

Filter binding assay.....197, 201, 202
Flavin adenine dinucleotide (FAD).....12, 174,
184, 186, 187, 192–193
Flow cytometry.....423, 464, 465
Fluorescence-assisted cell sorting analysis
(FACS) 328, 330–331, 333, 335, 337
Frameshifting 14, 15, 40, 60, 132, 237,
238, 244–245, 262, 263
Free fatty acids (FAA) 144

G

Gas chromatography (GC).....24, 89, 351,
352, 371, 427–435, 440, 442
Gas chromatography-mass spectrometry
(GC-MS) 24, 428–430, 432–435, 440, 442
Gastric epithelial cell.....19, 409, 411
Gastritis 409
Gating 113
Gene
delivery337, 497–499
duplication..... 42, 221, 222, 230
expression..... 9, 13, 20, 51, 67–78, 130,
131, 137, 144, 475
fusion..... 46
pbex.....161, 168
spermine synthase (SMS)20, 40, 160–162,
165, 438, 441
Genomics
comparative 39–48
functional..... 39–48
Glucose
homeostasis.....144, 145, 148
metabolism 143–157
tolerance 144–148, 153–155, 157
Glutathione220, 241, 253

H

Hair growth.....21
Helicobacter pylori.....19, 409–424
Heparan sulfate proteoglycan (HSPG), blockage..... 328
Heparinase III lyase treatment 328, 329, 332, 334
Hepatic shock..... 379
Heptafluorobutyric acid (HFBA).....507, 509,
511–513, 516
Heritable disease.....20
High-performance liquid chromatography
(HPLC)23, 89–90, 103, 175–177,
179, 186, 189, 190, 197, 201, 202, 209, 213, 224,
228, 304, 341–342, 345–346, 351–353, 355–360,
362, 363, 368, 371, 374, 375, 383–385, 392–393,
403, 428, 440, 442, 463–465, 469, 471–473, 509
Histone acetyltransferase (HAT)..... 475

Histone deacetylase (HDAC)..... 23, 475–490
HuR..... 9, 68–71, 73, 75–77, 280, 281, 283, 286, 290
Hydrogen peroxide (H₂O₂)..... 13, 173–174, 176,
183, 185, 188, 201, 396, 401, 410, 463
Hydroxycinnamoyl conjugates..... 48
Hypusine 8, 9, 13–14, 21, 60, 195, 196,
202, 207–209, 212–215

I

Immunoassays 351
Immunochemistry 238–239, 245–249
Immunofluorescence 306, 310
Immunoprecipitation..... 53–56, 58, 61, 68, 71, 73,
240, 243, 250–251, 259, 263, 264, 281, 283–286
Inducible nitric oxide synthase (iNOS) 409
Infection..... 19, 310, 328, 334, 337, 409–424
Inflammation..... 19, 144, 147, 149, 174, 386, 427
Insulin
 release 113
 sensitivity..... 144, 145, 148, 149, 155, 157
Inwardly-rectifying potassium channels
 (Kir)..... 9, 113–125
Inward rectifier 114
Ion channel..... 8, 9, 20, 21, 113, 114, 119–121,
123–125, 269, 350, 437
Ion exchange chromatography..... 197, 200–202,
209, 212–213
Ionizable 493, 494
Ionization. *See* ionizable
Ion-pairing 465, 506–508
Ischemia reperfusion injury (IRI) 19, 379–393

K

Kainate 20
Keratosis follicularis spinulosa decalvans (KFSD)..... 20
Kidney damage 393
Kinetic analysis 224–226, 228, 230, 234, 423
Knockout mice. *See* Mice
Knockout mutants 83, 88, 106
k-RAS. *See* Oncogene

L

Leeuwenhoek 3
Leishmania 14, 39, 310–312, 315, 324
Leishmania major..... 310, 311
Life span 62, 161
Lipid metabolism 11, 143–157
Lipoprotein..... 145
Liposome 115, 117–121, 123, 124
Liquid chromatography/mass spectrometry
 (LC-MS) 57, 505–517
Liver regeneration 21
Luminol..... 174–177, 185, 188, 414, 422

Lysine 4, 5, 8, 13, 40, 42, 43, 53, 57, 60,
195, 196, 239, 249, 296, 300, 305, 306, 311,
315, 347, 405, 485

M

Macrophage..... 19, 409–411, 414–417, 420–422
MEK 73, 76, 77
Membrane potential 9, 113
Membrane vesicles, inside-out 297, 299–303, 340–344
Mental retardation..... 20, 162, 438, 439
Methylthioadenosine (MTA) 436, 437, 440,
442–444
Mice
 conditional knockout 133
 Gyro (Gy)..... 159–169
 knockout..... 11, 19, 130, 133, 134, 139,
332, 333, 340, 345
 transgenic 10, 11, 20, 130, 133, 144,
156, 159–169, 327
Monooxygenase 207, 208
mRNA
 stability 14, 15, 61, 68
 translation 67, 68, 130
Myocardial infarction 379

N

*N*¹-acetylspermidine 12, 173, 464
*N*¹-acetylspermine 173, 179, 371, 401, 414, 464
N-acyltransferases..... 42, 48
NAD 7, 8, 195, 198, 199, 211
*N*¹-aminopropylspermidine 82, 86, 94, 99
N-carbamoylputrescine..... 5
N-carbamoylputrescine amidase 5
N-carbamoylputrescine amidohydrolase..... 40
*N*¹-dansylnorspermidine..... 465, 468
Neurological abnormalities..... 161
NMDA receptors 9, 20
*N*¹, *N*¹¹-didansylnorspermine 465, 466, 468
Nuclear magnetic resonance spectroscopy
 (NMR)..... 60, 86, 87, 102, 494, 496,
497, 500, 501

O

Obesity..... 19
Oligomerization state 221, 227
Oncogene
 c-Myc..... 10, 15
 k-RAS..... 17
Operon..... 47, 58, 302, 305
o-phthalaldehyde 23, 84, 89, 108, 300, 304,
341, 352, 442, 463
Ornithine 4, 40–42, 52, 144, 219, 241, 254, 263, 264,
271, 276, 296, 299–302, 305, 310, 410, 421

- Ornithine decarboxylase (ODC) 5, 6, 40, 53,
131, 160, 219, 220, 233, 237, 240–243, 252,
255–260, 269–271, 279–291, 305, 310, 327,
382, 393, 410
- Oxidase 12, 19, 174, 180
- P**
- Pancreatitis 11, 19, 21, 143–157, 450
- Patch clamp 115, 119–125
- Permease 309, 310, 318
- Peroxisome 19, 144, 183, 464
- Phex*. See Gene
- Phosphate 4, 5, 43, 52, 53, 125, 131, 145, 146, 161,
163–164, 167, 168, 192, 210, 213, 238, 239,
241, 242, 271, 274, 280, 299, 305, 312, 316,
329, 340, 341, 370, 381, 382, 389, 390, 413,
414, 440, 441, 444, 483, 490, 495, 496
- Phospholipids 144, 428, 496
- Phosphorylation 17, 250, 297, 298, 300, 301, 304, 306
- Phylogenetic
analysis 43, 44, 233
tree 43, 44, 222, 233
- pK_a 23, 478, 493–502
- Plasma membrane vesicles 340, 342
- Polyamine
analogs 10, 12, 16, 17, 21–23, 174, 178,
435, 505, 514, 516
analysis 23–24, 56, 83, 84, 89, 90, 174,
309–325, 340, 351, 354, 356, 428, 472, 505–517
backconversion 410
blockade 114, 123–125
branched 82, 83, 91, 99, 101, 102, 105
catabolism 12–13, 143, 174, 184, 191, 410
dansyl 356, 357, 371, 464, 469, 472, 473
deficiency/deficient cells 21, 54, 62, 63,
297, 438, 450
dietary 17, 18, 339, 349–363
efflux/excretion/exporter 12, 14–17, 296, 306, 367
fluorescent 17, 463–473
homeostasis 16, 219, 222
interconversion 12
methylated 449–460
modulon 9, 51–63
oxidase 174, 183–193, 350, 393, 396
protonation 494, 496
quaternary 8, 82, 89, 91, 99, 101, 104
requiring mutants 54, 55
RNA interaction 51
transport/transport system (PTS)/transporters 12,
15–18, 21, 234, 260–262, 271, 295–306,
309–325, 339–347, 463–473, 477, 478, 480
uptake 12, 14–17, 21, 237, 260, 262, 270,
277, 296, 301, 304–306, 327–337, 340, 342,
465, 484–485, 489–490
- Polyaminobenzamide (PABA) 23, 477–480, 487, 490
- Polyamino hydroxamic acid (PAHA) 23, 477, 478,
480, 487, 490
- Polymerase chain reaction (PCR) 20, 48, 55, 56,
58, 69, 70, 73, 74, 78, 107, 108, 131, 134, 138,
139, 163–166, 168, 186, 190, 226, 285, 286,
291, 412–413, 416–418, 423, 441
- Polysome 68, 69, 280–282, 286–290
- Posttranscriptional regulation 8, 9, 15, 67–78, 279–291
- Posttranslational modification 7, 9, 13, 475
- Potassium channel 9, 113–125
- Potentiometric titration. See Potentiometry
- Potentiometry 494, 496, 497, 500–501
- Prokaryotes 41, 51, 309
- Promoter
CMV-IE 161
metallothionein 144
region 15, 166, 413, 418
- Proteasome 14, 237, 255, 264
- Protein synthesis 9, 13, 51, 52, 54–60, 62,
87–88, 104–106, 186, 187, 305
- Protozoal. See Protozoan
- Protozoan 16, 309–313, 315–319, 324
- Prozyme 14, 221–223, 227, 230, 233, 234
- Putrescine 3–8, 12, 14, 16, 17, 40–42, 47,
48, 51, 52, 54–56, 60, 61, 68, 73–75, 81, 82, 84,
86, 90, 96, 100, 104, 159, 173, 185, 191, 198,
199, 221, 223, 227, 230, 232, 238, 244, 263,
269, 279, 296–306, 312, 327, 331, 340–347,
349–353, 355, 358–363, 392, 397, 405, 406,
410, 427–429, 431, 435, 437, 442, 451, 452, 464
- Pyruvate 5, 221, 311, 314, 411, 482
- R**
- Ras12V cells 279, 280, 286, 290
- Reactive oxygen species (ROS) 12, 19–22, 174
- Real time-polymerase chain reaction
(RT-PCR) ... 70, 72, 73, 382, 388, 411, 415–418
- Regenerative tissue growth 19
- Renal failure 19, 379, 395–406
- Reverse genetics 88, 106–108
- Ribonucleoprotein (RNP) 61, 68–73
- RNA binding proteins (RBPs) 9, 68–71, 73, 280, 286
- S**
- Saccharomyces cerevisiae* 39, 40, 295–306, 310, 340
- SDS-Polyacrylamide gel electrophoresis
(SDS-PAGE) 55, 75, 76, 188, 197,
199, 201–203, 223, 226, 227, 233, 243, 245,
248, 251, 255, 257, 258, 260, 263, 270, 272,
273, 275, 277, 390, 398, 402, 419, 424, 488
- Shine-Dalgarno 9, 58, 61
- Snyder-Robinson syndrome (SRS) 20, 162, 168,
437–444

- Spermidine 3, 40, 51, 68, 81, 131, 144, 159, 173, 185, 195, 208, 220, 238, 269, 279, 296, 312, 327, 342, 349, 379, 395, 410, 427, 437, 449, 464, 484, 496
- Spermidine/spermine-N1-acetyltransferase (SSAT) 10–14, 17–20, 22, 131, 132, 143–157, 173, 174, 379–393, 399, 404, 405, 410, 412, 414, 422, 449, 450, 464, 466, 469–471, 473
- Spermidine synthase 5, 10, 11, 40, 45, 220, 437, 440, 442
- Spermine 3, 40, 51, 68, 81, 124, 131, 143, 159, 173, 185, 198, 220, 238, 269, 279, 304, 312, 327, 342, 349, 379, 395, 410, 427, 437, 449, 464, 495, 516
- Spermine oxidase (SMO) 12, 13, 18–20, 22, 173–180, 382, 388, 395–397, 399, 401, 403–406, 410–412, 414–416, 421–422
- Spermine synthase 3, 5, 11, 20, 21, 40, 45, 159–169, 220, 221, 437–444, 497
- Stereospecificity 21, 450
- Sterility 160
- Stroke 19, 343, 379, 395–406
- Suicide 20, 219, 230–232, 427–429, 435
- Sym*-homospermidine 7, 48, 82, 90, 96, 101, 106
- Sym*-homospermidine synthase 84, 92–96
- Sym*-norspermidine 3, 6, 42, 48
- T**
- Tetracycline-regulated 133
- Tetrakis(3-aminopropyl)ammonium 8, 82, 83, 85, 90, 93, 97–99, 104, 105
- Thermine 3, 6, 82–84, 90–92, 96, 104, 109
- Thermophiles 3, 4, 6, 8, 9, 23, 81–109
- Thermospermine 3, 5, 12, 40, 42, 45, 46, 82–84, 89–92, 96, 103, 496, 497
- Thermus thermophilus* 83, 86–88, 90, 99–102, 104–109
- Thin layer chromatography (TLC) 23, 89, 96, 191, 351, 383, 451, 455, 456, 458–460
- Transcription 8, 9, 14, 20, 41, 52, 58–60, 67–70, 72, 74–75, 130, 133, 238, 241, 269, 272, 279, 313, 320, 350, 411, 437
- Transcription factor 9, 52, 58, 68
- Transfection 115, 121, 122, 239–240, 243, 244, 249, 250, 258, 259, 261–262, 274–275, 311, 315, 325, 411–412, 415–416, 419
- Transgene 130, 132–135, 137–140, 161, 165–167
- Transgenic. *See* Mice
- Transglutaminase 464
- Translation 9, 14, 15, 40, 41, 51, 52, 60–63, 67, 68, 104, 105, 130, 220, 221, 238, 241, 269, 271–273, 279–281, 350, 395, 410, 437
- Translational frameshifting 237, 238, 244–245
- Transporters 16, 17, 260, 296, 297, 304, 310, 313, 315, 318, 319, 322, 325, 328, 339, 340, 478
- Triamine 101, 104, 106, 498
- Trypanosoma brucei* 221–223, 230, 232–234, 310–312, 315, 324, 325
- Trypanosoma cruzi* 16, 221, 223, 232, 310–312, 315, 324
- Trypanosomatid. *See* Trypanosomes
- Trypanosomes 14, 39, 41, 43, 226, 229
- Trypanothione 220
- Trypanosoma. *See* Trypanosomes
- Tumor marker 137, 367–377
- Tumor suppressor 131, 480
- U**
- Ubiquitin 255
- Ubiquitination 270
- Ulcer 19, 140, 409
- 3'-Untranslated region (3'UTR) 68, 74
- 5'-Untranslated region (5'UTR) 241, 280
- V**
- Vacuoles 12, 297, 300, 303–304, 306
- Vesicles 17, 297, 299–303, 306, 340–344, 347
- Vibrio cholerae* 7, 45
- W**
- Western analysis 225, 232
- Western blotting/immunoblotting 20, 53–55, 57, 62, 76–77, 136, 167, 238–240, 243, 245–250, 260, 261, 398, 402, 411, 415, 419–420, 482–484, 487
- White adipose tissue (WAT) 144, 145
- X**
- Xenopus laevis* oocytes 310, 313, 319–324
- X-linked intellectual disability 437–444